Design of Connections in Timber Structures

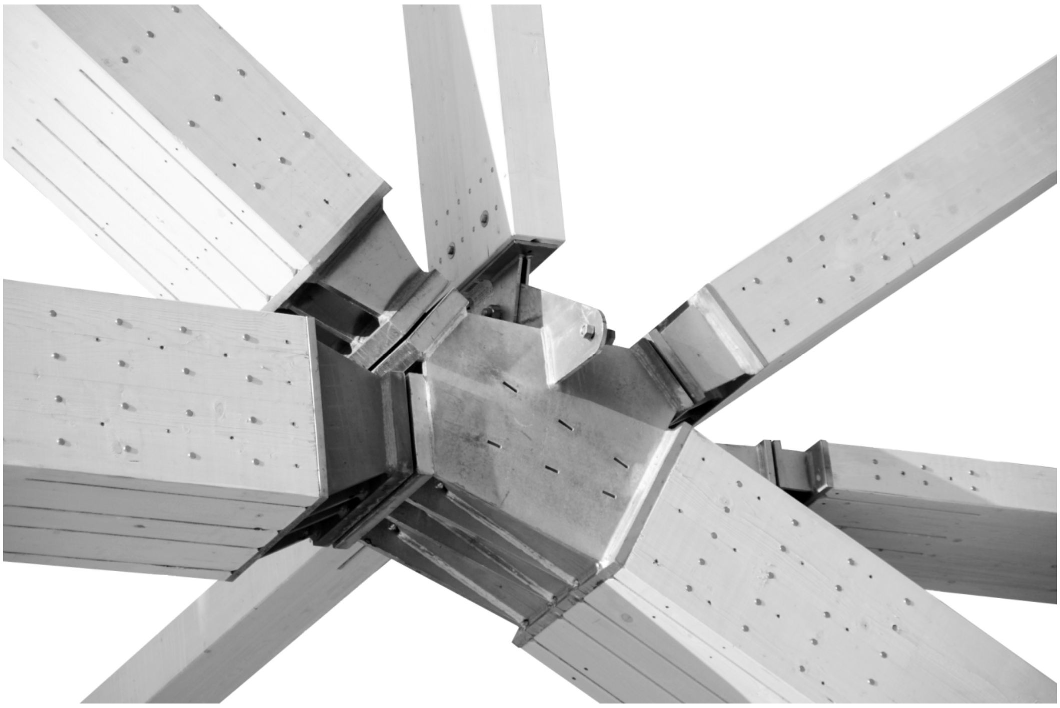

Editors:

Carmen Sandhaas, Jørgen Munch-Andersen, Philipp Dietsch

cost
EUROPEAN COOPERATION
IN SCIENCE & TECHNOLOGY

Design of Connections in Timber Structures

A state-of-the-art report by COST Action FP1402 / WG3

With contributions by:
Thomas K. Bader, Hans Joachim Blass, Jean-François Bocquet, Jorge M. Branco, Reinhard Brandner, José Manuel Cabrero, Kurt de Proft, Thierry Descamps, Philipp Dietsch, Bettina Franke, Steffen Franke, Rainer Görlacher, Robert Jockwer, André Jorissen, Marion Kleiber, Romain Lemaître, Jørgen Munch-Andersen, Tomaž Pazlar, Keerthi Ranasinghe, Andreas Ringhofer, Carmen Sandhaas, Michael Schweigler, Mislav Stepinac, Eero Tuhkanen, Maxime P. Verbist, Miguel Yurrita

Editors:
Carmen Sandhaas, Jørgen Munch-Andersen, Philipp Dietsch

EUROPEAN COOPERATION IN SCIENCE & TECHNOLOGY

Funded by the Horizon 2020 Framework Programme of the European Union

Bibliographic information published by the Deutsche Nationalbibliothek
The Deutsche Nationalbibliothek lists this publication in the Deutsche Nationalbibliografie; detailed bibliographic data are available in the Internet at http://dnb.d-nb.de.

This publication is based upon work from COST Action FP1402, supported by COST (European Cooperation in Science and Technology).
COST (European Cooperation in Science and Technology) is a funding agency for research and innovation networks. Our Actions help connect research initiatives across Europe and enable scientists to grow their ideas by sharing them with their peers. This boosts their research, career and innovation.
www.cost.eu

Funded by the Horizon 2020 Framework Programme of the European Union

Printed in Germany.

ISBN 978-3-8440-6144-4
ISSN 0945-067X

Shaker Verlag GmbH • P.O.Box 101818 • D-52018 Aachen
Phone: 0049/2407/9596-0 • Telefax: 0049/2407/9596-9
Internet: www.shaker.de • e -mail: info@shaker.de

CONTENTS

Introduction

This state-of-the-art report has been prepared within COST Action FP1402 *Basis of structural timber design – from research to standards*, Working Group 3 *Connections*. The Action was established to create an expert network that is able to develop and establish the specific information needed for standardization committee decisions. Its main objective is to overcome the gap between broadly available scientific results and the specific information needed by standardization committees. This necessitates an expert network that links practice with research, i.e. technological developments with scientific background. COST presents the ideal basis to foster this type of joint effort. Chapter 8 Connections presents an integral part of Eurocode 5 and is in need of revision. This state-of-the-art report shall provide code writers with background information necessary for the development of the so-called *Second Generation of the Eurocodes*, now aimed to be produced in 2022.

In Working Group 3 *Connections* there has been focus on the determination of the strength parameters needed to determine the load-carrying capacity of a single dowel-type fastener and on the load distribution among fasteners in a group as well as methods to avoid brittle failure modes in the timber around the fastener or group of fasteners. Also ease of use has been addressed. The design of carpentry joints is dealt with, too, as such connections now can take advantage of the precision of modern wood working.

The aim was reached through fruitful discussions during meetings, authoring of common papers and Short Term Scientific Missions, all of which have established new links between researchers and practitioners, both young and experienced and from many countries. The physical deliverables are this state-of-the-art report, the proceedings of the *International Conference on Connections in Timber Engineering – From Research to Standards* held at Graz University of Technology in 2017, reports from Short Term Scientific Missions and papers in proceedings and journals (see list of publications and STSM reports provided at the end of this report).

Results from a questionnaire for practitioners about the connections chapter of Eurocode 5

José Manuel Cabrero
Universidad de Navarra
Pamplona, Spain

Mislav Stepinac
University of Zagreb
Croatia

Keerthi Ranasinghe
University of Wales
Trinity Saint David, UK

Marion Kleiber
Harrer-Ingenieure GmbH
Karlsruhe, Germany

1. Introduction

Eurocode 5 is an integral part of the aimed European harmonization for product and design standards, allowing a common structural building market all around Europe. In 2012, through the Mandate M/515, the European Commission invited CEN to develop the work program for the preparation of the second generation of Eurocodes. The Mandate, among other objectives, called for a "Refinement to improve the 'ease of use' of Eurocodes by practical users" [1]. The CEN answer to the Mandate, "Response to Mandate M/515" [2], focuses on harmonization and state-of-the-art approaches and also on user confidence. The required ease-of-use has also been further clarified by defining that the Eurocodes are addressed to "Competent civil, structural and geotechnical engineers, typically qualified professionals able to work independently in relevant fields" [3].

The section on connections, the Chapter 8, takes up a long part of the current version of Eurocode 5. About 20% of the text is spent on connections, and yet, only the most common connection types are included in detail.

The COST Action FP1402 aims to bridge the existing gap in the timber construction world between the broadly available scientific results and the specific information needed by designers, industry, authorities and code committees, providing transfer for practical application in timber design and innovation [4]. Its results will provide some background knowledge for the development of the so-called Second Generation of the Eurocodes, aimed to be produced in 2020 [5].

Within the Working Group 3 (WG3) of the COST Action FP1402, it was thus decided to develop a questionnaire to get the opinion of the practitioners about the content and structure of the current Chapter 8 of Eurocode 5 [6], which includes most of the rules related to the design of structural connections. The idea was to understand the experiences of the practitioners, manufacturers and academia, and to point out general problems and issues concerning Chapter 8 and Eurocode 5.

2. Methodology

A questionnaire can be an excellent tool to get an insight in to the problems faced by the practitioners. Numerous studies had already been done in the past to gather consumer opinions towards timber as a construction material [7], architects' view on timber structures [8-10], trends in worldwide markets [11, 12] and future potential of wood construction [13, 14].

The design of connections in timber structures has long been identified as the most crucial component of the design process due to the complex stress transfer mechanisms exhibited by dowel type connections, the wood anisotropy, the potential for wood splitting arising out of excessive stresses perpendicular to grain, significant reduction of wood cross section in the connection region, lack of understanding of detailing and execution, manufacturing and construction [15]. A Nordic study presented in [16] identified that 23% of failures of timber structures were directly connected due to bad design of connections in structural elements and that 57% of cases reported were in dowel-type connections.

The idea of this questionnaire therefore was to get feedback about the problems faced by practitioners in using the connections section to make our engagements with the code writers more meaningful. The questionnaire was sent to engineering practitioners, manufacturers and academia in the hope that key problems would be identified. As mentioned above, the focus was primarily on practitioners. Taught by experience that practitioners do not meet and complete the surveys if they are not in their native language, online questionnaire was translated into 12 different European languages (English, German, Spanish, Portuguese, Italian, French, Croatian, Slovenian, Slovakian, Estonian, Finnish and Dutch). Information was gathered in all above mentioned languages and later translated in English by an experienced domestic structural engineer who knows the code and professional terminology in English.

The questionnaire was divided into four parts: general information about the respondents, general issues of Eurocode 5, issues with Chapter 8 and specific issues with fasteners. The first part of the questionnaire asked information about the work experience in the field of timber structures, common types of structures and engineered wood products which are commonly used. The second part of the survey was focused on the general knowledge of the Eurocode 5 standard, in particular on the familiarity with the standard, possible problems, mistakes and issues of the standard, also asking for recommendations for improvement. Of interest was also to get knowledge about other standards or guidelines often used when information is not found in Eurocode 5. The third part was questions about satisfaction about the Chapter 8, problems and disadvantages. Questions were also asked about the organization of the Chapter. The fourth part asked about specific issues with fasteners. Overall, a total of 35 questions with 36 sub questions were asked. Parts of the contents in this chapter have first been published by the same authors in the journal *Engineering Structures* **170**:135-145 (2018) [17].

3. Results

3.1 Respondents' profile

The questionnaire was filled out by 412 respondents from 28 European countries and 5 non-European countries (Fig. 1). As seen from the Fig. 1, most answers came from Germany (23.8 %), France (10.4 %) and Spain (9.0 %), but a significant number of respondents came from other parts of Europe as well [17]. Only 7% of the respondents have less than 3 years of work experience and only 11% have less than 3 years of work experience in timber structures, which proves the quality of the answers and their familiarity with the standard (Figs. 2 and 3).

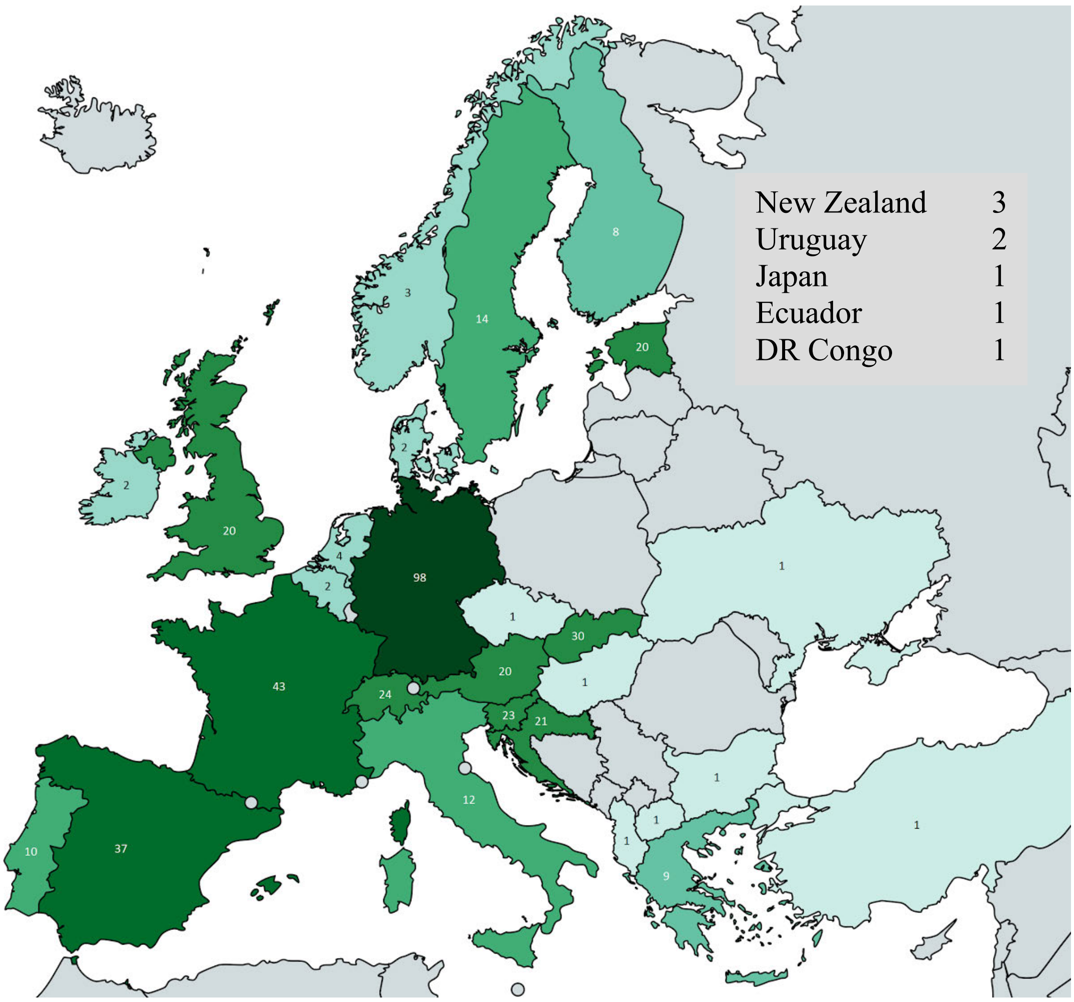

Fig. 1. Geographical distribution of answers (darker colour = more answers) [17].

More than 72% of respondents are working as practitioners and manufacturers, while 18% are coming from Academia and 10% are from professions connected to the timber industry (Fig. 4). Respondents were mainly working in medium to big design offices (with more than 10 employees, Fig. 5) and in a respectful percentage of companies (40%) timber structures were their main point of interest (Fig. 6), identified as having more than 70% of the daily work dedicated to timber structures.

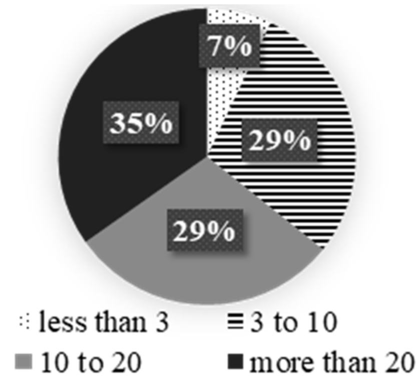

Fig. 2. *Work experience of respondents*

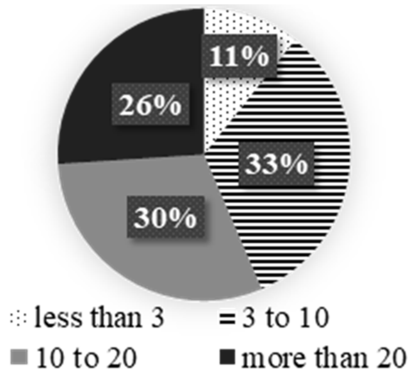

Fig. 3. Work experience in timber structures of respondents

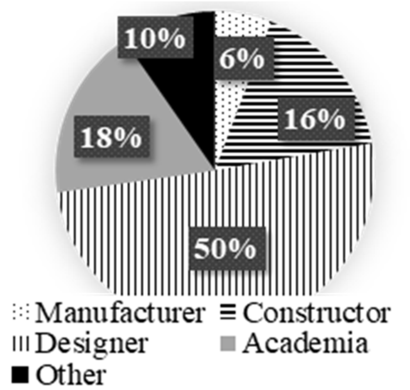

Fig. 4. Respondent's employment

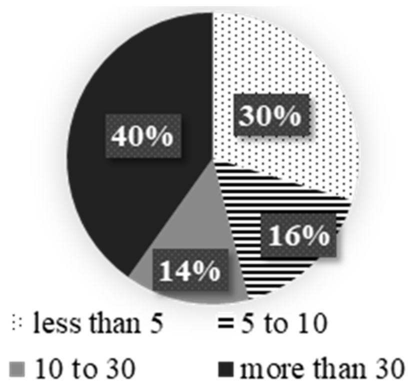

Fig. 5. Number of employees

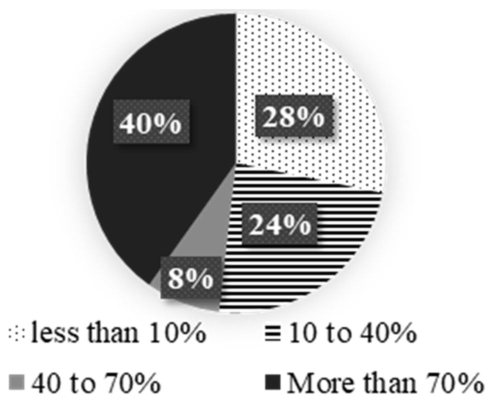

Fig. 6. Percentage of timber structures designed by your company

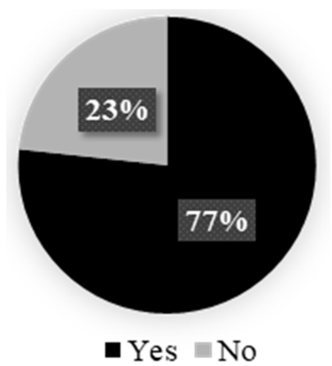

Fig. 7. Did you study timber engineering as part of your studies?

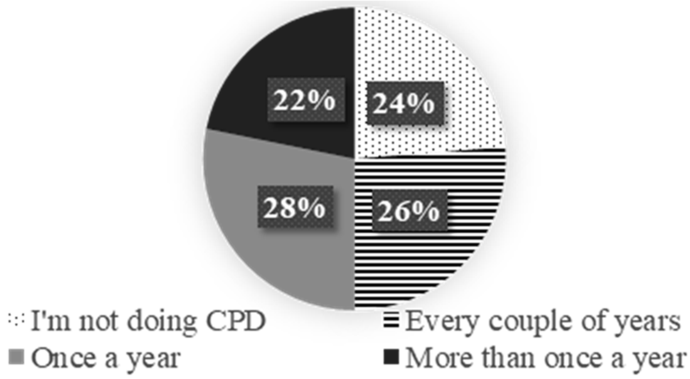

Fig. 8. How often do the respondents participate in Continued Professional Development (CPD) courses on timber engineering?

A great number of respondents were studying timber engineering during their education (Fig. 7) and 50% is participating at least once a year in continued professional development courses (Fig. 8). Respondents have an experience in designing simple timber structures but there was a significant number of respondents who have experience with more complicated structures (Fig. 9). Respondents are more often using glulam and softwood, but also have experience in design with other materials (Fig. 10).

Using a 5-point Likert scale [18] from "I'm not familiar" to "I'm really familiar", the average grade for familiarity with the standard was 3.8 and for satisfaction 3.0. Only 1.9 % of respondents were completely satisfied with the code, which points to an underlying unease with using the standard (Fig. 11).

Using a 5-point Likert scale [18] from "I'm not satisfied" to "I'm really satisfied", the average grade for satisfaction with the National Annexes (NA) for Eurocode 5 is around 3.0. In Fig. 12, satisfaction with the NAs is compared for the different countries.

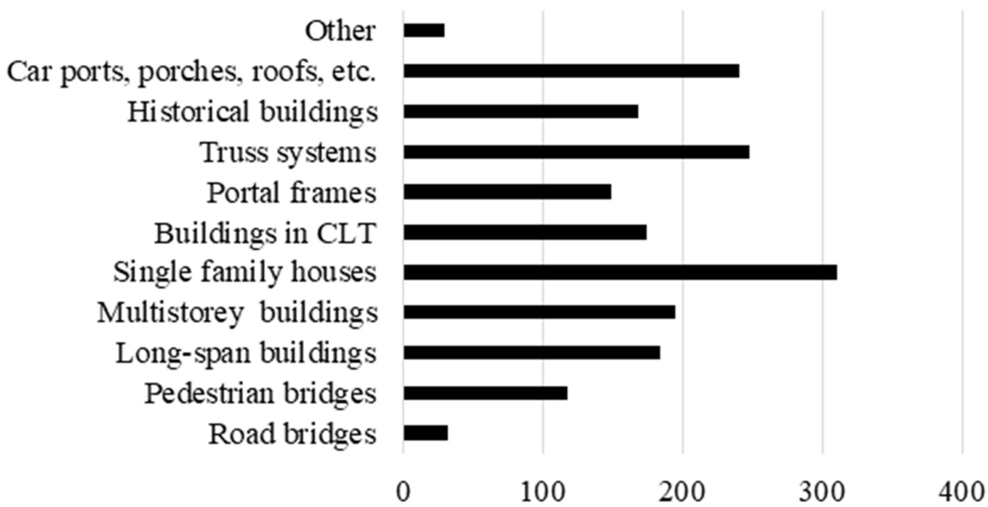

Fig. 9. Type of structures respondents have experience with

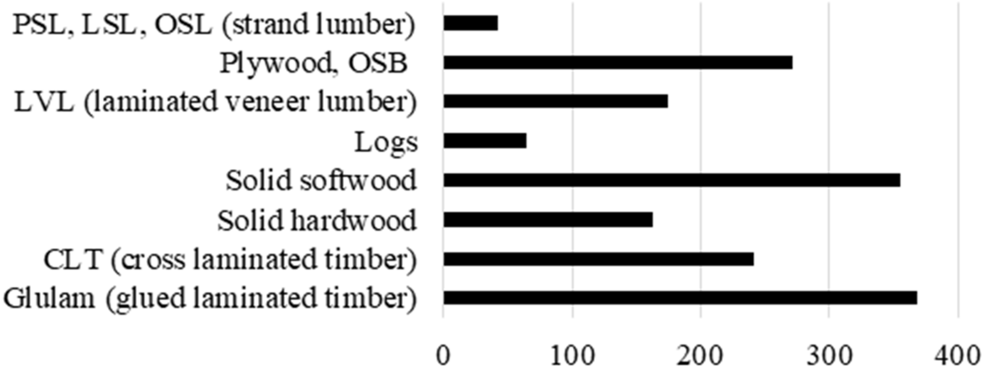

Fig. 10. Which timber products do you use?

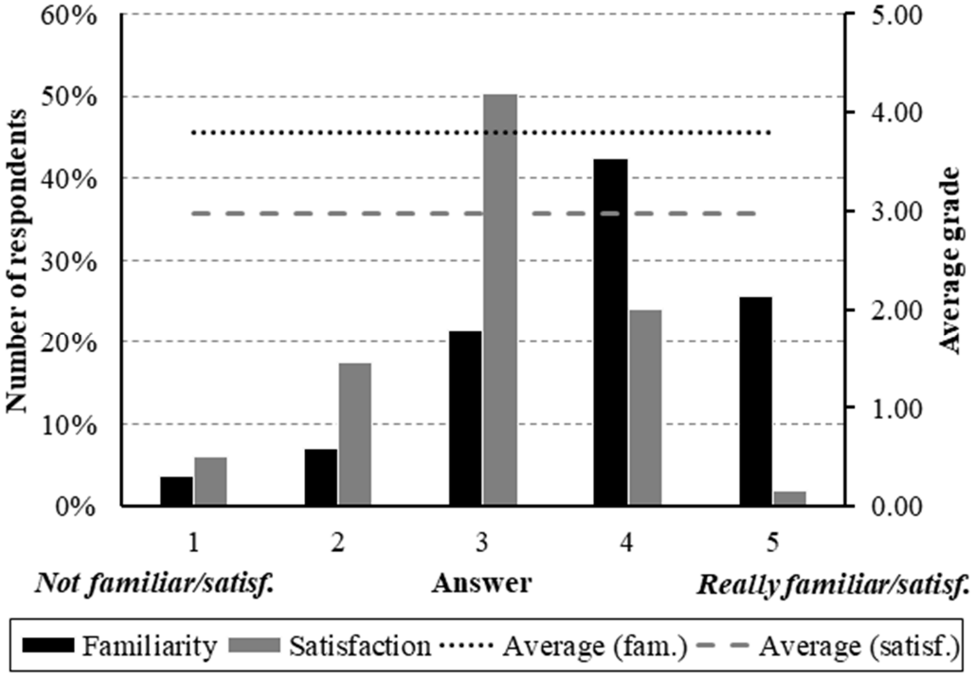

Fig. 11. Level of satisfaction and knowledge of the present Eurocode 5 (1 – I'm not familiar, I'm not satisfied at all, 5 – I'm really familiar, I'm pretty satisfied). [17]

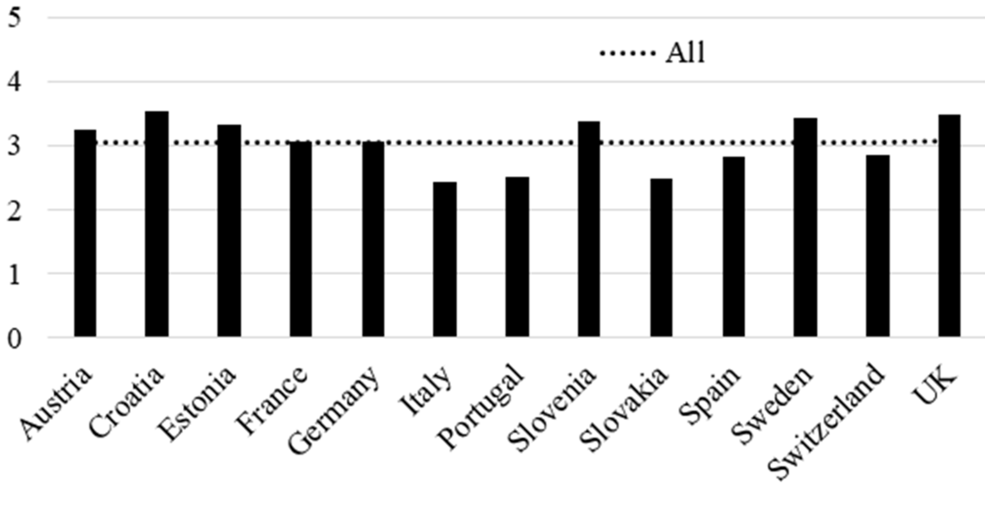

Fig. 12. Level of satisfaction on country's National Annex for Eurocode 5 (1 – I'm not satisfied at all, 5 –I'm pretty satisfied)

3.2 General issues of Eurocode 5

Inquiries on perceived general problems of Eurocode 5 and the need for improvement of the code were summarized in three descriptive questions where respondents could freely express their opinions on such matters as obvious mistakes in the code, parts that require excessive design effort to apply and parts that could lead to uneconomic construction. These are summarized in Tables 1 to 4 below. Unsurprisingly, connections top the lists in all these tables by some significant margins.

Table 1. Parts in the Eurocode 5 that require excessive design effort to apply

Topic	Frequency
Connections	64
Vibrations and deflections	14
Stability of members	12
Stresses perp to grain and shear	8
Timber-concrete composites, components and assemblies	7
Load duration classes and service classes	7
Structural fire design	2
Seismic design	2

Table 2. Parts in the Eurocode 5 that that could lead to uneconomic construction

Topic	Frequency
Connections	26
Stresses perp to grain and shear	21
Stability of members	14
Structural fire design	13
Vibrations and deflections	13
Load duration classes and service classes	7
Material properties and partial safety factors	3

Table 3. Parts of the Eurocode 5 where whole solution of the problem is not covered or there is a lack of provided information

Topic	Frequency
Connections	7
CLT	5
Stability of members	4
Vibrations and deflections	4
EWP	3
Timber-concrete composites, components and assemblies	2

Table 4. Erroneous parts in the Eurocode 5 according to respondents

Topic	Frequency
Connections	22
Stability of members	6
Stresses perp to grain and shear	5
Vibrations and deflections	4
Load duration classes and service classes	3
Timber-concrete composites, components and assemblies	2

Using a 5-point Likert scale from “it must be changed completely” to “it doesn't need any change” respondents were leaving opinions about satisfaction with technical content, organization of the content and figures in Eurocode 5 (Fig. 13).

A significant number of respondents were using the code for the design and/or checking of existing structures (62%, Fig. 14). When there is a lack of information in Eurocode 5, respondents said they refer their former national standards, but also the standards of other countries (Fig. 15).

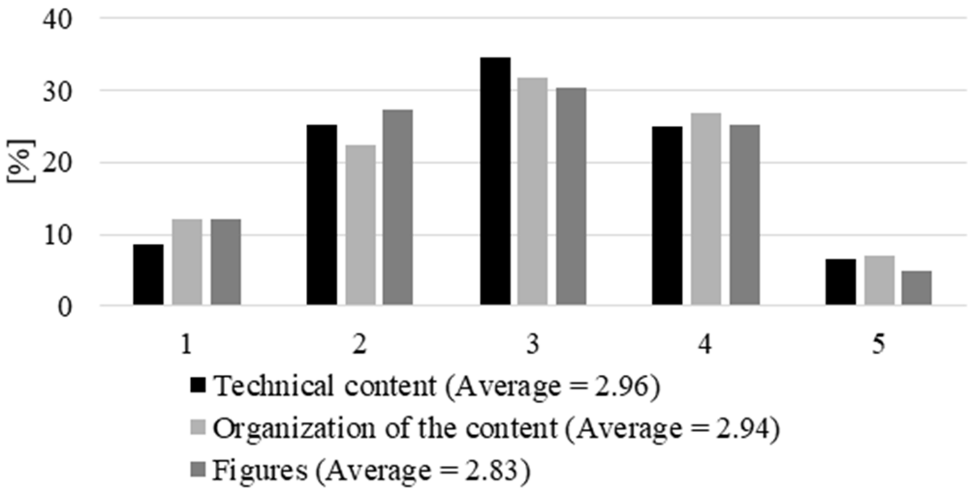

Fig. 13. Satisfaction with technical content, organization of the content and figures in Eurocode 5 (1 –I'm not satisfied at all, 5 –I'm pretty satisfied)

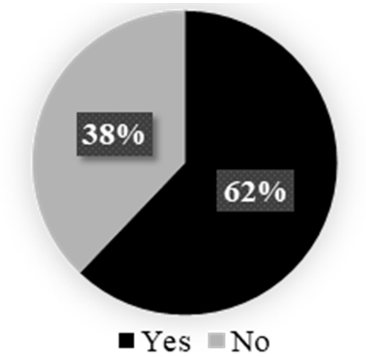

Fig. 14. Do you use the code for the design and/or checking of existing structures?

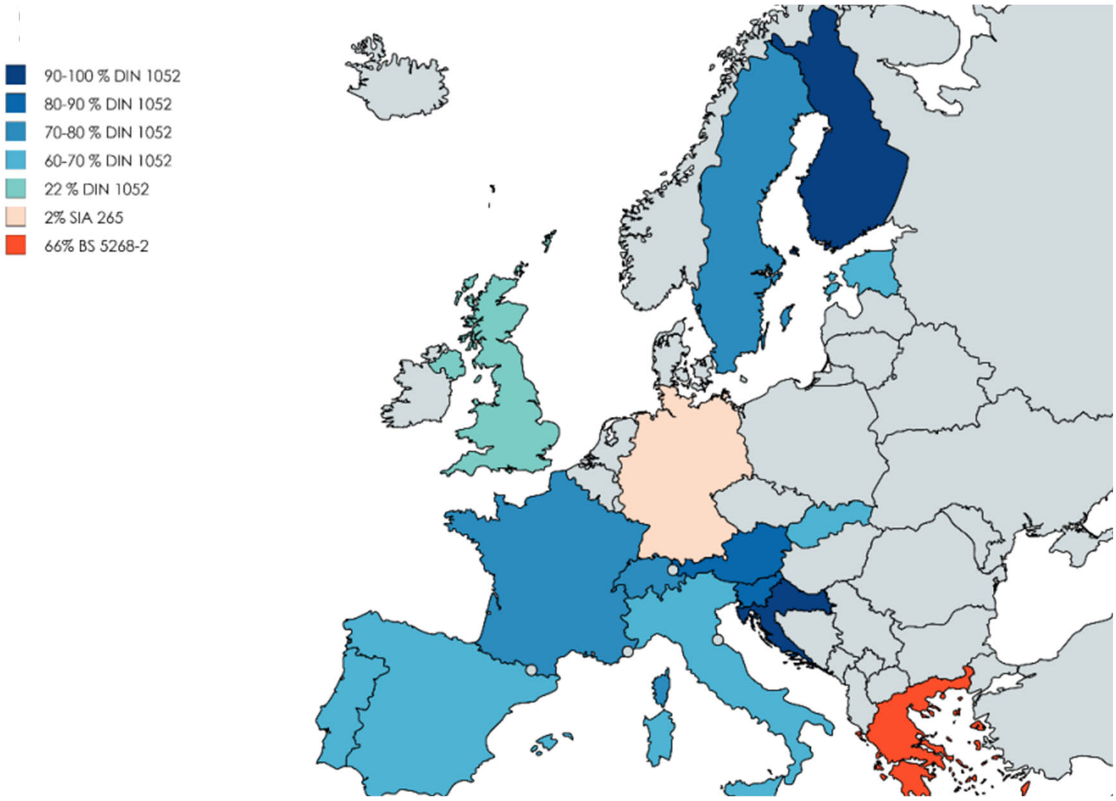

Fig. 15. If you don't find information in Eurocode 5 for a specific item of work, which other standard are you using? [17]

3.3 Issues with Chapter 8, Connections of Eurocode 5

As seen from the previous Chapter and the Tables 1 to 4, most of the problems were identified in the Chapter 8 of the Eurocode 5. The main problems with the current version of Chapter 8 are summarized in Table 5. The most common opinions were regarding the problems in the structure of the code and difficulties in navigation through the Chapter (Table 5).

Table 5. Main problems with the current version of Chapter 8 (N_{all} = 410, $N_{experts}$ = 184). Multiple responses were possible.

Problem	Number of responses – all	Number of responses – experts
Difficulties in navigating	223 (54%)	123 (67%)
Confusing statements	156 (38%)	89 (48%)
Lack of information	143 (35%)	64 (35%)
Poor presentation of technical content	134 (33%)	71 (39%)
Dependency on other standards	87 (21%)	46 (25%)
Lack of consistency	68 (17%)	41 (22%)
Other	43 (10%)	21 (11%)
No problem	34 (8%)	3 (1.6%)

Using a 5-point Likert scale [18] from “I’m not satisfied” to “I’m satisfied”, academics with an average of 3.0 were slightly more satisfied than practitioners with an average of 2.8. This can be seen in the Fig. 16. Only 0,5% of the respondents are completely satisfied with the structure of Chapter 8.

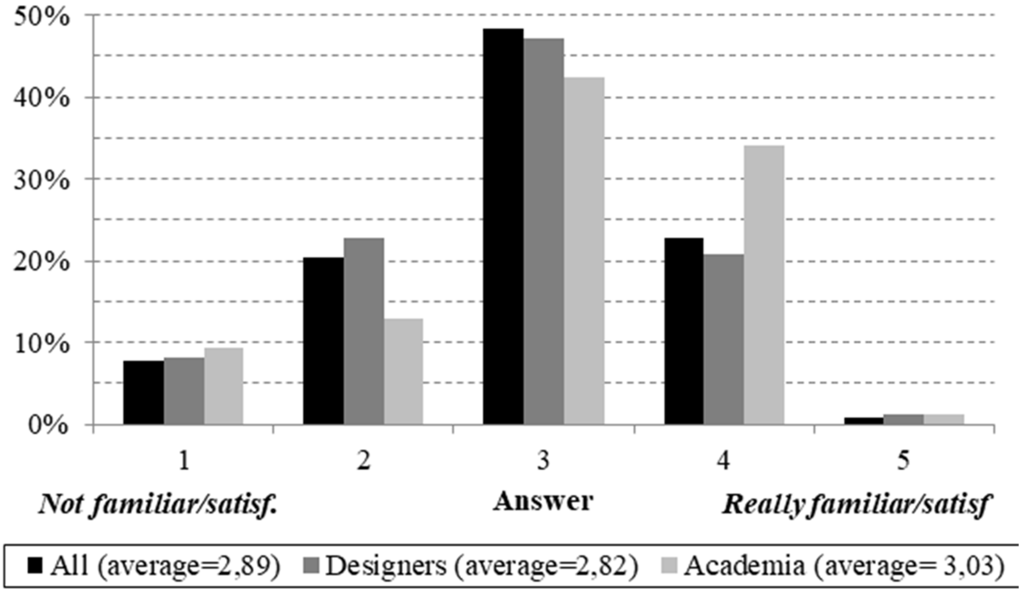

Fig. 16. Overall satisfaction with the structure of Chapter 8 [17].

More than 80% of the respondents agreed that there are a lot of missing details, such as on glued-in rods, carpentry joints, reinforced connections, self-tapping screws with large diameters and fastener in axial compression. They also considered that design rules regarding new types of fasteners and connections in Engineered Wood Products (EWP’s) should also be added. Other things highlighted as missing in the Chapter 8 were; the rules for moment transmitting connections and modern screws, improved rules for effective number of fasteners and methods for calculation of slip in connections, combined effects of lateral and tension loads, new and brittle failure modes, better explanations of methods for obtaining ductility in the connections, etc. 55% of the respondents did not consider spacing rules as understandable!

From a practical point of view respondents agree that parts of the Chapter such as punched metal plate connectors, minimum spacing of fasteners dependent on the density, tension perpendicular to grain, geometrical requirements in multiple shear and spacing requirements are too complicated or too confusing and better explanations and clarification of the problems are needed. Also, nearly 50% of respondents experience problems with the definition of loaded and unloaded edges for distances, differentiation between thin and thick plates (steel-to-timber connections), rope effect, explanation of fastener capacities for double shear, i.e., practitioners forgetting to multiply by 2 etc. Regarding the reorganization of the Chapter, all respondents agree on the following statements: yield moment equations for all fastener types should be written in one place, embedment equations for all fasteners should be written in one place, Johansen equations, rope effect limits and failure mode diagrams should all be in one table, spacing requirements for different fastener types should be in one table (Fig. 17). Other parts that should not be scattered inside Chapter 8 were identified as slip moduli and stiffness parameters, spacing, end and edge distances for dowel type connectors (Table 6).

Table 6. Parts of Chapter 8 which should not be scattered inside the code

Topic	Frequency
Spacing, end and edge distances	12
European Yield Model	6
Slip moduli and stiffness parameters	8
Mechanical parameters of dowel type connectors	8
Whole Chapter in general	7
Embedment strengths	3

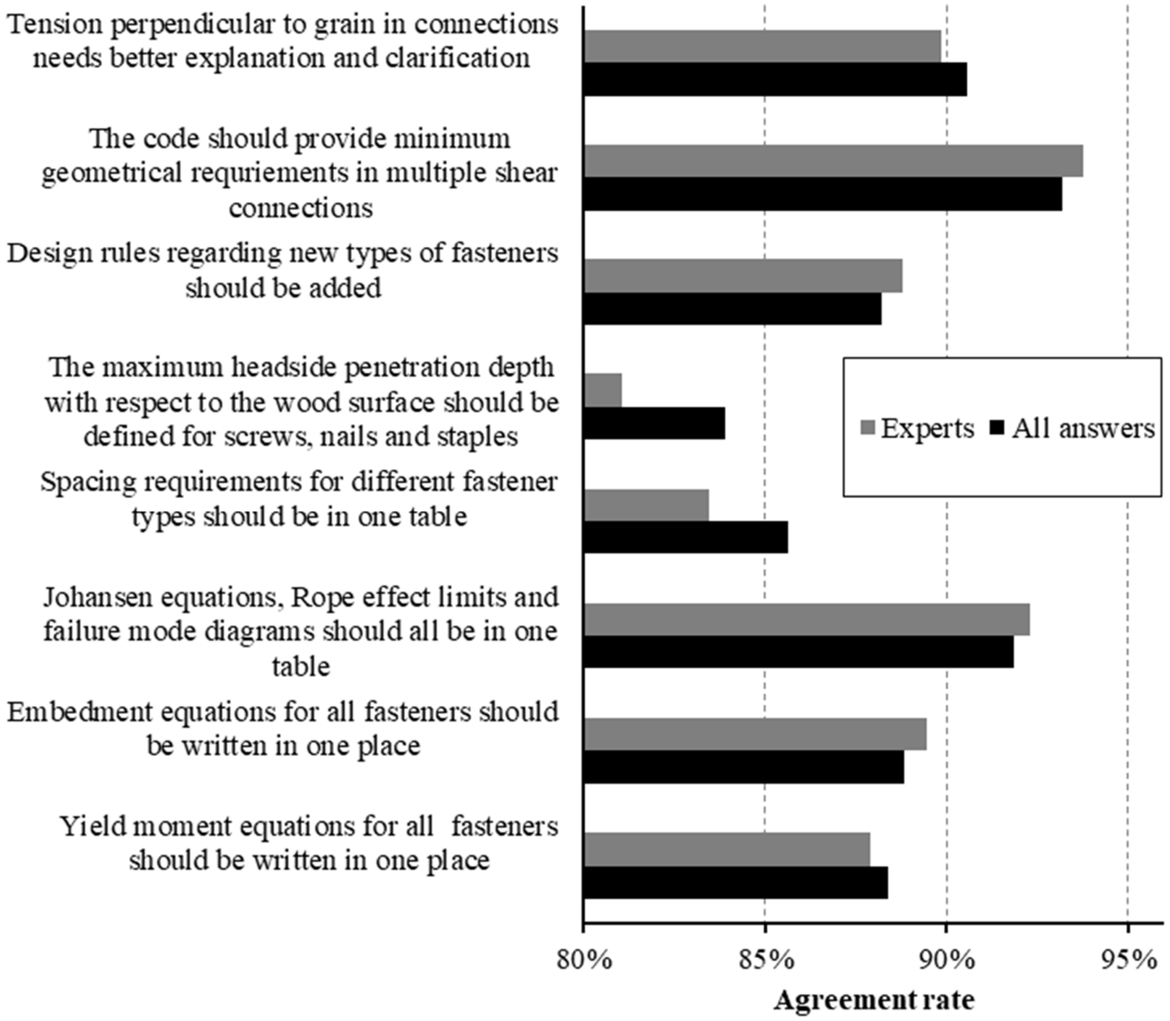

Fig. 17. Respondents' agreement about several questions of the reorganization of the Chapter [17]

People are mostly using modern connection techniques such as screws, dowels, bolts and nails (Fig. 18). A majority of respondents (56%) would prefer to use technical classes for fastener properties instead of declared properties and a huge majority (82%, Fig. 19) wish there were more simple design rules for connections in addition to existing rules. 88% of respondents express the need and an interest in European Guidelines for the Chapter 8 of Eurocode 5 (Fig. 20).

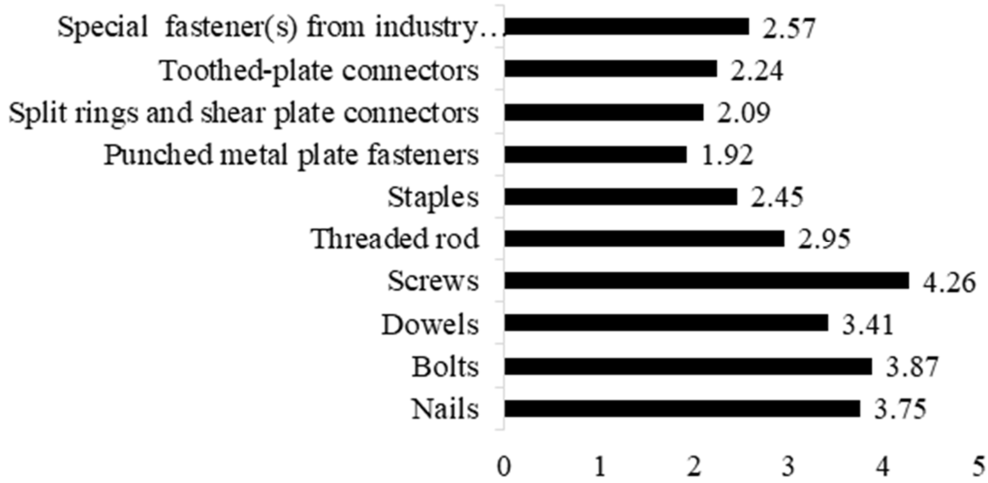

Fig. 18. Most common types of fasteners used (1 - Never, 5 - Often)

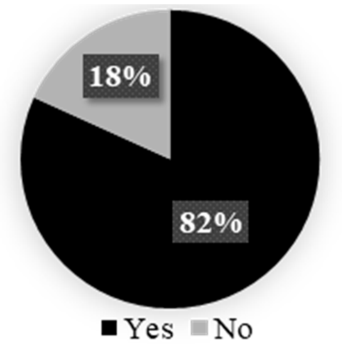

Fig. 19. In addition to existing rules, do you wish there were more simple design rules for connections?

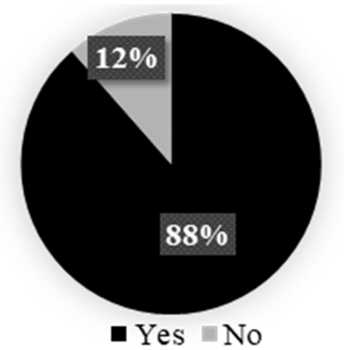

Fig. 20. Would you be interested in European Guidelines for EN1995, Chapter 8?

4. Conclusions

CEN/TC250/SC5, in "Response to Mandate M/515" [2], **focuses** on further harmonization of design principles, inclusion of state-of-the-art design approaches and enhancing user confidence in using the standard as priorities to be achieved in the next revision to Eurocode 5. In this regard, clarity and understandability, ease of navigation, state-of-the-art information and consistency with product and **execution** standards have been identified as key elements to the next revision.

A Europe-wide survey of practitioners, from both the industry and the academia was thus conducted to identify the end-user's perspective on the standard, especially in relation to the above key elements. The survey was prepared to cover Eurocode 5 in general and more specifically the connections chapter. The survey was translated in to 12 European languages to broaden the feedback received.

The section on connections, the Chapter 8 of the current Eurocode 5, takes up a significant number of pages, which is in line with the importance of the section. However, through the survey conducted and the results discussed above, it could be seen that significant gaps still exist within this section. A clear understanding of the problems that the practitioner is facing every day when using this standard to design timber structures has been gained. Respondents to the survey agree that the Chapter lacks information, contains confusing statements and poorly presented technical content, making it difficult to navigate through and use. Most felt that the Chapter is unacceptable for day-to-day use in a design practice, where the commercial pressures do not allow much time to complete a design.

Acknowledgements

This article is based upon work of Working Group 3 of the COST Action FP1402, supported by COST (European Cooperation in Science and Technology). Authors wish to place on record their thanks to all of the translators; Elke Mergny, Jaroslav Sandanus, Tomaž Pazlar, Matteo Izzi, Robert Jockwer, Eero Tuhkanen, Kurt de Proft and Pedro Palma, all respected members of the engineering communities within their individual countries, for their kind help. We also wish to express our immense gratitude to Prof. Hans Blass of Karlsruhe Institute of Technology, for reviewing a version of this paper sent to him at the last minute. Parts of the contents in this chapter have first been published in the article "Proposal for reorganization of the connections chapter of Eurocode 5", *Engineering Structures*, Volume 170, 2018, pages 135–145 [17].

References

[1] The European Commission (2012) *Mandate M/515* – Mandate for amending existing Eurocodes and extending the scope of structural Eurocodes.

[2] CEN/TC250 (2013) *Response to Mandate M/515* – Towards a second generation of Eurocodes.

[3] CEN/TC250 (2015) *N1239* – Position paper on enhancing ease of use of structural Eurocodes.

[4] https://www.costfp1402.tum.de/en/home/. Homepage of COST Action FP1402: Basis of Structural Timber Design - from research to standards.

[5] Dietsch P, Winter S (2012) Eurocode 5 – Future developments towards a more comprehensive code on timber structures. *Structural Engineering International* **22**(2):223-231.

[6] http://tiny.cc/woodForm. Homepage of questionnaire: Connections with metal fasteners, Chapter 8, EN 1995-1-1.

[7] Gold S, Rubik F (2009) Consumer attitudes towards timber as a construction material and towards timber frame houses - selected findings of a representative survey among the German population. *Journal of Cleaner Production* **17**(2):303-309.

[8] Hemström K, Mahapatra K, Gustavsson L (2011) Perceptions, attitudes and interest of Swedish architects towards the use of wood frames in multi-storey buildings. *Resources, Conservation and Recycling* **55**(11):1013-1021.

[9] Arnautovic-Aksic D (2016) A comparative analysis of architects' views on wood construction. *Spatium* **36**:100-105.

[10] Laguarda Mallo MF, Espinoza O (2015) Awareness, perceptions and willingness to adopt Cross-Laminated Timber by the architecture community in the United States. *Journal of Cleaner Production* **94**:198-210.

[11] Ganguly I, Eastin IL (2009) Trends in the US decking market: A national survey of deck and home builders. *Forestry Chronicle* **85**(1):82-90.

[12] Riala M, Ilola L (2014) Multi-storey timber construction and bioeconomy – barriers and opportunities. *Scandinavian Journal of Forest Research* **29**(4):367-377.

[13] Hurmekoski E, Jonsson R, Nord T (2015) Context, drivers, and future potential for wood-frame multi-story construction in Europe. *Technological Forecasting and Social Change* **99**:181-196.

[14] Wang L, Toppinen A, Juslin H (2014) Use of wood in green building: A study of expert perspectives from the UK. *Journal of Cleaner Production* 65:350-361.

[15] Frühwald E, Thelandersson S (2008) *Design of safe timber structures - How can we learn from structural failures in concrete, steel and timber?* 10th World Conference on Timber Engineering, proceedings vol. 4., pp. 1962–1969.

[16] Frühwald Hansson E (2011) Analysis of structural failures in timber structures: Typical causes for failure and failure modes. *Engineering Structures* **33**(11):2978-2982.

[17] Stepinac M, Cabrero JM, Ranasinghe K, Kleiber M (2018) Proposal for reorganization of the connections chapter of Eurocode 5. *Engineering Structures* **170**:135-145.

[18] Likert R (1932) A technique for the measurement of attitudes. *Archives of Psychology* **22**(140):1-55.

Proposal for new structure of the connections chapter

Keerthi Ranasinghe
University of Wales
Trinity Saint David, UK

José Manuel Cabrero
Universidad de Navarra
Pamplona, Spain

Mislav Stepinac
University of Zagreb
Croatia

Marion Kleiber
Harrer-Ingenieure GmbH
Karlsruhe, Germany

1. Introduction

The section on connections, the Chapter 8, takes up a long part of the current version of the Eurocode 5. About 20% of the text is spent on connections, and yet, only the most common connection types are included in detail. In the former 1987 version [1] approximate expressions were used for connections, but the final version adopted the "Johansen model" [2]. Discussions related to the development of the model included in the final version of the Eurocode 5 may be found in the CIB-W18 proceedings [3]. Parts of the contents in this chapter have first been published by the same authors in the journal *Engineering Structures* **170**:135-145 (2018) [4].

2. Structure of the Chapter 8 of EN 1995-1-1

As shown in the previous chapter, one of the key items that surfaced as a result of the questionnaire was that the structure of the current Chapter 8 in Eurocode 5 is unacceptable for the daily use of the standards in practice. Therefore, a new structure to the Chapter 8 of Eurocode 5 is considered necessary. The following table (Table 1) shows the existing structure of Chapter 8 against a proposal that came out of many discussions during WG3 meetings. The aim was to get a structure which the designer can follow through from the beginning to the end, during connection design.

In the first two sections some general information and rules for the basis of design are given. The third section includes the fastener properties which are needed for the next steps. Section 4 has been retained as the one that discusses durability as it reflects the general structure of all Eurocodes. The design of a single dowel-type fastener is described in part 5. In contrast to the old structure, in the proposal fasteners are not differentiated by the type, but their diameter. Section 6 is new as it deals with the design of a connection. Within this section spacing, group effects, timber failure, block-shear, plug shear and forces at an angle to the grain are all considered. Section 7 covers the serviceability aspects. Traditional connectors and punched metal plate fasteners have been moved to Sections 8 and 9.

Table 1. Existing and proposed structure of Chapter 8

Existing Eurocode 5	New Eurocode 5
8.1 GENERAL 8.1.1 Fastener requirements 8.1.2 Multiple fastener connections 8.1.3 Multiple shear plane connections 8.1.4 Connection forces at an angle to the grain 8.1.5 Alternating connection forces	8.1 GENERAL 8.1.1 Fastener requirements 8.1.2 Multiple fastener connections
8.2 LATERAL LOAD-CARRYING CAPACITY OF METAL DOWEL-TYPE FASTENERS 8.2.1 General 8.2.2 Timber-to-timber and panel-to-timber connections 8.2.3 Steel-to-timber connections	8.2 BASIS OF DESIGN 8.2.1 General 8.2.2 Alternating connection forces 8.2.3 Limits for connection capacities 8.2.4 Miscellaneous rules
8.3 NAILED CONNECTIONS 8.3.1 Laterally loaded nails 8.3.2 Axially loaded nails 8.3.3 Combined laterally and axially loaded nails	8.3 FASTENER PROPERTIES 8.3.1 General 8.3.2 Correction for wood type 8.3.3 Conditions for connection capacities (execution) 8.3.3.1 Need for predrilling 8.3.4 Strength parameters 8.3.4.1 Embedment strength 8.3.4.2 Yield moment 8.3.4.3 Head pull-through strength 8.3.4.4 Withdrawal strength
8.4 STAPLED CONNECTIONS	8.4 DURABILITY 8.4.1 Corrosivity of timber and atmospheric environment
8.5 BOLTED CONNECTIONS 8.5.1 Laterally loaded bolts 8.5.2 Axially loaded bolts	8.5 DESIGN OF SINGLE DOWEL-TYPE FASTENERS 8.5.1 General 8.5.1.1 Combined laterally and axially loaded fasteners 8.5.2 Axial load-carrying capacity 8.5.3 Lateral load-carrying capacity 8.5.4 Rope-effect 8.5.5 Johansen contribution 8.5.5.1 Timber-to-timber and panel-to-timber connections 8.5.5.2 Steel-to-timber connections 8.5.5.3 Multiple shear plane connections
8.6 DOWELLED CONNECTIONS	8.6 CONNECTION DESIGN 8.6.1 Spacing 8.6.2 Group effect 8.6.3 Timber failure 8.6.3.1 Block shear and plug shear, steel-to-timber connections 8.6.3.2 Connection forces at an angle to the grain
8.7 SCREWED CONNECTIONS 8.7.1 Laterally loaded screws 8.7.2 Axially loaded screws 8.7.3 Combined laterally and axially loaded screws	8.7 SERVICEABILITY
8.8 CONNECTIONS MADE WITH PUNCHED METAL PLATE FASTENERS 8.8.1 General 8.8.2 Plate geometry 8.8.3 Plate strength properties 8.8.4 Plate anchorage strengths 8.8.5 Connection strength verification	8.8 CONNECTORS 8.8.1 General 8.8.2 Split ring and shear plate connectors 8.8.3 Toothed-plate connectors
8.9 SPLIT RING AND SHEAR PLATE CONNECTORS	8.9 PUNCHED METAL PLATE FASTENERS
8.10 TOOTHED-PLATE CONNECTORS	

It is the authors' view that the proposed new structure to the connections chapter of Eurocode 5 is more in line with the design philosophy of a connection in practice, and that it makes the navigation through the chapter much easier. The approach taken to arrange the design rules according to the diameter rather than the fastener types as in the current version also minimizes repetition of and looping for information.

Furthermore, the order of the sub sections of the chapter has also been changed, the benefits of which become quite evident when shown through an example of designing the lateral load-carrying capacity of a connection with screws (Figs. 1 and 2).

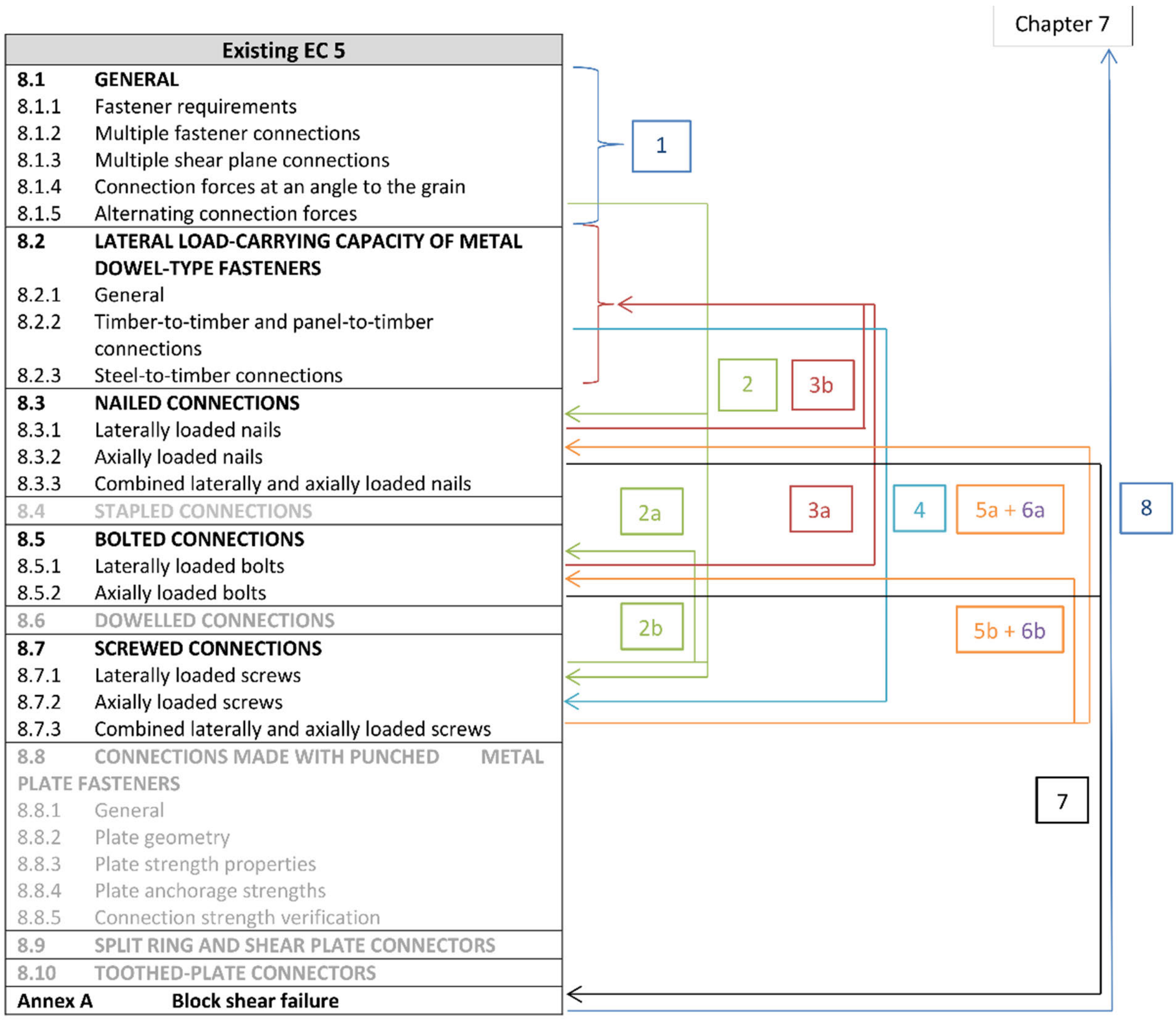

Fig. 1. Example of designing the lateral load-carrying capacity of a connection with screws – procedure in existing Eurocode 5 [4]

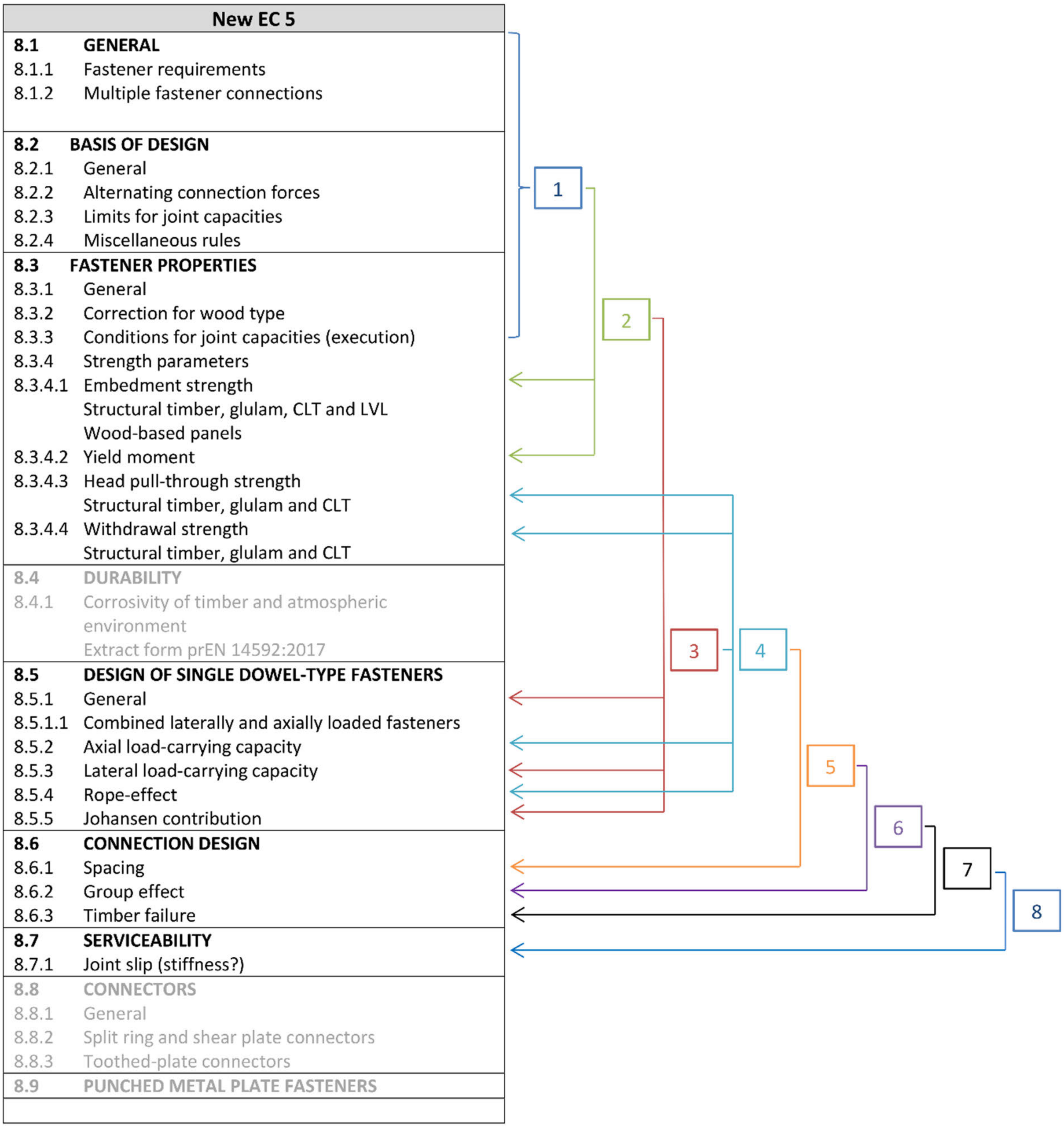

Fig. 2. Example of designing the lateral load-carrying capacity of a connection with screws – procedure in proposed version of Eurocode 5 (EC 5) [4]

In steps 1 to 8 in the diagram above, the approach taken when designing the lateral load-carrying capacity of a connection with screws is described. When this approach is superimposed on the existing chapter, it becomes very clear how confusing the current structure can be. In the proposed structure on the other hand, the design logic in steps 1 to 8 is broadly followed.

3. Conclusions

Designing a connection and realizing this design in practice has long been considered as the most important aspect of timber design. It has been shown that most failures occurring in timber structures were caused by failures in connections.

A new structure to the Chapter is been presented. Most of the user concerns that were found through the survey have been taken into account in preparing this proposal. Through the use of a simple example, the design flow of a simple connection has been studied, and the benefits are examined with a comparison to the existing structure of Chapter 8.

Acknowledgements

This article is based upon work of Working Group 3 of the COST Action FP1402, supported by COST (European Cooperation in Science and Technology). Parts of the contents in this chapter have first been published in the article "Proposal for reorganization of the connections chapter of Eurocode 5", *Engineering Structures*, Volume 170, 2018, pages 135–145 [4].

References

[1] Crubile P, Ehlbeck J, Brüninghoff H, Larsen HJ, Sunley JG (1987) Common Unified Rules for Timber Structures. Eurocode No. 5. *Report EUR9887*, Brussels.

[2] Larsen HJ (1992) An introduction to Eurocode 5. *Construction and Building Materials* **6**(3):145-150.

[3] Larsen HJ, Munch-Andersen J (2011) *Part 4: Connections*. In: CIB-W18 Timber Structures – A review of Meetings 1-43, Danish Timber Information.

[4] Stepinac M, Cabrero JM, Ranasinghe K, Kleiber M (2018) Proposal for reorganization of the connections chapter of Eurocode 5. *Engineering Structures* **170**:135-145.

Technical specifications for fasteners

Tomaž Pazlar
Slovenian National Building and Civil Engineering Institute (ZAG)
Ljubljana, Slovenia

Summary

(Dowel-type) fasteners used in timber structures are according to the Commission regulation (EU) No 305/2011 considered as construction products. Therefore, they should be CE marked and together with the Declaration of Performance it should be possible for users to check the performance of the specific product and compare it with other products under the same technical approach. This paper presents the possibilities of declaring the performance of dowel-type fasteners (screws) including the comparison when using different technical specifications.

1. Introduction

Commission regulation (EU) No 305/2011 of the European Parliament and of the Council (CPR) [1] was in 2013 probably the most significant change in a decade in the way how the quality of the construction products is assured and how they are placed or made available on the market. CPR replaced the Construction Products Directive 89/106/EEC as amended by the Directive 1993/68/EEC (CPD) establishing the harmonized rules for expressing the performance of construction products through the seven basic requirements for construction works (BWR 1-7): mechanical resistance and stability, safety in case of fire, hygiene, health and environment, safety and accessibility in use, protection against noise, energy economy and heat retention, and sustainable use of natural resources.

In the terms of CPR the BWR of construction products can be expressed through the harmonized technical specifications: harmonized standards (hEN) and European Assessment Documents (EAD).

Harmonized standards are established by the European standardization bodies (European Committee for Standardization – CEN for example) on the basis of the request issued by the Commission. The result of a Commission mandate is that all harmonized standards have an additional Annex ZA, which defines the harmonized characteristics and the Assessment and Verification of Constancy of Performance system (AVCP). The CPR (Delegated regulation (EU) No 568/2014) defines five different AVCP systems (marked as 1+, 1, 2+, 3 and 4) which in detail define the tasks under the responsibility of the manufacturer and the tasks / involvement of the third party - notified certification body / notified laboratory (Fig. 1). The AVPC system is defined with the Commission mandate concerning the execution of standardization work (in case of timber fasteners with the mandate M/112).

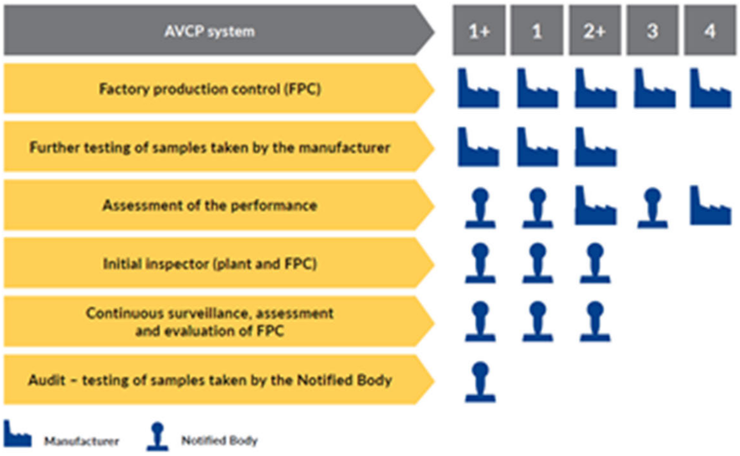

Fig. 1. AVCP systems and tasks of parties involved [2].

Currently there are more than 400 harmonized European standards covering a wide range of construction products. The list of standards is periodically published in the Official Journal of the EU, including the important dates: date of applicability and date of the end of the co-existence period with previous issues, if relevant. The dowel type fasteners (nails, staples, screws, dowels, bolts and nuts) are subject of the harmonized standard EN 14592:2008+A1:2012 *Timber structures – Dowel-type fasteners – Requirements* [3] (below referred to as EN 14592+A1). The use of this standard release is mandatory from 01.07.2013. Currently the standard is under revision. The AVCP system defined in the Annex ZA is 3: the notified laboratory has to perform the initial type testing (ITT); the manufacturer has to set up and implement the factory production control (FPC). After fulfilling all listed requirements, the manufacturer has to mark the products with a CE marking and issue a Declaration of Performance (DoP) as requested by the CPR. The DoP must express the performance of the construction product in relation to the essential characteristics as specified in the harmonised technical specification and should contain the information as defined in Commission delegated regulation (EU) No 574/2014.

A European Technical Assessment (ETA), based on European Assessment Document (EAD) can be in general issued for any construction product not covered or not fully covered by a harmonized standard or for which the performance of product cannot be completely assessed using an existing harmonized standard. EAD and ETA are prepared by the Technical Assessment Body (TAB). Although established in 1990 under different legal frames (and name) the European Organisation for Technical Assessment (EOTA) is today a non-profit organisation, bringing together Europe's Technical Assessment Bodies. Although the EADs are publicly available documents (they are available on EOTA website and such as the harmonized standards their list is published in the official journal of the EU), the ETAs are property of the manufacturer since they are related to specific product(s). In case a relevant EAD does not exist the TAB first has to prepare this document which has to be – before issuing any ETA – approved by the Commission. For specific dowel type fasteners, the EAD is already available: EAD 130118-00-0603 – *Screws for use in timber construction* [4] (below referred to as EAD). Currently 26 ETAs based on the discussed

EAD were already published. Some valid ETAs also exist, but in this case Approvals, not Assessments, which were issued under the CPD. The approvals – they will all expire on 30.06.2018 – also provide information about the load-carrying capacity of single fasteners or groups of fasteners.

It also has to be taken into consideration that some properties of dowel-type fasteners can be calculated according to the provisions of EN 1995-1-1:2005 *Eurocode 5: Design of timber structures – Part 1-1: General – Common rules and rules for buildings* (below referred to as EN 1995) [5]. Even the harmonized standard EN 14592+A1 with some characteristics offers a choice of testing or calculation according to EN 1995-1-1. Compared with the specific dowel-type fastener characteristics from a CE marking or DoP the Eurocode equations in general provide the characteristics of fasteners not taking into consideration specific product characteristics (like thread type).

2. Dowel-type fasteners – screws

Screws are the most widely used products among the dowel-type fasteners listed in EN 14592+A1. This is also somehow confirmed with the existence of EAD which suggests that the manufacturers of fastener would like to define the characteristics of products beyond the requirements of the standard. Therefore, this paper focuses on this specific type of fasteners. Through the comparison of two types of technical specifications their prospects and constrains are pointed out.

2.1 Material and geometry properties

Screws can be according to the standard EN 14592+A1 and relevant EAD produced of carbon or stainless steel. EN 14592+A1 is furthermore referencing to relevant EN standards and allows use of alternative steel grades with the equivalent mechanical characteristics which in many cases proved to be relevant due to the location of manufacturing sites – most of the dowel-type fasteners are produced in Asia.

Both technical specifications, EN 14592+A1 and relevant EAD, allow that screws can be either corrosion protected, lubricated or coated for withdrawal enhancement.

Both technical specifications have similar requirements regarding the geometry ratios (d = 2.4-24 mm, $\ell_g \geq 4d$, $0.6d$ [EAD $0.5d$] $\leq d_1 \leq 0.9d$), where d is threaded diameter, d_1 inner diameter and ℓ_g threaded length.

With the tolerances, the standard is more strict (ℓ and d (2.5%), other dimensions (5%)) than EAD. Even larger tolerances can be specified in an ETA.

With the corrosion protection the EN 14592+A1 requirement is only the definition of the grade of the parent material or thickness of coating. EAD is more detailed in defining the relevant standards for corrosion protection according to the examples given in EN 1995-1-1 and allowing the alterative corrosion protection by introducing the verification test procedures relating to the relevant corrosion protection standards.

Compared with the standard the EAD, is more detailed in the definition of special geometric attributes (drill tips, shank ribs, double thread), penetration length and also regarding the intended use.

2.2 Mechanical characteristics

Table 1 presents the relevant mechanical characteristics of screws and test / calculation methods – although there is a question of suitability of EN 1995 equations for modern self-tapping screws. Test methods are in detail elaborated in [6]. The added values of the EAD are additional essential characteristics within the BWR 1 - mechanical resistance and stability: 1.) Bending angle, 2.) Characteristic yield strength, 3.) Spacing, end and edge distances of the screws and minimum thickness of the wood based material and 4.) Slip modulus for mainly axially loaded screws.

Table 1. Relevant mechanical characteristics of screws and test methods

	Test	Calculation
Characteristic yield moment ($M_{y,k}$)	EN 409	EN 1995-1-1
Characteristic withdrawal parameter ($f_{ax,k}$):	EN 1382	EN 1995-1-1
Characteristic head pull-through parameter ($f_{head,k}$)	EN 1383	
Characteristic tensile capacity ($f_{tens,k}$)	EN 1383	
Characteristic torsional ratio ($f_{tor,k}$ / $R_{tor,k}$)	EN ISO 10666 & EN 15737	

With the characteristic *yield moment* both technical specifications relate to standard EN 409: the principle involves the simple four-point bending test of fasteners with predefined distances between supports / loading in relation to the fastener diameter. EN 14592+A1 requires that both smooth and threaded part shall be tested where the EAD focuses only on the weakest point within the screw length. The bending angle is the same ($\alpha = 45/d^{0.7}$), only the distance between imposed forces is with EAD limited to $2 \cdot d$. EN 14592+A1 defines that cracks have to be checked at angle α + 10°, but there are no detailed instructions (only bare eye inspection?). The EAD uses a different approach; screws have to be bended over a bending mandrel with a diameter $2 \cdot d$ measuring the bending angle at an extent that it will not break off. Characteristic yield moment can also be calculated according to EN 1995-1-1, but in some cases the values might differ from the value obtained in tests.

With characteristic *withdrawal parameter* both technical specifications refer to the testing procedure defined in standard EN 1382: fasteners shall be driven to a penetration depth of between $8 \cdot d$ and $20 \cdot d$ and pulled out. Relatively strict criteria are given for the timber density (EN ISO 8970). The EAD additionally offers a correction factor in relation to the characteristic density of the strength class used. The important influencing parameter with the solid timber is also the orientation of growth rings. However due to the cracks in solid timber and dimension of screws the glue laminated timber is often used in testing. Different orientation of layer scatters the results and with low number of samples causes relatively low characteristic values. The EAD additionally offers calculation principles for the calculation of characteristic withdrawal capacity $F_{ax,\alpha,k}$ for angles α between 15 and 45 degrees. Similar as with the characteristic yield moment, the characteristic withdrawal parameter can also be calculated according to EN 1995-1-1 but in most cases the values might differ from the value obtained in tests.

For the characteristic *head pull through parameter* both technical specifications refer to standard EN 1383: a fastener has to be pulled through a timber based material with thickness less than or equal to 7d. The parameter is defined as a ratio between maximum measured force and square of head diameter. As with the characteristic withdrawal parameter the criteria for timber density are relatively strict with this test method too. The screw axis should be perpendicular to the timber surface, knots and other imperfections should be avoided. Also the orientation of growth ring is recognized as an important parameter. The EAD approach is slightly different: three different methods are possible. For some specific timber based material the EAD gives values of $f_{head,k}$ (1) while for solid and glulam material at least 20 tests are foreseen for each influencing parameter (2). In the most general case at least 100 tests are required (3).

In the characteristic *tensile capacity* test, the timber is replaced with the steel plate. The hole has a diameter d + 1 mm, the result ($f_{tens,k}$) is a force in [N]. The steel plate shall have a sufficient thickness to introduce either a pull-off failure of the head, or a tensile failure of the shank. EN 14592+A1 requires at least 10 samples, while the number of samples in EAD is not given. An additional requirement of the EAD is also the evaluation of characteristic yield strength determined by using the strength elongation diagram from the characteristic tensile capacity test.

The characteristic *torsional ratio* is in EN 14592+A1 declared as a ratio between the characteristic torsional strength ($f_{tor,k}$) and characteristic torsional resistance to insertion into timber ($R_{tor,k}$). Characteristic *torsional strength* shall be determined by testing in accordance with the method given in EN ISO 10666:1999, 4.2.3. Screws shall be clamped in the area of thread in such a way that the thread is not damaged and the torque should be applied. Torsional resistance to insertion shall be determined by testing in accordance with the method given in EN 15737:2009. Screws have to be screwed into the timber piece until the screw is fully embedded along its entire length in the timber specimen with the density between 400 and 500 kg/m^3. By using the moment/penetration depth diagram the maximum value of the screw *insertion moment* ($R_{tor,\rho}$) has to be evaluated. Insertion moment has to be adjusted to a common timber density of 450 kg/m^3. The EN 14592+A1 requires that the ratio $f_{tor,k}$ / $R_{tor,k}$ should be bigger than 1.5. The basic principles of evaluating the characteristic torsional ratios in the EAD are similar, only the number of required samples is bigger and the density adjustment is slightly different.

Additionally, the EAD gives instructions for spacing, end, edge distances and the minimum thickness of wood based material with reference to EN 1995-1-1 or to a test method defined in the EAD, Annex A. However, this topic is out of scope of this paper.

2.3 Quality control

The AVCP defined in the standard and in EAD is 3, although the initial proposal for the EAD was 2+. Consequently, no third party is involved in the production control. With the standard, the notified laboratory is involved only with the ITT testing, all production control is the responsibility of the manufacturer. The EAD also contains the basic frame of tasks of the manufacturer (cornerstones) which have to reflect in the Control plan document as a part of each issued ETA.

Regarding the initial type testing the EN 14592+A1 mentions the grouping of products in families although no detailed instructions are given. EAD does not discuss this issue, but according to already issued ETAs the grouping is taken into consideration. The minimum number of samples per ITT testing is clearly defined in the standard, although the number (10) seems to be relatively low, especially where tests are performed on solid / glulam timber or on timber based products. The EAD in general requires more samples, at least 20, for each influencing parameter.

Corrosion protection – where required – has to be declared as the grade of parent material or thickness of coating. Since there is a requirement only for declaration and not for testing in most cases this characteristic is not tested in the process of ITT.

Furthermore, the EAD is more detailed regarding the factory production control. EN 14592+A1 defines the minimum number of specimen per each steel consignment (for example 5 samples per geometry), but does not specify the number of samples for mechanical tests in each steel or coating consignment and the number of samples for durability in each steel or coating consignment. The EAD cornerstones for control plan are more clearly defined: minimum number of samples (5 or 10 depending on the type of test) and minimum frequency of control is given. The frequency of control also has a logical background (for example bending angle is defined per production or heat treatment batch).

Similar as with the ITT the corrosion protection in FPC tasks is foreseen only as a supplier declaration, for both technical specifications.

It also has to be pointed out that due to the AVCP system 3 where no third party is involved in the factory production control the establishment and performance of regular FPC is not always the case, at least with smaller (overseas) manufacturers.

3. Conclusions

In the frame of the CPR two types of technical specifications for dowel-type fasteners – screws exist: A harmonized standard EN 14592+A1 and EAD 130118-00-0603. Although in general the EAD is more detailed than standard the following issues should be considered when updating the documents:

- Detailed instructions for grouping / selecting specimens,
- Detailed definition of material / geometry characteristics,
- Defining acceptance criteria („minimum and maximum values“),
- Number of specimens / influence parameters,
- Adjustment factors for widely used materials,
- Relations between measured / calculated values (relation to EN 1995-1-1),
- Yield moment - definition of detailed criteria for inspection of cracks,
- Clear instructions for evaluating the corrosion protection (declaring / testing).

Additionally, it has to be pointed out that EN 14592+A1 is currently under revision. Although tests for evaluating basic mechanical characteristics will not change, there are some differences suggested in the geometry requirements. Also the area of corrosion protection is elaborated more in details. Additionally, tests for evaluating the ductility, characteristic tensile yield stress and seismic performance are suggested.

References

[1] *Commission regulation (EU) No 305/2011* of the European Parliament and of the Council of 9 March 2011 laying down harmonized conditions for the marketing of construction products and repealing Council Directive 89/106/EEC

[2] *European Commission: CE marking of construction products – Step by step*. https://ec.europa.eu/growth/content/ce-marking-construction-products-step-step-guide-now-available-all-eu-languages-0_en

[3] *EN 14592:2008+A1:2012*. Timber structures – Dowel-type fasteners – Requirements. CEN, Brussels.

[4] *EAD 130118-00-0603*. Screws for use in timber construction. www.eota.eu.

[5] *EN 1995-1-1:2005/A2:2014* (Eurocode 5). Design of timber structures – Part 1-1: General – Common rules and rules for buildings. CEN, Brussels.

[6] Franke S, Franke B, Tuhkanen E (2018) *Test methods for determination of design parameters of fasteners*. Design of connections in timber structures, state-of-the-art report, COST Action FP1402.

Test methods for determination of design parameters of fasteners

Steffen Franke
Bern University of Applied Science
Biel/Bienne, Switzerland

Bettina Franke
Bern University of Applied Science
Biel/Bienne, Switzerland

Eero Tuhkanen
Tallinn University of Technology
Estonia

Summary

The quality and safety of connections with dowel-type fasteners depend on the design method/equation and the strength parameters of the materials. The focus of this chapter is on the parameters of the timber and the fasteners themselves and their determination as international standards provide different methods for the test setup and the evaluation of the strength values. These different methods lead to different and non-comparable values. An overview, comparison and discussion will be presented on the performance of the wooden material and the steel fastener itself. The primary focus is on dowels and screws.

1. Introduction

Connections using mechanical fasteners play an important role in timber structures. Their performance must therefore be estimated with high reliability. The behaviour of connections is exhaustively characterized by stiffness and capacity, and for most calculations, the European Yield Model (EYM) based on Johansen [1] is widely accepted nowadays. This model breaks down the overall behaviour of the connection into two components. The first, the fastener yield capacity, is independent of the properties of the wood. The second component, however, the embedment strength, is directly linked to the wood. For both failure cases, the test setups and evaluation of parameters are described. Further on, the withdrawal capacities as well as the head pull-through capacity are important parameters for the description of the performance of connections, especially for the use of self-tapping screws or drilled-in rods for high-performing timber connections where the fasteners are also loaded in tension parallel to the fastener axis.

Variances in testing and evaluation of these performance parameters result in significant differences for both capacity and stiffness depending on the load-to-grain direction. This renders impossible comparisons or the evaluation of reliable calculation methods using available test data. Therefore, a review of different test setups and evaluation methods has been carried out. The results highlight the major differences between American, European and international standards and their subsequent influence on the values obtained.

For fasteners not fully covered under a harmonized standard, the ETA documents (European Technical Assessments, prior to 30 June 2013 European Technical Approvals) give direct values for relevant parameters. To determine these values for ETA, an EAD (European Assessment Document) applies. A comprehensive overview of the EAD development and interpretation is given in the previous chapter of this report.

Currently, three EADs for fasteners are available, where approaches for the determination of design parameters are presented:

- EAD 130118-00-0603: Screws for use in timber constructions [2]
- EAD 130019-00-0603: Dowel-type fasteners with resin coating [3]
- EAD 130033-00-0603: Nails and screws for use in nailing plates in timber structures [4]

The first EAD is for screws made from special stainless or carbon steel. The second covers staples in timber structures, and the third is for annular ringed shank nails, square twist nails and screws for use in nailing plates and three-dimensional nailing plates in timber structures.

2. Material, parameters and test methods

2.1 Material

The determination of reliable performance parameters for connections must be carried out for the fasteners itself (steel properties) and the timber member (system properties). The steel properties comprise the tension strength f_t, the yield moment M_y, and the torsional moment capacity $f_{tor,k}$. The system properties contain the thickness of the timber member t, the embedment strength f_h, the withdrawal parameter f_{ax}, and the head pull-through parameter f_{head}. Further the system properties should be determined for the different materials used in timber structures such as softwood, hardwood, and wood products e.g. glued laminated timber, cross-laminated timber, and laminated veneer lumber. For softwood such as spruce, comprehensive test series have been carried out over several decades. However, there are far fewer series for hardwood, hence less data is available. Due to the natural higher strength potential, modifications in the test setups and evaluation methods may be necessary.

2.2 Embedment strength

2.2.1 General

The current European standard EN 1995-1-1:2004 (Eurocode 5) [5] provides empirical formulas for the calculation of embedment strength. Eurocode 5 describes the embedment strength of wood as a function of the:

- Wood species (softwood or hardwood)
- Wood density ρ [kg/m^3]
- Fastener diameter d [mm]
- Load-to-grain angle α [°]

All formulas were established based on experimental results from extensive embedment testing. However, the test of the embedment strength can nowadays be performed according to different standards, where different test setups/methods and evaluation methods are given. These test setups and evaluations have been used by different researchers [6-13].

These variances in testing and evaluation result in significant differences for both embedment strength f_h and stiffness K depending on the load-to-grain direction. Consequently, comparisons and the use of all available test data to evaluate reliable calculation methods are impossible. The main testing standards for embedment strength are the American ASTM D5764-97a:2013 [14], the European EN 383:2007 [15], and the international ISO/DIS 10984-2:2008 [16]. They specify different test methods, sample sizes, loading procedures and evaluation methods.

2.2.2 Test setup, specimen and loading procedure

2.2.2.1 ASTM D5764-97a:2013

The ASTM D 5764-97a:2013 [14] standard provides a full-hole (FH) and a half-hole (HH) testing setup, as shown in Fig. 1 and Fig. 2. The minimum specimen dimensions are 38 mm or 2d in thickness and the maximum is 50 mm or 4d in width and length, independent of the load-to-grain angle α, where d is the dowel diameter, see Fig. 3.

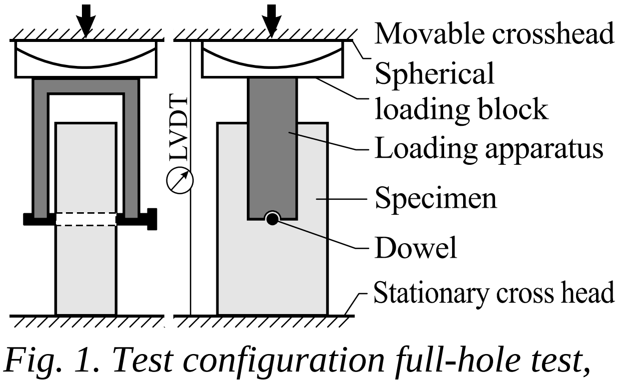

Fig. 1. Test configuration full-hole test, [14]

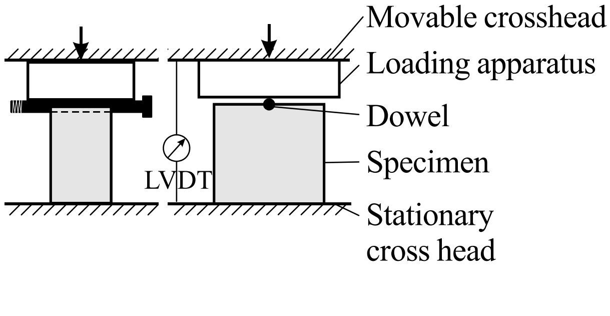

Fig. 2. Test configuration half-hole test, [14]

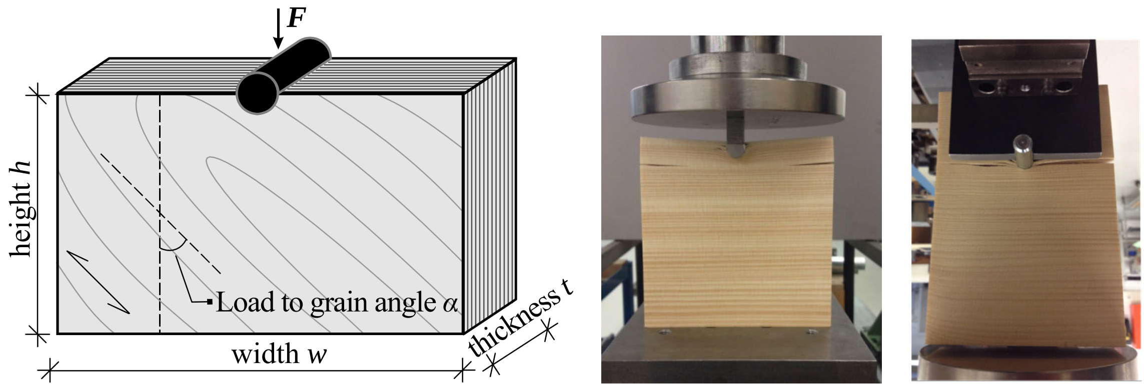

Fig. 3. Specimen sizes, variables and samples HH90-ASTM and FH90-EN383

The test is conducted so as to reach the maximum load in 1 to 10 min, using a constant rate of testing of usually 1.0 mm/min. There is no further information on the loading procedure. The results are given as yield load F_{yield}, determined using the 5% offset method (see Fig. 7), proportional limit load F_{prop} and ultimate load $F_{ultimate}$. The embedment strength f_h calculated from the yield load is given as follows:

$$f_h = \frac{F_{yield}}{d \cdot t} \tag{1}$$

with dowel diameter d and thickness of the test specimen t. There is no information about the determination of foundation modulus (stiffness) K provided.

2.2.2.2 ISO/DIS 10984-2:2008

Tests under the international standard ISO/DIS 10984-2:2008 [16] are carried out using a full-hole test shown in Fig. 4, but the test needs to avoid bending of the fastener under test. Thus, it also allows the use of the half-hole test shown in Fig. 4. The minimum specimen dimensions for tests parallel and perpendicular to the grain can be found in Fig. 5.

The loading procedure consists of one preload cycle from $0.4 \cdot F_{max,est}$ to $0.1 \cdot F_{max,est}$ with $F_{max,est}$ as an estimated maximum load, and the force is increased or decreased at a constant rate, as shown in Fig. 6. The maximum load must be reached within 300 ± 120 s. The standard includes formulas to calculate the embedment strength f_h, Eq. (2), where $F_{\max}$ is either the ultimate load or the load at 5 mm displacement, and the foundation modulus K_s, Eq. (3), where w are the displacements at $0.4 \cdot F_{max}$ and $0.1 \cdot F_{max}$.

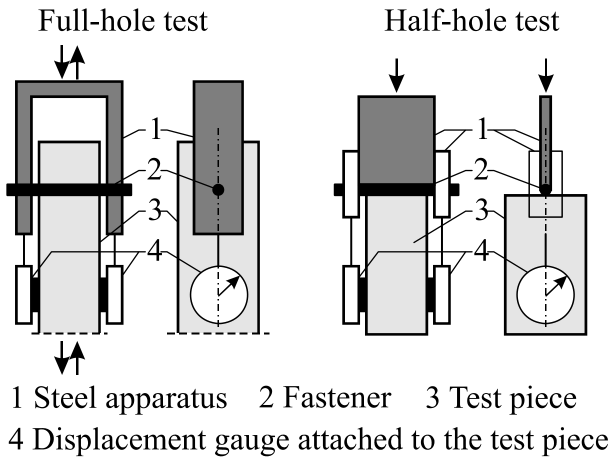

Fig. 4. Test configuration, [16]

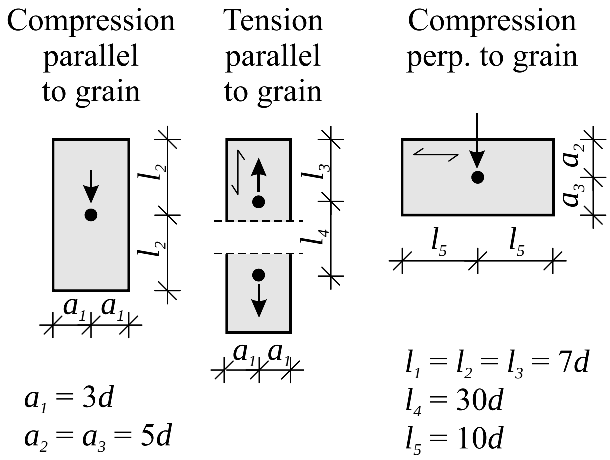

Fig. 5. Sizes of test specimens, [16]

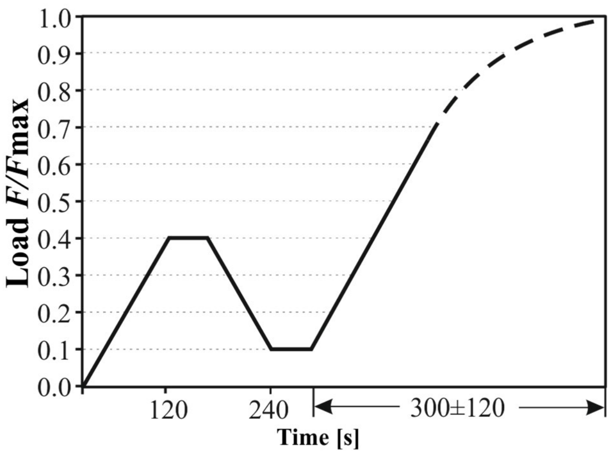

Fig. 6. Loading procedure, [16]

$$f_h = \frac{F_{\max}}{d \cdot t} \tag{2}$$

$$K_s = \frac{0.4 \cdot f_{h,est}}{w_{i,\text{mod}}} = \frac{0.4 \cdot f_{h,est}}{4/3 \cdot \left(w_{0.4 \cdot F} - w_{0.1 \cdot F}\right)} \tag{3}$$

2.2.2.3 EN 383:2007

The European EN 383:2007 [15] testing standard is equal to the ISO/DIS 10984-2:2008 [16], except that it does not allow the half-hole test alternative.

2.2.2.4 Evaluation of test results

Similarly, embedment strength can be evaluated from the experimental stress-strain curves using two main principles: either by taking the load value corresponding to an absolute displacement of 5 mm as recommended by EN 383:2007 [15] and ISO/DIS 10984-2 [16] ($f_{h,5mm}$) or by offsetting the elastic-linear part of 5% of the fastener's diameter as suggested in ASTM D5764-97a [14] ($f_{h,5\%}$). Furthermore, evaluating the results at 2.1 mm ($f_{h,2.1mm}$) has been used as well. These variations in evaluation methods have a significant influence on the embedment strength of up to 23% even for the same evaluation method and up to 76% between the evaluation methods depending on the load-to-grain direction as shown in Fig. 9 and in [17]. There is also more than 100% in differences for the stiffness evaluation. This has led to incompatibility in experimental results.

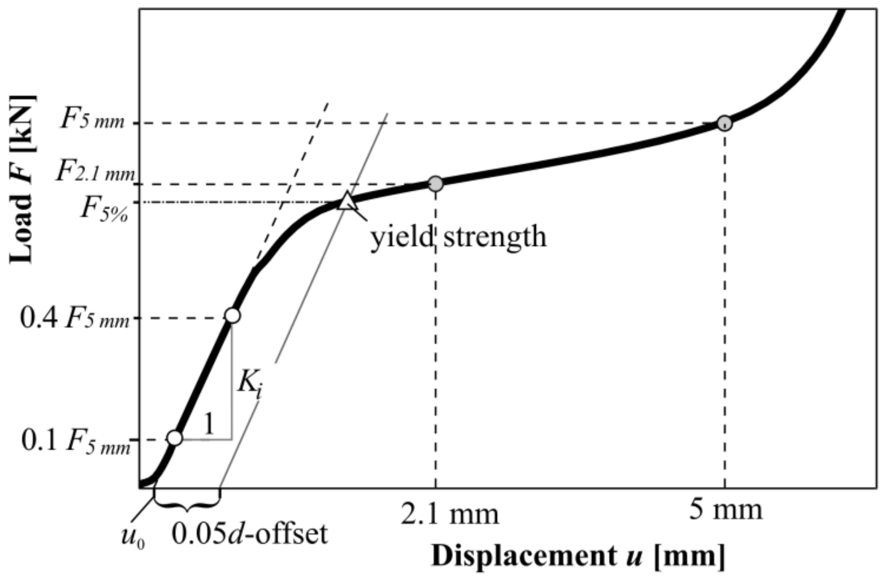

Fig. 7. Evaluation methods

2.2.3 Summary of test and evaluation methods

The full-hole (ASTM, ISO and EN) and half-hole (ASTM and ISO) test methods are used in the standards. The main resulting difference between these methods is the different deformation behaviour of the dowel and therefore the stiffness and stress distribution under the dowel. Furthermore, fixing the loading plate to the dowels, as in the ASTM full-hole test, will influence the deformation as well. Table 1 provides a summary of the different methods and their details.

These details highlight the major differences between the three standards and their subsequent consequences on the embedment strength values obtained. For example, the half-hole test applies the load on the full length of the fastener. This allows a result free from any influence of the fastener's bending to be obtained. This gives a realistic result for the embedding strength but does not reflect the realistic stiffness of a connection due to the bending deformation of the fasteners in real connections. In contrast, the full-hole test rather includes the bending of the fasteners, but does not lead to uniform stress under the dowel, which was used in the development of EYM. Sandhaas et al. [13] have stated that there are no differences between compression and tension tests. Evaluation of embedment test results has been a point of discussion among experts, and various methods were used in the past (see for instance, the summary in [22]). Table 2 summarizes the evaluation methods found in the literature and highlights the inconsistent use and therefore non-comparable results.

Table 1. Summary of test method details

Method / detail	ASTM D 5764-97a	ISO/DIS 10984-2	EN 383
Full-hole test (FH)	(yes) only for specimens that tend to split in HH test	yes	yes
Half-hole test (HH)	yes	yes	no
Loading plate fixed to dowels (full-hole test)	no	yes	yes
Specimen: Thickness t, cp. Fig. 3	≥ min (38 mm or 2d)	not specified	1.5d – 4d
Width w, cp. Fig. 3	≥ max (50 mm or 4d)	6d for $\alpha = 0°$ 20d for $\alpha = 90°$	6d for $\alpha = 0°$ 40d for $\alpha = 90°$
Length resp. height h (loaded end), cp. Fig. 3	≥ max (50 mm or 4d)	7d for $\alpha = 0°$ 5d for $\alpha = 90°$	7d for $\alpha = 0°$ 5d for $\alpha = 90°$
Loading procedure, cp. Fig. 6	Monotonic. displ. controlled within 1 to 10 min	Preloading cycle. displ. controlled within 300 ± 120 s	Preloading cycle. displ. controlled within 300 ± 120 s
End of loading	0.5d displacement or after max load	5 mm displ. or after max load	5 mm displ. or after max load
Evaluation of load resp. embedment strength, cp. Eq. (1) and (2)	yield load (5%-off set) or max. load	max. load or load at 5 mm	max. load or load at 5 mm
Evaluation of stiffness K, cp. Eq. (3)	no	yes: K_i, K_s, K_e	yes: K_i, K_s, K_e

Table 2. Embedment test designs and evaluation methods found in literature

Author	Test set up	Evaluation method		
	Full-hole (FH), half-hole (HH)	5% offset	5 mm	2.1 mm
Whale et al. [6]	Equivalent to EN 383:2007 - FH	Until failure		
Ehlbeck & Werner [7]				x
Sawata & Yasumura [9]	EN 383:2007 – FH	x	x	
Hübner et al. [10]	EN 383:2007 – FH		x	
Franke & Quenneville [11, 12, 19]	ASTM D5764-97a – HH	x	x	

2.2.4 Discussion

As mentioned before and shown in Fig. 9, the variations in the test and evaluation methods have a significant influence on the embedment strength of up to 76% between the evaluation methods. For the stiffness, the influence can even rise to 200% [17]. This shows the need for standardisation; respectively, equalizing the test and evaluation methods for both the determination of the embedment strength and stiffness for reliable use within the design standards, and creating comparability between the results of different researchers and/or species.

The following points, marked in red in Fig. 8, require discussion and agreement:

- Determination of embedment strength:
  - Which test method: Full-hole, Half-hole
  - What evaluation method: $f_{5\%}$, $f_{h,2.1mm}$, $f_{h,5mm}$
- Determination of foundation modulus (stiffness):
  - Which test method: Full-hole, Half-hole
  - Which modulus: Initial foundation modulus K_i, Foundation modulus K_s, Elastic foundation modulus K_e
- Determination of u_0: first slope. second slope
- Specimen size: EN 383:2007 [15] with $t \geq$ min (40, 4d) or ASTM D5764-97a:2013 [14]

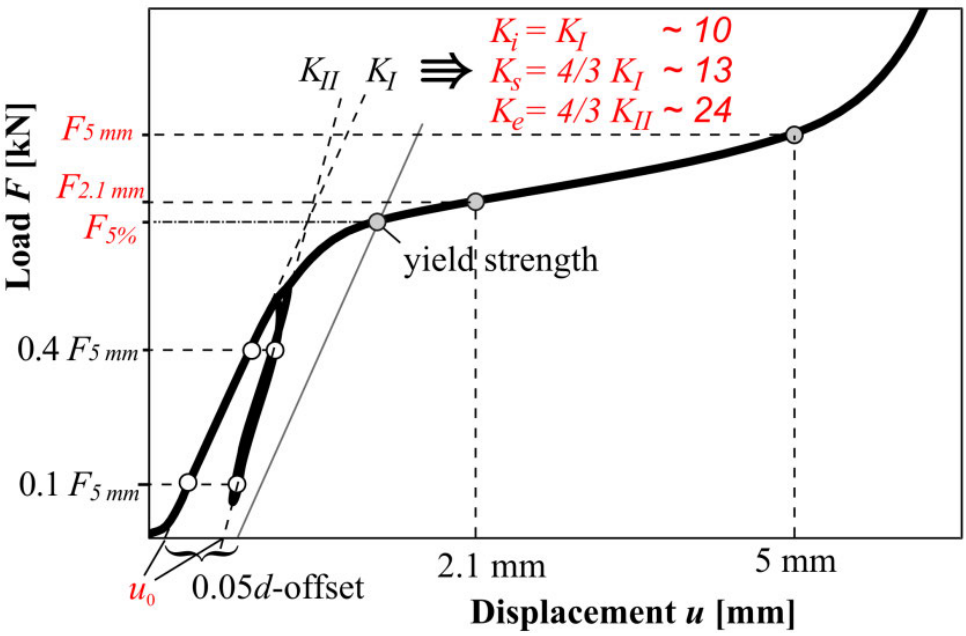

Fig. 8. Evaluation methods for discussion

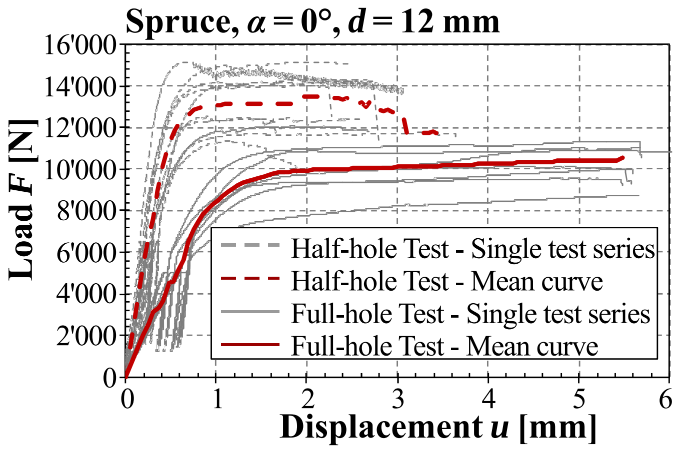

Fig. 9. Comparison half-hole and full-hole test results for Spruce, d = 12 mm

2.3 Withdrawal capacity

2.3.1 EN 1382:2016

The withdrawal capacity of nails, staples, and screws is determined using direct testing of at least 10 specimens (EN 14592:2008+A1, Tables 2, 3 and 4 [20]) according to EN 1382:2016 [21] or for nails and screws through analysis according to equations given in EN 1995-1-1:2004 [5]. The test specimens are prepared with the equilibrium moisture content related to 20 ± 2° temperature and 65 ± 5% relative humidity (EN ISO 8970 [25]). The fasteners must be inserted into the wood according to practice, e.g. with pre-drilling. The withdrawal capacity of fasteners can be determined for application parallel, perpendicular and under angle to grain. For solid test specimens and tests perpendicular to grain, half of the fasteners must be oriented in a radial and the other half in a tangential direction. The specimen sizes are summarized in Fig. 10.

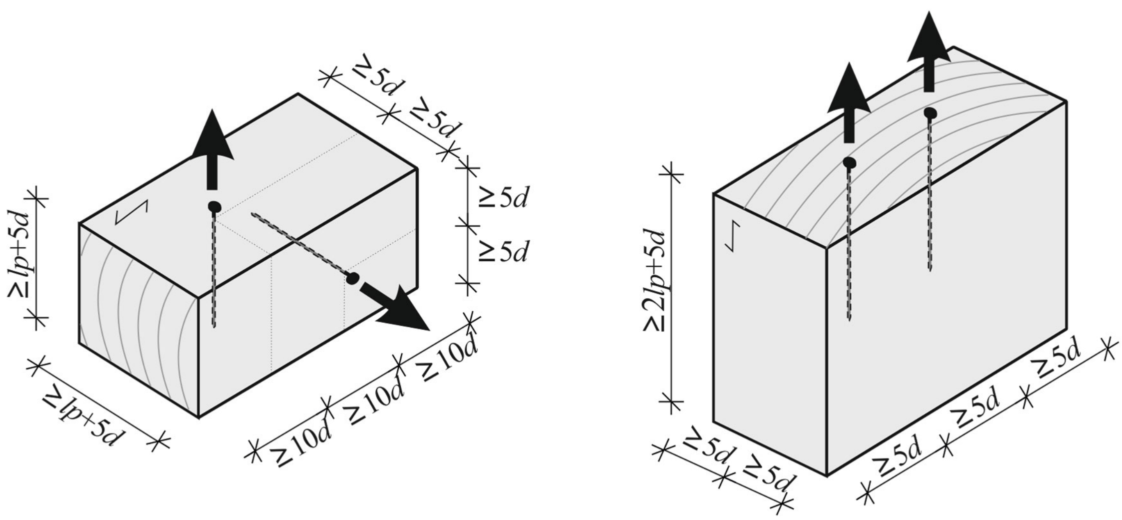

Fig. 10. Specimen sizes and distances, [21]

Before testing, the penetration depth of the fastener needs to be determined. The fastener is pulled axially with a test machine according to EN 26891:1991 [23]. Bearing supports must be at a distance less than 3*d* from the fastener. The test must be done with a constant load rate. The maximum load F_{max} must be reached within 90 ± 30 s with an accuracy of 1%. The pulling device should be strong enough to exclude head deformations. The withdrawal parameter for nails and screws is determined by the following equation:

$$f_{ax} = \frac{F_{max}}{d \cdot l_p} \tag{4}$$

where

F_{max}	Maximum load [N]
d	Diameter of the smooth shank of the fastener [mm]
l_p	Penetration depth [mm]

The resulting strength values have to be corrected to the characteristic density (EN 14592:2008+A1, [20]).

2.3.2 European Assessment Document (EAD)

2.3.2.1 Screws

In the EAD for screws [2], two methods to determine withdrawal capacity are given.

Method 1

Method 1 refers to the test method given in EN 1382:2016 [21] and is valid for screws inserted in the timber with an angle α between the screw axis and grain direction of at least 15° with the following exceptions:

- At least 20 tests for every influencing parameter (outer thread diameter; drill tip; secondary rough thread; angle α) are required
- The characteristic density ρ_k must fulfil the requirements of EN ISO 8970 [25]
- If necessary, the withdrawal parameter of each test needs to be corrected with factor k_ρ:

  $$k_p = \left(\frac{\rho_k}{\rho}\right)^{0.8} \tag{5}$$

  where

ρ_k	Characteristic density of the strength class of the timber to which the test results should be related
ρ	Density of the specimen

From the possibly corrected withdrawal parameters for all test results the characteristic value of the withdrawal parameter is to be calculated according to EN 14358 [26]. This characteristic withdrawal parameter corresponds to the chosen characteristic density of the timber.

For angles α between screw axis and grain direction $15^\circ \leq \alpha \leq 45^\circ$, the characteristic withdrawal capacity $F_{ax,\alpha,Rk}$ is determined according to following equation:

$$F_{ax,\alpha,Rk} = k_{ax} \cdot f_{ax,90,k} \cdot d \cdot l_{ef} \left(\frac{\rho_k}{\rho} \right)^{0.8} \tag{6}$$

where

k_{ax}	Factor to consider the influence of the angle between screw axis and grain direction and the long-term behaviour: $k_{ax} = 0.3 + (0.7\alpha)/45^\circ$ (7)
$f_{ax,90,k}$	Short-term characteristic withdrawal parameter for an angle α between screw axis and grain direction of 90º [N/mm²]
l_{ef}	Penetration length of the threaded part of the screw in the timber member [mm]
d	Outer thread diameter of the screw [mm]
ρ_k	Characteristic density of the wood based member

Equations (6) and (7) may be used for angles $0^\circ \leq \alpha \leq 15^\circ$ if the following requirements are satisfied:

- $f_{ax,0,k} / f_{ax,90,k} \geq 0.6$
  $f_{ax,0,k}$ short-term characteristic withdrawal parameter for an angle α between screw axis and grain direction of 0º determined on test specimens made from solid softwood.
- The penetration length of the threaded part of the screw is:

$$l_{ef,req} = \min \begin{cases} \dfrac{4 \cdot d}{\sin \alpha} \\ 20 \cdot d \end{cases} \tag{8}$$

- At least four screws must be used in connections with screws inserted in the timber with an angle between screw axis and grain direction of less than 15º.

Method 2

In all other cases not fulfilling the requirements of Method 1, the characteristic withdrawal parameter is determined by testing according to the test method given in EN 1382 [21]. The provisions are valid for screws inserted in the timber member with an angle α between screw axis and grain direction of at least 15º. The timber or the wood-based materials for the test specimens represent the density distribution of the strength class for which the withdrawal parameter is determined. For timber, generally at least 100 tests for each wood species with different timber specimens are required. For wood-based panels produced from veneers, strands or particles, a minimum of 20 specimens is required. All parameters influencing the withdrawal parameter must be examined (e.g. outer thread diameter; drill tip; secondary rough thread;

angle α). The characteristic value of the withdrawal parameter for the tested screw in the corresponding strength class or wood based materials is calculated according to EN 14358 [26].

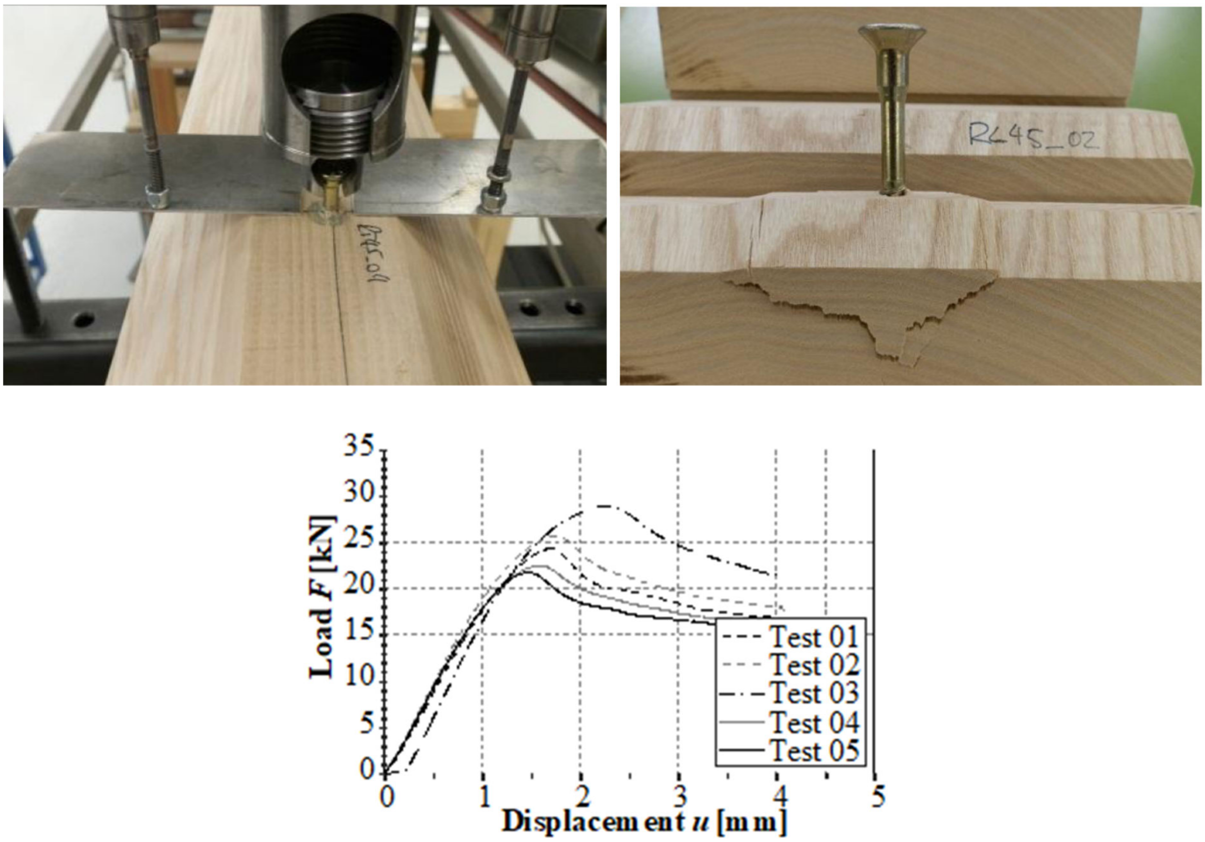

Fig. 11. Test setup, specimen failure for load to grain angle 45° and load-displacement curves for fully threaded screw 8 x 120 mm with penetration depth of 10d, loaded perp. to grain in ash [24].

2.3.2.2 Staples

For staples [3], withdrawal capacity is divided into short-term/medium-term and long-term/permanent load.

Short-term and medium-term load

For short-term and medium term, the test method given in EN 1382:2016 [2110] applies. The standard for selection of timber specimens is EN ISO 8970 [25]; tests are carried out with solid timber or softwood according to EN 338/EN 14081-1 ([27], [28]) and characteristic density ρ_k = 350 kg/m^3 for the supporting material.

At least 20 tests for each different diameter and type of steel of the raw wire, as well as each different kind of resin, are required. Staples must be driven through the connected material with a thickness of at least $t_1 = 40d$ into the test specimen with the axis of the fasteners perpendicular to the grain (not parallel) to a penetration of at least 14d or 20 mm, but not more than 20d, and not more than the stated minimum of the length of the resin coating.

After manufacturing, the test pieces must be stored for at least one week at (20 ± 2) º C and (65 ± 5) % relative humidity. The characteristic withdrawal parameter for the tested staple is calculated according to EN1382 [21] with following additional condition:

$$f_{ax,k} \geq 40 \cdot 10^{-6} \cdot \rho_k^2 \geq 4.9 \text{ N/mm}^2$$

where ρ_k characteristic density of the wood based member.

The withdrawal parameter of each test has to be corrected with

$$k_\rho = \frac{\rho_k}{\rho} \tag{9}$$

Long-term and permanent load

Complementary tests for long-term and permanent loads meet the requirements for the short-term/medium-term test; only the conditioning will be different: temperature (60 ± 2) ºC and relative humidity (75 ± 5) %. At least 20 tests for each kind of resin is required.

If the withdrawal parameter meets the requirements of equation (9), the design withdrawal capacity for service class 1 and 2 for long-term and permanent loads can be taken to $R_{ax,d}$ = 70 N (with γ_M = 1.3).

This capacity can be applied if the following requirements on the thickness t_1 of the connected material are met:

$\rho_k \leq 400$ kg/m³	$t_1 \leq 80$ mm (e.g. solid timber or softwood)
400 kg/m³ < $\rho_k \leq 650$ kg/m³	$t_1 \leq 60$ mm (e.g. wood-based panel and solid timber or hardwood)
650 kg/m³ < $\rho_k \leq 900$ kg/m³	$t_1 \leq 40$ mm (e.g. wood-based panels and gypsum boards)
900 kg/m³ < $\rho_k \leq 1200$ kg/m³	$t_1 \leq 25$ mm (e.g. hardboards, gypsum fibreboards, cement-bonded particleboards)
1200 kg/m³ < $\rho_k \leq 1600$ kg/m³	$t_1 \leq 20$ mm (e.g. highly compressed gypsum fibreboards)

with ρ_k characteristic density of the connected material.

Wood fibre insulation material:

$t_1 \leq 70 \cdot$d, with d = nominal diameter of raw staple wire

2.3.2.3 Nails and screws for use in nailing plates

The EAD for nailing plates [4] is referenced fully under EN 1382:2016 [21] or EN 1995 1-1:2004 [5].

2.4 Head pull-through resistance of wood

2.4.1 EN 1383:2016

The head pull-through resistance $f_{head.k}$ is relevant for nails, staples and screws. The parameter describes the resistance of wood against the head pull-through of a fastener or the crown pull-through of a staple. The head pull-through resistance needs to be determined with direct testing of at least 10 specimens (EN 14592:2008+A1, Tables 2, 3, 4 [20]) according to EN 1383:2016 [29], or through analysis for nails according to equations given in EN 1995-1-1:2004 [5].

The wood for the test specimens must be selected according to EN ISO 8970 [25] and prepared with the equilibrium moisture content related to 20 ± 2° temperature and 65 ± 5% relative humidity. The axis of the fastener must be perpendicular to the surface and grain direction of the wood, as shown in Fig. 12. The fasteners need to be inserted into the wood according to practice, e.g. with or without pre-drilling. The specimen sizes are summarized in Fig. 12. For test specimens and tests perpendicular to the grain, one part of the fasteners must be oriented in a radial and one part in a tangential direction. For staples, one part of the connections must be carried out for an angle between the staple crown and grain direction of $\alpha_{cm} = 0°$ and the other part for $\alpha_{cm} = 90°$.

The test must be carried out according to the test setup shown in Fig. 13. The test machine must fulfil the requirements of EN 26891:1991 [23]. The maximum load F_{max} must be reached with constant speed in 300 ± 120 s. F_{max} must be pre-calculated with 1 % accuracy.

Strength values are always given in relation to density and moisture content and determined according to Eq. (10) for nails and screws and Eq. (11) for staples:

$$f_{head} = \frac{F_{\max}}{d_h^2} \tag{10}$$

$$f_{head} = \frac{F_{\max}}{a \cdot d_h} \tag{11}$$

where

F_{max}	Maximum head pull-through load [N]
a	Width of staple [mm]
d	Nominal diameter of fastener [mm]
d_h	Head diameter of fastener for nails, screws or width of staple crown [mm]

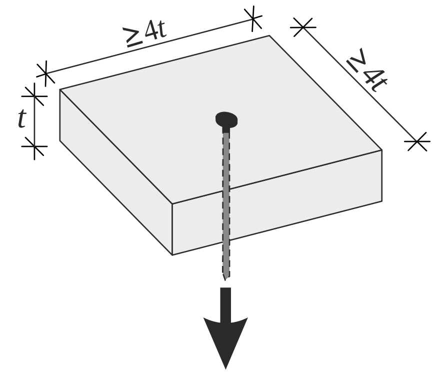

Fig. 12. Test specimen for head pull-through resistance, [29]

Table 3 Specimen sizes, [29]

Type	Specimen size
Solid wood	$4t \cdot 4t$ with $t \leq 7d$
Wood products	$4t \cdot 4t^{*}$
* *t is thickness of plate as produced*	

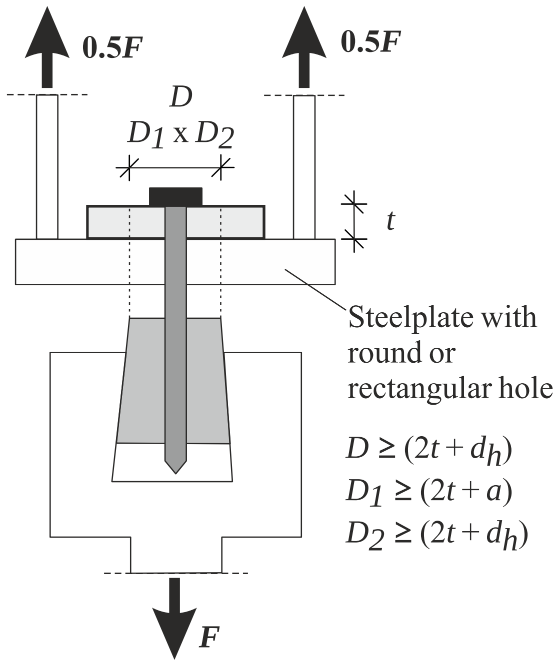

Fig. 13. Test setup for head pull-through resistance, [29]

2.4.2 European Assessment Document

2.4.2.1 Screws

The EAD for screws [2] offers 3 methods to determine head pull-through parameters.

Method 1

For screws with a head diameter at least 1.8 times the shank or inner thread diameter, the characteristic head pull-through parameter may be determined by calculation (minimum timber strength classes C24 and GL24 according to EN 14081-1 [28] and EN 14080 [30]).

The characteristic value of the head pull-through parameter for a characteristic density of 380 kg/m^3 of the timber and the following wood-based panel is as follows:

- Plywood: EN 636 [31] and EN 13986 [32]
- OSB: EN 300 [33] and EN 13986 [32]
- Solid wood panel: EN 13353 [34] and EN 13986 [3]
- Particleboard: EN 312 [35] and EN 13986 [3]
- Fibreboards: EN 622-2 [36], EN 622-3 [37] and EN 13986 [3]

With thickness more than 20 mm:

$f_{head,k} = 10$ N/mm^2

For wood-based panels with a thickness between 12 mm and 20 mm:

$f_{head,k} = 8$ N/mm^2

For wood-based panels with a thickness of less than 12 mm, the characteristic head pull-through capacity is based on a characteristic value of the head pull-through parameter of 8 N/mm^2, and limited to 400 N complying with the minimum thickness of the wood-based panels of $1.2d$ with d as outer thread diameter. In addition, minimum thickness as set out in Table 4 applies:

Table 4. Minimum thickness of wood-based panels

Wood-based panel	Minimum thickness [mm]
Plywood	6
OSB	8
Solid wood panels	12
Particleboards	8
Cement-bonded particle boards	8
Fibreboards (hard and medium)	6

Method 2

For screws in solid wood according to EN 14081-1 [28], or glued laminated timber made from softwood according to EN 14080 [30], which do not fulfil the requirements for using Method 1, or for screws with special design of the head which may influence the head pull-through capacity, the head pull-through parameter is determined by testing according to the test method given in EN 1383 [29]. At least 20 tests for each influencing parameter are required. For one chosen characteristic density ρ_k, the density of the test specimens must fulfil the requirements of EN ISO 8970 [25]. If necessary, the head pull-through parameter of each test must be corrected by the following factor k_ρ:

$$k_\rho = \left(\frac{\rho_k}{\rho}\right)^{0.8} \tag{12}$$

where

ρ_k Characteristic density of the strength class of the timber to which the test results should be related

ρ Measured density of the specimen

Characteristic values of the head pull-through parameter must be calculated according to EN 14358 [26].

Method 3

Method 3 is for cases, where the requirements of methods 1 or 2 are not fulfilled, i.e. it must be used for screws with a head diameter less than 1.8 times the shank or inner thread diameter, and lower timber strength classes.

Using method 3, the characteristic head pull-through parameter is determined by testing according to the test method given in EN 1383 [29]. The timber or wood-based materials for the test specimens represent the density distribution of the strength class for which the head pull-through parameter is determined. For timber, generally at least 100 tests for each wood species with different timber specimens are required. For wood-based panels produced from veneers, strands or particles, a minimum of 20 specimens is required.

All parameters influencing the head pull-through must be examined. The characteristic value of the head pull-through parameter is calculated according to EN 14358 [26].

2.4.2.2 Staples

For staples, the head pull-through parameter is determined by testing according to the test method given in EN 1383 [29]. Testing is not required for staples flush with the surface, a cross-sectional area within 1.7 mm^2 and 3.5 mm^2, a maximum anchoring length t_2 of 20d, a characteristic withdrawal parameter $f_{ax,k} = 40 \cdot 10^{-6} \cdot \rho_k^2$ and a minimum thickness t_1 of the connected material according to Table 5, because this failure is not significant.

Table 5. Minimum thickness of wood-based panels

Wood or based panel	Minimum thickness [mm]
Solid timber	24
Solid wood panels	7d*
Plywood	6*
OSB	8*
Resin-bonded particleboards	8*
Cement-bonded particle boards	8*

* *increased by 2 mm if staple crown is countersunk*

The head pull-trough parameter determined by the tests must be stated in accordance with the characteristic density of the connected material.

The characteristic head pull-through capacity $R_{ac,2,k}$ [N] may be calculated as follows:

$$R_{ac,2,k} = f_{head,k} \cdot b \cdot d \tag{13}$$

Where

$f_{head,k}$ Characteristic head pull-through parameter [N/mm^2]

b Width of staple crown in mm

d Nominal diameter of raw staple wire [mm]

2.5 Yield moment of fastener

2.5.1 General

The European standard EN 1995-1-1:2004 (Eurocode 5) [5] specifies the yield moment as a function of fastener diameter d [mm] and tensile strength f_u [N/mm^2]. Several types of fasteners are distinguished: round and square nails, staples and bolts. For dowels and screws, formulae for bolts and nails apply depending on diameter. All empirical formulae were established based on experimental results. The main available standards for determining yield moment capacity are the European EN 409:2009 [38], American ASTM F1575-17 [39], and the International ISO 10984-1:2009 [40]. They specify different test methods, sample sizes, loading procedures and evaluation methods.

For fasteners not covered under a harmonized standard, the ETA document (European Technical Assessment, prior to 30 June 2013: European Technical Approval) gives direct values of M_y or formulae related to the diameter (e.g., cf. [41] and [42]). To determine these values, the EAD (European Assessment Document) applies.

2.5.2 Test setup, specimen and loading procedure

2.5.2.1 EN 409:2009

EN 409:2009 [38] is intended for use with all dowel-type fasteners. The principle of the test is shown in Fig. 14. Loading is carried out in such a manner that the loading points do not move along the fastener and the load remains normal to the axis of the dowel-type fastener during the test.

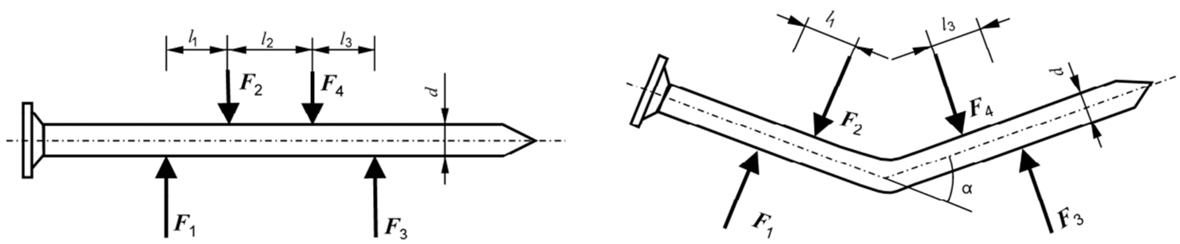

Fig. 14. Loading principle for nails [38]

The loads F_2 and F_4 may not deviate by more than 5% of each other. The following boundary conditions for the setup are given:

$$l_1; l_3 \geq 2d$$

$$d \leq l_2 \leq 3d$$

with fastener diameter d in mm.

The load is increased at such a rate that the required rotation angle given for the tested fastener type is reached in 10 ± 5 seconds.

Rotation angles that are required to be achieved during that time are a function of fastener diameter and tensile strength:

- for nails and staples α = 45º
- for screws, dowels and bolts used in wood-based products α = 110/d degree [*Note: in standard EN 14592:2008+A1:2012 [20], the following limitation for the rotation angle applies:*

  $$\alpha = 45 / d^{0.7} \tag{14}$$

  For screws intended for use in load-bearing timber structures, no cracks shall be observed at angle +10°]
- for screws, dowels and bolts with a tensile strength of 1000 N/mm^2 used in timber with a characteristic density of 360 kg/m^3, Fig. 15 applies
- for different tensile strength values or/and different characteristic timber density, the rotation angle is:

  $$\alpha = \alpha_1 \left(\frac{2.78 \rho_k}{f_t} \right)^{0.44} + \alpha_2 \tag{15}$$

  Where:

  α Rotational angle to be used to determine the yield moment, [°]
  α_1 Rotational angle in Fig. 15, [°]
  α_2 10° for nails, staples and screws and 0º for dowels and bolts
  ρ_k Char. density of the timber where the fastener is to be applied, [kg/m^3]
  f_t Tensile strength of the fastener, [N/mm^2]

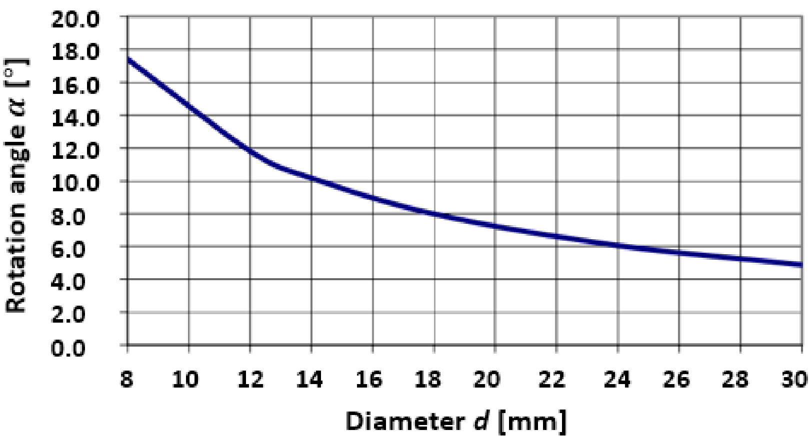

Fig. 15. Rotation angle versus fastener diameter [38]

The yield moment calculation follows the following formula:

$$M_y = \max \begin{cases} F_1 \cdot l_1 \\ F_3 \cdot l_3 \end{cases} \tag{16}$$

2.5.2.2 ASTM F1575-17

The standard ASTM F1575-17 [39] is intended only for nails used in engineered connection applications and based on three-point loading, see Fig. 16. Cylindrical loading and bearing points should not deform during loading and have diameter $d = 10$ mm. The length between nail bearing points is shown in Table 6.

[*Note: Values in the standard are given in inch-pound units. A conversion to SI units is provided for clarity.*]

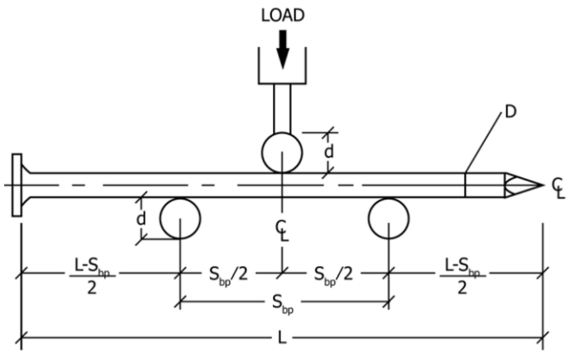

Fig. 16. Three-point loading for smooth shank and fully threaded shank nails [39]

Smooth shank, partly and fully threaded shank, and diameter measurements are distinguished. Modifications of the loading setup for several types of the shank are given, see Fig. 17.

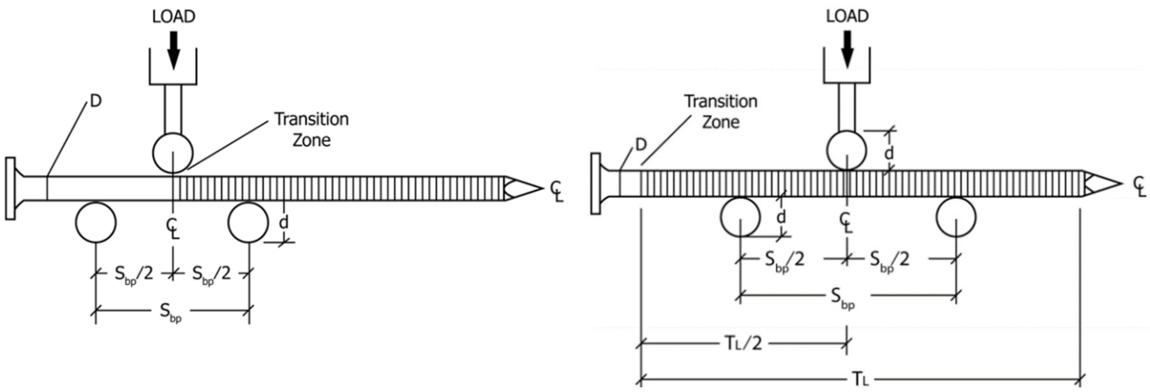

Fig. 17. Load-bearing point locations for partially threaded or insufficient smooth shank [39]

Table 6. Length between nail bearing points

Nominal nail diameter [mm]	Length between bearing points s_{bp} [mm]
2.5	28
2.8	33
3.0	35
3.3	38
3.7	43
4.1	48
4.8	55
Larger than 4.8	1.5 times the nail diameter, rounded to the nearest tenth of 2.5 mm

* *Length between bearing points for nails with diameters other than shown in Table 6 are the lengths for the next smaller listed diameter.*

A minimum of 15 specimens must be tested for each size or type of nail and for coated nails. The coating must be removed before the test. The maximum constant rate of loading r_L is as follows:

r_L = 6.5 mm/min, which is roughly one nail diameter per minute

The bending yield moment is determined from the load-deformation curve, which is intermediate between the proportional limit load and the maximum load for the nail. It is calculated by the intersection of the load-deformation curve with a line represented by the initial tangent modulus offset 5% from the fastener diameter, see Fig. 18. In cases where the offset line does not intersect the load-deformation curve, the maximum load is to be used as the yield load. The bending yield moment will then be the average of the specimens tested.

As an alternative to the establishment of a load-deformation curve, initial tests are performed to establish a relationship between the maximum load and the 5% offset value. Only then is the maximum load recorded for subsequent tests. The nominal bending yield strength is determined as follows:

$$F_{y,b} = \frac{M_y}{S} \tag{17}$$

Where

$F_{y,b}$	Nominal fastener yield strength [N/mm^2]
S	Effective plastic section modulus [mm^3] for full plastic hinge (for circular, prismatic nails, $S = D^3/6$, where D is nail diameter)
M_y	Calculated load based on test load [Nmm]

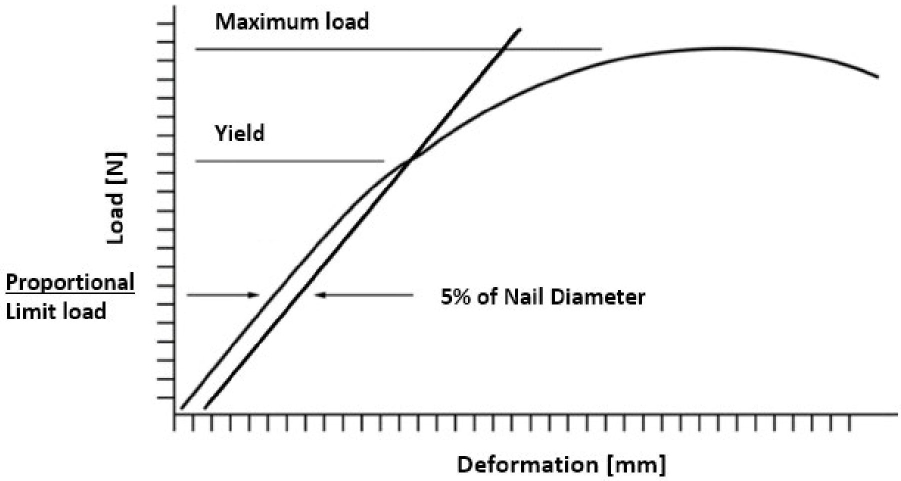

Fig. 18. Load-deformation diagram from nail bending test [39]

$$M_{y,b} = \frac{P \cdot s_{bp}}{4} \qquad (18)$$

where

P test load determined from the load-deformation curve [N]

s_{bp} cylindrical bearing point spacing [mm]

2.5.2.3 ISO 10984-1:2009

ISO 10984-1:2009 [40] specifies methods for determining the yield moment of all dowel-type fasteners. In principle, it covers both standards – EN 409:2009 [38] and ASTM F1575-17 [39] – referred to as Method A and Method B accordingly. No suggestions have been given to the user regarding which method to use.

In Method A, in addition to EN 409:2009 [38], the diameter of the shank is defined as “without coating;” all other principles remain the same.

Method B follows the ASTM F1575-17 [39] standard with several differences:

- it is intended to be used for all dowel-type fasteners, not only for nails
- all units are in SI system and rounded as converted in the previous section
- the length between bearing points is at least 11*d* for nails and staples and 4*d* for bolts
- length from bearing point to the top of the fastener is not less than 2*d* for nails, staples and bolts
- loading is not defined as speed-related, but as the minimum time to achieve maximum load (not less than approx. 30 s)
- only M_y value must be calculated, not bending yield strength $F_{y,b}$

2.5.2.4 European Assessment Document (EAD)

EADs for screws [2] and staples [3] refer to EN 409:2009 [38] for finding M_y values for fasteners. The following clauses and remarks apply:

For screws

- the free length between bearing points in Fig. 14 is restricted to $l_2 = 2d$
- a minimum number of tested specimens is given (10 pcs)
- it is clearly indicated that the weakest point within the length of the screw must be tested
- the bending angle according to EN 14592:2008+A1 [20] is given: $\alpha = 45°/d^{0.7}$
- the characteristic value of the yield moment is calculated according to EN 14358:2015 [26]

For staples

- a minimum tensile strength 900 N/mm^2 is given (c.f. EN 14592:2008+A1 [20] 800 N/mm^2)
- the free length between bearing points in Fig. 14 is restricted to $l_2 = 3d$
- a minimum number of tested specimens is given (10 pcs)
- the characteristic value of the yield moment is calculated according to EN 14358:2015 [26]

In EAD 130033-00-0603 [4], nails and screws are specifically developed for use together with three-dimensional nailing plates (as a kit) and the yield moment is not determined separately. The lateral load-carrying capacity of the whole connection is calculated using the relevant parts of EN 1995-1-1:2004 (Eurocode 5) [5] or determined by testing in accordance with EN 1380 [43].

2.5.3 Summary of test and evaluation methods

Despite the fact that there are several standards to determine M_y values for dowel-type fasteners, two main test principles are used: a four-point bending test, and a three-point bending test. When evaluating results, different approaches apply: one is based on effective bending angles, the other on proportional limit load.

2.5.4 Discussion

As shown previously, there are two different test methods available, a four-point and a three-point bending test. These are difficult to compare due to the context in which these values are used – the European standard Eurocode 5 [5] refers to the four-point bending test and American National Design Specification (NDS) for wood construction [45] to the three-point bending test. Standard ISO 10984-1:2009 [40] allows both methods to be used.

2.6 Torsional moment of fastener

2.6.1 EN 14592:2008+A1 [20] and European Assessment Document (EAD)

Torsional moment capacity $f_{tor,k}$ is relevant only for screws. Both EN 14592:2008 +A1 [20] and EAD 130118-00-0603: “Screws for use in timber constructions” [2] state that the parameter is tested in accordance with EN ISO 10666:1999 [44]. The latter sets the minimum amount of tests (ten) and for each outer thread diameter for the longest screw required. The principle of the test is shown in Fig 19. The screw to be tested must be clamped in a clamping device in such a way that the clamped portion of thread is not damaged. Torque is applied to the screw until failure occurs.

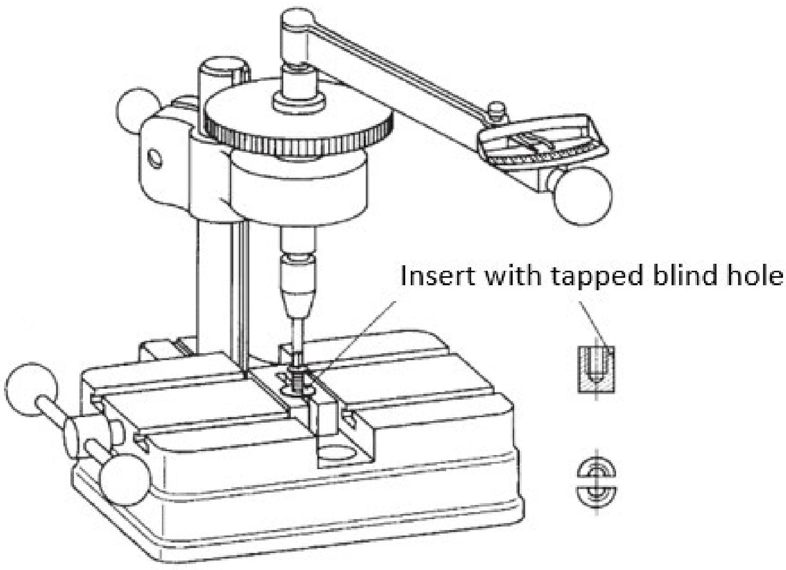

Fig. 19. Testing appliance for torsional test [44]

2.7 Tensile capacity of fastener

2.7.1 EN 14592:2008+A1

The shank tensile capacity (or head pull-off capacity) $f_{tens,k}$ is relevant only for nails and screws. EN 14592:2008+A1 [20] states the parameter is tested with direct testing of at least ten specimens according to EN 1383:2016 [29] as described in Chapter 2.3.2. Fig. 13 shows the test setup; the head side timber is replaced with a steel plate of sufficient thickness. The pre-drilled hole in the steel plate may not exceed the outer diameter of the nail or screw d + 1 mm. For partially threaded screws and profiled nails, the area of transition from the profiled to the smooth part of the shank must be located within the free length in testing and have a clear distance from the jaws of the testing equipment of at least $3d_1$ and $3d$ accordingly. The ultimate load F_{max} must be reached with a constant speed of 10 ± 5 s.

2.7.2 European Assessment Document (EAD)

EAD 130118-00-0603: “Screws for use in timber constructions” [2] defines tensile strength according to EN 14592:2008+A1 [20]. In addition, characteristic yield strength is determined by the same procedure. The elongation is to be measured in the middle of each screw using a strain gauge. The start length of the specimen should be 50 mm or 80 mm. After exceeding the yield strength of the screw, the applied load is reduced to 10% of the yield load. Then, the load is increased to more than the original load.

Determination of the characteristic yield strength is done as follows: a midline should be drawn through the hysteresis loop. A further line is constructed by drawing a parallel graph from the midline through the 0.2%-elongation point. The yield load is the ordinate value of the intersection from this line with the strength-elongation curve. The yield load is divided by the value of the core cross-section of the screw, resulting in the yield strength. The characteristic value is calculated according to EN 14358 [26].

3. Conclusions

This paper aims to summarize and to give an overview of the test methods to determine the strength parameters of dowel-type fasteners and timber material concerning connections, and comparison and discussion of the different methods of test and evaluation. There are different ways and means to determine fastener parameters. Furthermore, the manufacturer may declare the relevant values partly outside the harmonised standards. This could lead to the situation where results from different researchers/institutes are not comparable. Hence, there is a need for harmonisation of test and evaluation methods, or, in some cases, for clarification of condition of use.

References

[1] Johansen K (1949) Theory of Timber Connections. *International Association for Bridge and Structural Engineering Publications* **9**:249-262.

[2] *EAD 130118-00-0603*. Screws for use in timber constructions. www.eota.eu, October 2017.

[3] *EAD 130019-00-0603*. Dowel-type fasteners with resin coating. www.eota.eu, September 2017.

[4] *EAD 130033-00-0603*. Nails and screws for use in nailing plates in timber structures. www.eota.eu, March 2015.

[5] *EN 1995-1-1:2008* (Eurocode 5). Design of timber structures – Part 1-1: General – Common rules and rules for buildings. CEN, Brussels.

[6] Whale L, Smith I, Hilson B (1986) *Behaviour of nailed and bolted joints under short-term lateral load – Conclusions from some recent research*. CIB-W18 Meeting 19, Paper 19-7-1, Florence, Italy.

[7] Ehlbeck J, Werner H (1992) *Tragfähigkeit von Laubholzverbindungen mit stabförmigen Verbindungsmitteln*. Tech. Report. Versuchsanstalt für Stahl, Holz und Steine der Universität Karlsruhe, Abt. Ingenieurholzbau, Karlsruhe, Germany.

[8] Rammer D, Winistorfer S (2001) Effect of moisture content on dowel-bearing strength. *Wood and Fiber Science* **33**(1):126-139.

[9] Sawata K, Yasumura M (2002) Determination of embedding strength of wood for dowel-type fasteners. *Journal of Wood Science* **48**:138-146.

[10] Hübner U, Bogensperger T, Schickhofer G (2008) *Embedding strength of European hardwoods*. CIB-W18 Meeting 41, Paper 41-7-5, St. Andrews, Canada.

[11] Franke S, Quenneville P (2010) *Investigation of the embedding strength of Radiata Pine and LVL*. World Conference on Timber Engineering, Riva del Garda, Italy.

[12] Franke S, Quenneville P (2012) *Embedding behaviour of Douglas Fir*. World Conference on Timber Engineering, Auckland, New Zealand.

[13] Sandhaas C, Ravenshorst GJP, Blass HJ, van de Kuilen JWG (2013) Embedment tests parallel-to-grain and ductility aspects using various wood species. *European Journal of Wood and Wood Products* **71**(5):599-608.

[14] *ASTM D5764-97a* (2013) Standard test method for evaluating dowel-bearing strength of wood and wood-based products. West Conshohocken, United States.

[15] *EN 383:2007*. Timber structures – Test methods. Determination of embedding strength and foundation values for dowel type fasteners. CEN, Brussels.

[16] *ISO/DIS 10984-2:*2008. Timber structures – Dowel type fasteners – Part 2: Determination of embedding strength and foundation values. International Organization for Standardization, Geneva.

[17] Franke S, Magnière N (2014) *Discussion of testing and evaluation methods for the embedment behaviour of connections*. INTER Meeting 47, Paper 47-7-1, pp. 93-102, Bath, UK.

[18] Franke S, Magnière N (2013) The embedment failure of European beech compared to spruce wood and standards. *Materials and Joints in Timber Structures*, Springer, pp. 221-229.

[19] Franke S, Quenneville P (2011) Bolted and dowelled connections in Radiata pine and laminated veneer lumber using the European yield model. *Australian Journal of Structural Engineering* **12**(1):13-27.

[20] *EN 14592:2008+A1*. Timber structures – Dowel type fasteners – Requirements. CEN, Brussels.

[21] *EN 1382:2016*. Timber structures – Test methods – Withdrawal capacity of timber fasteners. CEN, Brussels.

[22] Leijten A, Köhler J, Jorissen A (2004) *Review of probability data for timber connections with dowel-type fasteners*. CIB-W18 Meeting 37, Paper 37–7–13, Edinburgh, UK.

[23] *EN 26891:1991*. Timber structures – Joints made with mechanical fasteners – General principles for the determination of strength and deformation characteristics. CEN, Brussels.

[24] Christiandl U (2013) *Ausziehwiderstände von Schrauben im Eschen Brettschichtholz*. BA thesis, Bern University of Applied Sciences.

[25] *EN ISO 8970:2010*. Timber structures – Testing of joints made with mechanical fasteners – Requirements for wood density. CEN, Brussels.

[26] *EN 14358:2015*. Timber structures – Calculation and verification of characteristic values. CEN, Brussels.

[27] *EN 338:2016*. Structural Timber – Strength Classes. CEN, Brussels.

[28] *EN 14081-1:2016*. Timber structures – Strength graded structural timber with rectangular cross section – Part 1: General requirements. CEN, Brussels.

[29] *EN 1383:2016*. Timber structures –Test methods – Pull through resistance of fasteners. CEN, Brussels.

[30] *EN 14080:2013*. Timber structures – Glued laminated timber and glued solid timber – Requirements. CEN, Brussels.

[31] *EN 636:2012*. Plywood – Specifications. CEN, Brussels.

[32] *EN 13986:2004*. Wood-based panels for use in construction – Characteristics, evaluation of conformity and marking. CEN, Brussels.

[33] *EN 300:2006*. Oriented Strand Boards (OSB) – Definitions, classification and specifications. CEN, Brussels.

[34] *EN 13353:2008*. Solid wood panels (SWP) – Requirements. CEN, Brussels.

[35] *EN 312:2010*. Particleboards – Specifications. CEN, Brussels.

[36] *EN 622-2:2004*. Fibreboards – Specifications – Part 2: Requirements for hardboard. CEN, Brussels.

[37] *EN 622-3:2004*. Fibreboards – Specifications – Part 3: Requirements for medium boards. CEN, Brussels.

[38] *EN 409:2009*. Timber structures – Test methods – Determination of the yield moment of dowel type fasteners. CEN, Brussels.

[39] *ASTM F1575-17:*2017. Standard test method for determining bending yield moment of nails. West Conshohocken, United States.

[40] *ISO 10984-1:*2009. Timber structures – Dowel type fasteners – Part 1: Determination of yield moment. International Organization for Standardization, Geneva.

[41] *ETA-12/0063* (2012). SFS self-tapping screws WT. Österreichisches Institut für Bautechnik, Vienna, Austria.

[42] *ETA-11/0030* (2016). Rotho Blaas self-tapping screws WT. ETA-Danmark A/S, Nordhavn, Denmark.

[43] *EN 1380:2009*. Timber structures – Test methods – Load bearing nails, screws. dowels and bolts. CEN, Brussels.

[44] *EN ISO 10666:1999*. Drilling screws with tapping screw thread – Mechanical and functional properties. CEN, Brussels.

[45] *ANSI/NDS 2018 Edition*. American National Design Specification for Wood construction, American Wood Council, Leesburg.

Nailed connections: Investigation on parameters for Johansen model

Carmen Sandhaas
Karlsruhe Institute of Technology
Germany

Rainer Görlacher
Karlsruhe Institute of Technology
Germany

This contribution has already been published in the proceedings of the INTER Meeting 50, Paper 50-7-3, pp. 95-109, Kyoto, Japan

Summary

A comprehensive database containing more than 8000 tests carried out for certification purposes of nails has been analysed with regard to parameters needed for design of nailed connections. An equation to calculate the characteristic yield moment covering all nail types has been proposed. Investigations on the withdrawal and head pull-though parameters revealed that the correlation with the density is weak and the scatter is significant. Consequently, at the current state of knowledge, tests to obtain declared values need to be carried out.

1. Introduction

In Eurocode 5, nailed connections are designed using the Johansen model extended with the rope effect, the so-called European Yield Model (EYM). Necessary input parameters are hence, apart from geometrical data, embedment strength f_h, yield moment M_y and withdrawal and head pull-through capacity F_{ax} resp. F_{head}. Generally, empirical equations based on regression analyses have been derived for all four parameters f_h, M_y, F_{ax} and F_{head}. However, especially for ring shank nails, no consistent rules are given in the current version of Eurocode 5. Values for yield moments or withdrawal parameters, for instance, must be taken from technical documents of the single nails. This is not only cumbersome for practitioners, it also requires a considerable testing effort from producers.

The aim of this contribution is to propose more straightforward equations regarding the parameters wire tension strength f_u, nail tension capacity F_t, yield moment M_y, withdrawal parameter f_{ax} and head pull-through parameter f_{head}, which have to be experimentally established in current certification practice. Based on an extensive database comprising more than 8000 test results carried out for certification purposes, regression analyses have been carried out. Potential benefits are more robust design models covering a large range of nails, reduced testing and simplified design equations. Prerequisite to all derived equations are sufficient spacings and end and edge distances to avoid splitting.

2. State-of-the-art

Connection design in the current Eurocode 5 is based on Johansen's model [1] that firstly had been applied to nailed connections by Moeller [2]. Since then, considerable research effort has been put into further development of methods to establish the ultimate characteristic load and deformation behaviour as discussed in Ehlbeck [3], who gives a concise and comprehensive summary of the state of the art in the late seventies. Ehlbeck already discussed input parameters necessary for the design of nailed connections such as embedment strength and yield moment as well as the contribution of the rope effect to the connection capacity and hence the withdrawal performance of non-smooth shank nails. The background discussed by Ehlbeck is still representative today as research efforts concerning bolted and screwed connections have been and still are in the focus whereas nailed connections are less represented in current research. An exception to this is the work done by Whale and Smith in the eighties concerning embedment strength [4, 5] and investigations by Blaß in the early nineties concerning group effects in nailed connections [6, 7].

In current certification practice, all five parameters, f_u, M_y, F_t, f_{ax} and f_{head}, are tested according to EN 14592 where a minimum value for the wire strength of f_u = 600 MPa is required. The evaluated values on the characteristic level are then declared in technical documents. For smooth shank nails however, the characteristic yield moment $M_{y,Rk}$ can also be calculated. For round nails for instance, Eurocode 5 gives the following Eq. (1):

$$M_{y,Rk} = 0.3 \cdot f_u \cdot d^{2.6} \quad (1)$$

where f_u is the wire tension strength and d is the nominal nail diameter.

Eq. (1) is based on work done by Werner and Siebert [8] and it is valid only when a tension strength of the wire of 600 MPa is inserted. This value of 600 MPa is mandatory even if the actual value is higher which is the case for diameters less than 4 mm. The exponent of 2.6 in Eq. (1) reflects an observed increase of yield strength (up to 1000 MPa for 2 mm nails) with decreasing nail diameter which can be explained with work hardening due to cold drawing.

Also for the parameters f_{ax} and f_{head}, regression equations are given in Eurocode 5 for smooth shank nails under short-term load:

$$f_{ax,k} = 20 \cdot 10^{-6} \cdot \rho_k^2 \quad \text{and} \quad f_{head,k} = 70 \cdot 10^{-6} \cdot \rho_k^2 \quad (2)$$

The withdrawal and head pull-through parameters for non-smooth shank nails are, analogously to M_y and F_t, defined in the individual declarations of performance of the producers. Considering the head pull-through parameter, this applies as well although the head shape may be the same for non-smooth and smooth shank nails.

3. Database

The global database consists of in total 8416 tests taken from 96 reports on mostly ring shank nails (rings 77%, spiral nails with threads 5%) and wires (11%). Special ring shank nails with smooth intermediate shanks as shown in Fig. 1 on the left constituted 5.3% of the overall database, whereas smooth shank nails constituted only 1% of the database and square nails only 0.3%. For smooth shank nails, only wire strength was tested and no other parameters are available. Nails from 33 different producers were considered and the tests were carried out between 1997 and 2013. It is not considered useful to enlarge the database with older results as both steel grades and production technologies may have changed since then and any analyses would not be representative of modern nails. The geometrical properties given in Fig. 1 on the right are also recorded in the database. The number of tests per parameter is given in Table 1 As properties of nails made from stainless steel do not differ significantly from all other nails, see for example Fig. 2, no difference will be made in analyses.

With regards to the individual parameters, wire strength f_u, calculated with the wire diameter, and nail tension capacity F_t are measured maximum values. The given yield moment M_y is the value at a measured deformation angle of 45° or the reached maximum bending angle before rupture of the nails. It should be noted that issues concerning test execution and precision of measured angles lead to uncertainties about the measured values as for instance, machine slip as well as elastic bending is included in the measurement during testing [9]. Withdrawal capacity F_{ax} and head pull-through capacity F_{head} were evaluated using softwood (*Picea abies*), stored at 65/20 and with the recorded densities. F_{ax} again is the measured maximum value whereas F_{head} is the maximum value or the value at a deformation of the testing machine of 15 mm.

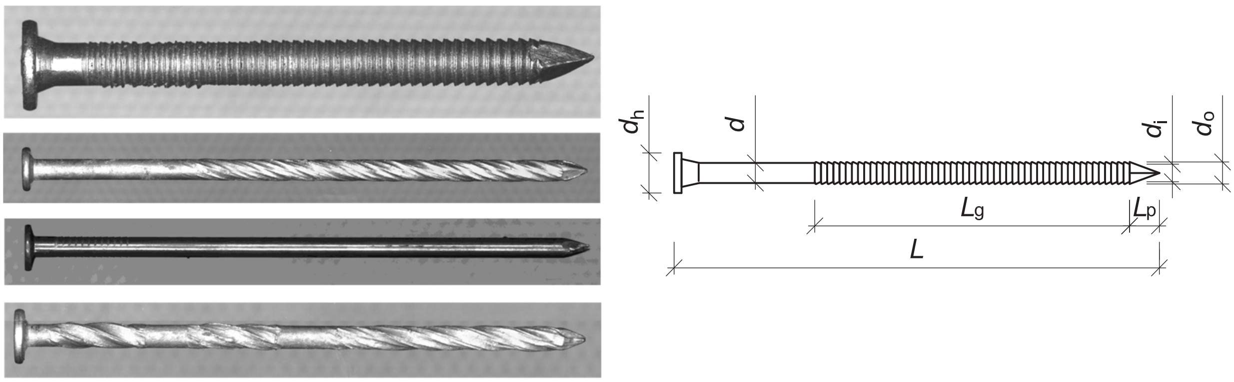

Fig. 1. Left: Nail shapes in database. From top to bottom: ring shank nail, spiral nail, smooth shank nail, special spiral nail. Right: Geometrical properties with d = nominal nail diameter, d_i = inner diameter, d_o = outer diameter, d_h = head diameter, L_g = length of non-smooth shank, L_p = tip length.

Table 1. Composition of database.

	Wire tension strength f_u	Yield moment M_y	Nail tension capacity F_t	Withdrawal capacity F_{ax}	Head pull-through capacity F_{head}
No. of tests	1076	2844	1160	2316	1020
Of which stainless steel	203	369	195	300	60
Of which hdg*	-	265	178	310	220

* hdg = hot-dip galvanised nails

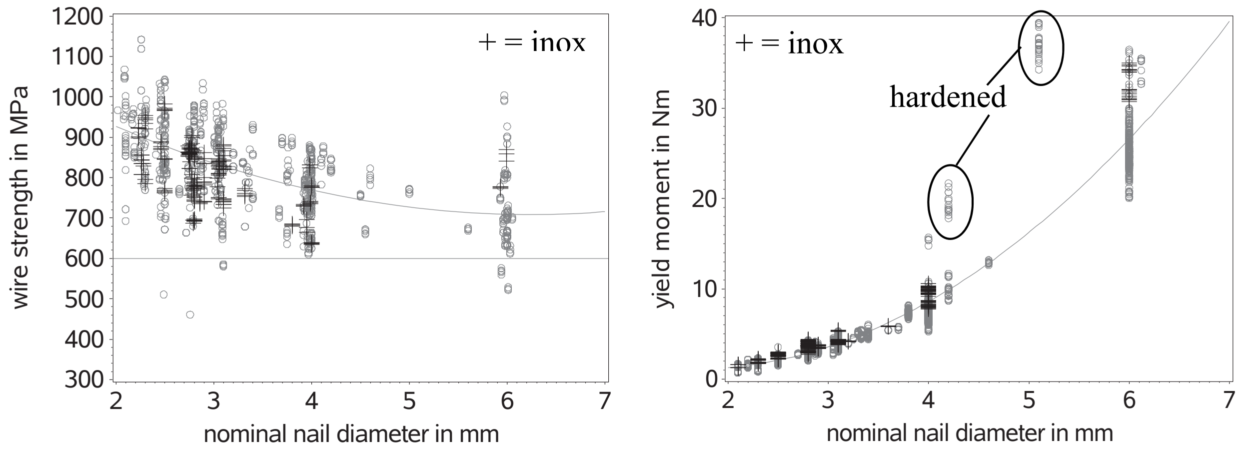

Fig. 2. Influence of stainless steel on wire strength (left) and on yield moment (right). Experimental values are shown and on the right, hardened nails are identified.

4. Analysis and discussion

4.1 Wire strength and tension capacity

Similar to Werner and Siebert [8], a decrease of wire and nail strength with increasing diameter can observed in Fig. 3 where the nail strength $f_{u,nail}$ has been calculated using the tension capacity F_t and the nominal diameter d. The nail tension strength calculated with the nominal diameter d (and not with the inner diameter d_i) is slightly lower than the original wire strength. The decrease of tension strength with increasing diameter can be explained with work hardening due to cold drawing. As multiple passes are needed for smaller diameter nails, strength values are increasing with decreasing diameter.

For design purposes, wire strength tests are not needed. Tension tests on nails are sufficient to guarantee tension properties, calculated with the nominal diameter *d*. Producers may need wire tests however in order to control delivered steel grades. Furthermore, the significant difference between bright wire tension strength and subsequent tension strength of hot-dip galvanised (hdg) nails, the crosses in Fig. 3, is obvious, especially for small diameter nails where a major part of the diameter is affected by heat. For hot-dip galvanised nails, it is indispensable to carry out tension tests on finished nails as wire strength has no significance. The same applies to hardened nails (special nails) where the wire strength is not correlated to the nail strength.

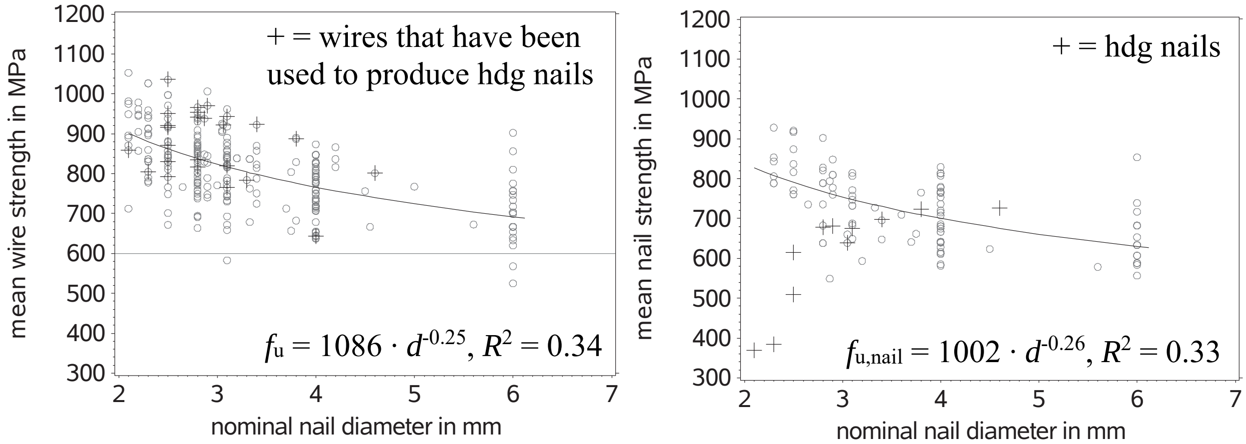

Fig. 3. Left: Mean tension strength of wire versus nominal nail diameter d. Right: Mean tension strength of nail calculated with F_t and nominal diameter d. Data from 78 test series (403 single tests f_u, 916 single tests F_t). Regression excludes hdg nails.

4.2 Yield moment

A nonlinear regression analysis to derive an expression for M_y has been carried out. The dependent variables have been the nominal diameter *d* and $f_{u,nail}$ which is the tension strength calculated from the nail tension capacity F_t and the nominal diameter *d*. Only such a procedure is realistic as both inner diameter d_i and yield strength f_y are unknown values in practice. As an assignment of single M_y values to single F_t values within one testing series is not possible, mean values of both M_y and $f_{u,nail}$ form the basis of the regression analysis. The influence of nail types and steel qualities on the resulting regression equation has been investigated and no significant differences were observed (differences in independent variables of max 1.6%). Therefore, no differentiation has been made within the database, e. g. with respect to different nail types or normal and stainless steel. The hardened nails highlighted in Fig. 2 on the right could not be included in the analysis as on these nails, only My has been tested and no data was available to calculate $f_{u,nail}$. It is expected that they would fit in the following equations if their actual tension strength would be used, which could be experimentally determined very easily. The nonlinear regression based on mean values of 105 test series resulted to (with $R^2 = 0.995$):

$$M_y = 0.185 \cdot f_{u,nail} \cdot d^{2.99} \tag{3}$$

Fig. 4 on the left shows the experimental versus the predicted values. The very good agreement between tests and model resulting in a bisect line with small scatter can be seen. Eq. (3) is similar (with a difference in the pre-factor of 0.9) to the mechanical equation for a full plastic moment of a round section, Eq. (4):

$$M_{\mathrm{pl}} = \frac{1}{6} \cdot f_{\mathrm{y}} \cdot d^3 \tag{4}$$

Blaß and Colling [10] proposed Eq. (4) to calculate the yield moment of dowels defining an effective yield strength $f_{\mathrm{y,ef}}$. A good agreement between test results and calculated values was found when $f_{\mathrm{y,ef}}$ is put to $f_{\mathrm{u,nail}}$ and the following Eq. (5) is proposed for nails:

$$M_{\mathrm{y}} = \frac{1}{6} \cdot f_{\mathrm{y,ef}} \cdot d^3 \quad \text{with} \quad f_{\mathrm{y,ef}} = f_{\mathrm{u,nail}} \tag{5}$$

Fig. 4 on the right shows the ratio between the individual experimental results and the calculated values using Eq. (5) and the mean nail tension strength $f_{\mathrm{u,nail}}$, mean per series. The observed 5$^{\mathrm{th}}$-percentile of the ratio is 0.995 (64 of 1034 ratios are smaller than 1) and therefore, the 5-percentile is slightly exceeded.

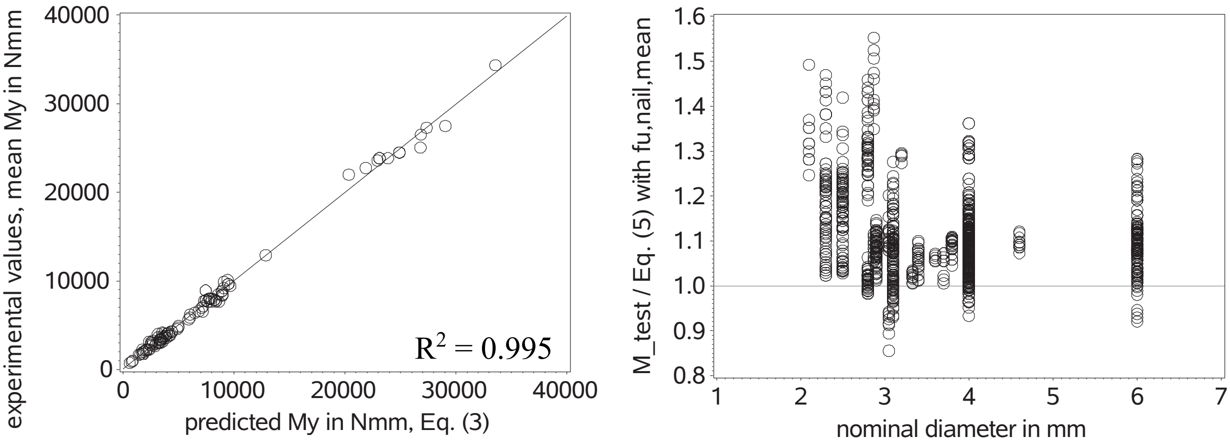

Fig. 4. Left: Experimental and predicted values (Eq. (3)) for the yield moment M_y. Right: The y-axis shows the ratio of individual experimentally determined yield moments over calculated yield moments using Eq. (5) and the mean nail tension strength values $f_{u,nail,mean}$ per series. The x-axis shows the nominal nail diameter. Data from 105 test series (1034 single tests M_y, 1035 single tests F_t).

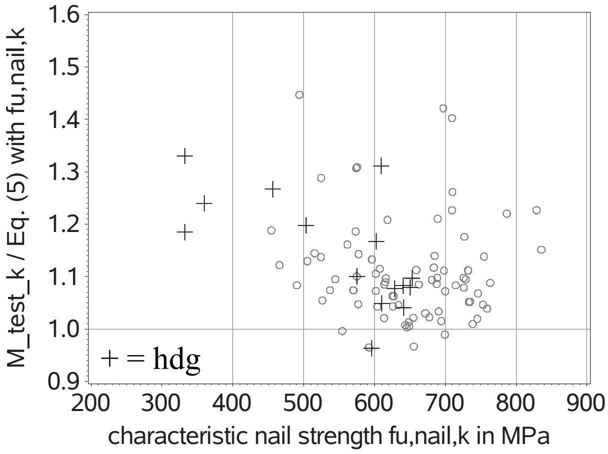

Fig. 5. Ratio between characteristic experimental and characteristic calculated yield moments (Eq. (5)) in dependence of the characteristic nail tension strength $f_{u,nail,k}$. Data from 105 test series (1034 single tests M_y, 1035 single tests F_t).

Based on the procedure prescribed in EN 14358 [11], 5th-percentile values have been estimated. The characteristic values were calculated from the test values assuming a lognormal distribution and a standard deviation of $s_y = 0.05$ for both the yield moment and the tension strength. This makes sense because both values are describing the same steel property and the differences in the variation are random. Fig. 5 shows the ratio between experimental and calculated yield moments using Eq. (5) versus the characteristic nail tension strength $f_{u,nail,k}$. The ratio is based on characteristic values $M_{y,k}$ per test series and Eq. (5) with $f_{u,nail,k}$. The 5th-percentile of the ratio is 1.00. Eq. (5) is therefore reflecting accurately the relationship between tension strength, nail diameter and yield moment and it is able to predict the characteristic yield moment $M_{y,k}$ using $f_{u,nail,k}$ as characteristic effective yield strength.

Fig. 5 also shows that the characteristic tension strength of the nails varies in a wide range and it would hence not be economically efficient to define a minimum tension strength for all nails. It would rather be reasonable to define technical classes to calculate the characteristic yield moment with a characteristic effective yield strength $f_{y,ef,k}$ which is based on characteristic tension strength values, see vertical lines in Fig. 5.

Concerning Eurocode 5, three options to regulate the yield moment of nails exist:

- No equation is given and the practitioners have to take the characteristic yield moments from the individual declarations of performance.
- Eq. (5) is inserted in Eurocode 5 where the characteristic tension strength $f_{u,nail,k}$ has to be taken from the declarations of performance.
- Technical classes are defined prescribing different characteristic tension strength values, where however, additional notes need to be given similar to prEN 14592 [12]. For instance, it must be clearly stated that small diameter nails may have significantly higher tension strength values than 6 mm nails (see also Fig. 3 on the right). Table 2 gives some examples on how such classes could be defined.

Table 2. Possible definition of technical yield strength classes (YSC) for effective yield strength $f_{y,ef}$ (in MPa) of dowel-type fasteners.

YSC1	YSC2	YSC3	YSC4	YSC5	YSC6	YSC7
300	400	500	600	700	800	900
Mild steel dowels						
hdg nails	-	d = 6 mm ⟶			d = 2 mm	
						Staples

4.3 Withdrawal parameter

For dowel type fasteners, the withdrawal parameter fax is calculated from the withdrawal capacity F_{ax} by the following equation:

$$f_{ax} = \frac{F_{ax}}{d \cdot L_{ef}} \tag{6}$$

where d is the nominal diameter and L_{ef} is defined as the length of the threaded part in the pointside member ($L_{ef} = t_{pen}$ (acc. Eurocode 5 [13]) = l_d (acc. EN 1382 [14])). That means that the tip of the nails has to be subtracted from the penetration length. Fig. 6 shows the tip length L_p versus the nail diameter d of all test data. The tip length is between d and $2 \cdot d$ with a mean value of $1.4 \cdot d$.

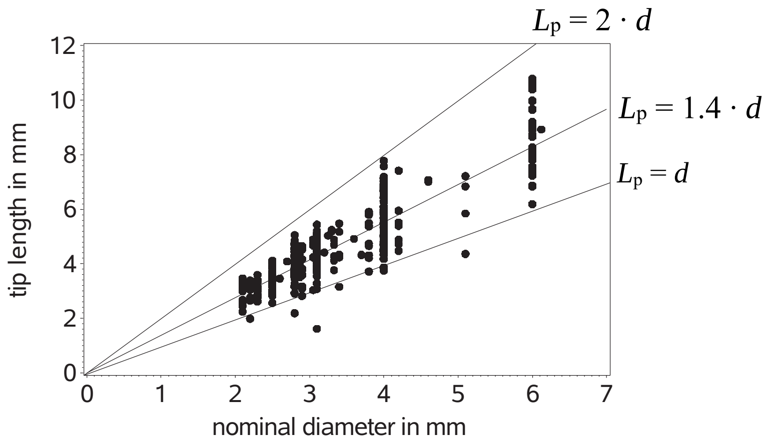

Fig. 6. Tip length L_p versus nominal diameter d, 5483 values (L_p has not always been recorded).

Pearson's correlation coefficients of f_{ax} are given in Table 3. The influence of L_{ef}, L_p and d is weak and also the ring depth, which is expressed as the ratio between inner (d_i) and outer (d_o) diameter, shows no correlation (R = 0.00) with f_{ax}. Only the density ρ correlates with f_{ax} (R = 0.33). For most types of fasteners, the withdrawal parameter is indeed a function of the wood density, as can be seen in Eq. (2). Fig. 7 shows f_{ax} in dependence of the density ρ. It can be seen that the range of tested densities is not fully representative for all softwood strength classes according to EN 338 [15] where classes with densities below 300 kg/m^3 and higher than 500 kg/m^3 exist, while the test values are between 329 and 472 kg/m^3.

In order to give a closer look at the relationship between f_{ax} and ρ, a nonlinear regression has been carried out ($R^2 = 0.11$) which is shown in Fig. 7 and where the exponent of 1.38 corresponds to the correction factors proposed in prEN 14592 [12] (there Table D.1):

$$f_{ax} = 3.6 \cdot 10^{-3} \cdot \rho^{1.38} \tag{7}$$

Table 3. Correlation matrix for withdrawal parameter.

	ρ	L_{ef}	L_p	ratio d_i/d_o	d
f_{ax}	0.33	-0.02	-0.20	-0.00	-0.18

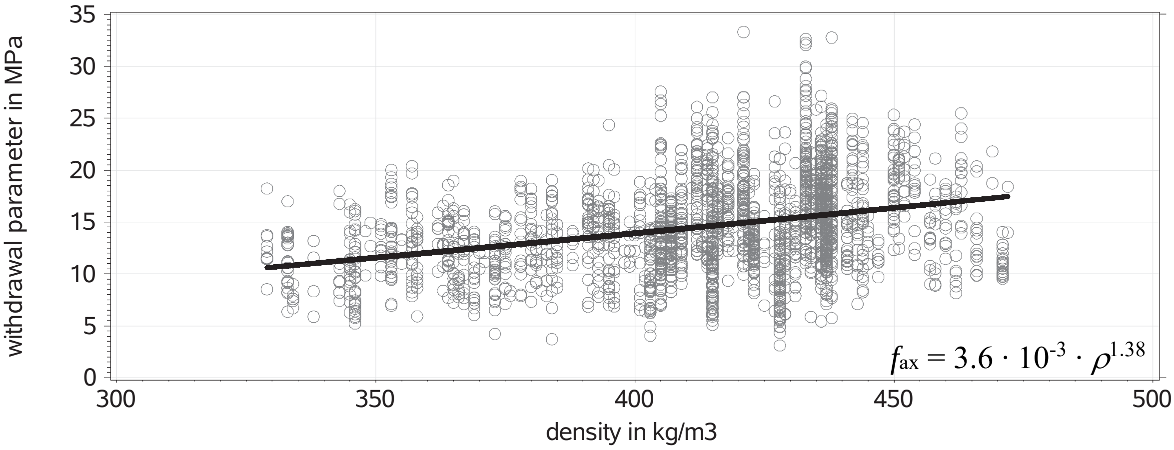

Fig. 7. Withdrawal parameter versus density, 2316 tests.

Still, with a correlation coefficient of 0.33 and a R^2-value of 0.11, the scatter is rather high and the relationship between f_{ax} and ρ is not very strong. One reason for this is that the differences between the nails of different producers are much higher than the differences caused by the density. This is visualised in Fig. 8 were the withdrawal parameters are given per test series with increasing nominal diameters. In Fig. 8, it can also be seen that the scatter within one test series is smaller for 4 to 6 mm nails than for smaller diameter nails. Additional influence effects were observed during testing. For instance, it has been observed that rather non-measurable factors guarantee good withdrawal parameters. Above all, the sharpness of the rings that can be felt when passing the nails through the fingers defines good performance. In the database, no information is available concerning the quality and sharpness of the rings or threads, and measuring it would increase testing efforts considerably.

Based on the procedure prescribed in EN 14358 [11], 5th-percentile values have been estimated assuming a lognormal distribution. The individual withdrawal parameters have been adjusted to a reference density of ρ_{ref} = 350 kg/m^3 using Eq. (7):

$$f_{ax,corr} = f_{ax} \cdot \left(\frac{350}{\rho} \right)^{1.38} \tag{8}$$

Fig. 9 shows the characteristic withdrawal parameter $f_{ax,k}$ per test series versus the nominal diameter and the five nail types are identified. Spiral, special spiral and square nails did not reach characteristic values larger than 8 MPa. Furthermore, the scatter is higher for smaller diameter nails which has already been seen in Fig. 8.

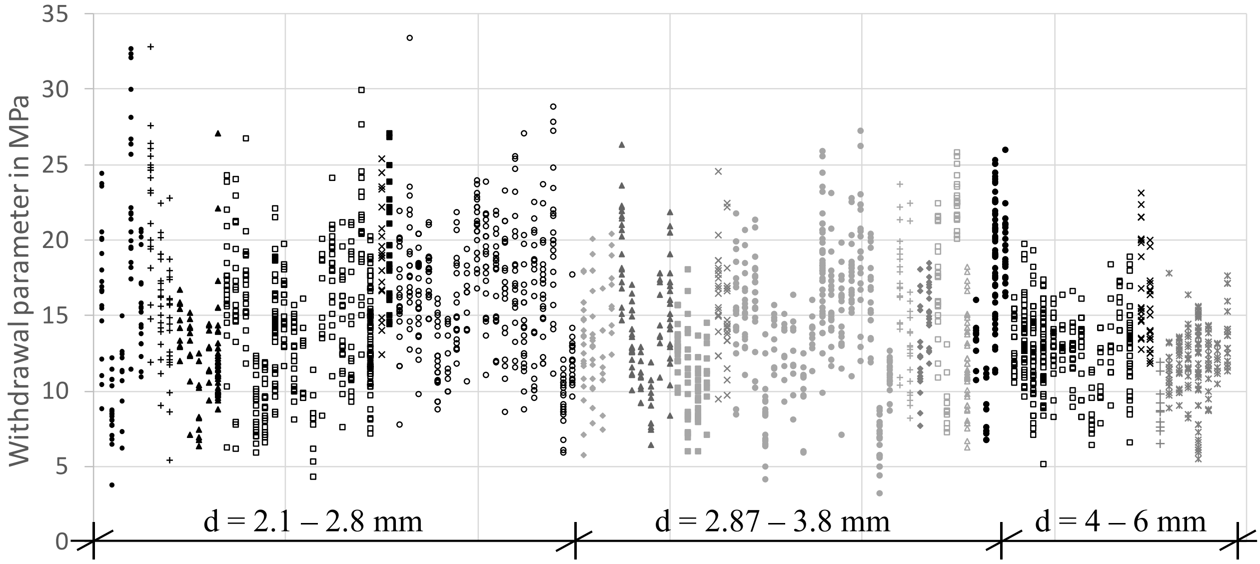

Fig. 8. 2316 withdrawal parameters are shown per test series and with increasing diameters.

Based on the actual database and the analyses shown, it can be concluded that also in future, tests have to be carried out and values for f_{ax} have to be taken from technical documents. At the moment, no test results are available where one nail type has been tested using a large range of wood densities or where the detailed nail geometry including information on the ring sharpness has been measured. Consequently, no thorough analyses can be carried out concerning these influence parameters.

With regard to code implementation, technical classes could be introduced so that designers do not need to consult declarations of performance to get withdrawal parameters. The horizontal lines in Fig. 9 correspond to the withdrawal classes for all fastener types in accordance with prEN 14592 [12], where values of 4.5, 6, 7, 8, 10 and 12 MPa are given. The decrease of variation with increasing diameter is observed also on the 5th-percentile level. Considering the still persistent high scatter in Figs. 7 to 9, the necessity of determining f_{ax} with the effective penetration depth (i. e. subtracting the tip length) for connection design purposes remains worth discussing. If a nonlinear regression is carried out where f_{ax} is calculated with the full penetration depth, differences of 10% to 20% to Eq. (7) are evaluated which disappear in the scatter within one diameter or density range.

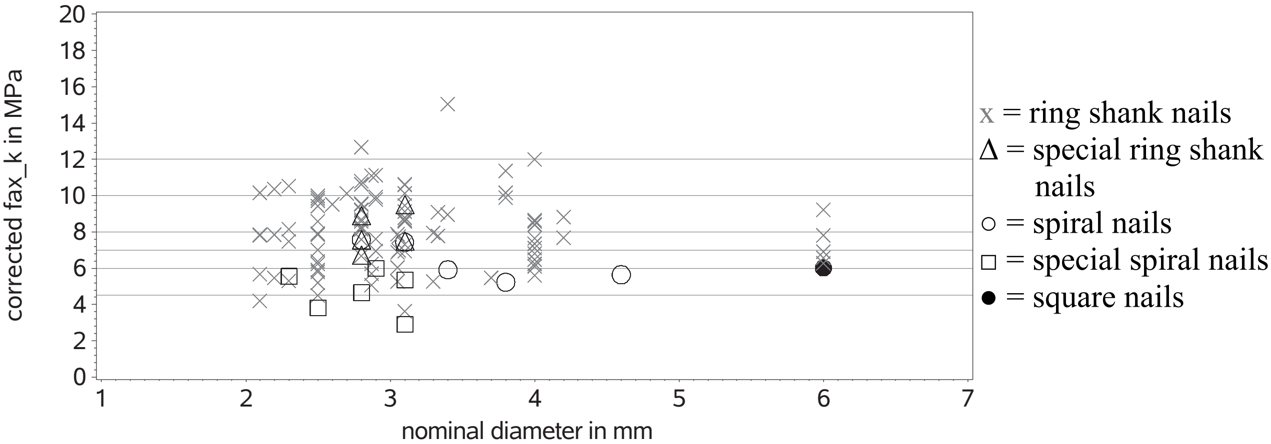

Fig. 9. Characteristic withdrawal parameter f_{ax} versus nominal diameter. f_{ax} has been corrected with $(350/\rho)^{1.38}$. Withdrawal classes from prEN 14592 [12] are shown, see horizontal lines at 4.5, 6, 7, 8, 10 and 12 MPa. Data from 118 test series (2316 single tests f_{ax}).

4.4 Head pull-through parameter

Similar to the withdrawal parameter, also the head pull-through parameter is considered to be a function of the wood density, Eq. (2). Therefore, again a correlation between head pull-through parameter f_{head} and density ρ, Table 4 and Fig. 10, has been carried out, where f_{head} has been calculated as follows with d_{h} = head diameter:

$$f_{\text{head}} = \frac{F_{\text{head}}}{d_{\text{h}}^2} \tag{9}$$

Table 4. Correlation matrix for head pull-through.

	ρ	d_{h}	d	d_{h}/d
f_{head}	0.52	-0.27	-0.27	0.08

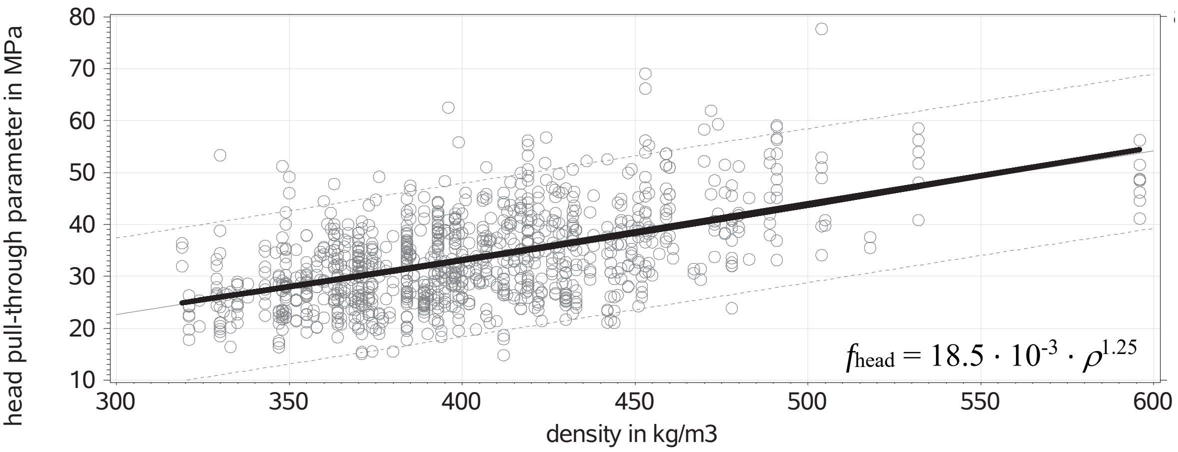

Fig. 10. Head pull-through parameter versus density, 1020 single tests.

Considering Table 4, the ratio of head diameter d_h over nominal diameter d (where d_h is approximately $2 \cdot d$) shows no influence on f_{head}. The head shape however may have an influence, but this parameter has not been recorded. No head pull-through tests were carried out using standard ring shank nails with trumpet heads that are used to fasten steel plates. Table 4 gives a Pearson's correlation coefficient for the density ρ of $R = 0.52$ and Eq. (10) gives the result of a nonlinear regression considering the complete database of 1020 results (with $R^2 = 0.28$). Eq. (10) is shown in Fig. 10.

$$f_{head} = 18.5 \cdot 10^{-3} \cdot \rho^{1.25} \tag{10}$$

If the same regression is carried out excluding the few results for high densities > 550 kg/m³, Eq. (10) does not change significantly and gives slightly lower values of f_{head} for higher densities (difference at 500 kg/m³ is 6%). These slight differences are included in the 95%-confidence interval shown in Fig. 10.

Again, based on the procedure prescribed in EN 14358 [11], 5th-percentile values have been estimated assuming a lognormal distribution. The individual head pull-through parameters have been adjusted to a reference density of $\rho_{ref} = 350$ kg/m³ using Eq. (10):

$$f_{head,corr} = f_{head} \cdot \left(\frac{350}{\rho}\right)^{1.25} \tag{11}$$

Fig. 11 shows the characteristic head pull-through parameter $f_{head,k}$ per test series versus the nominal diameter and the four nail types are identified. Again, the scatter is higher for smaller diameter nails. Fig. 11 also shows a decrease of f_{head} with increasing nail diameter which can be also concluded from Table 4 where the correlation coefficient for d (and its related parameter d_h) is -0.27 indicating a relationship between f_{head} and diameter.

Similar to the withdrawal parameter and based on the actual database and the analyses shown, it can be concluded that also in future, tests have to be carried out and values for f_{head} have to be taken from technical documents. With regard to code implementation, technical classes could be introduced also for head pull-through. The horizontal lines in Fig. 11 correspond to the withdrawal classes for all fastener types in accordance with prEN 14592 [12], where values of 10, 12.5, 15, 18, 20, 25 and 30 MPa are given. Considering the persistent scatter of f_{head} in Fig. 11 although head shapes do not differ significantly (round and flat shape and d_h approx. $2 \cdot d$), the random selection of the used timber seems to have a significant influence. Parameters such as annual ring widths and orientation of tangential and radial directions may have an influence on the experimental values and the question remains if high f_{head} values above 20 MPa are reliable. A lower bound value of 15 MPa seems to be possible which could be used, without further testing, for all nails with non-smooth shanks as long as $d_h/d > 1.8$.

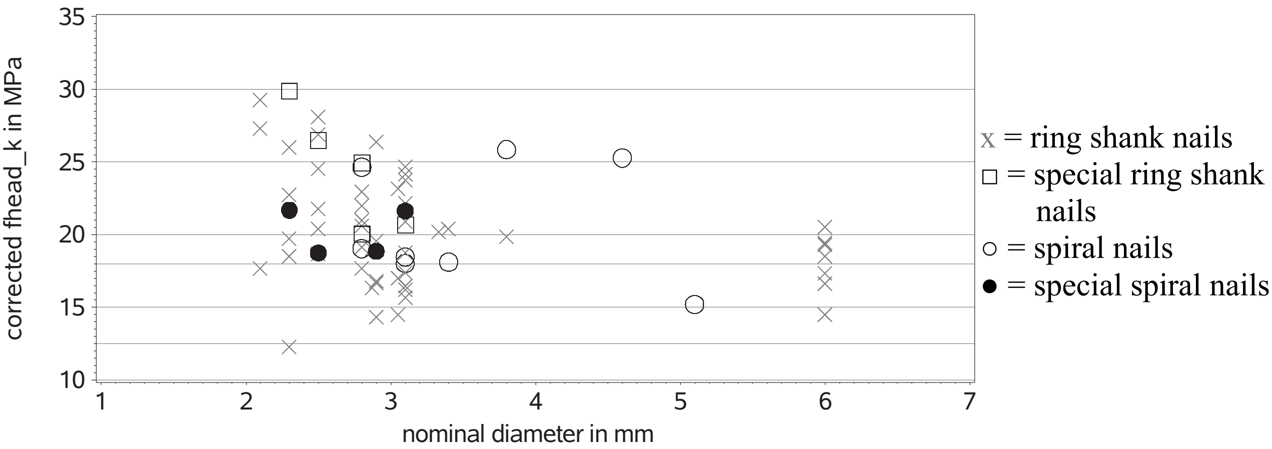

Fig. 11. Characteristic head pull-through parameter f_{head} versus nominal diameter. f_{head} has been corrected with $(350/\rho)^{1.25}$. Head pull-through classes from prEN 14592 [12] are shown, see horizontal lines at 10, 12.5, 15, 18, 20, 25 and 30 MPa. Data from 67 test series (1020 single tests f_{head}).

5. Conclusions

A comprehensive database containing test results on mainly ring shank nails has been analysed. The following recommendations can be given concerning input parameters for connection design in accordance with the European Yield Model:

- Wire tension strength: These tests are not needed. However, producers may still require wire tests to control delivered steel grades.
- Nail tension capacity F_t: Tension tests on nails need to be carried out and subsequently, a nail tension strength $f_{u,nail}$ can be calculated using the nominal diameter. This tension strength corresponds to an "effective yield strength $f_{y,ef}$"
- Yield moment M_y: The equation defining the theoretical full plastic bending capacity using an effective yield strength, Eq. (5), can be inserted in Eurocode 5 for all nail types except square nails where no tests were available. It would be no longer necessary to determine M_y by tests, where the results are often different between the testing institutes because of not clearly defined testing conditions (e. g. free bending length between $1 \cdot d$ and $3 \cdot d$ or technical difficulties of measuring the exact bending angle). The nominal diameter and the nail tension strength are needed to calculate the yield moment according to Eq. (5). The nail tension strength, which can be determined with a repetitious accuracy, must be taken from individual DoPs. Additionally, yield strength classes could be defined giving different nail tension strength values.
- Withdrawal parameter: Considering the database with its limitations, it is proposed to include technical classes in Eurocode 5 to facilitate design of nailed connections. For design purposes, it is recommended to limit the characteristic withdrawal parameter for nails with small diameters to a certain limit (e. g. 8 N/mm^2) even if tested values are higher (see Fig. 9), because the withdrawal strength is very sensible to wood characteristics (not totally explained by the density) and production tolerances.

- Head pull-through parameter: The conclusions are analogous to those for the withdrawal parameter. Also here, the insertion of technical classes is proposed.

Acknowledgements

This work has been carried out within COST Action FP1402 and the authors would like to thank Elke Mergny, who started to assemble the database in the framework of a Short Term Scientific Mission which was paid by the same COST Action.

An extended version of this chapter has been published in: "Sandhaas C, Görlacher R (2018) Analysis of nail properties for joint design. *Engineering Structures* **173**:231-240."

References

[1] Johansen KW (1949) *Theory of timber connections.* Publication 9, International Association of Bridge and Structural Engineering (IABSE), Basel, Switzerland.

[2] Moeller T (1951) *En ny metod foer beraekning av spikfoerband.* Handlingar no. 117, Chalmers Tekniska Hoegskola, Göteborg, Sweden.

[3] Ehlbeck J (1979) *Nailed joints in wood structures.* Bulletin no. 166, Wood Research and Wood Construction Laboratory, Virginia Polytechnic Institute and State University, USA.

[4] Whale LRJ, Smith I (1986) *Mechanical timber joints.* Report 18/86, TRADA, High Wycombe, UK.

[5] Whale LRJ, Smith I (1986) *The derivation of design clauses for nailed and bolted joints in Eurocode 5*. CIB-W18 Meeting 19, Paper 19-7-6, Florence, Italy.

[6] Blaß HJ (1990) *Load distribution in nailed joints*. CIB-W18 Meeting 23, Paper 23-7-2. Lisbon, Portugal.

[7] Blaß HJ (1991) Traglastberechnung von Nagelverbindungen. *Holz als Roh- und Werkstoff* **49**(3):91-98. doi:10.1007/BF02614345.

[8] Werner H, Siebert W (1991) Neue Untersuchungen mit Nägeln für den Holzbau. *Holz als Roh- und Werkstoff* **49**(5):191-198.

[9] Steilner M, Blaß HJ (2014) *A method to determine the plastic bending angle of dowel-type fasteners*. In: Aicher S, Reinhardt HW, Garrecht, H (eds) RILEM bookseries. Materials and joints in timber structures. Recent developments in technology. Stuttgart, Germany, pp. 603-613.

[10] Blaß, HJ, Colling, F (2015) *Load-carrying capacity of dowelled connections*. INTER Meeting 48, Paper 48-7-3, pp. 115-129. Sibenik, Croatia.

[11] *EN 14358:2007*. Timber structures – Calculation of characteristic 5-percentile values and acceptance criteria for a sample. CEN, Brussels.

[12] *prEN 14592:*2017. Timber structures – Dowel-type fasteners – Requirements. CEN, Brussels.

[13] *EN 1995 1-1:2010 (Eurocode 5)*. Design of timber structures – Part 1-1: General – Common rules and rules for buildings. CEN, Brussels.

[14] *EN 1382:2016*. Timber structures – Test methods – Withdrawal capacity of timber fasteners. CEN, Brussels.

[15] *EN 338:2009*. Structural timber – Strength classes. CEN, Brussels.

Database of staples

Kurt de Proft
wood.be
Brussels, Belgium

Carmen Sandhaas
Karlsruhe Institute of Technology
Germany

Summary

A database has been assembled using available test data from Karlsruhe Institute of Technology (KIT) where many tests have been done to characterise the properties of staples. In the context of the forthcoming revision of Eurocode 5, the objective of this database is to collect and analyse a maximum of data on the following topics:

- Mechanical properties of staples
- Load-carrying capacity of connections using staples
- Edge distances in connections using staples

However, only few test results on both staple properties and stapled connections were available. Also only one single research report [1], dating from 1973, is available concerning staples and stapled connections. Only 86 test series were available concerning wire strength, 20 series concerning the yield moment, 89 series concerning withdrawal and no series concerning head pull-though. Also embedment tests are not usually carried out using staples.

1. Mechanical properties of staples

1.1 Introduction

Over the years, a certain number of certification tests were performed on staples at KIT which were documented in 32 reports. All 32 reports from 1997 to 2012 are included here. The following parameters were reported, see also Fig. 1:

- Geometrical properties: length of the staple L_n, width of the crown b_r, width b and thickness a of staple legs
- Length of the resin coated parts L_h
- Wire diameter d which corresponds to the nominal diameter of the staple
- Tensile strength of the wire $f_{u,wire}$ (in a few reports, the tensile strength of the staple leg is measured)
- Withdrawal capacity F_{ax} of the staple for a certain penetration length L_{ef} and a certain density ρ at a moisture content u

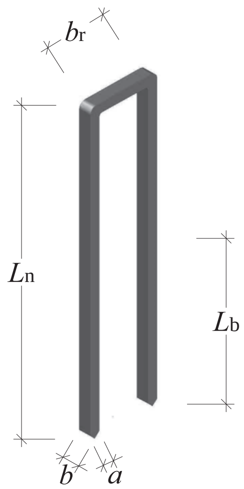

Fig. 1. Geometry of a staple.

It is furthermore reported if the staples were galvanized or if stainless steel has been used. Only in six reports, also the yield moment M_y was measured. Only mean values and standard deviations were included in the database and not the individual test values. Generally, 20 tests were carried out to evaluate the withdrawal capacity (10 tangential, 10 radial), 5 tests to evaluate the yield moment and 5 tests to evaluate the wire tension strength. In the following, the three measured mechanical properties wire strength $f_{u,wire}$, yield moment M_y and withdrawal capacity F_{ax} are discussed. No results on the head pull-through parameter were available. All data has been inserted in spreadsheets.

1.2 Wire strength

Fig. 2 shows the results of the wire tension tests where the mean values of 86 test series are given. A slight influence of the wire diameter on the wire tension strength can be observed. The decrease of tension strength with increasing diameter can be explained with hardening due to cold forming as thinner wires have to be passed through the dye more often. The mean wire tension strength of all 86 values is 965 MPa with a coefficient of variation COV = 8.3% (values < 800 MPa are included). No difference between carbon and stainless steel could be observed.

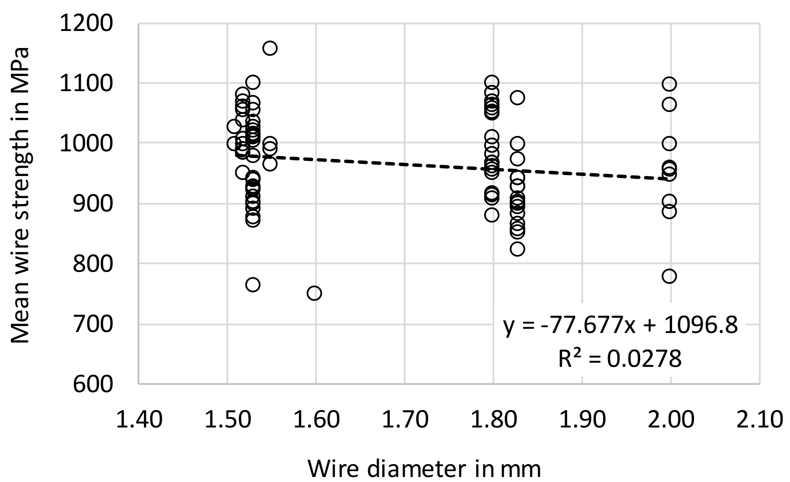

Fig. 2. Wire strength $f_{u,wire,mean}$ versus wire diameter d. Mean values of 86 series.

1.3 Yield moment

Only six reports contained data on the yield moment of staples and only 20 different test series were available. Both the mean and the characteristic yield moment is shown in Fig. 3 versus the nominal diameter (= wire diameter). Fig. 3 also contains some characteristic values taken from Declarations of Performance (DOP) of different producers and it also shows Eq. (1) from Eurocode 5 (Amendment A2):

$$M_{\mathrm{y,k}} = 150 \cdot d^3 \tag{1}$$

Eq. (1) is derived from Eq. (2) using a fixed yield strength for the staples of f_y = 900 MPa:

$$M_{\mathrm{y,k}} = \frac{1}{6} \cdot f_{\mathrm{y}} \cdot d^3 \tag{2}$$

It can be seen in Fig. 3 that all characteristic values derived from experimental results, the red crosses, lie above Eq. (1) and thus on the safe side. However, no thorough analyses can be carried out due to the very limited number of test results.

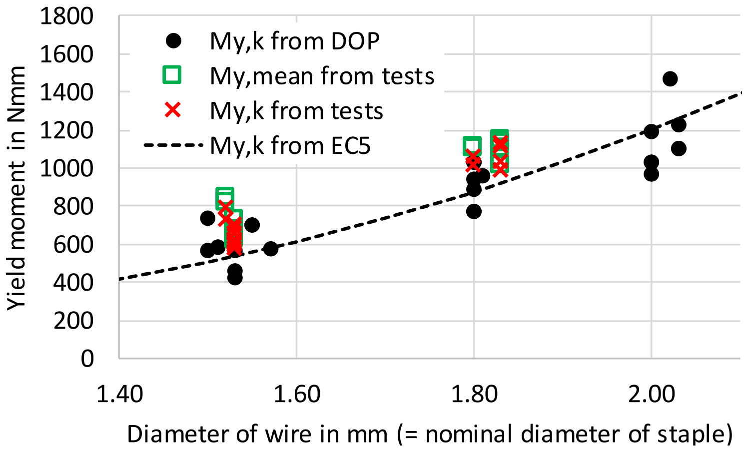

Fig. 3. Yield moment M_y versus wire diameter d. Mean and characteristic values of 20 series, characteristic values from DOPs and equation from Eurocode 5.

1.4 Withdrawal capacity

89 series evaluating the withdrawal capacity were available where the mean density amounted to 427 kg/m^3 at a mean moisture content of 11.8%. All tested staples were resin-coated. In order to analyse the withdrawal tests, the capacity has been transformed into the withdrawal parameter f_{ax} using Eq. (3) with the penetration depth L_{ef} and the nominal diameter d:

$$f_{ax,k} = \frac{F_{ax}}{d \cdot L_{ef}} \tag{3}$$

Fig. 4 shows the mean withdrawal parameter $f_{ax,mean}$ versus the mean density ρ_{mean} per test series. The scatter is high and a very low dependency of f_{ax} on ρ can be observed. In the current version of Eurocode 5, axial loading of staples is not regulated (contrarily to the German National Annex which explicitly allows for axial loading). Looking at Fig. 4, this seems to be too conservative. As a conservative starting point, a constant value of f_{ax} = 8 MPa could be used, however more testing data for a more thorough analysis should be evaluated.

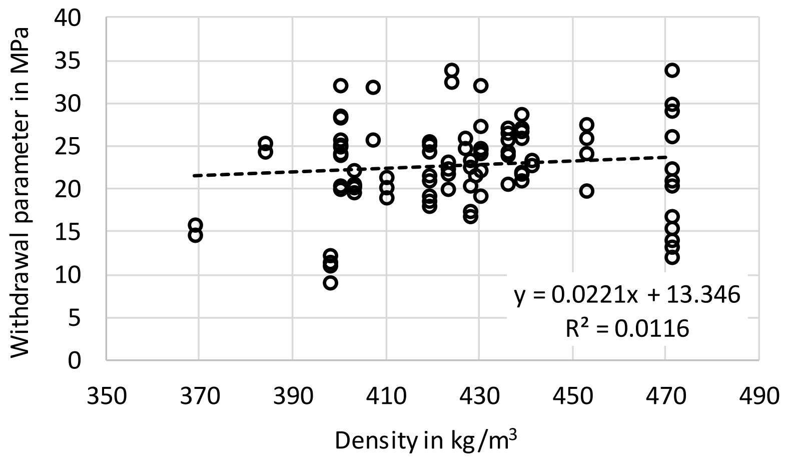

Fig. 4. Withdrawal parameter $f_{ax,mean}$ versus density ρ_{mean}. Mean values from 89 test series

2. Load-carrying capacity of connections using staples

2.1 Introduction

Apart from test data for the individual fasteners, KIT also performed a number of tests on stapled connections. The six available test reports are all dated between 1976 and 1983. There are no recent reports available. All reports have a similar content where three types of tests are reported:

- Tests to determine the load-carrying capacity of the stapled connection where the staples are laterally loaded
- Tests to determine the withdrawal capacity of the staple
- Tests to determine the head pull-through capacity of the staple through a wood-based panel

In the following, only the shear tests are presented; it is considered useless to further boost the previously presented database using very old withdrawal and head pull-though tests (these data however is included in the spreadsheets).

2.2 Shear tests

The shear tests were performed in tension and both timber-to-timber as well as timber-to-wood-based panel tests were carried out. The first series of tests concerned timber-to-timber connections where the staples were positioned in two different ways:

- The angle between the crown of the staple and the grain direction of the timber is 0° (Fig. 5)
- The angle between the crown of the staple and the grain direction of the timber is 45° (Fig. 6)

The tests were performed with staples that have different wire diameters. The dimensions of the specimen were chosen as a function of the staple dimensions (edge distances). For example, the distance between the staple and the edge of the timber (distance e_3 in Fig. 5 and distance e_4 in Fig. 6) was chosen to $5 \cdot d$.

Another parameter in the tests was the moisture content of the timber at fabrication of the specimen and at testing. One series was tested with a moisture content of the timber between 12% and 14%, both during fabrication as well as testing. A second series was tested with a moisture content of the timber between 25% and 30% at the time of fabrication of the specimen and moisture content between 12% and 14% at the time of testing.

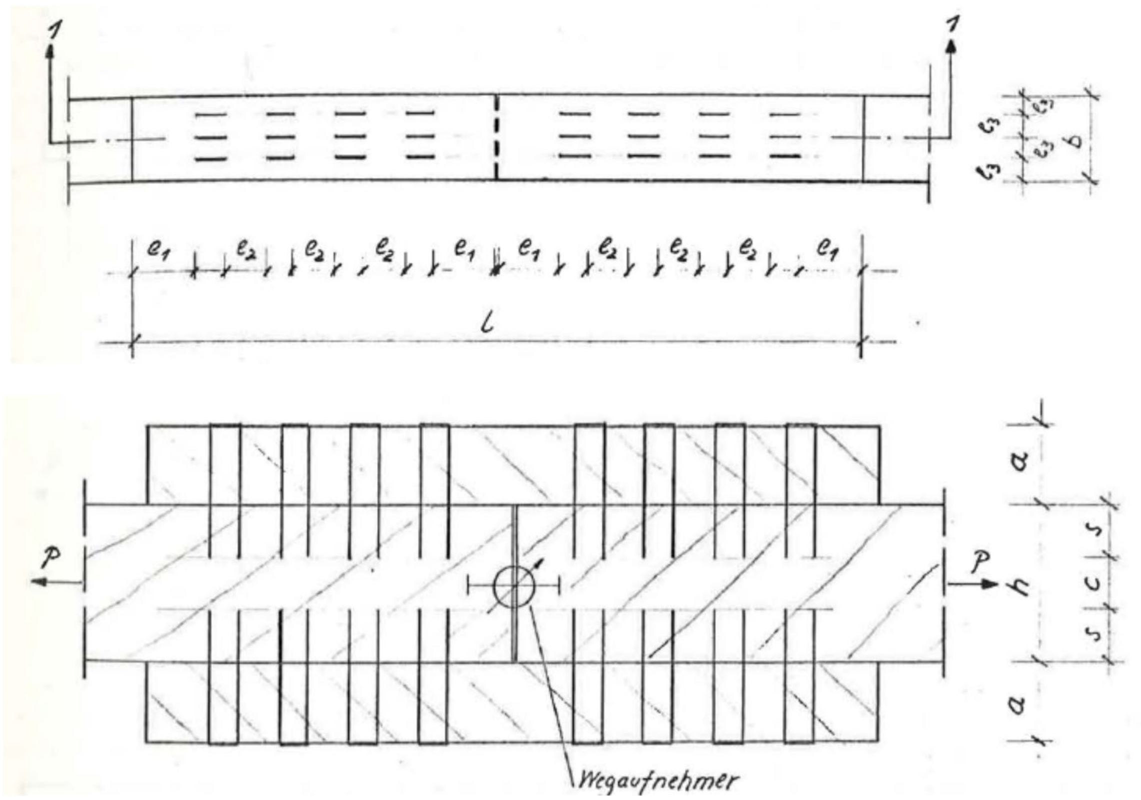

Fig. 5. The angle between the crown of the staple and the grain direction of the timber is 0°.

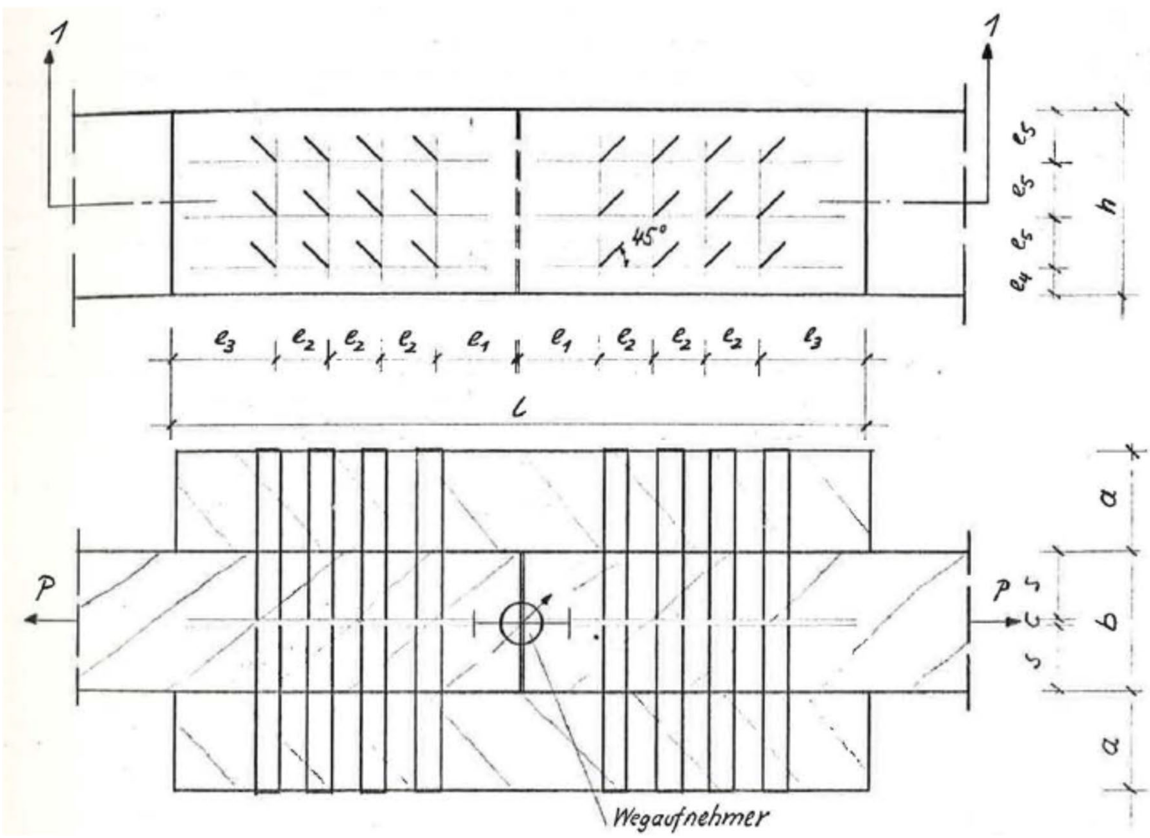

Fig. 6. The angle between the crown of the staple and the grain direction of the timber is 45°.

In a second series of tests, timber-to-wood-based panel connections were tested, see Fig. 7. Three types of panels were used:

- High density fibre boards (density around 1000 kg/m^3) with a thickness of 4 or 6 mm
- Plywood (spruce) (density around 500 kg/m^3) with a thickness of 7.5 and 12.5 mm
- Particle board (density around 700 kg/m^3) with a thickness of 8 or 13 mm

The connection was tested with the angle between the crown of the staple and the grain direction of the timber equal to 45°. The distance from the side of the timber member to the first leg of the staple was again 5 · *d*.

Table 1 presents all shear test results contained in the reports where mean values are given (5 tests per series have been carried out). For the time being, no further analyses have been carried out.

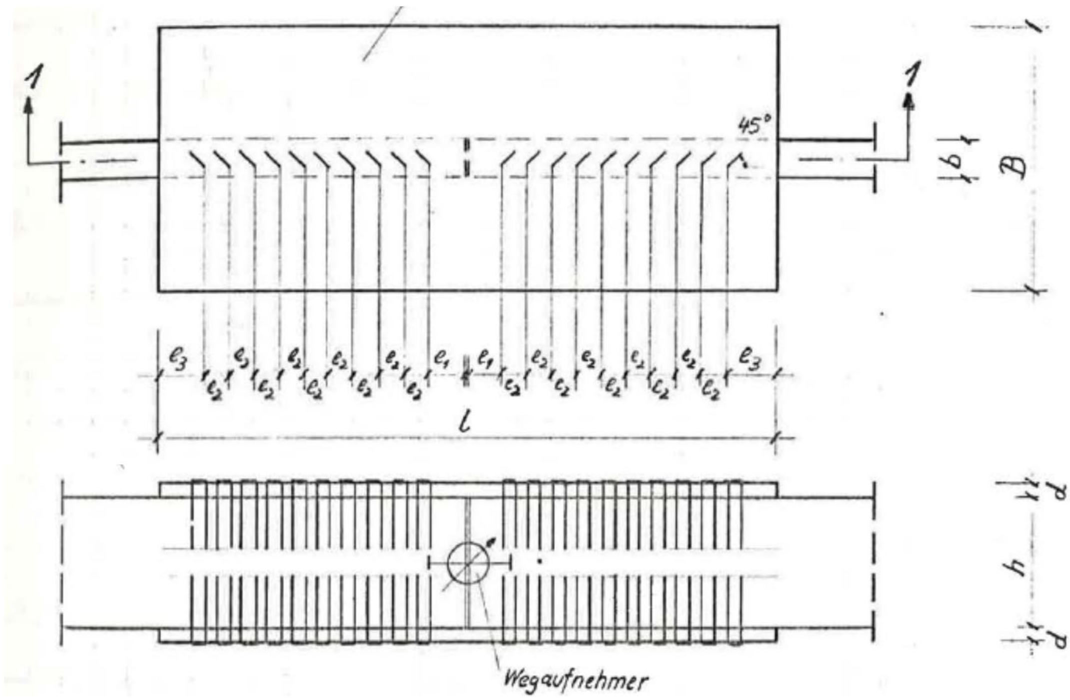

Fig. 7. Specimen to test the load-carrying capacity of a timber-to-wood-based panel connection.

Table 1. Results of reported shear tests on stapled connections, mean values of 5 tests per series.

report	u at prod.	u at test	no. staples	L_n (mm)	d (mm)	L_h (mm)	b_r (mm)	Side 1	$\rho_{m,1}$ (kg/m³)	t_1 (mm)	Side 2	$\rho_{m,2}$ (kg/m³)	t_2 (mm)	α (°)	F_m (kN)
A	12%	12%	24	75.0	2.00	41.0	12.2	timber	462	51.0	timber	476	24.0	0	20
A	12%	12%	24	75.0	2.00	41.0	12.2	timber	463	51.0	timber	491	24.0	45	31
A	25-30 %	12%	24	75.0	2.00	41.0	12.2	timber	478	51.0	timber	485	24.0	0	22
A	12%	12%	20	75.0	2.00	41.0	12.2	HDF	1030	6.0	timber	472	69.0	45	24
A	12%	12%	20	75.0	2.00	41.0	12.2	PB	760	8.0	timber	492	67.0	45	24
B	12%	12%	24	63.5	1.53		12.6	timber	440	43.5	timber	440	20.0	45	19
C	12-14%	12-14%	24	51.0	1.83	27,5-29	11.7	timber	512	29.0	timber	512	22.0	0	21
C	12-14%	12-14%	24	51.0	1.83	27,5-29	11.7	timber	512	29.0	timber	512	22.0	45	22
C	25-30%	12-14%	24	51.0	1.83	27,5-29	11.7	timber	512	29.0	timber	512	22.0	0	26
C	25-30%	12-14%	24	51.0	1.83	27,5-29	11.7	timber	512	29.0	timber	512	22.0	45	31
C			20	44.2	1.83	22-24	11.7	HDF	1020	4.0	timber	512	40.2	45	13
C			20	44.2	1.83	22-24	11.7	PB	657	8.0	timber	512	36.2	45	22
D	12-14%	12-14%	24	50	1.58	19-21	11.5	timber	465	30	timber	465	20	45	16
D	28.60%	13%	24	50	1.58	19-21	11.5	timber	465	30	timber	465	20	45	14
D	12-14%	12-14%	24	50	1.58	19-21	11.5	timber	465	30	timber	465	20	45	18
D	28.60%	13%	24	50	1.58	19-21	11.5	timber	465	30	timber	465	20	45	14
D	12-14%	12-14%	12	63.9	1.58	33-34	11.3	timber	465	24	timber	465	13	45	15
D	28.60%	13%	12	63.9	1.58	33-34	11.3	timber	465	24	timber	465	13	45	13
D	12-14%	12-14%	12	63.9	1.58	33-34	11.3	timber	465	24	timber	465	13	45	18
D	28.60%	13%	12	63.9	1.58	33-34	11.3	timber	465	24	timber	465	13	45	16
E	12-14%	12-14%	24	50.2	1.56	0	12.2	timber	421	30.2	timber	421	20	0	19
E	25-30%	12-14%	24	50.2	1.56	0	12.2	timber	421	30.2	timber	421	20	0	19
E	12-14%	12-14%	24	50.2	1.56	0	12.2	timber	421	30.2	timber	421	20	45	23
E	25-30%	12-14%	24	50.2	1.56	0	12.2	timber	421	30.2	timber	421	20	45	22
E	12-14%	12-14%	24	50.3	1.83	0	12.7	timber	421	28.3	timber	421	22	0	21
E	25-30%	12-14%	24	50.3	1.83	0	12.7	timber	421	28.3	timber	421	22	0	22
E	12-14%	12-14%	24	50.3	1.83	0	12.7	timber	421	28.3	timber	421	22	45	26
E	25-30%	12-14%	24	50.3	1.83	0	12.7	timber	421	28.3	timber	421	22	45	27
E	-	-	20	50.2	1.56	0	12.2	HDF	1011	4	timber	421	37	45	15
E	-	-	20	50.3	1.83	0	12.7	HDF	1011	4	timber	421	46	45	14
E	-	-	20	50.3	1.83	0	12.7	HDF	995	6	timber	421	44	45	30
E	-	-	20	50.3	1.83	0	12.7	plywood	477	7.5	timber	421	43	45	29
E	-	-	20	50.3	1.83	0	12.7	PB	657	8	timber	421	42	45	20
F	-	-	20	49.9	2.00	24/30	12.0	HDF	995	6	timber	426	43.9	45	25
F	-	-	20	49.9	2.00	24/30	12.0	plywood	477	7.5	timber	426	42.4	45	25
F	-	-	20	49.9	2.00	24/30	12.0	PB	657	8	timber	426	41.9	45	25
F	12-14%	12-14%	24	75	2.00	24/27	12.0	timber	426	51	timber	426	24	45	28
F	25-30%	12-14%	24	75	2.00	24/27	12.0	timber	426	51	timber	426	24	45	27

u = moisture content, L_n = length of staple, d = nominal diameter, L_h = length of resin-coated part, b_r = width of crown, $\rho_{m,1/2}$ = mean density of member 1/2, $t_{1/2}$ = thickness of member 1/2, α = angle between crown and grain direction, F_m = mean load-carrying capacity per connection.

3. Edge distances in connections using staples

No reports were available where the focus of the investigations lay on the evaluation of the minimum edge distances of stapled connections. No indication could be found as to where the current rules on minimum distances and spacings stem from. They seem to be rules deriving from experience and judgement of carpenters and timber designers. This is curious to note seeing the manifold practical issues and problems surrounding especially the minimum edge distances. In practice, sheeting panels will have connections on vertical timber frame members where practical member thicknesses are often just thick enough to fulfil current rules.

4. Conclusions

The first surprising conclusion is the sheer lack of test results on both staple properties and stapled connections. Also only one single research report [1], dating from 1973, is available concerning staples and stapled connections. Only 86 test series were available concerning wire strength, 20 series concerning the yield moment, 89 series concerning withdrawal and no series concerning head pull-though. Also embedment tests are not usually carried out using staples. Analysing this small database however, a couple of conclusions can be drawn:

- The current Eurocode 5 equation to calculate the characteristic yield moment of staples holds.
- A constant withdrawal parameter of 8 MPa could be used to calculate the withdrawal capacity of resin-coated staples.

The available tests on stapled connections are even less and date back to the late seventies/early eighties. Production methods and steel qualities may have changed and it is hard to judge whether these old tests can provide useful data. However, seeing the general lack of test results, the connection tests could be used to backwards calculate yield moment and embedment strength.

References

[1] Möhler K, Ehlbeck J, Köster P (1973). *Untersuchungen über das Trag- und Verformungsverhalten von Heftklammerverbindungen bei Tafelelementen*. Mitteilung aus der Versuchsanstalt für Stahl, Holz und Steine, Abt. Ingenieurholzbau der Universität Karlsruhe (TH), Germany.

Database of screws

Carmen Sandhaas
Karlsruhe Institute of Technology
Germany

Summary

In the framework of this COST Action and analogously to the nail database presented here (*Nailed connections: Investigation on parameters for Johansen model*), an extensive database comprising more than 18,000 test results on screws carried out for certification purposes has been assembled. This database still has to be validated and will be analysed only after this COST Action.

1. Short presentation of database

Data from 84 test reports and 26 different producers has been assembled. Table 1 shows the distribution of the individual test results. A total of 18105 tests results, of which 2800 screws made from stainless steel, are part of the database. Fig. 1 shows some examples of screw types.

Table 1. Composition of screw database.

	Insertion moment R_{tor}	Torsional capacity F_{tor}	Yield moment M_y	Tension capacity F_t	Withdrawal capacity F_{ax}	Head pull-through capacity F_{head}
No. of tests	4200	3056	2396	3365	3068	2020

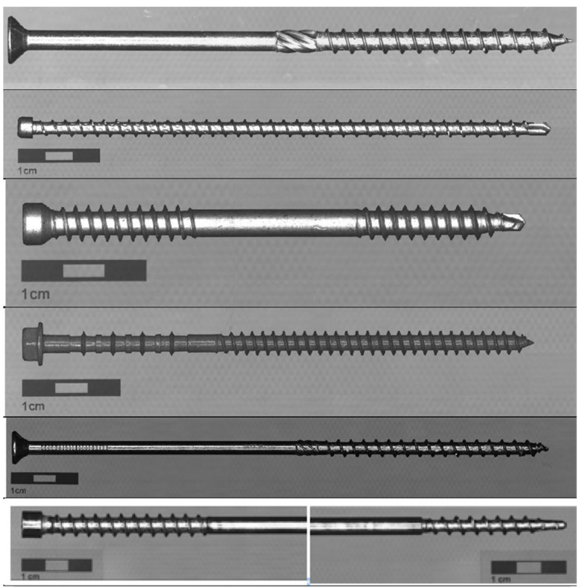

Fig. 1. Some screw types in the database

Database and parameterization of embedment slip curves

Michael Schweigler
Department of Building Technology, Linnaeus University
Växjö, Sweden

Carmen Sandhaas
Karlsruhe Institute of Technology
Germany

Summary

Currently, work is undergoing to develop novel modelling approaches based on beam-on-foundation (BOF) formulations that can be used to design complex timber connections (see also chapter "Numerical modeling of the load distribution in multiple fastener connections"). For BOF models, load-displacement data derived from embedment tests are needed, with which nonlinear springs representing the embedment of the fastener in the surrounding timber matrix can be defined. First efforts were undertaken to identify possible data sources that include displacement data in addition to embedment strength. Parameterized equations can be used to describe corresponding experimental embedment slip curves analytically, so that they can be used as input to BOF-models. Methods for parameterization of embedment slip curves are shortly presented, and necessary parameters for an analytical description are listed. A proposal for revisions of the European standard for embedment testing, EN 383 [1] is given. Finally, a first overview of embedment data, including relevant literature references is presented. The literature list is based on a BSc thesis from TU Wien [2] and a Master thesis from KIT [3].

1. Parameterization of embedment slip data

Using parameterized equations for the embedment slip data gives direct access to the embedment stress f_h as a function of various parameters, such as displacement of the fastener u, load-to-grain angle α, fastener diameter d, wood density ρ, moisture content MC, … (see Fig. 1). Using parameterized embedment slip curves in BOF-models is advantageous. Compared to application of tabulated embedment data in BOF-models, the computational time decreases considerably if analytical functions are used, since embedment strength and stiffness can be directly determined for arbitrary displacements. Furthermore, embedment slip data can be easily adjusted to the above listed influence parameters.

In most cases, embedment slip curves can be well described analytically by three parameters, namely one strength parameter and two stiffness parameters, see Fig. 1. The latter are addressed to the initial, i.e. elastic stiffness k_0, and to the final, i.e. elasto-plastic stiffness k_f. The strength parameter could be defined either as f_h at u

equal to 5 mm, which corresponds to the current definition of the embedment strength in EN 383 [1], or as $f_h = f_{h,\ inter}$ at the intersection of the tangent k_f with the vertical axis (see Fig. 1). In addition, some parameterization models require information on the unloading stiffness k_{unload}. These four parameters, i.e. $f_{h,inter}$, k_0, k_f, and k_{unload}, are a function of the other influence parameters like e.g. α, d, ρ and MC. A summary of parameterization methods for experimentally determined slip data is given in [4], in which the authors focused on an analytical definition of f_h depending on u and α. In [4], a three-step approach is presented. In a first step, parameterized embedment slip curves for a certain α are defined by application of exponential, polynomial or exponential-polynomial functions, as proposed by e.g. Foschi [5], Richard/Abbott [6] and Sauvat [7]. Secondly, the trend of parameters derived in the first step are fitted over the load-to-grain angle α, by application of regression functions. For this purpose, trigonometric functions, e.g. Hankinson formula [8], or functions from statistics, e.g. an adapted version of the Gaussian function [9] can be applied. In a third step, regression equations from step one and two are combined, resulting in a parameterized equation for the embedment stress as a function of u and α. For further details the reader is referred to [4].

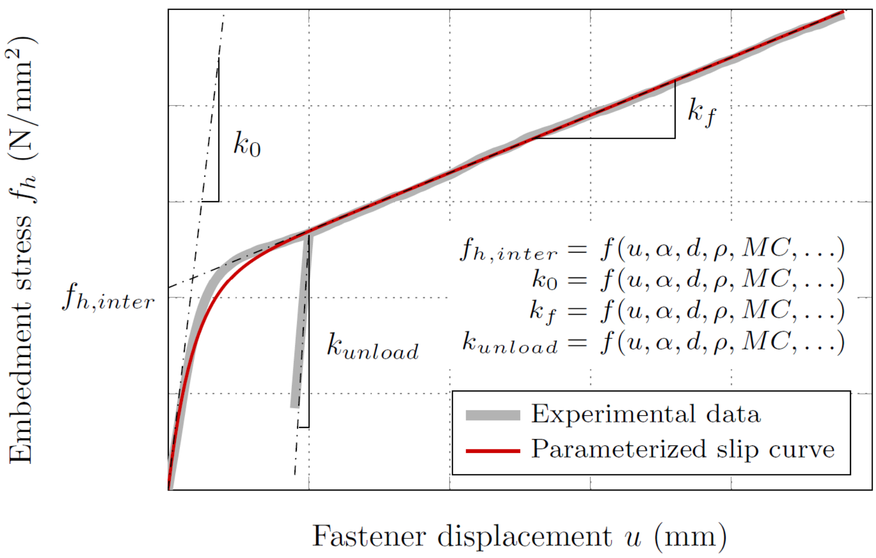

Fig. 1. Schematic illustration of a parameterized embedment slip curve, including required parameters.

To define parameterized embedment slip curves, existing embedment data (see table in Section 3) could be used. However, currently available data are incomplete, especially with regards to information on the elasto-plastic stiffness k_f, and there are hardly any embedment curves for load-to-grain angles α in-between the principal material directions (i.e. $\alpha = 0°$ and 90°). This fact can be mainly addressed to missing regulations in the corresponding testing standard EN 383 and its application, where the embedment strength was in the focus rather than corresponding displacements. Thus, a revision of EN 383 is proposed in the following.

2. Revision of the embedment testing standard EN 383

To allow for parameterization of embedment data through analytical equations, i.e. the definition of curve functions that represent the embedment slip behavior, and the subsequent use of these curve functions in BOF-models, documentation of the required parameters from embedment tests is essential. A revised definition of the initial elastic loading stiffness k_0 should be given. Stiffness parameter k_0, named k_s in EN 383 [1], should be determined based on the measured embedment strength f_h, instead of the estimated embedment strength $f_{h,est}$. Furthermore, regulations for determination of the unloading stiffness k_{unload} should be included as well. In addition, a parameter for the final elasto-plastic loading stiffness k_f must to be included for parameterized equations of ductile connections. This is important since extrapolation of tests data up to 5 mm displacement limit to larger displacements is not possible (see discussion in [4]). Stiffness k_f could be defined as secant loading stiffness between two points in the elasto-plastic region of the slip curves. These two points on the slip curve could be defined by the embedment stress at certain fastener displacements u, determined relative to the dowel diameter d, like e.g. at $u = 0.5 \cdot d$ and $1.5 \cdot d$. Therefore, the displacement limit u_{max} in embedment testing should be increased as well (see discussion in [4]). A combined definition, i.e. a displacement limit given by an absolute displacement and a limit defined relative to the fastener diameter, is proposed. The absolute definition is of importance for small fastener diameters like nails, while the relative limit applies for larger diameters. A relative limit of one and a half or two times the fastener diameter could be used.

Especially in embedment testing parallel to the grain, brittle failure due to splitting must be avoided before the ultimate limit of embedment stress is reached. For testing up to displacements larger than the current 5 mm limit, reinforcement of test specimens is a prerequisite, in order to avoid premature failure due to splitting. Preferably, EN 383 should include regulations for the position and strength of reinforcement measurements as well. Furthermore, regulations for the geometry of test specimens for load application at an angle to the grain have to be included. The surface quality of the steel fastener should be documented as well, since it was shown to have strong influence on the embedment behaviour (see e.g. [28]).

3. Overview of available data

ID	Author	Wood species	Fastener type	Fastener diameter [mm]	Experimental standard	load-to-grain angle [°]	load-displacement curve [yes/no]
-	Anonymous_1	spruce/pine LVL	dowel, screw, nail	4; 6; 8; 16	EN 383	0, 90	Yes (in [2])
-	Anonymous_2	spotted gum, radiata pine, radiata pine LVL	screw	8	EN 383	0, 90	Yes (in [2])
10	Awaludin et al.	Shorea obtusa	bolt	12; 4	?	0, 30, 45, 60, 90	No
11	Bader et al.	spruce LVL	dowel	12; 20	EN 383	0, 45, 90	Yes
12	Blaß et al._1	spruce	screw	6; 8; 10; 12	EN 383	0, 30, 45, 60, 90	Yes (in [2])
13	Blaß et al._2	spruce CLT, spruce OSB	dowel, screw, nail	4,2; 6; 8; 12; 16; 20; 24	EN 383	0, 45, 90	Yes
14	Bléron et al.	fir	dowel	10; 12; 14; 16; 18; 20	?	0, 15, 30, 45, 60, 75	No
15	Claisse et al.	?	bolt, dowel	12	EN 26891	0	Yes
16	Dias et al.	Spruce, pine, chestnut	dowel	10	EN 383	0, 90	No
17	Ehlbeck and Werner	Beech, oak, teak, merbau, afzelia, bongossi	dowel	8, 12, 16, 24, 30	prEN 383	0, 30, 45, 60, 90	Yes
18	Franke et al._1	spruce	dowel	12	EN 383 ASTM D5764	0, 90	Yes
19	Franke et al._2	Spruce, beech	dowel	6; 12; 20; 30	ASTM D5764	0, 25, 55, 90	No
20	Franke et al._3	Pine, pine LVL	dowel, bolt	6; 8; 12; 16; 20; 25; 30	ASTM D 5764	0, 22.5, 45, 67.5, 90	No
21	Gattesco	spruce GL	bolt	16	?	0, 90	Yes
22	Hong	Douglas-fir	nail, bolt	3,3; 12,7; 19,1; 25,4	ASTM D 5764	0, 45, 90	Yes
23	Hübner et al.	Beech, ash, black locust	dowel	6, 8, 12, 16, 20	EN 383	0, 30, 60, 90	No
24	Hwang et al.	Pine LVL, Douglas-fir PSL, aspen LSL	dowel	6, 8, 10, 12, 14, 16, 18, 20, 22, 24	ASTM D 5764	0, 90	No
25	Kobel et al.	beech LVL	dowel, bolt	8; 12; 16; 20	EN 383	?	Yes
26	Moraes et al._1	pine	bolt	10	EN 383	0	Yes
27	Moraes et al._2	pine	dowel	8	EN 383	0, 90	No
28	Moses	aspen LSL	dowel	9,5; 13; 19	ASTM D5764	0, 45, 90	Yes
29	Parsons et al.	Pine WPC, maple WPC	dowel	9,525; 6,35; 4,76	ASTM D5764	0	No
30	Pedersen	spruce GL	dowel	12	EN 383	0, 30, 60, 90	Yes
31	Rammer et al.	Douglas Fir-Larch Southern Pine Spruce-Pine-Fir	bolt, nails	12,7; 3,33	ASTM D5764	0	No
32	Reynolds et al.	Douglas fir	dowel	20	ASTM D5764	0, 90	No
33	Sandhaas	Spruce, beech, Purpleheart, Cumaru, Azobé	dowel	12; 24	EN 383	0	Yes (in [2])
34	Santos et al._1	pine	dowel	14	EN 383	0	Yes
35	Santos et al._2	pine	dowel	14	EN 383 ASTM D5764	0, 90	Yes
36	Sawata et al.	spruce GL, pine GL	dowel	8; 12; 16; 20	EN 383	0, 90	No
37	Schickhofer et al._1	spruce pine	dowel	8; 12; 20	prEN 383	0, 10, 20, 25, 30, 40, 50, 60, 70, 80, 90	No

38	Schickhofer et al._2	ash	dowel	6; 8; 12; 16; 20	prEN 383	0, 15, 30, 45, 60, 75, 90	No
39	Schoenmakers et al._1	spruce	dowel	6; 12; 24	EN 383	90	No
40	Schoenmakers et al. _2	spruce	dowel	8; 16	EN 383	90	No
41	Sjödin et al.	pine	dowel	20	EN 383	0	Yes
42	Sosa Zitto	Eucalyptus grandis	nail, bolt, dowel	5,5; 12,7	EN 383	0, 90	No
43	Whale and Smith_1	spruce-pine-fir, pine plywood, birch plywood, Douglas-fir plywood	nail, bolt	2,65; 3; 3,35; 3,75; 4; 5; 6; 8; 12; 16; 20	-	0, 90	No
44	Whale and Smith_2	Spruce, pine, Keruing, Greenheart, tempered hardboard	nail, bolt	2,65; 3,35; 4; 5; 6; 8; 12; 16; 20	-	0, 90	No
45	Wilkinson	Douglas-fir GL	bolt	12,7; 19; 25,4	ASTM D1761-88	0, 90	No
46	Xu et al.	? (GL28h)	dowel	16	ASTM D 5764	0, 45, 90	(Yes)
47	Zink-Sharp et al.	maple oak	bolt	12,7	ASTM D1761	?	(No)

ID = see following literature list

References

[1] *EN 383:2007*. Timber structures – Test method – Determination of embedement strength and foundation values for dowel type fasteners. CEN, Brussels.

[2] Hackl RE (2016) *Literaturstudium zur experimentellen Untersuchung des Lochleibungsverhaltens von stiftförmigen Verbindungsmitteln im Ingenieurholzbau*. BSc thesis, Vienna University of Technology.

[3] Przybilla S (2017) *Study on embedment test data and its possible use in novel joint design approaches.* MSc thesis, Karlsruhe Institute of Technology.

[4] Schweigler M, Bader TK, Hochreiner G, Lemaître R (2018) Parameterization equations for the nonlinear connection slip applied to the anisotropic embedment behavior of wood. *Composites Part B: Engineering* **142**:142–158

[5] Foschi R (1974) Load-slip characteristics of nails. *Wood Science* **7**(1):69–76.

[6] Richard RM, Abbott BJ (1975) Versatile elastic-plastic stress-strain formula. *Journal of Engineering Mechanics-ASCE* **101**(4):511–5.

[7] Sauvat N (2001) *Résistance d'assemblages de type tige en structure bois sous chargements cycliques complexes*. PhD thesis, LERMES/CUST, Université Blaise Pascal-Clermont II, France.

[8] Hankinson RL (1921) Investigation of crushing strength of spruce at various angles to the grain. *Air Service Information Circular*, McCook Field Report Serial No. 1570, **III**(253):1-15.

[9] Casella G, Berger RL (2002) *Statistical inference*. Vol. 2. Duxbury Pacific Grove, CA.

[10] Awaludin A, Smittakorn W, Hirai T, Hayashikawa T (2007) Bearing properties of *Shorea obtusa* beneath a laterally loaded bolt. *Journal of Wood Science* **53**(3):204-210.

[11] Bader TK, Schweigler M, Serrano E, Dorn M, Enquist B, Hochreiner G (2016) Integrative experimental characterization and engineering modeling of single-dowel connections in LVL. *Construction and Building Materials* **107**:235-246.

[12] Blass HJ, Bejtka I, Uibel T (2006) *Tragfähigkeit von Verbindungen mit selbstbohrenden Holzschrauben mit Vollgewinde*. Karlsruher Berichte zum Ingenieurholzbau Bd. 4, Universität Karlsruhe.

[13] Blass HJ, Uibel T (2007) *Tragfähigkeit von stiftförmigen Verbindungsmittel in Brettsperrholz*. Karlsruher Berichte zum Ingenieurholzbau Bd. 8, Universität Karlsruhe.

[14] Bléron L, Bocquet JF, Duchanois G, Triboulet P (2001) *Contribution to the optimization of timber joints performances: Analysis of dowel type fasteners embedment strength*. Joints in Timber Structures, Bd. 22, RILEM Publications. Cachan, France.

[15] Claisse PA, Davis TJ (1998) High performance jointing systems for timber. *Construction and Building Materials* **12**:415-425.

[16] Dias AMPG, van de Kuilen JWG, Cruz HMP, Lopes SMR (2010) Numerical modeling of the load-deformation behavior of doweled softwood and hardwood joints. *Wood and Fiber Science* **42**(4):480-489.

[17] Ehlbeck J, Werner H (1992) *Tragfähigkeit von Laubholzverbindungen mit stabförmigen Verbindungsmitteln*. Forschungsbericht der Versuchsanstalt für Stahl, Holz und Steine, Universität Karlsruhe.

[18] Franke S, Magnière N (2014) *Discussion of testing and evaluation methods for the embedment behaviour of connections*. INTER Meeting 47, Paper 47-7-1, pp. 92-102, Bath, UK.

[19] Franke S, Magnière N (2014) *The embedment failure of European beech compared to spruce wood and standards*. In: Aicher S, Reinhardt HW, Garrecht, H (eds) RILEM bookseries. Materials and joints in timber structures. Recent developments in technology. Stuttgart, Germany.

[20] Franke S, Quenneville P (2011) Bolted and dowelled connections in Radiata pine and laminated veneer lumber using the European Yield Model. *Australian Journal of Structural Engineering* **12**(1):13-27.

[21] Gattesco N (1998) Strength and local deformability of wood beneath bolted connectors. *Journal of Structural Engineering* **124**(2):195-202.

[22] Hong JP (2007) *Three-dimensional nonlinear finite element model for single and multiple dowel-type wood connections*. PhD thesis, University of British Columbia.

[23] Hübner U, Bogensperger T, Schickhofer G (2008) *Embedding strength of European hardwoods*. CIB-W18 Meeting 41, Paper 41-7-5, St. Andrews, Canada.

[24] Hwang K, Komatsu K (2002) Bearing properties of engineered wood products – effects of dowel diameter and loading direction. *Journal of Wood Science* **48**(4):295-301.

[25] Kobel P, Steiger R, Frangi A (2014) *Experimental analysis on the structural behaviour of connections with LVL made of beech wood*. In: Aicher S, Reinhardt HW, Garrecht, H (eds) RILEM bookseries. Materials and joints in timber structures. Recent developments in technology. Stuttgart, Germany.

[26] Moraes PD, Rodrigues JPC (2012) Behavior of bolted timber joints subjected to high temperatures. *European Journal of Wood and Wood Products* **70**:225-232.

[27] Moraes PD, Rogaume Y, Bocquet JF, Triboulet P (2005) Influence of temperature on the embedding strength. *European Journal of Wood and Wood Products* **63**:297–302.

[28] Moses DM (2000) *Constitutive and analytical models for structural composite lumber with applications to bolted connections*. PhD thesis, University of British Columbia.

[29] Parsons WR, Bender DA (2004) Energy-based design of dowel connections in wood-plastic-composites hollow sections. *Journal of Structural Engineering* **130**(4):681-689.

[30] Pedersen MU (2001) *Dowel-type timber connections – Strength modelling*. PhD thesis, Danmarks Tekniske Universitet.

[31] Rammer DR, Winistorfer SG (2001) Effect of moisture content on dowel-bearing strength. *Wood and Fiber Science* **33**(1):126-139.

[32] Reynolds T, Harris R, Chang WS (2013) An analytical model for embedment stiffness of a dowel in timber under cyclic load. *European Journal of Wood and Wood Products* **71**:609-622

[33] Sandhaas C, Ravenshorst G, van de Kuilen JWG (2013) Embedment tests parallel-to-grain and ductility aspects using various wood species. *European Journal of Wood and Wood Products* **71**(5):599-608.

[34] Santos CL, de Jesus AMP, Morais JJL, Lousada JLPC (2009) Quasi-static mechanical behaviour of a double-shear single dowel wood connection. *Construction and Building Materials* **23**:171–182

[35] Santos CL, de Jesus AMP, Morais JJL, Lousada JLPC (2010) A comparison between the EN 383 and ASTM D5764 test methods for dowel-bearing strength assessment of wood – Experimental and numerical investigations. *Strain* **46**(2):159-174.

[36] Sawata K, Yasumura M (2002) Determination of embedding strength of wood for dowel-type fasteners. *Journal of Wood Science* **48**(2):138-146.

[37] Schickhofer G, Traetta G (2007) *Einflussfaktoren auf die Lochleibungsfestigkeit von Fichte und Kiefer für Stabdübelverbindungen*. In: Pirnbacher G: Verbindungstechnik im Ingenieurholzbau, Verlag der Technischen Universität Graz.

[38] Schickhofer G, Hübner U (2007) Die Festigkeitskenngröße „Lochleibung“ für die Laubholzart Esche, In: Pirnbacher G: Verbindungstechnik im Ingenieurholzbau, Verlag der Technischen Universität Graz.

[39] Schoenmakers JCM, Svensson S (2011) Embedment tests perpendicular to the grain – optical measurements of deformation fields. *European Journal of Wood and Wood Products* **69**(1):133-142.

[40] Schoenmakers JCM, Jorissen AJM, Leijten AJM (2010) Evaluation and modelling of perpendicular to grain embedment strength. *Wood Science and Technology* **44**(4):579-595.

[41] Sjödin J, Serrano E, Enquist B (2008) An experimental and numerical study of the effect of friction in single dowel joints. *European Journal of Wood and Wood Products* **66**(5):363-372.

[42] Sosa Zitto MA, Köhler J, Piter JC (2012) Embedding strength in joints of fast-growing Argentinean Eucalyptus grandis with dowel-type fasteners. Analysis according to the criterion adopted by European standards. *European Journal of Wood and Wood Products* **70**(4):433-440.

[43] Whale LRJ, Smith I (1968) *Mechanical joints in structural timber - Information for probabilistic design*. TRADA Research Report Nr. 17, TRADA, UK.

[44] Whale LRJ, Smith I (1968) *Mechanical timber joints*. TRADA Research Report Nr. 18, TRADA, UK.

[45] Wilkinson TL (1992) *Strength of bolted timber connections with steel side members*. Research Paper FPL-RP-513, Forest Products Laboratory.

[46] Xu BH, Bouchair A, Taazount M, Racher P (2013) Numerical simulation of embedding strength of glued laminated timber for dowel-type fasteners. *Journal of Wood Science* **59**:17-23.

[47] Zink-Sharp A, Stelmokas JS, Gu HM (1991) Effects of wood anatomy on the mechanical behavior of single-bolted connections. *Wood and Fiber Science* **31**(3):249-263.

Stiffness and deformation of connections with dowel-type fasteners

Robert Jockwer
ETH Zürich
Switzerland

André Jorissen
Technical University Eindhoven
The Netherlands

Summary

Connections are important details in timber structures. Their non-linear load-deformation behaviour has a considerable impact on the deformation of timber structures and on the stress distribution in statically indeterminate structures. Recommendations for the stiffness values of connections can be found in different standards. The background of these recommendations is presented in this chapter. An evaluation of a large data set of test results from dowelled connections reveals the impact of additional parameters on the stiffness of connections not yet considered in the design codes. In addition, test data analyses from different sources are presented as well.

1. Introduction

1.1 Background

Connections with laterally loaded steel dowels are widely used in timber structures. The load-carrying capacity of these connections can be estimated using the design equations in Eurocode 5 EN 1995-1-1:2004 [1] based on the so called European Yield Model. For a reliable design of structures not only the load-carrying capacity but also the load-deformation behaviour (e.g. stiffness and ductility) of the connections are of importance, especially in situations where sufficient deformation capacity (and energy dissipation) of the connection is of importance, e.g. in earthquake situations. The design equations and recommendations for stiffness of connections given in the current version of Eurocode 5 are very basic, only applicable in linear calculations (which is in fact sufficient when designing in the serviceability limit states) and do not allow for a more sophisticated design with regard to deformations. Furthermore, the background of these design equations for stiffness is unclear; especially the stiffness determination of a multiple fastener connection with dowel type fasteners, for which according Eurocode 5 simply the stiffness of a connection with one fastener in single shear should be multiplied by the number of shear planes, lacks background.

1.2 General

The deformation between two or more members that are connected results from elastic and non-elastic deformation in the connecting members (wood and/or steel) and the fasteners.

Depending on the configuration of the connection, the relative deformation strongly depends of the location of the measurement. In Fig. 1 the deformation of the connection is defined as the relative deformation of the centres of the fasteners in the original members. Due to the stronger embedment (or fixed clamping in the ideal case) of the fastener in the steel member, the relative deformation of the wood-steel connections is considerably smaller compared to the wood-wood connection.

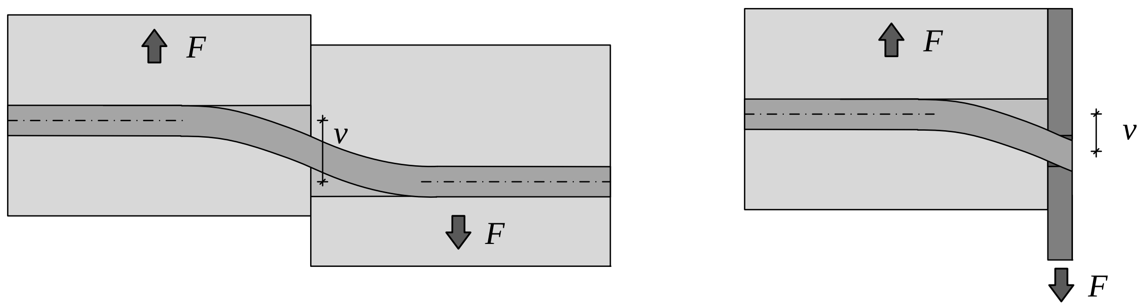

Fig. 1. Deformation measured at a dowelled wood-wood and wood-steel connection.

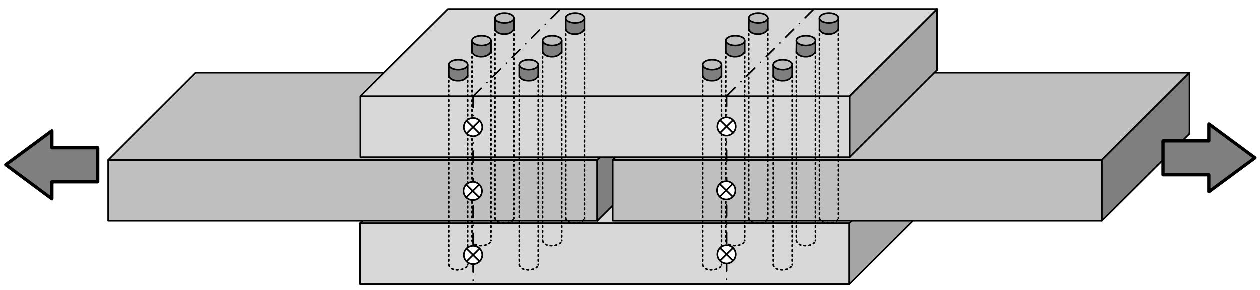

Fig. 2. Measurement of the deformations between points ⊗ at a connection with multiple fasteners.

1.3 Geometry

The general denotations of the geometry of a connection are given in Fig. 3: the diameter of the fasteners d, the spacing of the fasteners in direction parallel (a_1) and perpendicular to the grain (a_2), the end distance a_3 and edge distance a_4; the thickness of the side members t_s and middle member t_m. The density of the timber members is denoted by ρ.

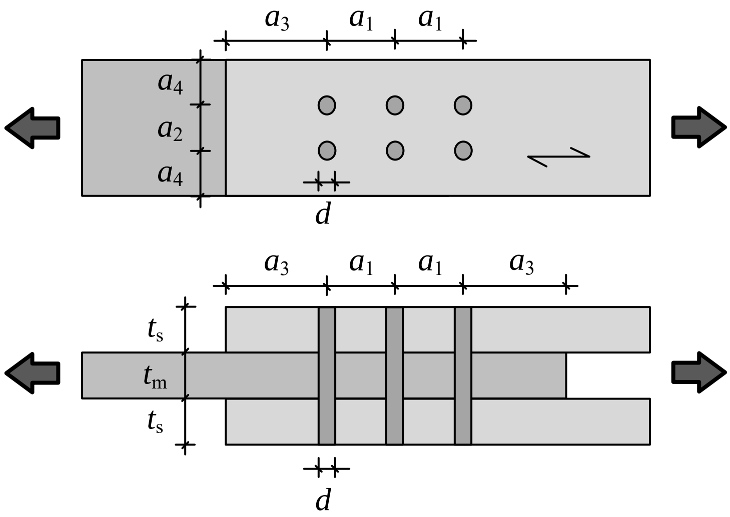

Fig. 3. Denotation of geometry at a dowelled wood-wood connection.

1.4 Terminology

The non-linear load-deformation behaviour of connections is complex to describe. An example of a load-deformation curve is shown in Fig. 4. At low load levels a rather soft behaviour is observed with large initial deformations. These initial deformations are more pronounced for connections exhibiting large tolerances. With increasing deformation the load increases and shows an approximately linear load-deformation behaviour at midrange load levels. At higher load levels a non-linear load-deformation behaviour can be observed if sufficient ductility is available. The maximum load and the ultimate load can be distinguished, the latter being defined as the load at a certain ultimate displacement or a certain drop of load. Various denotations and terms are used to describe this behaviour. An example is the term for the description of slope of the load-deformation curve: in Eurocode 5 this term is called *slip modulus* whereas in Granholm [2] the term *modulus of deformation* is used. In other literature the term *slip* is used for the description of the deformation of structures at load levels of little or no load [3].

Within this paper the following terms are used as presented in Fig. 4:

- Stiffness: slope of the load-deformation curve in N/mm.
- Slip: deformation of a connection at zero or low load-levels in mm.

In Dubas [3] it is highlighted that the initial slip is commonly smaller for connection tested in laboratory due to the higher precision compared to connections produced in practice.

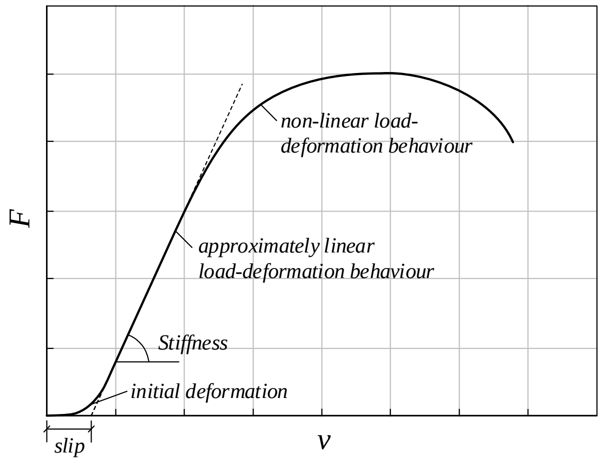

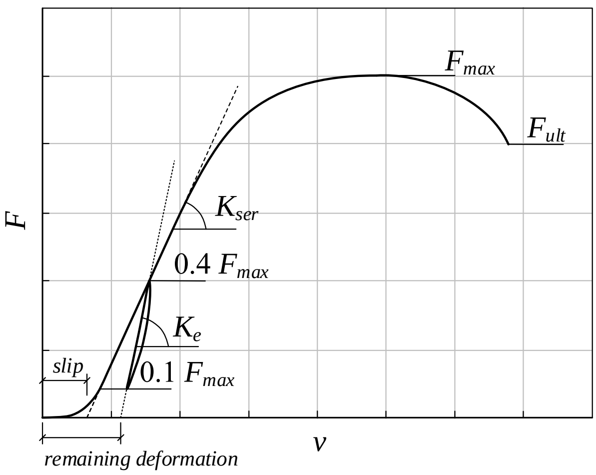

Fig. 4. Characteristics of the load-deformation diagram of the connection.

1.5 Stiffness of connections

When analysing the load-deformation curve the tangential and the secant stiffness can be determined. The tangential stiffness can be calculated at a single point whereas the secant stiffness is determined between two points or load-levels. As an example the stiffness at serviceability load level could be determined as a tangential stiffness whereas the stiffness describing the ultimate load could be represented as a secant stiffness.

A simplified diagram showing the load-deformation behaviour of a connection is given in Fig. 4.

The stiffness is not constant along the non-linear load-deformation dependency of the connection. Depending on the respective load-level(s) different values can be observed. In general a decrease of stiffness can be observed with increasing deformation.

Graholm [2] determined the tangential and secant stiffness along the entire load-deformation curve of a nailed connection as given in Fig. 5. The curves where calculated based on results from 70 tests on nails d = 5.6 mm and length 150 mm. Graholm highlights the problem how to account for the friction between the timber elements. In the case of a collapse of a bridge formwork evaluated by Graholm [2] the stiffness at failure due to instability of the system was only approximately 20-25% of the initial values.

Gehri states in [3] that if only the ultimate load level is considered in the standard, the corresponding stiffness at fastener failure would be too conservative for the serviceability limit states due to the strong dependency of the relevant stiffness value on the respective load level.

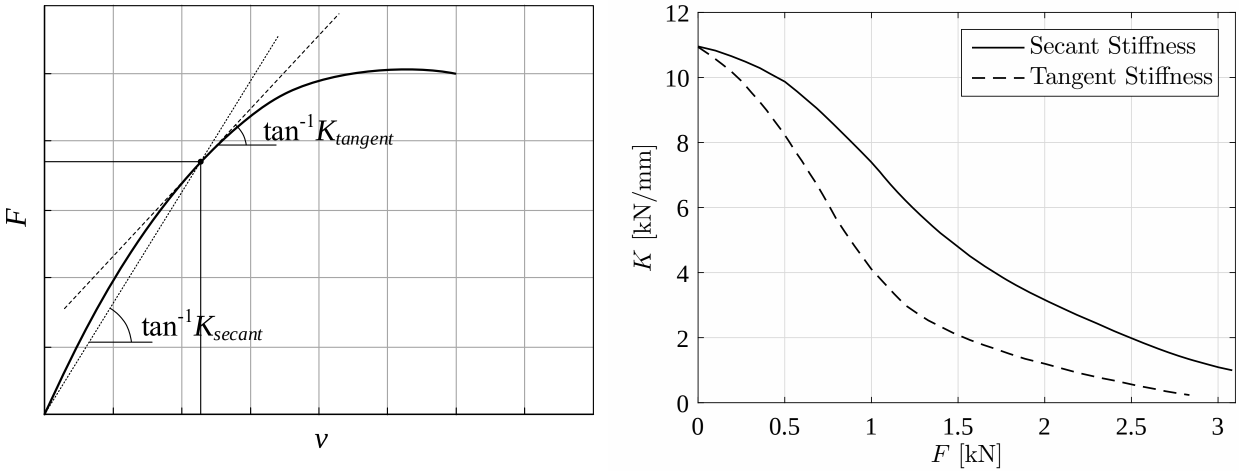

Fig. 5. The secant and tangent stiffness per nail studied by Graholm [2].

1.6 Importance of stiffness of connections

The slip of connections is of special importance for highly undetermined structures or combined elements with non-rigid connections such as trusses, built-up columns or timber frames. Examples of failure of structures due to the non-considered deformation of connections are e.g. the failure of the formwork of the Sandö-bridge in the 1930s [2]. The importance of the different characteristics of the load-deformation curve of a connection can be discussed for the example of the simple beam with a combined cross-section (Fig. 6) taken from [3]:

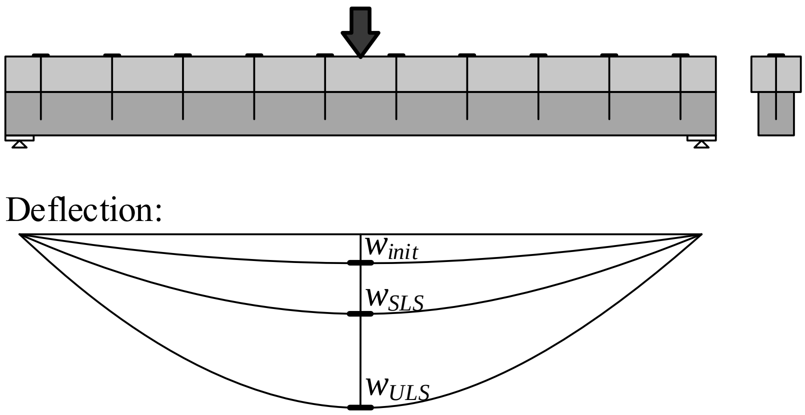

Fig. 6. Simplified model and deflection of a beam with combined cross-section.

- The initial deformation under self-weight and at low load-levels is influenced by the slip of the connections.
- The deformation at serviceability limit state (SLS) can be determined by the tangential stiffness at the respective load level between approximately 10% and 40% of ultimate load.
- The deformation relevant for the ultimate limit state (ULS) can be calculated using the secant modulus of the connection. Ultimate failure of the entire beam will occur by failure of the individual timber members: the combined cross section without fasteners is the limit case that even after failure of the individual fasteners is carrying the load.

For other cases, such as structures and systems exhibiting stability problems, the tangential stiffness of the fasteners might be used for the determination of the critical load.

1.7 Influences on the joint performance

As stated by Ehlbeck in [4] the following parameter can be identified with an impact of the load-deformation behaviour and performance of the joints:

- *fastener dimensions and material properties:*
  - size, length, diameter,
  - point, head, and thread dimensions,
  - clean, smooth, or rough surface,
  - plating, galvanizing, or other coating,
  - fastener stiffness and flexural properties;
- *the properties of the fastened and fastening members:*
  - compressive and embedding strength,
  - elastic and creep moduli,
  - displacement modulus and elastic or plastic bearing constant,
  - (all these properties are related to density, grain direction, moisture content)
  - friction between fastener and its surrounding material,
  - relaxation;
- *the joint configuration:*
  - single and multiple fasteners per joint,
  - single, double, or multiple shear,
  - thickness of members,
  - distances of the fastener from the member sides and ends,
  - fastener spacing,
  - predrilling,
  - fasteners driven into side-grain or end-grain wood,
  - depth of nail or screw penetration,
  - clinching of protruding nail points;
- *the loading conditions:*
  - static, repetitive, or dynamic loading,
  - short or long-term loading,
  - rate and range of loading,
  - time interval between fastener insertion and load application.

2. Test standards

For testing of connections a reloading cycle is used in order to determine the elastic stiffness without the impact of slip.

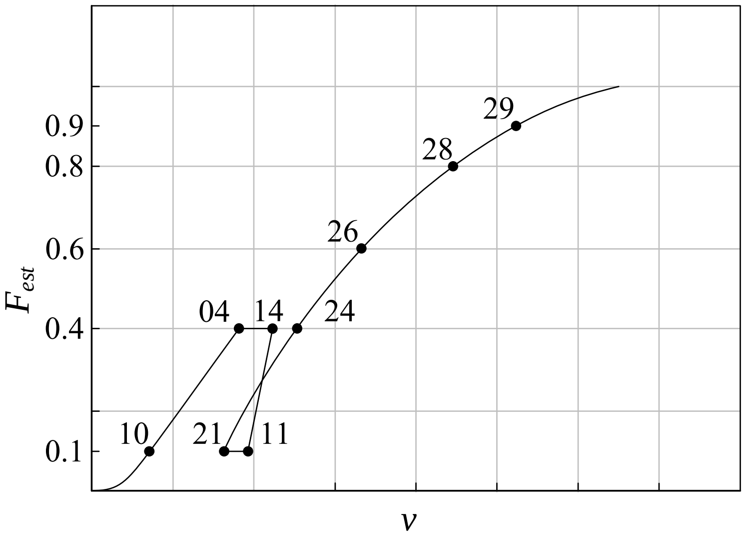

Fig. 7. Idealized load and deformation curve of a loading procedure with pre-loading cycle according to EN 26891 [5].

2.1 EN 26891

According to Eurocode 5 the stiffness K_{ser} is related to the parameter k_s specified in EN 26891 [5]. The initial stiffness k_i (called initial slip modulus in EN 26891) is specified as the secant stiffness at 40% of the estimated maximum load F_{est} using the initial deformation v_i.

$$k_i = \frac{0.4 \cdot F_{est}}{v_i} \qquad \text{where} \qquad v_i = v_{04} \tag{1}$$

The stiffness k_s is derived using a modified initial deformation $v_{i,mod}$.

$$k_s = \frac{0.4 \cdot F_{est}}{v_{i,mod}} \qquad \text{where} \qquad v_{i,mod} = \frac{4}{3} \cdot \left(v_{04} - v_{01}\right) \tag{2}$$

In elastic stiffness k_e can be determined for the elastic reloading cycle.

$$k_e = \frac{0.4 \cdot F_{est}}{v_e} \qquad \text{where} \qquad v_e = \frac{2}{3} \cdot \left(v_{14} + v_{24} - v_{11} - v_{21}\right) \tag{3}$$

3. Regulations and design rules for stiffness and load-deformation behaviour of connections

3.1 Eurocode 5

In Eurocode 5 [1] the stiffness of fasteners is specified in Table 7.1 in Section 7.1.

Table 1. Values of K_{ser} for fasteners and connectors in N/mm in timber-to-timber and wood-based panel-to-timber connections

Fastener type	K_{ser}
Dowels Bolts with or without clearance Screws Nails (with predrilling)	$\dfrac{\rho_{\mathrm{m}}^{1.5} \cdot d}{23}$
Nails (without predrilling)	$\dfrac{\rho_{\mathrm{m}}^{1.5} \cdot d^{0.8}}{30}$

Additional recommendations are given as follows:

If the mean densities $\rho_{m,1}$ and $\rho_{m,2}$ of the two jointed wood-based members are different then ρ_m in the above expressions should be taken as

$$\rho_{\mathrm{m}} = \sqrt{\rho_{\mathrm{m},1} \cdot \rho_{\mathrm{m},2}} \tag{4}$$

For steel-to-timber or concrete-to-timber connections, K_{ser} should be based on ρ_m for the timber member and may be multiplied by 2.0.

3.1.1 Background and derivation of equations: Ehlbeck and Larsen (1993)

Background on the derivation of the equations given in Table 1 can be found in Ehlbeck and Larsen [6].

General

A value for the stiffness *enables the designer to calculate the joint deformation at different load levels. However, the* stiffness *normally decreases with increasing load. Therefore, Eurocode 5 gives different values for serviceability limit state design and for ultimate limit state design.*

The instantaneous stiffness *for serviceability limit state design – denoted K – is assumed to be the secant modulus of the load*-deformation *curve at a load level of approximately 40 percent of the maximum load (load-carrying capacity) of the joint. In this low load range from zero to 0.4 · $F_{max,k}$, a linear load*-deformation *relationship based on K_{ser} is assumed to be acceptable for design purposes.* This definition of stiffness corresponds to K_{i} according to EN 26891.

The instantaneous stiffness *for ultimate limit state design – denoted K_u – is assumed to be the secant modulus of the load*-deformation *curve at a load level of approximately 60 to 70 percent of the maximum load. As a reasonable simplification applicable for design procedures, K_u may be taken as:*

$$K_{\mathrm{u}} = \frac{2}{3} \cdot K_{\mathrm{ser}} \tag{5}$$

Nails may be driven into the members with or without predrilled holes. Nailed joints with predrilled holes are stiffer than those without predrilled holes (splitting effect). This should be taken into consideration in the design.

Thick nails in predrilled holes may behave approximately as thin dowels driven into tight-fitting predrilled holes. Therefore, there should be no difference between the design stiffness *of thin dowels and thick nails in predrilled holes.*

***Estimation of* stiffness**

The load-carrying capacity of nailed joints is in most cases governed by Eq.(6):

$$R = \sqrt{\frac{2 \cdot \beta}{1+\beta}} \sqrt{2 \cdot M_{\mathrm{y}} \cdot f_{\mathrm{h}} \cdot d} \tag{6}$$

With $\beta = 1$, the embedding strength values $f_{h,k} = 0.082 \cdot (1 - 0.01 \cdot d) \cdot \rho_k$ (predrilled holes) and $f_{h,k} = 0.082 \cdot \rho_k \cdot d^{0.3}$ (not predrilled), the yield moment $M_{y,Rk} = 180 \cdot d^{2.6}$ for nails ($M_{y,Rk} = 0.3 \cdot f_{u,k} \cdot d^{2.6}$ in Eurocode 5), the load-carrying capacity of a nailed joint can be calculated as:

$$R = \sqrt{30 \cdot (1 - 0.01 \cdot d) \cdot d^{3.6} \cdot \rho_{\mathrm{k}}} \tag{7}$$

for joints with predrilled holes, and

$$R = \sqrt{30 \cdot d^{3.3} \cdot \rho_{\mathrm{k}}} \tag{8}$$

for joints without predrilled holes.

The instantaneous deformation *at approximately 40 percent of the load-carrying capacity has been estimated from many tests available from various test laboratories:*

$$u_{\mathrm{inst}} = 40 \cdot \frac{d^{0.8}}{\rho_{\mathrm{k}}} \tag{9}$$

with predrilled holes, and

$$u_{\mathrm{inst}} = 60 \cdot \frac{d^{0.8}}{\rho_{\mathrm{k}}} \tag{10}$$

without predrilled holes.

The instantaneous stiffness *for serviceability limit state design then becomes:*

$$K_{\mathrm{ser,inst}} = \frac{0.4 \cdot R}{u_{\mathrm{inst}}} \tag{11}$$

For nails in predrilled holes, this leads to

$$K_{\mathrm{ser,inst}} = \frac{0.55}{100}\sqrt{(100-d)} \cdot \rho_{\mathrm{k}}^{1.5} \cdot d \tag{12}$$

and with the nail diameter ranging from 2 to 8 mm it can be simplified to:

$$K_{\mathrm{ser,inst}} = \frac{\rho_{\mathrm{k}}^{1.5} \cdot d}{20} \tag{13}$$

For nailed joints without predrilled holes from Eq. 8:

$$K_{\mathrm{ser,\,inst}} = \frac{\rho_k^{1.5} \cdot d}{27.4 \sim 25} \tag{14}$$

On the basis of further research data, the values given in Table 2 for dowel-type fasteners in general were found. These values are suitable for estimating instantaneous deformation *values under service conditions (serviceability limit state).*

If the characteristic densities of the joint members are different ($\rho_{k,1}$ and $\rho_{k,2}$), then ρ_k for calculating the stiffness *may be taken as*

$$\rho_{\mathrm{k}} = \sqrt{\rho_{\mathrm{k,1}} \cdot \rho_{\mathrm{k,2}}} \tag{15}$$

For bolted joints the instantaneous deformation *under service load should be taken as*

$$u_{\mathrm{inst}} = \frac{F}{K_{\mathrm{ser}}} + 1\mathrm{mm} \tag{16}$$

Table 2. Values for K_{ser} for dowel-type fasteners in N/mm [6]

Fastener type	Timber-to-timber Panel-to-timber	Steel-to-timber
Dowels Screws with $d \geq 8$ mm	$\frac{\rho_k^{1.5} \cdot d}{20}$	$\frac{\rho_k^{1.5} \cdot d}{30}$
Nails (with predrilling) Screws with $d < 8$ mm	$\frac{\rho_k^{1.5} \cdot d}{20}$	$\frac{\rho_k^{1.5} \cdot d}{20}$
Nails (without predrilling)	$\frac{\rho_k^{1.5} \cdot d^{0.8}}{25}$	$\frac{\rho_k^{1.5} \cdot d^{0.8}}{25}$

3.1.2 Background: Ehlbeck (1979)

In [4] it is mentioned that the stiffness values tabulated in design codes are only rough estimates of the real behaviour of timber joints due to the large variability of the material properties. This should be accounted for especially when analysing complex structures or when performing sophisticated models.

Ehlbeck refers to Norén [7] with regard to the proportional limit (or "flow limit") as *that load beyond which it does not increase more than 10% at a* deformation *increment of 1 mm per member*. This proportional limit can be interpreted as the yield load F_y as shown in Fig. 8.

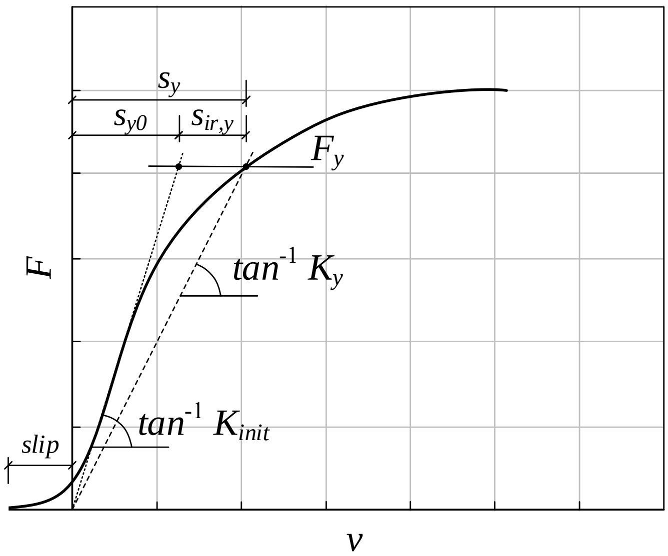

Fig. 8. Definition of the proportional limit F_y, the residual deformation $s_{ir,y}$ and the secant stiffness K_y, the from [4].

Further *As a distinct proportional limit is difficult to assign to the load*-deformation *curve, an agreement may be reached to define this point as being located at a small value of residual* deformation, $s_{ir,y}$. *This proportional limit can be a basis for determining a secant stiffness,* K_y*, for the lowest load range. Such a stiffness varies with the stipulated residual* deformation *value,* $s_{ir,y}$ *and may coincide with the* proportional *limit discussed above.*

It is stated that *The ultimate load,* F_u*, is observed only at a relatively large* deformation. *It has been proposed that a practical and meaningful ultimate load be defined at that load where the* deformation *between adjacent members does not exceed a certain maximum value, such as 7.5 mm*, being the summation of the deformations in both member (excluding slip). *This definition may, however, not suit to the modern safety concepts.*

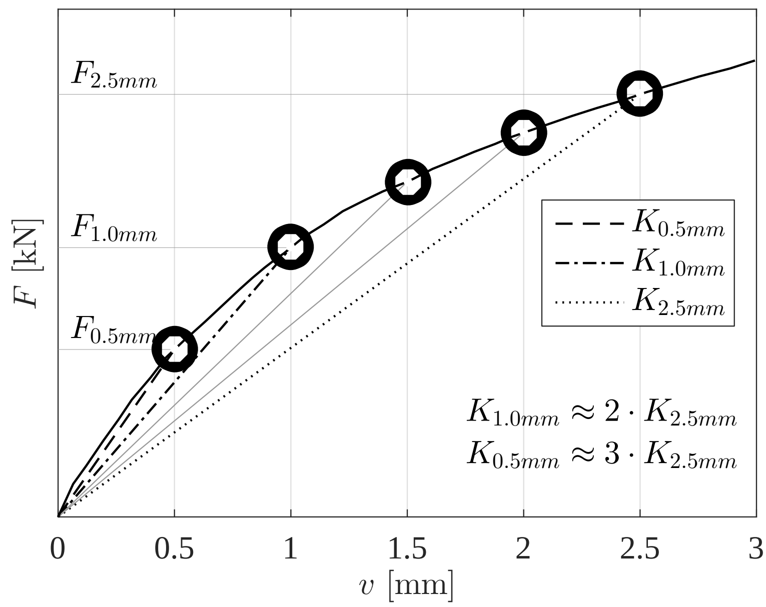

Fig. 9. Schematic load-deformation curve and secant stiffness for different values of deformation [4].

Following the specifications shown in Fig. 9 the relation between the stiffness $k_{0.5}$ and $k_{1.0}$ of the load at deformations at 0.5 mm and 1.0 mm can be derived as follows:

$$k_{1.0} \approx 2 \cdot k_{2.5} \approx \frac{2}{3} \cdot k_{0.5} \qquad (17)$$

3.2 DIN 1052:2008

In the former German standard for timber structures DIN 1052 [8] the stiffness of fasteners is specified in Appendix G given in Table 3. For bolts with clearance an additional slip of 1 mm should be accounted for.

Table 3. Values of K_{ser} for fasteners and connectors in N/mm in timber-to-timber, wood-based panel-to-timber and steel-to-timber connections; values per shear plane

Fastener type	K_{ser}
Dowels Bolts without clearance	$\dfrac{\rho_k^{1.5} \cdot d}{20}$
Nails (with predrilling)	$\dfrac{\rho_k^{1.5} \cdot d}{20}$
Nails (without predrilling)	$\dfrac{\rho_k^{1.5} \cdot d^{0.8}}{25}$

3.2.1 DIN 1052-2:1988

In the 1988 version of DIN 1052 [9] the stiffness K in N/mm is given in dependency of the permissible load F_{perm}. In addition values for the deformation at permissible load level are given.

Table 4. Values of stiffness K in N/mm and deformation v in mm at permissible load level F_{perm} for fasteners in timber-to-timber and steel-to-timber connections; values per shear plane

Fastener and connection type		K	v
Dowels and bolts without clearance		$1.2 \cdot F_{perm}$	0.8
Nails in single shear in timber-to-timber and steel-to-timber connections	without predrilling	$5.0 \cdot \dfrac{F_{perm}}{d}$	$0.2 \cdot d$
	with predrilling	$10 \cdot \dfrac{F_{perm}}{d}$	$0.1 \cdot d$
Nails in multiple shear in timber-to-timber connections	With and without predrilling	$10 \cdot \dfrac{F_{perm}}{d}$	$0.1 \cdot d$
Nails in multiple shear in steel-to-timber connections	with predrilling	$20 \cdot \dfrac{F_{perm}}{d}$	$0.05 \cdot d$

The permissible load F_{perm} in N of a nail is given for conventional softwood timber in [9] with:

$$F_{perm} = \frac{500 \cdot d^2}{10 + d} \tag{18}$$

The permissible load of nails inserted in holes predrilled with 0.9*d* may be increased by 25%.

A comparison of the stiffness values for nails with and without predrilling given in Tab. 3 and 4 is given in Fig. 10. The stiffness values according to DIN 1052:1988 in Tab. 4 are considerably higher compared to the values in Tab. 3.

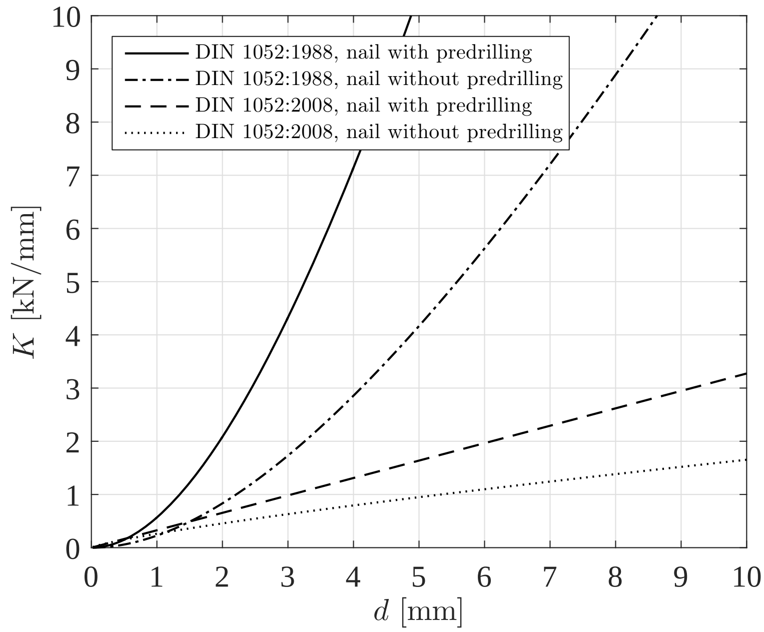

Fig. 10. Comparison of stiffness values K_{ser} in Tab. 3 and 4 for ρ_k = 350 kg/m³.

3.3 SIA 265:2012

In the Swiss standard for timber structures SIA 265 [10] the stiffness of connections is specified for dowels, bolts, predrilled nails and predrilled screws in Table 5 and for non-predrilled nails in Table 6.

Table 5. Stiffness K_{ser} per dowel and shear plane for moisture content Class 1

Load direction	Timber-to-timber Panel-to-timber	Steel-to-timber
Parallel to grain $K_{ser,0}$	$3 \cdot \rho_k^{0.5} \cdot d^{1.7}$	$6 \cdot \rho_k^{0.5} \cdot d^{1.7}$
Perpendicular to grain $K_{ser,90}$	$1.5 \cdot \rho_k^{0.5} \cdot d^{1.7}$	$3 \cdot \rho_k^{0.5} \cdot d^{1.7}$

Table 6. Stiffness K_{ser} per nail and shear plane for moisture content Class 1 for nails without predrilling (Table 25 from SIA (2012))

Load direction	Timber-to-timber Panel-to-timber	Steel-to-timber
Parallel to grain $K_{\mathrm{ser},0}$	$60 \cdot d^{1.7}$	$120 \cdot d^{1.7}$
Perpendicular to grain $K_{\mathrm{ser},90}$	$30 \cdot d^{1.7}$	$60 \cdot d^{1.7}$

In addition to the individual stiffness values explanations regarding the load-deformation behaviour and ductility of connections are given. The ductility factor D_s and the stiffness K_{ser} are defined in Fig. 11 and Eqs. (19) and (20). The definition is similar to that in EN 12512.

$$D_s = \frac{v_u}{v_y} \tag{19}$$

$$K_{ser} = \frac{F_y}{v_y} \tag{20}$$

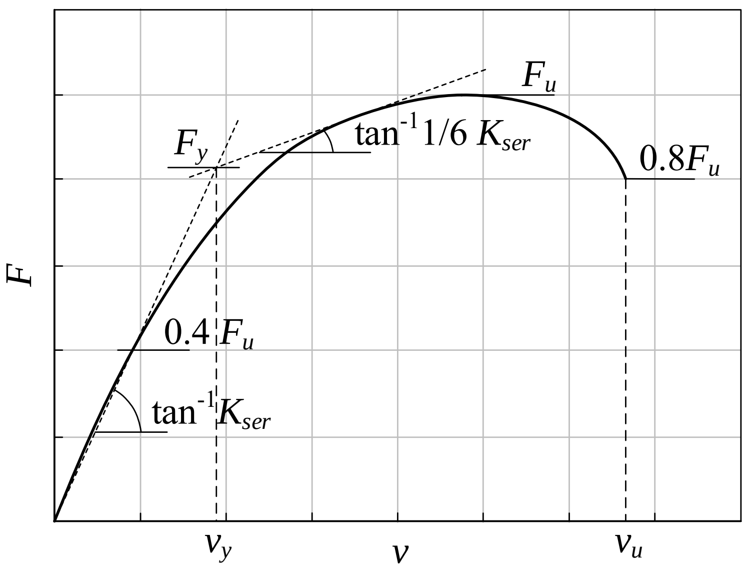

Fig. 11. Schematic load-deformation curve for the definition of ductility factor D_s and the stiffness K_{ser}.

The required ductility factor of the connection is a function of the desired structural behaviour and exploitation of plastic force redistributions in the system. The assignment of ductility factor is given in Table 7 for standard types of connection.

Table 7. Ductility factor for timber connections

Ductility factor D_s	Type of connection
$D_s = 1…2$	Shear connections with dowel-type fasteners and timber thickness less than those defined for achieving a failure mode with two plastic hinges in the fastener. Nails, screws and glued-in dowels subject to withdrawal forces. Ring connectors. Single-sided and double-sided toothed-plate connectors. Punched metal plate fasteners. Glued connections
$D_s = 3$	Shear connection with dowel-type fasteners and timber thickness sufficient for achieving a failure mode with two plastic hinges in the fastener. Nailed connections with nail penetration $s \geq 9 \cdot d$. Stapled connections with minimum timber thickness. Screwed connections with screw penetration $s \geq 9 \cdot d$

The stiffness for the serviceability limit state, K_{ser}, and the stiffness for the ultimate limit state, K_u, or the deformation v_u as defined in Fig. 12 are determined on the basis of tests (e.g. according to the provisions of SIA 265/1). Standard values for K_{ser} are given in Table 5 and Table 6 for each fastener for moisture content Class 1 and for short-term loading.

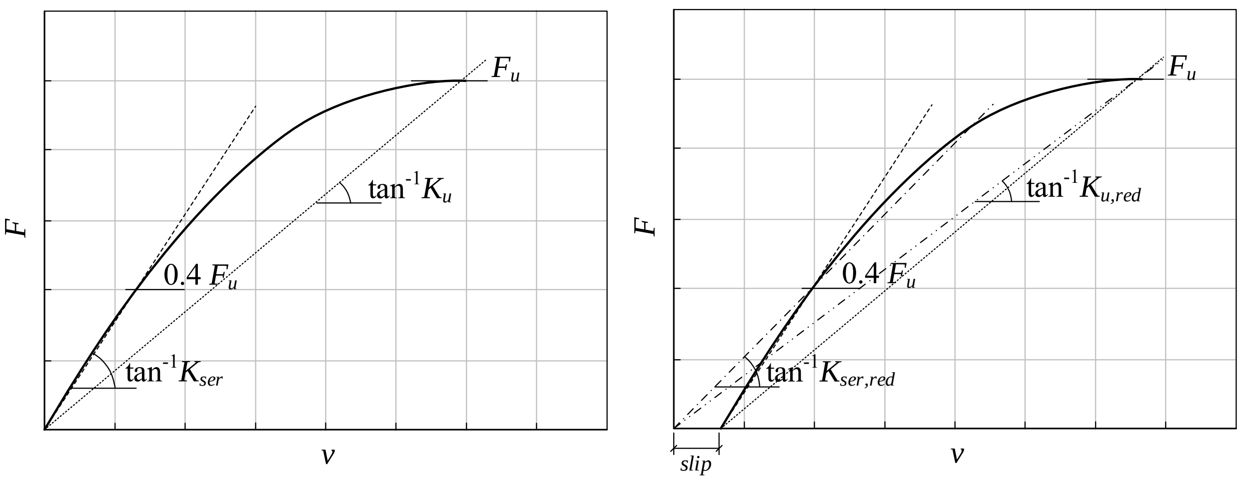

Fig. 12. Definition of the stiffness of a connection for serviceability limit state and ultimate limit state as well as the reduced stiffness in the connection to take into account slip.

3.3.1 Background: SIA 164:1981

In the former standard for timber structures SIA 164 [11] from 1981 it is pointed out that for the determination of deformations and of stresses and action effects of statically indeterminate structures the slip and the elastic and creep deformations of connections have to be considered. In Table 8, stiffness values for connections with different fasteners are given.

Table 8. Stiffness K_{ser} per fastener and shear plane for moisture content Class 1

Type	Load direction	Timber-to-timber	Slip
Nails without predrilling	All loading directions	$40 \cdot d^{1.7}$	0.5…1 mm
Nails with predrilling	Parallel to grain	$60 \cdot d^{1.7}$	
Dowels	Parallel to grain	$60 \cdot d^{1.7}$	
Bolts	Parallel to grain	$60 \cdot d^{1.7}$	0.5…1 mm hole clearance
Screws	Parallel to grain	$60 \cdot d^{1.7}$	0.6…0.9 mm
Split rings, etc.	Parallel to grain	d^2	1.0 mm

According to [3] relatively low stiffness values were chosen in standard SIA 164 due to the higher creep in the connection compared to the other timber members (equal creep factors are used both for connections and timber members). The values for nails without predrilling are based on the tests by Möhler and Ehlbeck [12].

Fontana [13] states that the stiffness values for dowels are based on loading parallel to the grain at a load level of approximately 1.5-2 times the serviceability level. On serviceability level the stiffness can be up to twice the declared values. Fontana mentions that Scheer [14] determined a stiffness value of $60 \cdot d^{1.7}$ from tests on nailed beams (without predrilling) and observed 0.45 mm remaining deformation (slip) after unloading from serviceability load level. Hence, the stiffness observed is approximately 50% higher than specified in Table 8.

3.4 CIB - Structural Timber Design Code

In the fifth draft of the CIB Structural Timber Design Code from 1980 [15] the following regulation for the deformation u of a nailed connection is given for a load F not exceeding one third of the characteristic load-carrying capacity F_k of the connection $F \leq F_k/3$:

$$u = 0.5 \cdot d \cdot \left(\frac{F}{F_k} \right)^{1.5} \tag{21}$$

The deformation of bolted connections at $F = F_k/3$ is suggested to be approximately $0.1 \cdot d + 1$ mm, for dowelled connection and screw connections a deformation $0.1 \cdot d$ is proposed.

For the design of mechanically jointed components such as built up columns stiffness values of nailed connections are proposed as given in Table 9.

Table 9. Stiffness in N/mm in dependency of modulus elasticity of the timber in N/mm²

Fastener	Stiffness
Round nails with $d < 5$ mm	$0.02 \cdot E_0 \cdot d$
Round nails with $d > 5$ mm	$0.1 \cdot E_0$

4. Experimental studies and evaluations

4.1 Dubas (1981)

Dubas [3] states that slip can be observed for all types of connections even for predrilled fasteners. For nailed connections without predrilling a slip under permissible load can expected to be between 0.5 mm for small diameter and 1 mm for larger diameter or subsequent drying of the timber. In the CIB-proposal [15] a slip under permissible load is approximately $0.1 \cdot d$, which is between 0.3 mm and 0.8 mm for nails.

Dubas evaluates the tests by Möhler and Ehlbeck [12] and by Egner [16] with regard to the impact of fastener diameter d in stiffness K. The tests by Möhler and Ehlbeck [12] on nailed connections without predrilling are given in Table 10. The permissible load $F_{\mathrm{II,perm}}$ in DIN 1052:1969 is equal to the values given in DIN 1052:1988 in Eq. (18). The test results by Egner [16] performed on bolted connections are given in Table 11.

Table 10. Stiffness values $K_{II,perm}$ at permissible load level and $K_{1.5mm}$ at a deformation of 1.5 mm from tests on nailed connections with smooth and ring shank nails without predrilling from Möhler and Ehlbeck [12].

d [mm]	Type	$F_{\mathrm{II,perm}}$ DIN 1052 [N]	$K_{\mathrm{II,perm}} = F_{\mathrm{II,perm}} / v_{\mathrm{II,perm}}$ [N/mm]	$K_{1.5\mathrm{mm}} = F_{1.5\mathrm{mm}} / v_{1.5\mathrm{mm}}$ [N/mm]
2.8	Ring shank 28/33 x 60	300	500 / 400 / 750	342 / 300 / 350
2.8	Smooth 25 x 65	300	786 / 625 / 811	342 / 300 / 329
4.2	Ring shank 42/50 x 90	625	1894 / 1250 / 1645	729 / 625 / 694
4.2	Smooth 42 x 110	625	3125 / 1786 / 2083	700 / 672 / 625
5.2	Ring shank 52/58 x 180	975	1625 / 1950 / 1523	1021 / 1125 / 975
5.5	Smooth 55 x 160	975	3482 / 3482 / 4643	1138 / 1117 / 1108

Table 11. Stiffness values $K_{II,perm}$ at permissible load level and $K_{1.5mm}$ at a deformation of 1.5 mm from tests on bolted connections from Egner [16] .

d	$F_{\mathrm{II,perm}}$ DIN 1052	$K_{\mathrm{II,perm}}$	$K_{\mathrm{1.5mm}}$
[mm]	[N]	[N/mm]	[N/mm]
12	2735	39100	5210
16	4865	16200 / 12500	8870 / 7130
24	10950	73000	19080

The deformation of v = 1.5 mm corresponds to 1.5-2 times the serviceability load level as shown in Fig. 13.

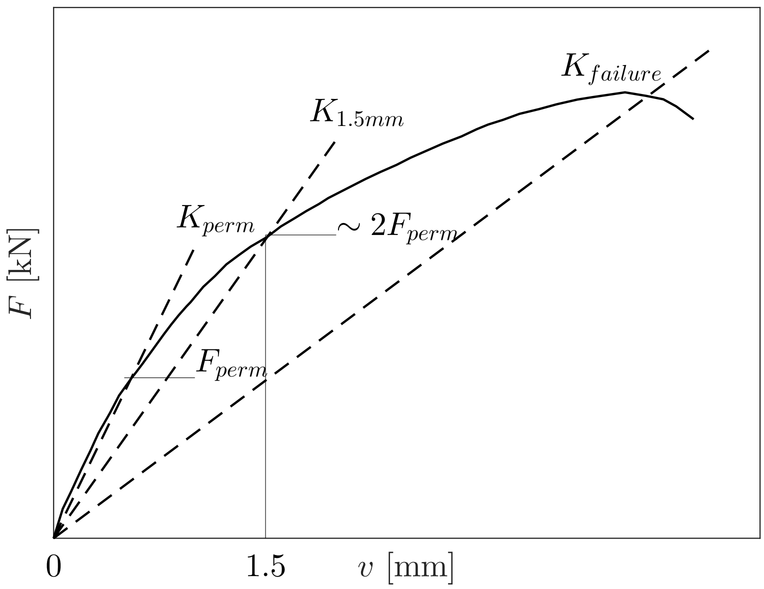

Fig. 13. Load-deformation diagram and stiffness K for different load levels for short term loading.

Dubas suggests to represent the test results in Table 10 and Table 11 by a constant factor and a size dependency on the dowel diameter $d^{1.7}$ as shown in Eq. (22) and Fig. 14.

$$K = \mathrm{constant} \cdot \mathrm{d}^{1.7} \tag{22}$$

The fit of all data to the proposed model yields a constant of 46.9 and an exponent 1.87 for the diameter.

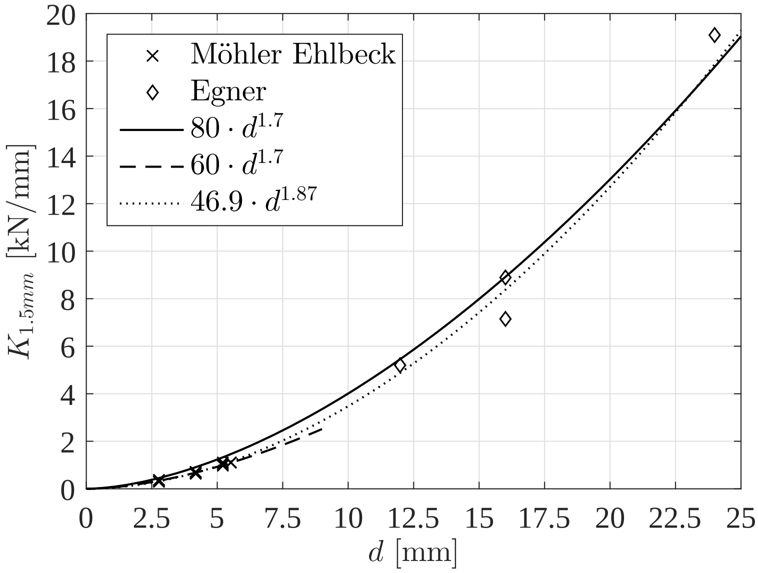

Fig. 14. Size dependency of the test results on nails in Table 10 (dashed line) and on dowels in Table 11 (solid line) for a deformation v = 1.5 mm.

Test carried out at ETH Zurich by Gehri and Fontana [17] on dowelled connections show a similar dependency as shown in Fig. 15.

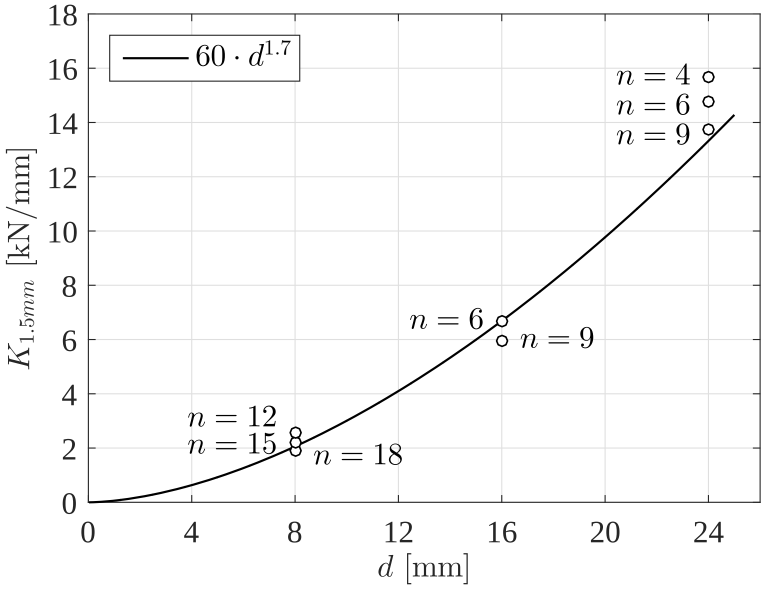

Fig. 15. Stiffness values $K_{1.5mm}$ for timber-timber connections on spruce glulam with dowel slenderness $\lambda = t/d = 6$ and steel strength $f_u = 500$ N/mm^2.

As a conclusion the following values are given in Dubas [3] based on the above test results for short term loading:

- Nails without predrilling $50 \cdot d^{1.7}$
- Nails with predrilling $60 \cdot d^{1.7}$
- Dowels and bolts $60 \cdot d^{1.7}$

If the stiffness values are compared with the values and equations for load-carrying capacity, the following statements can be made:

- The compliance of the connections shows only a minor dependency on the diameter of the fastener
- Connections with bolts show a smaller deformation compared to connections with nails of equal diameter due to the lower load level for bolts caused by the lower yield strength of the bolts ($f_{y,bolt} \approx 235$ N/mm^2 vs. $f_{y,nail} \approx 500$-600 N/mm^2).

4.2 Ehlbeck and Werner (1988)

In the tests reported in Ehlbeck and Werner [18] it was observed that the deformation at the permissible load according to DIN 1052 increases with increasing diameter *d*. For softwood the following equation was derived:

$$K_{ser} = (1.2 \cdot d - 1.6) \cdot \rho_k \tag{23}$$

The stiffness for hardwood is approximately 25% higher.

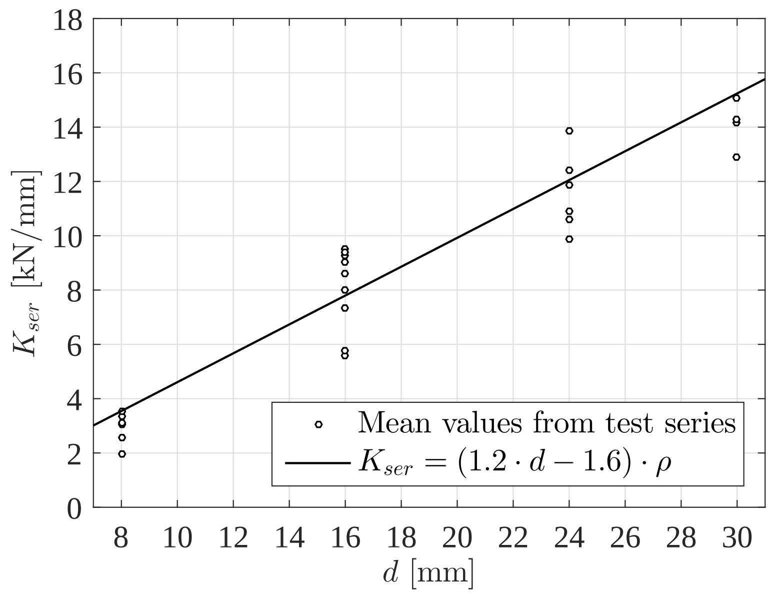

Fig. 16. Stiffness K_{ser} per shear plane and dowel (f_y = 600 N/mm^2) of a three-member joint based on a total number of 108 tests from [18] for an average density ρ = 443 kg/m^3.

A slip of 0.2 mm for softwood and of 0.1 mm for hardwood is suggested. The load-deformation behaviour of a connection is suggested to be linear by Eq. (23) for $F \leq F_{max}$ /2.75 (see Fig. 4). Especially for dowel diameter d > 16 mm the deformation was larger than reported by Möhler (1986) [19].

4.3 Jorissen (1998)

Jorissen [20] observed in the tests on multiple bolted connections considerably lower stiffness values as compared to those suggested in Eurocode 5. This is explained by the individual hole clearances, i.e. the fastener slip at 40% of the failure load is often smaller than the hole clearance and some bolts do not contribute to the load and to the connection stiffness. The following equation for connections with multiple bolts is proposed by Jorissen:

$$K_{\text{ser}} = k_{\text{bolt}} \cdot \frac{\rho_{\text{k}}^{1.5} \cdot d}{20} = 0.3 \cdot \frac{\rho_{\text{k}}^{1.5} \cdot d}{20} \tag{24}$$

4.4 Impact of moisture content on connection stiffness

Only very few test results exist for evaluating the impact of wood moisture content on connection stiffness. The test by Möhler and Ehlbeck reported in [12] were carried out on timber with a moisture content between MC ≈ 16-21%. Dubas [3] assumes that in the connection the majority of the deformation occurs in the wood and, hence, the same moisture dependency as for clear wood members can be applied also to the stiffness of connections.

5. Evaluation of the test results from TU Delft

5.1 General, geometry and configurations

A large number of tests on dowelled connections was performed at TU Delft by Jorissen [20]. One of the goals of the study by Jorissen was to determine the effect of number of fasteners in a row n and of spacing a_1 on the load-carrying capacity of connections. The results of the study led to the reduction factor for n_{ef} in Eurocode 5.

The connections tested are timber-timber connections with dowels loaded in double shear. A summary of the geometry and configurations of the connections is summarized in Table 12 and illustrated in Fig. 17. The following parameters were varied: member thickness of the side (t_{s}) and middle (t_{m}) members, dowel diameter d, number of fasteners in a row n, number of rows of fasteners m, spacing of the fasteners a_1, end-distance a_3. The steel quality of the dowels was between 4.6 and 6.8 and the yield strength calculated from the bending moment was approximately $f_{\text{y}} \approx$ 514-680 N/mm^2, respectively. The density of the timber members was recorded. Most of the test series include 10-30 specimens, but some test series only 5-6.

The specimens were tested mainly in compression but also in tension as shown in Fig. 17. To reduce friction, two Teflon sheets were placed in both interfaces and steel strips were added to avoid a gap between the middle and side members – see Fig. 18.

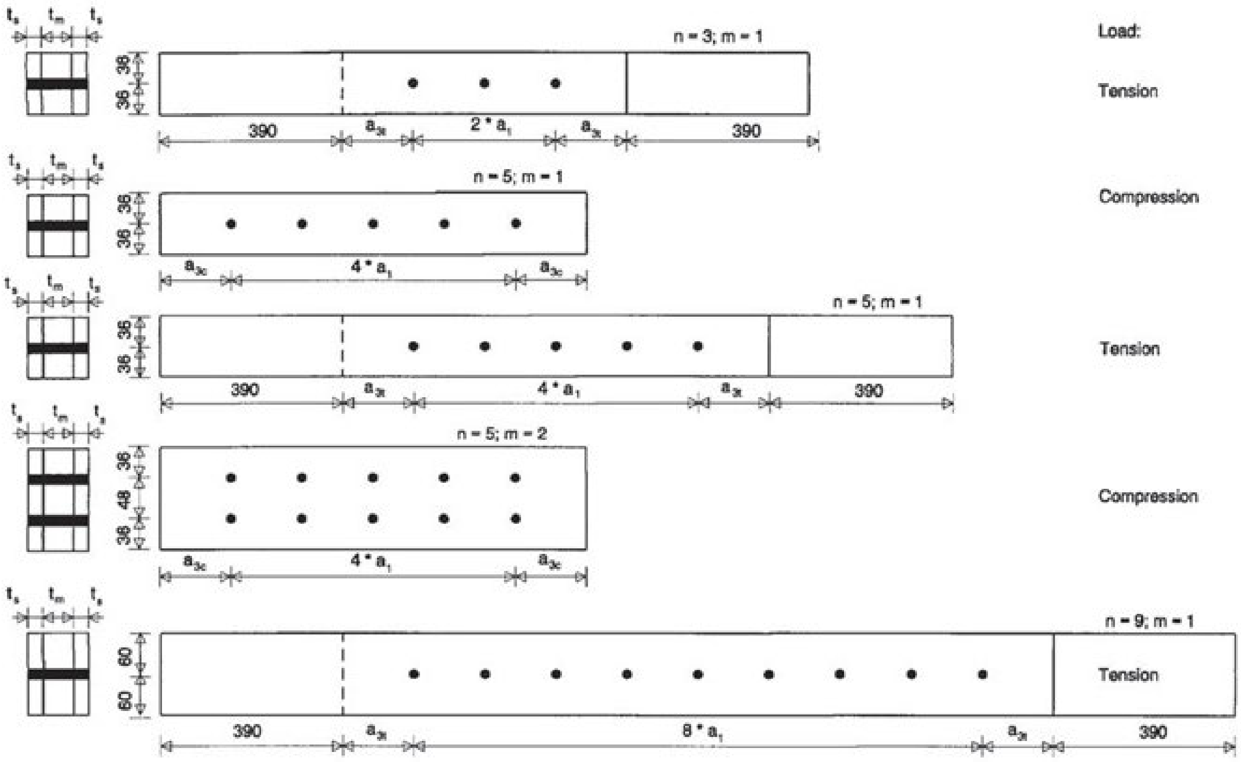

Fig. 17. Specimen configurations of connections with multiple dowels loaded in tension and compression from [20].

Table 12. Test series with variation of parameters.

Series	Type	t_s/d	t_m/d	n	m	a_1/d	a_3/d	d	#
1	1	1.021	2.043	1	1	0	7	11.75	30
2	1	1.021	2.043	3	1	2	7	11.75	10
3	1	1.021	2.043	3	1	3	7	11.75	10
4	1	1.021	2.043	3	1	5	7	11.75	10
5	1	1.021	2.043	5	1	1	7	11.75	21
6	1	1.021	2.043	5	1	2	7	11.75	18
7	1	1.021	2.043	5	1	3	7	11.75	20
8	1	1.021	2.043	5	1	5	7	11.75	20
9	1	1.021	2.043	5	2	1	7	11.75	19
10	1	1.021	2.043	5	2	3	7	11.75	20
11	1	3.087	4.116	5	1	5	7	15.55	10
12	1	1.021	2.043	9	1	2	7	11.75	20
13	1	1.021	2.043	9	1	3	7	11.75	20
14	2	3.038	4.051	5	1	5	7	19.75	10
15	3	2.254	4.507	1	1	0	7	10.65	25
16	3	2.133	4.267	3	1	2	5	11.25	10
17	3	2.133	4.267	3	1	2	7	11.25	10
18	3	2.400	4.267	3	1	3	7	11.25	10
19	3	2.133	4.267	3	1	5	7	11.25	10
20	3	2.043	4.085	5	1	1	7	11.75	20
21	3	2.043	4.085	5	1	2	5	11.75	19
22	3	2.043	4.085	5	1	2	7	11.75	20
23	3	2.043	4.085	5	1	3	5	11.75	20
24	3	2.043	4.085	5	1	3	7	11.75	20
25	3	2.043	4.085	5	1	5	7	11.75	20
26	3	2.180	4.359	5	2	1	7	11.035	20
27	3	2.254	4.507	5	2	3	7	10.65	20
28	3	2.043	4.085	9	1	2	5	11.75	19
29	3	2.064	4.127	9	1	2	7	11.64	20
30	3	2.137	4.275	9	1	3	5	11.255	20
31	3	2.085	4.169	9	1	3	7	11.53	20
32	3	2.043	4.085	9	1	5	7	11.75	10
33	4	3.380	4.507	1	1	0	7	10.65	10
34	4	3.380	4.507	5	1	1	7	10.65	21
35	4	3.380	4.507	5	1	3	7	10.65	20
36	4	3.380	4.507	5	1	5	7	10.65	20
37	4	3.380	4.507	5	2	1	7	10.65	22
38	4	3.380	4.507	5	2	3	7	10.65	20
39	6	4.507	4.507	1	1	0	7	10.65	10
40	6	4.085	4.085	5	1	1	7	11.75	5
41	6	4.085	4.085	5	1	3	7	11.75	6
42	6	4.085	4.085	5	1	5	7	11.75	7
43	6	4.085	4.085	5	2	1	7	11.75	6
44	6	4.085	4.085	5	2	3	7	11.75	6
45	8	5.021	6.128	1	1	0	7	11.75	20
46	8	5.540	6.761	3	1	2	5	10.65	10
47	8	5.540	6.761	3	1	2	7	10.65	10
48	8	5.540	6.761	3	1	3	7	10.65	10
49	8	5.540	6.761	3	1	5	7	10.65	10
50	8	5.021	6.128	5	1	1	7	11.75	19
51	8	5.021	6.128	5	1	2	5	11.75	20
52	8	5.021	6.128	5	1	2	7	11.75	20
53	8	5.021	6.128	5	1	3	5	11.75	20
54	8	5.021	6.128	5	1	3	7	11.75	20
55	8	5.021	6.128	9	1	2	5	11.75	20
56	8	5.021	6.128	9	1	2	7	11.75	20
57	8	5.021	6.128	9	1	3	5	11.75	20
58	8	5.021	6.128	9	1	3	7	11.75	20
59	8	5.021	6.128	9	1	5	7	11.75	10

5.2 Test procedure, measurements and evaluation

The following parameters were determined in the tests: time, load, machine deformation, deformation of LVDT on both sides of the connection. For the further evaluation the mean deformation measured by the LVDT was used. An illustration of a specimen with location of the measurement of the deformations is given in Fig. 18.

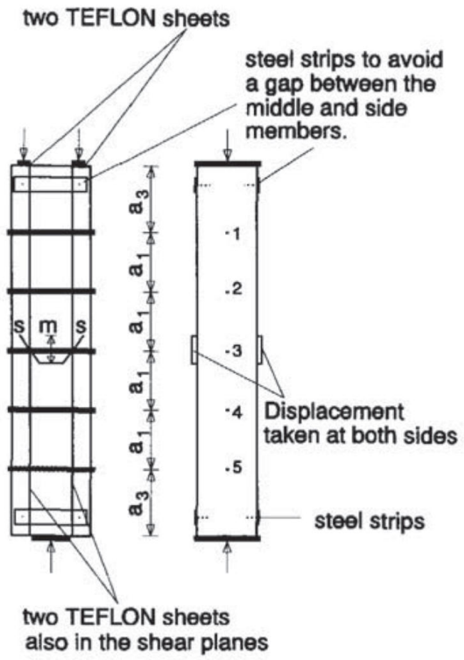

Fig. 18. Test set-up of a connection with multiple dowels from [20].

A reloading cycle was performed according to EN 26891 [4] – see Fig. 7. A typical evaluation of stiffness values is shown in Fig. 19.

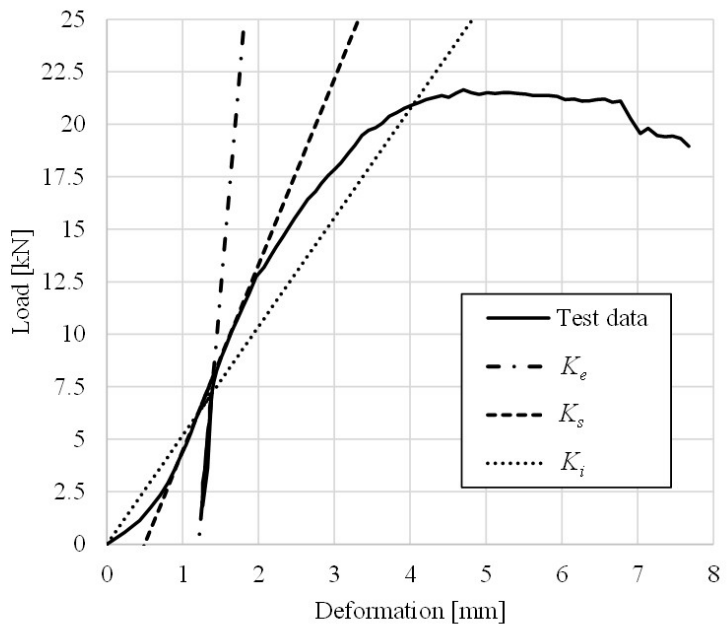

Fig. 19. Examples of a typical load-deformation curve and evaluation of stiffness values.

5.3 Impact of individual parameters

For the evaluation of the impact of individual parameters on the stiffness of connections the test series where sampled into groups of equal configurations. The following non-linear regression model was used for the evaluation of the impact of parameter X (diameter and row of fasteners) on the stiffness K:

$$K = a \cdot X^{b} \tag{25}$$

5.3.1 Diameter d

The test series selected for the evaluation of the impact of dowel diameter on stiffness are given in Table 13. Since only a limited number (10) of test configurations with 16 and 20 mm dowels were tested, the tests with 12 mm dowels in the regression analyses for the results presented in Fig. 20 were limited as well to the same configurations as for the 16 and 20 mm tests.

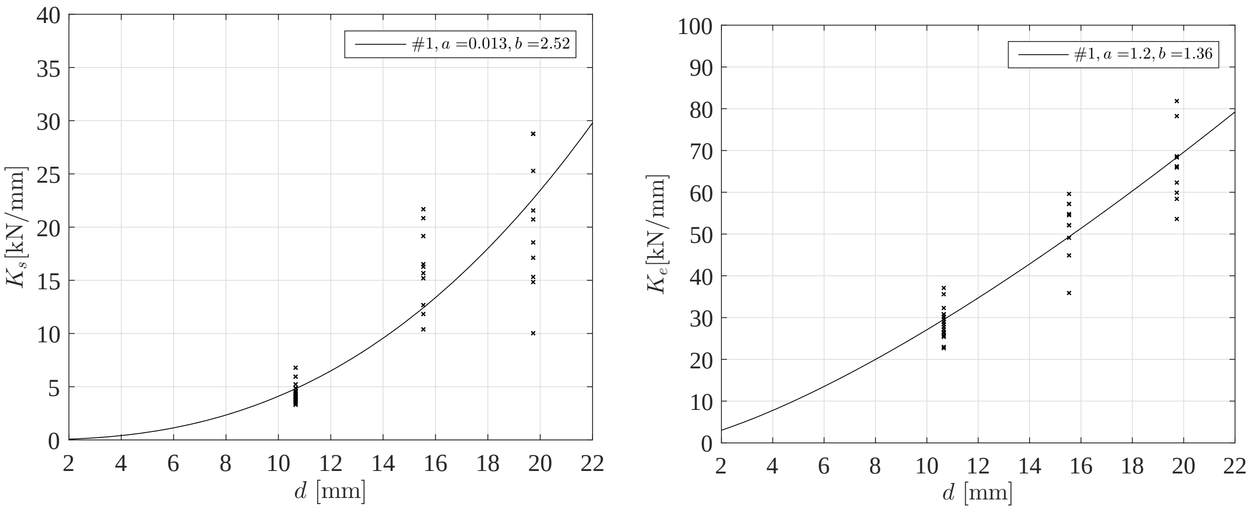

Fig. 20. Impact of diameter d on stiffness K_s and elastic stiffness K_e.

Based on the test series 11, 14 and 36 the following regressions can be fitted:

$$K_s = 0.013 \cdot d^{2.6} \tag{26}$$

$$K_e = 1.17 \cdot d^{1.36} \tag{27}$$

Table 13. Test series selected for evaluation of the impact of diameter.

Series	Type	t_s/d	t_m/d	n	m	a_1/d	a_3/d	d	#
Group No. 1:									
11	1	3.087	4.116	5	1	5	7	15.55	10
14	2	3.038	4.051	5	1	5	7	19.75	10
36	4	3.380	4.507	5	1	5	7	10.65	20

5.3.2 Number of fasteners in a row *n*

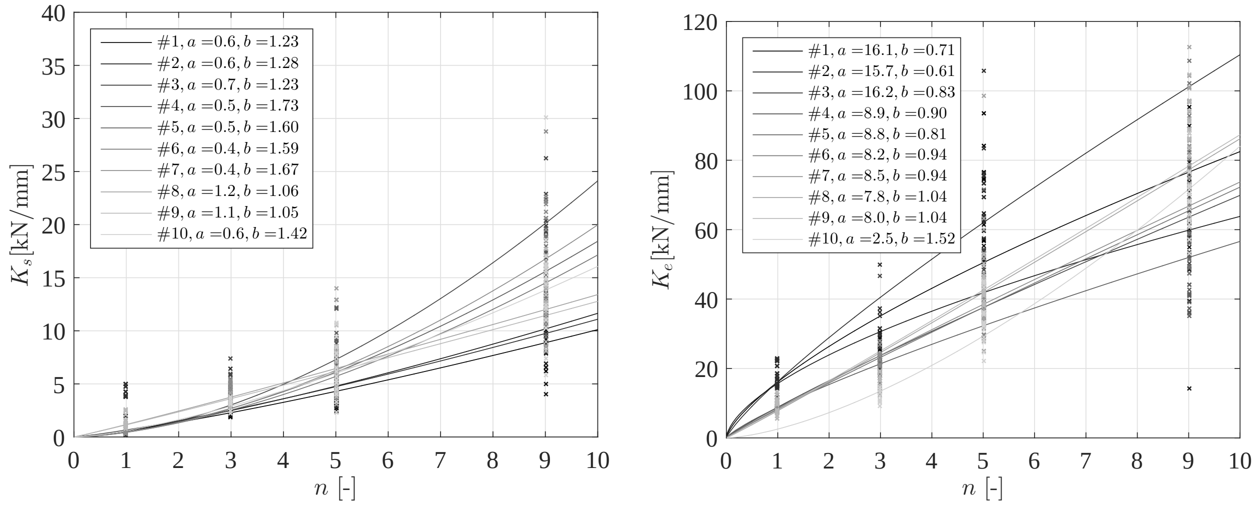

Fig. 21. Impact of number of fasteners in a row n on stiffness K_s and elastic stiffness K_e.

The following mean regressions can be fitted:

$$K_s = 0.657 \cdot d^{1.39} \tag{28}$$

$$K_s = 10.08 \cdot d^{0.934} \tag{29}$$

Table 14. Test series with variation of parameters.

Series	Type	t_s/d	t_m/d	n	m	a_1/d	a_3/d	d	#
Group No. 1:									
1	1	1.021	2.043	1	1	0	7	11.75	30
3	1	1.021	2.043	3	1	3	7	11.75	10
7	1	1.021	2.043	5	1	3	7	11.75	20
13	1	1.021	2.043	9	1	3	7	11.75	20
Group No. 2:									
1	1	1.021	2.043	1	1	0	7	11.75	30
2	1	1.021	2.043	3	1	2	7	11.75	10
6	1	1.021	2.043	5	1	2	7	11.75	18
12	1	1.021	2.043	9	1	2	7	11.75	20
Group No. 3:									
1	1	1.021	2.043	1	1	0	7	11.75	30
4	1	1.021	2.043	3	1	5	7	11.75	10
8	1	1.021	2.043	5	1	5	7	11.75	20
Group No. 4:									
15	3	2.254	4.507	1	1	0	7	10.65	25
17	3	2.133	4.267	3	1	2	7	11.25	10
22	3	2.043	4.085	5	1	2	7	11.75	20
29	3	2.064	4.127	9	1	2	7	11.64	20
Group No. 5:									
15	3	2.254	4.507	1	1	0	7	10.65	25
16	3	2.133	4.267	3	1	2	5	11.25	10
21	3	2.043	4.085	5	1	2	5	11.75	19
28	3	2.043	4.085	9	1	2	5	11.75	19
Group No. 6:									
15	3	2.254	4.507	1	1	0	7	10.65	25
18	3	2.400	4.267	3	1	3	7	11.25	10
24	3	2.043	4.085	5	1	3	7	11.75	20
31	3	2.085	4.169	9	1	3	7	11.53	20
Group No. 7:									
15	3	2.254	4.507	1	1	0	7	10.65	25
19	3	2.133	4.267	3	1	5	7	11.25	10
25	3	2.043	4.085	5	1	5	7	11.75	20
32	3	2.043	4.085	9	1	5	7	11.75	10
Group No. 8:									
45	8	5.021	6.128	1	1	0	7	11.75	20
47	8	5.540	6.761	3	1	2	7	10.65	10
52	8	5.021	6.128	5	1	2	7	11.75	20
56	8	5.021	6.128	9	1	2	7	11.75	20
Group No. 9:									
45	8	5.021	6.128	1	1	0	7	11.75	20
48	8	5.540	6.761	3	1	3	7	10.65	10
54	8	5.021	6.128	5	1	3	7	11.75	20
58	8	5.021	6.128	9	1	3	7	11.75	20
Group No. 10:									
46	8	5.540	6.761	3	1	2	5	10.65	10
51	8	5.021	6.128	5	1	2	5	11.75	20
55	8	5.021	6.128	9	1	2	5	11.75	20

5.3.3 Selected parameters and density of the timber members ρ

The side member thickness t_s/d and middle member thickness t_m/d have only a small impact on stiffness K_s and elastic stiffness K_e. The following parameters are selected for further evaluation: number of fasteners in a row n, number of rows of fasteners m, diameter d and density ρ.

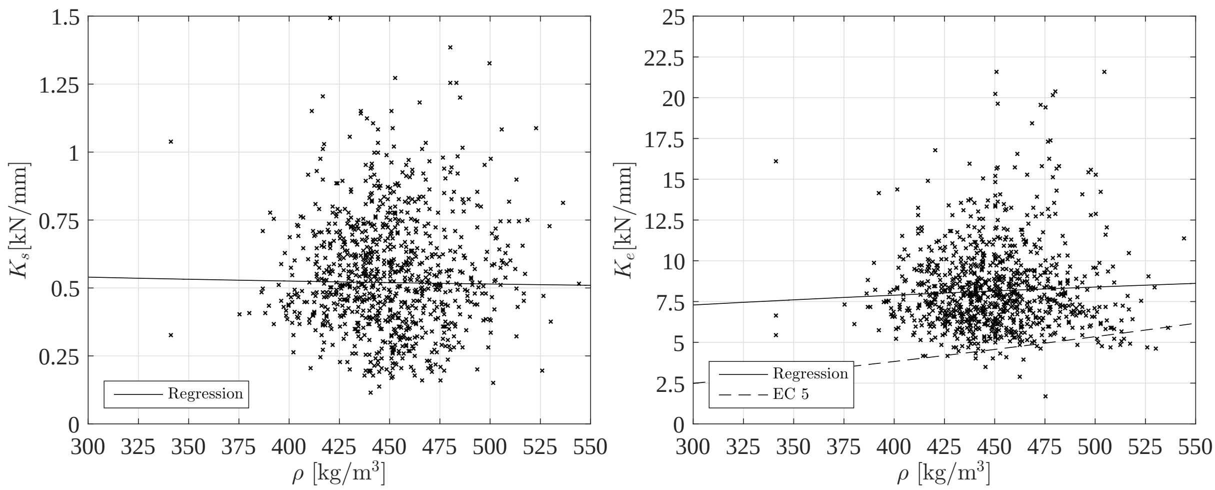

Fig. 22. Impact of mean density of the timber member ρ on stiffness K_s and elastic stiffness K_e.

The following regressions can be fitted:

$$K_\mathrm{s} = 0.0018 \cdot n^{1.4} \cdot m^{0.8} \cdot d^{2.6} \cdot \rho^{-0.094} \tag{30}$$

$$K_\mathrm{e} = 0.053 \cdot n^{0.9} \cdot m^{0.65} \cdot d^{1.4} \cdot \rho^{0.275} \tag{31}$$

The impact of density on the stiffness of a connection is rather small according to Eqs. (30) and (31). In the test series analysed in this study, only softwood timber with a rather small range of density was used. A more detailed study of the impact of density requires a broader range of densities including the results of different hardwood species.

5.3.4 Variability of stiffness

The variability of the stiffness values is evaluated by using only n, m and d as follows:

$$K_\mathrm{s} = 0.001 \cdot n^{1.4} \cdot m^{0.8} \cdot d^{2.6} \tag{32}$$

$$K_\mathrm{e} = 0.284 \cdot n^{0.9} \cdot m^{0.65} \cdot d^{1.4} \tag{33}$$

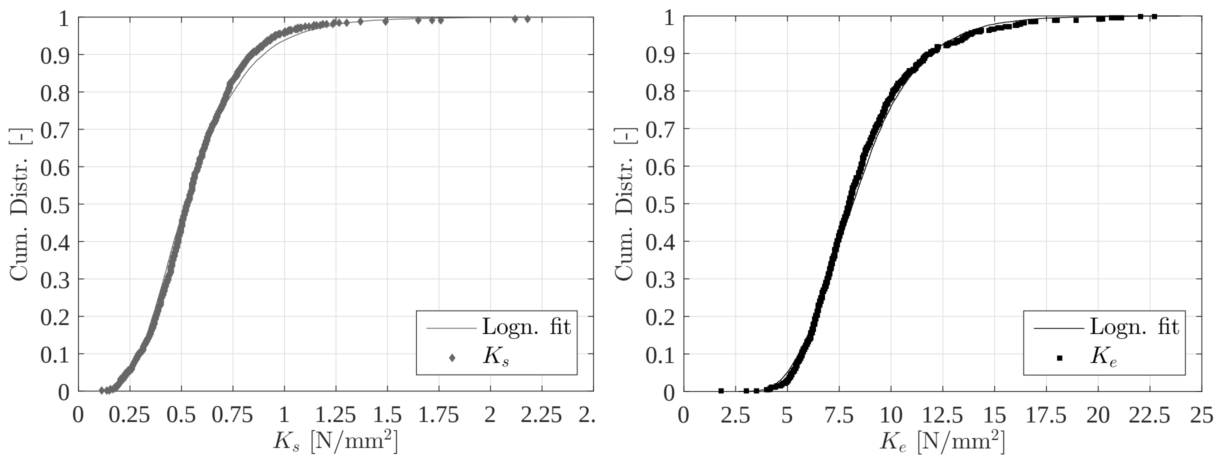

Fig. 23. Cumulative distribution of stiffness K_s and elastic stiffness K_e for n = 1,

m = 1 and d = 11 mm.
The percentile values and the variability of the stiffness K_s and elastic stiffness K_e are summarized in Table 15.

Table 15. Percentile values and coefficient of variation of stiffness values in N/mm for a connection with n = 1, m = 1 and d = 11 mm.

Stiffness	5%-quantile	50%-quantile	95%-quantile	CoV
K_s	0.254	0.54	1.06	45.8%
K_e	4.96	8.14	13.4	30.9%

6. Conclusions

6.1 Summary

From the studies presented in this chapter, the following conclusions with regard to the performance of the design approaches can be summarized:

- The background of the equations for stiffness in Eurocode 5 is vague
- The equations for stiffness in Eurocode 5 are partly based on simplified assumptions
- Different standards and studies suggest different equations for stiffness
- The relation between stiffness for serviceability and ultimate limit states is not in line with the safety format in Eurocode 5
- The evaluation of test data from TU Delft on connections with dowels shows considerable differences compared to the stiffness values suggested in Eurocode 5
- There is a non-linear impact of number of fasteners in a row and number of rows of fasteners
- The side and middle member thickness of the timber members of the connection shows only a minor impact
- The density of the timber members shows only a minor impact on stiffness for the observed sample of tests on softwood specimens

6.2 Outlook and need for further research

Further research is needed for the following topics:

- Impact of density of timber members for a broader range of soft- and hardwoods
- Stiffness of different types of timber-timber and steel-timber connections
- Stiffness of different types of fasteners
- Evaluation of the entire load-deformation behaviour
- Evaluation of the ductility of connections in dependency of failure mode
- Relation between initial and elastic stiffness
- Relation between stiffness with relevance for serviceability and ultimate limit states
- Percentile values of relevant stiffness values and recommendations for design

Acknowledgements

The work presented in this paper was developed during a Short Term Scientific Mission at Technical University of Eindhoven supported by COST Action FP 1402 (European Cooperation in Science and Technology) (www.costfp1402.tum.de).

References

[1] *EN 1995-1-1:2004* (Eurocode 5) Design of timber structures – Part 1-1: General – Common rules and rules for buildings. CEN, Brussels.

[2] Granholm H (1963) *Der Einsturz des Bogengerüstes der Sandöbrücke*. Verlag der Akademie der Wissenschaften und der Literatur, Mainz, Germany.

[3] Dubas P, Gehri E, Steurer T (1981) *Einführung in die Norm SIA 164 (1981) – Holzbau*. Publication No. 81-1, Baustatik und Stahlbau, ETH Zürich, Switzerland.

[4] Ehlbeck J (1979) *Load-carrying capacity and deformation characteristics of nailed joints*. CIB-W18 Meeting 12, Paper 12-7-1, Bordeaux, France.

[5] *EN 26891:1991*. Timber structures – Joints made with mechanical fasteners – General principles for the determination of strength and deformation characteristics (ISO 6891:1983). CEN, Brussels.

[6] Ehlbeck J, Larsen HJ (1993) *Eurocode 5 design of timber structures: Joints*. In: Barnes M, Brauner A, Galligan W, Leichti R, Soltis L (eds) Proc. of the International Workshop On Wood Connectors, Forest Products Society.

[7] Norén B (1968) *Nailed joints – their strength and rigidity under short-term and long-term loading*. Tech. Rep. 22, National Swedish Institute for Building Research.

[8] *DIN 1052:2008*. Entwurf, Berechnung und Bemessung von Holzbauwerken – Allgemeine Bemessungsregeln und Bemessungsregeln für den Hochbau. Deutsches Institut für Normung e.V., Berlin, Germany.

[9] *DIN 1052-2:1988*. Holzbauwerke; Mechanische Verbindungen. Deutsches Institut für Normung e.V., Berlin, Germany.

[10] *SIA 265:2012*. Timber Structures. SIA Swiss Society of Engineers and Architects, Zurich, Switzerland.

[11] *SIA 164:1981*. Timber Structures. SIA Swiss Society of Engineers and Architects, Zurich, Switzerland.

[12] Möhler K, Ehlbeck J (1973) Untersuchungen über das Tragverhalten von Sondernägeln bei Beanspruchung auf Abscheren und Ausziehen. *Berichte aus der Bauforschung* Heft 91.

[13] Fontana M (1984) *Festigkeits- und Verformungsverhalten von hölzernen Fachwerkträgern unter besonderer Berücksichtigung der Knotenausbildung*. Publication No. 84-1, Baustatik und Stahlbau, ETH Zürich, Switzerland.

[14] Scheer C (1980) *Berechnung von Fachwerkkonstruktionen unter Berücksichtigung des durchlaufenden Ober- und Untergurtes*. Technische Universität Berlin, Germany.

[15] *CIB – Structural Timber Design Code*. Fifth edition, August 1980.

[16] Egner K (1955) Versuche mit Bolzenverbindungen (Schraubenbolzen). *Fortschritte und Forschungen im Bauwesen*, Reihe D, Heft 20.

[17] Gehri E, Fontana M (1983) *Betrachtungen zum Tragverhalten von Passbolzen in Holz-Holz-Verbindungen*. Publication No. 83-1, Baustatik und Stahlbau, ETH Zürich, Switzerland.

[18] Ehlbeck J, Werner H (1988) Untersuchungen über die Tragfähigkeit von Stabdübel-verbindungen. *Holz als Roh-und Werkstoff* **46**(8):281–288

[19] Möhler K (1986) Verschiebungsgrößen mechanischer Holzverbindungen der DIN 1052 Teil 2 (Entwurf 1984). *Bauen mit Holz* 4:206–214

[20] Jorissen A (1998) *Double shear timber connections with dowel type fasteners*. PhD thesis, Delft University of Technology, The Netherlands

A review of the existing models for brittle failure in connections loaded parallel to the grain

J.M. Cabrero
Universidad de Navarra
Pamplona, Spain

M. Yurrita
Universidad de Navarra
Pamplona, Spain

Summary

In the current normative version of Eurocode 5, brittle failure of connections loaded parallel to the grain is not included. The informative Annex A includes methods for the determination of the block-shear and plug-shear failures. This paper provides information on the most relevant models dealing with brittle failure of connections loaded parallel to the grain, organized by the different failure mechanisms, with special attention to how they are included in Eurocode 5 and the draft of the New Zealand code.

1. Introduction

The capacity of timber connections is usually defined by means of the European Yield Model, EYM. Those plastic mechanisms are based on the assumption of yielding in steel and embedment behavior in timber, which both are ductile mechanisms.

Hence, it is usually assumed that the plastic mechanism described by the EYM mirrors the total capacity of the connection. However, in some cases, brittle failure of the wood member may happen before such plastic mechanism is produced. The failure mechanism of a timber connection with mechanical fasteners among other things depends on the geometry of the connection and the type of fastener.

Failure modes different from the ductile embedment may happen in a timber connection. Typical failure modes for dowelled connections loaded parallel to the grain are shown in Fig. 1. The first one (a, left) is embedment (as described in the EYM model). The remaining four are brittle failure modes: splitting, row-shear plug or block shear, and tensile failure. Embedment (a) is the only one supposed to be ductile, although when the bolt displacement is larger, it usually results in splitting (b), which is usually related to perpendicular to grain tension; row-shear failure (c) is usually related to stocky fasteners which protrude the whole element; group tear-out failure (d) is usual for both bolted (block shear, failing the whole thickness of the member) or nailed (plug shear, with a bottom failure plane); finally, the net tension failure (e) is a tensile failure of the plane where the connection ends, usually related to an insufficient net area.

This document reviews the existing proposals for the different brittle failure mechanisms in connections loaded parallel to the grain. The different models are ordered according to the previously described brittle failure modes in Figure 1: splitting, row-shear and block-shear. For consistency, the different equations have been rewritten according to a common nomenclature, which is given in Fig. 2.

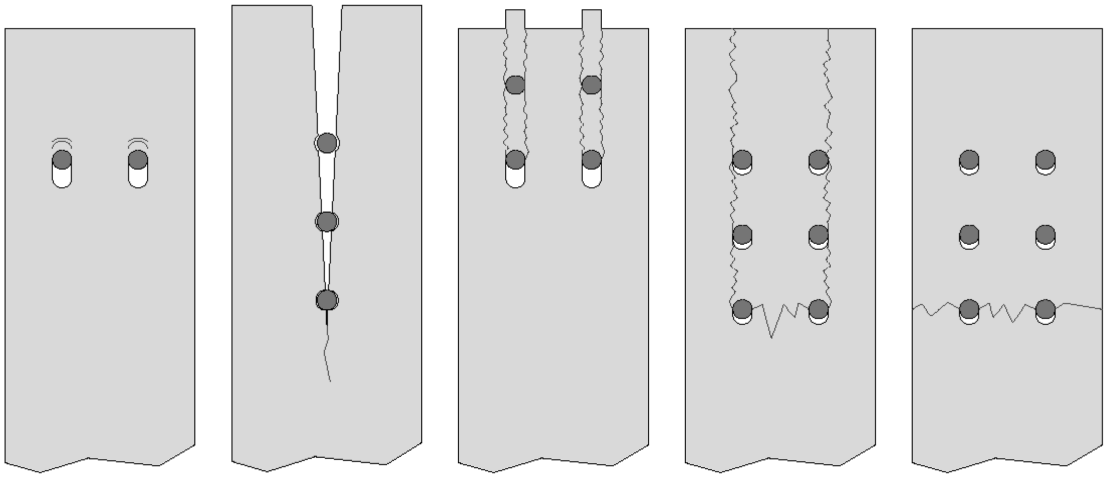

(a) Embedment (b) Splitting (c) Row shear (d) Block shear (e) Net tension

Fig. 1. Failure modes in a connection. Image from [1].

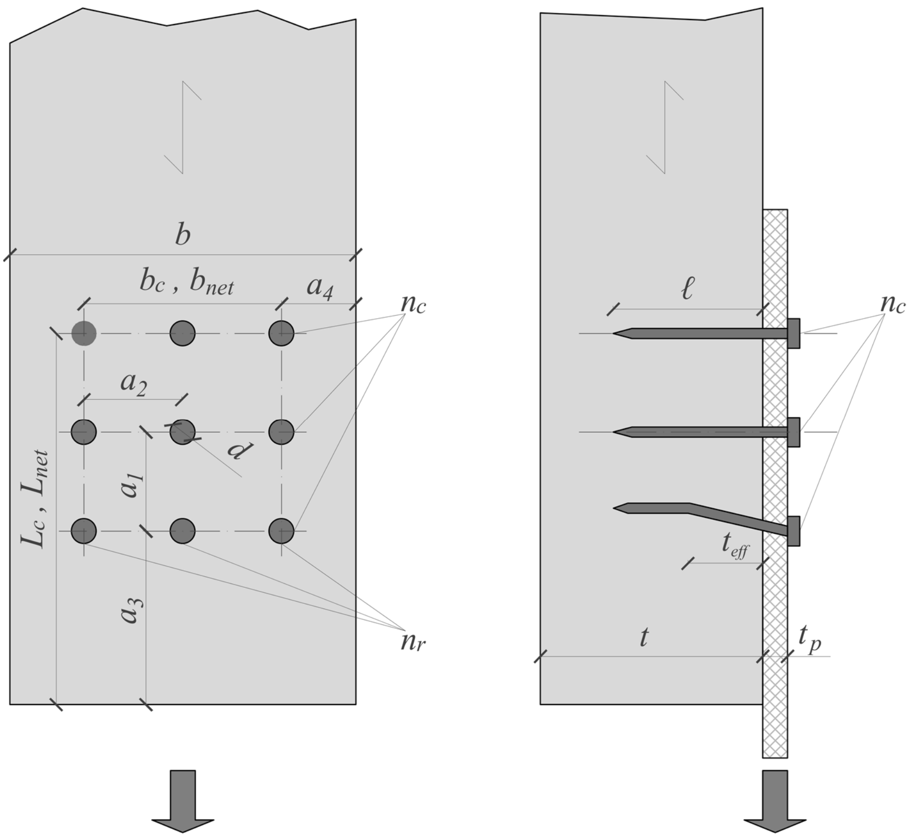

Fig. 2. Denotation of geometrical parameters used in this chapter. Image from [1].

2. Splitting

2.1 Eurocode 5 (EC5)

Splitting failure is not explicitly considered in Eurocode 5 [2]. It is, however, implicitly included in the reduction factor n_{ef}, which reduces the number of fasteners to be used in the calculations for the connection capacity. The effective number n_{ef} for nails is given as $n_{ef} = n_c^{kef}$, where k_{ef} is given in Table 1, with values ranging from 0.5 to 1.0.

Table 1. Values of k_{ef} for the effective number of nails

Spacing*	k_{ef}	
	Not predrilled	Predrilled
$\geq 14d$	1.0	1.0
$a_1 = 10d$	0.85	0.85
$a_1 = 7d$	0.7	0.7
$a_1 = 4d$	-	0.5

* For intermediate spacings, linear interpolation of k_{ef} is permitted.

For dowels, it is given as:

$$n_{ef} = \min\begin{cases} n_c \\ n_c^{0.9} \cdot \sqrt[4]{\dfrac{a_1}{13 \cdot d}} \end{cases} \tag{1}$$

where n_c is the number of fasteners in a row, and a_1 the spacing between them.

Initially, the factor was considered to account only for the load distribution between fasteners, but it later included splitting failure. It is mainly based on the work by Jorissen [3, 4], who developed an analytical model based on a beam on elastic foundation model to obtain the perpendicular to grain stresses and the Volkersen model [5] for the shear stress. The splitting failure is supposed to begin in the fastener's hole.

2.2 New Zealand draft

There are no considerations about the splitting in the parallel-to-grain direction in the New Zealand draft standard [6].

2.3 Hanhijärvi and Kevarinmäki

The model from Hanhijärvi and Kevarinmäki [7] does not only propose an equation for splitting failure. It is a comprehensive calculation model which integrates all possible brittle failure modes for connections with dowels.

In this first reference to it, the whole proposal of the model is explained. Otherwise, it would be difficult to understand it in the following sections. They divide the connection in two parts: outer and inner part of the connection, as shown in Fig. 3. The considered failure planes of the inner part are drawn with continuous lines while the outer part is represented with dashed lines. Capacities for the outer and inner parts are obtained independently as the minimum capacity for each part. Then the sum of these two capacities leads to the capacity of the connection. They consider a possible interaction among the different stresses, and they therefore propose interaction terms between some of those failure planes.

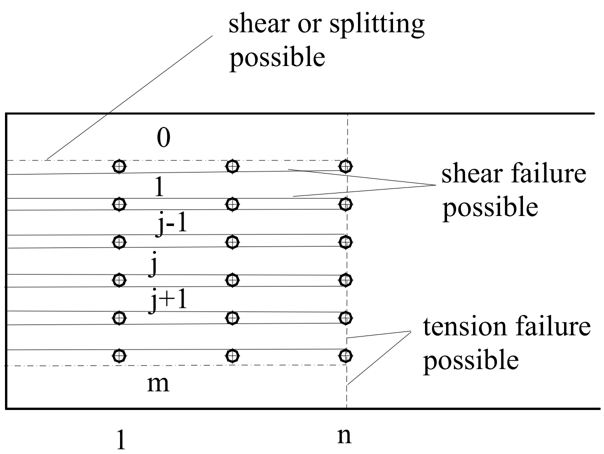

Fig. 3. Failure planes considered by Hanhijärvi and Kevarinmäki [7].

Splitting is considered only in the outer part of the connection. Hanhijärvi and Kevarinmäki [7] used the same Volkersen model which was used by Jorissen [4], but instead of a reduction factor, they obtained the following expressions for the splitting of a row of fasteners, depending on whether it originates in the hole, $F_{spl,hole,Rd}$, or in the end, $F_{spl,end,Rd}$, of the member.

$$F_{spl,hole,Rd} = \frac{k_{t90,cnctr} \cdot n_{ef} \cdot 10 \cdot f_{t,90,k} \cdot t_{ef} \cdot a_3}{s_{t90,hole}} \tag{2}$$

$$F_{spl,end,Rd} = \frac{k_{t90,cnctr} \cdot n_{ef} \cdot 10 \cdot f_{t,90,k} \cdot t_{ef} \cdot a_3}{s_{t90,end}} \tag{3}$$

where $k_{t,90,cnctr}$ is a stress concentration factor (set to 0.7 in their work), $f_{t,90,k}$ is the perpendicular-to-grain tensile strength, t is the thickness of the specimen, a_3 is the end-distance, and a_4 is the edge distance. The factor 10 corresponds to the wedging factor estimated in 1/10 by Jorissen [4]. The s_t parameters are the ratio between the maximum and average perpendicular to grain stress, and were curve-fitted to the results from the Volkersen model, and is defined as:

$$s_{t90,hole} = \max \begin{cases} 1 \\ 0.65 \cdot \dfrac{a_3}{a_4} \end{cases} \tag{4}$$

$$s_{t90,end} = \frac{2.7}{\cosh\left(\dfrac{a_3}{a_4} - 1.4\right)} \tag{5}$$

They assume a load distribution factor, called n_{ef} (similar in its expression to that in the Eurocode 5), but simplified to $n_{ef} = n^{0.9}$, and a dowel deformation effect, which in fact reduces the thickness of the loaded plane in timber, t_{ef}.

The t_{ef} parameter takes into account the dowel deformation by reducing the thickness of the failure plane, similarly as it will be done by means of the effective thickness in other proposals:

$$t_{1,ef} = t_1 \cdot \min \begin{cases} 1 \\ \dfrac{d}{0.6 \cdot d_{gr,1}} \end{cases} \quad \text{where} \quad d_{gr,1} = 2.45 \cdot \sqrt{\frac{f_{h,m}}{f_{y,m}}} \cdot t_1 \quad \text{(side members)} \tag{6}$$

$$t_{2,ef} = t_2 \cdot \min \begin{cases} 1 \\ \dfrac{d}{0.5 \cdot d_{gr,2}} \end{cases} \quad \text{where} \quad d_{gr,2} = 1.23 \cdot \sqrt{\frac{f_{h,m}}{f_{y,m}}} \cdot t_2 \quad \text{(middle members)} \tag{7}$$

where d_{gr} is the limit above which the dowel is rigid according to the Johansen theory; $f_{h,m}$ is the mean embedment strength equal to $1.5 \cdot f_{h,0,k}$ and $f_{y,m}$ is the nominal yield strength of the dowel.

Regarding the previously referred interaction between the different stresses: since the maximum value of the stress components does not act in the same location, the usual condition (that is, assume that the sum of the utilization rates of the different components must not exceed 100%) could be relaxed and parameterized. When two stress components affect the capacity of a part, the interaction is considered by reducing the lower capacity by subtracting an amount proportional to the ratio of the lower capacity to the higher. $k_{interaction}$ is a parameter, which could be varied depending on interaction type. In their work, they consider it with a value of 0.3.

Interaction of splitting is only considered for the case of $F_{spl,hole,Rd}$, which should be combined with row shear of the outer parts with the interaction equation (8), replacing the subscripts 1 and 2 by the corresponding of the considered forces. In this case, $F_{spl,hole,Rd}$ and $F_{shear,out,Rd}$, which is defined in equation (12). As a result, $F_{spl,hole+shear,out,Rd}$ is obtained.

$$F_{1+2} = \begin{cases} F_1 \cdot \left(1 - k_{interaction} \cdot \dfrac{F_1}{F_2}\right), \text{ if } F_1 \leq F_2 \\ F_2 \cdot \left(1 - k_{interaction} \cdot \dfrac{F_2}{F_1}\right), \text{ if } F_2 < F_1 \end{cases} \quad \text{with} \quad k_{interaction} = 0.3 \tag{8}$$

3. Row-shear failure

3.1 Eurocode 5

There is no provision on row-shear failure in the Eurocode. It could be considered that the previously described effective number of fasteners n_{ef} implicitly deals with this type of failure, since it was considered in the original work by Jorissen [4].

3.2 New Zealand draft

The design for row-shear strength in the New Zealand standard draft [6] is given by:

$$F_{row,Rd} = \phi_w \cdot RS_i \cdot n_r \cdot k_1 \cdot k_{12} \tag{9}$$

where RS_i is the characteristic row shear strength along two shear planes of a row i, given as follows:

$$RS_i = 0.75 \cdot f_{v,k} \cdot K_{LS} \cdot n_c \cdot 2 \cdot a_{cri} \cdot h \tag{10}$$

where a_{cri} is the minimum between a_1 or a_3; K_{LS} is the loading surface factor equal to 1.00 for inner members, and 0.65 for outer members of a connection. The k and ϕ are code calibration parameters.

3.3 Hanhijärvi and Kevarinmäki

Hanhijärvi and Kevarinmäki [7] consider row shear failure in the related planes in a simple manner by calculating the shear capacity as the shear area multiplied by the shear strength of wood, which is reduced by multiplying it by a factor $k_{v,cnctr}$ (0.7) which accounts for stress concentration. As in their proposal for splitting, the n_{ef} factor considers the load distribution among fasteners. This proposal is similar to the formula for the failure of the shear plane of the Eurocode 5 [2] in its Annex A.

It should be pointed out that they do not consider row shear as the failure of the row as a whole, but as part of a system. As a result, they consider in the inner part the shear of the adjacent planes of the wood contained between two rows instead of the two shear planes of a row. As a consequence, they consider two shear formulae, one for the inner part, $F_{shear,in,Rd}$, and another for the outer part, $F_{shear,out,Rd}$, which has only one shear plane, and it thus is divided by two. Note that each formula is for only one failure plane, not for the whole connection.

$$F_{shear,in,Rd} = k_{v,cnctr} \cdot \frac{n_{ef}}{n_c} \cdot A_{v,j} \cdot f_{v,k} = k_{v,cnctr} \cdot \frac{n_{ef}}{n_c} \cdot 2 \cdot \left[(n_c - 1) \cdot a_1 + a_3 \right] \cdot t_{ef} \cdot f_{v,k} \tag{11}$$

$$F_{shear,out,Rd} = k_{v,cnctr} \cdot \frac{n_{ef}}{n_c} \cdot A_{v,j} \cdot f_{v,k} = k_{v,cnctr} \cdot \frac{n_{ef}}{n_c} \cdot \left[(n_c - 1) \cdot a_1 + a_3 \right] \cdot t_{ef} \cdot f_{v,k} \tag{12}$$

The stress concentration factor $k_{v,cnctr}$ has a factor lower than one to take into account the unevenness of the stress distribution. The area $A_{v,j}$ of the outer part is half that of the inner part. Actually, the shear part of the inner part has been described in the row shear failure section, to which somehow it resembles.

As previously explained, the t_{ef} parameter takes into account the dowel deformation by reducing the thickness of the plane, similarly to the effective thickness in other proposals. The n_{ef} factor takes into account the effect of load distribution between the dowels.

As already seen in Section 2.3, there is an interaction between $F_{row,out,Rd}$ and $F_{spl,hole,Rd}$ given by equation (8). The same equation is applied for the interaction between shear and tensile forces, as will be explained in 4.2.3.

3.4 Jensen and Quenneville

Jensen and Quenneville [8, 9] developed a model based on the same Volkersen theory [5], where the row shear problem is treated as a pure shear problem with no interaction between shear stresses and perpendicular-to-grain tensile stresses. They propose two different solutions, depending on the assumed failure criterion. The row shear failure load for a single fastener connection may approximately be given by the following equation if using a mean stress failure criterion:

$$F_{row,Rd} = \min \begin{cases} 2 \cdot n_c \cdot t \cdot f_v \cdot a_3 \\ 2 \cdot n_c \cdot t \cdot f_v \cdot a_1 \end{cases} \tag{13}$$

If using a maximum stress failure criterion, the solution becomes

$$F_{row,Rd} = \phi \cdot 2 \cdot t \cdot f_v \cdot a_3 \tag{14}$$

where

$$\phi = \frac{\tanh \omega}{\omega} \tag{15}$$

$$\omega = f_v \cdot a_3 \cdot \sqrt{\frac{2}{G_f \cdot d \cdot E}} \tag{16}$$

4. Block-shear failure/ Plug-shear

Block-shear failure (also known as group-tear-out) and plug-shear refer to the same failure mode, in which the failure is produced in the outer perimeter of the connection area. The difference between them is mainly due to the dimensions of the fasteners, as described below, which result in the failure of an additional bottom plane when small-diameter fasteners which do not protrude the whole timber member are used.

4.1 Plug-shear failure

In nailed or screwed connections where the fastener does not protrude the whole timber thickness, plug shear failure can occur, in which an entire block defined by the perimeter of the connection is torn away from the timber. The failure is defined by the failure of three different planes, head tensile H, lateral shear L, and bottom shear B (as shown in Fig. 4).

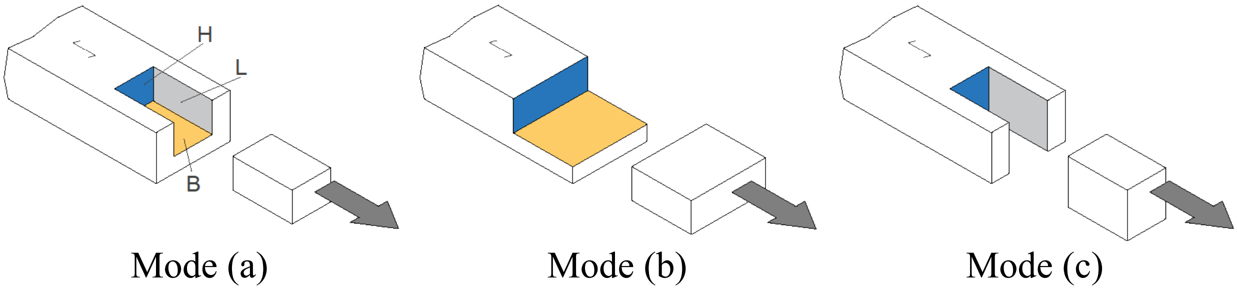

Fig. 4. Different possible failure modes of wood block tear-out: (a) mode a [head tensile (H), lateral (L) and bottom (B) shear planes]; (b) mode b [head tensile (H) and bottom shear (B) planes]; (c) mode c [head tensile (H) and lateral shear (L) planes] [1].

4.1.1 Eurocode 5

In the 2004 version of the Eurocode 5, in Annex A of Eurocode 5 [2] the block shear failure is obtained as the maximum of:

- the tensile resistance of the end face (tensile side, T),
- the sum of the shear resistances of the side (L) and bottom (B) faces corresponding to the effective wood depth, t_{ef}, which depends on the governing ductile failure mode.

$$P_w = \max \begin{cases} 1.5 \cdot A_{net,t} \cdot f_{t,0,k} \\ 0.7 \cdot A_{net,v} \cdot f_{v,k} \end{cases} \tag{17}$$

where

$$t_{ef} = \begin{cases} L_{net,v} \cdot t_1 & \text{embedment failure or steel-timber-steel connection} \\ \dfrac{L_{net,v}}{2} \cdot \left(L_{net,t} + 2 \cdot t_{ef} \right) & \text{other cases} \end{cases} \tag{18}$$

4.1.1.1 Effective thickness

The effective thickness t_{ef} depends both on the steel plate thickness and the number of plastic hinges. Steel plates of thickness $t_p \leq 0.5d$ are classified as thin plates and steel plates of thickness $t_p \geq d$ as thick. For intermediate values of thickness, interpolation is needed.

For thin steel plates (for failure modes given in brackets):

$$t_{ef} = \begin{cases} 0.4 \cdot t_1 & \text{(a)} \\ 1.4 \cdot \sqrt{\dfrac{M_{y,Rk}}{f_{h,k} \cdot d}} & \text{(b)} \end{cases} \tag{19}$$

For thick steel plates (for failure modes given in brackets):

$$t_{ef} = \begin{cases} 2 \cdot \sqrt{\dfrac{M_{y,Rk}}{f_{h,k} \cdot d}} & \text{(e), (h)} \\ t_1 \cdot \left[\sqrt{2 + \dfrac{M_{y,Rk}}{f_{h,k} \cdot d \cdot t_1^2}} - 1 \right] & \text{(d), (g)} \end{cases} \tag{20}$$

4.1.2 New Zealand draft

Zarnani and Quenneville [6, 11-14] developed a spring model, based on the stiffness of each plane, as shown in Fig. 4. It is the approach included in the proposal for the New Zealand standard draft [6].

The applied load transfers from the wood member to the failure planes according to the relative stiffness ratio of each resisting adjacent volume to the individual failure plane. K_h, K_b and K_l are the stiffness of the wood blocks loading the head, bottom and lateral failure planes. By predicting the stiffness of the corresponding wood volume, one can derive the portion of the connection load that is channelled to each resisting plane and from the resistance of each failure planes, one can determine which failure plane triggers the connection failure.

The connection resistance is obtained as an addition of the critical plane failure load plus the load carried by the other planes:

$$F_{plug,Rd} = \min \begin{cases} F_h = f_{t,m} \cdot A_{th} \cdot \left(1 + \dfrac{K_b}{K_h} + \dfrac{K_l}{K_h}\right) & \text{(tensile head } T\text{)} \\ F_b = \min\left(f_{v,m} \cdot C_{ab} \cdot A_{sb},\ f_{t,m} \cdot X_l \cdot d_z\right) \cdot \left(1 + \dfrac{K_h}{K_b} + \dfrac{K_l}{K_b}\right) & \text{(bottom plane } B\text{)} \\ F_l = \min\left(f_{v,m} \cdot C_{al} \cdot A_{sl},\ 2 \cdot f_{t,m} \cdot t_{ef} \cdot d_e\right) \cdot \left(1 + \dfrac{K_h}{K_l} + \dfrac{K_b}{K_l}\right) & \text{(lateral plane } L\text{)} \end{cases} \tag{21}$$

With the failure planes:

Head tensile plane stiffness (T): $K_h = \frac{2 \cdot E \cdot A_{th}}{L}$

Bottom shear plane stiffness (B): $K_b = (1-H) \cdot (K_{sb} + K_{tb})$ (22)

Lateral shear plane stiffness (L): $K_l = (1-F) \cdot (K_{sl} + K_{tl})$

where the shear planes are divided in two different contributions, pure shear K_{si} and tension K_{ti}; H and F are reduction factors related to the reduction of the bottom (H) and lateral (F) distance.

The wood load-carrying capacity of the connection is the load which results in the earlier failure of one of the resisting planes due to being overloaded and equals to the minimum of P_{wh} (head failure), P_{wb} (bottom failure) and P_{wl} (lateral failure).

A_{th}, A_{sb} and A_{sl} are the areas of the head, bottom and lateral resisting planes with respect to the wood effective thickness, t_{ef}, subjected to tension and shear stresses. Also, C_{ab} and C_{al} are the ratios of the average to maximum stresses on the bottom and lateral shear planes respectively. n_p is the number of the plates equal to 1 and 2 for one-sided and double-sided connections, respectively. X_l is the maximum effective edge distance (equal to two times the half of the distance between the first and the last rows, which is comparable to $X_b = 2t_{ef}$).

By accounting different area configurations, the different possible failure modes depicted in Fig. 5 can be checked and verified.

4.1.2.1 Effective thickness

For brittle failure before yielding of the fasteners, the effective wood thickness is determined from the elastic deformation, which is determined from a beam on an elastoplastic foundation model.

For mixed modes – those where yielding in the fasteners has begun – the effective thickness may be derived from the EYM mode:

$$t_{ef,y} = \begin{cases} L_p & \text{Mode I} \\ \sqrt{\dfrac{M_{y,l}}{f_{h,0} \cdot d_l} + \dfrac{L_p^2}{2}} & \text{Mode III} \\ 2 \cdot \sqrt{\dfrac{M_{y,l}}{f_{h,0} \cdot d_l}} & \text{Mode IV} \end{cases} \qquad (23)$$

The algorithm is originally proposed for rivets. It may be used for nails and screws that are inserted into predrilled holes, provided the area corresponding to the cutting diameter is subtracted from the resisting plane surfaces. This affects the strength of the tensile and shear resisting planes and not their stiffness.

The proposed model has been extended for its use in CLT [15].

4.1.3 Kangas and Vesa

Kangas and Vesa [16] proposed the resistance of the connection as the lowest value of the total embedding failure and the plug shear capacity:

$$F_{plug,Rd} = \min \begin{cases} n_r \cdot n_c \cdot R_{nail} \\ R_t + R_v = t_{ef} \cdot f_{t,0} \cdot b_c + b_c \cdot l_c \cdot f_v \end{cases} \tag{24}$$

where t_{ef} is the distance between the two plastic hinges in a nail, calculated from the plastic yield-mode given in the EYM and neglecting any contribution from the rope effect:

$$t_{ef} = 2 \cdot \sqrt{\frac{M_y}{f_h \cdot d}} \tag{25}$$

The effective width b_c is the sum of the distances between fasteners perpendicular to grain:

$$b_c = b_w - \left(2 \cdot a_4 + n_c \cdot d\right) \tag{26}$$

The part denoted as R_t in equation (24) corresponds to the tensile plane T, and the R_v to the bottom shear plane (L). The lateral shear planes are not considered in this proposal.

4.1.4 Foschi and Longworth

Foschi and Longworth [17] defined the capacity as the minimum of both lateral l and head h planes:

$$F_{plug,Rd} = \min \begin{cases} R_t = \dfrac{f_{t,0} \cdot t \cdot b}{K_t \cdot \beta_t \cdot \alpha_t \cdot \gamma_h} \\ R_v = \dfrac{2 \cdot f_v \cdot t \cdot l}{K_s \cdot \beta_s \cdot \gamma_h} \end{cases} \tag{27}$$

The numerically derived factors $K_{t/s}$, $\beta_{t/s}$, α_t and γ_h account for the number of nail rows (n_r) and columns (n_c), timber thickness (h) and penetration depth (t), respectively. As previously, the part denoted as R_t corresponds to the tensile plane T, and the R_v to the lateral shear planes (L). In this case, the bottom shear plane is not considered.

4.1.5 Johnson and Parida

Johnson and Parida [18] analysed plug-shear failure in short-term experiments on nailed steel-to-timber connections with five different connection geometries. Using spring models, it is shown that the load distribution creates pronounced stresses at the last nail in the connection, which probably initiates the plug shear failure. Fasteners placed in groups can be a successful way of reducing the risk of plug shear failure. The failure is probably initiated at the nail farthest from the free end, where tensile stresses perpendicular to grain occur.

The work checks different hypotheses of active load-carrying areas, and finally proposes:

$$F_{plug,Rd} = \max \begin{cases} R_t = b_c \cdot t_{ef} \cdot f_t \\ R_v = b \cdot l \cdot f_v \end{cases} \tag{28}$$

4.2 Block shear

For large fasteners such as bolts and dowels, the fastener protrudes the whole timber member, so that no bottom failure plane is activated. Usually, the block-shear failure activates the lateral *L* and head *H* planes.

4.2.1 Eurocode 5

The same procedure as the already described in section 4.1.1 for the case of plug shear is proposed for the case of large fasteners.

4.2.2 New Zealand draft

The design block-shear or group-tear-out strength in the New Zealand standard draft [6] defines a head tensile plane (R_T) and two lateral shear planes (R_V) based in the row-shear calculations:

$$F_{block,Rd} = \phi_w \cdot \left(R_v + R_t\right) \cdot k_1 \cdot k_{12} = \phi_w \cdot \left(RS_i + 1.25 \cdot f_{t,0,k} \cdot A_{GT-net}\right) \cdot k_1 \cdot k_{12} \tag{29}$$

where RS_i is the characteristic row shear strength along two shear planes of the outer row of the connection and $A_{GT\text{-}net}$ is the net tension area between the two outer rows. The k and ϕ are code calibration parameters.

4.2.3 Hanhijärvi and Kevarinmäki

As already explained, Hanhijärvi and Kevarinmäki [7] do not consider failure modes acting separately. Forces are considered to act together leading to a complex stress situation. Hence, no block shear is proposed, but they consider an interaction between the shear and tensile forces as part of this complex unitary model.

However, a block-shear failure can be obtained from their equations as follows. The capacity of the inner (inside the rows) tensile plane is given as:

$$F_{ten,in,Rd} = k_{t,cnctr} \cdot \frac{n_{ef}}{n_c} \cdot A_{t,i} \cdot f_{t,0,k} = k_{t,cnctr} \cdot \frac{n_{ef}}{n_c} \cdot (a_2 - d) \cdot t \cdot f_{t,0,k} \tag{30}$$

The capacity of the outer tensile plane must be considered as well, and it is given as:

$$F_{ten,out,Rd} = k_{t,cnctr} \cdot \frac{n_{ef}}{n_c} \cdot A_{t,i} \cdot f_{t,0,k} \cdot k_{t,outer} = k_{t,cnctr} \cdot \frac{n_{ef}}{n_c} \cdot (a_2 - d) \cdot t \cdot f_{t,0,k} \cdot k_{t,outer} \tag{31}$$

The outer plane adds a reduction factor $k_{t,outer}$ to take into account the asymmetry of the tensile stress distribution.

$k_{t,outer}$ is defined as:

$$k_{t,outer} = \frac{1}{1+\frac{A_{t,j}}{A_{v,j}}} = \frac{1}{1+\frac{\left(a_4 - \frac{d}{2}\right)\cdot h}{\left[(n_c - 1)\cdot a_1 + a_3\right]\cdot t}} \tag{32}$$

$k_{t,cnctr}$ is a stress concentration factor higher than one (they proposed 1.5, similar to Eurocode). The tensile plane is thus divided in two parts, the inner and the outer.

Tensile forces of outer and inner part of the connection are then combined with the corresponding shear forces with the interaction formula (8) obtaining the forces $F_{ten+shear,out,Rd}$ and $F_{ten+shear,in,Rd}$.

Then forces of each element of inner and outer part are obtained:

$$F_{in,Rd,i} = \min\left(F_{ductile,in}\ ,\ F_{ten+shear,in,Rd}\right) \tag{33}$$

$$F_{out,Rd,i} = \min\left(F_{ductile,in}\ ,\ F_{spl,end,Rd}\ ,\ F_{spl,hole+shear,out,Rd}\ ,\ F_{ten+shear,out,Rd}\right) \tag{34}$$

The connection capacity is obtained by the sum of the outer and inner parts:

$$F_{Rd} = \sum_i F_{in,Rd,i} + \sum_i F_{out,Rd,i} \tag{35}$$

5. Net tensile failure

The tensile failure has been already covered as part of the block failure. It can be indeed analysed as a block-shear failure excluding the lateral failure planes, and considering the net tensile area. It is thus not explicitly covered as such by any code, except for the New Zealand draft.

5.1 Eurocode 5

Although in the 2004 version of Eurocode 5 [2] there is no explicit definition of net tensile failure, it is established in section 6.1.2 that:

$$\sigma_{t,0,d} \le f_{t,0,d} \tag{36}$$

Which means that in any timber member loaded in tension parallel-to-the-grain, the design tensile stress along the grain $\sigma_{t,0,d}$ must be lower or equal to the design strength along the grain $f_{t,0,d}$. This condition should be also accomplished in the connection.

5.2 New Zealand draft

The design net tensile strength in the New Zealand standard draft [6] defines a head tensile plane (R_T) as:

$$F_{net,Rd} = \phi_w \cdot R_t \cdot k_1 \cdot k_{12} = \phi_w \cdot f_{t,0,k} \cdot A_n \cdot k_1 \cdot k_{12} \tag{37}$$

where A_n is the member net cross-sectional area and must be $\ge 0.75A_g$, the member gross cross-sectional area. The k and ϕ are code calibration parameters.

6. Conclusions

The assessment of brittle capacity, which actually is the capacity of the timber members of the connection, is of utmost importance. However, till recently, the capacity of the connections has usually been assumed as that derived from the EYM model, which is the ductile capacity (provided that the capacity of the timber members is higher).

Brittle failure of connections loaded parallel to the grain have not yet been covered in detail in the Eurocode, which includes a model for block-shear failure in its Annex A [2], and does not explicitly consider splitting and row-shear.

This paper provides a detailed description of some of the existing proposals for the different brittle failure modes. Special attention is given to those proposals which are to be included in the future New Zealand standard [6], which tries to include all the different brittle failure modes.

A detailed performance analysis, based on the benchmarking of the existing proposals, has been done in the accompanying paper published by the same authors in the framework of the COST Action FP1402 [1].

Acknowledgements

The second author is supported by a PhD fellowship from the Programa de Becas FPU del Ministerio de Educación y Ciencia (Spain) under the grant number FPU15/03413. He would also like to thank the Asociación de Amigos of the University of Navarra for their help with a fellowship in early stages of this research. Both authors would like to acknowledge the contribution of the COST Action FP1402 for the development of this work.

Parts of the contents in this chapter have first been published in the scientific paper "Performance assessment of existing models to predict brittle failure modes of steel-to-timber connections loaded parallel-to-grain with dowel-type fasteners" by J.M. Cabrero and M. Yurrita (Engineering Structures, 2018) [1].

References

[1] Cabrero JM, Yurrita M (2018) Performance assessment of existing models to predict brittle failure modes of steel-to-timber connections loaded parallel-to-grain with dowel-type fasteners. *Engineering Structures*, in press. DOI: 10.1016/j.engstruct.2018.03.037.

[2] *EN 1995-1-1:2004 (Eurocode 5)* Design of timber structures – Part 1-1: General – Common rules and rules for buildings. CEN, Brussels.

[3] Jorissen AJM (1997) *Multiple fastener timber connections with dowel type fasteners*. CIB-W18 Meeting 30, Paper 30-7-5, Vancouver, Canada.

[4] Jorissen AJM (1998) *Double shear timber connections with dowel type fasteners*. PhD thesis, Delft University of Technology.

[5] Volkersen O (1938) Die Nietkraftverteilung in zugbeanspruchten Nietverbindungen mit konstanten Laschenquerschnitten. *Luftfahrtforschung* **35**:4-47.

[6] Quenneville P, Zarnani P (2017) *Proposal for the connection chapter of the New Zealand code "Design of Timber Structures"*.

[7] Hanhijärvi A, Kevarinmäki A (2008) *Timber failure mechanisms in high-capacity dowelled connections of timber to steel – experimental design and results*. VTT Publication vol. 677, VTT Technical Research Centre of Finland.

[8] Jensen JL, Quenneville P (2011) Experimental investigations on row shear and splitting in bolted connections. *Construction and Building Materials* **25**(5):2420-2425.

[9] Jensen JL, Quenneville P (2010) Fracture mechanics analysis of row shear failure in dowelled timber connections. *Wood Science and Technology* **44**(4):639-653.

[10] Jensen JL, Quenneville P (2011) Fracture mechanics analysis of row shear failure in dowelled timber connections: asymmetric case. *Materials and Structures* **44**(4):351-360.

[11] Zarnani P, Quenneville P (2014) Wood block tear-out resistance and failure modes of timber rivet connections: A stiffness-based approach. *Journal of Structural Engineering* **140**(2):04013055.

[12] Zarnani P, Quenneville P (2014) Splitting strength of small dowel-type timber connections: Rivet joint loaded perpendicular to grain. *Journal of Structural Engineering* **2**(10):04014064.

[13] Zarnani P, Quenneville P (2012) *A stiffness-based analytical model for wood strength in timber connections loaded parallel to grain: Riveted joint capacity in brittle and mixed failure modes*. CIB-W18 Meeting 45, Paper 45-7-1, Växjö, Sweden.

[14] Zarnani P, Quenneville P (2014) Strength of timber connections under potential failure modes: An improved design procedure. *Construction and Building Materials* **60**:81-90.

[15] Zarnani P, Quenneville P (2014) *Resistance of connections in cross-laminated timber (CLT) under block tear-out failure mode*. INTER Meeting 47, Paper 47-7-3, pp. 117-129, Bath, UK.

[16] Kangas J, Vesa J (1998) *Design on timber capacity in nailed steel-to-timber joints*. CIB-W18 Meeting 31, paper 31-7-4, Savonlinna, Finland.

[17] Foschi R, Longworth J (1975) Analysis and design of griplam nailed connections. *Journal of the Structural Division* **101**(12):2537-2555.

[18] Johnsson H, Parida G (2013) Prediction model for the load-carrying capacity of nailed timber joints subjected to plug shear. *Materials and Structures* **46**(12):1973-1985.

Brittle failure of connections loaded perpendicular to grain

Robert Jockwer
ETH Zürich
Switzerland

Philipp Dietsch
Technical University of Munich
Germany

Summary

Connections loaded perpendicular to grain are prone to brittle failure due to fracture induced by tension perpendicular to grain stresses. Different approaches can be found in design codes and literature to account for the reduction of load-carrying capacity in the design of the structure. In this paper selected design approaches are discussed and their behaviour with regard to different geometrical parameters is analysed. The structural behaviour of connections loaded perpendicular to grain is evaluated on the basis of a test series carried out at ETH Zurich and based on test results from literature. The impact of different geometrical parameters on the load carrying capacity is demonstrated and the design approaches are benchmarked by the large number of individual test results. Recommendations for a safe design are given at the end of the paper.

1. General

1.1 Geometry of connections loaded perpendicular to the grain

The geometrical properties and denotations of a connection loaded perpendicular to the grain are illustrated in Fig. 1. The relevant geometrical properties are the dimensions of the beam ($b \cdot h$), relative connection height α, connection width a_r and height h_m. In addition, the geometry of the connection can be described by the number of columns m and rows n of fasteners. The height of the connection and the position of specific fasteners can be specified by the distance between the n^{th}-row of fasteners to the loaded edge. In case of multiple connections, the distance between each other is l_l or l_1. The distance to the end grain is denoted by a_1.

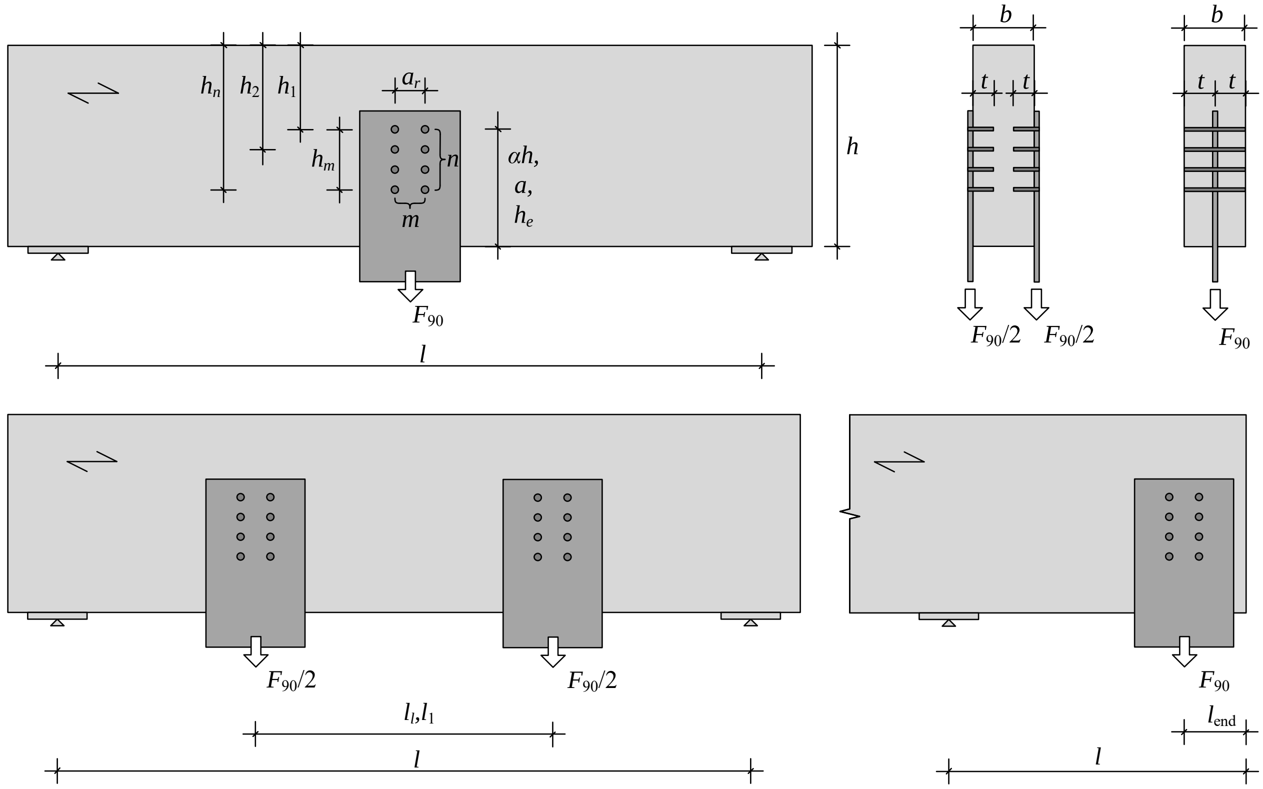

Fig. 1. Denotation at connections loaded perpendicular to grain.

1.2 Types of connections loaded perpendicular to the grain

Connections loaded perpendicular to the grain are often made by means of e.g. nails, dowels, bolts, (self-tapping) screws, glued-in rods or shear connectors. The number of fasteners in a connection depends on the type of fastener used. Small diameter fasteners like nails or rivets are often used with a larger quantity within one connection whereas large diameter fasteners like bolts, glued-in rods or shear connectors are also used individually.

Connections can be either made as timber/timber connections like in the case of many shear connectors, or can be made in combination with steel plates like for (3D) nailing plates or dowelled slotted in metal steel plates. Glued-in rods or self-tapping screws can be directly loaded in tension and do not need additional elements for hanging loads.

2. Design approaches

The existing design approaches for connections loaded perpendicular to grain can be separated into approaches based on stress criteria or fracture mechanics theory. A good review on existing approaches can be found in e.g. [1, 2].

An overview of the background and relation of the existing design approaches is illustrated in Fig. 2. In this chapter all the illustrated design approaches will be presented and discussed more in detail.

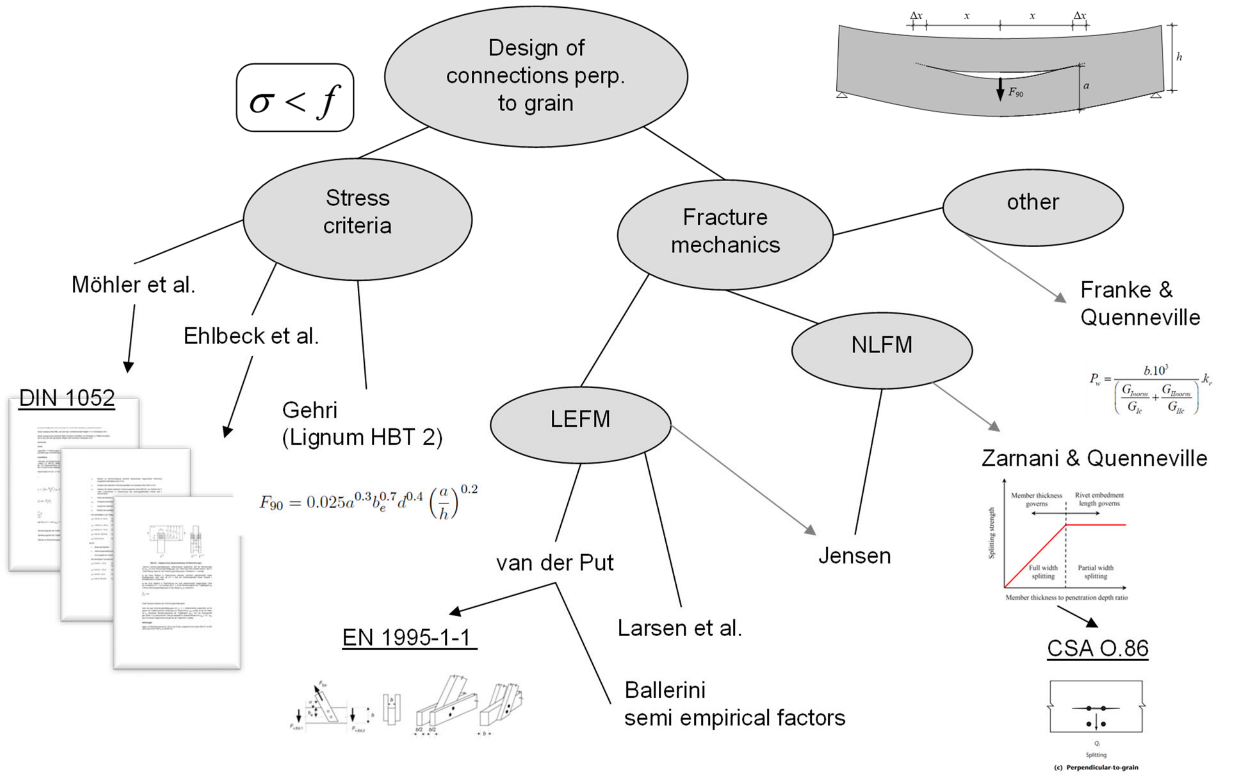

Fig. 2. Illustration of the background of design approaches for connections loaded in tension perpendicular to the grain.

2.1 Approaches based on stress criteria

2.1.1 Möhler and Siebert

A first approach based on stress criteria was presented by Möhler and Siebert [3, 4]. The approach is based on the test series reported in [3, 5]. The volume loaded in tension perpendicular to the grain is based on the studies on volume effect by Barrett et al. [6].

$$F_{90,mean} = \frac{f(a,h)}{10} \cdot \frac{\left(b_{eff} \cdot W' \cdot h_1\right)^{-0.2} \cdot b_{eff} \cdot W'}{s} \quad [\text{kN}] \tag{1}$$

with b_{eff}, W' and h_1 in [cm].

$$\frac{f(a,h)}{10} = 0.68 + 1.37 \cdot \frac{h}{100} \cdot 0.2 \cdot \frac{a}{h} + 0.4 \cdot \frac{a}{100} \tag{2}$$

with a and h in [cm].

Factor s for consideration of the connection height h_m is based on the assumption of stress distribution above of the fasteners according to Fig. 3. The distance h_i of the fastener i from the unloaded beam edge.

$$s = \frac{1}{n}\sum_{i=1}^{n}\left(\frac{h_1}{h_i}\right)^2 \tag{3}$$

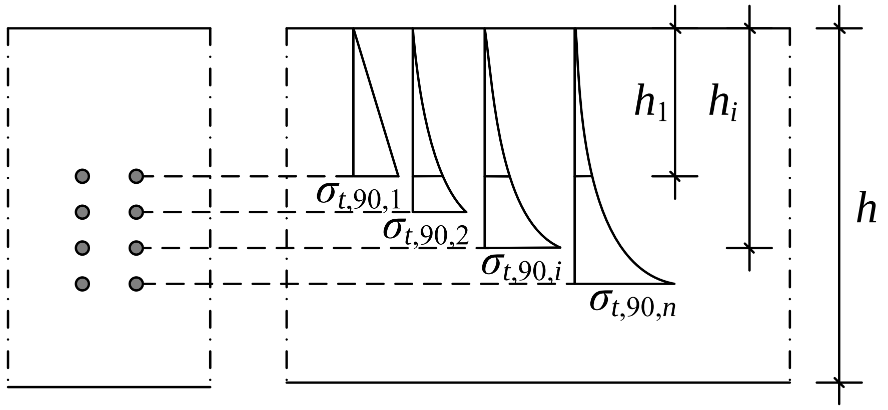

Fig. 3. Distribution of tension perpendicular to grain stresses in different rows n of the connection according to Möhler and Siebert [3].

The effective beam width b_{eff} was equal to the beam width b. If the beam is loaded only partially over the beam width due to e.g. a small penetration depths of the fasteners the effective beam width should be reduced $b_{eff} \leq b$. The connection width W' is specified as follows:

$W' = m \cdot 2.15 \cdot d$	For shear connectors type Appel
$W' = m \cdot 5 \cdot d$	For dowels
$W' = m \cdot 5 \cdot d$	For nails

2.1.2 Ehlbeck et al.

The approach in Eq. (1) was further developed by Ehlbeck [7, 8]. An additional parameter accounting for the connection width was included. The approach was limited to relative connection heights $\alpha \leq 70\%$ based on the observation from tests [3, 5, 9]. In the tests it was observed that connections with stiffer fasteners reach higher load-carrying capacities. The basic equation is based on a verification of tension perpendicular to grain stresses:

$$\sigma_{t,90,d} = \eta \cdot k_r \cdot \frac{F_{90,d}}{A_{ef}} \leq 15 \cdot A_{ef}^{-0.2} \cdot f_{t,90,d} \quad (4)$$

The factor η describes the amount of tension perpendicular to the grain stresses that result from the portion of shear stresses according to beam theory:

$$\eta = 1 - 3 \cdot (\alpha)^2 + 2 \cdot (\alpha)^3 \quad (5)$$

The factor k_r is similar to Equation (3) by [3].

$$k_r = \frac{1}{n} \sum_{i=1}^{n} \left(\frac{h_1}{h_i} \right)^2 \quad (6)$$

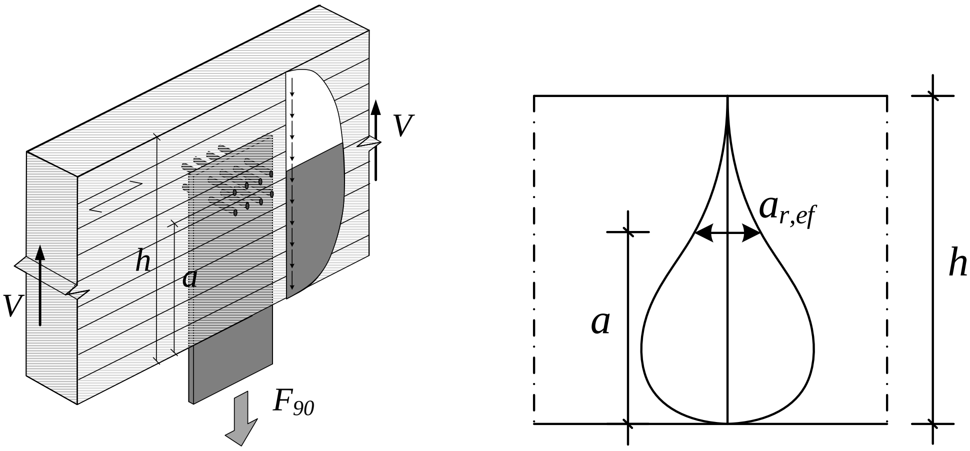

Fig. 4. Impact of the relative connection height α on tension perpendicular to grain stresses (left) and impact of the width of the connection (right) according to Ehlbeck et al. [7].

The width of the effective width is accounted for by the area loaded in tension perpendicular to grain $A_{ef} = a_r \cdot b$ and an additional factor c_h.

$$a_{r,ef} = \sqrt{a_r^2 + (c_h)^2} \tag{7}$$

For connections with only one column of fasteners the theoretical width $a_r = 0$ is increased by the empirically determined value c_h for the effective width $a_{r,ef}$ as follows:

$$c = \frac{4}{3}\sqrt{\alpha \cdot (1-\alpha)^3} \tag{8}$$

Factor c is derived from the assumed stress distribution according to Fig. 4. For two single connections with a distance l_l between each other the effective total width can be derived as follows.

$$a_{r,ef,total} = a_{ef,r} \cdot \left(1 + \frac{l_l}{l_l + a_r}\right) \tag{9}$$

For connections at a cantilever only half of the effective width of the connection is accounted for in case the connection has a distance less than half the beam height from the beam end.

2.1.3 Lignum HBT 2

A fully empirical approach was given in Lignum Holzbautabellen 2 [10], that was calibrated from experiments from [3, 4, 11] as discussed in [12]. The approach was developed mainly for the purpose to give information for the design of 3D nail plates like hold-down or joist hangers and not for larger connection loaded perpendicular to the grain. The approach accounts for different types of fasteners (Fig. 5).

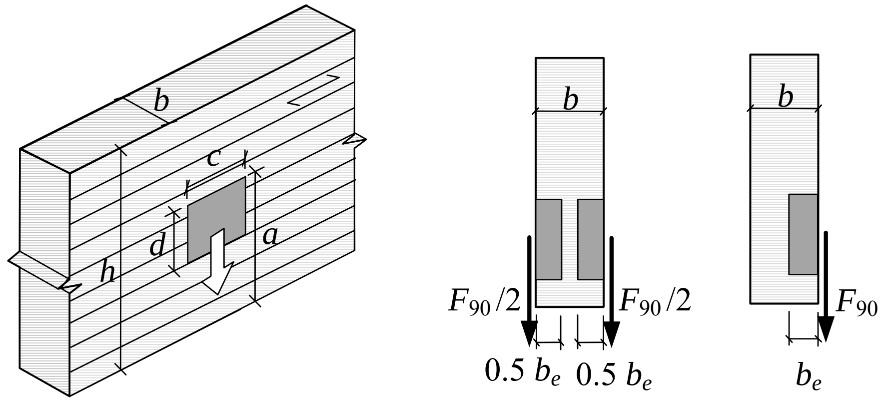

Fig. 5. Denotations of the geometrical parameters at a connection loaded perpendicular to the grain according to [10].

The effective width be of the beam in dependency of the diameter and type of the fastener for double sided connections:

$b_e = \min\{b; 2 \cdot t; 24 \cdot d\}$	Nails
$b_e = \min\{b; 0.6 \cdot d\}$	Split rings
$b_e = \min\{b; d\}$	Shear connectors
$b_e = \min\{b; 6 \cdot d\}$	Dowels or bolts

The effective width be of the beam in dependency of the diameter and type of the fastener for single sided connections:

$b_e = \min\{0.5 \cdot b; t; 12 \cdot d\}$	Nails
$b_e = \min\{0.5 \cdot b; 0.3 \cdot d\}$	Split rings
$b_e = \min\{0.5 \cdot b; 0.5 \cdot d\}$	Shear connectors

The strength parameter 0.025 was calibrated based on test results for a safety margin of 4.

$$F_{90} = 0.025 \cdot a^{0.3} \cdot b_e^{0.7} \cdot d^{0.4} \cdot \left(\frac{a}{h}\right)^{0.2} \qquad (10)$$

With a, b_e, d, h in [mm]; F_{90} in [kN]

The impact of the width of the connection is stated to be low and could be accounted for by the factor $(1 + c/a)^{0.1}$ in case more detailed design is required. For connections at cantilever beams only half the load-carrying capacity is accounted for.

2.2 Fracture mechanics based approaches

2.2.1 van der Put

A design approach for connections loaded perpendicular to the grain was presented by van der Put [13, 14]. The model is based on the crack formation and propagation starting at a single dowel as shown in Fig. 6. Hence, the geometry of the connection is not accounted for. The approach is based on a 2D model and assumes a linear dependency from the beam width.

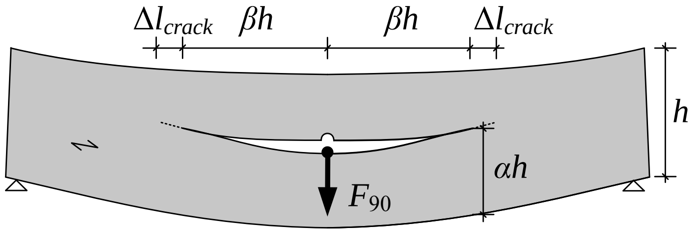

Fig. 6. Model of a beam with a connection perpendicular to the grain and a crack propagating at a single fastener.

The critical load for crack progression was derived by van der Put from the equilibrium of energies during infinitesimal crack growth by Δl_{crack} for a crack length $\beta h = 0$.

$$F_{90} = 2 \cdot b \cdot \sqrt{\frac{G \cdot G_c \cdot \alpha h}{\frac{3}{5}(1-\alpha)}} \tag{11}$$

A more generalized approach was presented by Jensen et al. [15] for crack length $\beta h > 0$. In addition Jensen et al. proposed design equations for adjacent connections with different distance, see also Fig. 7.

$$F_{90} = 2 \cdot b \cdot \sqrt{\frac{G \cdot G_c \cdot \alpha h}{\frac{3}{5}(1-\alpha) + \frac{3}{2}\left(\frac{\beta}{\alpha}\right)^2 \frac{G}{E}\left(1-\alpha^3\right)}} \tag{12}$$

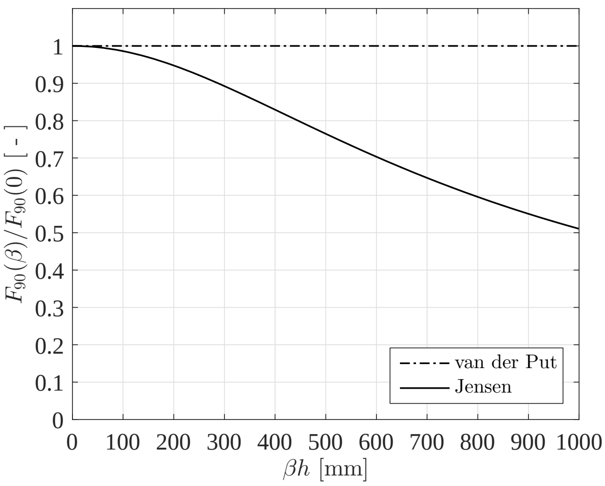

Fig. 7. Relative reduction of crack propagation load with increasing crack length βh for $\alpha = 0.6$, $E = 11500$ N/mm^2 and $G = 650$ N/mm^2.

The calibration of the parameter $G \cdot G_c$ is matter of ongoing discussion. Values in the range of $C_{1,c} \approx 10$ N/mm$^{1.5}$ are discussed in [14, 16]. The value currently given in EN 1995-1-1 [17] is considered to overestimate the load-carrying capacity of connection loaded perpendicular to the grain (e.g. [1, 18, 19]).

2.2.2 Larsen and Gustafsson

The duration of load (DOL) effect on the material parameter $C_{1,c}$ was studied in a test series by [20] on tension specimens loaded by dowel connections perpendicular to the grain. The parameter was calculated from the tests according to Eq. (13).

$$F_{ult} = 2 \cdot b \cdot C_{Larsen} \cdot \sqrt{\alpha \cdot h} \tag{13}$$

where

$$C_{Larsen} = \sqrt{\frac{2}{\beta_s} \cdot G \cdot G_f} \tag{14}$$

The shear correction factor β_s varies between $\beta_s = 1$ for the tests on single rows of fasteners ($m = 1$) in the tests by [20] and the common values according to beam theory $\beta_s = 6/5$ for the evaluation of test results from literature yielding to $C_{Larsen} = C_1$.

2.3 Jensen et al.

Jensen did extensive studies on various problems related to fracture due to loading perpendicular to the grain. A summary of different models for connections loaded perpendicular to the grain based on quasi-nonlinear fracture mechanics (QNLFM) theory is given in [21]. The theory can be illustrated as the theory of a beam on elastic foundation. The softening behaviour during fracture is accounted for by this approach, which yields to more complex equations.

$$P_{90} = \lambda \cdot P_{90,LEFM} \tag{15}$$

$$\lambda = \frac{\sqrt{2 \cdot \varsigma + 1}}{\varsigma + 1} \tag{16}$$

$$P_{90,LEFM} = 2 \cdot b \cdot C_1 \cdot \sqrt{\frac{\alpha h}{1 - \alpha}} \tag{17}$$

and

$$C_1 = \sqrt{\frac{5}{3} \cdot G \cdot G_c} \tag{18}$$

and

$$\varsigma = \frac{C_1}{f_{t,90}} \cdot \sqrt{\frac{10 \cdot G}{\alpha h \cdot E}} \tag{19}$$

For a connection at a cantilever beam a modification of the approach given in Jensen [22] is proposed:

$$P_{90} = P_{90,LEFM} \cdot \min \begin{cases} \dfrac{1}{2 \cdot \sqrt{2\varsigma + 1}} + \dfrac{b \cdot f_t \cdot l_e}{P_{90,LEFM}} \\ \dfrac{2 \cdot \sqrt{2\varsigma + 1}}{\varsigma + 1} \end{cases} \tag{20}$$

This equation was verified for moment connections in spans between two beam parts.

2.3.1 Ballerini

Ballerini [23, 24] included parameters f_w and f_r accouting for the width (a_r) and the height (h_m), respectively, in modified versions of the design approach by van der Put [13] and Jensen et al. [25]. A different power of the relative connection height was based on a better fit with experiments.

$$F_{ult} = 2 \cdot b \cdot C_1 \cdot \sqrt{\frac{\alpha h}{\left(1 - \alpha^3\right)}} f_w \cdot f_r \tag{21}$$

where:

$$f_w = \min \begin{cases} 1 + 0.75 \cdot \left(\dfrac{a_r + l_l}{h} \right) \\ 2.0 \end{cases} \tag{22}$$

$$f_r = 1 + 1.75 \cdot \frac{\kappa}{1 + \kappa} \tag{23}$$

$$\kappa = \frac{n \cdot h_m}{1000} \tag{24}$$

2.3.2 Franke and Quenneville

The distinction between mode 1 and mode 2 fracture modes was accounted for in the design approach proposed by Franke and Quenneville [26], which is based on numerical models.

$$F_{90} = \frac{b}{\dfrac{G_{norm}^{I}}{G_c^{I}} + \dfrac{G_{norm}^{II}}{G_c^{II}}} \cdot k_r \tag{25}$$

G^I_c and G^{II}_c are the critical energy release rates of mode 1 (tension perpendicular to grain) and mode 2 (shear) failure. The normalized fracture energies G^i_{norm} are developed based on numerical studies and calibrated by tests.

$$G_{norm}^{I} = e^{\left(h^{-1}\left(200-10\cdot(\alpha h)\cdot h^{-0.25}-a_r\right)\right)} \quad \text{for solid timber and glulam} \tag{26}$$

$$G_{norm}^{I} = e^{\left(0.8-1.6\cdot(\alpha h)\cdot h^{-0.1}-10^{-3}\cdot a_r\right)} \quad \text{for LVL} \tag{27}$$

$$G_{norm}^{I} = 0.05 + 0.12\cdot\alpha + 10^{-3}\cdot a_r \quad \text{for solid timber and glulam} \tag{28}$$

The impact of the number of rows n of fasteners is accounted for by factor k_r:

$$k_r = \begin{cases} 1 & \text{for } n=1 \\ 0.1+(\arctan(n))^{0.6} & \text{for } n>1 \end{cases} \tag{29}$$

2.3.3 Zarnani and Quenneville

Zarnani and Quenneville [27] presented an approach that considered the crack length along the fibre direction. Depending on the slenderness of the fasteners, full (corresponding to $P_{s,b}$) or partial cracking over the width (corresponding to $P_{s,tef}$) of the beam can be assumed. For very stout dowels embedment failure can be expected. The effective width of the connection is denoted $w_{net} = a_r - m \cdot d$ and the distance of the connection to the unloaded end-grain to the left or right is denoted as $a_{3c,L}$ or $a_{3c,R}$, respectively.

$$P_w = n_P \cdot \min\begin{cases} P_{s,tef} \\ P_{s,b} \end{cases} \tag{30}$$

$$P_{s,tef} = C_t \cdot f_{tp} \cdot t_{ef} \cdot \left[w_{net} + \min\left(\beta\alpha h, a_{3c,L}\right) + \min\left(\beta\alpha h, a_{3c,R}\right)\right] \tag{31}$$

where

$$C_t = \begin{cases} 1.264\cdot\varsigma^{-0.37} & \text{, for } \varsigma<1.9 \\ 1 & \text{, for } \varsigma\geq 1.9 \end{cases}, \quad \text{where } \varsigma = \frac{a_{1c}}{a_2\left(n_e-1\right)} \tag{32}$$

$$P_{s,b} = \eta\cdot b\cdot C_{fp}\cdot\sqrt{\frac{\alpha h}{1-\alpha}} \tag{33}$$

where

$$\eta = \frac{\min\left(w_{net}+\gamma\alpha h, a_{3c,L}\right)+\min\left(\gamma\alpha h, a_{3c,R}\right)}{2\gamma\alpha h} \tag{34}$$

The parameter η amounts $\eta = 1$ for a single fastener in midspan. A reduction of load-carrying capacity can be observed at a distance to the beam end in cantilever beams of $a_{3c}/(\alpha h) = 4$ (for LVL) and $a_{3c}/(\alpha h) = 2.7$ (for glulam). Therefore, the effective crack length coefficient γ for full separation is $\gamma = 4$ for LVL and $\gamma = 2.7$ for glulam.

2.3.4 Additional design approaches

Additional, mostly empirical design approach can be found e.g. in Lehoux and Quenneville [28], Quenneville and Mohammad [29]. These approaches are quite specific with regard to the type of connection used and the timber properties. They are not considered in the further analysis.

2.4 Design approaches in standards

2.4.1 DIN 1052

The approach in DIN 1052 [30] is based on the studies by Möhler and Lautenschläger [5], Möhler and Siebert [3] and Ehlbeck et al. [7].

$$F_{90,d} \leq R_{90,d} = k_s \cdot k_r \cdot \left(6.5 + 18 \cdot \alpha^2\right) \cdot \left(t_{ef} \cdot h\right)^{0.8} \cdot f_{t,90,d} \tag{35}$$

$$k_s = \max \begin{cases} 1 \\ 0.7 + \dfrac{1.6 \cdot a_r}{h} \end{cases} \tag{36}$$

$$k_r = \frac{n}{\sum_{i=1}^{n} \left(\dfrac{h_1}{h_i}\right)^2} \tag{37}$$

In addition the following specifications are made:

- Connections with small relative connection height $a < 0.2$ are only allowed for short duration of load (e.g. uplift by wind actions)
- Highly loaded connections with very large connection width $a_r/h > 1$ and $F_{90,d} > 0.5 \cdot R_{90,d}$ have to be reinforced.
- For multiple connections along the direction of the beam axis with a distance $l_l \geq 2 \cdot h$ the individual resistance $R_{90,d}$ can be assumed for each connection.
- For multiple connections along the direction of the beam axis with a distance $0.5 \cdot h \geq l_l$ the total resistance of the group of connections must not exceed $R_{90,d}$.
- For two connections with a distance along the direction of the beam axis of $0.5 \cdot h < l_l < 2 \cdot h$ the individual resistance $R_{90,d}$ of each connection has to be reduced by the factor k_g according to Equation (38).

  $$k_g = \frac{l_1}{4 \cdot h} + 0.5 \tag{38}$$

- Two or more adjacent connections with a distance along the direction of the beam axis of $l_l < 2 \cdot h$ have to be reinforced if $F_{90,d} > 0.5 \cdot k_g \cdot R_{90,d}$.
- Connections at cantilever beams with an end grain distance $a_1 < h$ have to be reinforced if $F_{90,d} > 0.5 \cdot R_{90,d}$.

The effective penetration depth t_{ef} of the fasteners is for double sided connections:

$t_{ef} = \min\{b; 2 \cdot t; 24 \cdot d\}$	Timber/Timber connections with nails or screws
$t_{ef} = \min\{b; 2 \cdot t; 30 \cdot d\}$	Steel/Timber connection with nails
$t_{ef} = \min\{b; 2 \cdot t; 12 \cdot d\}$	Dowelled or bolted connections
$t_{ef} = \min\{b; 100\text{ mm}\}$	Connections with shear or split ring connections etc.
$t_{ef} = \min\{b; 6 \cdot d\}$	Connections with glued-in rods

The effective penetration depth t_{ef} of the fasteners is for single sided connections:

$t_{ef} = \min\{b; t; 12 \cdot d\}$	Timber/Timber connections with nails or screws
$t_{ef} = \min\{b; t; 15 \cdot d\}$	Steel/Timber connection with nails
$t_{ef} = \min\{b; t; 6 \cdot d\}$	Dowelled or bolted connections
$t_{ef} = \min\{b; 50\text{ mm}\}$	Connections with shear or split ring connections etc.

2.4.2 EN 1995-1-1

The approach given in EN 1995-1-1 [17] is based on the studies by van der Put [13]. The approach is based on a verification of shear stresses in the beam cross-section as shown in Fig. 8. Hence, for connections outside midspan with an unsymmetric spread of shear force the higher of the shear force values on the sides ($F_{v,Ed,1}$) or ($F_{v,Ed,2}$) is decisive for the load carrying capacity of the connection. For connections at a cantilever the force transmitted to the support is taken into account directly.

$$F_{v,Ed} \leq F_{90,Rd} \tag{39}$$

$$F_{v,Ed} = \max\begin{cases} F_{v,Ed,1} \\ F_{v,Ed,2} \end{cases} \tag{40}$$

$$F_{90,Rd} = 14 \cdot b \cdot w \cdot \sqrt{\frac{\alpha h}{1-\alpha}} \tag{41}$$

For punched metal plate fasteners an increase of load-carrying capacity can be accounted for.

- for punched metal plate fasteners, where w_{pl} is the with d of the nailing plate:

$$w = \max\left\{\left(\frac{w_{pl}}{100}\right)^{0.35}; 1\right\} \tag{42}$$

- for all other fasteners:

$$w = 1 \tag{43}$$

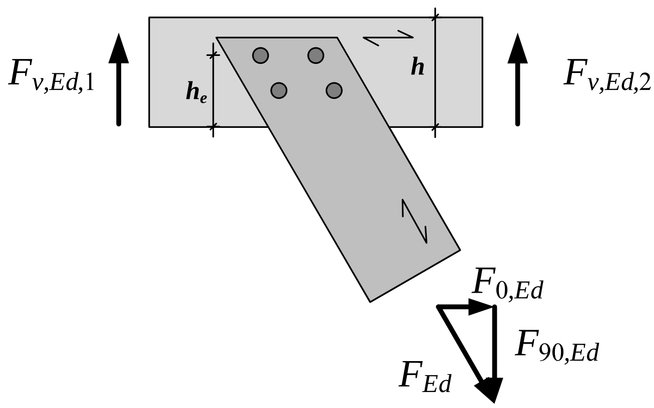

Fig. 8. Connection loaded at an angle to the grain according to Eurocode 5 [17].

3. Evaluation of design approaches

3.1 Material properties

The different approaches depend on different material parameters because of the theory they are based on. The empirically based approaches by Möhler and Siebert [4] and Gehri [12] use the strength theory, namely the tension perpendicular to the grain strength. In order to account for the special loading situation at perpendicular to the grain connections Ehlbeck et al. [7] proposes a specific tension perpendicular to the grain strength value $f_{t,90}$ in contrast to the general strength value determined according to 408 [32]. This value accounts for different effects such as the size effects [33, 34] and duration of load (DOL) and variations in moisture content [35, 36]. The application of the general strength value $f_{t,90,k}$ according to EN 338 [37] or EN 14080 [38] should be avoided for the special situation of a connection loaded in tension perpendicular to the grain.

The fracture energy G_f for the crack opening mode 1 and the in plane crack shearing mode 2 is used in the approaches on basis of fracture mechanics [13, 15]. Values for the fracture energy for the mode 1 can be found e.g. in [20], for the mode 2 in [39].

3.2 Impact of geometrical parameters

3.2.1 Beam height *h* and beam width *b*

A square root dependency of the member size is accounted for by the linear elastic fracture mechanics based approaches [13, 23], i.e. $h^{1/2}$. The impact of beam with is linear in these approaches. The approaches by Jensen et al. [21] and by Franke and Quenneville [26] use a more complex height effect due to the underlying non-linear fracture mechanics theory or due to the fit to numerical simulations. Approaches considering volume effects [3, 7] also account for the impact of beam width and result in a height effect $h^{0.8}$. The different impact of beam height and beam width is shown in Fig. 9 where the load-carrying capacity is normalized to the beam height $h = 600$ mm and a (theoretical) beam width $b = 10$ mm and $d = 12$ mm. The approaches based on a limited number of tests [12] or simulations [26] show for very large and very small beams a considerably different behaviour.

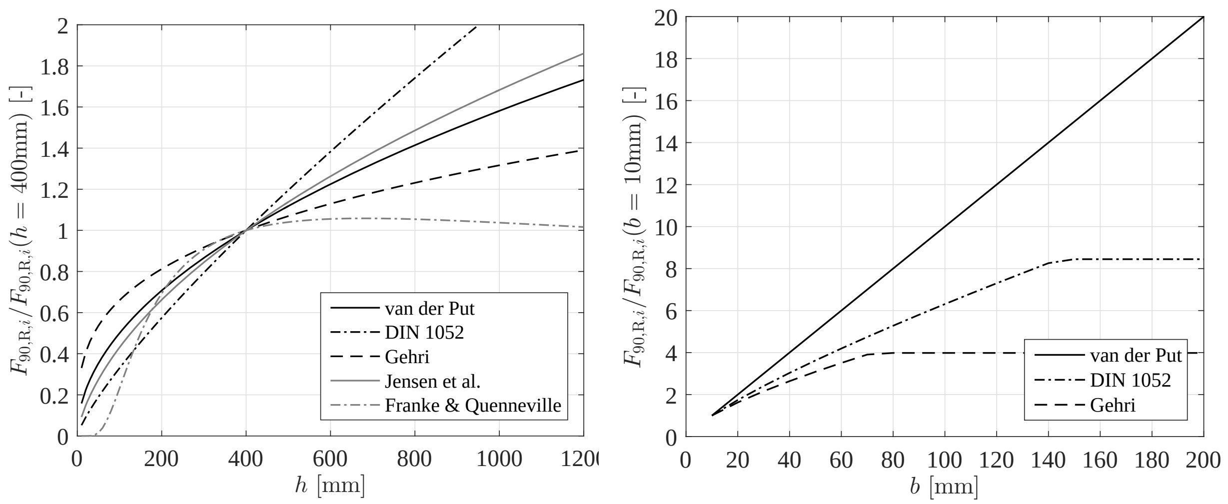

Fig. 9. Impact of the beam height h and beam width b on the relative load-carrying capacity $F_{90,R,i}/F_{90,R,i}(ref)$ for a reference of h = 600 mm, b = 10 mm and d = 12 mm.

Only the approaches by Möhler and Siebert [3] and Ehlbeck et al. [7] accounting for a volume effect and the approach by Gehri [12] consider a non-linear impact of the beam width. The approach in HBT 2 and in DIN 1052 set maximum values of effective beam width in dependency of the fastener type and diameter, which leads to a limitation of load-carrying capacity for beams of large width. This limitation of beam width accounts for the effect of early splitting around the fastener as discussed by e.g. Schoenmakers [1] and Zarnani and Quenneville [27].

3.2.2 Relative connection height α

The different impact of the relative connection height α on the load-carrying capacity is shown in Fig. 10. Especially for very large and very small values of α the differences increase drastically. Some approaches set limits of the range of application of these approaches such as DIN 1052 [30] and HBT 2 [10] ($0.2 \leq \alpha \leq 0.7$).

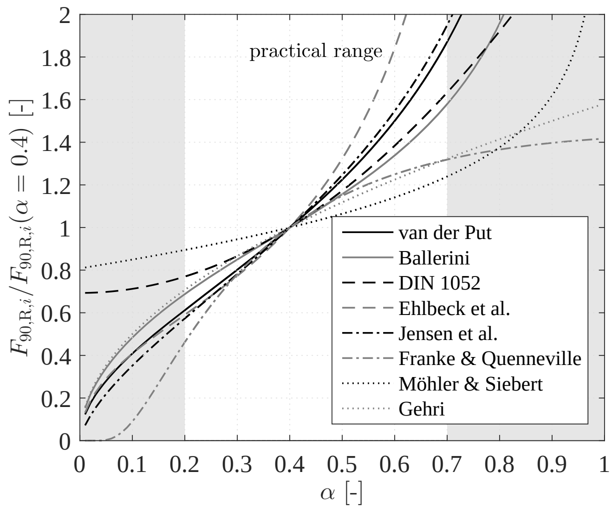

Fig. 10. Impact of α on the relative load-carrying capacity $F_{90,R,i}/F_{90,R,i}(ref)$.

3.2.3 Number of rows *n* and columns *m* of fasteners

The impact of the geometry of the connections is accounted for in the approaches based on strength theory [3, 7, 12, 30] and the semi-empirical approaches [23, 26]. The comparison of the impact of connection geometry is shown in Fig. 11.

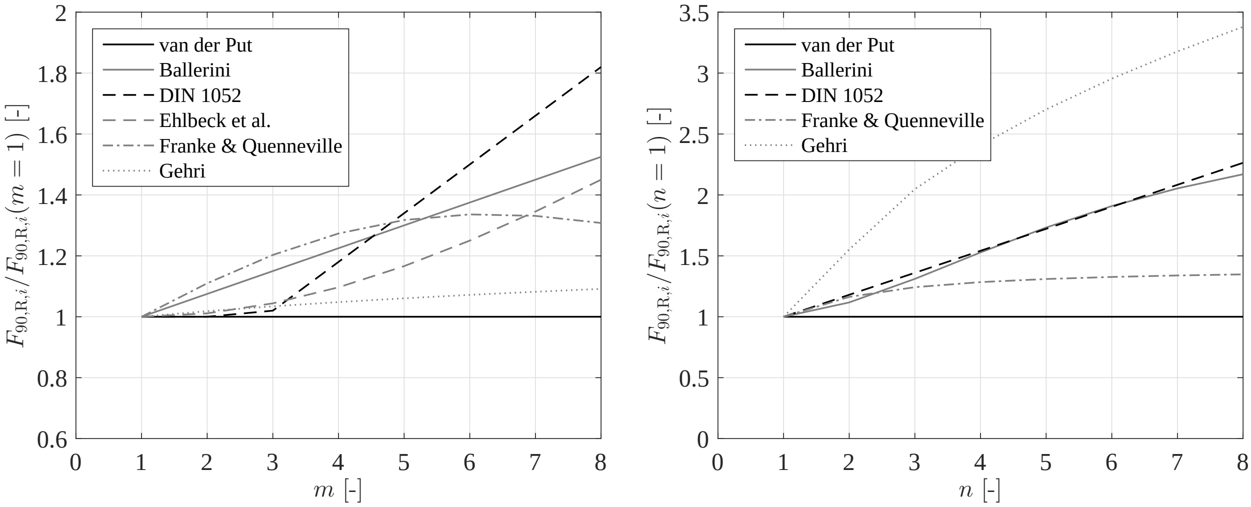

Fig. 11. Impact of the number of fastener columns m (left) and the number of fastener rows n (right) on the relative load-carrying capacities $F_{90,R,i}/F_{90,R,i}(ref)$.

4. Summary

4.1 Benchmarking against results from experiments

A detailed study and comparison of design approaches and test results can be found in Jockwer and Dietsch [31].

4.2 Conclusions

From the studies performed during the STSM at TU Munich, the following conclusions can be drawn:

- The height *h* and width *b* of the beam, relative connection height α, connection width a_r and connection height h_m are the most relevant geometrical parameters in order to estimate the load-carrying capacity of connections loaded perpendicular to the grain. The distance l_l between adjacent connections has an important impact on the load-carrying capacity as well. Of minor importance are the position of a connection along the span fo the beam or for connections on cantilever beams.
- The existing design approaches given in literature are based on strength criteria or fracture mechanics theory. When using such approaches in design standards the relevant material properties used in these approaches should be in line with the values specified in the corresponding material standards.

- Schoenmakers [1] and Jockwer et al. [19] showed the beneficial effect of reinforcement in order to restore the load-carrying capacity of beams with connections loaded perpendicular to the grain. When implementing a design approach for unreinforced connections loaded perpendicular to the grain into a design code, the benefit of reinforcement of such connections should be pointed out and design equations for the design of the reinforcement should be given.

4.3 Outlook and need for further research

From the evaluation in this contribution and from the studies during the STSM the following need for further research can be identified:

- Bolts, dowels, nails or shear connectors are the fastener types used in most experiments. The structural behavior also of other types of fasteners should be studied.
- The impact of multiple adjacent connections should be evaluated. Special emphasis should be paid to the potential higher risk of failure due to size or volume effects.
- Most approaches consider a linear impact of beam width on load-carrying capacity. The risk of early splitting in the vicinity of the fastener and a resulting effective width should be evaluated.
- Duration of load effects and effects from moisture variations are constant matter of concern for situations with tension perpendicular to the grain.

Reinforcement is an easy and efficient measure to restore the load-carrying capacity of beams with connections loaded perpendicular to grain.

Acknowledgements

The work presented in this paper was developed during a Short Term Scientific Mission at Technical University of Munich supported by COST Action FP 1402 (www.costfp1402.tum.de). The students C. Thiede and D. Gisler are thanked for their contributions in the frame of their master thesis.

A detailed evaluation of the contents in this chapter have been published in the scientific paper [31]: "Jockwer R, Dietsch P (2018). Review of design approaches and test results on brittle failure modes of connections loaded at an angle to the grain. *Engineering Structures* **171**: 362-372, DOI: 10.1016/j.engstruct.2018.05.061."

References

[1] Schoenmakers JCM (2010) *Fracture and failure mechanisms in timber loaded perpendicular to the grain by mechanical connections*. PhD thesis, Technische Universiteit Eindhoven, The Netherlands.

[2] Jockwer R (2016) *Review of design recommendations for connections loaded perpendicular to the grain*. COST Action FP1402 “Basis of Structural Timber Design” – from research to standards, in: Report of Short Term Scientific Mission at Technical University Munich, TU Munich, Germany.

[3] Möhler K, Siebert W (1980) *Ausbildung von Queranschlüssen bei angehängten Lasten an Brettschichtträgern oder Vollholzbalken*. Forschungsbericht der Versuchsanstalt für Stahl, Holz und Steine, Universität Fridericiana Karlsruhe, Germany.

[4] Möhler K, Siebert W (1981) Queranschlüsse bei Brettschichtträgern oder Vollholzbalken. *Bauen mit Holz* **83**:84-89.

[5] Möhler K, Lautenschläger R (1978) *Großflächige Queranschlüsse bei Brettschichtholz*. Forschungsbericht der Versuchsanstalt für Stahl, Holz und Steine, Universität Fridericiana Karlsruhe, Germany.

[6] Barrett JD, Foschi RO, Fox SP (1975) Perpendicular-to-grain strength of Douglas fir. *Canadian Journal of Civil Engineering* **2**:50-57.

[7] Ehlbeck J, Görlacher R, Werner H (1989) *Determination of perpendicular-to-grain stresses in joints with dowel-type fasteners – A draft proposal for design rules*.CIB-W18 Meeting 22, Paper 22-7-2, Berlin, Germany.

[8] Ehlbeck J, Görlacher R (1991) Empfehlung zum einheitlichen genaueren Querzugnachweis für Anschlüsse mit mechanischen Verbindungsmitteln. *Bauen mit Holz* **93**:825-828.

[9] Ehlbeck J, Görlacher R (1983) *Tragverhalten von Queranschlüssen mittels Stahlformteilen, insbesondere Balkenschuhen, im Holzbau*. Forschungsbericht der Versuchsanstalt für Stahl, Holz und Steine, Universität Fridericiana Karlsruhe, Germany.

[10] Lignum (1990) *Holzbau-Tabellen HBT 2*, Zürich, Switzerland.

[11] Ehlbeck J, Görlacher R (1985) Zum Querzugnachweis bei Anschlüssen mittels Stahlblechformteilen. *Bauen mit Holz* **87**:468-473.

[12] Gehri E (1988) *Tragmodell für Queranschlüsse*.

[13] van der Put TACM (1990) *Tension perpendicular to the grain at notches and joints*. CIB-W18 Meeting 23, Paper 23-10-1, Lisbon, Portugal.

[14] van der Put TACM, Leijten AJM (2000) *Evaluation of perpendicular to grain failure of beams caused by concentrated loads of joints*. CIB-W18 Meeting 33, Paper 33-7-7, Delft, The Netherlands.

[15] Jensen JL (2003) *Splitting strength of beams loaded by connections*. CIB-W18 Meeting 36, Paper 36-7-8, Colorado, USA.

[16] Leijten AJM, Jorissen A (2001) *Splitting strength of beams loaded by connections perpendicular to grain, model validation*. CIB-W18 Meeting 34, Paper 34-7-1, Venice, Italy.

[17] *EN 1995-1-1:2004 (Eurocode 5)* Design of timber structures – Part 1-1: General – Common rules and rules for buildings. CEN, Brussels.

[18] Jensen JL, Quenneville P (2011) Experimental investigations on row shear and splitting in bolted connections. *Construction and Building Materials* **25**(5):2420–2425.

[19] Jockwer R, Frangi A, Steiger R (2015) *Evaluation of the reliability of design approaches for connections perpendicular to the grain*. INTER Meeting 48, Paper 48-7-4, Šibenik, Croatia.

[20] Larsen H, Gustafsson P (2001) *Dowel joints loaded perpendicular to grain*. CIB-W18 Meeting 34, Paper 34-7-3, Venice, Italy.

[21] Jensen JL, Quenneville P, Girhammar UA, Källsner B (2012) *Beams loaded perpendicular to grain by connections – Combined effect of edge and end distance*. CIB-W18 Meeting 45, Paper 45-7-2, Växjö, Sweden.

[22] Jensen JL (2005) Quasi-non-linear fracture mechanics analysis of splitting failure in simply supported beams loaded perpendicular to grain by dowel joints. *Journal of Wood Science* **51**(6):577-582.

[23] Ballerini M (2004) *A new prediction formula for the splitting strength of beams loaded by dowel-type connections*. CIB-W18 Meeting 37, Paper 37-7-5, Edinburgh, Scotland.

[24] Ballerini M, Rizzi M (2007) Numerical analyses for the prediction of the splitting strength of beams loaded perpendicular-to-grain by dowel-type connections. *Materials and Structures* **40**(1):139–149.

[25] Jensen JL, Gustafsson PJ, Larsen HJ (2003) *A tensile fracture model for joints with rods or dowels loaded perpendicular-to-grain*. CIB-W18 Meeting 36, Paper 36-7-9, Colorado.

[26] Franke B, Quenneville P (2011) *Design approach for the splitting failure of dowel-type connections loaded perpendicular to grain*. CIB-W18 Meeting 44, Paper 44-7-5, Alghero, Italy.

[27] Zarnani P, Quenneville P (2013) *Wood splitting capacity in timber connections loaded transversely: Riveted joint strength for full and partial width failure modes*. CIB-W18 Meeting 46, Paper 46-7-5, Vancouver, Canada.

[28] Lehoux MCG, Quenneville P (2004) *Bolted wood connections loaded perpendicular-to-grain, a proposed design approach*. CIB-W18 Meeting 37, Paper 37-7-4, Edinburgh, Scotland.

[29] Quenneville P, Mohammad M (2001) *A proposed Canadian design approach for bolted connections loaded perpendicular-to-grain*. Proceedings of the International RILEM symposium on joints in timber structures, pp 61-70.

[30] *DIN 1052:2008-12*. Entwurf, Berechnung und Bemessung von Holzbauwerken – Allgemeine Bemessungsregeln und Bemessungsregeln für den Hochbau. Deutsches Institut für Normung e.V., Berlin, Germany.

[31] Jockwer R, Dietsch P (2018) Review of design approaches and test results on brittle failure modes of connections loaded at an angle to the grain. *Engineering Structures* **171**: 362-372, https://doi.org/10.1016/j.engstruct.2018.05.061.

[32] *EN 408:2010*. Timber structures – Structural timber and glued laminated timber – Determination of some physical and mechanical properties. CEN, Brussels.

[33] Mistler HL (2016) Design of glulam beams according to EN 1995 with regard to perpendicular-to-grain tensile strength: comparison with research results. *European Journal of Wood and Wood Products* **74**:169–175.

[34] Aicher S, Dill-Langer G, Klöck W (2002) *Evaluation of different size effect models for tension perpendicular to grain strength of glulam*. CIB-W18 Meeting 35, Paper 35-6-1, Kyoto, Japan.

[35] Aicher S, Dill-Langer G (1997) *DOL effect in tension perpendicular to grain of glulam depending on service classes and volume*. CIB-W18 Meeting 30, Paper 30-9-1, Vancouver.

[36] Aicher S, Dill-Langer G, Ranta-Maunus A (1998) Duration of load effect in tension perpendicular to the grain of glulam in different climates. *European Journal of Wood and Wood Products* **56**(5):295-305.

[37] *EN 338:2009*. Structural timber – Strength classes. CEN, Brussels.

[38] *EN 14080:2013*. Timber structures – Glued laminated timber and glued solid timber – Requirements. CEN, Brussels.

[39] Aicher S, Boström L, Gierl M, Kretschmann D, Valentin G (1997) *Determination of fracture energy of wood in mode II*. RILEM TC 133 Report, SP Swedish National Testing and Research Institute, Borås, Sweden.

Design approaches for dowel-type connections in CLT structures and their verification

Andreas Ringhofer *)
Institute of Timber Engineering and Wood Technology
Graz University of Technology, Austria

Reinhard Brandner *)
Institute of Timber Engineering and Wood Technology
Graz University of Technology, Austria

Hans Joachim Blass
Karlsruhe Institute of Technology
Germany

*) Joint first authorship

This contribution has already been published in the proceedings of the International Conference on Connections in Timber Engineering – From Research to Standards, COST FP1402, Graz, Austria.

Summary

Within the last 20 years, cross laminated timber (CLT) has become one of the most important building products in modern timber engineering. By the end of this decade its annual worldwide production volume is expected to exceed 1,000,000 m³. There is a strong interest of the industry, engineers, architects and contractors to implement CLT in European product, design and execution standards. This is part of the currently ongoing revision of Eurocode 5, supported by COST Action FP1402. In this context and in addition to the ULS and SLS verification of the panels themselves, provisions regarding the design of connections in CLT composed by dowel-type fasteners are of utmost importance.

Within this contribution, we aim on collecting, discussing and validating related approaches for characteristic values in literature for connections and single dowel-type fasteners in CLT. In addition, these models – especially dedicated to the withdrawal and embedment strength of dowels, nails and self-tapping screws – are compared with current regulations on dowel-type fasteners for solid timber and glulam as given in Eurocode 5. These comparisons are made in order to identify a pending need of modification of current Eurocode 5 equations and state-of-the-art regulations. Regarding the connection design, minimum spacing, edge and end distances as well as additional geometrical conditions, regulations on the effective number of fasteners in a group and minimum penetration depths are summarized. Finally, conclusions with respect to the single fastener properties, withdrawal and embedment strength,

are made together with comments on regulations ensuring the integrity of CLT structures. Overall, we aim on presenting a compilation of the current state-of-the-art knowledge on dowel-type fasteners in CLT as basis for implementing design provisions for CLT in the new connections chapter of Eurocode 5.

1. Introduction

Cross laminated timber (CLT) is a planar, large dimension engineered timber product, designed for structural purposes and capable of bearing loads in- and out-of-plane. CLT, with dimensions $t_{CLT} \times w_{CLT} \times \ell_{CLT}$, is commonly composed of an uneven number N of orthogonal layers ($t_\ell \times w_\ell$) of finger-jointed laminations or wood-based panels. Adjacent laminations within the same layer may also feature narrow face bonding; without narrow face bonding gaps between the laminations may occur. The orthogonal layers are typically bonded at their side face forming rigid composite elements; flexible composites featuring layers connected by nails, staples or other fasteners are also on the market but not focused on within this contribution. Current approvals of European CLT products allow gaps in width (w_{gap}) up to 6 mm. Some CLT products feature also laminations with one or more stress reliefs, usually 2.5 mm wide; see Fig. 1 and EN 16351 [1].

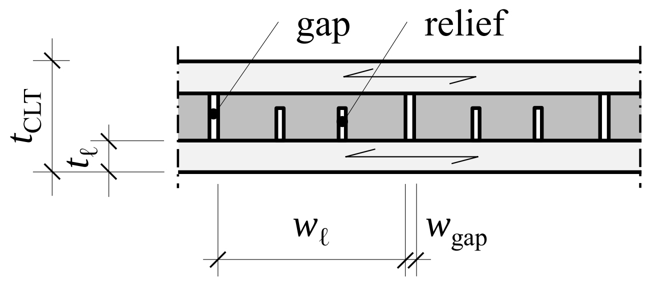

Fig. 1. (left) Principal CLT layup and some definitions of geometry and execution; (right) typical five-layer CLT element.

CLT has been used in manifold applications but primary as large dimension wall, floor and roof element in single and multi-story buildings, halls and bridges. Although only 20 years on the market, this product has been changing the timber engineering sector in many ways, e.g.:

- by allowing architects thinking rather in planes and volumes than in lines;
- by supporting the timber engineering sector with a stand-alone structural element enabling assembling of constructions amazingly fast, dry, clean and with high precision;
- by providing all subsequent crafts conditions for easy and fast mounting and manipulation, e.g. of additional layers (e.g. insulation as well as installation layer and façade) and building services in general; and
- by offering end-users and investors highest building quality and a sustainable, natural living and working environment.

CLT has been revolutionizing the timber engineering sector in analogy to the invention of particle boards in furniture industry which at that time initiated also big changes. There are several analogies between CLT and particle boards e.g. the homogeneity of both products in comparison with the base material, i.e. a reduced variation in physical / mechanical properties. Both products are planar, feature a significantly reduced swelling and shrinkage in-plane and utilize base material (quality) which would be hard to use otherwise. Their industrial production processes are relatively simple and the final products can be relatively easy manipulated and assembled.

Apart from all these mutualities, differences in respect to scale, reliability and safety requirements, service life and exposure shall be considered as well.

At the time the particle board entered the market also a significant change in furniture design could be observed, again by thinking in planes and volumes (boxes) rather than in lines and frames. New connection and fastener solutions, which were optimized for particle boards, together with a high degree in standardizing products and processes enabled extensive industrialization and economically prized furniture production.

CLT is on the way to catch up also these two very important steps: standardization (e.g. of layer thicknesses (t_ℓ = 20, 30, 40 mm), layups, base material quality and design approaches) and by developing a connection technique optimized for CLT; in respect to the latter, there is still much room for further developments and improvements. Aiming on versatile applicable connection solutions in CLT structures, a first step could be differentiating into principal connection lines (see also Fig. 2).

Considering this and looking at structures as a whole, the possibilities in realizing integral CLT structures also depend on the principle construction system. Single family houses, residential, office and school buildings up to three to five stories are commonly erected as platform-frame systems (indirect vertical load transfer between wall elements of vertically adjacent stories via soft floor elements).

Higher or heavily-loaded buildings are commonly designed as balloon-frame systems (direct vertical load transfer between wall elements of vertically adjacent stories).

Although CLT is currently used in superstructures hardly possible in timber one decade ago, a connection technique underlining the possibilities building with CLT is still widely missing. In fact, current commonly applied fastener and connection solutions, like angle brackets and hold-downs, are borrowed from light-weight timber constructions; these connectors together with a wall-floor-wall connection in a typical platform-frame CLT structure are shown in Fig. 3. In optimizing angle brackets for CLT structures a first step could be adapting the geometry to resist both, shear and uplift forces, consolidating the tasks of current angle brackets (shear load transmission) and hold-downs (transmission of uplift forces) in one connector (Flatscher and Schickhofer [3]).

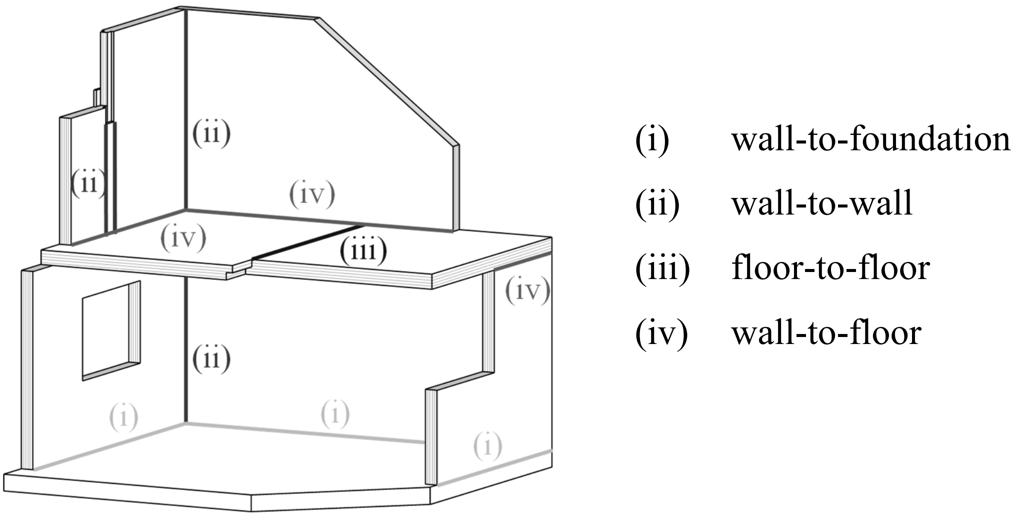

Fig. 2. Definition of connections exemplarily for a CLT platform-frame structure (Brandner et al. 2016 [2]; adapted).

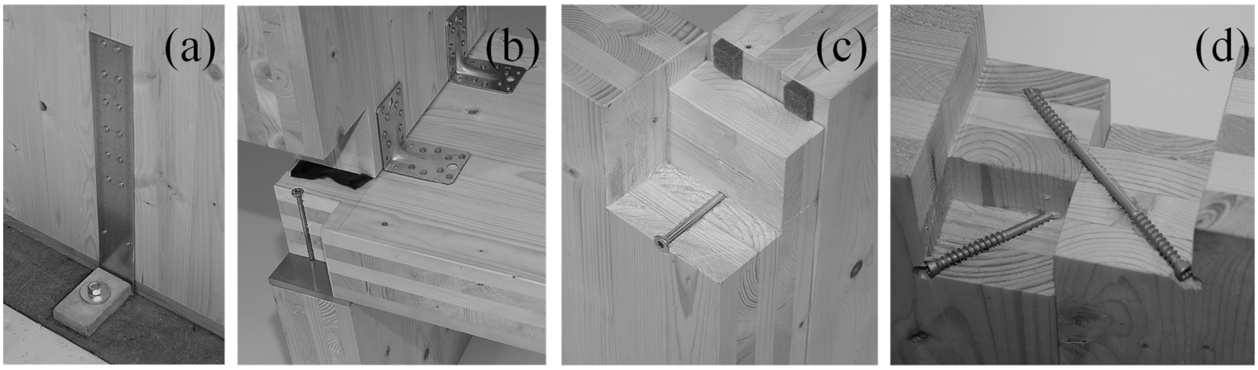

Fig. 3. (a) wall-foundation connection with hold-down; (b) wall-floor-wall connection with angle brackets and partially-threaded self-tapping screws; (c) wall-wall edge-connection with partially-threaded self-tapping screws, (d) wall-wall connection with double-threaded self-tapping screws; Schickhofer et al. (2010) [4].

Apart from angle brackets, hold-downs and line connections realized by means of partially, fully- or double-threaded self-tapping screws (see Fig. 3), for CLT structures also other connection solutions and first CLT system connectors are available; e.g. solutions with (self-drilling) smooth dowels / tight-fitting bolts and inner metal plates (e.g. Bernasconi [5]), the system connectors X-RAD (Polastri et al. [6], [7]; http://www.rothoblaas.com/products/fastening/x-rad 2017-07-07) or SHERPA CLT Connector (Kraler et al. [8]; http://de.sherpa-connector.com/clt_connector 2017-07-07), as well as special connection solutions, e.g. embedded steel tubes in combination with glued- or screwed-in rods (Schickhofer et al. 2010 [4]); see Fig. 4.

All these connection solutions have in common a connection between metal elements and CLT achieved via dowel-type fasteners, e.g. profiled nails (annular ringed shank nails or helically threaded nails), fully-, partially- or double-threaded self-tapping screws, smooth dowels or tight-fitting bolts as well as screwed- or glued-in rods, which are either loaded axially, laterally or combined. Retailers like Rothoblaas, Simpson Strong Tie, etc. support engineers with comprehensive (software) design tools and tabularized characteristic performance-based connection properties; a detailed verification of the single dowel-type fasteners themselves – fixing angle brackets, hold-downs or system connectors to CLT – is thus not required. However, the anchorage potential of single fasteners in CLT as described e.g. by the embedment strength and the withdrawal strength are essential parameters for the development of CLT connectors and for verification of line connections realized with self-tapping screws or (self-drilling) dowels as well as individual connection solutions.

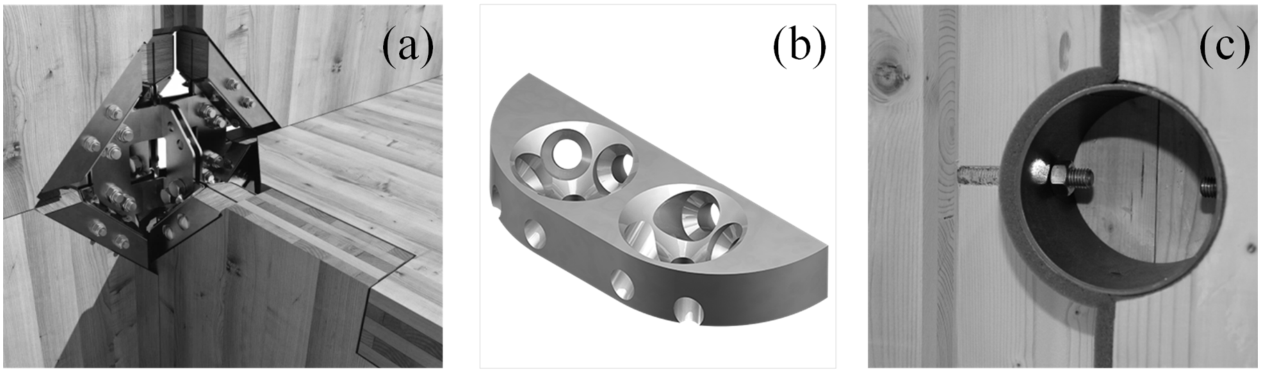

Fig. 4. (a) X-RAD system connector for balloon-frame CLT structures (Rothoblaas © [9]); (b) SHERPA CLT-connector (Sherpa © [10]); (c) embedded steel tube and glued-in rods (Schickhofer et al. 2010 [4]).

Connections decisively impact the behavior of CLT structures. Whereas in lightweight timber structures wall and floor diaphragms behave more flexible, CLT diaphragms (walls and floors) are characterized by high stiffness and high resistance in shear, tension and compression in-plane. Consequently, in CLT structures ductility and energy dissipation have to be provided by adequate connection solutions, the contribution from CLT itself is negligible. Considering the main requirements on connections, as they are high resistance, high stiffness and high ductility, the significant difference in the behavior of light-frame and CLT diaphragms is necessitating new ways of thinking in developing adequate connection solutions for CLT.

In view of ongoing harmonization and standardization processes and the upcoming new version of the European Timber Design Code, Eurocode 5 (series of standards EN 1995-x-x), it is intended to reorganize the chapter on connections by providing a tool-box, supporting the engineer step-by-step with required basic characteristic values for different anchoring materials. A prerequisite therefore are generic approaches instead of models limited to each individual timber product.

In view of that, the next chapters are organized by providing at first some general notes on dowel-type fastener behavior in CLT; what is special and what can be treated equally to solid timber and glulam. In that respect potential failure modes are listed and discussed in conjunction with CLT. Following this, we summarize and discuss the state-of-the-art of axially and laterally loaded dowel type fasteners anchored in CLT, emphasizing the withdrawal and embedment behavior, respectively.

Some suggestions for harmonization of current regulations on solid timber and glulam with CLT are made. Finally, we summarize also current suggestions and regulations on the connection design and requirements for securing structural integrity before summary and concluding remarks are given.

2. CLT characteristics common with glulam and solid timber

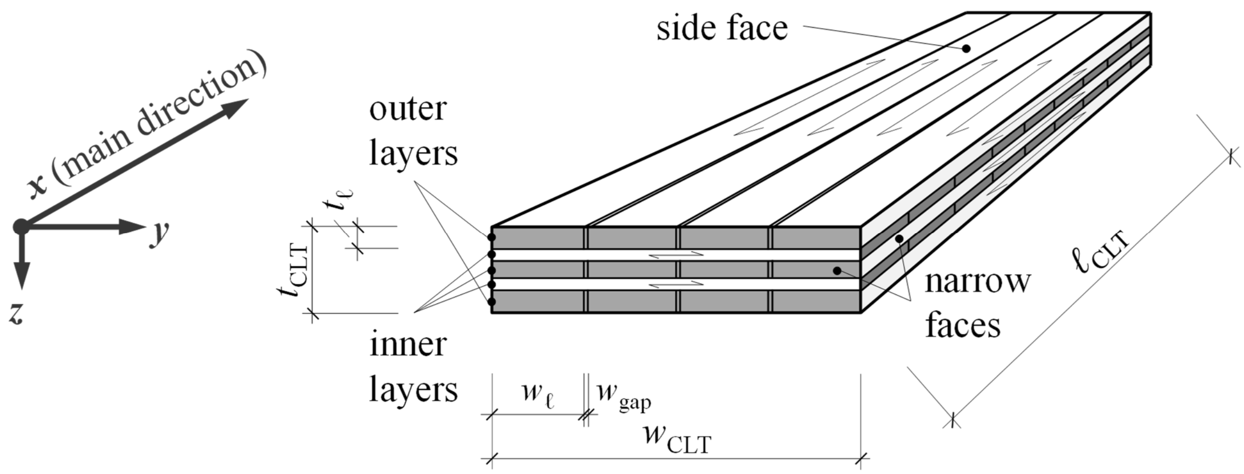

Fig. 5. Principal CLT element: terms, dimensions, coordinate system.

CLT as well as glued laminated timber (glulam; GLT) are composed of solid timber laminations, typically of board dimension. Similarities in design provisions between solid timber (ST), CLT and GLT are expected, but the orthogonal layup of CLT demands additional attention. At first, differentiation in the positioning of fasteners in CLT side face (fastener axis oriented out-of-plane) and narrow face (fastener axis oriented in-plane) is necessary; see Fig. 5 (we will see later in a proposed generic approach for withdrawal properties that this differentiation would also make sense for glulam and other laminated products). Furthermore, the influence of gaps and potential stress reliefs has to be taken into account as placement of fasteners in gaps, in particular if inserted in the narrow face and parallel to the grain, may lead to significant losses in fastener performance. According to approvals of current European CLT products, in the outer (top) layers gap widths up to 4 mm are allowed whereas in the inner (core) layers the gap width is limited to 6 mm. The European product standard for CLT, EN 16351 [1], limits gap widths generally to 6 mm. CLT producers aim on minimizing gap widths which is reflected already in Blaß and Uibel [11], Uibel and Blaß [12, 13] where inner layers featured a mean and 95 %-quantile gap width of 0.6 to 2.0 mm and 1.8 to 4.5 mm, respectively, whereas the 95 %-quantile in the outer layers was only 1.0 to 1.6 mm.

Fasteners inserted via the CLT side face and loaded laterally behave rather ductile, facilitating that all fasteners in a group of fasteners contribute to the load-bearing capacity to their full extent, i.e. the effective number n_{ef} is equal to n, the number of fasteners inserted; see also Fig. 6. This ductile behavior is due to the orthogonal layup where transverse layers act as reinforcement and prevent early failures in tension perpendicular to grain and block or row shear.

Apart from a generally observed minor influence of gaps (Blaß and Uibel [11] and Uibel and Blaß [12, 13]), fasteners inserted via the CLT side face can be designed similar to solid timber and glulam. Considering also that typical insertion angles are (30°) 45° to 90°, the influence of the angle β between load and grain orientation of outer layers in case of laterally loaded fasteners, as well as the thread-grain angle α in case of axially loaded fasteners (see Fig. 7), is small and with some conservatism even negligible; more on that later.

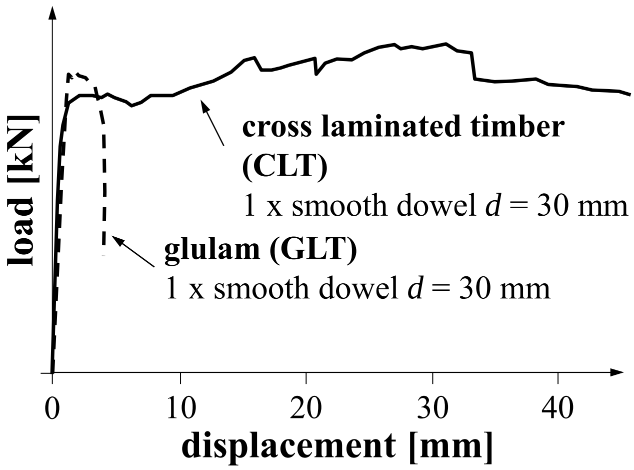

Fig. 6. Load-displacement behaviour of laterally loaded smooth dowels in the CLT side face (Schickhofer et al. 2010 [4]; adapted).

To reduce the influence of gaps on fastener performance, i.e. to reduce the probability that the effective anchorage length of a fastener is solely placed in gaps, it is suggested to penetrate a minimum of three layers (M = 3, with M as the number of penetrated CLT layers); see Blaß and Uibel [11].

By anchoring fasteners in the CLT narrow face, the possibility of penetrating layers with grain oriented parallel to the fastener axis has to be taken into account. This circumstance influences also the probability that a fastener is inserted in a gap, i.e. the influence of gaps on the fastener performance in the narrow face is higher than in the side face. Furthermore, in a group of fasteners or even for one single fastener different thread-grain angles are possible; see Fig. 8.

Laterally loaded fasteners in the CLT narrow face can either be loaded in-plane, i.e. by being loaded parallel to the CLT side face, or out-of-plane, i.e. by being loaded perpendicular to the CLT side face. In the latter case the possibility of tension perpendicular to grain failures, before reaching the capacity of fasteners, shall be taken into account.

In general, when discussing the performance of a connection composed by laterally or axially loaded dowel-type fasteners, the following potential failure mechanism can be differentiated; see Table 1.

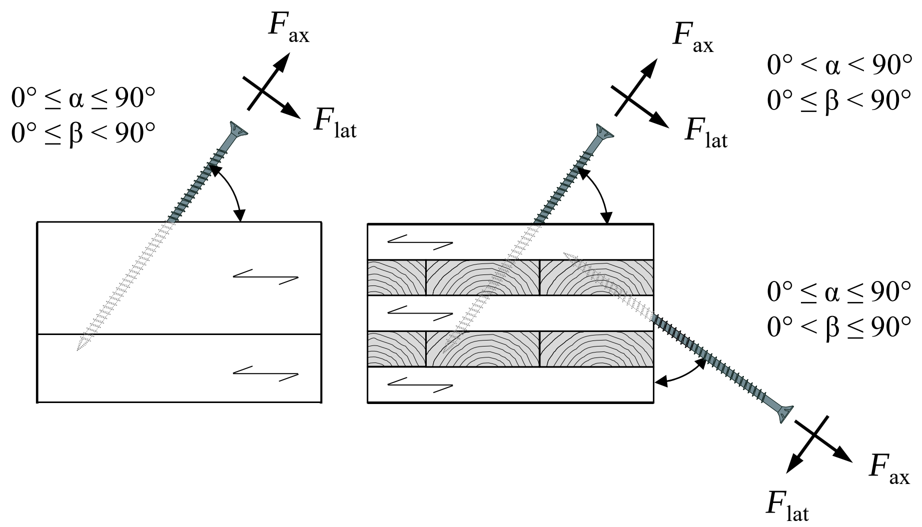

Fig. 7. Definition of thread-grain angle α and the angle between load and grain orientation of outer layers β, exemplarily for a screw inserted in side and narrow face of CLT.

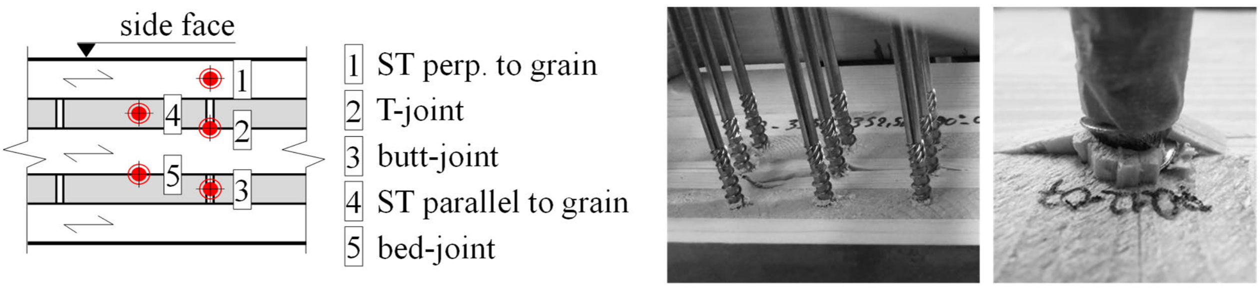

Fig. 8. (left) possible positions of dowel-type fasteners oriented perpendicular to the grain of outer layers in the CLT narrow-face; (middle) group of axially loaded self-tapping screws in the CLT narrow face, and (right) single screw featuring different thread-grain angles (Brandner [14]; adapted); ST = solid timber.

Table 1. Summary of potential failure mechanism in case of axially or laterally loaded single or group of fasteners

Loading	Failure mode	Failing material
Axial	Withdrawal	Timber
	Head pull-through	Timber
	Fastener tension	Steel
	Tension perpendicular to grain (splitting)	Timber
	Block shear and row shear	Timber
Lateral	Embedment	Timber
	Yield in bending	Steel
	Block shear, row shear, plug shear	Timber
	Tension perpendicular to grain (splitting)	Timber

As failures of the fastener itself (steel failures) do not depend on the applied timber products we focus further on failure modes of CLT surrounding the fastener, in particular on the embedment and withdrawal capacity, as the related properties are of major importance for the description of laterally and axially loaded fasteners, respectively.

The density as indicating property for fastener performance in timber has to be differentiated between side and narrow face insertion. For fasteners in the side face, penetrating several layers, the characteristic density of CLT is proposed; see Blaß and Uibel [11] and Uibel and Blaß [13] who defined the characteristic density of CLT, based on laminations with strength class C24 and a characteristic density of $\rho_{12,\ell,k} = 350$ kg/m³ according to EN 338 [15], with $\rho_{12,CLT,k} = 400$ kg/m³. Following the proposal of PT SC5.T1 [16] for the new version of EN 1995-1-1 [17], for CLT made of C24 or T14 laminations according to EN 338 [15] a value of $\rho_{12,CLT,k} =$ 385 kg/m³, based on the relationship $\rho_{12,CLT,k} = 1.1 \cdot \rho_{12,\ell,k}$, analogously to glulam, is proposed. For adjustment of models for withdrawal and embedment properties to density, corresponding corrections are presented. As fasteners inserted via the CLT narrow face anchor mostly only in one lamination, for calculation of embedment and withdrawal capacity the characteristic density of the laminations themselves applies, e.g. for C24 or T14 according to EN 338 [15]: $\rho_{12,\ell,k} = 350$ kg/m³.

3. Withdrawal strength of axially loaded dowel-type fasteners in CLT

3.1 Definitions, general comments and overview

Within this section, we focus on threaded or profiled dowel-type fasteners, enabling a composite action with the surrounding timber material and thus an appropriate performance when loaded in axial direction, i.e. self-tapping screws and profiled nails. Note: glued-in rods or glued-in metal plates, which also show a reasonable performance in case of axial loading, are not discussed in this paper. The composite action between the axially loaded fastener and the timber component is expressed by the withdrawal strength f_{ax}. In contrast to the withdrawal parameter, $f_1 = f_{ax}\,\pi$, the withdrawal strength f_{ax} is defined as

$$f_{ax} = \frac{F_{ax,max}}{\ell_{ef} \cdot d \cdot \pi} \tag{1}$$

with $F_{ax,max}$ as the fastener's capacity in axial direction (equal to the withdrawal resistance $F_{ax,\alpha,Rk}$ according to Eurocode 5 [17]), d as its relevant (nominal) diameter and ℓ_{ef} as its effective inserted thread length; the latter either including the fastener's tip length or not – as it is discussed later on.

Blaß and Uibel [11] (also published in Uibel and Blaß, [12, 13, 18]) were the first who investigated the performance of dowel-type fasteners, situated in different positions in the side and narrow face of CLT. Their analyses comprised variations in fastener type (dowels, self-tapping screws and nails), both angles α and β, different layups of Central European CLT (also including solid wood-based panels,

$N = 3 \div 7$), randomly distributed gap widths $w_{gap,mean}$ up to 2.0 mm and different nominal diameters d. With regard to single fastener properties, outcomes were used for determining empirical regression functions as well as characteristic approaches for withdrawal and embedment strength as basis for the design of dowel-type fasteners inserted in CLT.

In respect to self-tapping screws and their axial load-bearing behavior in CLT, within the last years further comprehensive studies were conducted at Graz University of Technology, c.f. Ringhofer [19]. Amongst other topics, several experimental campaigns are compiled dealing with a detailed analysis of selected parameters relevant for the screws' load-bearing behavior. This especially concerns the following parameters, the number of penetrated layers M (Reichelt [20]; Ringhofer et al. [21]), the thread-grain angle α and the gap configuration (gap type and width; see Grabner [22]; Brandner [14]; Brandner et al. [23] and Silva et al. [24]). Based on a detailed statistical analysis on available comprehensive data on screw withdrawal tests an empirical, generic approach, presented in Ringhofer et al. [25]) and Ringhofer [19], was established and successfully validated by means of independently derived data sets.

In the following Sections 3.2 and 3.3 we summarize the main findings and recommendations of both research programs dedicated to the withdrawal behavior of dowel-type fasteners as carried out at KIT and Graz University of Technology. Furthermore, we compare related models with those currently given in Eurocode 5 [17] for determining the characteristic withdrawal strength particularly of axially loaded self-tapping screws situated in solid timber or glulam.

Apart from the European research programs also the work done by Kennedy et al. [26] is worth being mentioned since it represents one of the few non-European research activities regarding the determination of mechanical properties of single fasteners situated in (the side face of) CLT elements.

3.2 Axially loaded self-tapping screws in CLT elements

The experimental program presented in Blaß and Uibel [11] and dedicated to the withdrawal strength of axially loaded self-tapping single screws with outer thread diameters $d = \{6, 8, 12\}$ mm can be separated into two campaigns: one where the focus was on CLT side face insertion and one where the screws were situated in the CLT narrow face. The impact of gaps between laminations of one layer on the mechanical screw performance was investigated by four alternative possibilities of screw insertion, covering the number of penetrated gaps $N_{gap} = \{0, 1, 2, 3\}$ (CLT side face) as well as the gap type (CLT narrow face, insertion in T- and butt-joints, c.f. Fig. 8) while the mean gap width $w_{gap,mean}$ varied randomly between 0.2 and 2.0 mm. For screws situated in the CLT side face, this was exclusively done for perpendicular-to-grain insertion while for those situated in the CLT narrow face, both limits of screw axis position to the single layer's grain direction, $\alpha = \{0, 90\}°$ were examined. Specimens made of 3- and 5-layered CLT panels with five different layups were used for 387 withdrawal tests. Subsequently, empirical regression functions for predicting the withdrawal strength f_{ax} were determined based on the test results; the characteristic approach is presented in Eq. (2):

$$f_{\text{ax,k}} = \frac{9.02 \cdot d^{-0.2} \cdot \ell_{\text{ef}}^{-0.1}}{1.35 \cdot \cos^2 \varepsilon + \sin^2 \varepsilon} \quad \text{and} \quad f_{\text{ax,k,corr}} = f_{\text{ax,k}} \cdot \left(\frac{\rho_{\text{k}}}{350} \right)^{0.75} \tag{2}$$

and ε as primary insertion angle, e.g. for screws in CLT narrow face: $\varepsilon = 0°$ (on a conservative but general basis), and for screws in CLT side face $\varepsilon = 90°$. As given in Eq. (2), for this approach a multiplicative power model is applied. Apart from ε, it identifies the outer thread diameter, the timber density as well as the effective inserted thread length as influencing parameters. While influences from diameter and density were adapted to the test results (both have a disproportional influence on f_{ax} respectively), Blaß and Uibel [11] adopted the impact of ℓ_{ef} on f_{ax} from the results of a previous testing campaign conducted in solid timber, c.f. Blaß et al. [27] and Eq. (4). Note: with regard to the definition of f_{ax} given in Eq. (1), it is worth mentioning that Blaß and Uibel [11] determined their experimental withdrawal strengths with ℓ_{ef} including the tip length, thus leading to a conservative interpretation of test results.

Due to material homogenization, the smaller probability of gap insertion along ℓ_{ef} as well as the fact that parallel-to-grain insertion is impossible, the withdrawal strength of screws situated in the CLT side face is of course significantly higher than of screws situated in the CLT narrow face. This is expressed by the factor 1.35 in Eq. (2), whose magnitude results from a data fit to those CLT narrow face test series with the worst results for withdrawal strength (parallel-to-grain insertion in gaps).

The examinations carried out at Graz University of Technology base on similar parameter configuration as in Blaß and Uibel [11] but additionally comprised variations in thread-grain angle α within the limits {0, 90}° for CLT side and narrow face insertion, as well as systematic examinations of the number of penetrated layers' (and their orientation) and the gap width's (for the types shown in Fig. 8). Amongst others, corresponding outcomes were applied for deriving a new generic approach for determining the withdrawal capacity of axially loaded self-tapping screws as presented in Ringhofer et al. [25] and Ringhofer [19] and shown in Eqs. (3-5):

$$f_{\text{ax,k}} = k_{\text{ax,k}} \cdot k_{\text{sys,k}} \cdot 8.67 \cdot d^{-0.33} \quad \text{and} \quad f_{\text{ax,k,corr}} = f_{\text{ax,k}} \cdot \left(\frac{\rho_{\text{k}}}{350} \right)^{k_\rho} \tag{3}$$

$$k_{\text{ax,k}} = \begin{cases} 1.00 & \text{for } 45° \leq \alpha \leq 90° \\ 0.64 \cdot k_{\text{gap,k}} + \dfrac{1 - 0.64 \cdot k_{\text{gap,k}}}{45} \cdot \alpha & \text{for } 0° \leq \alpha \leq 45° \end{cases}, \quad k_{\text{sys,k}} = \begin{cases} 1.00 & \text{ST} \\ 1.10 & \text{CLT}, N \geq 3 \\ 1.13 & \text{GLT}, N \geq 5 \end{cases} \tag{4}$$

$$k_{\text{gap,k}} = \begin{cases} 0.90 & \text{CLT narrow face} \\ 1.00 & \text{else} \end{cases}, \quad k_\rho = \begin{cases} 1.10 & 0° < \alpha \leq 90° \\ 1.25 - 0.05 \cdot d & \alpha = 0° \end{cases} \tag{5}$$

This new generic approach comprises the following features, which are different from current approaches:

- Firstly, density correction by the power factor k_ρ is kept more flexible; in-depth analyses identified thread-grain angle and outer thread diameter as important influencing parameters.
- Secondly, for screws penetrating more than one layer when applied in laminated timber products a significant homogenization was found. Apart from the density, so far the only parameter indicating the anchorage material, a stochastically determined system factor k_{sys} is introduced, see Eq. (4). It allows adjusting the withdrawal capacity related to the base material density, i.e. the density of the laminations, according to the screw application, i.e. it increases the withdrawal capacity the more layers are penetrated by the screw. This circumstance neither can be covered by inserting the product density instead of the base material density nor would this procedure be meaningful. This commitment – aimed to cover screw application in laminated timber products in general – reflects the generic character of this approach as opportunity to decrease the number of models for different applications without a loss of accuracy due to simplification.
- Thirdly, the systematic variation of gap width and type, especially in case of CLT narrow face insertion, enabled the determination of a probabilistic model quantitatively and explicitly describing the related negative impact on withdrawal strength f_{ax}, c.f. Brandner [14]. Considering currently given limits with regard to gaps and stress reliefs, c.f. Chapter 1, and further assumptions (e.g. the variabilities of density and withdrawal strength), a corresponding simplification in form of the multiplicative factor k_{gap} is applied; see Eq. (5).

Besides the explained differences, the impact of both remaining influencing parameters, the outer thread diameter and thread-grain angle, is treated in a traditional way, i.e. diameter adjustment by a negative power parameter and a bilinear model with discontinuity at $\alpha = 45°$ for considering the influence of the thread-grain angle. In line with Blaß and Uibel [11], the placement of screws in the side face of CLT elements leads to significantly higher withdrawal strengths than that in their narrow face. Deviating from Blaß and Uibel [11], Eq. (3) does not contain ℓ_{ef} as influencing parameter since no related impact on f_{ax} could be observed (Note: This is only valid if tip length is not part of ℓ_{ef}).

We now compare quantitatively the approaches given in Eq. (2) and Eq. (3), with special focus on screw insertion in CLT elements, with the current model for determining the characteristic withdrawal strength according to Eurocode 5 [17]; see Eq. (6), which is based on Blaß et al. [27] and 1212 withdrawal tests on axially loaded screws inserted in solid timber at different outer thread diameters, effective insertion lengths (counted by neglecting the tip length) and axis-to-grain angles.

$$f_{\mathrm{ax,k}} = \frac{18.0 \cdot d^{-0.5} \cdot \ell_{\mathrm{ef}}^{-0.1} \cdot k_{\mathrm{d}}}{1.2 \cdot \cos^2 \alpha + \sin^2 \alpha} \quad \text{with} \quad f_{\mathrm{ax,k,corr}} = f_{\mathrm{ax,k}} \cdot \left(\frac{\rho_{\mathrm{k}}}{350}\right)^{0.80} \quad \text{and} \quad k_{\mathrm{d}} = \min\begin{cases} d/8 \\ 1 \end{cases} \tag{6}$$

In fact, the approach in Eq. (6) is very similar to Eq. (2) (the impact of d is more pronounced while the density is considered in a quite similar way). In comparison to Eq. (4), the influence of the thread-grain angle is modelled according to Hankinson [28] instead of a bi-linear approach, and there is the additional coefficient k_{d}, which decreases f_{ax} in case of $d < 8$ mm, which, together with the limitation to thread-grain angles $\alpha \geq 30°$ in Eurocode 5 [17] is not part of Blaß et al. [27]. Since the product CLT is not covered by the current version of Eurocode 5 [17], Eq. (6) does not specifically consider a related application. Nevertheless, selected parameter characteristics enable a reasonable model comparison, which is illustrated in Fig. 9 to Fig. 11 in dependence of representative characteristic densities (which means single lamella strength classes; for CLT side face insertion, the relationship $\rho_{12,\mathrm{CLT,k}} = 1.1 \cdot \rho_{12,\ell,\mathrm{k}}$, was applied) and outer thread diameters. Furthermore, ℓ_{ef} was constantly set to $10 \cdot d$, as a related specification is necessary when applying Eq. (2) and Eq. (6).

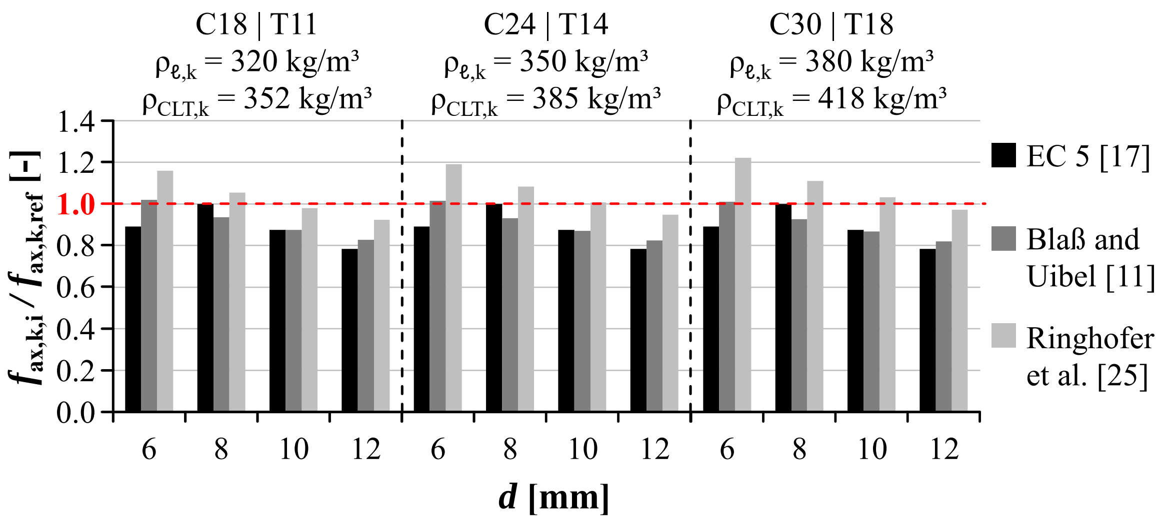

Fig. 9. Comparison of characteristic withdrawal strength according to Eurocode 5 [17], Blaß and Uibel [11] and Ringhofer et al. [25] for varying outer thread diameters of self-tapping screws related to that of Eurocode 5 [17] for d = 8 mm; CLT side face and perpendicular-to-grain insertion (α = 90°).

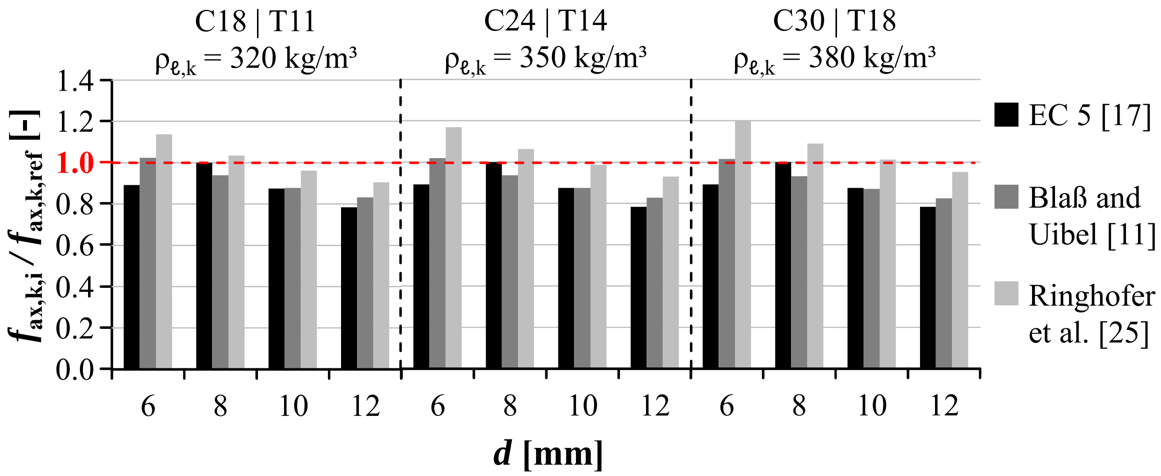

Fig. 10. Comparison of characteristic withdrawal strength according to Eurocode 5 [17], Blaß and Uibel [11] and Ringhofer et al. [25] for varying outer thread diameters of self-tapping screws related to that of Eurocode 5 [17] for d = 8 mm; CLT narrow face and perpendicular-to-grain insertion (α = 90°).

With regard to the comparison of characteristic withdrawal strengths for perpendicular-to-grain insertions, once through several layers (CLT side face, Fig. 9) and once into one layer (CLT narrow face, Fig. 10), two points are worth being discussed in detail:

Firstly, even though input parameter treatment differs in the magnitude of the power values to some extent, characteristic withdrawal strengths determined by Eq. (2) and Eq. (6) result in a nearly equal value if practically relevant outer thread diameters $d = \{8, 10, 12\}$ mm are considered.

Secondly, the new approach presented in Eq. (3) leads to remarkably higher values of $f_{ax,k}$ if compared to the two others. Furthermore, this is independent from timber density and outer thread diameter and – in case of Fig. 9 – it confirms the aforementioned statement of increased withdrawal strength due to the application of k_{sys} according to Eq. (4).

In Fig. 11, which displays the parallel-to-grain insertion in the CLT narrow face and thus only comprises approaches which take the impact of gaps on f_{ax} into account, the situation is different: here, the generic approach presented in Eq. (3) results in significantly smaller withdrawal strengths than those determined by Eq. (2), irrespective of conducted parameter variations. This conservative estimation can be explained by a less pronounced relationship between density and withdrawal strength in case of $\alpha = 0°$ combined with a higher difference of f_{ax} between perpendicular- and parallel-to-grain insertion, c.f. Eq. (4) and Eq. (5).

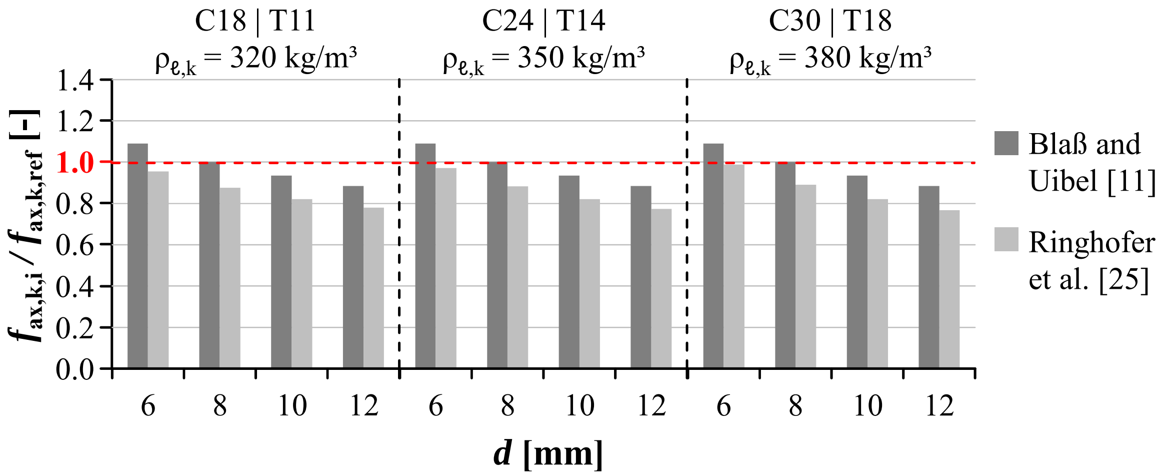

Fig. 11. Comparison of characteristic withdrawal strength according to Blaß and Uibel [11] and Ringhofer et al. [25] for varying outer thread diameters of self-tapping screws related to that of Blaß and Uibel [11] for d = 8 mm; CLT narrow face and parallel-to-grain insertion.

3.3 Axially loaded profiled nails in CLT elements

With regard to the performance of axially loaded, profiled nails situated in the side and narrow face of CLT elements, examinations comparable to those for self-tapping screws were not conducted at Graz University of Technology. Thus, the study presented in Blaß and Uibel [11] is the exclusive source for withdrawal properties of nails in CLT discussed in this section. Since this program did not distinguish between self-tapping screws and nails, it is referred to Section 3.2 for a related explanation. The sole deviations to self-tapping screws are of course the smaller nominal diameters $d = \{3.1, 4.0, 6.0\}$ mm of the nails (loadbearing class III, according to DIN 1052, 1988) as well as the higher number of tests (523) carried out in three- and five-layered CLT panels with in total five different layups. The characteristic approach proposed by Blaß and Uibel [11] again bases on an empirical regression model adjusted to the test results and is shown in Eq. (7):

$$f_{\text{ax,k}} = \frac{4 \cdot d^{-0.4}}{3.33 \cdot \cos^2 \varepsilon + \sin^2 \varepsilon} \quad \text{with} \quad f_{\text{ax,k,corr}} = f_{\text{ax,k}} \cdot \left(\frac{\rho_{\text{k}}}{350}\right)^{0.80} \tag{7}$$

and ε as primary insertion angle, e.g. for nails in CLT narrow face: $\varepsilon = 0°$ (on a conservative but general basis), and for nails in CLT side face $\varepsilon = 90°$. For CLT featuring gaps and/or stress reliefs, Blaß and Uibel [37] recommend to reduce the withdrawal capacity according to Eq. (7) to 80 % for nails with $d < 6$ mm and to apply only nails with $d \geq 4$ mm and $\ell_{\text{ef}} \geq 8 \cdot d$. Apart from the pre-factor 3.33, which is significantly higher than that for self-tapping screws in Eq. (2) – possibly caused by smaller nominal diameters while the average gap width was kept constant – the considered influencing parameters as well as their treatment are similar to those given in Eq. (2).

Fig. 12 compares characteristic withdrawal strengths of profiled nails determined according to Eq. (7) in dependence of the nominal diameter, the single layer's characteristic density as well as the position in the CLT panel (side vs. narrow face). It again highlights the significant difference of withdrawal strength in dependence of the nail location, which is not only caused by the aforementioned pre-factor but also by applying a higher characteristic (product) density $\rho_{12,\mathrm{CLT,k}} = 1.1 \cdot \rho_{12,\ell,\mathrm{k}}$, for CLT side face if compared to narrow face insertion.

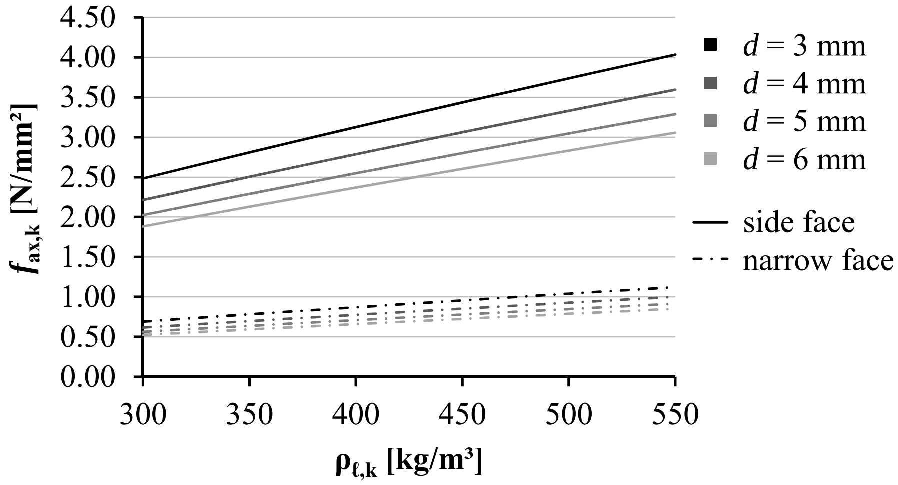

Fig. 12. Characteristic withdrawal strength vs. characteristic density $\rho_{\ell,k}$ of profiled nails: comparison between CLT side and narrow face insertion in dependence of the nominal nail diameter; according to Blaß and Uibel [11].

In contrast to self-tapping screws or smooth shank nails, the currently valid version of Eurocode 5 [17] refers to design values published in the manufacturers' declarations of performance (DoP) instead of providing a product-independent approach for determining the characteristic withdrawal strength of profiled nails. This can be explained by significant differences in withdrawal strength of nails from different producers, which are higher than the ones caused by a variation of common influencing parameters such as the timber density or the nominal diameter [29]. In this recently published source, it is reported that the related variability disabled the derivation of a reasonable generic approach. With regard to the average withdrawal strength of profiled nails, Sandhaas and Görlacher [29] determined a nonlinear, empirical regression model for estimating this property, which is based on a comprehensive test database available at KIT and given in Eq. (8), see:

$$f_{\mathrm{ax,k}} = 3.60 \cdot 10^{-3} \cdot \rho^{1.38} \tag{8}$$

with ρ as the density of solid timber as material applied for the tests. According to Sandhaas and Görlacher [29], this approach has a rather limited predictive quality due to a poor correlation between density and withdrawal strength. Nevertheless, it represents the average declared withdrawal strength of profiled nails in solid timber and shall be applied for a comparison with the one for CLT as published by Blaß and Uibel [11], see Eq. (9).

$$f_{ax} = \frac{0.16 \cdot d^{-0.4} \cdot \rho^{0.8}}{3.1 \cdot \cos^2 \varepsilon + \sin^2 \varepsilon} \tag{9}$$

This comparison is subsequently illustrated in Fig. 13 in dependence of the nominal nail diameter and the layer density at $\varepsilon = 90°$ and identifies remarkably higher values of f_{ax} determined by Eq. (8), especially for average timber densities of common softwood strength classes (C24 and above) according to EN 338 [15].

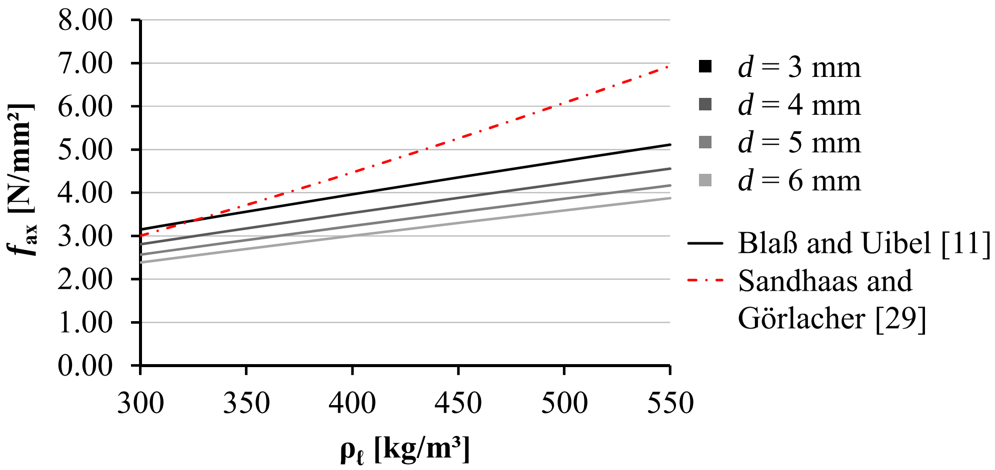

Fig. 13. Comparison of withdrawal strength of profiled nails estimated by Eq. (7) with the approach published in Sandhaas and Görlacher [29] (Eq. (8)) in dependence of nominal diameter and layer density; $\varepsilon = 90°$.

4. Embedment strength of laterally loaded dowel-type fasteners in CLT

4.1 General comments and overview

Blaß and Uibel [11] and Uibel and Blaß [12, 13, 18] were the first investigating laterally-loaded dowel-type fasteners in CLT side and narrow faces of Central European CLT and solid wood-based panels. More recently, Kennedy et al. [26] report on investigations conducted in North America on laterally-loaded threaded-fasteners inserted in CLT side face.

In the following we summarize the main findings from the comprehensive report of Blaß and Uibel [11] as introduced in Section 3.1 and compare the proposed relationships with current design provisions for solid timber and glulam as given in Eurocode 5 [17].

In general, the embedment strength represents a system property, the resistance of timber against laterally loaded fasteners. In cases of fasteners penetrating several layers in CLT side face or two or more different laminations in the CLT narrow face, featuring different angles between fastener axis and load, this kind of system property even comprises different contributions of layers and laminations as different load-grain angles may be concerned.

4.2 Laterally loaded dowel-type fasteners in CLT side face

4.2.1 Smooth dowels and tight-fitting bolts

Blaß and Uibel [11] tested smooth dowels with diameters $d = 8$ to 24 mm in three- and five-layer CLT elements, positioned apart or in gaps involving one to three layers, and loaded at 0°, 45° and 90° in respect to the outer layer's grain orientation. Thereby, a minor influence of the number of gaps on the embedment strength was observed together with homogenized properties with increasing number of penetrated layers.

By means of regression analysis, for the characteristic embedment strength $f_{\mathrm{h,k,CLT}}$ of dowels inserted in CLT side face two models were found: the first, considering explicitly the CLT layup, and the second, more simplified approach, representing the investigated CLT layups and tested configurations on an average basis, see Eq. (10).

$$f_{\mathrm{h,k,CLT}} = \frac{32 \cdot (1 - 0.015 \cdot d)}{1.1 \cdot \sin^2 \beta + \cos^2 \beta} \quad \text{with} \quad f_{\mathrm{h,k,CLT,corr}} = f_{\mathrm{h,k,CLT}} \cdot \left(\frac{\rho_{\mathrm{k}}}{400} \right)^{1.2} \tag{10}$$

with β as angle between load and grain of outer layers and $\rho_{\mathrm{k}} = 400$ kg/m³. This regression model is limited to the investigated parameters, the layup parameter of tested panels, i.e. the sum of layer thicknesses oriented parallel to outer layers vs. the sum of layer thicknesses oriented perpendicular to outer layers, $\Sigma t_{\ell,\mathrm{x,i}} / \Sigma t_{\ell,\mathrm{y,i}}$, which was between 0.95 and 2.1, and the maximum layer thickness, which was max $[t_{\ell,\mathrm{i}}]$ = 40 mm.

The influence of density on the embedment strength was found to be equal to solid timber; see additional tests in Blaß and Uibel [11] as well as Blaß et al. [27]. An adjustment of Eq. (10) to $\rho_{\mathrm{CLT,k}} = 385$ kg/m³, as currently proposed by PT SC5.T1 [16], would lower the resistance by 4 %.

Fig. 14 compares the characteristic embedment strength according to Eq. (10) with the current regulation for solid timber and glulam according to Eurocode 5 [17]; see Eq. (11). In both equations, a similar relationship between dowel diameter and embedment strength is observed. In contrast, the influence of the load-grain angle β on the embedment strength is found to be much smaller for dowels inserted in CLT side face than in solid timber and glulam. This is because the embedment strength determined on dowels inserted in CLT side face comprises both, the influence of layers oriented parallel and perpendicular to loading direction.

$$f_{\mathrm{h,k,EC5}} = \frac{0.082 \cdot (1 - 0.01 \cdot d) \cdot \rho_{\mathrm{k}}}{k_{90} \cdot \sin^2 \beta + \cos^2 \beta} \xrightarrow[\text{softwood}]{\text{with } \rho_{\mathrm{k}} = 400 \text{ kg/m}^3} f_{\mathrm{h,k,EC5}} = \frac{32.8 \cdot (1 - 0.01 \cdot d)}{(1.35 + 0.015 \cdot d) \cdot \sin^2 \beta + \cos^2 \beta} \tag{11}$$

Furthermore, the characteristic embedment strength of dowels with smaller diameters is closer to current regulations for dowels at $\beta = 0°$ whereas the characteristic embedment strength of dowels with larger diameters is in-between current regulations for dowels at $0° \leq \beta \leq 90°$. This outcome may be explained in two ways: at first, splitting failures, as being more frequent for dowels with smaller diameter and loaded parallel to grain, are prevented in CLT by the orthogonal layup. Secondly, an influence of gaps on the embedment strength of dowels with smaller diameter could not be observed; the smallest diameter tested was d = 8 mm.

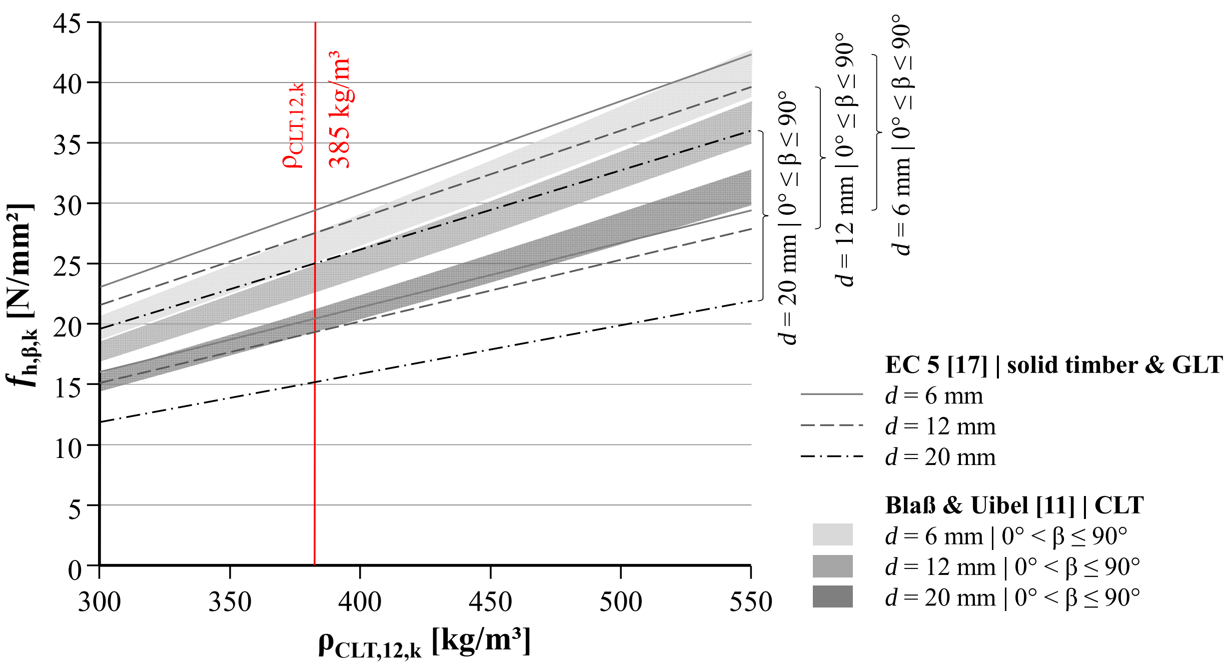

Fig. 14. Characteristic embedment strength vs. characteristic density of smooth dowels and tight-fitting bolts: comparison between Eurocode 5 [17] (solid timber and GLT) with Blaß and Uibel [11] and Uibel and Blaß [12], [13]; CLT side face).

Overall, regulation of embedment strength for smooth dowels and tight-fitting bolts inserted in CLT side face is suggested equal to solid timber and glulam, with adjustment factors for very small dowel diameters, accounting for a potential negative influence of gaps, and an adapted k_{90}-factor (see Eq. (11)), taking into account the joint action of layers featuring different load-grain angles in CLT.

4.2.2 Profiled nails and self-tapping screws

Blaß and Uibel [11] and Uibel and Blaß [12, 13] report also on embedment tests with self-tapping screws and smooth nails in the side face of wood-based panels with layer thicknesses $t_{\ell,i} \leq 7$ mm. The thin layers together with the reinforcing transverse layers lead to rather high characteristic embedment strengths $f_{h,k,CLT}$ in comparison with $f_{h,k,EC5}$ for glulam and solid timber according to Eurocode 5 [17], see

$$f_{h,k,CLT} = 60 \cdot d^{-0.5} \quad \text{with} \quad f_{h,k,CLTcorr} = f_{h,k,CLT} \cdot \left(\frac{\rho_k}{400}\right)^{1.05} \tag{12}$$
$$f_{h,k,EC5} = 0.082 \cdot \rho_k \div d^{-0.3} \xrightarrow{\text{with } \rho_k = 400\,\text{kg/m}^3} f_{h,k,EC5} = 32.8 \cdot d^{-0.3}$$

In CLT all nails and screws were inserted without predrilling. Although the embedment tests were conducted with smooth nails, Eq. (12) for CLT is limited to profiled nails, e.g. helically threaded nails and annular ringed shank nails.

As already observed in previous investigations, for dowel-type fasteners without predrilling, no influence of load-grain angle on embedment strength is observed.

In their design proposal, Blaß and Uibel [11] and Uibel and Blaß [13] limit Eq. (12) to layer thicknesses of $t_{\ell,i} \leq 9$ mm. Thus, for common CLT with standard layer thicknesses of $t_{\ell,ref} = 20$, 30 and 40 mm this equation is of minor concern. In case of CLT featuring layers with $t_{\ell,i} > 9$ mm, Blaß and Uibel [11] suggest calculating the embedment strength of laterally loaded profiled nails and self-tapping screws, inserted without predrilling, equal to solid timber. This again allows harmonizing regulations for solid timber, glulam and CLT.

4.3 Laterally loaded dowel-type fasteners in CLT narrow face

4.3.1 General comments

In contrast to CLT side face, in CLT narrow face positioning of fasteners parallel and / or perpendicular to grain within and between single laminations as well as between layers is possible. Furthermore, gaps may have a more significant influence on the embedment strength of fasteners positioned in narrow face than in side face.

Laterally loaded dowel-type fasteners positioned in the CLT narrow face can be loaded in-plane, out-of-plane or a combination of both; see Fig. 15. If loaded out-of-plane, tension perpendicular to grain stresses potentially causing early splitting and delamination of layers have to be considered; minimum requirements on layer and CLT thickness are presented later in Chapter 5. As the fasteners are inserted in or between laminations, for calculation of the characteristic embedment strength the characteristic density of the laminations, $\rho_{\ell,k}$, applies.

Although Uibel and Blaß in Schickhofer et al. [4] recommend not using smooth dowels, tight-fitting bolts or profiled nails in the narrow face of CLT, neither for bearing axial nor lateral loads, the models derived from testing are briefly presented.

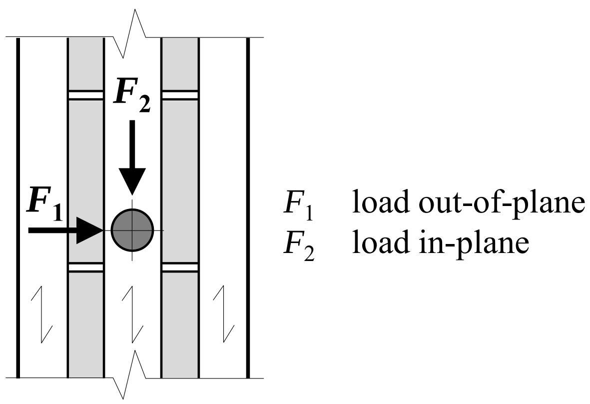

Fig. 15. Laterally loaded dowel-type fasteners in CLT narrow face: principal load directions.

4.3.2 Smooth dowels and tight-fitting bolts

For laterally loaded dowels in CLT narrow face the following relevant parameters were identified (Blaß and Uibel [11]):

- angle between dowel axis and grain of the penetrated CLT layer;
- ratio between dowel diameter and thickness of the penetrated CLT layer, $d / t_{\ell,i}$;
- position of dowels relative to longitudinal and lateral gaps as well as stress reliefs.

During testing, Blaß and Uibel [11] frequently observed splitting failures, due to tension stresses perpendicular to grain, in combination with rolling shear of the penetrated layer in case of dowels inserted parallel to grain. Low resistances were found for dowels inserted perpendicular to grain, featuring a diameter d close to the penetrated layer thickness $t_{\ell,i}$ and loaded out-of-plane. This is because of the adjacent layers with grain oriented parallel to dowel axis, which are activated in compression perpendicular to grain.

From all tested configurations (dowels inserted parallel / perpendicular to grain, in / close to gaps within / between layers) the lowest resistances were observed when dowels with diameter $d < t_{\ell,i}$ were inserted parallel to grain and loaded in-plane. Based on these outcomes and by means of regression analysis the following conservative but universally applicable approach, independent of the load-grain angle, was defined:

$$f_{\mathrm{h,k,CLT}} = 9 \cdot (1 - 0.017 \cdot d) \quad \text{with} \quad f_{\mathrm{h,k,CLT,corr}} = f_{\mathrm{h,k,CLT}} \cdot \left(\frac{\rho_{\mathrm{k},\ell}}{350} \right)^{0.91} \tag{13}$$

4.3.3 Profiled nails and self-tapping screws

By testing the embedment strength of dowel-type fasteners in the CLT narrow face, smooth nails and self-tapping screws, inserted without predrilling, were used; see Blaß and Uibel [11] and Uibel and Blaß [13, 18]. The embedment strength of screws was determined for the threaded part.

By testing the same load configurations as for dowels, the lowest resistances were again observed when nails or screws with diameters $d < t_{\ell,i}$ were inserted parallel to grain and loaded in-plane. Based on these outcomes and by means of regression analysis the following conservative but universally applicable approach, independent of the load-grain angle, was defined:

$$f_{\mathrm{h,k,CLT}} = 20 \cdot d^{-0.5} \quad \text{with} \quad f_{\mathrm{h,k,CLT,corr}} = f_{\mathrm{h,k,CLT}} \cdot \left(\frac{\rho_{\mathrm{k},\ell}}{350} \right)^{0.56} \tag{14}$$

In contrast to Eurocode 5 [17] where the effective (core) diameter of screws, d_{ef}, shall be used, according to Eq. (14) the nominal (outer) diameter d applies for both, nails and screws.

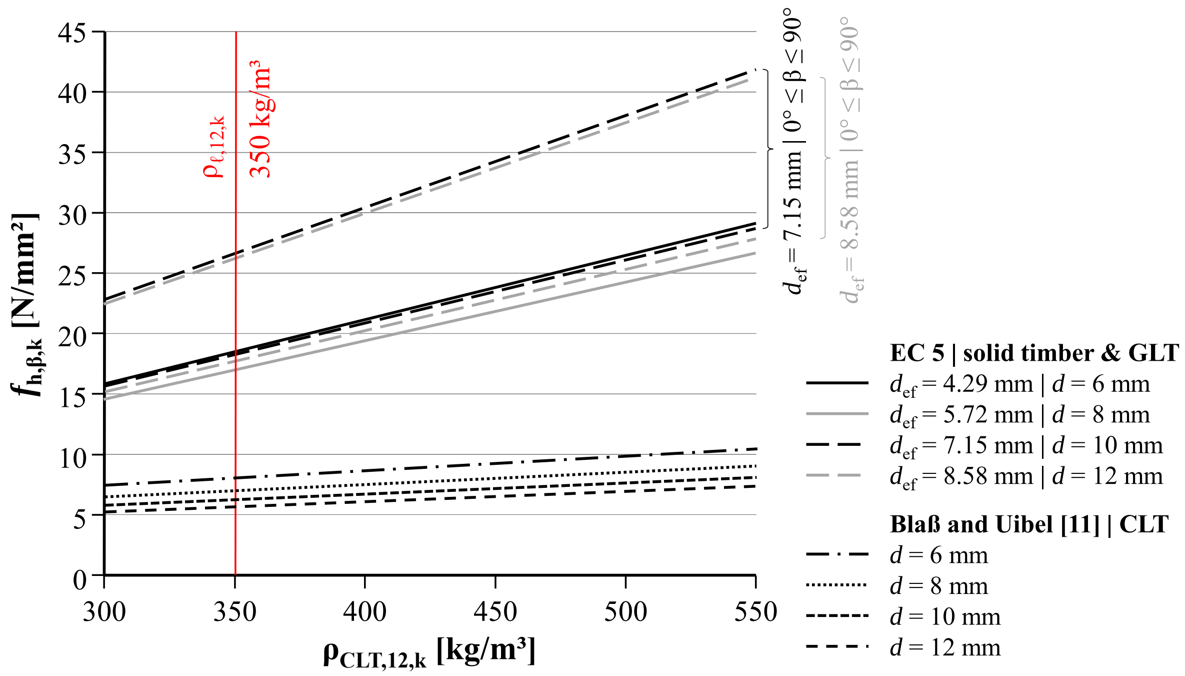

Fig. 16. Characteristic embedment strength vs. characteristic density of self-tapping screws: comparison between Eurocode 5 [17] (solid timber and GLT) with Blaß and Uibel [11] (CLT narrow face); d_{ef} = 1.1 · (0.65 · d) assumed; note: acc. to Eurocode 5 [17] screws with $d_{ef} \leq 6$ mm are treated like nails (inserted without predrilling; no influence of load-grain angle), with $d_{ef} > 6$ mm as dowels (inserted with predrilling; influence of load-grain angle).

In comparison to the embedment strength of nails and screws positioned in CLT side face (see Eq. (12)), in CLT narrow face only 1/3 of the resistance can be utilized. This is also reflected in Fig. 16 were a comparison between the approach of Blaß and Uibel [11] and Uibel and Blaß [13] with that in Eurocode 5 [17] for screws inserted in solid timber and glulam is presented.

Aiming on harmonizing the regulations for embedment strength of fasteners positioned in solid timber, glulam and CLT, for laterally loaded self-tapping screws (and nails) in CLT narrow face an additional coefficient $k_{lat,CLT,NF}$, taking into account the load configuration delivering the lowest embedment strength, and by additionally neglecting the influence of the load-grain angle, as anchored in Eurocode 5 [17], is proposed, see

$$f_{h,k,CLT,NF} = k_{lat,CLT,NF} \cdot f_{h,k,0,ST\,\&\,GLT} \quad \text{with} \quad k_{lat,CLT,NF} = 0.25 \tag{15}$$

with $f_{h,k,CLT,NF}$ and $f_{h,k,0,ST\,\&\,GLT}$ as the characteristic embedment strength of laterally loaded self-tapping screws in the narrow face of CLT and the characteristic embedment strength in solid timber and glulam (GLT) at a load-grain angle of $\beta = 0°$, respectively.

5. Connection design

5.1 Introduction and overview

For an appropriate design of connections comprising groups of fasteners in CLT, further specifics are required in addition to withdrawal and embedment strength, which are necessary for determining the single fastener's load-bearing capacity (according to Eq. (10) for axial and e.g. according to Johansen [30] for lateral loading). These additional specifics and verifications are often directly linked to connection failure modes. One required verification is the resistance of the component's net cross-section. Another verification is the load-bearing capacity of the group of fasteners, which concerns their effective number, n_{ef}, as well as the minimum spacing and the edge and end distances, a_i. It is worth pointing out that both properties, n_{ef} and a_i, are closely related to each other, i.e. $n_{ef} = n$ can only be achieved if the single fastener in conjunction with the anchorage material provides enough ductility for load redistribution and the minimum spacing (especially parallel to grain, a_1) is fulfilled, preventing unfavorable failure modes such as splitting parallel-to-grain or block shear.

With regard to the state-of-the-art knowledge on both, n_{ef} and a_i, many aspects are already covered by the report of Blaß and Uibel [11]. This source contains a comprehensive study aiming on the lateral load-bearing behavior of connections composed by dowels, nails and screws, situated in the side and narrow faces of CLT elements. Further and more recent publications, focusing on predominately axially loaded connections, are e.g. Mahlknecht and Brandner [31], Plüss and Brandner [33] and Brandner [14]. The main outcomes and recommendations from these publications are summarized and discussed in the following Sections 5.2 and 5.3.

Other publications which frequently examine dowel-type connections in CLT are more related to their cyclic load-bearing behavior and not to n_{ef} and a_i, e.g. Flatscher et al. [34] and Gavric et al. [35].

5.2 Laterally loaded dowel-type connections in CLT

Blaß and Uibel [11] conducted a comprehensive test program on laterally loaded connections in order to validate the applicability of their approaches for the characteristic embedment strength of dowels, self-tapping screws and nails for design purposes as well as for determining dowels and verifying nails and screws minimum spacing for CLT; see Fig. 17.

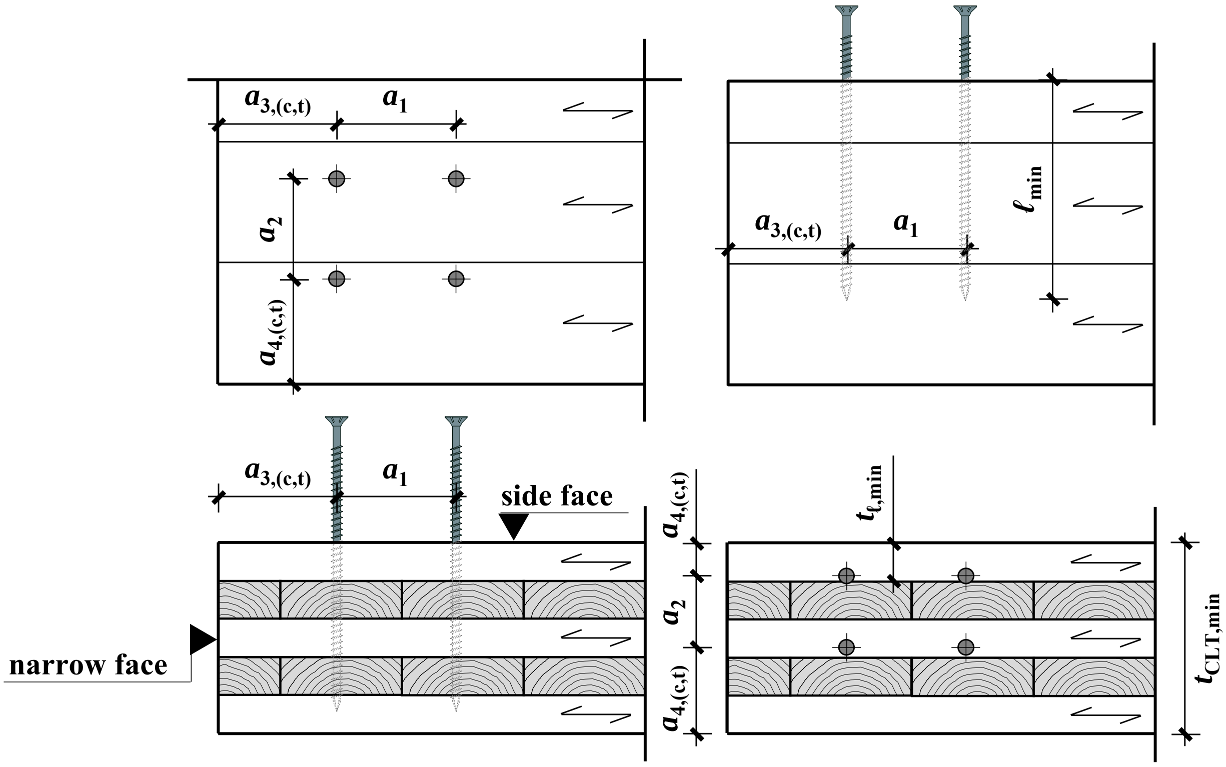

Fig. 17. Definition of minimum spacing, edge and end distances and further geometrical boundary conditions, exemplarily for self-tapping screws; according to Blaß and Uibel [11].

Apart from the applied fasteners and their position within the CLT element (side vs. narrow face), Blaß and Uibel [11] also varied the type of connection (steel-to-timber connections with inner and outer steel plate as well as CLT-CLT lap joints, both with one or two shear planes), the fastener diameter (dowels: d = {8, 12, 16, 20, 24} mm; screws: d = {8, 12} mm; profiled nails: d = {4, 6} mm), the number of fasteners in the group, n, as well as their spacing, edge and end distances and further geometrical boundary conditions, which are illustrated in Fig. 17.

The observations made by Blaß and Uibel [11] during testing connections of laterally loaded dowel-type fasteners in the CLT side face are summarized briefly:

- Apart from some specimen which failed in the zone of load introduction, other failure modes observed by testing connections with dowels were tension failure in layers close to the shear plane, successive shear & rolling shear failures and some block shear failures, whereby block shear failure emerged without regularity.
- As the number of dowels placed parallel to the outer layer's grain direction did not influence the load-bearing capacity, Blaß and Uibel [11] concluded that the effective number of fasteners n_{ef} can be set equal to their total number n.

- The load-carrying capacity of connections with dowels was predicted by means of the theory of Johansen [30] and the characteristic embedment strength $f_{h,k}$ according to Eq. (10). This characteristic embedment strength $f_{h,k}$ only implicitly represents an inhomogeneous stress distribution along the fastener axis due to penetrated alternating orthogonal layers. Despite these circumstances and although the connection's failure modes differed widely from failure modes observed by testing single dowels, overall good to conservative predictions of the load-carrying capacity of dowelled connections were made.
- Good validation for the embedment strength as input parameter in Johansen's [30] theory was also achieved for the majority of tested connections with self-tapping screws and nails. This also concerned the withdrawal strength as basis for the rope effect. The regulation of $n_{ef} = n$ is also proposed for these fasteners.

Similar to connections in CLT side face, proposals made by Blaß and Uibel [11] for the CLT narrow face could also successfully be validated. Two important observations made during testing are summarized in brief:

- Connections with dowels situated in layers perpendicular to grain and loaded parallel to grain failed by splitting already at small deformations. However, due to the implicit conservatism in predictions according to Blaß and Uibel [11] even these failure modes are covered but it is pointed out that the given recommendations are only proven for tested CLT layups and configurations.
- Tests with laterally loaded self-tapping screws situated in the CLT narrow face showed that for some configurations minimum spacing determined by insertion tests in advance were too small. Consequently, Blaß and Uibel [11] increased the corresponding values.

Minimum spacing, edge and end distances and further geometrical boundary conditions, as defined in Fig. 17, as outcome of the comprehensive test campaigns and proposal in Blaß and Uibel [11, 37] are summarized in Table 2 and Table 3.

Table 2. Minimum spacing, edge and end distances of dowel-type fasteners in CLT; according to Blaß and Uibel [11, 37].

Fastener	**Position**	a_1	a_2	$a_{3,t}$	$a_{3,c}$	$a_{4,t}$	$a_{4,c}$
Self-tapping screws	Side face	4 d	2.5 d	6 d	6 d	6 d	2.5 d
	Narrow face	10 d	3 d	12 d	7 d	–	5 d
(Profiled) nails	Side face	(3 + 3 cos β) d	3 d	(7 + 3 cos β) d	6 d	(3 + 4 sin β) d	3 d
Dowels	Side face	(3 + 2 cos β) d	3 d	5 d	4 d sinβ (min 3 d)	3 d	3 d
	Narrow face	4 d	3 d	5 d	3 d	–	3 d

Table 3. Further geometrical boundary conditions for dowel-type fasteners in the narrow face of CLT; according to Blaß and Uibel [11, 37].

Fastener type	$t_{CLT,min}$	$t_{\ell,min}$	ℓ_{min}^*
Self-tapping screws	10 d	$d \leq 8$ mm: 2 d $d > 8$ mm: 3 d	10 d
Dowels	6 d	d	5 d

* Dowels: minimum timber thickness, screws: minimum insertion depth

5.3 Axially loaded dowel-type connections in CLT restricted to self-tapping screws

With respect to axially-loaded fasteners, it has to be outlined that a_i, n_{ef} and additional geometrical boundary conditions in Blaß and Uibel [11] are only based on insertion tests (in respect to a_i for nails and screws) as well as tested lap-joints. Additional experimental campaigns were conducted at Graz University of Technology in order to validate the recommendations given by Blaß and Uibel [11] also for axially loaded (concentrated) connections in CLT. This concerned connections with self-tapping screws since these fasteners are exclusively applied for the transmission of heavy loads as well as for efficient system connectors, c.f. Chapter 1. The related studies are summarized separately in dependence of the screw position in the CLT panel:

Mahlknecht and Brandner [31] investigated concentrated connections of screws inserted via the CLT side face, by varying the minimum spacing $\{a_1, a_2\}$, the insertion depth ℓ_{min} as well as the number of screws, n. Despite the orthogonal layup of CLT and although the screws penetrated several layers, brittle block shear failure modes, as combination of rolling shear failure and failure in tension perpendicular to grain, were observed up to spacing $a_1 = a_2 < 7 \cdot d$ and depending on ℓ_{min}; c.f. Fig. 18. This failure mode, which is perhaps even more relevant for solid timber and GLT, misses so far a verification approach; a first proposal for solid timber and glulam is presented in Mahlknecht et al. [32].

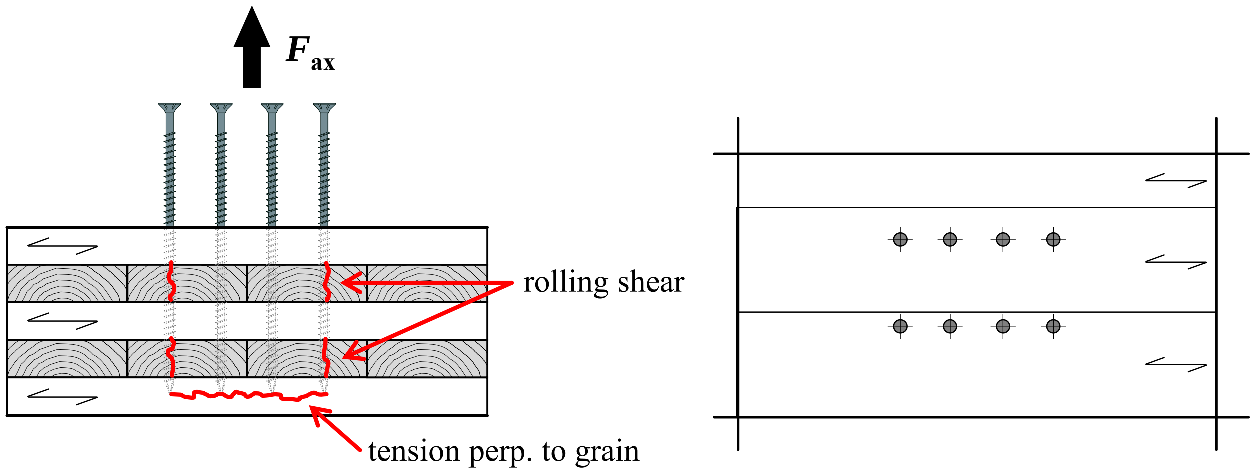

Fig. 18. Block shear failure of axially loaded groups of self-tapping screws situated in the CLT side face.

Plüss [36] conducted comprehensive tests on concentrated groups of axially-loaded screws in the CLT narrow face. The CLT layup, the number of fasteners, the thread-grain angle α as well as the spacing between the fasteners were varied. Table 4 summarizes recommendations for a_i as given by Plüss and Brandner [33]. Not surprisingly, a_1 decreasing with α was observed. Comparing the recommendations given in Table 2 for lateral and in Table 4 for axial loading for the worst case of $\alpha = 90°$, Table 4 gives slightly smaller minimum requirements.

Table 4. Minimum spacing of axially loaded self-tapping screws situated in the narrow face of CLT in dependence of α; according to Plüss and Brandner [33].

α	a_1	a_2
0°	2.5 d	
45°	5 d	
90°	7 d	5 d / 2.5 d *
0° | 90°	5 d	
45° | 45°	5 d	

* 5 d if inserted in the same layer, 2.5 d if inserted in different layers

With regard to the effective number of axially loaded self-tapping screws situated in CLT and basing on a successful verification by Mahlknecht and Brandner [31] (so far block shear failure can be prevented) and Plüss and Brandner [33], Brandner et al. 2016 [2] propose Eq. (16) for a related determination:

$$F_{\mathrm{ax,n}} = 0.90 \cdot \sum_{i=1}^{R} F_{\mathrm{ax,ref,i}} \cdot n_{\mathrm{i}} \tag{16}$$

with R as the number of different thread-grain angles, n_{i} as the number of screws per thread-grain angle and $F_{\mathrm{ax,ref,i}}$ as reference withdrawal capacity of a single fastener for a specific thread-grain angle. Note: laboratory tests indicated even $n_{\mathrm{ef}} \geq n$, which is dedicated to the homogenization occurring with increasing number of screws in a group. The pre-factor 0.9 shall cover inevitable inaccuracies in practical connection execution.

6. Conclusions

Based on the compiled state-of-knowledge on axially and laterally loaded dowel-type fasteners in CLT as well as the comparisons made with current regulations on dowel-type fasteners in solid timber and glulam according to Eurocode 5 [17], the following conclusions are made:

- It is suggested to regulate the embedment as well as the withdrawal strengths of dowel-type fasteners in CLT in analogy to solid timber and glulam. Therefore, generic approaches as exemplarily presented for the withdrawal capacity of self-tapping screws in Eqs. (3–5), should be defined. Some suggestions how to regulate the embedment strength of dowel-type fasteners in CLT based on that of solid timber are presented in Chapter 4. For profiled nails, recent studies as well as the provisions in Eurocode 5 [17] indicate the necessity of performance testing for axial loading.
- Based on current test experience the following suggestions can be made for applications of dowel-type fasteners in respect to loading and positioning in CLT:

Table 5. Dowel-type fasteners in CLT side and narrow face: recommended applications according to Schickhofer et al. [4].

	Side face	**Narrow face**
Profiled nails	for axial and lateral loads	not applicable
Smooth dowels and tight-fitting bolts	only for lateral loads	not applicable
Self-tapping screws	for axial and lateral loads	for axial and lateral loads

- With respect to laterally loaded connections composed by dowel-type fasteners in CLT, the ductile behavior in case of side face insertion, which is due to the orthogonal reinforcing layup of CLT, enables $n_{ef} = n$. For laterally loaded fasteners in the CLT narrow face, n_{ef} should be calculated according to the design provisions for solid timber, as e.g. given in Eurocode 5 [17]. For axially loaded self-tapping screws inserted in CLT side or narrow face a suggestion for n_{ef} is given in Eq. (16).

Regulations on minimum spacing and edge and end distances have to consider the specific structure of CLT, i.e. the orthogonal layup and the influence of gaps. Proposals together with additional geometrical regulations can be found in

- Table 4.
- Apart from regulations on single fastener properties and connections, to ensure the integrity of solid timber constructions with CLT the following maximum spacing e_{max} between connections are recommended:

Table 6. Execution requirements for CLT connections according to ÖNORM B 1995-1-1 [38].

connection type	**e_{max} [mm]**
CLT to CLT with screws	500
CLT to GLT with screws	500
CLT to steel girders with screws	750
CLT to solid components with angle brackets	1,000

Acknowledgements

The publication, as part of the proceedings from the Conference of COST Action FP1402 "International Conference on Connections in Timber Engineering – From Research to Standards", held on the 13th September 2017 at Graz University of Technology, Graz, Austria, was written in the framework of the COST Action FP1402 "Basis of Structural Timber Design – from Research to Standards", chaired by Philipp Dietsch, Technische Universität München (www.costfp1402.tum.de).

References

[1] *EN 16351:2015*. Timber structures – Cross laminated timber – Requirements. CEN, Brussels.

[2] Brandner R, Flatscher G, Ringhofer A, Schickhofer G, Thiel A (2016) Cross laminated timber (CLT): Overview and development. *European Journal of Wood and Wood Products* **74**:331–351. DOI 10.1007/s00107-015-0999-5.

[3] Flatscher G, Schickhofer G (2016) *Displacement-based determination of laterally loaded cross laminated timber (CLT) wall systems*. INTER Meeting 49, Paper 49-12-1, pp. 131-150, Graz, Austria.

[4] Schickhofer G, Bogensperger T, Moosbrugger T. (eds., 2010) *BSPhandbuch: Holz-Massivbauweise in Brettsperrholz – Nachweise auf Basis des neuen europäischen Normenkonzepts*. Verlag der Technischen Universität Graz, Graz, Austria, (in German).

[5] Bernasconi A (2012) *Überbauung Via Cenni Mailand – 4 Holzhochhäuser mit je 9 Geschossen*. Internationales Holzbau-Forum, Garmisch Partenkirchen, Germany (in German).

[6] Polastri A, Angeli A, Gianni DR (2014) *A new construction system for CLT structures*. World Conference on Timber Engineering (WCTE), Quebec City, Canada.

[7] Polastri A, Giongo I, Angeli A, Brandner R (2017) Mechanical characterization of a pre-fabricated connection system for cross laminated timber structures in seismic regions. *Engineering Structures* (in press). DOI 10.1016/j.engstruct.2017.12.022.

[8] Kraler A, Kögl J, Maderebner R, Flach M (2014) *SHERPA-CLT-Connector for cross laminated timber (CLT) elements*. World Conference on Timber Engineering (WCTE), Quebec City, Canada.

[9] *Rothoblaas* (2015) Wood Connectors and Timber Plates. Catalogue.

[10] *Sherpa* (2013) Sherpa Manual. Catalogue.

[11] Blaß HJ, Uibel T (2007) *Tragfähigkeit von stiftförmigen Verbindungsmitteln in Brettsperrholz*. Karlsruher Berichte zum Ingenieurholzbau, Band 8, Universitätsverlag Karlsruhe, ISBN 978-3-86644-129-3 (in German).

[12] Uibel T, Blaβ HJ (2006) Load carrying capacity of joints with dowel type fasteners in solid wood panels. CIB-W18 meeting 39, Paper 39-7-5, Florence, Italy.

[13] Uibel T, Blaß HJ (2013) *Joints with dowel type fasteners in CLT structures*. In: Harris R, Ringhofer A, Schickhofer G (eds.). COST Action FP1004: focus solid timber solutions – European conference on cross laminated timber (CLT), University of Bath, UK.

[14] Brandner R (2016) *Group action of axially loaded screws in the narrow face of cross laminated timber*. World Conference on Timber Engineering (WCTE), Vienna, Austria.

[15] *EN 338:2016*. Structural timber – Strength classes. CEN, Brussels.

[16] *PT SC5.T1* (2018) Final draft of design of cross laminated timber in a revised Eurocode 5-1-1, Version: 2018-01-30.

[17] *EN 1995-1-1:2004+AC:2006+A1:2008+A2:2014*. Eurocode 5: Design of timber structures – Part 1-1: General – Common rules and rules for buildings. CEN, Brussels.

[18] Uibel T, Blaβ HJ (2007) *Edge joints with dowel type fasteners in cross-laminated timber*. CIB-W18 meeting 40, Paper 40-7-2, Bled, Slovenia.

[19] Ringhofer A (2017) *Axially Loaded Self-Tapping Screws in Solid Timber and Laminated Timber Products*. Dissertation, Graz University of Technology, Austria.

[20] Reichelt B (2012) *Einfluss der Sperrwirkung auf den Ausziehwiderstand selbstbohrender Holzschrauben*. Master thesis, Graz University of Technology, Austria (in German).

[21] Ringhofer A, Brandner R, Schickhofer G (2015) Withdrawal resistance of self-tapping screws in unidirectional and orthogonal layered timber products. *Journal of Material Structures* **48**:1435–1447.

[22] Grabner M (2013) *Einflussparameter auf den Ausziehwiderstand selbstbohrender Holzschrauben in BSP-Schmalflächen*. Master thesis, Graz University of Technology, Austria (in German).

[23] Brandner R, Ringhofer A, Grabner M (2017) Probabilistic Models for the Withdrawal Behavior of Single Self-Tapping Screws in the Narrow Face of Cross Laminated Timber. *European Journal of Wood and Wood Products* **76**(1):13-30, DOI 10.1007/s00107-017-1226-3.

[24] Silva C, Branco JM, Ringhofer A, Lourenco PB, Schickhofer G (2016) The influences of moisture content variation, number and width of gaps on the withdrawal resistance of self tapping screws inserted in cross laminated timber. *Construction and Building Materials* 125:1205-1215.

[25] Ringhofer A, Brandner R, Schickhofer G (2015) *A universal approach for withdrawal properties of self-tapping screws in solid timber and laminated timber products*. 2nd INTER-Meeting, Paper 48-7-1, pp. 79-96, Sibenik, Croatia.

[26] Kennedy S, Salenikovich A, Munoz W, Mohammad M (2014) *Design equations for dowel embedment strength and withdrawal resistance for threaded fasteners in CLT*. World Conference on Timber Engineering (WCTE), Quebec City, Canada.

[27] Blaß HJ, Bejtka I, Uibel T (2006) *Tragfähigkeit von Verbindungen mit selbstbohrenden Holzschrauben mit Vollgewinde*. Karlsruher Berichte zum Ingenieurholzbau, Band 4, Universitätsverlag Karlsruhe, ISBN 3-86644-034-0 (in German).

[28] Hankinson RL (1921) Investigation of crushing strength of spruce at various angles to the grain. *Air Service Information Circular*, McCook Field Report Serial No. 1570, **III**(253):1-15.

[29] Sandhaas C, Görlacher R (2017) Nailed joints: Investigation on parameters for Johansen model. 4th INTER-Meeting, Paper 50-7-3, pp. 95-109, Kyoto, Japan.

[30] Johansen KW (1949) Theory of timber connections. *International Association for Bridge and Structural Engineering* **9**:249–262.

[31] Mahlknecht U, Brandner R (2013) *Untersuchungen des mechanischen Verhaltens von Schrauben-Verbindungsmittelgruppen in VH, BSH und BSP*. Research Report, holz.bau forschungs gmbh, Graz, Austria (in German).

[32] Mahlknecht U, Brandner R, Ringhofer A, Schickhofer G (2014) *Resistance and failure modes of axially loaded groups of screws*. In: Aicher S, Reinhardt HW, Garrecht H (eds), Materials and joints in timber structures, RILEM Book series 9, DOI 10.1007/978-94-007-7811-5_27.

[33] Plüss Y, Brandner R (2014) *Untersuchungen zum Tragverhalten von axial beanspruchten Schraubengruppen in der Schmalseite von Brettsperrholz (BSP)*. Internationales Holzbau-Forum IHF, Garmisch-Partenkirchen, Germany (in German).

[34] Flatscher G, Bratulic K, Schickhofer G (2014) *Screwed joints in cross laminated timber structures*. World Conference on Timber Engineering (WCTE), Quebec City, Canada.

[35] Gavric I, Fragiacomo M, Ceccotti A (2015) Cyclic behavior of typical screwed connections for cross-laminated (CLT) structures. *European Journal of Wood and Wood Products* **73**:179–191, DOI 10.1007/s00107-014-0877-6.

[36] Plüss Y (2014) *Prüftechnische Ermittlung des Tragverhaltens von Schraubengruppen in der BSP-Schmalfläche*. Master thesis, Graz University of Technology, Austria (in German).

[37] Blaß HJ, Uibel T (2009) Bemessungsvorschläge für Verbindungsmittel in Brettsperrholz. *Bauen mit Holz* **111**:46-53 (in German).

[38] *ÖNORM B 1995-1-1:2015 (Eurocode 5)*. Design of timber structures – Part 1-1: General – Common rules and rules for buildings – National specifications for the implementation of ÖNORM EN 1995-1-1, national comments and national supplements”, ASI, Austria (in German).

Dowelled connections and glued-in rods in beech wood

Steffen Franke
Bern University of Applied Science
Biel/Bienne, Switzerland

Bettina Franke
Bern University of Applied Science
Biel/Bienne, Switzerland

Summary

Hardwood is becoming more and more important in timber structures. The natural higher strength potential increases the potential of timber structures and power to compete with steel or concrete. However, for applying the typical carpentry joints or connections with mechanical fasteners, the performance parameters, stiffness and load-carrying capacity, defined by e.g. embedment capacity or withdrawal capacity are less standardized compared to softwood. Therefore, structural systems, parameters and relations for connections in beech wood are summarized and discussed with focus on European hardwood.

1. Introduction

There is lot of discussion and ambition in Europe about the use of hardwood as construction material. More wood is being growing than being used e.g. in the Swiss forest. Especially the hardwood stock has increased since 1995. In Switzerland, 31% of the entire wood stock is hardwood, where the biggest part with 18% counts for beech wood [1]. On the one hand, hardwood provides excellent mechanical strength properties but on the other hand the strength parameters are less investigated and standardized for the design of carpentry joints or connections with mechanical fasteners. The current design equations are developed and mainly valid for softwood. Details and explanations for hardwood are mostly missing. Hence, designers may avoid designing with hardwood [2]. However, connections play an important role in timber structures and can be classified according to the structure and loading situation (shown in Fig. 1) in:

- Tension or compression connections (parallel or under an angle to grain)
- Rigid and flexible joints
- Shear connections, mainly as main-sub girder joint
- Transverse connections under tension, including reinforcement
- Transverse connections under compression, including bearing and reinforcement

or according to the type, and/or fastener used:

- Glued connections
- Carpentry connections
- Connections with mechanical fasteners, e.g. nails, screws, dowels, glued-in rods

The performances of connections in modern hardwood constructions must be determined with high reliability. The behaviour of connections is characterized by its stiffness and its capacity. The European Yield Model (EYM) is widely accepted for the calculation of the load-bearing capacities of multiple shear plane connections with dowel-type fasteners based on specific material properties and joint dimensions. For hardwood connections, the research shows still open queries even if partly comprehensive investigations are carried out.

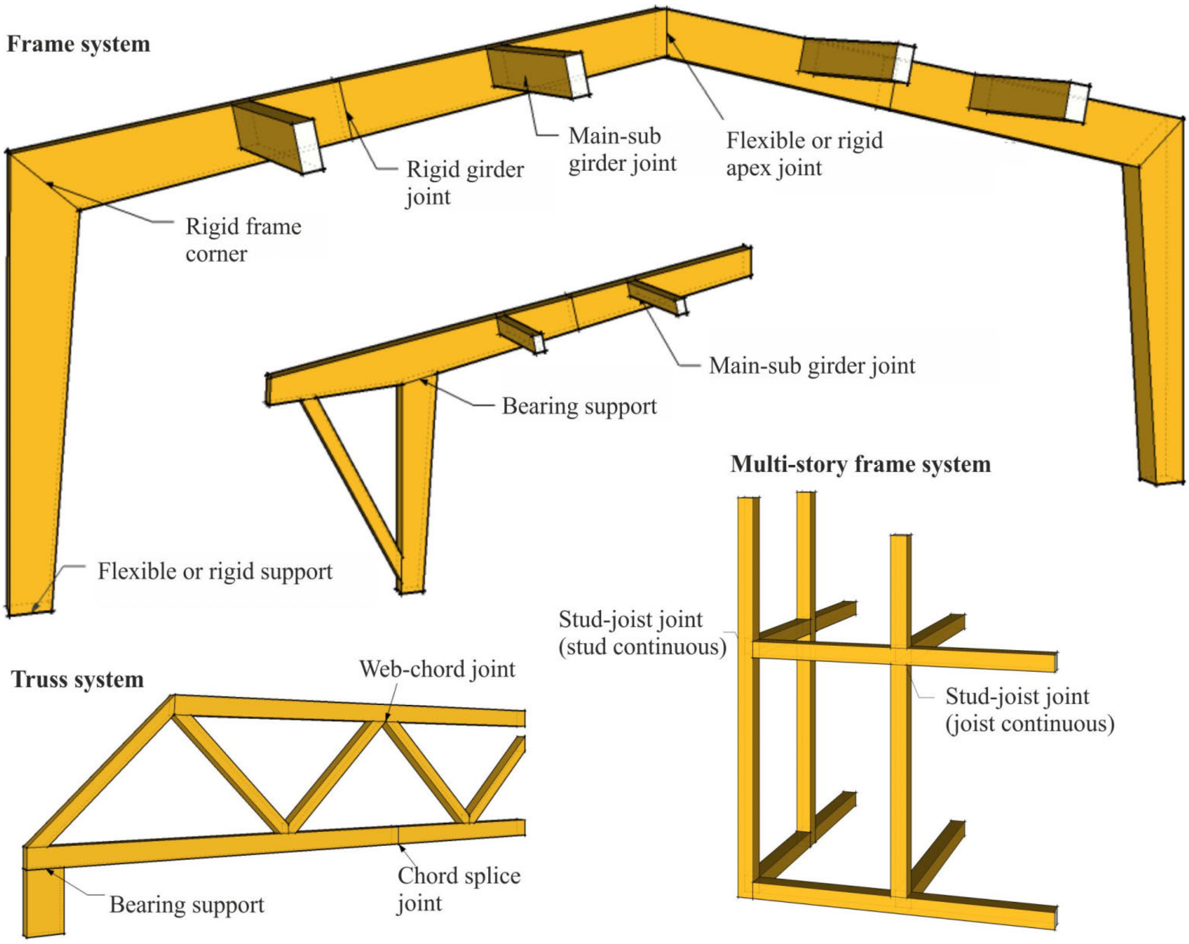

Fig. 1. Typical connection situations at frame constructions, truss systems or multi-story timber structures

2. Connections in hardwood

2.1 Characterization of connection types

Within the framework of a research project "Investigation and development of design parameters and methods for connections in hardwood", financed by the Swiss Federal Office for the Environment FOEN, a workshop with engineers, architects and practitioners was carried out to define beech-relevant (high performing) connection types. The background for the discussion was the study of different timber structures made of hardwood, which included single and multi-span beams, frames, trusses, frame systems (stud, joist), and shell structures. The categories of joints regarding the loading situation in Fig. 1 were evaluated according to their practical appearance, possibilities and acceptance. The main criteria were as following:

- Potential of practical application for hardwood structures
- Load-carrying capacity and performance rate
- Flexibility/rigidity/compliance, robustness and ductility

The sub criteria were:

- Manufacturing
- Transport and logistics
- Erection
- Fire resistance
- Aesthetics

Table 1 shows the matrix of joints against the loading situations including the realization and relevance of joints. As a result, the main relevant (ranking 2 and 3) connections in hardwood were defined as connections with or as:

- Glued in rods
- Long screws, $l > 200$ mm (self-tapping or pre-drilled) and drilled in rods
- Short screws $l \leq 200$ mm (without pre-drilling, self-tapping)
- Dowels/bolts
- Carpentry connections

Hereafter, the focus is on connections with steel dowels and connections with glued-in rods. Following, the load-carrying capacity and failure behaviour is described in relation to the necessary design parameters.

Table 1. Matrix of joints and their practical relevance (ranking) of acceptance

Connection / Loading situation	Glued	Glued-in rods	Selftapping Screws/ Drilled-in rods	Nails or short Screws	Dowels, Bolts	System-connectors	Carpenter/ Contact Joints
Tension/Compression (‖, ∢ to grain)	1	3	3	2	3	0	3
Moment	1	3	-	0	3	-	-
Shear (Main/sub girder)	-	1	2	2	2	2	3
Tension perp. to grain Reinforcement	0	3	3	-	-	-	-
Compression perp. to grain, Bearing, Reinforcement	-	3	3	-	-	-	-

2.2 Steel dowel-type connections

Steel bolts and dowels are commonly used in tension, shear and moment connections with slotted-in steel plates or outer steel plates, as shown in Fig. 2. The connection is based on transfer of tension, compression or shear forces through shear loading of the fastener and embedment of the wood. The load-carrying capacity depends on the material characteristic of the fastener, the embedment strength of the wood, load to grain angle, diameter of fastener and the connection layout regarding the effective number of fasteners. To avoid splitting the edge and end distances as well as the distances between must be well considered. Reinforcements with transversely insert screws are possible. The following failure mechanisms can appear:

- Shear failure of bolt/dowel
- Embedment failure of wood
- Wood failure in tension of the net cross section or in compression due to buckling or kink banding

EN 1995-1-1:2004 [3] provides design equations for bolts and dowels. The design considers the yield moment of the fastener and the embedment strength of the wood. The load-carrying capacity of bolted connections can increase when accounting for the rope effect. However, the specifications for hardwood are currently less investigated compared to softwood. The following material parameters or dimensions are necessary for the design:

- Embedment strength $f_{h,k}$
- Stiffness K_{ser}
- Load to grain angle α
- Diameter d
- Minimum thickness t
- Layout of the connection, spacings and edge distances
- Group effect

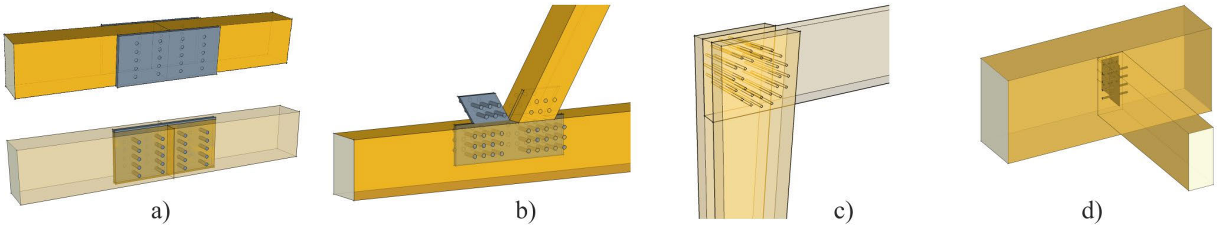

Fig. 2. Application of dowels or bolts: a) tension connection, b) truss knot, c) semi-rigid frame corner, and d) main to sub girder connection

2.3 Glued-in rods

Glued-in rods are mainly efficient for the transfer of tension and compression loads in axial direction. Moments can be split in tension and compression actions. Shear forces will be carried by the embedment of the timber and steel cross-section. Tension forces will be transferred from the wood through the glue to the rod where compression can also be transferred by direct contact. Depending on the connection type, the glued-in rods will be arranged parallel, inclined or perpendicular to grain. They can be applied in frame edges, as tension member extension as well as reinforcement for transverse tension or compression stress, as shown in Fig. 3. The following failure mechanisms can appear:

- Steel failure of rod
- Glue (bonding) failure
- Buckling of the rod

During the design, the composite of wood and rod as well as the strength of the bond line must be checked. In connections with a group of fasteners, the group effect must be considered, too. The spacing and edge distances influence the load-carrying capacity. DIN EN 1995-1-1/NA:2010 [4] provides design equations for glued-in rods. The load-carrying capacity depends on the following material parameters or dimensions:

- Embedment strength $f_{h,k}$
- Withdrawal resistance $R_{ax,k}$
- Load to grain angle α
- Rod diameter d
- Minimum thickness and embedding length l
- Layout of the connection, spacing and distance
- Group effect.

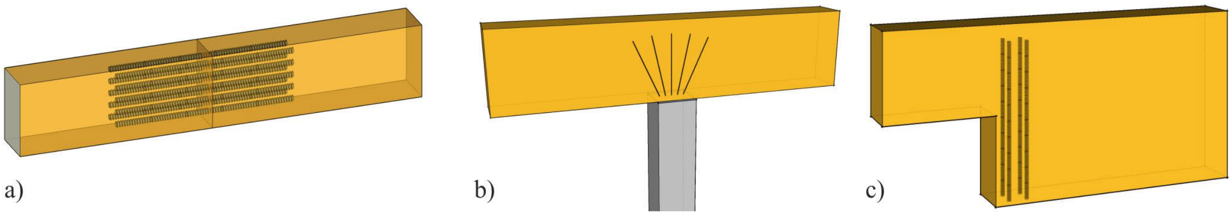

Fig. 3. Application of glued-in rods: tension member extension, transverse tension or compression reinforcement (from left to right)

3. Material and parameters for the design

3.1 Material

This paper comprises information regarding hardwood as solid wood and wood products like glulam or cross-laminated timber made of European beech. For glulam made from beech, the density and the main strength and stiffness parameters currently used are based on properties defined by a leading timber construction company as shown in Table 2. These properties will further be specified and extended for standardised products of beech glulam within a current research project.

Table 2. Current material characteristics of beech glulam from manufacturer [5]

Material properties		GL40k	GL40h	GL48k	GL48h
Bending strength	$f_{m,d}$ [MPa]	26.5	26.5	32.0	32.0
Tension parallel to grain	$f_{t,0,d}$ [MPa]	20.0	22.0	22.0	25.0
Compression parallel to grain	$f_{c,0,d}$ [MPa]	22.0	25.0	25.0	28.0
Tension perp. to grain	$f_{t,90,d}$ [MPa]	0.25	0.25	0.25	0.25
Compression perp. to grain	$f_{c,90,d}$ [MPa]	4.5	4.5	5.0	5.0
Shear	$f_{v,d}$ [MPa]	3.0	3.0	3.0	3.0
Modulus of elasticity	$E_{0,mean}$ [MPa]	14’000	14’000	15’000	15’000
	$E_{90,mean}$ [MPa]	1’000	1’000	1’000	1’000
Modulus of shear	G_{mean} [MPa]	1’000	1’000	1’000	1’000
Density	$f_{m,d}$ [kg/m^3]	550	580	600	620

3.2 Embedment strength

The European standard EN 1995-1-1:2004 [3] provides values for embedment strength in dependency of the density. The empirical equations for embedment strength were proposed by Whale et al. [6-8] based on tests on softwood and tropical hardwood. Various other researchers investigated the embedment strength for European hardwoods e.g. ash, beech or oak and derived equations, [9-14]. The parameters observed show a range of 20 MPa depending on the density and fastener diameters, as shown in Fig. 4. Recent research results by Hübner [12] or Sandhaas et al. [13] lead both to different approximations and confirm the complexity of the determination of the embedment strength because of different test setups and analysis methods, Franke & Magnière [15]. The European standard covers mostly the mean range of the embedment strength depending on the density and fastener diameter and will be used for the following approximations of the load-carrying capacities of connections in beech wood. The research results for the embedment strength show a wider spread according to the load to grain angle, as shown in Fig. 4. Here the assumption of the European standard is more conservative.

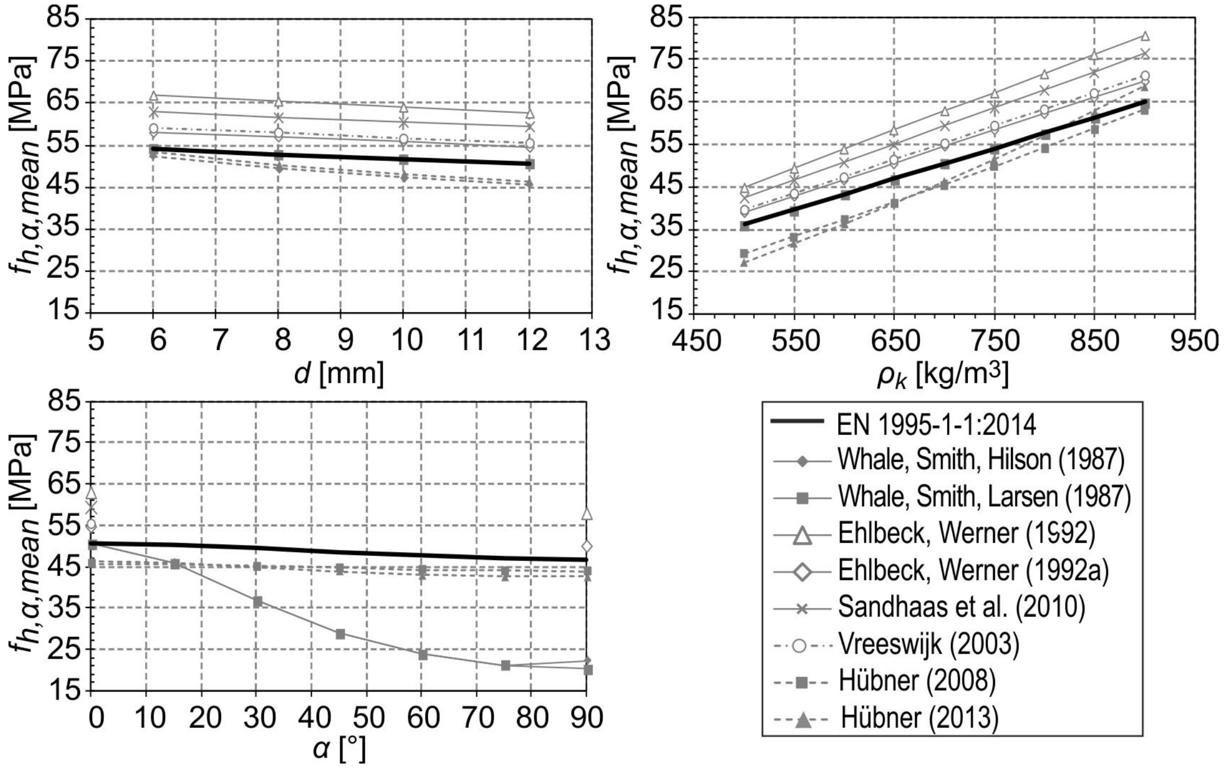

Fig. 4. Embedment strength on mean level for hardwoods in relation to the diameter d, the density ρ and the load to grain angle α, where ρ = 700 kg/m^3, α = 0°, d = 12 mm, resp.

4. Investigation on the assembling of connections in beech wood

4.1 Steel dowel-type connections

According to EN 1995-1-1:2004 [3], the holes for dowel-type fasteners must be predrilled to reduce the risk of splitting during insertion of the fasteners. However, information about the predrilling diameter for dowels is not provided. Practically, predrilling diameters smaller than the nominal dowel diameter are used for softwood but that is not possible in beech wood. Therefore, small test series with single and double part specimens and different predrilling diameters were carried out firstly under practical conditions with manual insertion and secondly by using a testing machine to quantify the insertion force [16]. Fig. 5 shows the summary of the penetration loads and that predrilling with a diameter of d + 0.1 mm is recommended for use. Predrilling with greater diameters will lead to too loose settings of the dowels and smaller predrilling diameters can lead to insertion problems or premature cracks where the load-carrying capacity of the connection could be reduced.

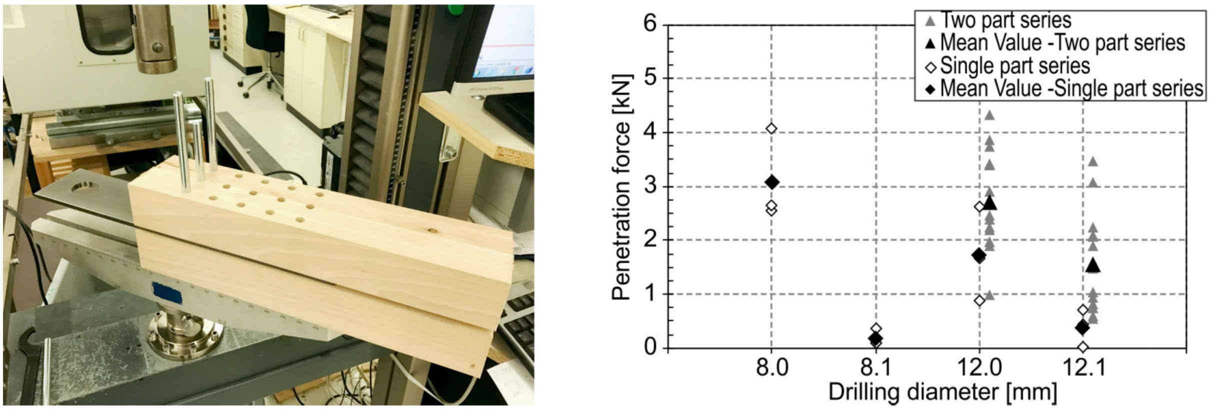

Fig. 5. Test setup for the investigation of penetration forces in two-part series, a double shear plane connection with slotted in steel plate (left), and comparison of penetration forces observed (right)

4.2 Glued-in rods

For glued-in rods, predrilling diameters D of $D = d + 2$ mm and $D = d + 4$ mm (d as nominal rod diameter was 16 mm) were used to assess the assembling conditions regarding successful distribution of adhesives over complete length and around the rod and the influence on the capacity and failure behaviour. Therefore, a symmetric pull-out test configuration with single rods oriented in parallel to grain direction ($\alpha = 0°$, bond length 10d) were used. Glulam of GL40h of European beech (*Fagus sylvatica*) from Swiss forests with average density of about 710 kg/m^3 and moisture content of 10.5% was used for the specimens. Threaded steel rods with a strength class of 8.8 were glued-in using a two-component PUR glue.

Testing series with the predrilling diameter $D = d + 4$ mm show a higher capacity (F_{mean} = 132.8 kN, CoV = 8.7%) and higher ductility compared to $D = d + 2$ mm (F_{mean} = 112.0 kN, CoV = 5.9%) as shown in Fig. 6. The differences can be found in the failure behaviour, where the series with $D = d + 2$ mm tend to fail in adhesion or wood shear failure, the $D = d + 4$ mm show cohesion failure within the bond line, see Fig. 6. Therefore, predrilling diameters of $D = d + 4$ mm are recommended for use of glued-in rods in beech.

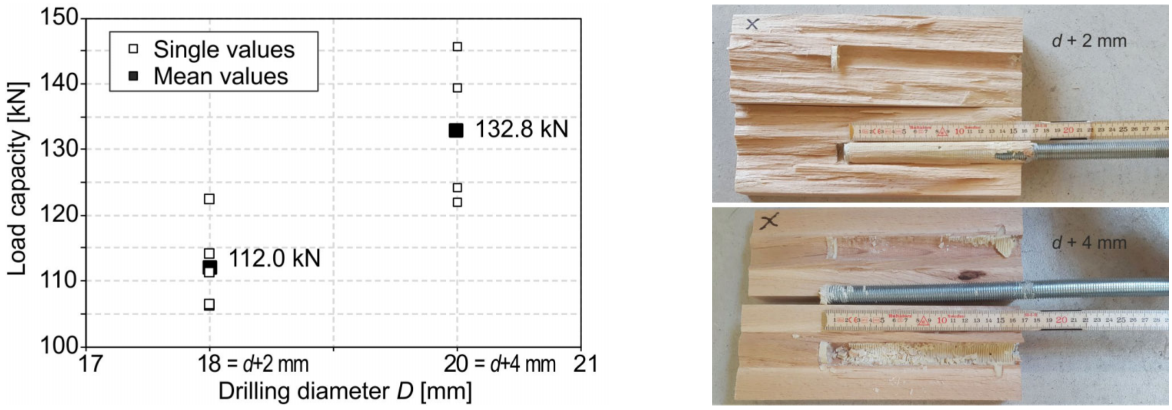

Fig. 6. Comparison of pull-out strength for drilling parameters investigated (left), and typical failure of glued-in rods under axial loading (right)

5. Load-carrying behaviour of connections

5.1 Steel dowel-type connections

The load-carrying capacity and failure behaviour of dowel-type connections are described by splitting of side members, embedment failure, yielding of fastener or shear of fasteners. For high performing connections a ductile failure is intended. For the characterization of the current design in EN 1995-1-1:2004 [3], test series with double-shear dowel-type connections with slotted-in steel plates were realised. EN 1995 -1-1:2004 [3] provides no specific regulations for spacing and edge distances of fasteners in beech wood. The current regulations depend only on the diameter of the fastener whereby the specific strength behaviour of beech wood is not considered. Therefore, the testing program carried out considers a variation of the dowel diameter, fastener spacing, number of fasteners perpendicular and in load direction and timber member thickness. The principle connection was a double-shear dowel-type connection with dowels of 8 mm diameter, one slotted-in steel plate and layout of m x n by 2 x 3, as shown in Fig. 7. Glulam of GL40h of European beech (*Fagus sylvatica*) from Swiss forests with an average density of about 710 kg/m^3 and a moisture content of 10.6% was used for the specimens. The steel dowels with a strength class of S355 were inserted prior to testing. The steel plate thickness was 8 mm. The tests were carried out according to EN 26891:1991 as symmetric pull-pull configuration, as shown in Fig. 7. Fig. 8 shows the evaluation method used for the determination of the maximum load-carrying capacity of the connection according to EN 26891:1991 [17]. The results are given per fastener (including two shear planes) and grouped according to the fastener spacings a_1 and a_2, the member thickness t, and number of rows in load direction n, as shown in Fig. 9 to Fig. 12.

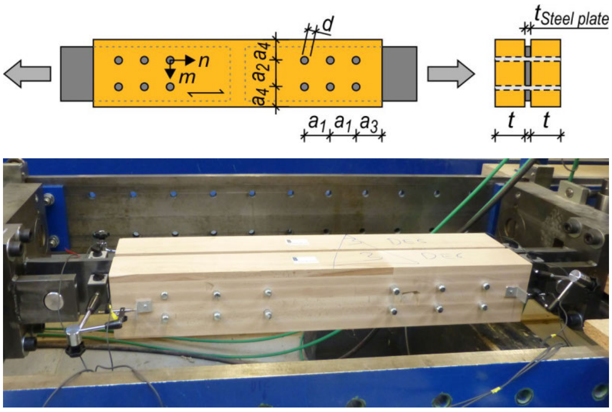

Fig. 7. Double-shear connection layout and test setup

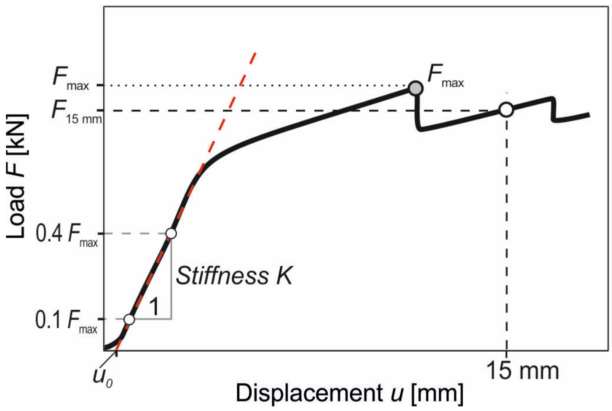

Fig. 8. Evaluation principle for load-carrying capacity and stiffness

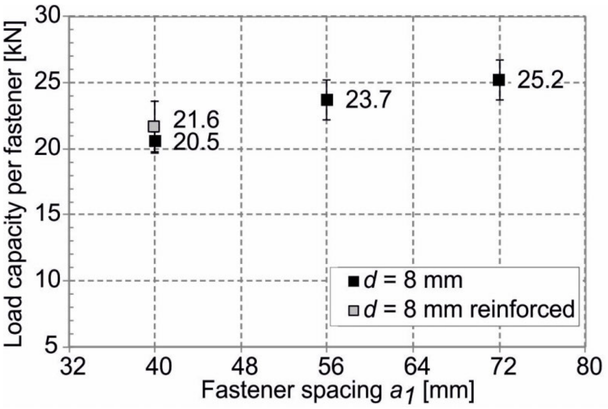

Fig. 9. Load-carrying capacity of dowel-type connections depending on fastener spacing a_1, spacing a_2 and a_4 with 3d, and a_3 with 7d

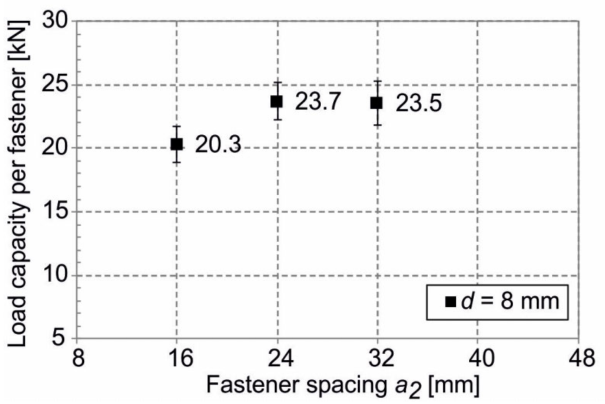

Fig. 10. Load-carrying capacity of dowel-type connections depending on fastener spacing a_2, spacing a_1 and a_3 with 7d, and a_4 with 3d

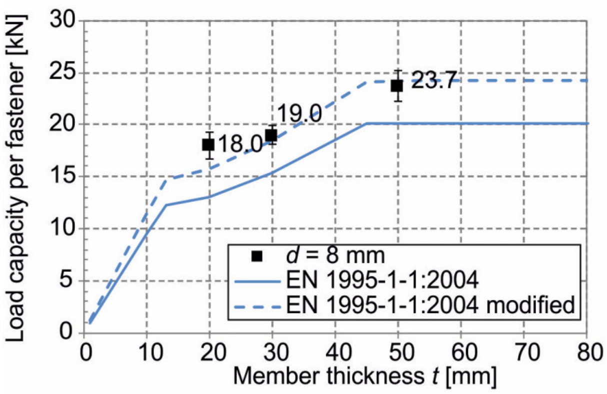

Fig. 11. Load-carrying capacity of dowel-type connections depending on member thickness t, the spacings are a_1 and a_3 with 7d, a_2 and a_4 with 3d

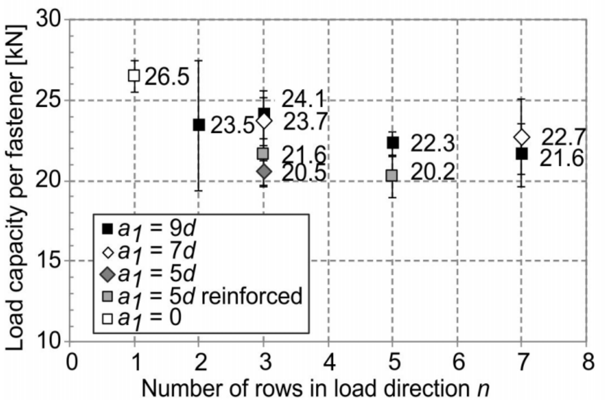

Fig. 12. Load-carrying capacity of dowel-type connections depending on number of rows n (see Fig. 7)

The load-carrying capacities per fastener observed show a certain linear increase with increasing spacing between the dowel parallel to grain a_1 from 5d to 9d and with increasing spacing perpendicular to grain a_2 from 2d to 3d.

For the dependency on the member thickness, Fig. 11, the three different failure mechanisms according to the theoretical approach (EYM by Johansen) can be seen. With increasing member thickness t, firstly embedment failure in timber member (linear increase of curve) governs, secondly one plastic hinge forms (concave part of curve) and finally two plastic hinges form (constant load-carrying capacity) where maximum capacity is observed. The load-carrying capacities reached fit to phase two and three and are higher than calculated load F_{mean} using the EN 1995-1-1:2004 [3] design equations considering the mean density for beech glulam with ρ_{mean} = 700 kg/m^3, steel plate strength of $f_{u,mean}$ = 560 MPa and steel dowel-type strength of $f_{u,mean}$ = 610 MPa (determined in tests according to ISO 6892-1). No rope effect is considered for dowelled connections. The curve "EN 1995-1-1:2004 modified" uses the same formulas and material parameters as before but the results are multiplied with a factor of 1.2 to see if the load-carrying capacities perform according to the EYM theory. The difference of about 20% between experimentally derived and calculated capacities are due to the scatter and uncertainties of density, embedment strength formula and the EYM itself.

5.2 Glued-in rods

The pull-out resistance was tested with single rods oriented in three different angles to grain direction: 0° – parallel to grain, 45° – angle to grain, and 90° – perpendicular to grain. The 0° orientation was done as symmetric pull-pull-test configuration and the 45° and 90° orientations were done in push-pull configuration, see Fig. 13. The variation includes rods with nominal diameters of 12, 16, and 20 mm with embedded thread lengths of 10d and 15d as well as different distances to the edge $a_{2,c}$ = 1.5d, 2.5d, 3.5d. For the assembly a predrilling diameter of the nominal diameter plus 4 mm was applied as specified before. Glulam of GL40h of European beech (*Fagus sylvatica*) from Swiss forests with an average density of about 710 kg/m^3 and a moisture content of 10.5% was used for the specimen. Threaded steel rods with a strength class of 8.8 were glued in using a two-component PUR glue.

The pull-out resistance calculated form the ultimate force and divided by the embedding surface using the nominal rod diameter of all series with pull-out failure are summarized for parallel to grain and 45° and 90° to grain direction in Fig. 14. Specimens with rods in parallel to grain direction with an embedment length of 10d lead to pull-out or cracking failure whereas embedment lengths of 15d and 20d always show steel failure. Small edge distances of 1.5d lead to splitting failure while edge distances of 2.5d and 3.5d lead to pull-out failure respectively steel failure. Test series with 45° and 90° to grain direction show pull-out failure only for the tests with 10d embedding length for rods with 16 mm and 20 mm in diameter.

Fig. 13. Test setup for glued in rods: principle sketch, photo for parallel to grain, 90° and 45° to grain (from left to right)

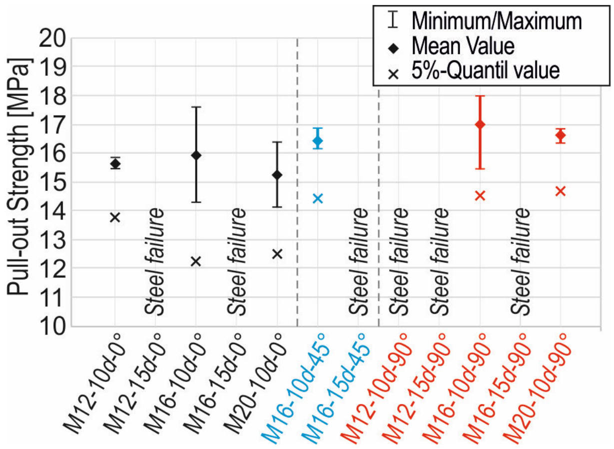

Fig. 14. Mean pull-out strengths for glued-in rods with different angle to grain directions

6. Discussion and conclusion

6.1 Dowels

The failure behaviour of steel to timber beech wood connections depends on the fastener slenderness ratio. For unreinforced connections slender fasteners lead to increased ductility while stout fasteners result in brittle failure. If minimum spacing requirements are satisfied, the effective number of fasteners only depends on the number of fasteners in a row parallel to the grain. It should further be noted that the effective number of fasteners as observed in multiple fastener steel-to-timber beech wood connections is based on a combination of failure behaviours both ductile and brittle. However, for the comparison of the test results with the EN 1995-1-1:2004 [3] prediction, n_{ef} according to EN 1995-1-1:2004 [3] was applied.

Fig. 15 shows that the test results of the beech connections show 46% higher capacity with a linear trend. The load-carrying capacities F_{mean} are calculated according to the EN 1995-1-1:2004 [3] design equations, considering the effective number of fastener n_{ef}, and material parameters as following: mean density for beech glulam $\rho_{mean} = 700$ kg/m^3, steel plate strength of $f_{u,mean} = 560$ MPa and steel dowel-type strength of $f_{u,mean}$ = 610 MPa, however the results are conservative. The material parameters used should be adjusted to react to the higher load-carrying capacities observed during the test series. The research work on embedment strength for beech wood show potential for an increase of the strength values, compare Fig. 15. Further tests with more complex connections and more shear planes are planned to give more information for the design on steel dowel-type connections in beech.

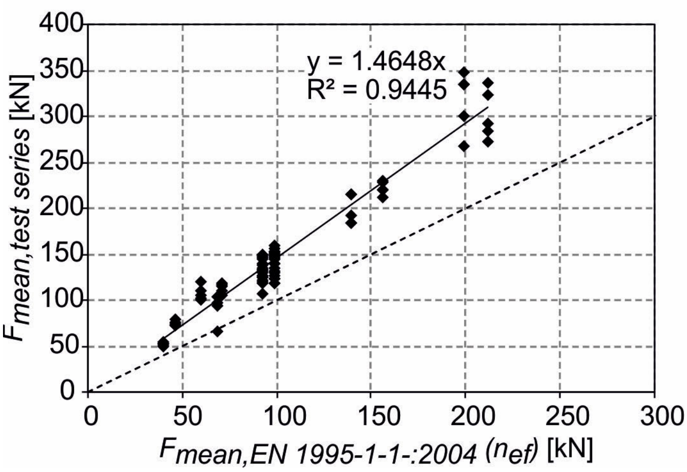

Fig. 15. Comparison of test results with EN 1995-1-1:2004 [3] predictions for dowel type connections

6.2 Glued-in rods

Although the state of the art in gluing threaded rods in wood recommends a minimum embedment length of 10*d* (based on softwood experiments), the connection using beech wood shows pull-out failure just up to 10*d* embedding length and steel failure for 15*d* or more for all load to grain directions using steel grade of 8.8. The maximum effective embedding length will be between 10*d* and 15*d* and needs to be defined by further tests and will depend on the steel grade. The pull-out resistance for 45° and 90° to grain direction is slightly higher than the parallel to grain one which is already more than double compared to the values used for softwood. A characteristic pull-out strength of 12 MPa for parallel to grain and of 14 MPa for perpendicular to grain could be used independent of diameter. Tests of connections with 4 or 6 glued-in rods will prove this assumption.

Acknowledgements

The present research results are part of the research project “Investigation and development of design parameters and methods for connections in beech wood”, financed by Swiss Federal Office for the Environment FOEN and industry partners.

References

[1] Eid. Forschungsanstalt für Wald Schnee u. Landschaft (2010) *Schweizerisches Landesforstinventar, Ergebnisse der dritten Erhebung 2004 –2006*. Birmensdorf, Switzerland

[2] Gehri E (2010) *Screw connections in hardwood structures*. 16. Internationales Holzbau-Forum, Garmisch Partenkirchen, Germany.

[3] *EN 1995-1-1:*2004 (Eurocode 5). Design of timber structures. CEN, Brussels.

[4] *DIN EN 1995-1-1/NA:2010* National Annex, Nationally determined parameters – Eurocode 5: Design of timber structures. Deutsches Institut für Normung e.V., Berlin, Germany.

[5] Strahm T (2012) *Esche und Buche im Ingenieurholzbau*. 2. Forum Holzbau, Beaune.

[6] Whale LRJ, Smith I (1986) *The derivation of design clauses for nailed and bolted joints in Eurocode 5*. CIB-W18 Meeting 19, Paper 19-7-6, Florence, Italy.

[7] Whale LRJ, Smith I, Hilson BO (1986) *Behaviour of nailed and bolted joints under short-term lateral load*. CIBW18 Meeting 19, Paper 19-7-1, Florence, Italy.

[8] Whale LRJ, Smith I, Larsen HJ (1987) *Design of nailed and bolted joints – Proposal for the revision of existing formulae in draft Eurocode 5 and the CIB code*. CIB-W18 Meeting 20, Paper 20-7-1, Dublin, Ireland.

[9] Ehlbeck J, Werner H (1992a) *Softwood and hardwood embedding strength for dowel-type fasteners*. CIB-W18 Meeting 25, Paper 25-7-2, Ahus, Sweden.

[10] Ehlbeck J, Werner H (1992b) *Tragfähigkeit von Laubholzverbindungen mit stabförmigen Verbindungsmitteln*. Technical Report. Versuchsanstalt für Stahl, Holz und Steine der Universität Karlsruhe.

[11] Hübner U, Bogensperger T, Schickhofer G (2008) *Embedding strength of European hardwoods*. CIB-W18 Meeting 41, Paper 41-7-5, St. Andrews, Canada.

[12] Hübner U (2013) *Mechanische Kenngrößen von Buchen-, Eschen- und Robinienholz für lastabtragende Bauteile*. PhD thesis, Technische Universität Graz.

[13] Sandhaas C, Ravenshorst GJP, Blass HJ, van de Kuilen JWG (2013) Embedment tests parallel-to-grain and ductility aspects using various wood species. *European Journal of Wood and Wood Products* 71:599–608.

[14] Vreeswijk B (2003) *Verbindingen in hardhout*. MSc thesis, Delft University of Technology.

[15] Franke S, Magnière N (2014) *Discussion of testing and evaluation methods for the embedment behaviour of connections*. INTER Meeting 47, Paper 47-7-1, Bath, UK.

[16] Franke S, Franke B (2018) Fundamentals and recent strength results of connections in modern hardwood timber structures. *Wood Material Science and Engineering*, under review.

[17] *EN 26891:1991*. Timber Structures; Joints with mechanical fasteners, General principles for the determination of strength and deformation characteristics. CEN, Brussels.

[18] *DIN 1052:2008*. Design of timber structures – General rules and rules for buildings. Deutsches Institut für Normung e.V., Berlin, Germany.

Beam-on-foundation modelling as an alternative design method for single fastener connections

Romain Lemaître
ENSTIB / LERMAB, University of Lorraine
Epinal, France

Jean-François Bocquet
ENSTIB / LERMAB, University of Lorraine
Epinal, France

Michael Schweigler
Department of Building Technology, Linnaeus University
Växjö, Sweden

Thomas K. Bader
Department of Building Technology, Linnaeus University
Växjö, Sweden

1. Introduction

Optimised manufacturing processes make the production of larger dimension timber products possible, which allow for the design of outstanding structures. In the last version of EN 1995-1-1 (Eurocode 5, [5]), which was developed during the 1990s, it seemed important to its drafters to propose design formulas to estimate the stiffness of connections in accordance with the needs of that time. Aware of the technical jump that had to be managed, the proposed rules remained simple. However, simple design equations became insufficient to cope with present-day challenges, which are e.g. related to the design of high-rise wooden buildings. In Eurocode 5, the load-carrying capacity of dowel-type timber connections is no longer determined by empirical formulas but it is based on the limit analysis proposed by Johansen [10]. This methodology however shows limits for complex connections even though many improvements have been made since its introduction [1]. In parallel with these analytical approaches, developments in computational mechanics made it possible to develop simple numerical methods [6, 7], which take into account even nonlinear phenomena. These approaches have remained unused in practical design due to their complex implementation and their high running time, at the time of their invention, while nowadays computational resources would allow for fast and efficient numerical methods-based design. Numerical modelling of connections can help engineers to fill the gaps of Eurocode 5 and to cope with variability in connection design. For this purpose, dowel-type fasteners are numerically modelled as elastoplastic beams on a nonlinear foundation in engineered wood-based products [8, 13]. This method is called Beam-On-Foundation (BOF) modelling and shows huge potential for engineering design. The purpose of this paper is to show how this method can substitute and complement limit analysis and empirical stiffness formulas of timber connections with dowel-type fasteners. Corresponding perspectives are exemplified after a comparison of BOF modelling with the limit state approach in Eurocode 5.

2. Description of the Beam-On-Foundation method

The complexity in the local deformation and stress state in wood close to the dowel suggests using a phenomenological approach to describe the embedment behaviour instead of using 3-dimensional continuum models. Thus, beam-on-foundation approaches have been developed (see Fig. 1), where nonlinear springs are used to model the contact between wood and steel dowel. Hirai, by making use of mathematical functions for the nonlinear relative displacement-embedment load behaviour (see [6, 7, 12, 15]. In most of these equations, the parameters can be related to physical properties derived from uniaxial embedment tests. The simplest approach would be to assume linear tangents with a continuous intermediate nonlinear transition. An initial nonlinear region with increasing stiffness is typically observed in test data. This is linked on the one hand to the quality and the precision of production and assembling, and on the other hand to the stochastic nature of the properties. Mathematical functions enable an integration of this initial behaviour, which would lead to a more realistic load distribution in multiple fastener connections. The dowel itself is modelled by 1-dimensional beam elements, which makes it possible to reduce the number of elements compared to a 3-dimensional model. An elastoplastic material behaviour is assigned to these beam elements. Prescription of displacements of the connected structural elements yield corresponding reactions forces, which gives access to the global load-displacement behaviour of the connection.

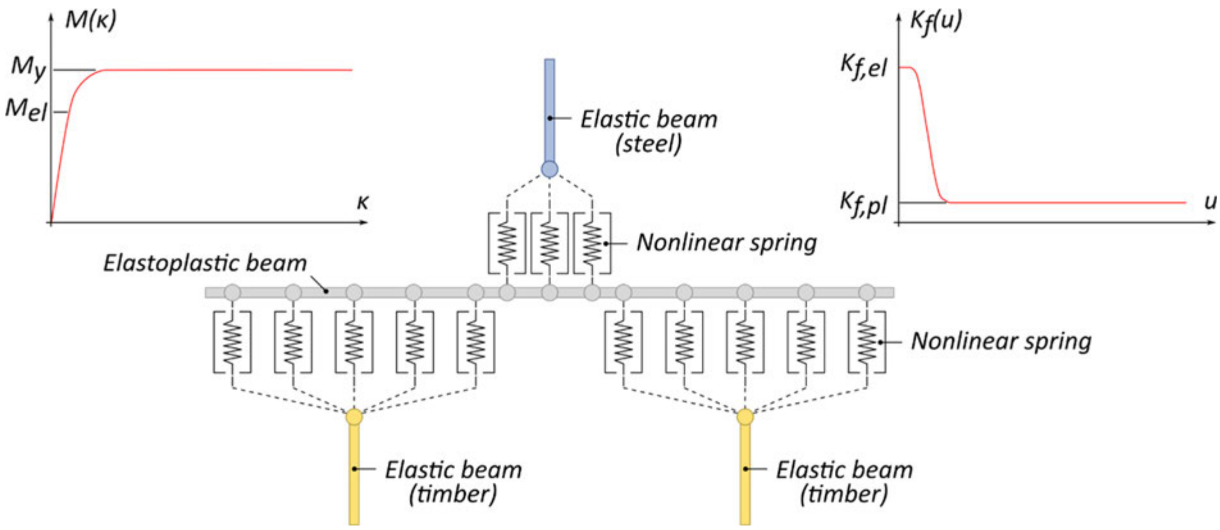

Fig. 1. Description of Beam-On-Foundation modelling for the design of timber connections with dowel-type fasteners (example of a meshing steel-to-timber connection with two shear planes)

The sensitivity of the discretization of the embedment behaviour, i.e., the number of spring elements and their distance along the dowel on the global load-displacement curve of the connection, were investigated by Hirai [7]. In this paper, rules are given to define the number of springs elements according to the slenderness of the connection t/d.

3. Comparison with European Yield Model

In this part, the load-bearing capacities and the stiffness of different types of connection assemblies computed with the analytical formulas of the European Yield Model (EYM) are compared with the numerical results of the BOF modelling.

In order to investigate the validity of the BOF modelling and to demonstrate that it can be used as an alternative to the EYM, results of these two methods will be compared for different connections with variation in connection parameters. In particular, load-bearing capacity, i.e. the connection load at a displacement equal to 5 mm, and the quasi-elastic stiffness of the connection were computed. Connection parameters were chosen to encompass all failure modes (see Figures 8-2 and 8-3 in Eurocode 5) and included the following variations:

- dowel diameter d = {8 mm; 12 mm; 24 mm};
- slenderness of the connection t/d = {1; 1.5; 2; 2.5; 3; 3.5; 4; 4.5; 5; 6; 7; 8; 9; 10}, where t is the thickness of the timber members;
- density of timber ρ = 420 kg/m^3;
- yield strength of the dowel f_y = 240 MPa.

The comparison is limited to timber-to-timber and steel-to-timber connections with two shear planes (equations (8.7), (8.11), (8.12) and (8.13) in Eurocode 5), see Fig. 2. Design equations specified in Fig. 2 are based on the EYM but contrary to Eurocode 5 equations, partial safety factors related to the uncertainties on the materials and the rope effect are neglected in order to be able to compare the mechanical models. Uncertainty considerations can be later added to the BOF model.

The BOF model was established with an elasto-plastic beam element representing the steel dowel. Young's modulus of steel equal to 210 GPa and a yield strength equal to 240 MPa (f_y) was used. The yield moment M_y included in the equations of Fig. 2 was equal to the theoretical expression for a circular cross-section. The non-linear behaviour of the dowel elements was defined from a moment-curvature relationship which allowed to calculate a new bending stiffness of the dowel for each step of calculation (equal to 0.02 mm).

The foundation modulus used to model the contact between wood and steel dowel was described by a pure elasto-plastic behaviour where the elastic limit f_h was equal to the empirical expression (8-16) of Eurocode 5. It was supposed that the behaviour remained elastic up to 1 mm of embedment. Therefore the elastic and plastic foundation moduli (named $K_{f,el}$ and $K_{f,pl}$) were respectively equal to f_h and zero.

The distance between embedment spring elements was equal to $0.4 \cdot d$. The nonlinear spring gave only loads parallel to the displacement direction, while the dowel was free to move along its axial direction (no friction was considered).

Load-bearing capacity according to the limit state approach ($F_{v,EC5}$) was compared to the reaction force in the BOF model for a relative displacement equal to 5 mm ($F_{v,BOF}$). The foundation modulus K_{ser} according to Eurocode 5 (see Fig. 2) was compared to the numerical simulations using two evaluations. In the first approach, stiffness was defined between 10% and 40% of the load-bearing capacity $F_{v,BOF}$ (empty forms of Fig. 3). In the second approach, the stiffness is defined between 0% and 10% of the load-bearing capacity $F_{v,BOF}$ to guarantee all material behaviours were linear (full forms of Fig. 3).

It was observed that the foundation modulus used to model the contact between steel and dowel influenced numerical results. Being difficult to quantify the elastic foundation modulus for that type of contact, different numerical simulations have been realised. Based on these simulations, an elastic behaviour with a foundation modulus equal to fifty times $K_{f,el}$ was retained in the rest of this study.

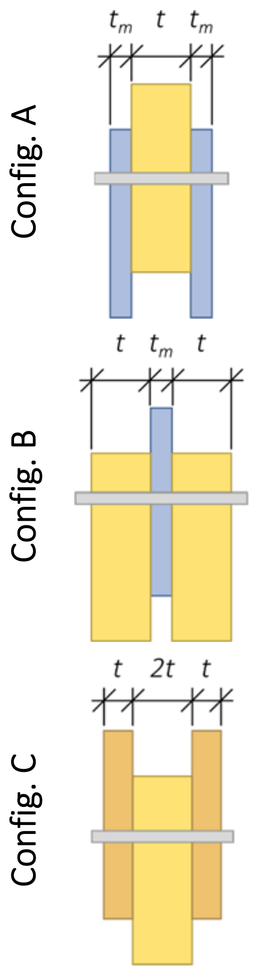

Config. A:

$$t_m = 0.5 \cdot d : \begin{cases} \text{mode (j)} : 0.5 \cdot f_h \cdot t \cdot d \\ \text{mode (k)} : \sqrt{2 \cdot M_y \cdot f_h \cdot d} \end{cases} \qquad K_{ser} = 2 \cdot \frac{\rho^{1.5} d}{23}$$

$$t_m = d : \begin{cases} \text{mode (l)} : 0.5 \cdot f_h \cdot t \cdot d \\ \text{mode (m)} : 2 \cdot \sqrt{M_y \cdot f_h \cdot d} \end{cases} \qquad K_{ser} = 2 \cdot \frac{\rho^{1.5} d}{23}$$

Config. B:

$$t_m = d : \begin{cases} \text{mode (f)} : f_h \cdot t \cdot d \\ \text{mode (g)} : f_h \cdot t \cdot d \cdot \left(\sqrt{2 + \frac{4 \cdot M_y}{f_h \cdot d \cdot t^2}} - 1 \right) \\ \text{mode (h)} : 2 \cdot \sqrt{M_y \cdot f_h \cdot d} \end{cases} \qquad K_{ser} = 2 \cdot \frac{\rho^{1.5} d}{23}$$

Config. C:

$$\begin{cases} \text{mode (f)} : f_h \cdot t \cdot d \\ \text{mode (g)} : \frac{f_h \cdot t \cdot d}{3} \cdot \left(\sqrt{4 + \frac{12 \cdot M_y}{f_h \cdot d \cdot t^2}} - 1 \right) \\ \text{mode (h)} : \sqrt{2 \cdot M_y \cdot f_h \cdot d} \end{cases} \qquad K_{ser} = \frac{\rho^{1.5} d}{23}$$

Fig. 2. Double-shear steel-to-timber and timber-to-timber connections and design equations according to Eurocode 5 without partial safety factors for comparison with BOF modelling.

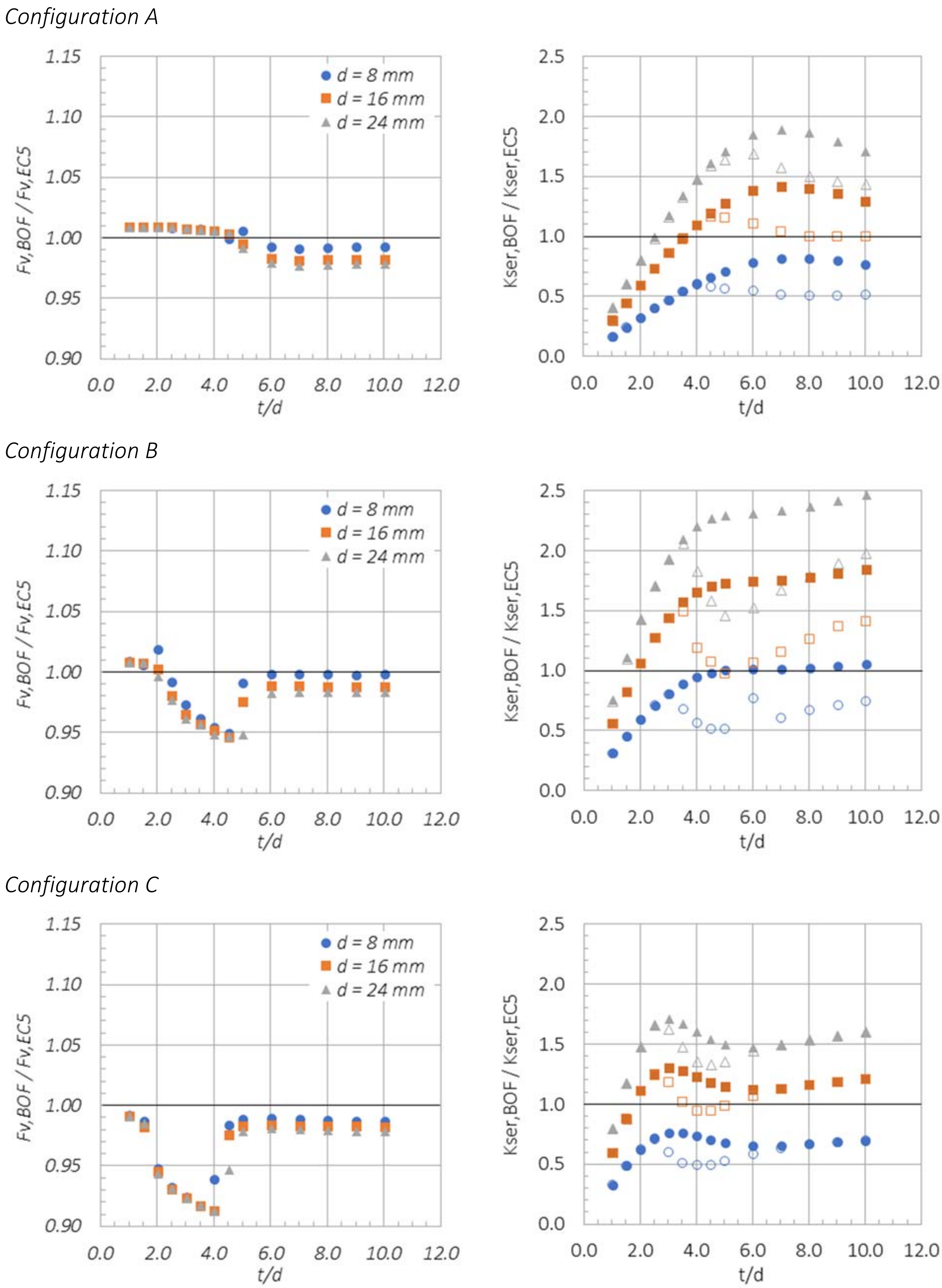

Fig. 3. Comparison of the load-bearing capacity and the empirical equation for K_{ser} in Eurocode 5 with BOF modelling results for each configuration.

The results are grouped in the different graphs in Fig. 3, where each point represents the ratio of numerical result to the analytical result. The numerical results show an evolution of the stiffness as a function of the slenderness t/d, which is not predicted by the empirical formula of Eurocode 5 for K_{ser}. It is observed that the evolution of the stiffness is more marked in the first approach for configurations B and C. It could be explained by the early emergence of the first plastic hinge on the dowel (in the inner part of the connection) decreasing its bending stiffness therefore the stiffness of the connection.

For the load-bearing capacity at 5 mm slip, the numerical results are in good agreement with the load calculated by the EYM. It becomes however obvious that differences evolve in accordance with the failure modes. Indeed, for the modes with one plastic hinge in the steel dowel, whatever the configuration and the dowel diameter, the differences between the numerical and the analytical results are lower than 10%. For the failure modes without plastic hinge or more than one, whatever the configuration and the dowel diameter, the differences are lower that 3%.

4. Perspectives of the method

Emergence of new engineering wood-based products (EWPs) led to the situations that design equations for connection in Eurocode 5 do not cover all EWPs. Moreover, only a limited number of connection layups are covered by Eurocode 5 equations. The BOF modelling can thus complement and extend Eurocode 5 equations and is intended to be a universal tool for estimating the mechanical behaviour of connections (load-bearing capacity, load distribution and stiffness). In the following, perspectives of this numerical tool for configurations which are not covered or only partially covered by Eurocode 5, will be shown. These configurations do not pretend to be exhaustive but are limited to the most common practically relevant cases.

4.1 Multiple-shear plane connections: analytical equations and BOF

To calculate multiple-shear planes connections, Eurocode 5 proposes to decompose the connection into series of three elements and to calculate for each decomposition the load-bearing capacity of each shear plane (§ 8.1.3 of Eurocode 5). However, checking the compatibility of failure modes (see Fig. 4) remains a tedious work for some configuration of connections. It is proposed here to check the consistency of the BOF modelling for a steel-to-timber connection with four shear planes. The connection is composed of two outer timber members with a thickness of t_1 equal to 95 mm and an inner timber member with thickness t_2 equal to 90 mm. The thickness of the steel plates is taken equal to the dowel diameter d = 16 mm. Finally, the material properties (embedding strength f_h and yield strength f_y) are identical to those specified in Section 3. For this design example, analytical formulas of the Johansen theory are given below and are associated with the failure modes shown in Fig. 4.

$$\text{mode (l + f)}: 0.5 \cdot f_h \cdot t_2 \cdot d + f_h \cdot t_1 \cdot d \tag{1}$$

$$\text{mode (l + g)}: 0.5 \cdot f_h \cdot t_2 \cdot d + f_h \cdot t_1 \cdot d \cdot \left(\sqrt{2 + \frac{4 \cdot M_y}{f_h \cdot d \cdot t_1^2}} - 1 \right) \tag{2}$$

$$\text{mode (l + h)}: 0.5 \cdot f \cdot_h t_2 \cdot d + 2 \cdot \sqrt{M_y \cdot f_h \cdot d} \tag{3}$$

$$\text{mode (m + f)}: 2 \cdot \sqrt{M_y \cdot f_h \cdot d} + f_h \cdot t_1 \cdot d \tag{4}$$

$$\text{mode (m + g)}: 2 \cdot \sqrt{M_y \cdot f_h \cdot d} + f_h \cdot t_1 \cdot d \cdot \left(\sqrt{2 + \frac{4 \cdot M_y}{f_h \cdot d \cdot t_1^2}} - 1 \right) \tag{5}$$

$$\text{mode (m + h)}: 2 \cdot \sqrt{M_y \cdot f_h \cdot d} + 2 \cdot \sqrt{M_y \cdot f_h \cdot d} \tag{6}$$

Results of the numerical simulation are shown in Fig. 5 in terms of the global load-relative displacement curve (displacement at the steel plate). In this graph, both load-slip curves of the outer parts and of the inner part are given. A substantially different behaviour in the timber members of the connection becomes obvious from the BOF model, which is not predicted by Eurocode 5 design equations. Load-bearing capacity for a dowel connection at a slip of 5 mm, as predicted by the numerical simulation, is 7% higher than Eurocode 5 predictions based on the EYM (predicted failure mode (m + f)).

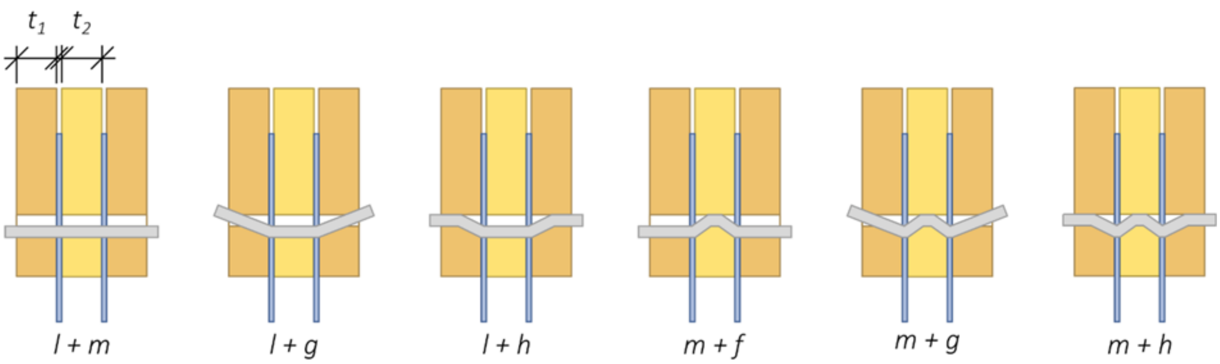

Fig. 4. Failure modes of multiple-shear planes for steel-to-timber connection.

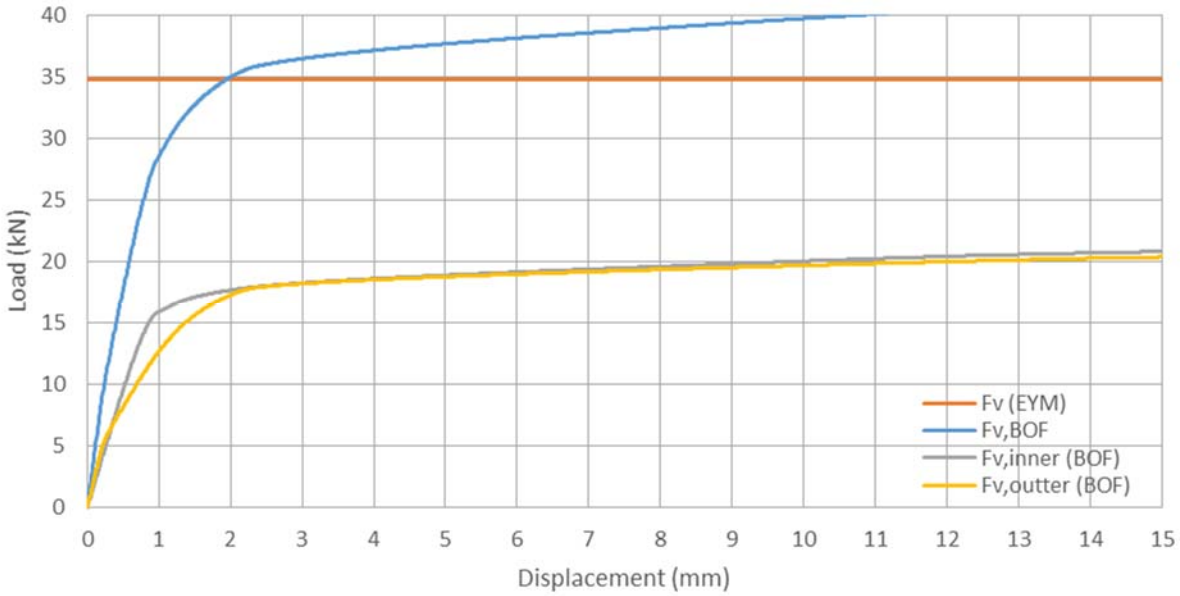

Fig. 5. BOF modelling results of one multiple-shear plane connection compared with EYM.

4.2 Multiple-material connections: Reinforcement with plywood

The addition of plywood as reinforcement significantly increases the resistance capacity of connections (see [3]). Analytical formulas based on the EYM, considering the contribution of plywood were derived in Werner [17]. It is proposed here to compare the BOF modelling with these formulas:

$$\text{mode (g)}: \left(f_{h,1}\cdot t_1 + f_{h,r}\cdot t_r\right)\cdot d \tag{7}$$

$$\text{mode (h)}: \left(0.5\cdot f_h\cdot t_2 + f_{h,r}\cdot t_r\right)\cdot d \tag{8}$$

$$\text{mode (j)}: \frac{\beta\cdot f_{h,1}\cdot d}{2+\beta}\left[\sqrt{\left(t_1+4t_r\right)^2+\frac{2+\beta}{\beta}\left(t_1^2-4\eta\cdot t_r^2+\frac{4M_y}{d\cdot f_{h,1}}\right)}-\left(t_1+4t_r\right)\right]+f_{h,r}\cdot t_r\cdot d \tag{9}$$

$$\text{mode (k)}: \frac{2\beta\cdot f_{h,1}\cdot d}{1+\beta}\left[\sqrt{t_r^2-\frac{1+\beta}{2\beta}\left(\eta\cdot t_r^2-\frac{2M_y}{d\cdot f_{h,1}}\right)}-t_r\right]+f_{h,r}\cdot t_r\cdot d \tag{10}$$

with $f_{h,r} = 0.11\ (1 - 0.01 \cdot d) \cdot \rho$, $\beta = f_{h,2}/f_{h,1} = 1$, and $\eta = f_{h,r}/f_{h,1} = 1.34$.

The connection is composed of two outer timber members with a thickness of t_1 equal to 32 mm and an inner timber member with a thickness of t_2 equal to 64 mm, on which plywood panels with a thickness of t_2 equal to 10 mm (see Fig. 6) were added at the inner shear planes. As the previous example, the material properties are identical to those mentioned in Section 3 and the dowel diameter was equal to 16 mm. The results of the numerical simulation are shown in Fig. 7. They show good agreement with Werner's equations (predicted failure mode (j)).

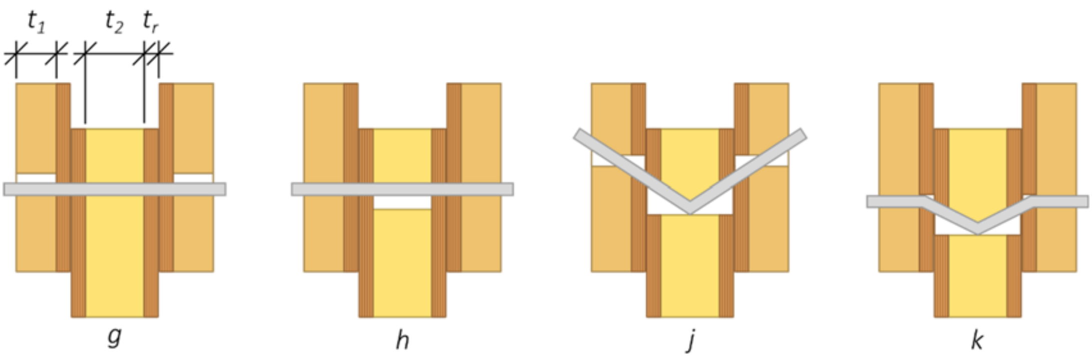

Fig. 6. Failure modes of timber-to-timber connection reinforced with glued-on wood-based panels.

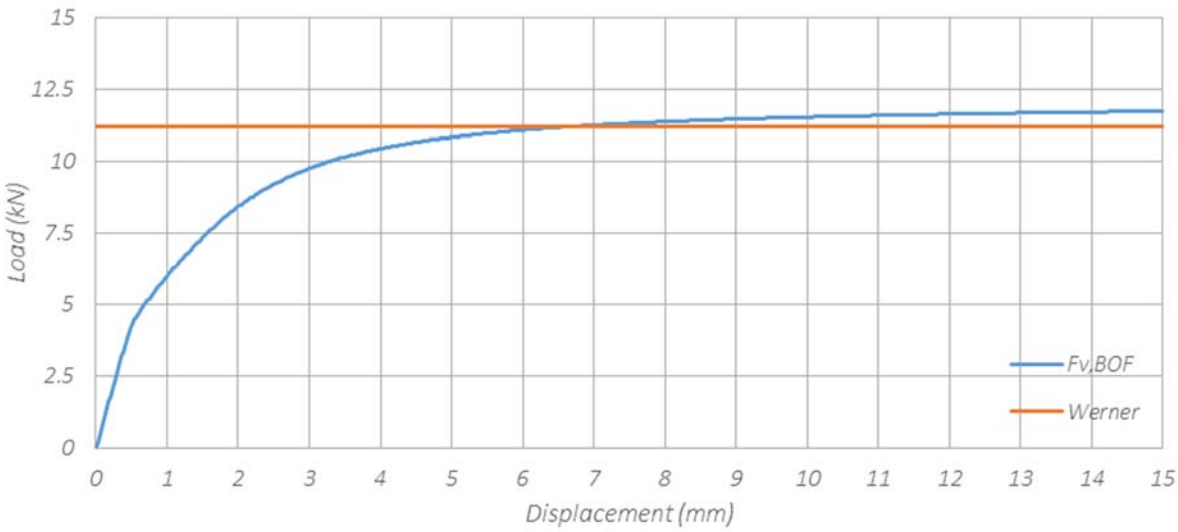

Fig. 7. BOF modelling result of one timber connection reinforced with glued-on wood-based panels and comparison with Werner equations [17].

4.3 Multiple-material connections: Cross laminated timber (CLT)

The last example of the BOF modelling is related to a CLT connection with one shear plane (three layers 19-22-19 for the CLT, thickness of the steel plate = dowel diameter = 16 mm). Uibel and Blaß [16] have proposed different analytical formulas for this type of connection. The results of the numerical simulation are shown in Fig. 9 (predicted failure mode (d.2)). They also show good agreement between the numerical results and the analytical equations.

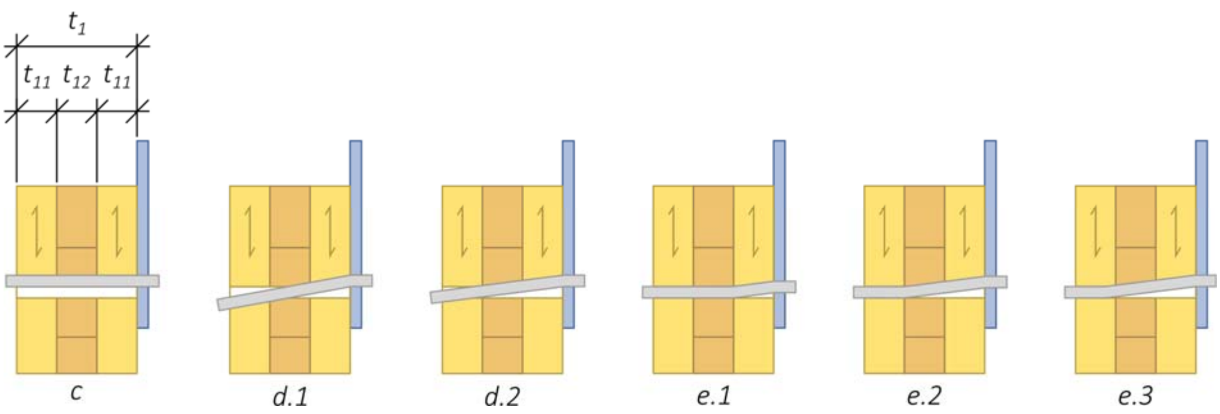

Fig. 8. Failure modes of one-shear plane for steel-to-CLT connection.

$$\text{mode (c)}: f_h \cdot t \cdot d \tag{11}$$

$$\text{mode (d.1)}: f_{h,1} \cdot t \cdot d \cdot \left[\sqrt{2} \cdot \sqrt{\beta \left(\beta \left(2 + \psi^2 - 2\psi + 1 \right) + 2\psi \left(1 - \psi \right) + \frac{2M_y}{f_{h,1} \cdot d \cdot t^2} \right)} - \beta \right] \tag{12}$$

$$\text{mode (d.2)}: f_{h,1} \cdot t \cdot d \cdot \left[\sqrt{2} \cdot \sqrt{\psi \left(2\beta - 2 \right) + 2 - \beta + \frac{2M_y}{f_{h,1} \cdot d \cdot t^2}} + 2\psi + \beta \left(1 - 2\psi \right) - 2 \right] \tag{13}$$

$$\text{mode (e.1)}: 2 \cdot \sqrt{M_y \cdot f_{h,1} \cdot d} \tag{14}$$

$$\text{mode (e.2)}: f_{h,1} \cdot t \cdot d \cdot \psi \cdot \left[1 - \beta + \sqrt{\beta \left(\beta - 1 + \frac{4M_y}{f_{h,1} \cdot d \cdot t^2 \cdot \psi^2} \right)} \right] \tag{15}$$

$$\text{mode (e.3)}: f_{h,1} \cdot t \cdot d \cdot \left[\beta \left(1 - 2\psi \right) + \sqrt{2\psi - 1 + 2\psi \left(\beta - 1 \right) - \beta + 1 + \frac{4M_y}{f_{h,1} \cdot d \cdot t^2}} \right] \tag{16}$$

Where:

$f_h = 0.112 \cdot d^{-0.5} \cdot \rho^{1.05}$, $f_{h,1} = 0.082 \cdot (1 - 0.01 \cdot d) \cdot \rho$, $f_{h,12} = f_{h,1} / (1.35 + 0.015 \cdot d)$;

$\beta = f_{h,12} / f_{h,1} = 0.629$, $\psi = t_{11} / t_1 = 0.317$.

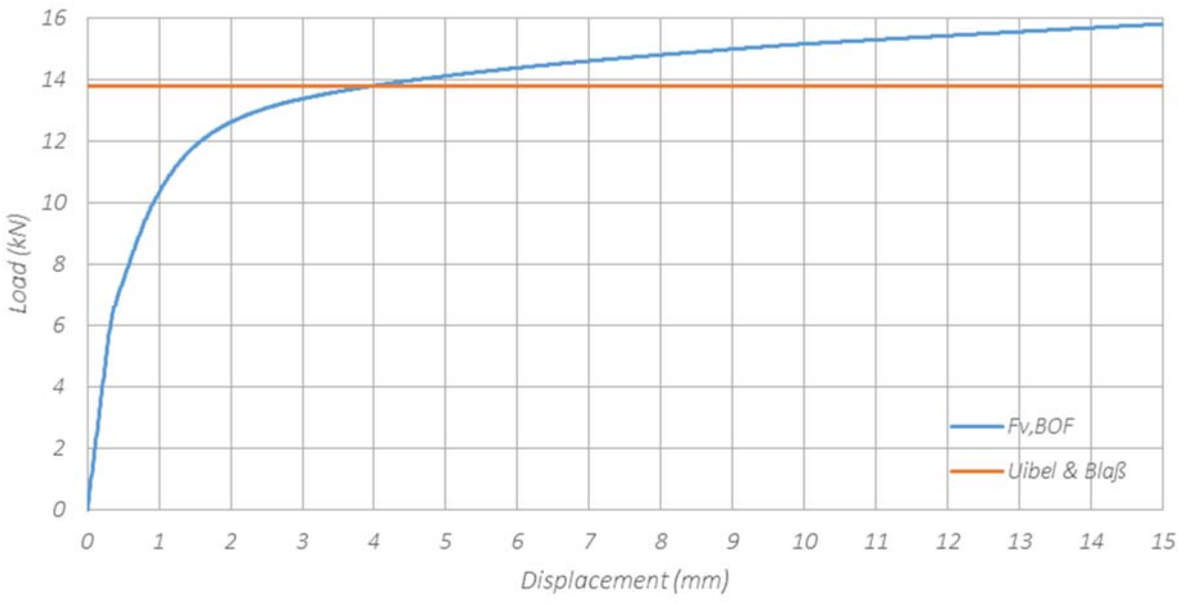

Fig. 9. BOF modelling result of one CLT connection (three layers 19-22-19) compared with Uibel and Blaß equations [16].

5. Proposed modifications for the EN 383 (2007)

The stress field of the timber around the dowel during an embedding test induces tensile stresses perpendicular to the grain of the wood. These stresses can cause splitting of the timber just after or even before the timber has entered its plastic domain (for tests with low load-to-grain angles, 0° to 30°). This phenomenon is more pronounced for timber with a high density and especially for hardwoods. However, at the scale of a connection, because of the mass of the material around the dowel or possible reinforcement (screws, plywood for example), the risk for splitting might be considerably reduced and ductile connection behaviour is achieved. In order to be able to predict the behaviour of these connections, there is a need to obtain experimental curves of embedment up to high dowel displacement (about 15 mm). For this purpose, embedment test specimens should be reinforced in order to avoid splitting. The reinforcement can be achieved by glued-on plywood at the end area of the specimen or by screws. The reinforcement must not alter the mechanics of the embedment and it must be placed sufficiently far from the drilling hole: $1.5 \cdot d$ (for reinforcement by plywood, see [11] and $3 \cdot d$ (for reinforcement by screw). The type of reinforcement to be favoured is a reinforcement by screw because it allows a simple and fast implementation. Screws should be placed perpendicular to the wood grain to ensure maximum transverse tensile strength.

By reinforcing embedment test specimens up to load-to-grain angles of equal to 30°, it becomes possible to idealize the experimental curves of embedment tests of wood or wood-based material by a nonlinear function with linear hardening (see Fig. 10) for all diameters, densities and load-to-grain angles. From this idealized shape, six physical parameters related to the embedding of timber can be defined. The proposed parameters are as follows:

- $f_{h,5mm}$: embedding strength defined at a displacement equal to 5 mm
- $f_{h,1mm}$: embedding strength defined at a displacement equal to 1 mm
- $K_{f,el,1}$: elastic foundation modulus defined between 10% and 40% of $f_{h,5mm}$ during the first loading
- $K_{f,el,2}$: elastic foundation modulus defined between 10% and 40% of $f_{h,5mm}$ during the first unloading
- $K_{f,pl}$: plastic foundation modulus defined between 3 mm and 15 mm displacement
- *gap*: gap between the dowel and the wood defined as the intersection of the x-axis and the line with the slope of $K_{f,el,1}$

These six parameters have the advantage of being easily measurable (regardless of the type of material tested: softwood, hardwood, CLT, LVL, plywood, etc.) and can be used in mathematical functions describing the nonlinear foundation; no matter which one is chosen by the users of the BOF modelling (see [15]).

Bléron and Duchanois [2] and Schweigler et al. [14] have shown that for embedding tests out of orthotropic axes, the relative displacement between the dowel and the wood is not collinear with the direction of the load. Both authors have used a set-up to leave free and measure the lateral displacement of the test specimen. This embedding mechanic is found in connections loaded by bending moments and that is why the embedding tests out of the orthotropic axes made to quantify the nonlinear foundation of the BOF modelling will have to take into account the previous remark.

Finally, the last proposal concerns the dimension of the test specimens for embedding tests with solid wood or glulam. The dimensions of the test specimens with load-to-grain angle tests are calculated by linear interpolation from the dimensions given in EN 383 [4] for 0° and 90° (see [9]).

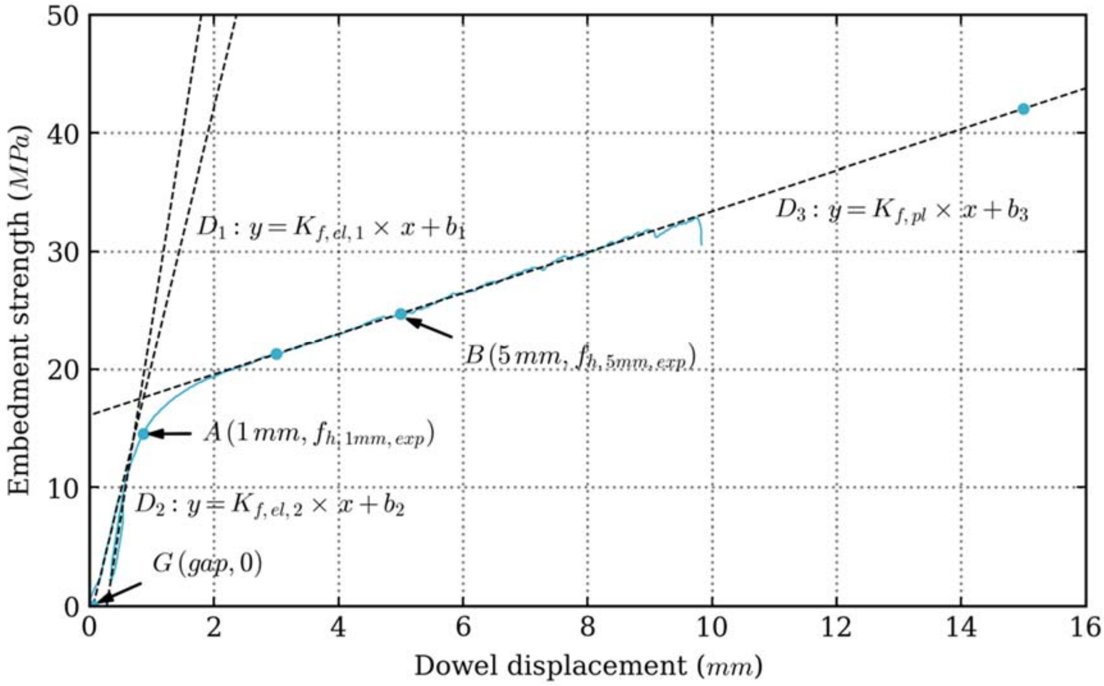

Fig. 10. Idealized shape of an experimental curve of an embedment test with the characteristic parameters necessary to quantify the nonlinear foundation.

6. Discussion and conclusions

In this paper, principles of modelling dowel-type fastener connections with beam-on-foundation (BOF) models using the finite element method, with special focus on influence parameters considered in the model, was described. A comparative study of the load-bearing capacity of single-dowel connections with two shear planes predicted by the Johansen theory with bearing capacity predicted by the BOF method was made. This comparison included effects of parameters included in the Yield Analysis Theory of Eurocode 5. The study was continued by the design of connections with more than two shear planes, as well as by connections with reinforcements and multiple-material layups in order to highlight possibilities of the BOF method compared to the Yield Analysis Theory, as regards practical engineering problems. Moreover, the BOF method was applied for prediction of the elastic behaviour of dowel-type fasteners for determination of elastic slip moduli, which are currently covered by an empirical equation in Eurocode 5.

BOF model calculations and their comparison to the design equations highlights the validity of the method and the advantage of a kinematically compatible model that allows prediction of the slip behaviour of connections in addition to the ultimate strength. Effects that are not explicitly covered in the empirical design equations, namely the influence of the slenderness on the elastic slip modulus, could be demonstrated.

Finally, recommendations for modifications of the timber engineering design standards were proposed. Since the BOF method requires additional input compared to the Yield Analysis Theory, namely kinematically compatible load-displacement data, proposed modifications mainly concern the embedment test standard EN 383 [4]. In the future, a study will also have to be done to quantify the foundation modulus of the contact between dowel and steel.

BOF calculations presented herein were limited to single dowel connections loaded parallel to the grain. The 2-dimensional model can however be applied to calculate connection behaviour for arbitrary load-to-grain angles and has been extended to a 3-dimensional foundation model. Their integration in multiple fastener connections is demonstrated in the next chapter of this state of the art report and can be used to predict load distribution.

References

[1] Blaß HJ, Laskewitz B (2000) *Load-carrying capacity of joints with dowel-type fasteners and interlayers*. CIB-W18 Meeting 33, Paper 33-7-6, Delft, Netherlands.

[2] Bléron L, Duchanois G (2006) Angle to the grain embedding strength concerning dowel type fasteners. *Forest Products Journal* **56**(3):44.

[3] Bouchaïr A, Racher P, Bocquet JF (2007) Analysis of dowelled timber to timber moment-resisting joints. *Materials and Structures* **40**(10):1127–41.

[4] *EN 383:2007*. Timber structures – Test methods – Determination of embedment strength and foundation values for dowel type fasteners. CEN, Brussels.

[5] *EN 1995-1-1: 2004* (Eurocode 5). Design of timber structures – Part 1-1: General and rules for buildings. CEN, Brussels.

[6] Foschi RO (1974) Load-slip characteristics of nails. *Wood Science* **17**:69-77.

[7] Hirai T (1983) Non-linear load-slip relationship of bolted wood-joints with steel side members –II – Application of the generalised theory of beam on elastic foundation. *Makusu Gakkaishi* **29**(12):839-844.

[8] Hochreiner G, Bader TK, de Borst K, Eberhardsteiner J (2013) Stiftförmige Verbindungsmittel im EC5 und baustatische Modellbildung mittels kommerzieller Statiksoftware. *Der Bauingenieur* **88**:275-289.

[9] Hübner U, Bogensperger T, Schickhofer G (2008) *Embedding strength of European hardwoods*., CIB-W18 Meeting 41, Paper 41-7-5, St. Andrews, Canada.

[10] Johansen KW (1949) Theory of timber connections. *International Association for Bridge and Structural Engineering* (ABSE) Pub. 9, 249-262.

[11] Sandhaas C (2012) *Mechanical behaviour of timber joints with slotted-in steel plates*. PhD thesis, Technische Universiteit Delft.

[12] Sauvat N (2001) *Résistance d'assemblages de type tige en structure bois sous chargements cycliques complexes*. PhD thesis, Université Blaise Pascal, Clermont-Ferrand.

[13] Sawata K, Yasumura M (2002) Determination of embedding strength of wood for dowel-type fasteners. *Journal of Wood Science* **48**(2):138-146.

[14] Schweigler M, Bader TK, Hochreiner G, Unger G, Eberhardsteiner J (2016) Load-to-grain angle dependence of the embedment behavior of dowel-type fasteners in laminated veneer lumber. *Construction and Building Materials* **126**:1020-1033.

[15] Schweigler M, Bader TK, Hochreiner G, Lemaître R (2018) Parameterization equations for the nonlinear connection slip applied to the anisotropic behaviour of wood. *Composites Part B: Engineering* **142**:142-158.

[16] Uibel T, Blaß HJ (2006) *Load-carrying capacity of joints with dowel type fasteners in solid wood panels*. CIB-W18 Meeting 39, Paper 39-7-5, Florence, Italy.

[17] Werner H (1993) *Untersuchungen von Holz-Verbindungen mit stiftförmigen Verbindungsmitteln unter Berücksichtigung streuender Einflußgrößen*. PhD thesis, Universität Karlsruhe.

Numerical modeling of the load distribution in multiple fastener connections

Thomas K. Bader
Department of Building Technology, Linnaeus University
Växjö, Sweden

Jean-François Bocquet
ENSTIB / LERMAB, University of Lorraine
Epinal, France

Michael Schweigler
Department of Building Technology, Linnaeus University
Växjö, Sweden

Romain Lemaître
ENSTIB / LERMAB, University of Lorraine
Epinal, France

This contribution is an extended version of the already published article in the proceedings of the International Conference on Connections in Timber Engineering – From Research to Standards, COST FP1402, Graz, Austria.

Summary

Numerical modeling approaches, for the determination of load distribution in laterally loaded connections, as well as for the assignment of stiffness properties of connections for the structural analysis, are summarized in this contribution. The effect of the nonlinearity and the load-to-grain orientation dependence of connection slip, of elastic deformation in the surrounding wood matrix, and of the deviation between load and displacement direction are discussed. Comparison of various models demonstrates the pronounced effect of the load-to-grain orientation dependence and the nonlinearity in connection slip on the load distribution, particularly in case of moment loading. The effect of elastic deformation in the wood matrix on the load distribution increases with increased size of connections, even more pronounced when connections are loaded by a shear force perpendicular to the grain. In case of normal force loading, the non-uniform load distribution due to elastic deformation in the wood matrix reduces rapidly with increased relative connection displacement. Pros and cons of the modeling approaches as well as necessary input data are discussed in relation to the design process and European standardization.

1. Introduction

In the design of timber structures, engineers are permanently facing the question of how to distribute loads in multiple fastener connections. Already for structural analysis, load distribution in connections must be considered, namely when calculating connection stiffness based on single fastener properties. Connection stiffness has to be considered in the structural analysis of timber structures when calculating internal forces and displacements. A corresponding set of internal forces acting in a connection needs subsequently to be distributed to single fasteners for the verification of single fasteners. The way how this is achieved, naturally depends on regulations in the timber engineering design standard (EN1995-1-1, Eurocode 5 [1]). The latter is currently primarily designed towards the verification of single fasteners, rather than towards the verification of multiple fastener connections. In practical applications, multiple fastener connections are mostly loaded by a combination of internal forces, which from a beam theory point of view includes normal forces (parallel to the grain), shear forces (perpendicular to the grain) and bending moments. Regarding standardization, load distribution in connections is currently not explicitly regulated in Eurocode 5.

Design regulations and assumptions on the single fastener connection behavior, however, strongly affect the possibilities of modeling the load distribution in connections. Eurocode 5, in its current version, prescribes a limit state approach for the determination of the strength of single fastener connections. Since the limit state approach does not give deformations, an empirical equation for their elastic stiffness in the serviceability limit state (SLS) is given. The stiffness however does not depend on the load orientation with respect to the grain, and consequently, an isotropic and most commonly elastic load distribution model is used in engineering practice. The use of an elastic and isotropic distribution model based on the polar moment of inertia for the prediction of nonlinear load-displacement behavior is a strong simplification and requires an adaption of the stiffness in relation to the load level. Thus in Eurocode 5, reduced stiffness of the fasteners in the ultimate limit state (ULS) design is prescribed. Ultimate limit loads of connections with pronounced yield plateau can be suitably estimated with limit state approaches. However, pronounced nonlinearities in the single fastener connection behavior with hardening under loading perpendicular to the grain are not accounted for. Thus, in order to enhance the modeling of load distribution in multiple fastener connections, also regulations for the modeling of the single fastener connection behavior must be improved.

Beam-on-nonlinear foundation models have shown to be able to predict nonlinear load-deformation behavior of connections with single fasteners based on a kinematically compatible experimental dataset of the embedment behavior of wood and the bending behavior of steel fasteners [2]. Thus, numerical modeling can give access to the *nonlinear slip behavior of connections* loaded under arbitrary angles to the grain. The nonlinear relationships can be exploited in the load distribution modeling, avoiding the need for assigning different linear stiffness for SLS and ULS design, respectively. Particularly when connections are subjected to a bending moment, fasteners are loaded at various angles to the grain. Consequently, load distribution is governed by the load-to-grain orientation dependence of the load-deformation behavior of the single fastener (Ohashi and Sakamoto, 1989 in [3]).

Another effect of the anisotropic material behavior of wood is the *deviation of the force and displacement orientation* in case of loading at an angle between the principal material orientations. This has been investigated experimentally for wood embedment behavior [4] and single dowel connection behavior [2] as well as numerically for a group of fasteners [5]. Not only 3dimensional Finite Element Method (FEM) modeling but also 3dimensional beam-on-foundation modeling with appropriate input datasets can be used to represent this behavior and its effect on the load distribution.

Fasteners typically introduce stress peaks in the wood, which lead to local plastic deformations and local relative displacements between the connected members, while the rest of the wooden matrix deforms elastically. Thus, finally, it is the effect of the *elastic deformations of the wooden matrix* in-between the fasteners of a connection, which affects the load distribution. Jorissen [6] showed that even the size of bending deformation of the steel fastener affects the load distribution in case of normal forces. This is related to the different degree of nonlinearity in the single fastener connection behavior, depending on the fastener bending failure mode. Thus, in case of unreinforced connections with a risk for brittle failure modes, the strength of multiple fastener connections *may be lower than the summation of the individual load-carrying capacities for each fastener* (Eurocode 5 8.1.2(2) [1]).

As outlined above, the load distribution in multiple fastener connections depends on the mechanical properties of their components, which can be simplified in the numerical model in many different ways, depending on the material models and the type of internal forces considered. Herein, we will focus on in-plane loading, namely bending moment M_y, shear force V_z (perpendicular to the grain) and normal force N_x (parallel to the grain), while out-of-plane loading is not considered. Previously proposed as well as novel 3dimensional and 2dimensional approaches will be reviewed and discussed. The contribution focuses on the load distribution in an integer wooden matrix without cracks. This is a prerequisite for the calculation of realistic stresses in the timber matrix, which allow assessing the risk for brittle failure.

The paper is organized as follows. Load distribution models including the effect of orientation dependent nonlinearity in the single fastener connection behavior, the elastic behavior of the wooden matrix, and the deviation of load and displacement direction will be reviewed and discussed, starting from the most general case with opportunities for simplification. This will show possibilities to reduce the amount of required input data and modeling efforts. Selected models will be applied to the cases of loading by an in-plane bending moment, normal force, shear force, and a combination of internal forces. Mechanical causalities in the above described cases of load distribution will be discussed, before recommendations for standardization and engineering design, including standardized material properties and consideration of the stochastic nature of component properties, will be proposed at the end of this paper.

2. Modeling of load distribution – approaches and simplification

2.1 General

Various numerical models for the determination of the load distribution and the corresponding input data are summarized in Fig. 1 and will be discussed in the following, starting with the most complex model and subsequently increasing simplifications.

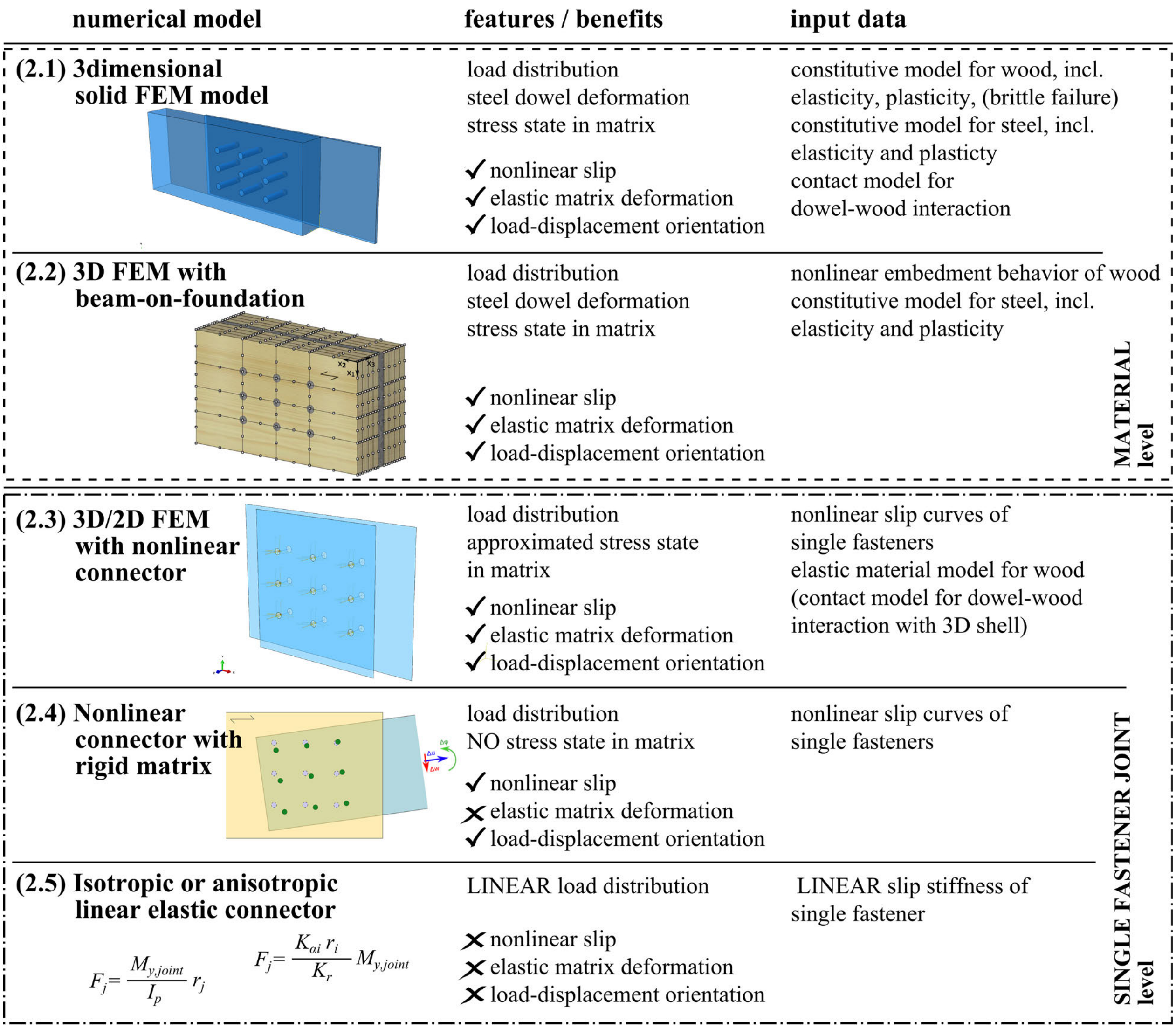

Fig. 1. Overview of models for the determination of load distribution in connections with laterally loaded fasteners.

There are basically two possible starting points with respect to modeling of load distribution in connections, which are either the *material level* (2.2 and 2.3 in Fig. 1) or the *single fastener connection level* (2.4-2.6 in Fig. 1). The former can either relate to basic material properties of wood or to a phenomenological modeling of the embedment behavior, as it is used in beam-on-foundation approaches [2]. In both cases, the single fastener connection behavior is derived as a consequence of the material properties and the global loading of the connection. Alternatively, load distribution modeling starts at the single fastener connection level, with knowledge about the nonlinear single fastener connection slip behavior, without accounting for local bending deformations of the fastener (see Fig. 1). In the latter case, a load-displacement relationship of single fastener connections (that takes into account anisotropy of timber) is used for calculation of multiple fastener connection properties.

In this contribution, in-plane loading situations of connections will be discussed, which requires knowledge of material properties or of laterally loaded single-fastener connection slip curves. Consequently, a coupling of properties in principal material directions parallel and perpendicular to the grain must be taken into account in constitutive and phenomenological material models. Input data used in example calculations within this contribution are visualized in Fig. 2. They encompass material properties of the components and single fastener slip curves typical for softwood glued laminated timber.

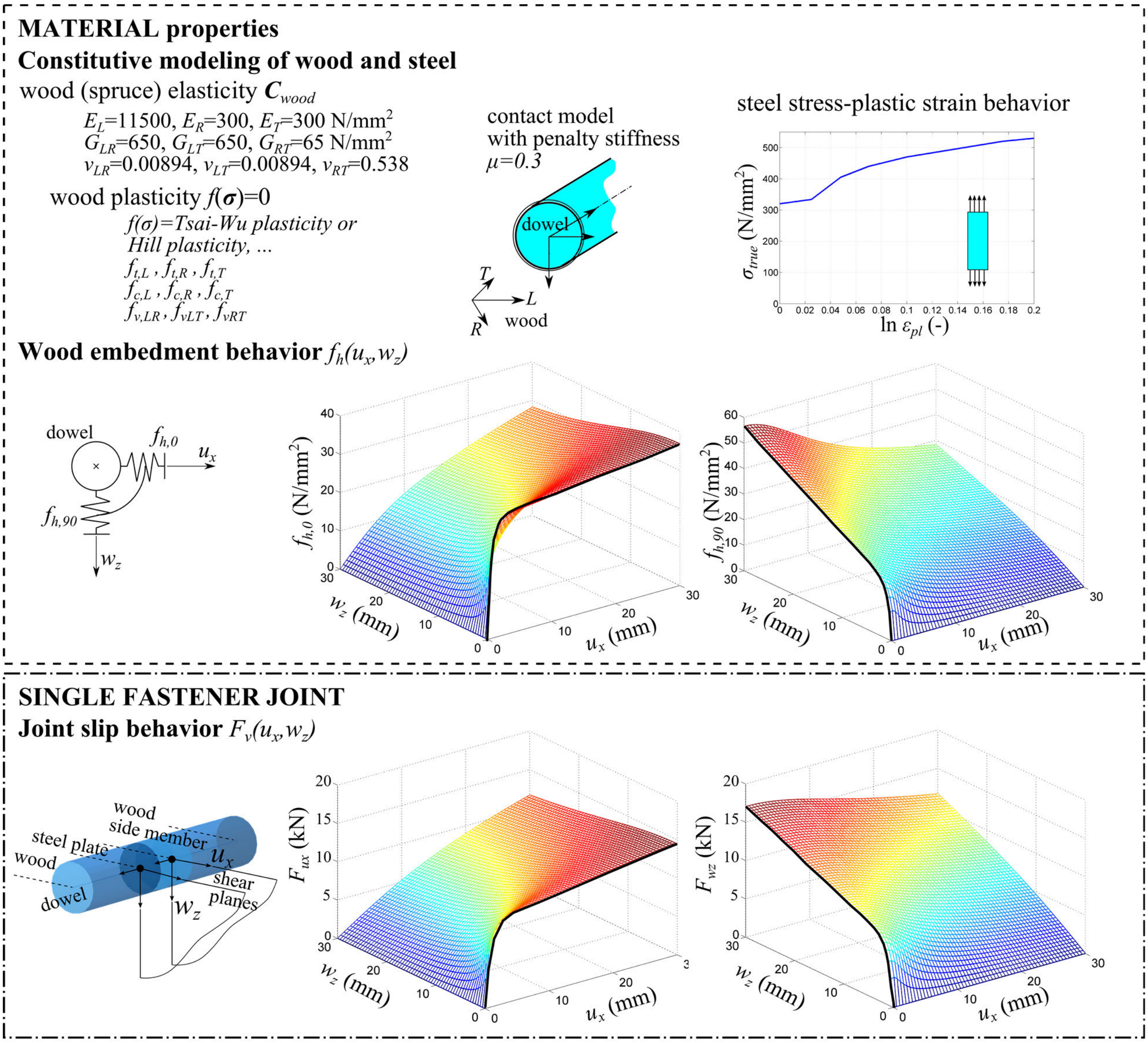

Fig. 2. Input data for numerical modeling of load distribution.

Stiffness properties of wood have been considered as mean values of glued laminated timber strength class GL24h [7] and Poisson's ratios were taken from literature [8]. A huge variability of Poisson's ratios of wood is reported in literature. However, a negligible effect of the Poisson effect on the load distribution is expected. Having at hand experimentally determined wood embedment behavior [4] and stress-strain relationship for steel [2], a beam-on-foundation model [2] has been used to determine single dowel connection slip curves, see Fig. 2.

2.2 3dimensional solid FEM model

The load distribution in connections can be studied by a 3dimensional discretization of the connection components with solid elements in FEM software. The interaction between the fasteners and the timber is then modeled with a contact criterion, typically by surface-to-surface contact encompassing a penalty friction formulation in the transverse plane and high contact stiffness in the normal direction. A pressure-overclosure relationship could be used to account for the local weakness of the interface (see [9] and [10]). Moreover, appropriate material models for wood and steel are required, which must at least account for elasticity and plasticity in order to reflect the plastic deformation of the timber member that causes plastic bending deformation of the mechanical fastener. The constitutive model for wood is the challenge in this case, since large strains are obtained close to the dowel-wood interface. Besides continuum damage mechanics models [11], classical failure criteria such as Tsai-Wu [9] or Hill [12] have been used to define yield functions, which have mainly been used in combination with ideal-plasticity in connection models. Most of the models were limited to small strain theory and small displacements and are thus most appropriate for the serviceability limit state. The main advantage of these models is naturally, in case of using an appropriate material model, the detailed information about local stresses and deformations. At the same time, this is their main drawback, since these models require long pre- and post-processing as well as long calculation times, which make them inflexible and unpractical for the engineering design of structures.

As another example, the deviation of the load and displacement direction in moment loaded connections has been studied by using a 3dimensional FEM model with an elastic material model for wood [5]. Load distribution was determined by integrating contact forces over the wood borehole surface. This work also included examples of how to combine beam models with 3dimensional solid FEM models.

2.3 3dimensional beam-on-foundation with wood matrix model

The complexity in the local deformation and stress state in wood close to the dowel suggests using a simpler, phenomenological approach to describe the embedment behavior. Thus, beam-on-foundation approaches have been developed (see Fig. 1), where nonlinear springs are used to model the contact between wood and steel dowel [13], by making use of mathematical functions for the relative displacement-embedment load behavior (see [14] and [15]). In most of these equations, the parameters can be related to physical properties derived from uniaxial embedment tests. The simplest approach would be to assume linear tangents with a continuous intermediate nonlinear transition [14]. An initial nonlinear region with increasing stiffness is typically observed in test data. This is linked on the one hand to the quality and the precision of production and assembling, and on the other hand to the stochastic nature of the properties. Mathematical functions enable an integration of this initial behavior [15], which would lead to a more realistic load distribution in multiple fastener connections.

The orthotropic behavior of wood is considered by using spring stiffness that depends on two orthogonal displacements (cf. Fig. 2), i.e., a coupling between the two springs for loading in-between the principal material directions is used (see e.g. [16] for modeling with coupled nonlinear springs). Thus, the steel dowel is 3dimensionally embedded in the wood. The discretization of the embedment behavior, i.e., the number of spring elements along the dowel, depends on the side member thickness. Hirai [13] proposed a law to determine the number of springs depending on the thickness of the wood and the dowel diameter. The dowel itself is modeled by 1dimensional beam elements, which makes it possible to reduce the number of elements compared to a 3dimensional model. An elastic-plastic material behavior is assigned to these beam elements.

The single fasteners are embedded in wood and steel members using 3dimensional solid elements with orthotropic elastic material behavior, in order to account for the elastic deformation of the wood matrix in the load distribution. Moreover, the non-uniform stress distribution over the thickness of the wood members is preserved in this model. However, the borehole in the timber as well as a contact behavior of the steel dowel to the wood is not explicitly accounted for.

2.4 Spring model (one spring per shear plane) with elastic wood matrix model

The local behavior of the steel dowel-wood interface could in a next step be simplified by a spring that accounts for the local relative displacement between the components (see Figs. 1 and 2). The spring element must however appropriately reflect the coupling between spring properties parallel and perpendicular to the grain [16], which herein is formulated in a nonlinear elastic manner using single dowel slip curves predicted by the beam-on-foundation approach (cf. Fig. 2 and [17]). The steel dowel is represented by quasi-rigid beam elements and the structural members could be reduced to 2dimensional elastic shell elements, since the non-uniform stress distribution over the thickness of the timber side members will be neglected in this model.

Another possible simplification relates to the local contact behavior of the steel dowel-wood interface, namely the loss of contact on one side due to plastic deformations in the wood. A surface-to-surface contact model is necessary for this purpose, which requires continuum shell elements for the timber side members in the numerical model. Alternatively, special grids with nonlinear springs could be designed (see [18] and [19]) or the contact could even be neglected and a kinematic coupling of the dowel and the surrounding wood could be applied. The latter has been used in the calculations presented herein. This introduces compression and tension stresses in the wood, and consequently, corrupts the stress state in the wood close to the interface with the dowel. It is however computationally much more efficient for the determination of the load distribution. The herein used spring behavior shown in Fig. 2 does not consider a deviation of the displacement and load direction, while a different set of spring forces could be used to predict this effect on the load distribution.

2.5 Spring model with rigid wood matrix

The wood matrix behavior is further simplified by neglecting its elastic deformations and assuming it to be rigid. The same applies to the steel plate in steel-to-timber connections (see [20] and [21]). Consequently, the load distribution modeling strongly simplifies and can be solved by kinematic compatibility and equilibrium considerations. An incremental procedure is however necessary for the calculation of multiple fastener connection slip curves, due to the nonlinearity in the single fastener connection slip behavior. A global relative displacement in two directions and a relative in-plane rotation of the connection is distributed to the individual fasteners, yielding relative displacements of fasteners and their direction with respect to the grain direction of the timber. The latter quantities are subsequently used to assign single fastener connection loads from their slip curve (cf. Fig. 2). Summing up of the loads finally yields internal forces of the connections, which are a consequence of the global relative displacement. On the contrary, calculation of load distribution for a given set of internal forces requires an iterative solution method. The procedure has been implemented in *Matlab* [20].

The main advantages of this model are its simple pre- and post-processing and short calculation times. Thus, the model can be integrated in the structural analysis of timber structures and even more, complex connection situations with different types of single fastener connections or end-grain contact situations can be considered using appropriate slip curves [20]. However, non-uniform load distribution under uniform normal force or shear force cannot be modelled with this approach, since the elastic deformation of the matrix is neglected.

2.6 Analytical models with linear single fastener connection slip

Assuming a linear instead of the nonlinear single fastener connection slip further simplifies the modeling. Preserving the orientation dependence in the single fastener connection slip behavior, i.e., linear elastic stiffness K_α depending on the load-to-grain angle, α, in-between parallel and perpendicular to the grain, the load of a single fastener connection $F_{M,i}$ due to an in-plane bending moment $M_{y,connection}$ is given by [3].

$$F_{M,i} = \frac{K_{\alpha,i} \cdot r_i}{K_r} \cdot M_{y,connection} \tag{1}$$

with the distance of the fastener to the center of rotation r_i and the rotational stiffness K_r of the connection,

$$K_r = \sum_{j=1}^{n} K_{\alpha,j} \cdot r_j^2 \tag{2}$$

K_α could be determined experimentally for single fastener connections or numerically based on embedment data (cf. with experimental data in [4]) with beam-on-foundation approaches. For standardization purposes, an analytical function with stiffness values parallel and perpendicular to the grain in combination with e.g. the Hankinson equation could be used.

As a final simplification, an orientation independent slip behavior of the single fastener connection could be assumed, which yields single fastener connection loads F_j due to an in-plane bending moment $M_{y,connection}$ from [3]

$$F_j = \frac{M_{y,connection}}{I_p} \cdot r_j \tag{3}$$

with I_P as the so-called polar moment of inertia calculated as the sum of squares of polar radii r_j, which are the radial distances of each fastener to the center of rotation. The rotational elastic stiffness $C_{ser,r}$ of the multi-fastener connection (in this case under serviceability conditions) is calculated as

$$C_{ser,r} = \sum_{j=1}^{n} K_{ser,j} \cdot r_j^2 \tag{4}$$

with $K_{ser,j}$ as the isotropic elastic slip modulus of dowel j.

3. Modeling load distribution in case of in-plane bending moment

In the following, selected numerical models described in section 2 will be applied to study the load distribution of multiple fastener connections. As reference single fastener connection, a double shear steel-to-timber connection with a 12 mm steel dowel, loaded by a center steel plate, is used. A wood side member thickness of 50 mm and a steel plate thickness of 12 mm were assumed together with material properties as summarized in Fig. 2. The spacing of the dowels was increased compared to Eurocode 5 minimum values by two times the dowel diameter, to account for plastic displacements in highly ductile or possibly reinforced connections, see Figs. 3 and 4. Regarding load distribution in case of bending moment, three different dowel groups have been calculated with 2x2, 3x3, and 5x5 dowels using the models described in subsections 2.4 and 2.5. Pure moment loading was ensured by using symmetric boundary conditions without constraining the timber matrix. The models give access to the global multiple fastener connection slip, as well as to the load distribution among the dowels, which is discussed in the following. Single dowel forces are given as forces per single fastener connection, which for the double shear steel-to-timber connection is twice the force per shear plane.

The effect of the elasticity of the wood matrix could be assessed. The rotational stiffness of the investigated connections as well as the obtained load distribution was found to hardly depend on the elastic deformation of the timber matrix (see Fig. 3). Only a slight increase in loads parallel to the grain combined with a slight decrease in loads perpendicular to the grain was observed in the Finite Element model with elastic wood matrix (see 5x5 dowels group in Fig. 3). However, the nonlinear orientation dependent slip curve of the fasteners is governing the load distribution. The high stiffness of the single fastener connections parallel to the grain (cf. fasteners 2&8 in Fig. 3 top right, and 3&23 in Fig. 3 bottom left) leads to a stronger loading of these dowels even compared to fasteners that are further away from the center of rotation (cf. fasteners 1&3&7&9 in Fig. 3 top right, and 1&5&21&25 in Fig. 3 bottom right). An analytical calculation based on the polar moment of inertia (see subsection 2.6) would yield a different load distribution in the initial loading path, since the load distribution would only be linearly related to the distance from the center of rotation, see Eq. (3).

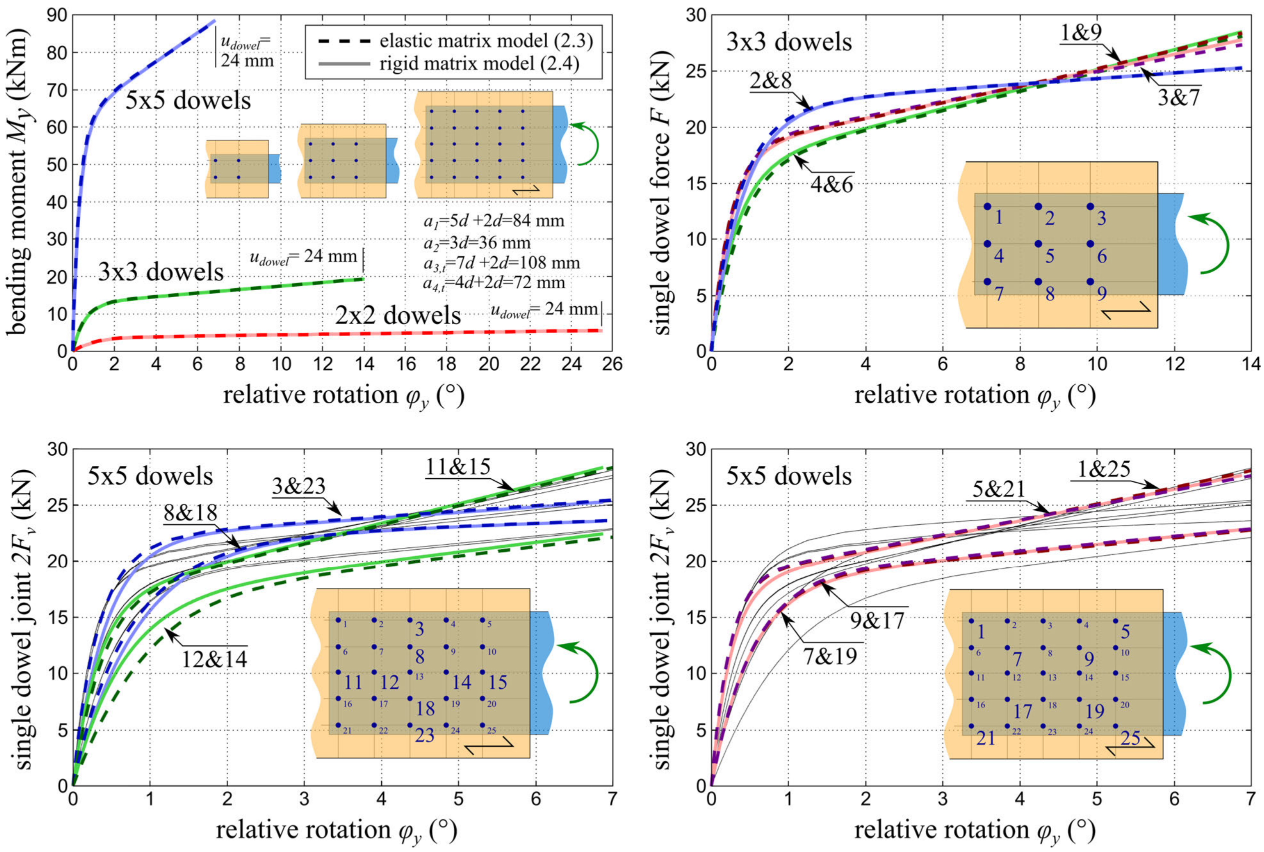

Fig. 3. Load distribution in case of in-plane bending moment – calculation examples; thin lines represente forces in dowels not discussed in the text.

Comparison of linear with nonlinear models is discussed in [17] and underlines that an isotropic calculation might lead to an underestimation of single fastener connection loads parallel to the grain. Using a load orientation dependent stiffness K_α would enhance the prediction quality of the linear elastic model, see Eq. (1). The load distribution in the plastic loading path subsequently depends on the limit loads, which are again a function of the load orientation. With respect to the rotational stiffness of multiple fastener connections, the modeling results suggest a negligible influence of the elasticity of the timber matrix in-between the dowels. Except for the very first part of the multiple fastener connection slip curve, the difference in dowel loads between the models with elastic (2.4) and rigid (2.5) wood matrix was found to be less than 10% (cf. Fig. 3).

The effect of lateral loads of the single dowels as a consequence of a prescribed displacement path, i.e. the fact that the load orientation does not necessarily follow the displacement orientation in anisotropic materials, could be neglected in the load distribution in case of a pure bending moment. This is due to the fact that these load components are pointing to the center of rotation and thus, they are not adding a contribution to the global moment. However, lateral loads might affect the stress distribution in the timber matrix predicted by the modeling approaches. This effect could be considered by adding the contribution of the lateral loads to the spring properties shown in Fig. 2, which would then yield a deviation of load orientation from the prescribed displacement orientation.

4. Modeling load distribution in case of forces parallel and perpendicular to the grain

Most research related to load distribution has been conducted for multiple fasteners in a row parallel to the grain, loaded by a normal force parallel to the grain. This was done to assess the risk for brittle failure as a consequence of load and stress accumulation [6]. The load distribution effect is however also present in multiple fasteners in a row perpendicular to the grain, loaded by a force at an angle of 90° to the grain, subsequently called shear force. Jorissen [6] used an elastic spring model with non-linear slip curves and even accounted for a random initial slip in the single fastener connections. Based on experimental and computational results, Jorissen proposed simplified design rules that comply with the effective number of fasteners concept for loading parallel to the grain. Effective number of fasteners in Eurocode 5 are based on the work of Jorissen and the elastic solution of Lantos (1969) (see [22] for a review of modeling approaches) taking into account longitudinal stiffness of the connected members, the number of fasteners, fastener spacing, and the slip modulus of the single fastener connection. Models are based on an effective flexibility of the wood between the fasteners, which is a function of the parallel and lateral spacing, the side member thickness and the Young's modulus of wood in the load direction [6].

Sjödin and Serrano [23] showed the influence of several rows of dowels and the effect of the unloaded edge distance (a_2 and $a_{4c,t}$ according to Eurocode 5) on the load distribution and proposed two numerical models (based on linear elastic fracture mechanics and based on Eurocode 5 single fastener strength values) for the calculation of the strength of such connections. The effect of lateral spacing and number of rows has also been investigated by means of a 2dimensional FEM model in [18] and [19].

The influence of the elastic deformation of the wood matrix on the load distribution in multiple fastener connections under forces parallel and perpendicular to the grain is exemplarily demonstrated in Fig. 4, using a beam-on-foundation modeling approach (subsection 2.3) for the single dowel, and an elastic FEM model (subsection 2.4) and a rigid matrix model (subsection 2.5) for multiple dowel groups. Input data is visualized in Fig. 2. Displacement boundary conditions in the numerical models have been set on the wood at a distance of 50 mm from the dowel, and on the steel plate at the height of the wood end grain. Slip curves of fastener groups are compared to the theoretical slip curve of the single dowel connections times the number of dowels (black curves related to model 2.5 in Fig. 4).

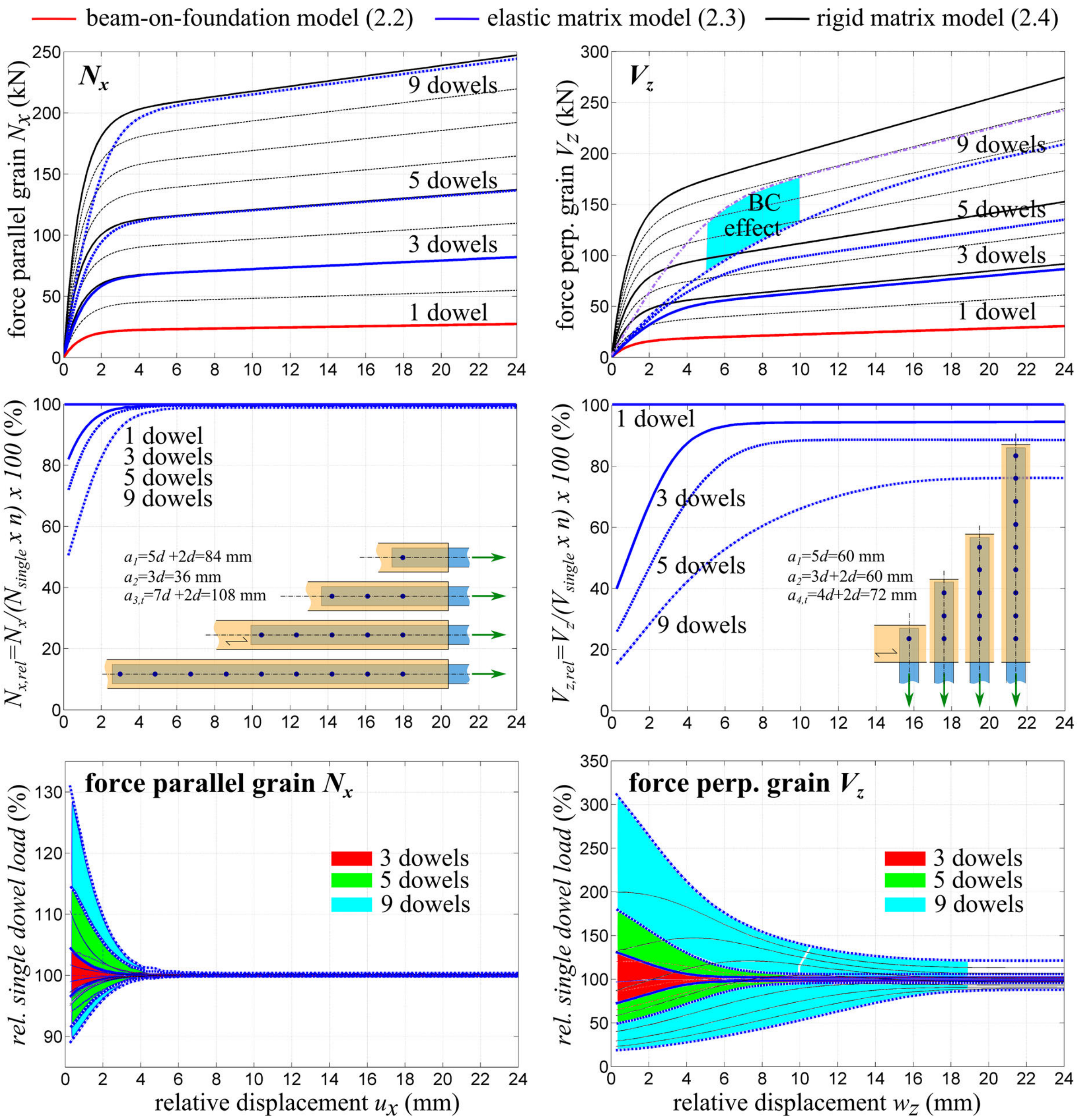

Fig. 4. Load distribution in case of forces parallel or perpendicular to the grain – calculation example.

In case of normal force loading, the non-uniform load distribution vanishes after some millimeters of relative displacement, while due to the low stiffness of wood perpendicular to the grain, in case of a force perpendicular to the grain, a non-uniform load distribution prevails and limits the strength of the multiple fastener connection. The group effect in the stiffness of connections is clearly visible, and much more dominant under shear loading perpendicular to the grain.

The load distribution, relative to a mean value of single dowel connection forces, is shown in Fig. 4 bottom and shows a load accumulation in the fastener closest to the displacement boundary condition of the wood, which in this case is the dowel furthest away from the end grain of the wood member. If all dowels had 100% of the mean value, a uniform load distribution would be given. The examples demonstrate the effect, but the load distribution naturally depends on the boundary conditions of the members. This is illustrated by the slip curve for 9 dowels under a force perpendicular to the grain (BC effect in Fig. 4 top). The upper line is calculated with constrained displacements at mid-height of the beam instead of at the top edge of the beam.

5. Modeling of load distribution in case of complex loading

In the most general case, a combination of internal forces acts on connections in timber structures. The combination of the above described special cases of single internal forces (sections 3 and 4) naturally depends on load cases of structures. All models presented in Fig. 1 could be used for this purpose to describe the interaction in the load distribution on the global behavior of connections. However, some of them are computationally very costly and thus not practical for an engineering design. Thus, calculations presented in the following, were done with the model described in subsection 2.5, i.e., without elastic deformations of the wood matrix.

Based on this model, limit surfaces of connections can be calculated based on limit state criteria. In the following, we are using maximum relative dowel displacements of 1.5 mm, 6 mm, 12 mm and 24 mm as limit criteria to determine limit states of two multiple dowel connections (3x3 and 5x5 dowels with same layup as shown in Fig. 2). Calculation results could be visualized in terms of relative displacements and rotation or, as in Fig. 5, by means of internal forces of the dowel group. Limit curves for pairs of internal forces (Fig. 5 bottom) clearly show the interaction as well as the hardening behavior, as a consequence of load redistribution in the case of moment loading or of displacement hardening for loading perpendicular to the grain. Neglecting the weak stiffness of wood perpendicular to the grain might slightly affect the interaction with the force perpendicular to the grain, particularly as regards the initial stiffness and for larger dowel groups.

The model predicted global behavior of the multiple fastener connection can be further used in the structural analysis of timber structures to account for the interaction of internal forces on the displacement behavior of the single fasteners and the load distribution among them, which finally governs the global behavior. Thus, each internal force (N_x, V_z, M_y) becomes a function of three degrees of freedom, namely the relative displacements u_x, w_z and the relative rotation φ_y. Alternatively, the relationship could be formulated in terms of a stiffness matrix, linking internal loads with relative displacements and rotation.

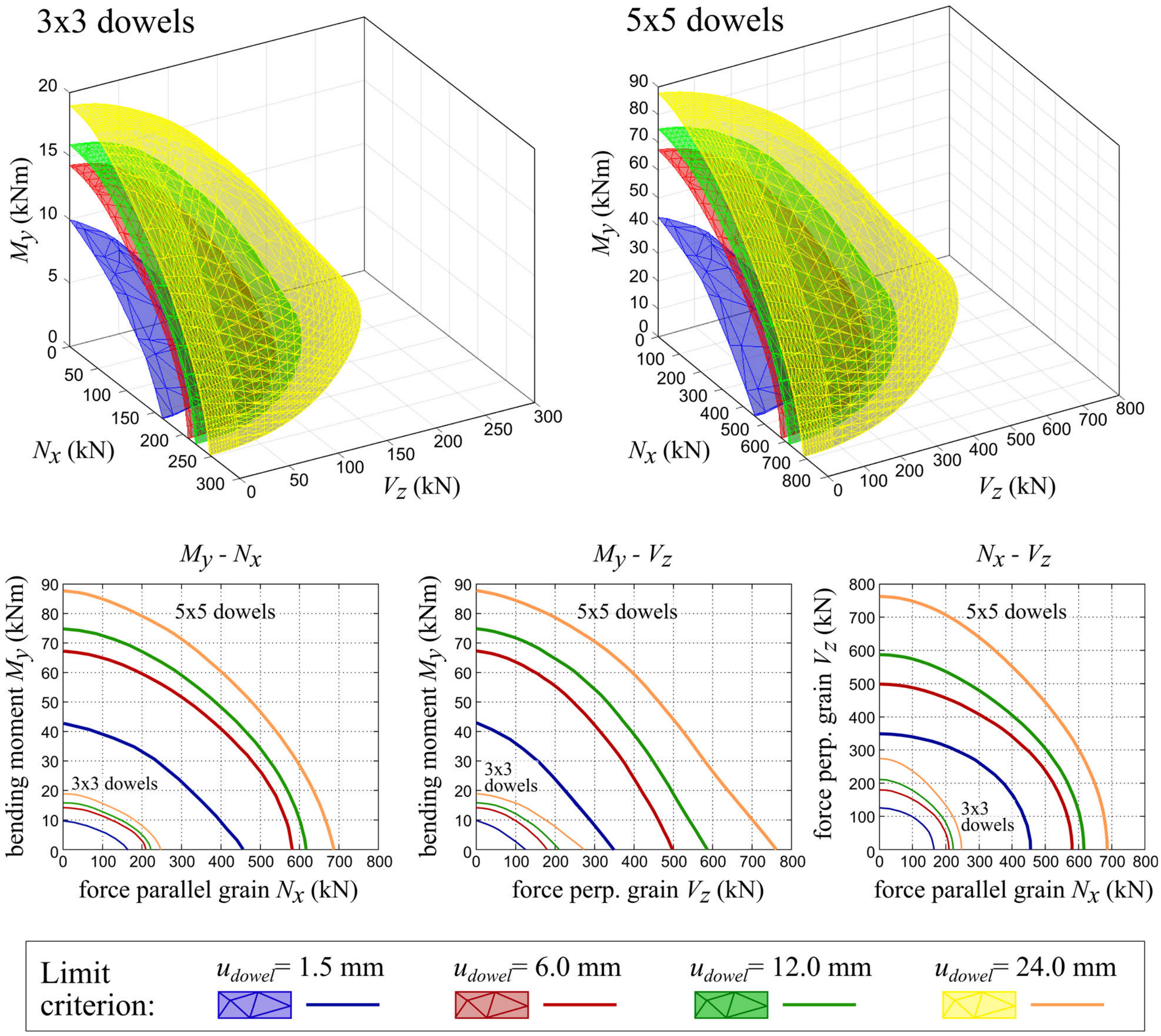

Fig. 5. Load distribution in case of combined force parallel to the grain (N_x), force perpendicular to the grain (V_x) and in-plane bending moment (M_y).

6. Load distribution in connections with glued-in steel rods

Since the withdrawal behavior, as well as the embedment behavior of the steel rods is almost linear until failure and the bending of the steel head is negligible, the axial force, $F_{ax,i}$, and the shear force, $F_{lat,i}$, in each glued-in rod are determined through the linear stiffness, $K_{ser,ax,i}$, and $K_{ser,lat,i}$, as (see Fig. 6)

$$F_{ax,i} = K_{ser,ax,i} \cdot dx \quad (5)$$

$$F_{lat,i} = K_{ser,lat,i} \cdot dz \quad (6)$$

with the displacement increments dx and dz.

Consequently, the normal force N_x and the shear force V_z are calculated as

$$N_x = \sum_{i=1}^{n} F_{ax,i} = \sum_{i=1}^{n} K_{ser,ax,i} \cdot dx \tag{7}$$

$$V_z = \sum_{i=1}^{n} F_{lat,i} = \sum_{i=1}^{n} K_{ser,lat,i} \cdot dz \tag{8}$$

The stiffness of the connection is assumed to be the sum of the corresponding single rods, which yields

$$K_{ser,x,ass} = \sum_{i=1}^{n} K_{ser,ax,i} \tag{9}$$

$$K_{ser,z,ass} = \sum_{i=1}^{n} K_{ser,lat,i} \tag{10}$$

The load distribution in case of a bending moment, M_y, can be calculated under the same assumption of a linear withdrawal behavior of the rods until failure by neglecting the bending of the steel head. Thus, the axial force in a rod, $F_{ax,i}$, becomes a function of the displacement, dx, due to a relative rotation, ϕ_y, and the distance from the assumed center of rotation, ρ_i, reading as

$$F_{ax,i} = K_{ser,ax,i} \cdot \rho_i \cdot \phi_y \tag{11}$$

Thus, the bending moment is derived as

$$M_y = \sum_{i=1}^{n} F_{ax,i} \cdot \rho_i = \sum_{i=1}^{n} K_{ser,ax,i} \cdot \rho_i^2 \cdot \phi_y \tag{12}$$

The rotational stiffness of the connection is then calculated as

$$C_{ser,r,ass} = \sum_{i=1}^{n} K_{ser,ax,i} \cdot \rho_i^2 \tag{13}$$

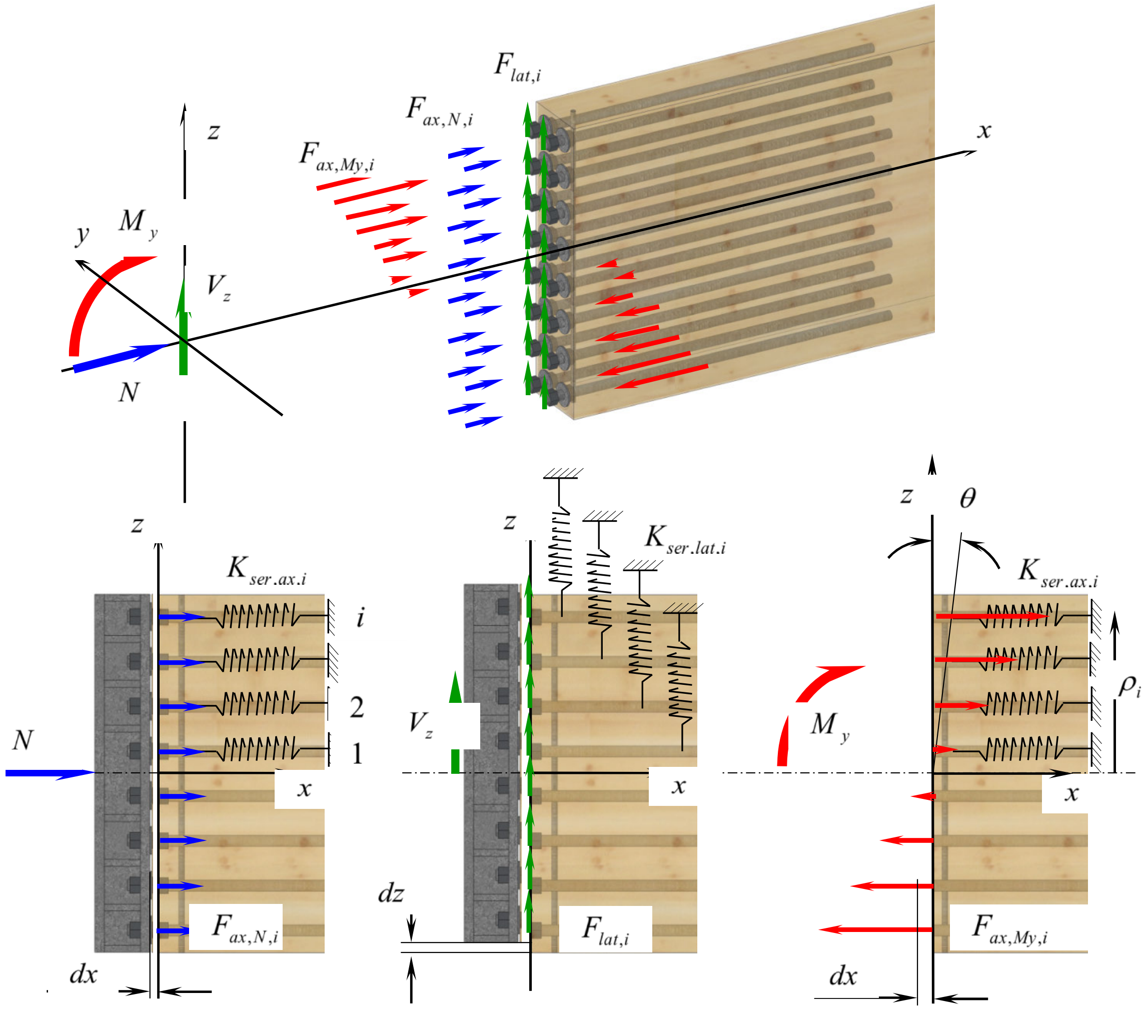

Fig. 6. Determination of load distribution in connections with laterally and axially loaded glued-in steel rods.

7. Suggestions for revisions and additions in design and testing standards

The presented numerical models of multiple fastener connections are essential for an improved design of connections based on a sound load distribution as a prerequisite for a realistic stress state in the timber matrix. The contribution highlights the need for improved knowledge of the nonlinear embedment and single fastener connection behavior as the main reason for non-uniform load distribution among fasteners, particularly under in-plane bending moment loading. Nonlinear embedment properties together with steel fastener material properties could be exploited in beam-on-foundation models to predict nonlinear slip curves of single fastener connections. This would avoid the need for comprehensive experiments for the assignment of stiffness properties of single fastener connections by means of derivation of empirical equations. Thus, a revision of embedment testing standards is required to prescribe embedment testing of connections up to large relative displacements and parameterization methods for the evaluation of test data. This would open up manifold possibilities for an advanced modeling and engineering design of connections, even including their seismic behavior.

The load distribution modeling is not only necessary for the determination of single fastener connection loads in the verification of connections, but also for the assignment of stiffness properties in the structural analysis of timber structures in the first step. The isotropic distribution model was previously shown to be a very crude simplification, underestimating single fastener connection loads parallel to the grain under moment loading. A more advanced analytical model using load-to-grain orientation dependent stiffness of single fastener connections would considerably enhance load distribution modeling. Moreover, multiple fastener connection stiffness parallel and perpendicular to the grain is reduced with increased number of fasteners, due to the weak elastic stiffness of the timber.

Compared to the currently pursued design of single fastener connections in Eurocode 5, models presented in this contribution would allow for an engineering design of multiple fastener connections. The design of connections is currently based on characteristic properties of the components, which yields lower limit strength below the characteristic strength of multiple fastener connections, since possible homogenization effects over the length scales are not accounted for. Herein, we propose to use mean values as input to the models, which consequently yields mean values on the single and multiple fastener connection level. The variability should subsequently be defined by taking into account the failure mode in combination with appropriate partial safety factors for connections. Since the modification factor only relates to the timber, it should be used to modify the mean values of the timber properties in the model instead of being assigned to the overall connection properties. Consequently, the single fastener connection failure modes will not be modified by uncertainty considerations. There is a potential for the presented models to considerable enhance the elastic-plastic design of timber structures exploiting the ductile capacity of reinforced multiple fastener connections.

Future standardization should provide regulations and allow for both, a simplified analytical as well as for a more advanced numerical modeling of load distribution. A comprehensive comparison of numerical modeling of load distribution with linear elastic load distribution models could be performed to determine errors, and consequently limits, of the simplified linear load distribution model, which should be made transparent in the design standard. A more advanced numerical design of connections should be supported by the standard by providing regulations and input data for beam-on-foundation and load distribution models.

Throughout this paper, we pointed out the need for assessment of brittle failure, which should rest on a reliable prediction of stresses in the matrix, taking into account the non-uniform load distribution. This forms the basis for the design of reinforcement measures to avoid brittle failure. Assessment of brittle failure, particularly in case of combined loading, should build upon the herein proposed numerical models that account for interactions of internal forces.

References

[1] *EN 1995-1-1:2004 + AC:2006 + A1:2008 (Eurocode 5)*. Design of Timber Structures – Part 1-1: General – Common Rules and Rules for Buildings. CEN, Brussels.

[2] Bader TK, Schweigler M, Serrano E, Dorn M, Enquist B, Hochreiner G (2016) Integrative experimental characterization and engineering modeling of single-dowel connections in LVL. *Construction and Building Materials* **107**:235-246.

[3] Racher P (1995) *Moment resisting connections*. Lecture C16 in Timber Engineering STEP 1, Centrum Hout, The Netherlands.

[4] Schweigler M, Bader TK, Hochreiner G, Unger G, Eberhardsteiner J (2016) Load-to-grain angle dependence of the embedment behavior of dowel-type fasteners in laminated veneer lumber. *Construction and Building Materials* **126**:1020-1033.

[5] Ormarsson S, Blond M (2012) *An improved method for calculating force distributions in moment-stiff timber connections*. World Conference on Timber Engineering, Auckland.

[6] Jorissen A (1998) *Double shear timber connections with dowel type fasteners*. PhD thesis, Delft University of Technology.

[7] *EN 14080:2013*. Timber structures. Glued laminated timber and glued solid timber. Requirements. CEN, Brussels.

[8] Gecys T, Daniunas A, Bader TK, Wagner L, Eberhardsteiner J (2015) 3D finite element analysis and experimental investigations of a new type of timber beam-to-beam connection. *Engineering Structures* **86**:134-145.

[9] Dorn M (2012) *Investigations on the serviceability limit state of dowel-type timber connections*. PhD thesis, Vienna University of Technology.

[10] Iraola B, Cabrero JM, Gil B (2016) *Pressure-overclosure law for the simulation of contact in spruce joints*. World Conference on Timber Engineering, Vienna.

[11] Sandhaas C (2012) *Mechanical behaviour of timber joints with slotted-in steel plates*. PhD thesis, Delft University of Technology.

[12] Dias AMPG, van de Kuilen JWG, Cruz HMP, Lopes SMR (2010) Numerical modelling of the load-deformation behavior of doweled softwood and hardwood joints. *Wood and Fiber Science* **42**:480-489.

[13] Hirai T (1983) Non-linear load-slip relationship of bolted wood-joints with steel side members – II – Application of the generalized theory of beam on an elastic foundation. *Makusu Gakkaishi* **29**(12):839-844.

[14] Foschi R (1974) Load-slip characteristics of nails. *Wood Science* **7**(1):69-76.

[15] Sauvat N (2001) *Résistance d'assemblages de type tige en structure bois sous chargements cycliques complexes*. PhD thesis, LERMES / CUST, Université Blaise Pascal-Clermont II.

[16] Vessby J, Serrano E, Olsson A (2010) Coupled and uncoupled nonlinear elastic finite element models for monotonically loaded sheathing-to-framing joints in timber based shear walls. *Engineering Structures* **32**:3433-3442.

[17] Bader TK, Schweigler M, Hochreiner G, Eberhardsteiner J (2016) *Load distribution in multi-dowel connections under moment loading – integrative evaluation of multiscale experiments*. World Conference on Timber Engineering, Vienna.

[18] Hochreiner G, Bader TK, Schweigler M, Eberhardsteiner J (2017) Structural behaviour and design of dowel groups Experimental and numerical identification of stress states and failure mechanisms of the surrounding timber matrix. *Engineering Structures* **131**:421-437.

[19] Hochreiner G, Riedl C, Schweigler M, Bader TK, Eberhardsteiner J (2016) *Matrix failure of multi-dowel type connections – engineering modelling and parameter study*. World Conference on Timber Engineering, Vienna.

[20] Schweigler M (2013) *A numerical model for slip curves of dowel connections and its application to timber structures*. Master's thesis, Vienna University of Technology.

[21] Jensen J (1994) *Dowel-type fastener connections in timber structures subjected to short-term loading*. PhD thesis, Danish Building Research Institute, SBI-Rapport 237.

[22] Blass HJ (1995) *Multiple fastener joints*. Lecture C15 in Timber Engineering STEP 1, Centrum Hout, The Netherlands.

[23] Sjödin J, Serrano E (2008) A numerical study of methods to predict the capacity of multiple steel-timber dowel joints. *Holz als Roh- und Werkstoff* **66**:447-454.

Design recommendations and example calculations for dowel-type connections with multiple shear planes

Jean-François Bocquet
ENSTIB / LERMAB, University of Lorraine
Epinal, France

Romain Lemaître
ENSTIB / LERMAB, University of Lorraine
Epinal, France

Thomas K. Bader
Department of Building Technology, Linnaeus University
Växjö, Sweden

1 Learning from the design by testing of Utopia pavilion of Lisbon

The main objective of COST FP1402 is to synthesize scattered research results into relevant, concise and reliable information about the design standard of interest, which in case of timber structures is Eurocode 5. As an introduction to this contribution, which aims for design recommendations for timber connections with multiple shear planes in order to guarantee their reliability, it seemed beneficial to summarize and to critically review design features of the Pavilion of Utopia. This building is now called Altice arena and was built in 1995 for the 1998 Lisbon World Exposition (Fig. 1). With a capacity of 16,000 seats, it is an exceptional timber roof structure, especially due to its complex geometry and wide span (from 52 to 115 m). The timber structure was built by Weisrock S.A., (France) following a European competition the company won. The roof structure is composed of latticework arches whose frames and diagonals were realized with glued laminated timber of strength class GL28h.

Fig. 1. The Utopia building (left) and the timber arches during erection (right) [2].

In the specifications of the construction, it was stated that the dimensioning of the timber structure was to be made based on the version of the Eurocode 5 under investigation during the year 1993. At that time, it was assumed that with the provisions of spacing and minimum edge distances for dowel-type connections, the dimensioning method of connections would ensure plasticization. This plastic limit could be estimated using the yield analysis model for dowel-type connections presented in the code and by taking into account the load distribution along a line of fasteners by an interaction criterion based on a Lantos or Cramer approach [4, 5]. In France, since the Spinetta law of January 4, 1978, it is mandatory that a control office verifies the proper implementation of regulations to ensure the insurability of a building. For the Pavilion of Utopia, the VERITAS control office in Paris was commissioned to follow the progress of the project. Given the size of the structure and the novelty of the regulation, it seemed appropriate for the control office and the prime contractor to verify the design of the joints by experimental analysis (Fig. 2).

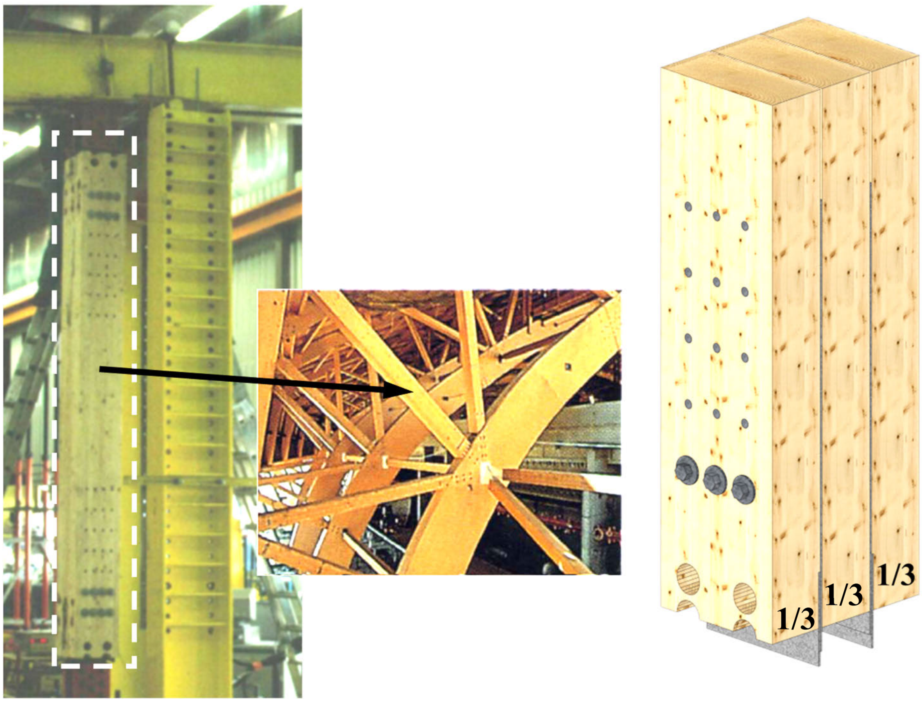

Fig. 2. The connections were tested in the Civil Engineering Department Laboratory LERMES in Clermont-Ferrand. The joints tested were situated at the ends of the diagonals of the main arches [1].

Connections of the diagonals of the main arch were selected for the experimental investigation. Based on the size of cross-sections determined by design calculation, the company Weisrock decided to produce the sections by gluing together three glued-laminated timber beams of identical dimensions. These diagonals were linked to the glued-laminated timber arches with slotted-in steel plates, and it appeared economical to insert the steel plates at the time of gluing of the cross-section. Machining was then provided in order to put the steel plates in the outer elements of the glued section. Thus, the geometry of the connection was fixed by favouring the production side. Since Eurocode 5 was used to evaluate the load-carrying capacity of the connection, the estimate should have been reliable regardless of the configuration adopted. Experimental testing was performed by the woodworking team of LERMES laboratory located in Clermont-Ferrand. The laboratory offered equipment able to load the diagonals of the arch in tension or in compression up to a maximum capacity of 3 MN [3]. In order to connect the steel plates with the three timber parts, continuous dowels penetrating all joint members were used. The principle of multiple shear plane connections was already present in ENV-1995-1-1:1993 and was expressed as given in the following paragraph:

6.2.3 Multiple shear plane connection

(1) In the case of more than two shear planes, the total capacity is generally determined by summing the minimum capacity of each shear plane, each shear plane being considered as part of a three-element connection.

It should be noted that in the current version of Eurocode 5, the principle has only been supplemented with rules of compatibility of modes between continuous shear planes.

The dowels were made of high grade steel 6.8. The number of dowels was variable according to the load in the elements, and bolts were added for some connections (participation in the load-carrying capacity) at the end of elements in order to ensure joint integrity.

The first tests highlighted different failure modes that were not described in ENV 1995-1-1. In the first case, splitting failure modes appeared while the number of fasteners was often less than 6 dowels along a line parallel to the grain. In that version of the ENV, the actual number of dowels was only decreased in case of more than 6 fasteners in a row, using the following rule and formula

6.5.1.2 Bolts stressed in shear

(3) For more than 6 bolts in line in the direction of the load, it is necessary to reduce by one third the load capacity of the additional bolts, that is to say that for n bolts the effective number of bolts is:

$$n_{ef} = 6 + \frac{2 \cdot (n-6)}{3} \tag{1}$$

Moreover, failure modes occurred where one or more timber parts were detached from the connection. Possibility of occurrence of these failure modes had been mentioned twice in the fundamental works summarised in STEP 1 [6] and STEP 2 [7] in 1994 (Chapters C1 and E6). However, these forecasts or relevant expectations did not give rise to specific recommendations in Eurocode 5 until today.

Although the row effect is integrated into Eurocode 5, as well as is the block shear failure, it is almost certain that an inexperienced designer would fall into the same sizing pitfalls if nothing is added in the code as related to designing multiple shear planes of connections. It is therefore important to clarify the problem encountered here and formulate design provisions that made the design of the connection reliable at that time. This design example can be used to enact rules that would lead to more reliable design of multiple fastener connections in the future.

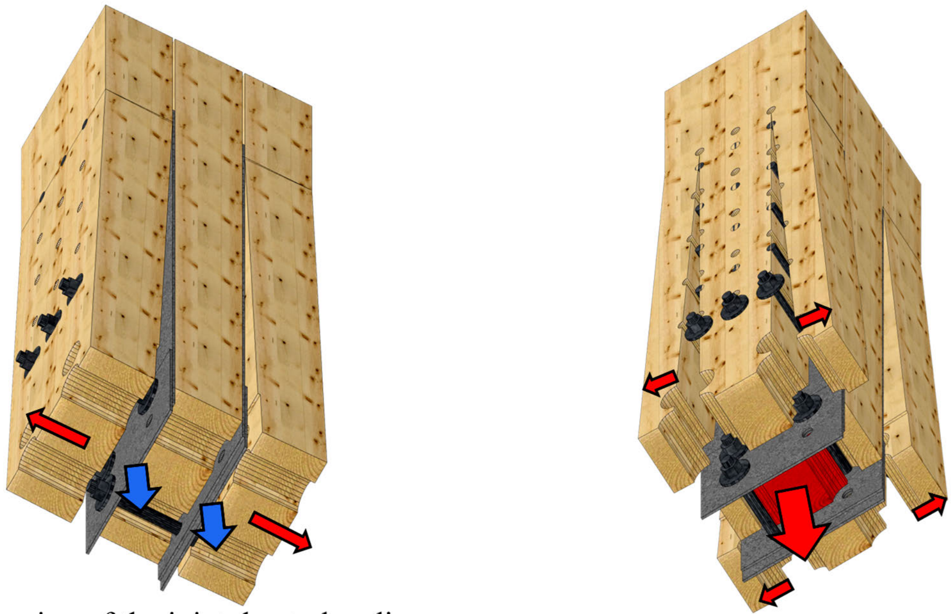

Opening of the joint due to bending of the dowels in the outer parts

Sequential failure starting by the tear out of the central block shear failure

Fig. 3. Opening of the joint during the loading and typical final failure modes with row shear failure and tear out block shear failure [1, 2, 3].

The connections in the diagonals of the arched truss structure of the Pavilion of Utopia, which consisted of three glued-laminated timber pieces of equal size, were mainly investigated in tensile tests. During tensile force loading, the outer timber elements of the section were not only subjected to tension but also to bending stresses, which could cause failure as well. Indeed, at the outer shear planes of the connection, the timber elements received a shearing force and a bending moment by each of the dowels on one side of the timber element. The shear at the interface acted with eccentricity with respect to the axis of the part and the timber parts were bent outward of the connection (Fig. 3). Bolts placed at the ends were used to balance this moment. At first glance, the number of these fasteners proved to be insufficient. The washers penetrated into the timber and allowed the timber elements to deform and to move away from the shear plane. Moving away from the shear plane, the timber released part of its tensile force, which was transferred to the central part and initiated failure. The distribution of the tensile force has therefore changed during loading. Central block shear failure occurred before plasticization of the dowel-type connection, it was followed by tensile failure which led to ultimate failure in a brittle manner at the end of this sequential failure process. Taking into account load redistribution phenomena during loading is much too complex for a simplified design method according to a structural design standard.

In order to increase the load-carrying capacity of the connection, it seemed essential to limit the opening effect explained above. In a first step, the number of bolts at the end of the connection was therefore doubled. Since splitting failure was not expected but observed for a number of fasteners in a row of less than or equal to 6, it was also chosen to reinforce the connections against splitting by threaded rods glued into the timber (at that time, glued-in rods were not developed as they are nowadays).

After having carried out further tests, it could be shown that all of these constructive reinforcement arrangements made it possible to reach the level of reliability required by Eurocode 0 for this project (Fig. 4). Fig. 4 shows that after the implementation of reinforcements, load distribution has been more uniform and generalized over the section when the failure appeared. It should be noted that the connection test carried out in compression led to a "ductile" block failure, of identical shape to the block failure in tension; the timber in compression at the bottom of the central block collapsed on itself.

Since realization of the Pavilion of Utopia, Eurocode 5 has been revised and the failure criterion taking into account the number of fasteners in a row has been modified. Moreover, a formulation to evaluate block shear failure was proposed in an annex to Eurocode 5; this formulation should be extended to emphasize that it is also necessary to verify this criterion when multiple fastener connections are subjected to compression.

The example of connections in the Pavilion of Utopia first of all highlights that it is important to implement constructive measures that make it possible to keep load distribution assumptions during loading. In other words, the initial geometry of the connection must be kept as long as possible during loading. Furthermore, when the capacity of a connection is found to be the result of the sum of the capacities of different parts, it is important to implement systems that limit sequential failure effects: in the example of the Pavilion of Utopia, the reinforcement by glued-in threaded rods have avoided splitting of the lines until the final failure of the connection in tension. Finally, it is possible to question the influence of the distribution of the width of timber between the shear planes: does this distribution have an influence on the reliability of the load-carrying capacity of the assemblies? Based on design examples, this research question and the aim for an optimized design of multiple shear plane connections with dowel-type fasteners will be discussed in this contribution.

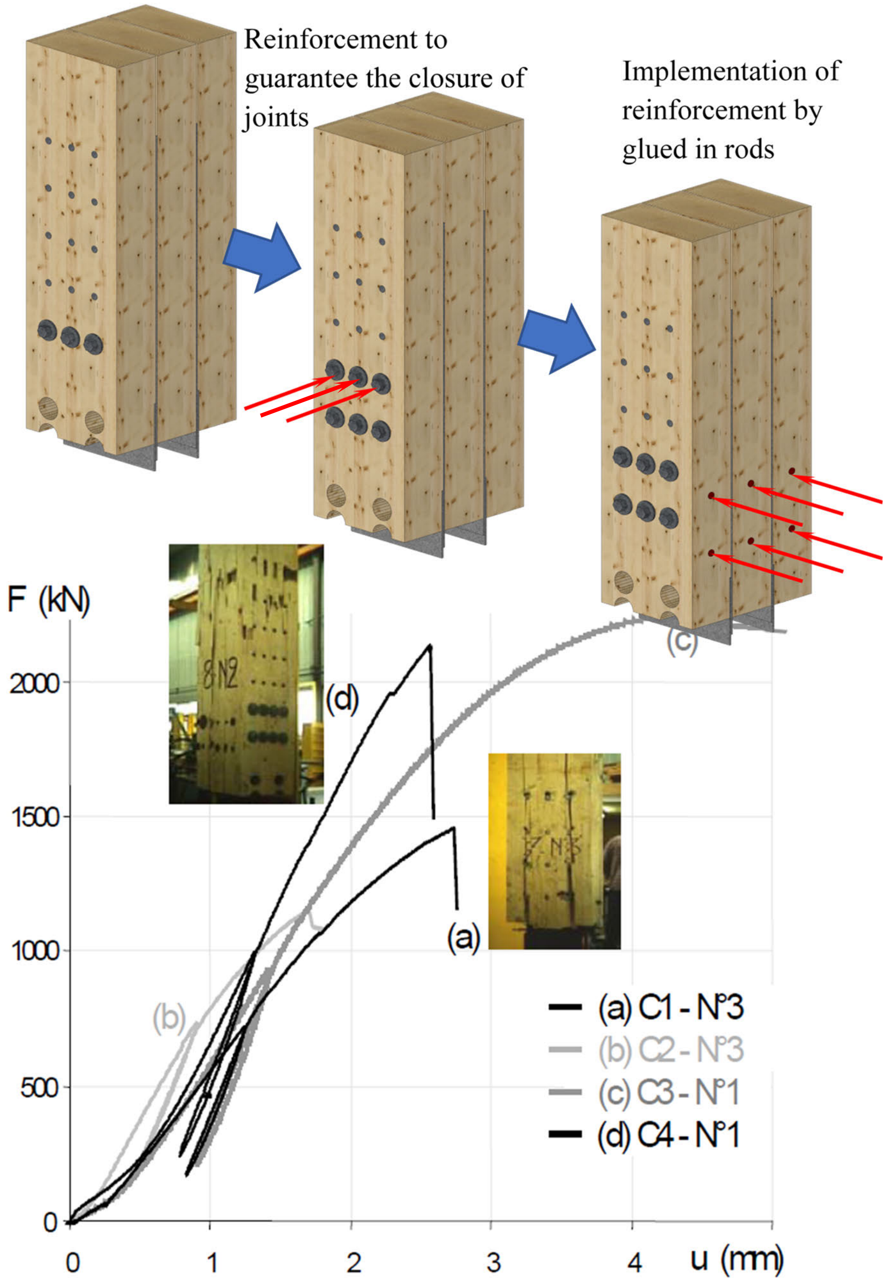

Series	n_r	n_f	Bolts	Dowels	loading
C1	3	4	--	12	Tension
C2	3	5-4-5	--	14	Tension
C3	3	5	6	9	Compression
C4	4	7	8	20	Tension

Fig. 4. Evolution of the design of the joints from the initial to the final configurations. Evolution of the stiffness during the tests in tension and compression in the initial and final configuration [3].

2 Approach to avoid the opening of joints

During the design phase of a timber connection, it is necessary to keep in mind that since it is possible to mobilize timber and steel plasticity, the connection can potentially deform considerably. In the situation where the connection shows a high ductility, this is not a problem. In the more frequent situation when the failure of the connection occurs in a brittle failure mode by splitting, shearing or block shear failure, precautions must be taken.

Some technical choices can enable deformation to the connection during loading. During load increase, these deformations will lead to a redistribution of stresses in particular for assemblies of high capacity. In the example presented in Section 1, it can be observed that the lack of transverse restraint at the end of the joint results in a drifting apart of the single parts perpendicular to the direction of loading. The moment induced by the shear force on the inner plane bends the timber element outwards. This bending will allow the dowels, that are bent by the shear force, to withdraw from the load they should bear (see Fig. 5).

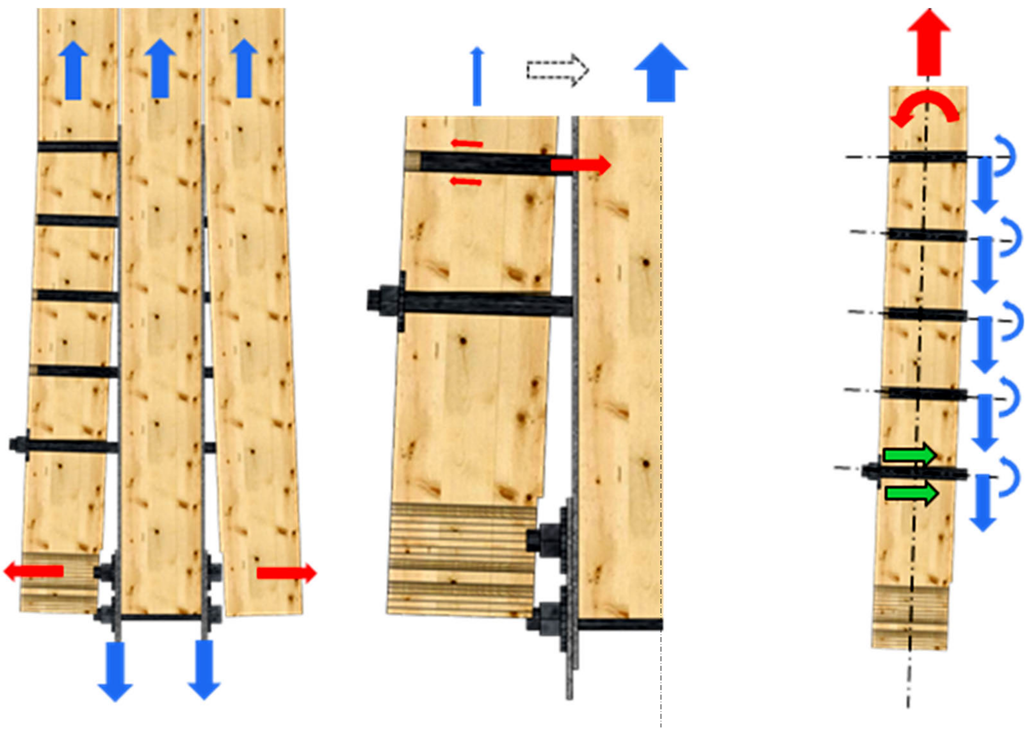

Fig. 5. Transfer of stresses and equilibrium in a deformed connection due to insufficient lateral restraint.

Since the bending of the lateral parts is not uniform along the element, the distribution of the loads along the row of fasteners is changed. This complicates prediction of the type of failure of the row. For these types of assemblies, the deformation at failure will be of the order of a few millimeters (see Fig. 4). The loss of elongation of the lateral elements, due to the sliding of the dowel, can rapidly transfer high quantities of load to the central part of the connection. The prediction of the load distribution at failure, in a deformed state of the connection, is neither conceivable nor realistic in current design. It seems already complex to take into account the stiffness of the shear planes in the design as it will be shown in the following sections. It is therefore necessary to prevent these phenomena by adding devices such as bolts (nuts and washers), screws or any other system, dimensioned during static calculations, that can deform during loading (Fig. 5).

3 Approach to ensure the sum of capacities

Although timber has shown and proven to be an engineered material with controllable variability, it is still a hygroscopic material. In a structure and in particular in a large structure, the assemblies can be exposed to hygroscopic conditions that are very variable and very different depending on where they are positioned in the structure. This leads more or less randomly, despite potential precautions, to occurrence of cracks after the opening of the building. Although design codes require to take cracking into account, not all design situations are covered.

In the early design phase, the designer needs to make choices to transfer loads, which are, as stated above, very often the multiplication of shear planes when dowel-type fasteners are implemented. Although this design choice appears quite naturally from calculations, the sum of the capacities of each plane to obtain the total load-bearing capacity is not as obvious as it seems. Particular care must be taken in the design, especially when brittle failure modes drive assemblies such as block shear failure.

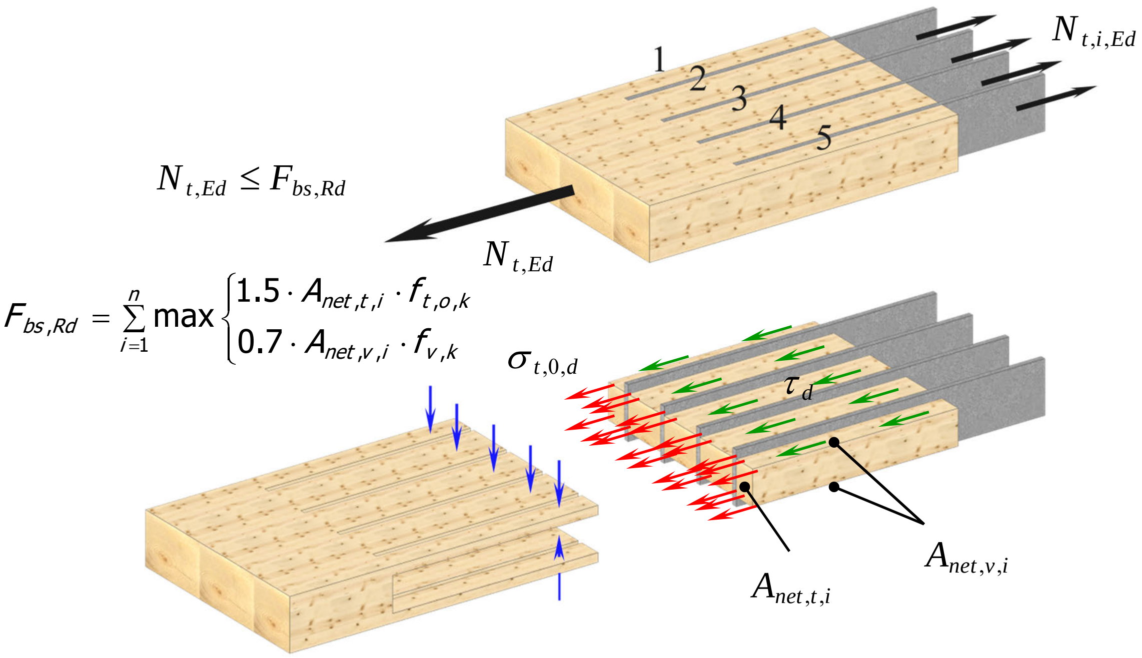

Fig. 6. Block shear failure in multiple shear plane connections in tension.

As will be shown in the next section, it is always preferable in connection design to focus on harmonisation of the stress distribution in the connection area. If the capacity at the bottom of the block drives the failure (Fig. 5), the failure will occur when one of the planes in tension reaches its maximum capacity. It is then very likely that this failure will trigger the failure of the other planes in tension. This indicates that the other planes will have reached a level of loading equivalent to the first plane that has failed. It then seems natural to estimate the load-carrying capacity of the connection by summing the capacities per plane, considering the lowest capacity.

For this calculation scheme to be realistic, it will be necessary to ensure that the distribution of the loads per plane remains, at a high level of loading, as close as possible to the initial hypotheses. Rigid (steel) fittings can provide this role of load distribution as shown in Fig. 7 and 8. Another solution is to reduce the hyperstaticity of the assemblies using e.g. dowels of half the required length and assembling the connections with shims. Adjustment of the assembly is then possible on site. These solutions generally reduce the necessary accuracy of execution, they however facilitate assembly on site and reduce costs.

Fig. 7. Multiple shear plane joints with rigid fitting and dowels in two pieces to ensure a homogeneous distribution of the normal forces. (Allianz Riviera Nice stadium)

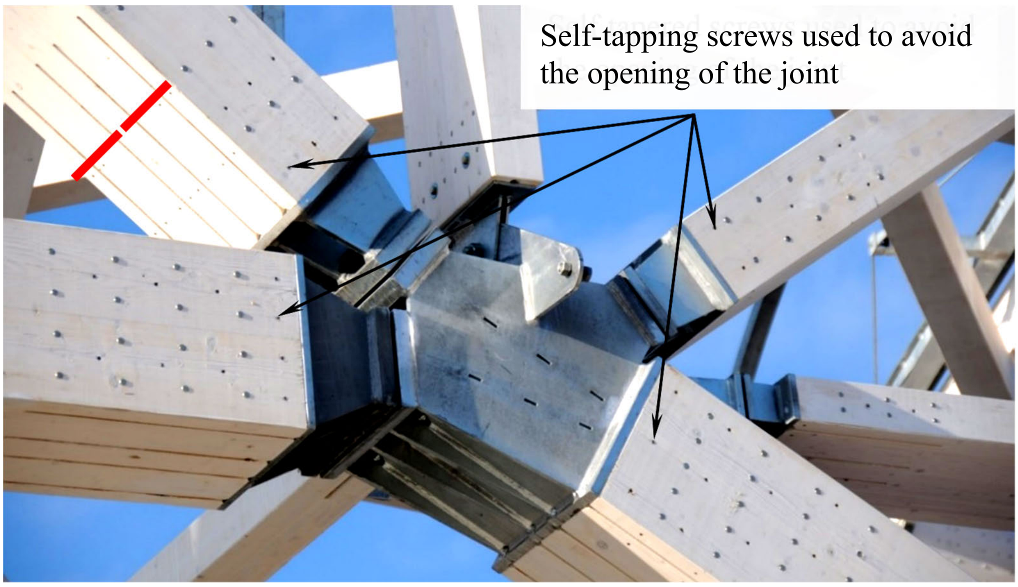

Fig. 8. Joints with eight shear planes and with dowels in two pieces, the rigid fittings are combined with thin steel wedges to control stress distribution. (Hall of Miramas Sports)

In the situation where the failure of the connection is governed by shear, the risk of a sequential failure is even greater. In fact, in an connection such as that presented in Fig. 6, the shear block capacity is given by the accumulation of 10 timber shear planes! Since the variability of the joint capacity is solely driven by shear, it is necessary to limit interaction with tensile stresses perpendicular to grain at the end of the connection when subject to a tensile force. The installation of self-tapping screws at the end of the connection is a good way to limit this risk, see Fig. 9.

Fig. 9. Reinforcement with self-tapping screws to avoid interaction between shear and tension perpendicular to the grain and following sequential failure in shear. (Hall of Miramas Sports)

4 Multiple shear plane timber connections and stress equilibrium

4.1 General

When it becomes necessary to transfer significant forces between the components of a structure and the size of the structural elements to be connected is equal, it is convenient to multiply the number of shear planes in dowel-type connections. Applying ultimate limit state analysis as proposed in Eurocode 5, it is easy to show that when mode 3 is reached, i.e. when the maximum number of plastic hinges is reached, the capacity of the connections cannot be increased with an increase of the thickness of the timber. This means that there is a limit at which large sizes become uneconomical. The multiplication of the number of shear planes is a way to optimize and to further increase the load-carrying capacity of the connection. For dimensioning of connections with multiple shear planes, Eurocode 5 does not propose a general formulation because on the one hand it is very complex to establish analytical formulas for an arbitrary number of shear planes and on the other hand because the number of configurations is not exhaustive. Eurocode 5 however proposes design principles which make it possible to use the formulas established for single and double shear connections to carry out calculations of multiple shear plane connections. The two principles in paragraph 8.1.3 of Eurocode 5 are as follows:

(1) In multiple shear plane connections the resistance of each shear plane should be determined by assuming that each shear plane is part of a series of three-member connections.

(2) To be able to combine the resistance from individual shear planes in a multiple shear plane connection, the governing failure mode of the fasteners in the respective shear planes should be compatible with each other and should not consist of a combination of failure modes (a), (b), (g) and (h) from Figure 8.2 or modes (e), (f) and (j/l) from Figure 8.3 with the other failure modes.

Although it seems apparently simple, these principles are not always easy to apply and do not always lead to reliable estimates of the plastic load-carrying capacity of connections. Although difficult, this issue can be solved by finite element calculations as will be shown at the end of this section. It does not constitute the core of the problem of design of connections with several shear planes if the brittle capacity of the connection limits the transmission of stresses. If the resistance to splitting or block failure limits the capacity of the connection, the distribution of member thicknesses in the multiple shear plane connection becomes the major problem to be solved. This raises the question of which principles should be applied in an optimisation analysis? The problem is not simple and it is difficult to solve without the implementation of advanced tools that can facilitate the calculations of the designer. In order to enable a large number of engineers to carry out design of multiple shear plane connections in timber structures without reducing the reliability of the calculation, it is essential to guide the designers to start their design by simple principles, before complicating their design and forcing them to use more advanced tools.

It will be shown in this section how the dimensioning of a connection with several shear planes can be solved in a simple and reliable way. Dimensioning principles will be given based on design calculations. The design example will furthermore serve as a reference and for comparison with more efficient design solutions in order to derive an optimisation principle. The optimisation approach is based on load distribution within the connection, and several approaches will be proposed in order to not limit the designer to the use of certain tools. The designer will be able to choose a certain technical level for a reliable design.

The connection with four shear planes as shown in Fig. 5 will serve as a reference example for design calculations. This connection is often encountered in timber construction. The connection consists of two steel plates and three pieces of timber. Estimation of the plastic load-bearing capacity of this connection can be carried out in full compliance with the principles mentioned above. Glued laminated timber with strength class GL24h and a thickness t equal to 280 mm are assumed. Thin steel plates are considered. Timber thicknesses of the outer, t_1, and inner part, t_2, are denominated according to Eurocode 5 (see Fig. 10), assuming a symmetric configuration. Steel dowels with a diameter of 16 mm and steel quality 4.6 with an ultimate tensile strength $f_{u,k}$ equal to 400 MPa are chosen.

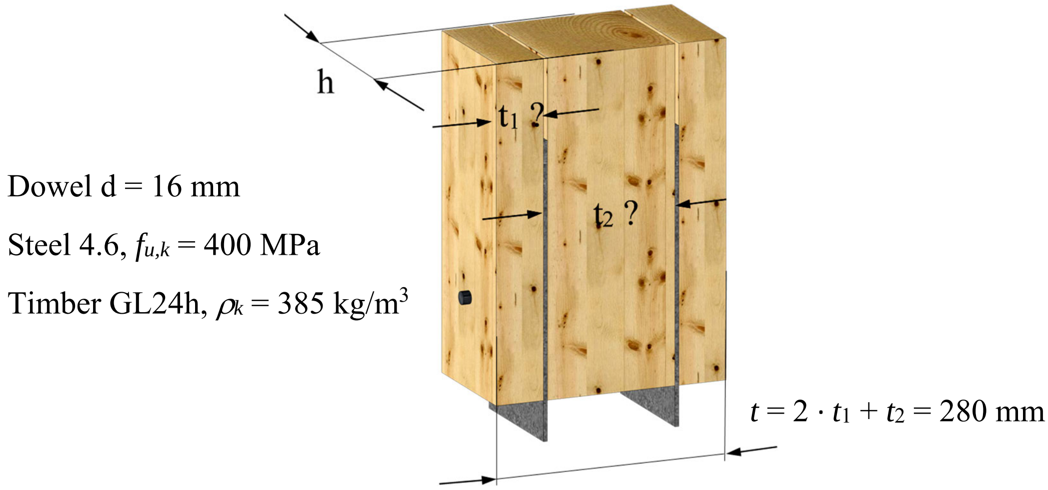

Fig. 10. Typical configuration of a connection with 4 shear planes with two steel plates inserted inside the timber.

4.2 Optimisation study for a single fastener connection

4.2.1 Discontinuity in load transfer: technical choice to cut the dowel

The fact that a connection has several shear planes does not necessarily require continuity of the fastener. By eliminating the continuity of the dowel in the central timber part of the connection, the connection with several shear planes reduces to a connection of two connections side by side, each with two shear planes with a central steel plate. Even if the principle seems simple and leaves little potential obtain an important load-bearing capacity, this technical choice allows to control directly the load distribution in the timber members, independent of the plastic failure modes of the half dowels (i.e. the dowels with half the total length). For this case, the distribution of the total thickness of timber in ¼ // ½ // ¼ is optimal because this transfers as much load to the central part as to the side parts regardless of the level of loading.

The dowels of half the total length (half dowels) can be inserted from each side, which facilitates assembling in particular when the gap in the connection must be minimised. As was shown in section 1, it will be necessary to hold the connection together in order to avoid the load redistribution between the outer parts and the central part using a suitable technical solution. When the connection comprises a large number of fasteners, some fasteners can be continuous to ensure the integrity of the connection without considerably changing load distribution in the timber members. Thus half dowels can be changed to bolts. Eurocode 5 proposes to estimate the load-bearing capacity of double shear dowel-type connections with a central steel plate by an ultimate limit state analysis (Fig. 11).

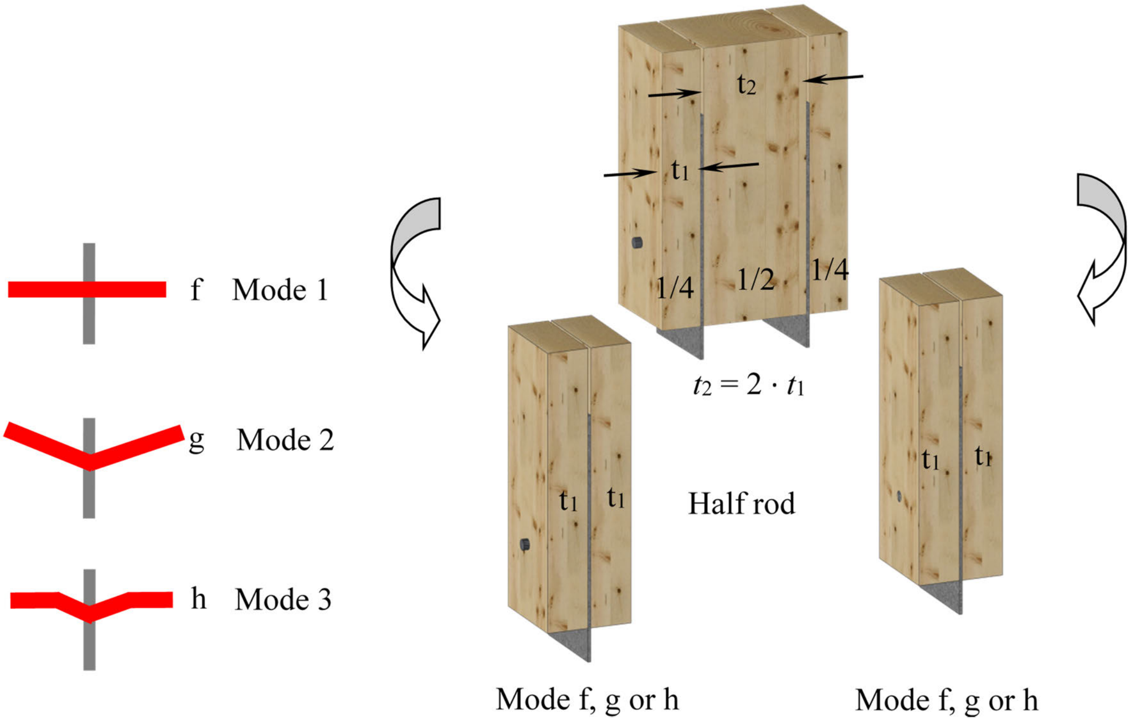

Fig. 11. Decomposition of a connection with four shear planes in two connections with two shear planes with two half dowels.

When the dowels have the same length on both sides of the steel plates, load-bearing capacity is independent of the thickness of the plate and the following design equations can be applied for calculating the load-bearing capacity per shear plane, $F_{v,Rk}$:

$$F_{v,Rk} = \min \begin{cases} f_{h,1,k} \cdot t_1 \cdot d & (f) \\ f_{h,1,k} \cdot t_1 \cdot d \cdot \left[\sqrt{2 + \dfrac{4 \cdot M_{y,Rk}}{f_{h,1,k} \cdot d \cdot t_1^{\,2}}} - 1 \right] + \dfrac{F_{ax,Rk}}{4} & (g) \\ 2.3 \cdot \sqrt{M_{y,Rk} \cdot f_{h,1,k} \cdot d} + \dfrac{F_{ax,Rk}}{4} & (h) \end{cases} \qquad (2)$$

where $f_{h,1,k}$ is the characteristic embedment strength of timber, t_1 is the timber side member thickness, d the fastener diameter, $M_{y,Rk}$ the characteristic yield moment of the fastener and $F_{ax,Rk}$ is the characteristic withdrawal capacity of the fastener for consideration of the so-called rope effect.

Even if the joints are large it is not always obvious that plastic failure of the connection can be achieved before brittle failure of the timber. This is why, as a first approach in this single fastener connection optimization, the rope effect will not be taken into account. This effect will be discussed later for multiple shear plane connections. In order to estimate the load-bearing capacity for each shear plane, it is considered that the plastic moment for doweled or bolted connections is calculated according to Eurocode 5 with $f_{u,k}$ as the characteristic ultimate tensile strength of steel:

$$M_{y,Rk} = 0.3 \cdot f_{u,k} \cdot d^{2.6} \qquad (3)$$

Embedment strength in the direction of the grain can be obtained by

$$f_{h,\alpha,k} = \frac{f_{h,0,k}}{k_{90}\sin^2\alpha + \cos^2\alpha} \tag{4}$$

$$f_{h,0,k} = 0.082 \cdot (1 - 0.01 \cdot d) \cdot \rho_k \tag{5}$$

with

$$k_{90} = \begin{cases} 1.35 + 0.015 \cdot d & \text{for softwoods} \\ 1.30 + 0.015 \cdot d & \text{for LVL} \\ 0.090 + 0.015 \cdot d & \text{for hardwoods} \end{cases} \tag{6}$$

where $f_{h,0,k}$ is the characteristic embedment strength parallel to the grain (in N/mm^2), ρ_k is the characteristic density of timber (in kg/m^3) and α is the load-to-grain angle.

4.2.2 Calculation of a multiple shear plane connection with discontinuous dowels

The calculations detailed below show the estimate of the load-carrying capacity of a timber part with discontinuous dowels, i.e., with two half-dowels.

For GL24h:

$$\rho_k = 385 \text{ kg/m}^3$$

$$f_{h,0,k} = 0.082 \cdot (1 - 0.01 \cdot d) \cdot \rho_k = 0.082 \cdot (1 - 0.01 \cdot 16) \cdot 85 = 26.52 \text{ MPa}$$

$$M_{y,Rk} = 0.3 \cdot f_{u,k} \cdot d^{2.6} = 0.3 \cdot 400 \cdot 16^{2.6} = 162141 \text{ Nmm}$$

$$t_1 = t/4 = 280/4 = 70 \text{ mm}$$

$$F_{v,Rk} = \min \begin{cases} 26.52 \cdot 70 \cdot 16 = 29.70\ kN & (f) \\ 26.52 \cdot 70 \cdot 16 \cdot \left[\sqrt{2 + \dfrac{4 \cdot 162141}{26.52 \cdot 70^2 \cdot 16}} - 1\right] = 15.46\ kN & (g) \\ 2.3 \cdot \sqrt{162141 \cdot 26.52 \cdot 16} = 19.08\ kN & (h) \end{cases}$$

The load-carrying capacity of one half of the connection, i.e. of one half dowel connection with two shear planes, is equal to:

$$F_{v,p,Rk} = 2 \cdot 15.46 = 30.92\ kN$$

4.2.3 Connections with multiple shear planes and continuous fasteners

The other mechanical choice that can be made is to introduce fasteners of any length into the connection. In this case, Eurocode 5 proposes to estimate the load-bearing capacity by limiting the analysis of dowel-type connections with several shear planes by first determining possible kinematically compatible failure modes. Then, the load-bearing capacity of each mode is obtained by decomposing them into a sum of connections with two shear planes for calculation of the capacity per shear plane. This principle applied to the previous discussed connection example leads to possible failure modes and decomposition as shown in Fig. 12. It should be noted that a multiple shear plane connection with thin steel plates is investigated.

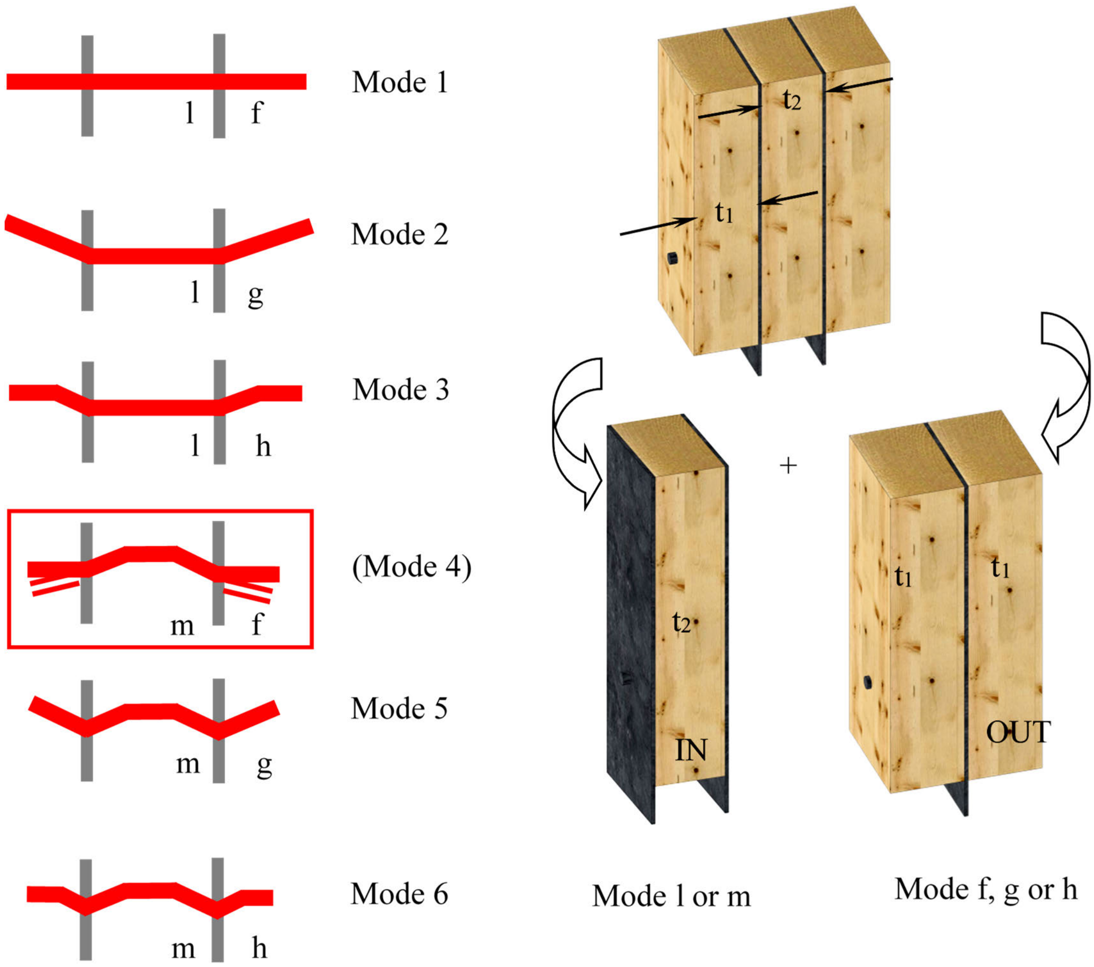

Fig. 12. Decomposition of the connection with four shear planes into connections with two shear planes.

Mode 4 shown in Fig. 12 is not a possible failure mode of the inner part of the connection (IN). For this mode, it is necessary that the steel plates are very thin or that the drilling clearance is important and the width of the external timber parts is small. This mode is rather uninteresting because it entails a connection configuration where two steel plates would be on the outer sides of one piece of timber, which is obviously not optimal.

It is interesting to recall after this decomposition that the equations of the European yield model, which are used to evaluate the capacity for the IN part of the connection area, are the ones for thick steel plates (i.e. the thickness of the outer timber part plus the steel plate are considered as a single thick steel plate). For the OUT part, the thickness of the steel plates has no significant impact on the failure modes.

Part IN:

$$F_{v,Rk} = \min \begin{cases} 0.5 \cdot f_{h,2,k} \cdot t_2 \cdot d & (l) \\ 2.3 \cdot \sqrt{M_{y,Rk} \cdot f_{h,2,k} \cdot d} + \dfrac{F_{ax,Rk}}{4} & (m) \end{cases} \tag{7}$$

Part OUT:

$$F_{v,Rk} = \min \begin{cases} f_{h,1,k} \cdot t_1 \cdot d & (f) \\ f_{h,1,k} \cdot t_1 \cdot d \cdot \left[\sqrt{2 + \dfrac{4 \cdot M_{y,Rk}}{f_{h,1,k} \cdot d \cdot t_1^2}} - 1 \right] + \dfrac{F_{ax,Rk}}{4} & (g) \\ 2.3 \cdot \sqrt{M_{y,Rk} \cdot f_{h,1,k} \cdot d} + \dfrac{F_{ax,Rk}}{4} & (h) \end{cases} \tag{8}$$

In order to be able to compare the calculation with the example of discontinuous dowels, the rope effect is also neglected. The load-bearing capacity per shear plane can thus be obtained based on 6 possible failure modes as follows:

Mode 1: $l + f$ $\quad F_{v,p,Rk} = 0.5 \cdot f_{h,2,k} \cdot t_2 \cdot d + f_{h,1,k} \cdot t_1 \cdot d$ (9)

Mode 2: $l + g$ $\quad F_{v,p,Rk} = 0.5 \cdot f_{h,2,k} \cdot t_2 \cdot d + f_{h,1,k} \cdot t_1 \cdot d \cdot \left[\sqrt{2 + \dfrac{4 \cdot M_{y,Rk}}{f_{h,1,k} \cdot d \cdot t_1^2}} - 1 \right]$ (10)

Mode 3: $l + h$ $\quad F_{v,p,Rk} = 0.5 \cdot f_{h,2,k} \cdot t_2 \cdot d + 2.3 \cdot \sqrt{M_{y,Rk} \cdot f_{h,1,k} \cdot d}$ (11)

(Mode 4: $m + f$ $\quad F_{v,p,Rk} = 2.3 \cdot \sqrt{M_{y,Rk} \cdot f_{h,2,k} \cdot d} + f_{h,1,k} \cdot t_1 \cdot d$, not possible) (12)

Mode 5: $m + g$ $\quad F_{v,p,Rk} = 2.3 \cdot \sqrt{M_{y,Rk} \cdot f_{h,2,k} \cdot d} + f_{h,1,k} \cdot t_1 \cdot d \cdot \left[\sqrt{2 + \dfrac{4 \cdot M_{y,Rk}}{f_{h,1,k} \cdot d \cdot t_1^2}} - 1 \right]$ (13)

Mode 6: $m + h$ $\quad F_{v,p,Rk} = 2.3 \cdot \sqrt{M_{y,Rk} \cdot f_{h,2,k} \cdot d} + 2.3 \cdot \sqrt{M_{y,Rk} \cdot f_{h,1,k} \cdot d}$ (14)

The load-bearing capacity of the multiple shear plane connection per shear plane is finally derived as the minimum value of the six failure modes, expressed as

$$F_{v,p,Rk} = \min \{ \text{mode 1, mode 2, mode 3, (mode 4), mode 5, mode 6} \} \tag{15}$$

For some modes, the load depends non-linearly on t_1 and t_2, which implies that an optimum can be determined. From the point of view of the designer, a layout of the steel plates can be found in such a way that it optimises the plastic load-bearing capacity of the connection; the connection is made as strong as possible.

4.2.4 Continuous fastener: optimisation for "maximum plastic load-bearing capacity per shear plane"

Although it is possible to do the optimisation of t_1 and t_2 numerically, it is chosen here for pedagogical purposes to make a graphical representation (Fig. 13) of the different modes (Eqs. (9) to (14)) by plotting the capacity of each of them as a function of t_1. t_2 can be obtained by $t_2 = 280 - 2 \cdot t_1$. The area delimited by the dotted line in Fig. 13 defines the dimensioning range since it delimits the minimum of the plastic failure modes [8-10]. Thus, it appears that with the same material parameters previously used and the same connection dimensions one optimum, i.e. a maximum load-bearing capacity exists.

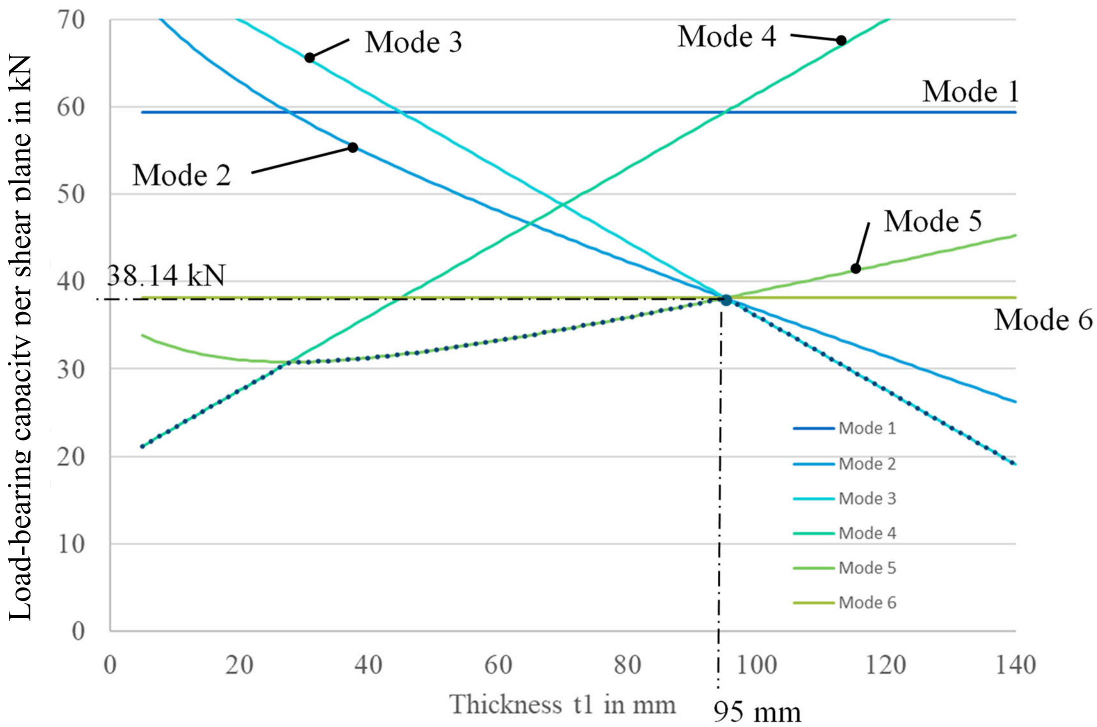

Fig. 13. Capacity per shear plane versus the thickness of the timber side member.

The timber thicknesses of the connection that give the maximum plastic capacity are close to t_1=95 mm and t_2=90 mm. Only for this specific connection configuration presented here, the maximum plastic capacity can be achieved by modes 2, 3, 5 or 6 (as they intersect at t_1 = 95 mm, randomly design), which gives the following calculation, e.g. for mode 6 according to Eq. (14).

$$F_{v,p,Rk} = 2.3 \cdot \sqrt{162141 \cdot 26.52 \cdot 16} + 2.3 \cdot \sqrt{162141 \cdot 26.52 \cdot 16} = 38.14\, kN \tag{16}$$

The technical choice to work with a continuous fastener in the connection, compared to a discontinuous fastener, allows to increase the plastic capacity per plane by

$$\eta(F_{v,p,Rk}) = \frac{(38.14 - 30.92)}{30.92} = 23\,\% \tag{17}$$

This can be considered as an interesting increase but leads to the appearance of a stress difference between the inner and outer timber parts, which gives rise to shear in the timber at the steel plates which remains difficult to control in the structure over time (Fig. 14). The timber of the inner part is inevitably more stressed than that of the outer parts.

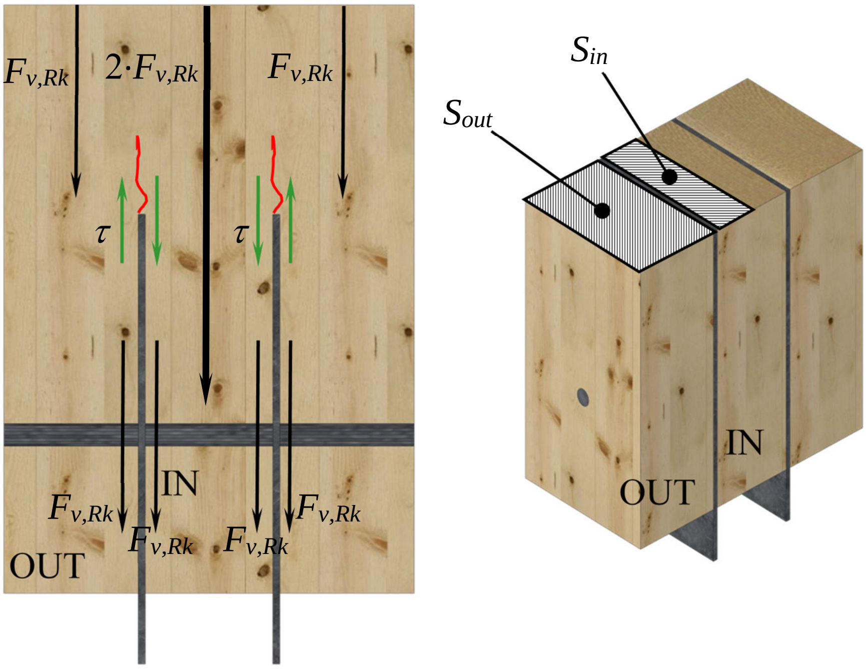

Fig. 14. Differential forces between inner and outer part that induce shear stress between the inner and outer part of the connection.

In order to quantify the differential forces between the inner part and the outer part of the connection, it is possible to calculate a uniform tensile stress acting on the outer part and the inner half-part by dividing the shear forces per plane by the gross area of the corresponding timber section as:

$$S_{OUT} = t_1 \cdot h \quad \text{for the outer parts,} \tag{18}$$

$$S_{IN} = t_2 / 2 \cdot h \quad \text{for the inner part,} \tag{19}$$

This yields the following tensile stresses:

$$\sigma_{t,0,OUT} = \frac{F_{v,Rk,OUT}}{S_{OUT}} \qquad \sigma_{t,0,IN} = \frac{F_{v,Rk,IN}}{S_{IN}} \tag{20}$$

$$\sigma_{t,0,OUT} = \frac{F_{v,Rk,OUT}}{t_1 \cdot h} \qquad \sigma_{t,0,IN} = \frac{F_{v,Rk,IN}}{t_2 / 2 \cdot h} \tag{21}$$

The stress difference between the outer parts and the inner part may be described as a relative value with respect to the stress on the outer part, which yields:

$$\delta = \frac{\sigma_{t,0,IN} - \sigma_{t,0,OUT}}{\sigma_{t,0,OUT}} \tag{22}$$

By inserting Eq. (15) into Eq. (22), stress differences between the timber parts occurring in mode 6 can be expressed as:

$$\delta = \left(\frac{2.3 \cdot \sqrt{M_{y,Rk} \cdot f_{h,2,k} \cdot d}}{t_2 / 2} - \frac{2.3 \cdot \sqrt{M_{y,Rk} \cdot f_{h,1,k} \cdot d}}{t_1} \right) \bigg/ \left(\frac{2.3 \cdot \sqrt{M_{y,Rk} \cdot f_{h,1,k} \cdot d}}{t_1} \right)$$

$$\delta = \left(\frac{2.3\sqrt{162141 \cdot 26.52 \cdot 16}}{90/2} - \frac{2.3 \cdot \sqrt{162141 \cdot 26.52 \cdot 16}}{95} \right) \bigg/ \left(\frac{2.3 \cdot \sqrt{162141 \cdot 26.52 \cdot 16}}{95} \right)$$

$$\delta = 111\% \tag{23}$$

Thus, by increasing the plastic yield of the connection by 23% (see Eq. (17)), the relative difference in stress between the inner and outer timber parts is increased by 111%. It seems inevitable that brittle failure will occur in the central part of the connection before the lateral parts might fail. As discussed in the previous section, if the connection is not properly held together and constrained against bending, the outer parts will redistribute the load to the central part. With these observations and keeping in mind the aim of this study to find an optimum connection design, the question of a uniform stress distribution in the timber with a continuous dowel in a multiple shear plane connection has to be investigated. This search for a uniform stress distribution will inevitably help to find an optimum for the connection configuration.

4.2.5 Continuous fastener: optimisation for “uniform stress distribution in timber parts”

To optimise the connection (i.e. to maximise the load-bearing capacity) and to balance the stresses in the different timber parts between the steel plates, it is necessary to add additional stresses to those previously stated:

$$F_{v,p,Rk} = \min\{\text{mode 1, mode 2, mode 3, (mode 4), mode 5, mode 6}\} \tag{24}$$

Based on calculations presented in section 4.2.4, the design principle considering different stresses between the outer and the inner part can be written for all possible plastic failure modes of the connection as:

$$\sigma_{t,0,IN} - \sigma_{t,0,OUT} = 0 \tag{25}$$

which yields the six possible failure modes:

Mode 1: $$2 \cdot 0.5 \cdot f_{h,2,k} \cdot d - f_{h,1,k} \cdot d = 0 \tag{26}$$

Mode 2: $$2 \cdot 0.5 \cdot f_{h,2,k} \cdot d - f_{h,1,k} \cdot d \cdot \left[\sqrt{2 + \frac{4 \cdot M_{y,Rk}}{f_{h,1,k} \cdot d \cdot t_1^2}} - 1 \right] = 0 \tag{27}$$

Mode 3: $$2 \cdot 0.5 \cdot f_{h,2,k} \cdot d - 2.3 \cdot \sqrt{M_{y,Rk} \cdot f_{h,1,k} \cdot d} \;/\; t_1 = 0 \tag{28}$$

(Mode 4: $$2 \cdot 2.3 \cdot \sqrt{M_{y,Rk} \cdot f_{h,2,k} \cdot d} \;/\; t_2 - f_{h,1,k} \cdot d = 0 \tag{29}$$)

Mode 5: $2 \cdot 2.3 \cdot \sqrt{M_{y,Rk} \cdot f_{h,2,k} \cdot d} \, / \, t_2 - f_{h,1,k} \cdot d \left[\sqrt{2 + \dfrac{4 \cdot M_{y,Rk}}{f_{h,1,k} \cdot d \cdot t_1^{\,2}}} - 1 \right] = 0$ (30)

Mode 6: $2 \cdot 2.3 \cdot \sqrt{M_{y,Rk} \cdot f_{h,2,k} \cdot d} \, / \, t_2 - 2.3 \cdot \sqrt{M_{y,Rk} \cdot f_{h,1,k} \cdot d} \, / \, t_1 = 0$ (31)

With regard to the six preceding criteria, it can immediately be noticed that the differential stress for mode 1 is independent of the widths t_1 and t_2. Failure mode 1 is thus always balanced whatever the size of t_1 and t_2 is, if the embedment strength of both parts is the same. This was expected since failure mode 1 is a composition of failure modes without plastic hinges for the parts IN and OUT of the decomposed connection. In mode 1, the force per shear plane is proportional to t_1 or t_2.

The maximum $F_{v,p,Rk}$, which is equal to the minimum capacity as formulated in Eq. (24), can be derived numerically. To clarify this, the relative differential stress with respect to the stress of the outer part as a function of the width of the timber is plotted in Fig. 15, in order to see if it is possible to find possible failure modes whose differential stress tends towards zero.

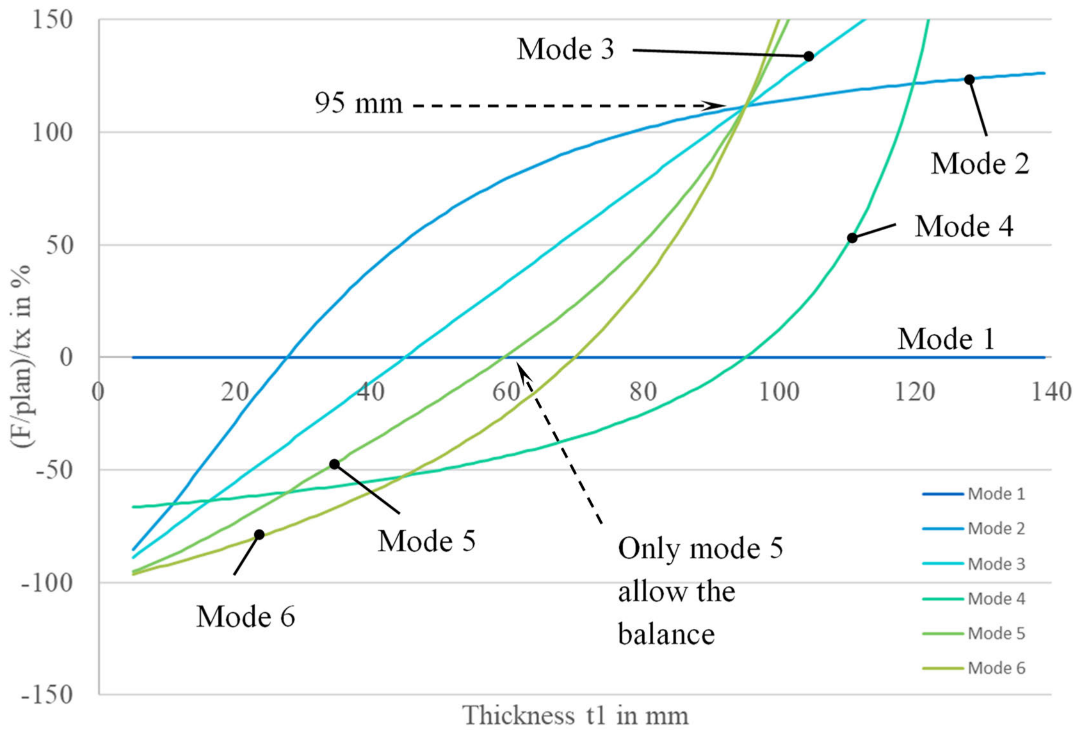

Fig. 15. Relative differential stress between the outer parts and the inner part for each of the failure modes versus the width of the outer timber parts.

Fig. 15 shows that a geometrical configuration exists for each of the modes that enables the balance of the stresses between the timber members, i.e. the relative differential stress is equal to 0. However, only one failure mode is possible to obtain this equilibrium, mode 5 (see also Fig. 16). When the thicknesses of the timber members are equal to t_1 = 59.6 mm and t_2 = 160.8 mm, the stress equilibrium is realized and mode 5 gives the lowest plastic load of all the possible modes as shown in Fig. 16.

Thus, with the same material parameters previously used and the same connection dimensions, the plastic load-bearing capacity of mode 5 according to Eq. (13) is:

$$F_{v,p,Rk} = 2.3 \cdot \sqrt{162141 \cdot 26.52 \cdot 16} + 26.52 \cdot 59.6 \cdot 16 \cdot \left[\sqrt{2 + \frac{4 \cdot 162141}{26.52 \cdot 16 \cdot 59.6^2}} - 1 \right]$$

$$F_{v,p,Rk} = 33.21\,\mathrm{kN} \tag{32}$$

The technical choice to work with a continuous dowel in the multiple shear plane connection and optimising the connection for uniform stress distribution allows to increase the plastic load-bearing capacity per shear plane by

$$\eta(F_{v,p,Rk}) = \frac{(33.21 - 30.92)}{30.92} = 7.5\,\% \tag{33}$$

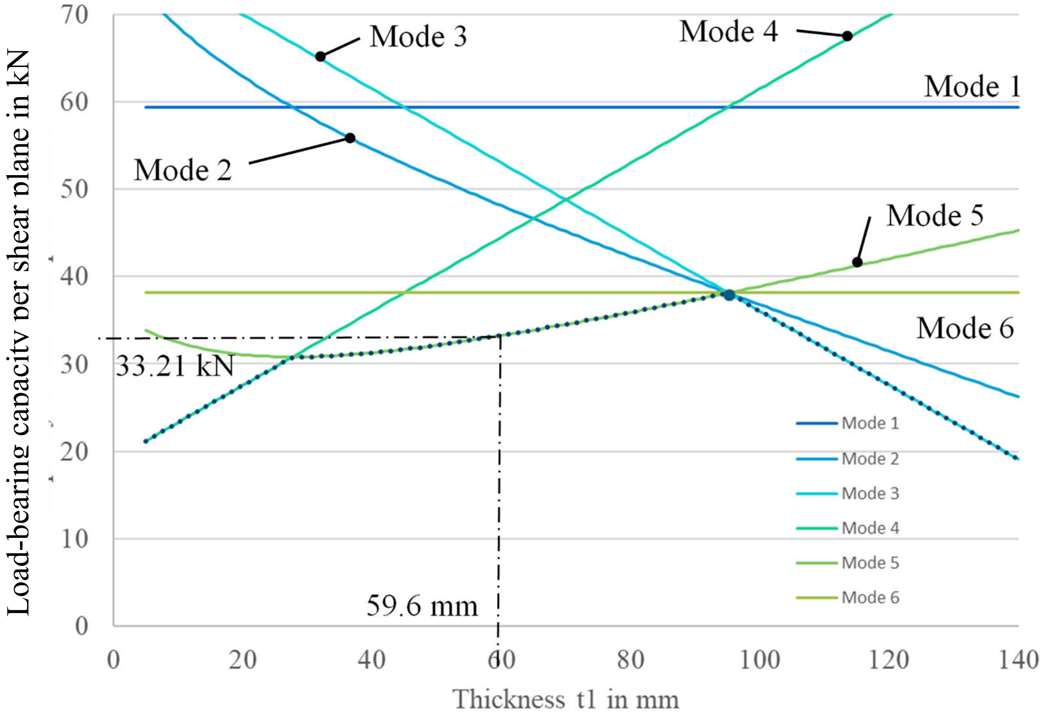

Fig. 16. Load-bearing capacity per shear plane versus timber width t_1.

For mode 5, the differential stress between timber parts can be expressed according to Eq. (22) and it is obviously equal to zero:

$$\eta = \frac{\left(2 \cdot 2.3 \cdot \sqrt{162141 \cdot 26.52 \cdot 16} / 160.8 - 26.52 \cdot 16 \left[\sqrt{2 + \frac{4 \cdot 162141}{26.52 \cdot 16 \cdot 59.6^2}} - 1 \right]\right)}{\left(26.52 \cdot 16 \left[\sqrt{2 + \frac{4 \cdot 162141}{26.52 \cdot 16 \cdot 59.6^2}} - 1 \right]\right)} = 0\% \tag{34}$$

4.2.6 Conclusions on the choice to use a continuous dowel

Table 1 summarises the presented calculations as an example of the application of the design experience presented in section 1. It can be observed that a uniform stress distribution allows for a comparably small increase in terms of plastic load-bearing capacity, in comparison with a solution where the dowel is discontinuous in the connection with multiple shear planes. Hence, for the designer, this discontinuous solution is simple, safe and easy to design.

This solution (i.e. half dowels) has been chosen for the construction of the building "*Fondation Louis Vuitton*" in Paris (2012) in order to control the distribution of loads. It facilitated the introduction of many dowels in steel plates with a gap reduced to 0.4 mm in diameter [12-14]. It can be noticed that the design accounted for holding the connection together by bolts, situated continuously on the periphery of the connections. Even on a prestigious building, this simplicity of execution may represent an optimum solution (Fig. 12).

Fig. 17. Connections (two slotted-in steel plates) of the "Fondation Louis Vuitton" (Frank Gehry) [11].

The search for the maximum plastic load-bearing capacity led to a significant imbalance of stresses in the timber parts of the connections. The major difference between both arrangements of connections with continuous dowels is that for the solution optimising with regard to a uniform stress distribution, the more the connection tends towards plasticisation, the more the homogenisation of the stresses in the timber parts is respected.

Table 1. Summary of the dimensions, yield and differential stresses of the three choices presented above.

	Thickness (in mm)		Load per shear plane $F_{v,Rk}$ (in kN)	η	δ
	t_1	t_2			
Discontinuous dowel	70	140	30.92	100	0%
Continuous dowel: Optimisation “maximum load-bearing capacity	95	90	38.14	123	110%
Continuous dowel: Optimization “uniform stress distribution”	60	160	33.21	107	0%

If timber would exclusively show plastic behaviour when exceeding strength limits in connections, the optimisation study of the multiple shear plane connection could stop here by choosing the solution which yields the highest load-bearing capacity with respect to the technological constraints of the specific study. However, even with a suitable reinforcement, connection assemblies often show brittle failure due to cracking of timber in the connection area (Fig. 18).

Fig. 18. Brittle failure mode of reinforced joints in bending [12].

This indicates that timber failure can occur before the plastic limit of the connection is reached, particularly in case of multiple fastener connections [16, 17]. What geometric layout of the fasteners is needed to achieve optimum dimensioning? It is the study of the load distribution in the "elastic" phase of the multiple fastener connection and of possible brittle failure modes that can answer this question. Consequently, corresponding investigations on the same connection example as before are presented in following.

4.3 Optimisation study of a multiple shear plane connection with 8 continuous dowels

4.3.1 Introduction

The previous part showed that a multiple shear plane connection with a continuous single fastener exhibits several optima: either in maximum plastic load-bearing capacity or in plastic load-bearing capacity with a uniform stress distribution. The question that now arises is which optimisation leads to the highest capacity in the so-called "elastic" loading phase, when brittle failure modes have to be considered. It is chosen to study a multiple fastener connection with fasteners similar to the previous example. In this connection, brittle failure of rows or blocks are possible. In a first step, the elastic phase will be investigated by estimating the stiffness of the inner and outer parts of the connection based on empirical equations provided by Eurocode 5. In a second step, the capacity will be estimated by an elastic model of a beam on elastic support, a so-called Beam-on-Foundation (BOF) model. Finally, the capacity will be estimated by considering a BOF model with nonlinear properties for steel and timber. Before presenting the analysis, calculations are presented, row effects and block shear failure capacity are estimated.

4.3.2 Geometry of the studied connection

Fig. 19 shows the general characteristics of the multiple fastener connection with 8 bolts and with multiple shear planes. Minimum distances and spacing are established following the specifications of Eurocode 5. Fig. 20 shows the geometry of the connection.

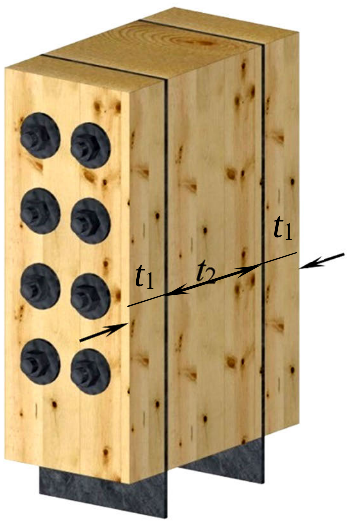

Fastener diameter d = 16 mm
Steel class 4.6
Elastic limit $f_{y,b}$ = 240 MPa
Characteristic tensile strength $f_{u,b}$ = 400 MPa
Number of rows n_{rows} = 2
Number of bolts per row: n = 4

Fig. 19. General characteristics of the studied connection.

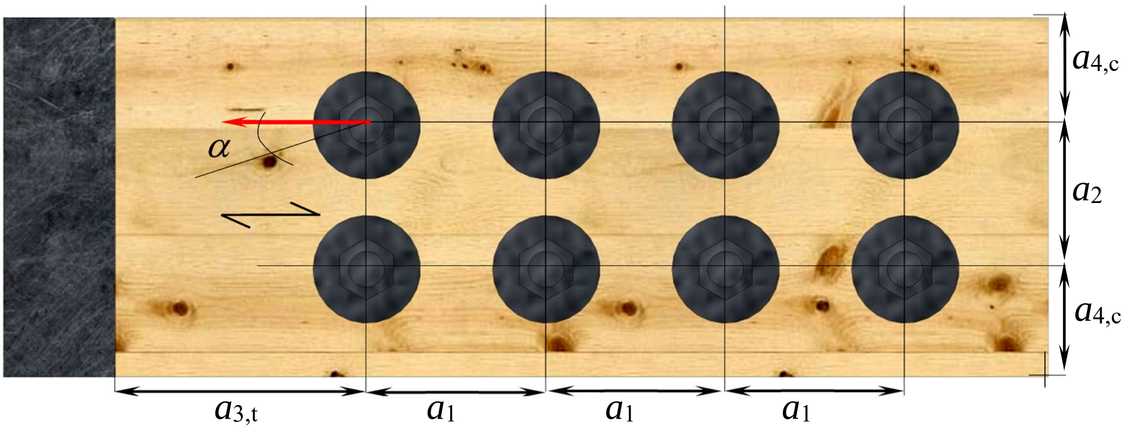

Fig. 20. Minimum distances and spacing of the connection.

Minimum distances and spacing are calculated as follows:

$$a_1 = \left(4+\left|\cos\alpha\right|\right)\cdot d = \left(4+\left|\cos 0\right|\right)\cdot 16 = 80\text{ mm} \tag{35}$$

$$a_2 = 4\cdot d = 4\cdot 16 = 64\text{ mm} \tag{36}$$

$$a_{3,t} = \max\left(80;7\cdot d\right) = \max\left(80;7\cdot 16\right) = 112\text{ mm} \tag{37}$$

$$a_{4,t} = \max\left(\left(2+2\cdot\sin\alpha\right)\cdot d;3\cdot d\right) = 3\cdot d = 3\cdot 16 = 48\text{ mm} \tag{38}$$

$$a_{4,c} = 3\cdot d = 3\cdot 16 = 48\text{ mm} \tag{39}$$

4.3.3 General characteristics of the connection

The embedding strength is given by the characteristic density of timber GL24h according to EN 14080 and Eq. (8.32) in Eurocode 5, which yields:

$$\rho_k = 385\ kg/m^3$$

$$f_{h,0,k} = 0.082\cdot(1-0.01\cdot d)\cdot\rho_k = 0.082\cdot(1-0.01\cdot 16)\cdot 385 = 26.52\text{ MPa} \tag{40}$$

The rope effect is given by the calculation of the timber compression under the flat washer as:

$$F_{ax,Rk} = \frac{\pi}{4}\left(D_{ext}{}^2 - D_{\text{int}}{}^2\right)\cdot 3\cdot f_{c,90,k} = \frac{\pi}{4}\left(50^2-18^2\right)\cdot 3\cdot 2.5 = 12817\ N \tag{41}$$

with the rope effect as the withdrawal capacity times a friction coefficient of ¼:

$$F_{ax,Rk}/4 = 12817/4 = 3204\text{ N} \tag{42}$$

The yield moment of the bolt is calculated according to Eq. (8.30) in Eurocode 5:

$$M_{y,Rk} = 0.3\cdot f_{u,k}\cdot d^{2.6} = 0.3\cdot 400\cdot 16^{2.6} = 162141\text{ Nmm} \tag{43}$$

4.3.4 Stiffness per shear plane applying Eurocode 5

In order to estimate the stiffness of each shear plane of the connection, it is necessary to use the average density of glued laminated timber GL24h with a mean density $\rho_m = 420$ kg/m^3 according to EN 14080. The slip modulus in the service limit state per fastener and shear plane is obtained by Eq. (7.1) in Eurocode 5:

$$K_{ser} = \rho_m^{1.5} d / 23 = 420^{1.5} \cdot 16 / 23 = 5987.78 \text{ N/mm} \tag{44}$$

For the timber-steel multiple fastener connection with 8 bolts and 4 shear planes and under consideration of 7.1(3) in Eurocode, this yields:

$$k_{type} = \begin{cases} 1 & \text{for timber / timber} \\ 2 & \text{for timber / steel or timber / concrete} \end{cases}$$

$$K_{ser,Jt} = n_{plan} \cdot n_{org} \cdot k_{type} \cdot K_{ser} = 4 \cdot 8 \cdot 2 \cdot 5987.78 = 383.22 \text{ kN/mm} \tag{45}$$

for the stiffness in inner part, called IN:

$$K_{ser,Jt,IN} = n_{plan} \cdot n_{org} \cdot k_{type} \cdot K_{ser} = 2 \cdot 8 \cdot 2 \cdot 5987.78 = 191.61 \text{ kN/mm} \tag{46}$$

for the stiffness in outer part, called OUT:

$$K_{ser,Jt,OUT} = n_{plan} \cdot n_{org} \cdot k_{type} \cdot K_{ser} = 1 \cdot 8 \cdot 2 \cdot 5987.78 = 95.81 \text{ kN/mm} \tag{47}$$

4.3.5 Capacity of the joint 95/90/95 (optimisation for "maximum plastic load-bearing capacity")

4.3.5.1 Capacity of a single dowel

Starting from the optimised dimensions of chapter 4.2.4 with side member thicknesses $t_1 = 95$ mm and thickness of the inner member $t_2 = 90$ mm, the capacity of a connection with steel plates constituting the external elements of a connection with two shear planes (part IN) can be determined according to Eq. (8.13) in Eurocode 5:

$$F_{v,Rk,Jhs} = \min \begin{cases} 0.5 \cdot f_{h,2,k} \cdot t_2 \cdot d & (l) \\ 2.3 \cdot \sqrt{M_{y,Rk} \cdot f_{h,2,k} \cdot d} & (m) \end{cases} \tag{48}$$

Application of the design equations for the IN part leads to:

$$F_{v,Rk,Jhs,IN} = \min \begin{cases} 0.5 \cdot 26.52 \cdot 90 \cdot 16 = 19093 \text{ N} & (l) \\ 2.3 \cdot \sqrt{162141 \cdot 26.52 \cdot 16} = 19077 \text{ N} & (m) \end{cases} \tag{49}$$

$$F_{v,Rk,IN} = 19.077 \text{ kN} \tag{50}$$

The capacity of a connection with a steel plate constituting the central element of a connection with two shear planes (part OUT) is determined according to Eq. (8.11) in Eurocode 5:

$$F_{v,Rk,Jhs} = \min \begin{cases} f_{h,1,k} \cdot t_1 \cdot d & \text{(f)} \\ f_{h,1,k} \cdot t_1 \cdot d \left[\sqrt{2 + \dfrac{4 \cdot M_{y,Rk}}{f_{h,1,k} \cdot d \cdot t_1^{\,2}}} - 1 \right] & \text{(g)} \\ 2.3 \cdot \sqrt{M_{y,Rk} \cdot f_{h,1,k} \cdot d} & \text{(h)} \end{cases} \tag{51}$$

Application of the design equations for the OUT part leads to:

$$F_{v,Rk,Jhs,OUT} = \min \begin{cases} 26.52 \cdot 95 \cdot 16 = 40308\,\text{N} & \text{(f)} \\ 26.52 \cdot 95 \cdot 16 \cdot \left[\sqrt{2 + \dfrac{4 \cdot 162141}{26.52 \cdot 95^2 \cdot 16}} - 1 \right] = 19061\,\text{N} & \text{(g)} \\ 2.3 \cdot \sqrt{162141 \cdot 26.52 \cdot 16} = 19077\,\text{N} & \text{(h)} \end{cases} \tag{52}$$

$$F_{v,Rk,Jhs,OUT} = 19.061\,\text{kN} \tag{53}$$

The capacity of half of the connection is obtained by mode 5 ($m + g$):

$$F_{v,p,Rk,Jhs} = F_{v,Rk,Jhs,IN} + F_{v,Rk,Jhs,OUT} = 19.077 + 19.061 = 38.14\,\text{kN} \tag{54}$$

4.3.5.2 Splitting failure

The characteristic brittle capacity, taking into account several fasteners in a row, is obtained according to Eq. (8.1) and (8.34) in Eurocode 5 by:

$$F_{v,ef,Rk} = n_{plaque} \cdot \sum_{i=1}^{n_{files}} n_{ef} \cdot F_{v,p,Rk,Jhs} \tag{55}$$

$$n_{ef} = \min \begin{cases} n \\ n^{0.9} \sqrt[4]{\dfrac{a_1}{13d}} \end{cases} = \min \begin{cases} 4 \\ 4^{0.9} \sqrt[4]{\dfrac{5}{13}} \end{cases} = 2.74 \tag{56}$$

$$F_{v,ef,Rk} = 2 \cdot 2 \cdot 2.74 \cdot 38.14 = 418.34 kN \tag{57}$$

where the capacity along the fastener row of the central part of the connection amounts to:

$$F_{v,ef,Rk,IN} = \frac{418.34}{38.14} \cdot 19.077 = 209.26\,\text{kN} \tag{58}$$

and the capacity along the fastener rows of the outer parts amounts to:

$$F_{v,ef,Rk,OUT} = \frac{418.34}{38.14} \cdot 19{,}06 / 2 = 104.54\,\text{kN} \tag{59}$$

4.3.5.3 Plastic failure

In case the connection can reach the plastic load-bearing capacity without brittle failure, the rope effect can be added to the capacity per shear plane as follows

$$F_{v,p,Rk} = F_{v,p,Rk,Jhs} + (\text{mode m})\min\begin{cases} F_{ax,Rk}/4 \\ 0.25 \cdot F_{v,Rk,Jhs,IN} \end{cases} + (\text{mode g,h})\min\begin{cases} F_{ax,Rk}/4 \\ 0.25 \cdot F_{v,Rk,Jhs,OUT} \end{cases} \tag{60}$$
$$= 38.14 + 2 \cdot 3.20 = 44.55 \text{ kN}$$

The maximum characteristic plastic capacity of the connection is therefore:

$$F_{v,Rk} = n_{plate} \cdot \sum_{i=1}^{n_{rows}} n \cdot F_{v,Rk} = 2 \cdot 4 \cdot 2 \cdot 44.55 = 712.75 \text{ kN} \tag{61}$$

where the plastic capacity of the central part of the connection amounts to

$$F_{v,Rk,IN} = \frac{712.75}{44.55} \cdot (19.08 + 3.20) = 356.50 \text{ kN} \tag{62}$$

and the plastic capacity of one of the outer parts of the connection amounts to

$$F_{v,Rk,OUT} = \frac{712.75}{44.55} \cdot (19.06 + 3.20)/2 = 178.12 \text{ kN} \tag{63}$$

4.3.5.4 Block shear failure

As a consequence of the connection layout with two rows of fasteners, a block shear failure is a possible brittle failure mode that needs to be evaluated according to Annex A in Eurocode 5 as follows:

$$F_{bs,Rk} = \max\begin{cases} 1.5 \cdot A_{net,t} \cdot f_{t,o,k} \\ 0.7 \cdot A_{net,v} \cdot f_{v,k} \end{cases} \tag{64}$$

with the characteristic tensile strength parallel to the grain and the characteristic shear strength of GL24h according to EN 14080:

$$f_{t,0,k} = 19.2 \text{ MPa} \quad \text{and} \quad f_{v,k} = 3.5 \text{ MPa} \tag{65}$$

The length of the tensile failure section in the connection is obtained by:

$$L_{net,t} = \sum_i l_{t,i} = a_2 - d_0 = 64 - (16 + 1) = 47 \text{ mm} \tag{66}$$

and the length of the shear failure section in the connection is obtained by:

$$\begin{aligned} L_{net,v} &= \sum_i l_{v,i} = 2 \cdot (a_{3,t} + 3 \cdot a_1 - 3.5 \cdot d_0) \\ &= 2 \cdot (112 + 3 \cdot 80 - 3.5 \cdot (16 + 1)) = 585 \text{ mm} \end{aligned} \tag{67}$$

The block shear capacity of the inner part (IN) is obtained after establishing the tensile and shear surfaces. Due to the connection being composed of bolts, it is considered that the failure will necessarily be of "block shear" type, i.e. over the entire width and thickness of the timber member, independent of the failure mode of the fastener. In the calculation of block shear failure, moisture induced cracking of the cross-section is considered by taking into account the reduction coefficient $k_{cr} = 0.67$, which yields:

$$A_{net,t} = L_{net,t} \cdot t_2 = 47 \cdot 90 = 4230 \text{ mm}^2 \tag{68}$$

$$A_{net,v} = L_{net,v} \cdot t_2 \cdot k_{\text{cr}} = 585 \cdot 90 \cdot 0.67 = 35276\, mm^2 \tag{69}$$

$$F_{bs,Rk,IN} = \max\begin{cases} 1{,}5 \times 4230 \times 19{,}2 \\ 0{,}7 \times 35276 \times 3{,}5 \end{cases} = \max\begin{cases} 121{,}82\, kN \\ 86{,}42\, kN \end{cases} = 121{,}82\, kN \tag{70}$$

Block shear failure is in this case controlled by the tensile strength of timber. The same procedure can be applied for the estimation of the block shear capacity of the outer parts (OUT):

$$A_{net,t} = L_{net,t} \cdot t_1 = 47 \cdot 95 = 4465 \text{ mm}^2 \tag{71}$$

$$A_{net,v} = L_{net,v} \cdot t_1 \cdot k_{cr} = 585 \cdot 95 \cdot 0.67 = 37235 \text{ mm}^2 \tag{72}$$

$$F_{bs,Rk,OUT} = \max\begin{cases} 1.5 \cdot 4465 \cdot 19.2 \\ 0.7 \cdot 37235 \cdot 3.5 \end{cases} = \max\begin{cases} 128.59 \text{ kN} \\ 91.23 \text{ kN} \end{cases} = 128.59 \text{ kN} \tag{73}$$

4.3.5.5 Stiffness estimation applying Eurocode 5

Fig. 21 shows the stiffnesses per shear plane of the IN and OUT part. It becomes obvious that failure occurs in a brittle way in the connection, since the block-shear capacity (part IN, governing as it is reached at a smaller connection slip than the splitting failure of the OUT part) is lower than the plastic limit of the connection. Since the steel plate deforms the bolts on both sides similarly, it can be considered that the same displacement is imposed on both sides (i.e. part IN fails). In order to evaluate the total load-bearing capacity of the connection when block shear failure occurs in the inner part (at 121.82 kN), it is necessary to take into account the load that is in the outer parts. Failure in one of the parts is considered to be the only possible scenario that can be verified in design, since it is unlikely to anticipate the evaluation of the connection capacity after one of its parts is broken. To control load distribution, the control of the stiffness of the shear planes appears to be essential.

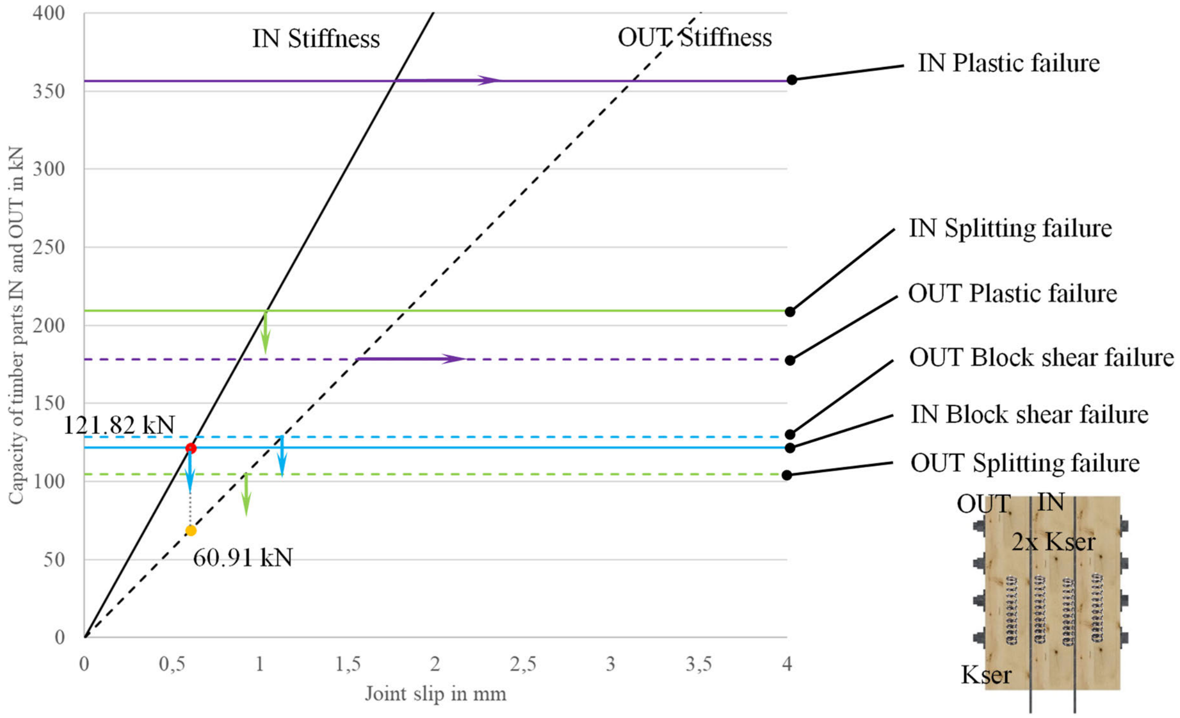

Fig. 21. Inner and outer stiffness of the 95/90/95 connection and estimated load-bearing capacity applying Eurocode 5.

The characteristic capacity to brittle failure of the multiple fastener connection is then obtained by, using the stiffness values calculated in Eqs. (46) and (47):

$$F_{v,Rk,Kser,EC5} = F_{bs,Rk,IN} + 2 \cdot \left(\frac{F_{bs,Rk,IN}}{K_{ser,IN}} \cdot K_{ser,OUT} \right) = 121.82 + 2 \cdot \left(\frac{121.82}{191.61} \cdot 95.81 \right) = 243.65 \text{ kN} \quad (74)$$

where the displacement at failure is equal to:

$$\delta_{Kser,\,EC5} = \frac{F_{bs,Rk,IN}}{K_{ser,IN}} = \frac{121.82}{191.61} = 0.63 \text{ mm} \quad (75)$$

4.3.6 Capacity of the joint 60/160/60 (optimisation for ”uniform stress distribution”)

4.3.6.1 Capacity of a single dowel

Starting from the optimised dimensions in section 4.2.5 with timber member thicknesses t_1 = 60 mm and t_2 = 160 mm, the capacity of a double-shear connection with steel plates constituting the external elements (part IN) can be determined according to Eq. (8.13) in Eurocode 5 by:

$$F_{v,Rk,Jhs} = \min \begin{cases} 0.5 \cdot f_{h,2,k} \cdot t_2 \cdot d & (l) \\ 2.3 \cdot \sqrt{M_{y,Rk} \cdot f_{h,2,k} \cdot d} & (m) \end{cases} \quad (76)$$

Application of the design equations to the IN part leads to:

$$F_{v,Rk,Jhs,IN} = \min \begin{cases} 0.5 \cdot 26.52 \cdot 160 \cdot 16 = 33944 \text{ N} & (l) \\ 2.3 \cdot \sqrt{162141 \cdot 26.52 \cdot 16} = 19077 \text{ N} & (m) \end{cases} \quad (77)$$

$$F_{v,Rk,IN} = 19.077 \text{ kN} \quad (78)$$

The capacity of a double-shear connection with a steel plate constituting the central element (part OUT) is determined according to Eq. (8.11) in Eurocode 5 by:

$$F_{v,Rk,Jhs} = \min \begin{cases} f_{h,1,k} \cdot t_1 \cdot d & (f) \\ f_{h,1,k} \cdot t_1 \cdot d \cdot \left[\sqrt{2 + \dfrac{4 \cdot M_{y,Rk}}{f_{h,1,k} \cdot d \cdot t_1^{\,2}}} - 1 \right] & (g) \\ 2.3 \cdot \sqrt{M_{y,Rk} \cdot f_{h,1,k} \cdot d} & (h) \end{cases} \quad (79)$$

Application of the design equations to the OUT part leads to:

$$F_{v,Rk,Jhs,OUT} = \min \begin{cases} 26.52 \cdot 60 \cdot 16 = 25458 \text{ N} & \text{(f)} \\ 26.52 \cdot 60 \cdot 16 \left[\sqrt{2 + \dfrac{4 \cdot 162141}{26.52 \cdot 60^2 \cdot 16}} - 1 \right] = 14182 \text{ N} & \text{(g)} \\ 2.3 \cdot \sqrt{162141 \cdot 26.52 \cdot 16} = 19077 \text{ N} & \text{(h)} \end{cases} \quad (80)$$

$$F_{v,Rk,Jhs,OUT} = 14.182 \text{ kN} \quad (81)$$

The capacity of half of the connection is obtained by mode 5 (m + g):

$$F_{v,Rk,Jhs} = F_{v,Rk,Jhs,IN} + F_{v,Rk,Jhs,OUT} = 19.077 + 14.182 = 33.26 \text{ kN} \quad (82)$$

4.3.6.2 Splitting failure

The characteristic capacity to brittle failure along a row of fasteners of the multiple fastener connection is obtained by:

$$F_{v,ef,Rk} = n_{plate} \cdot \sum_{i=1}^{n_{rows}} n_{ef} \cdot F_{v,p,Rk,Jhs} \quad (83)$$

$$n_{ef} = \min \begin{cases} n \\ n^{0.9} \sqrt[4]{\dfrac{a_1}{13 \cdot d}} \end{cases} = \min \begin{cases} 4 \\ 4^{0.9} \sqrt[4]{\dfrac{5}{13}} \end{cases} = 2.74 \quad (84)$$

$$F_{v,ef,Rk} = n_{plate} \cdot \sum_{i=1}^{n_{rows}} n_{ef} \cdot F_{v,Rk,Jhs} = 2 \cdot 2 \cdot 2.74 \cdot 33.26 = 364.83 \text{ kN} \quad (85)$$

The capacity along the row of fasteners of the central part of the connection amounts to:

$$F_{v,ef,Rk,IN} = \frac{364.83}{33.26} \cdot 19.08 = 209.26\ \text{kN} \tag{86}$$

and the capacity along the row of fasteners of the outer parts of the connection amounts to:

$$F_{v,ef,Rk,OUT} = \frac{364.83}{33.26} \cdot 14.18 / 2 = 77.78\ \text{kN} \tag{87}$$

4.3.6.3 Plastic failure

In case the connection can reach the plastic limit without brittle failure, the rope effect can be added to the capacity per shear plane as follows:

$$F_{v,Rk} = F_{v,Rk,Jhs} + \min\begin{cases} F_{ax,Rk} / 4 \\ 0.25 \cdot F_{v,Rk,Jhs,IN} \end{cases} + \min\begin{cases} F_{ax,Rk} / 4 \\ 0.25 \cdot F_{v,Rk,Jhs,OUT} \end{cases} = 33.26 + 2 \cdot 3.20 = 39.67\text{kN} \tag{88}$$

The maximum characteristic plastic capacity of the connection is then:

$$F_{v,Rk} = n_{plate} \cdot \sum_{i=1}^{n_{rows}} n \cdot F_{v,Rk} = 2 \cdot 2 \cdot 4 \cdot 39.67 = 634.70\ \text{kN} \tag{89}$$

whereby the plastic capacity of the central part amounts to:

$$F_{v,Rk,IN} = \frac{634.70}{39.67} \cdot \left(19.08 + 3.20\right) = 356.50\ \text{kN} \tag{90}$$

and the plastic capacity of one of the outer parts amounts to:

$$F_{v,Rk,OUT} = \frac{634.70}{39.67} \cdot \left(14.18 + 3.20\right) / 2 = 139.10\ \text{kN} \tag{91}$$

4.3.6.4 Block shear failure

Since the connection is composed of two rows of fasteners, a block shear failure is a possible failure that needs to be evaluated according to Appendix A of Eurocode 5 as follows:

$$F_{bs,Rk} = \max\begin{cases} 1.5 \cdot A_{net,t} \cdot f_{t,o,k} \\ 0.7 \cdot A_{net,v} \cdot f_{v,k} \end{cases} \tag{92}$$

For glued-laminated timber of strength class GL24h, the characteristic tensile strength parallel to the grain and the characteristic shear strength (according to EN 14080) are:

$$f_{t,0,k} = 19.2\ \text{MPa} \quad \text{and} \quad f_{v,k} = 3.5\ \text{MPa} \tag{93}$$

The length of the tensile failure area in the connection is obtained by:

$$L_{net,t} = \sum_i l_{t,i} = a_2 - d_0 = 64 - (16+1) = 47 \text{ mm} \tag{94}$$

and the length of the shear failure area is obtained by:

$$L_{net,v} = \sum_i l_{v,i} = 2 \cdot (a_{3,t} + 3 \cdot a_1 - 3.5 \cdot d_0) = 2 \cdot (112 + 3 \cdot 80 - 3.5 \cdot 17) = 585 \text{ mm} \tag{95}$$

The block shear capacity of the inner part (IN) is obtained after establishing the tensile and shear surfaces. Failure will necessarily be of "block shear" type, i.e. over the entire width and thickness of the timber member, independent of the failure mode of the fastener. In the calculation of block shear failure, moisture induced cracking of the cross-section is considered by taking into account the reduction coefficient $k_{cr} = 0.67$, which yields:

$$A_{net,t} = L_{net,t} \cdot t_2 = 47 \cdot 160 = 7520 \text{ mm}^2 \tag{96}$$

$$A_{net,v} = L_{net,v} \cdot t_2 \cdot k_{cr} = 585 \cdot 160 \cdot 0.67 = 62712 \text{ mm}^2 \tag{97}$$

$$F_{bs,Rk,IN} = \max \begin{cases} 1.5 \cdot 7520 \cdot 19.2 \\ 0.7 \cdot 62712 \cdot 3.5 \end{cases} = \max \begin{cases} 216.58 \text{ kN} \\ 153.64 \text{ kN} \end{cases} = 216.58 \text{ kN} \tag{98}$$

Block shear failure is in this case controlled by the tensile strength of timber. The same procedure can be applied for the estimation of the block shear capacity of the outer parts (OUT):

$$A_{net,t} = L_{net,t} \cdot t_1 = 47 \cdot 60 = 2820 \text{ mm}^2 \tag{99}$$

$$A_{net,v} = L_{net,v} \cdot t_1 \cdot k_{cr} = 585 \cdot 60 \cdot 0.67 = 23517 \text{ mm}^2 \tag{100}$$

$$F_{bs,Rk,OUT} = \max \begin{cases} 1.5 \cdot 2820 \cdot 19.2 \\ 0.7 \cdot 23517 \cdot 3.5 \end{cases} = \max \begin{cases} 81.22 \; kN \\ 57.62 \; kN \end{cases} = 81.22 \text{ kN} \tag{101}$$

4.3.6.5 Stiffness estimation applying Eurocode 5

Fig. 22 shows the stiffnesses per shear plane of the IN and OUT part. It becomes obvious that failure occurs in a brittle way in the connection, since the brittle capacity is lower than the plastic limit of the connection (here, the outer part fails due to splitting, at 77.78 kN). Since the steel plate deforms the bolts on both sides similarly, it can be considered that the same displacement is imposed on both sides. In order to evaluate the total load-bearing capacity of the connection when splitting failure occurs in the outer parts, it is necessary to take into account the load that is in the inner part. Failure in one of the parts is considered to be the only possible scenario that can be verified in design, since it is unlikely to anticipate the evaluation of the connection capacity after one of its parts is broken. To control load distribution, the control of the stiffness of the shear planes appears to be essential.

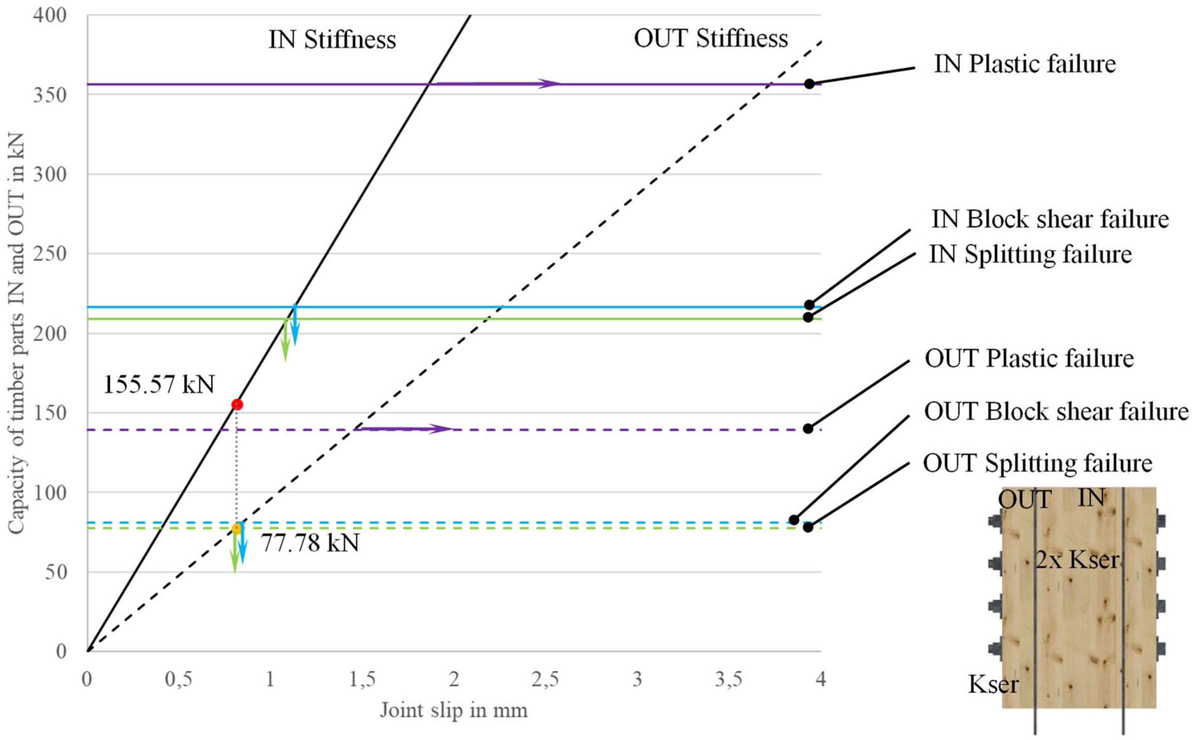

Fig. 22. Inner and outer stiffness of the 60/160/60 joint and estimated load-carrying capacity applying Eurocode 5.

The characteristic capacity to brittle failure of the multiple fastener connection is then obtained by:

$$F_{v,Rk,Kser,EC5} = 2 \cdot F_{v,ef,Rk,OUT} + \left(\frac{F_{v,ef,Rk,OUT}}{K_{ser,OUT}} \cdot K_{ser,IN} \right) = 2 \cdot 77.78 + \left(\frac{77.78}{95.81} \cdot 191.61 \right) = 311.15\,kN \quad (102)$$

where the displacement at failure is:

$$\delta_{Kser\ EC5} = \frac{F_{v,ef,Rk,OUT}}{K_{ser,OUT}} = \frac{77.78}{95.80} = 0.82\text{ mm} \quad (103)$$

4.3.7 Summary

Table 2 summarises the calculations concerning the multiple fastener connection with multiple shear planes. In the first row, Table 2 shows the plastic capacities of two different multiple shear plane connections with different member thicknesses. In this case, it was assumed that the plastic load-bearing capacity can be reached without splitting. In a second step, the capacity was estimated by taking into account load distribution effects and splitting, without taking into account the fact that failure must be sequential. Finally, splitting along a row and block shear failure were taken into account and yielded even lower capacities.

Table 2: Summary of estimated ultimate loads on 95/90/95 and 60/160/60 connections considering the stiffness per shear plane given by Eurocode 5.

	Optimization by plasticization, t_1 = 95 mm and t_2 = 90 mm	Optimization by uniform stresses ,t_1 = 60 mm and t_2 = 160 mm
Plastic failure: $F_{v,Rk}$	712.75 kN (Eq. (61))	634.70 kN (Eq. (89))
Splitting failure: $F_{v,ef,Rk}$	418.34 kN (Eq. (57))	364.83 kN (Eq. (85))
Block shear failure and splitting in a sequential failure scenario: $F_{v,Rk}$	243.65 kN (Eq. (75))	311.15 kN (Eq. (102))

4.4 Stiffness per plane estimated by a beam on elastic foundation model

4.4.1 General

The study in section 4.3 was based on a stiffness estimation using the empirical equations of Eurocode 5, which do not take into account side member thickness and fastener failure mode. Corresponding effects can however be estimated by means of a numerical model of the fastener embedded in timber, modelled as a beam on elastic foundation. In a first step, the stiffness per fastener and per shear plane will be calculated. In a second step, a global model of the multiple fastener connection is realised with beam-on-foundation elements, which allows taking into account stiffness of the timber in between fasteners and its influence on the global stiffness of the connection per shear plane. In order to establish this elastic model, it is necessary to assign stiffness to the steel plates of the connection. This is not considered in Eurocode 5 equations, where the stiffness of steel-to-timber connections is considered to be twice the stiffness of timber-to-timber connections. Tensile stiffness of steel plates is set equal to that of timber in the model presented in the following. This hypothesis makes it possible to obtain a uniform distribution of shear in the rows of fasteners of the connection. Thus, it is assumed that:

$$E_{timber} \cdot S_{timber} = E_{steel} \cdot S_{steel} \tag{104}$$

with

E_{timber} Elastic modulus of timber;

S_{timber} Cross section of timber in tension;

E_{steel} Elastic modulus of steel;

S_{steel} Cross section of steel in tension.

Assuming that the steel plate width is equal to the width of the timber part, yields:

$$e_{plate} = \frac{t_{timber}}{2} \cdot \frac{E_{timber}}{E_{steel}} = \frac{280}{2} \cdot \frac{11500}{210000} \approx 8 \text{ mm} \text{ (rounded to 10 mm)} \quad (105)$$

with

e_{plate} Thickness of one steel plate;

t_{timber} Total thickness of timber.

Thus, the following dimensions of the steel plate are chosen:

Thickness of the steel plate: e_{plate} = 10 mm

Width of the steel plate: l_{plate} = 64 mm

4.4.2 Modelling of a beam on elastic foundation: optimisation for "plastic load-bearing capacity"

4.4.2.1 Characteristics of timber: embedment behaviour

In order to model the bolted connection using a beam on elastic foundation approach, it is necessary to determine the foundation modulus of timber when it is subject to the diametrical pressure of a circular member. Even if this is not perfectly correct from a statistical point of view, an average modulus is estimated using the mean embedment strength of GL24h and a corresponding displacement of 1 mm. The average embedment strength is determined based on the empirical equation of Eurocode 5, using a mean value of timber density, yielding:

$$f_{h,0,mean} = 0.082 \cdot (1 - 0.01 \cdot d) \cdot \rho_m = 0.082 \cdot (1 - 0.01 \cdot 16) \cdot 420 = 28.93 \text{ MPa} \quad (106)$$

and by assuming a corresponding displacement of 1 mm [9], the foundation modulus is calculated by:

$$m_{fh} = \frac{f_h}{1} = 28.93 \text{ N/mm}^3 \quad (107)$$

4.4.2.2 Geometry of the model

The fastener is modelled by a steel beam with a circular section equivalent to that of the fastener, with a diameter of 16 mm. Since the problem is symmetrical, only one half of the connection is modelled and the rotation of the dowel at the plane of symmetry is constrained. The beam is then discretised using element lengths smaller than the bolt diameter [20]. Corresponding lengths of elements were, for the outer parts $l_{d,OUT}$ = 15.83 mm and for the inner part $l_{d,IN}$ = 15 mm. A gap of 1 mm with the timber is considered on both sides of the steel plate.

The stiffness of a spring can then be determined by:

$$K_d = m_{fh} \cdot d \cdot l_d \tag{108}$$

which yields the following stiffness values for each part:

$$K_{d\,OUT} = m_{fh} \cdot d \cdot l_{d\,OUT} = 28.93 \cdot 16 \cdot 15.83 = 7328.83 \text{ N/mm (Outer parts)} \tag{109}$$

$$K_{d\,IN} = m_{fh} \cdot d \cdot l_{d\,IN} = 28.93 \cdot 16 \cdot 15 = 6943.10 \text{ N/mm (Inner part)} \tag{110}$$

Fig. 23 presents a schematisation of this modelling approach, with properties applied in the calculation example.

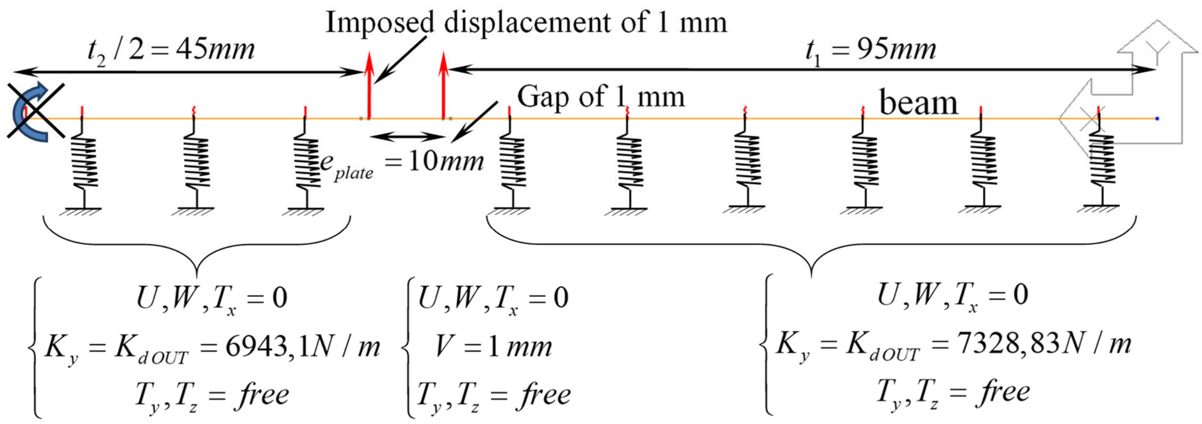

Fig. 23. Model of the bolt in the multiple shear plane connection 95/90/95 as a beam on an elastic foundation.

4.4.2.3 Deformation, shear force and stiffness per plane

A displacement of 1 mm is imposed on the bolt at the nodes of the plate. Fig. 24 shows the deformation of the bolt and the shear force diagram along the beam (= fastener axis).

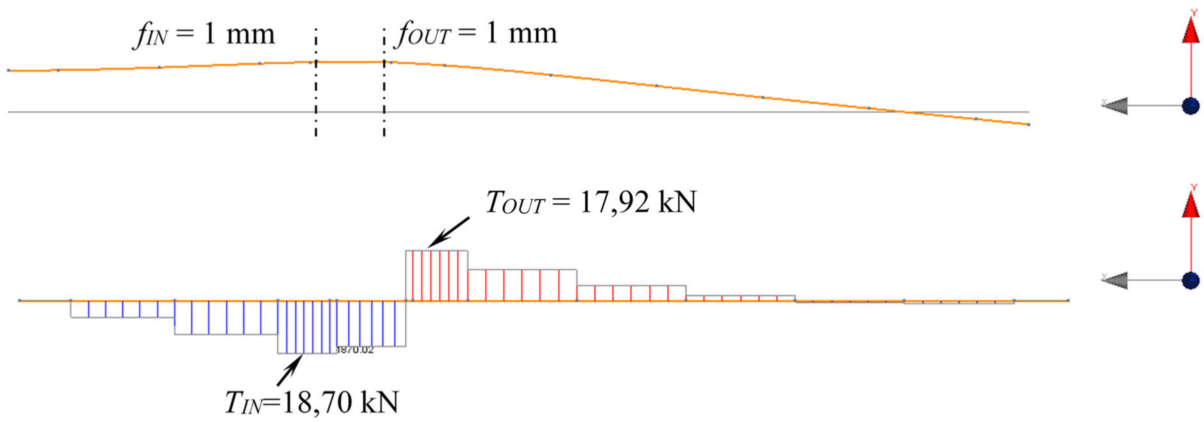

Fig. 24. Deformation of the fastener in the connection 95/90/95 with an imposed displacement of 1 mm at the steel plates and shear forces along the fastener axis.

The stiffness per shear plane can then be determined by dividing the shear forces by the imposed displacement of 1 mm. These calculations lead to the stiffness of each part:

$$K_{ser,OUT} = \frac{T_{OUT}}{f_{OUT}} = \frac{17.92}{1} = 17.92\ \mathrm{kN/mm}\ \text{(Outer parts)} \tag{111}$$

$$K_{ser,IN} = \frac{T_{IN}}{f_{IN}} = \frac{18.70}{1} = 18.7\ \mathrm{kN/mm}\ \text{(Inner part)} \tag{112}$$

These values are higher than the value obtained applying Eurocode 5, which was equal to (Eq. (44) times 2 = 2 · 5.987 = 11.97 kN/mm):

$$K_{ser} = 11.97\ \mathrm{kN/mm} \tag{113}$$

4.4.2.4 Modelling of the multiple fastener connection with 8 bolts

In order to determine the stiffness of the inner part of the connection and the stiffness of the outer parts, a symmetrical beam-type model is used. To account for the stiffness of the timber and steel parts, these are modelled as beams whose sections are equal to the actual dimensions of the parts without being affected by the drilling holes. The displacement of the steel plate is transmitted rigidly at the location of each bolt to the timber. The shear stiffness per shear plane (as calculated in the previous section) is introduced via spring elements. A displacement of 1 mm is applied to the plate. The shear force per bolt can thus be obtained as well as the sum of the normal force along the timber elements (see Fig. 25).

Assuming here that the slip of the connection represents the total deformation, the connection slip is equivalent to the displacement imposed on the connection, i.e., it is equal to 1 mm. The stiffness of the outer timber part is then:

$$K_{ser,Jt,OUT} = n_{row} \cdot K_{ser,row} = 2 \cdot \frac{N_{OUT}}{g} = 2 \cdot \frac{56.32}{1} = 112.64\ \mathrm{kN/mm} \tag{114}$$

with N_{OUT} the normal force in the outer part. Stiffness of the inner timber part is given by:

$$K_{ser,Jt,IN} = 2(\text{sym}) \cdot n_{row} \cdot K_{ser,row} = 2 \cdot 2 \cdot \frac{N_{IN}}{g} = 2 \cdot 2 \cdot \frac{52.13}{1} = 208.52\ \mathrm{kN/mm} \tag{115}$$

with N_{IN} the normal force in the outer part.

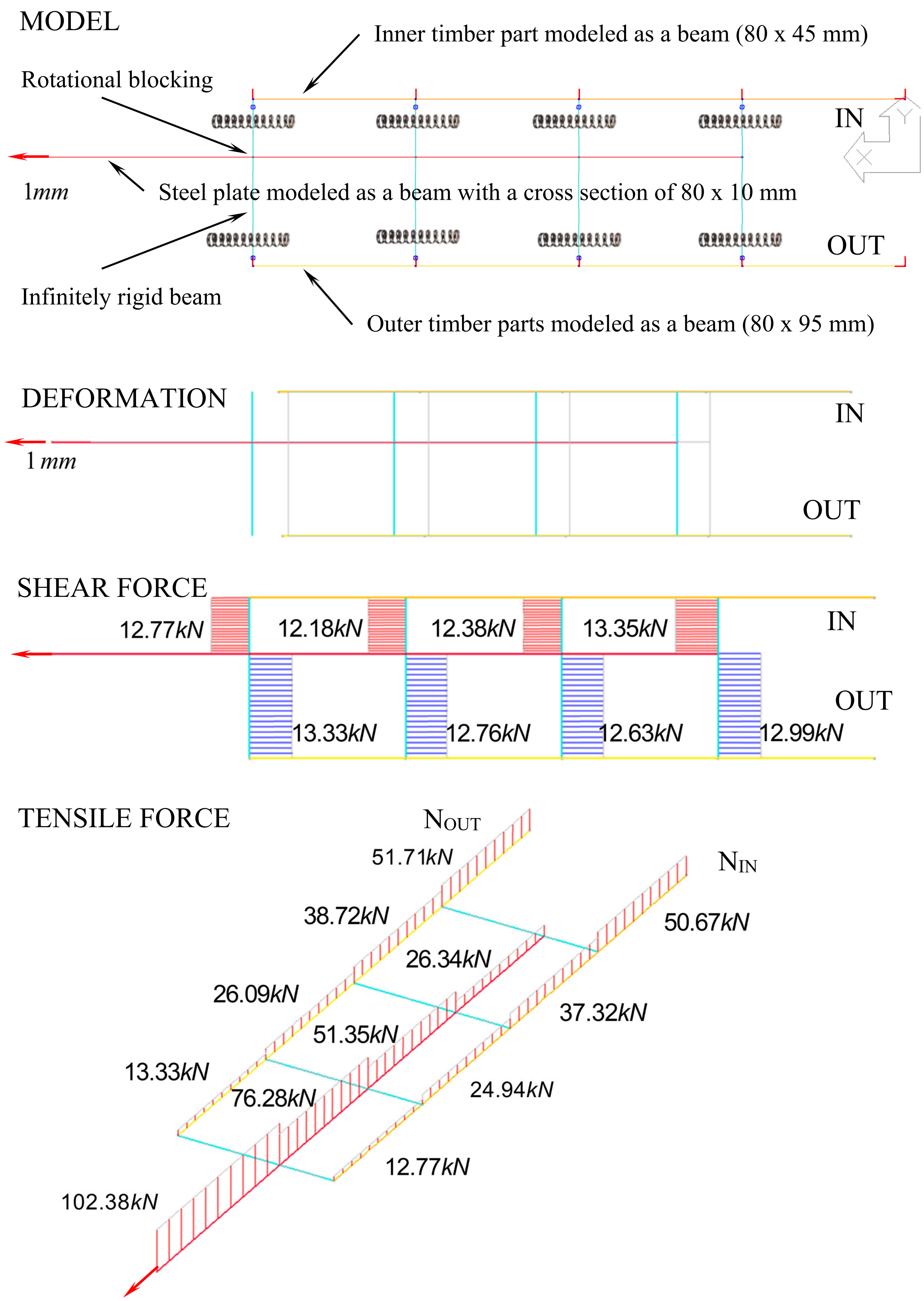

Fig. 25. From top to bottom: Model of the multiple fastener connection 95/90/95, deformation of the model with a displacement imposed on the plate of 1 mm, shear force per plane, and distribution of the tensile forces in the timber and steel beams.

4.4.2.5 Analysis of the failure of the connection

Fig. 26 shows the stiffnesses per shear plane of the IN and OUT part and the capacity limits to plastic and brittle failure modes. It becomes obvious that failure occurs in a brittle way in the connection (i.e. the inner part fails in block shear = capacity limit that is reached first, at smallest slip), since the brittle capacity is lower than the plastic limit of the connection. Since the steel plate deforms the bolts on both sides similarly, it can be considered that the same displacement is imposed on both sides. When failure occurs in the inner part through a block shear failure (at 121.82 kN), the load in the outer part needs to be known for calculating the total load of the connection. Failure in one of the parts is considered to be the only possible scenario to prove in terms of design, it is unlikely to anticipate the evaluation of the strength of the connection after one of its parts is broken. To control load distribution, controlling the stiffness of the planes appears to be essential.

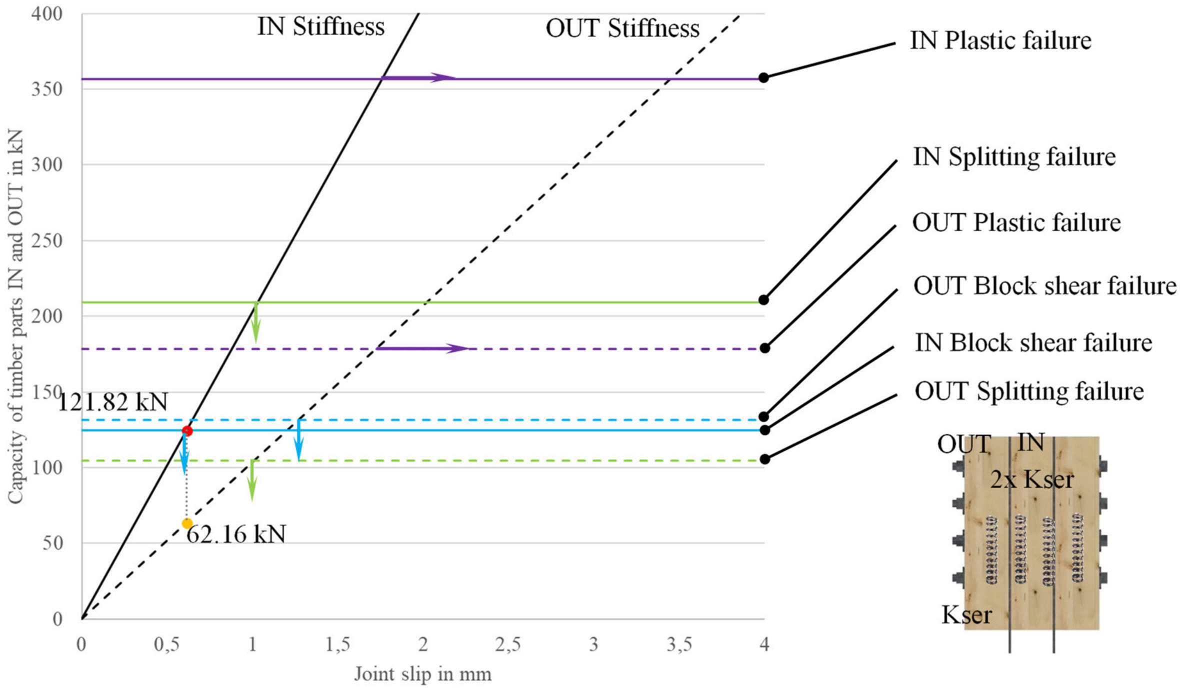

Fig. 26. Inner and outer stiffness of the multiple fastener connection 95/90/95 estimated with a model of beam on an elastic foundation and load-carrying capacity estimated with the Eurocode 5.

Ultimate brittle load-bearing capacity of the multiple fastener connection is then obtained by, considering the stiffnesses calculated in Eqs. (114) and (115):

$$F_{v,Rk,\text{model}} = F_{bs,Rk,IN} + 2 \cdot \left(\frac{F_{bs,Rk,IN}}{K_{ser,Jt,IN}} \cdot K_{ser,Jt,OUT} \right) = 121.82 + 2 \cdot \left(\frac{121.82}{208.52} \cdot 112.64 \right) = 253.43 \text{ kN} \quad (116)$$

and the displacement at failure is equal to:

$$\delta_{\text{beam model}} = \frac{F_{bs,Rk,IN}}{K_{ser,Jt,IN}} = \frac{121.82}{208.52} = 0.58 \text{ mm} \quad (117)$$

4.4.3 Modelling of a beam on elastic foundation: optimisation for "uniform stress distribution"

4.4.3.1 Characteristics of timber: embedment behaviour

The foundation modulus of timber embedment behaviour is assumed equal to that calculated in section 4.4.2.1, that is:

$$m_{fh} = \frac{f_h}{1} = 28.93\,\mathrm{N/mm^3} \tag{118}$$

4.4.3.2 Geometry of the model

The model presented in section 4.4.2.2 is adapted to the timber member thicknesses of 60/160/60 mm. Bolt element lengths are equal to $l_{d,OUT} = 15.83$ mm and $l_{d,IN} = 15$ mm for the outer and inner parts, respectively. A gap of 1 mm to the timber is considered on both sides of the steel plate. The stiffness of a spring is then:

$$K_d = m_{fh} \cdot d \cdot l_d \tag{119}$$

which yields the following stiffness values for each part:

$$K_{d\,OUT} = m_{fh} \cdot d \cdot l_{d\,OUT} = 28.93 \cdot 16 \cdot 15 = 6943.10\ \ \mathrm{N/mm}\ \text{(Outer parts);} \tag{120}$$

$$K_{d\,IN} = m_{fh} \cdot d \cdot l_{d\,IN} = 28.93 \cdot 16 \cdot 16 = 7406.08\,\mathrm{N/mm}\ \text{(Inner part)} \tag{121}$$

Fig. 27 presents the schematisation of this modelling approach, with properties applied in the calculation example.

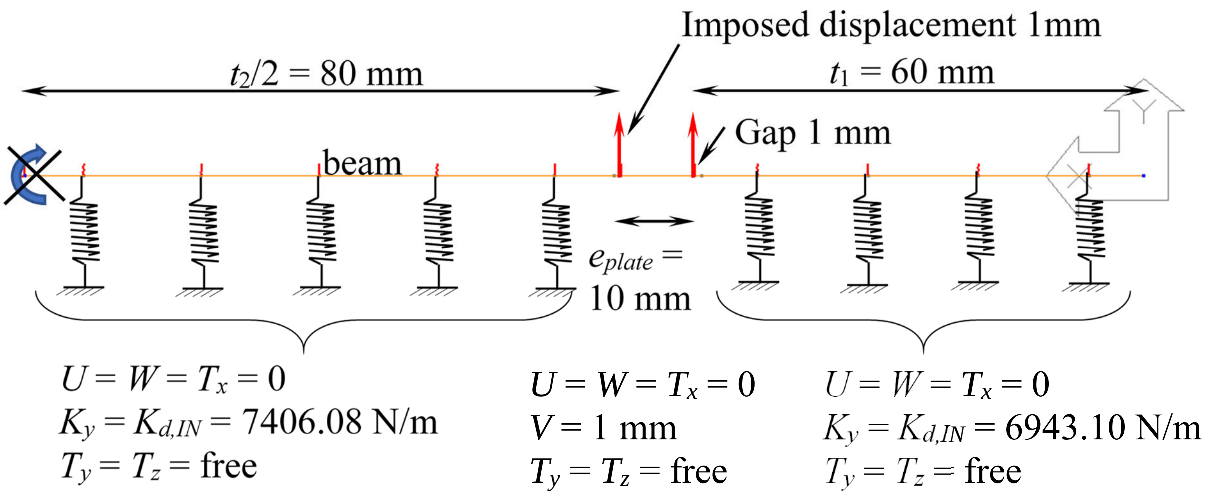

Fig. 27. Model of the fastener in the connection 60/160/60 as a beam on elastic foundation.

4.4.3.3 Deformation, shear force and stiffness per shear plane

A displacement of 1 mm is imposed on the bolt at the nodes of the plate. Fig. 28 shows the deformation of the bolt and the shear force diagram along the beam.

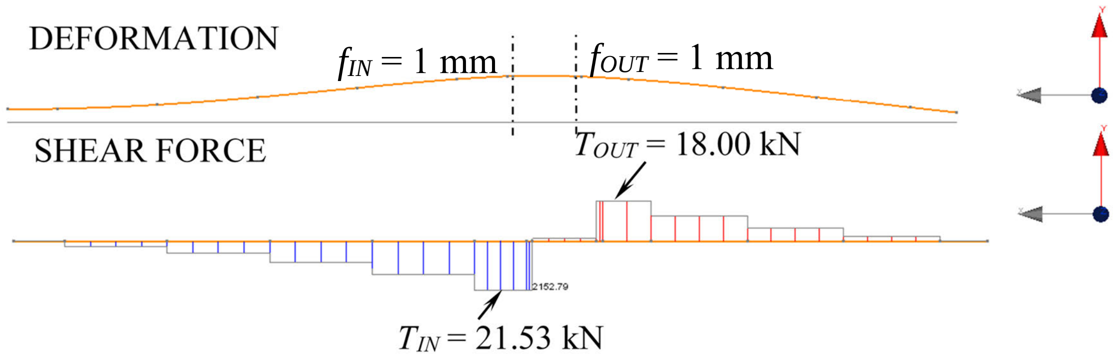

Fig. 28. Deformation of the fastener in the connection 60/160/60 with an imposed displacement of 1 mm at the steel plates and shear forces along the fastener axis.

The stiffness per shear plane can then be determined by dividing the shear forces by the imposed displacement of 1 mm. This leads to the stiffness of each part:

$$K_{ser,OUT} = \frac{T_{OUT}}{f_{OUT}} = \frac{18.00}{1} = 18.00 \text{ kN/mm (Outer parts)} \tag{122}$$

$$K_{ser,IN} = \frac{T_{IN}}{f_{IN}} = \frac{21.53}{1} = 21.53 \text{ kN/mm (Inner part)} \tag{123}$$

These values are higher than the value obtained applying Eurocode 5:

$$K_{ser} = 11.97 \text{ kN/mm} \tag{124}$$

4.4.3.4 Modelling of the multiple fastener connection with 8 bolts

In order to determine the stiffness of the inner part of the connection and the stiffness of the outer parts, a symmetrical beam-type model is used. To account for the stiffness of the timber and steel parts, these are modelled as beams whose sections are equal to the actual dimensions of the parts without being affected by the drilling holes. The displacement of the steel plate is transmitted rigidly at the location of each bolt to the timber. The shear stiffness per shear plane (as calculated in the previous section) is introduced via spring elements. A displacement of 1 mm is applied to the plate. The shear force per bolt can thus be obtained as well as the sum of the normal force along the timber elements (see Fig. 25).

Assuming here that the slip of the connection represents the total deformation, the connection slip is equivalent to the displacement imposed on the connection, i.e., it is equal to 1 mm. The stiffness of the outer timber part is then:

$$K_{ser,Jt,OUT} = n_{row} \cdot K_{ser,row} = 2 \cdot \frac{N_{OUT}}{g} = 2 \cdot \frac{49.98}{1} = 99.96 \text{ kN/mm} \tag{125}$$

with N_{OUT} the normal force in the outer part.

Stiffness of the inner timber part is given by:

$$K_{ser,Jt,IN} = 2(\text{sym}) \cdot n_{row} \cdot K_{ser,row} = 2 \cdot 2 \cdot \frac{N_{IN}}{g} = 2 \cdot 2 \cdot \frac{60.77}{1} = 243.77 \text{ kN/mm} \qquad (126)$$

with N_{IN} the normal force in the inner part.

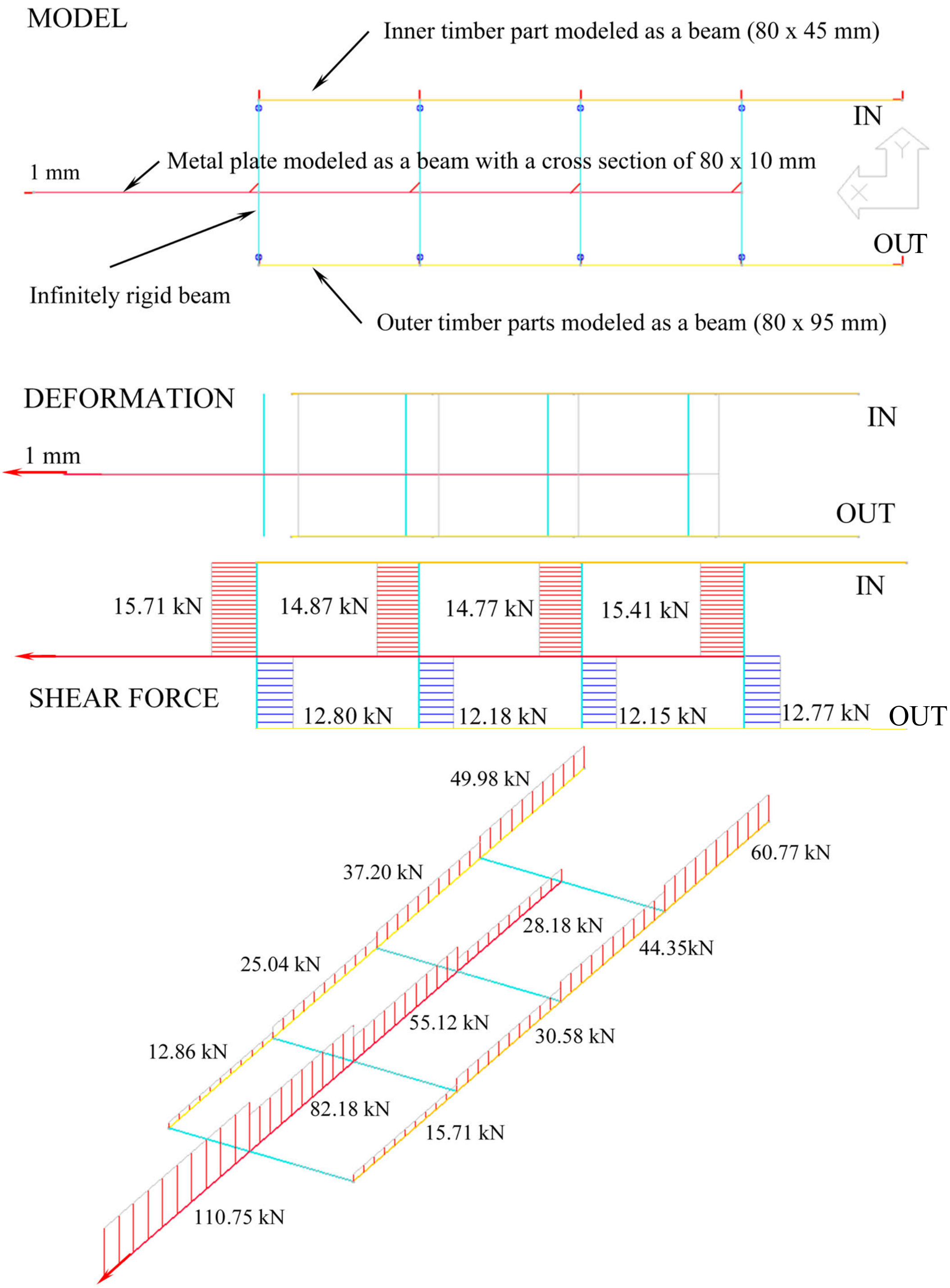

Fig. 29. From top to bottom: Model of the multiple fastener connection 60/160/60, deformation of the model with an imposed displacement of the plate of 1 mm, shear force per plane, and distribution of the tensile force in the timber and steel beams.

4.4.3.5 Analysis of the failure of the joint

Fig. 30 shows the stiffnesses per shear plane of the IN and OUT part and the capacity limits to plastic and brittle failure modes. It becomes obvious that failure occurs in a brittle way in the connection (i.e. the outer part fails in splitting), since the brittle capacity is lower than the plastic limit of the connection. Since the steel plate deforms the bolts on both sides similarly, it can be considered that the same displacement is imposed on both sides. When splitting failure occurs in the outer part (at 77.79 kN), the load in the inner part needs to be known for calculating the total load of the connection. Failure in one of the parts is considered to be the only possible scenario to prove in terms of design, it is unlikely to anticipate the evaluation of the strength of the connection after one of its parts is broken. To control load distribution, controlling the stiffness of the planes appears to be essential.

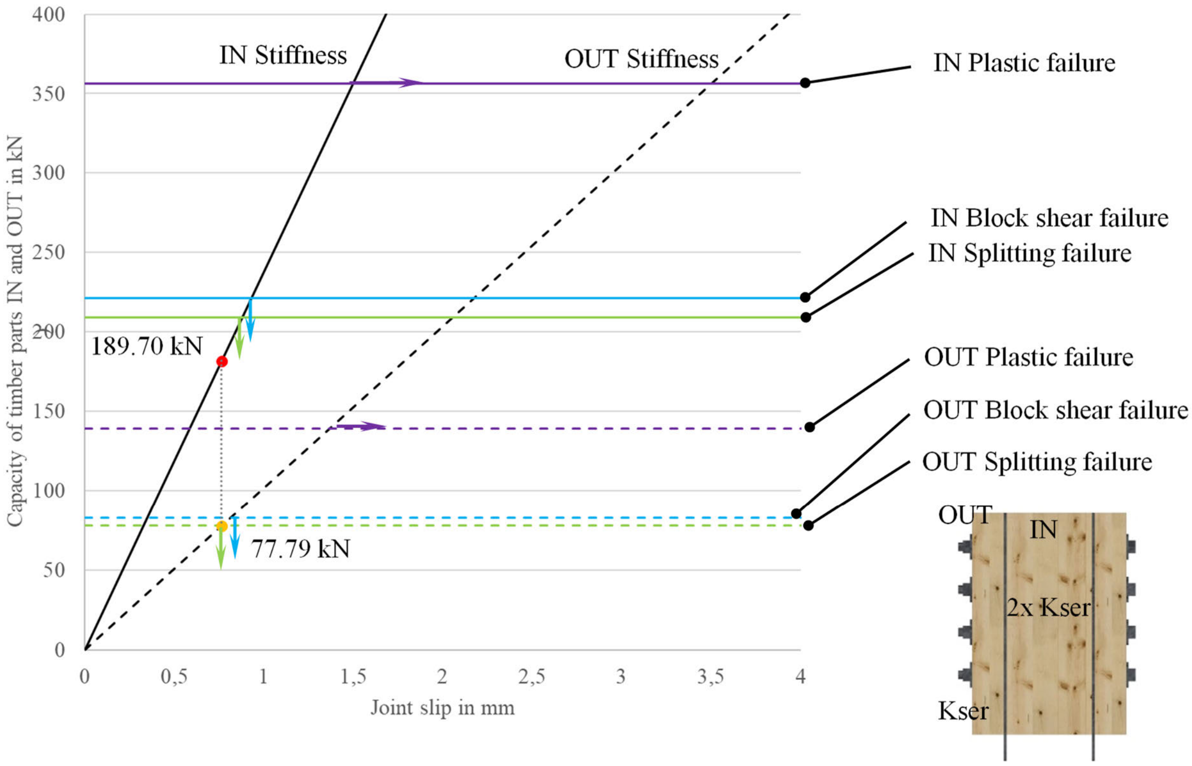

Fig. 30. Inner and outer stiffness of the connection 60/160/60 estimated with a beam on elastic model foundation and load-bearing capacity acc. to Eurocode 5.

The characteristic load-bearing capacity to brittle failure of the multiple fastener connection is then obtained by considering the stiffnesses given in Eqs. (125) and (126):

$$F_{v,Rk,\text{model}} = 2 \cdot F_{v,ef,Rk,OUT} + \left(\frac{F_{v,ef,Rk,OUT}}{K_{ser,Jt,OUT}} \cdot K_{ser,Jt,IN} \right) = 2 \cdot 77.79 + \left(\frac{77.79}{99.96} \cdot 243.77 \right) = 345.28 \text{ kN} \quad (127)$$

with the displacement at the failure equal to:

$$\delta_{\text{beam model}} = \frac{F_{v,ef,Rk,OUT}}{K_{ser,Jt,OUT}} = \frac{77.79}{99.96} = 0.78 \text{ mm} \quad (128)$$

4.4.4 Summary

The stiffness of a connection was calculated with a beam on elastic foundation model and compared to the stiffness based on Eurocode 5 equations. Higher stiffness was determined by the beam on elastic foundation model, which is able to take influences of fastener failure modes and timber member thickness into account. In the multiple fastener model, even load distribution effects due to stiffness of timber in between fasteners could be taken into account. Results of both approaches are given in Table 3. A dependence of capacities on the connection stiffness is obvious, i.e. different capacities are obtained depending on which approach is chosen to calculate the stiffness. Conclusions drawn in section 4.3.7 can be confirmed, i.e. the ultimate load-bearing capacity is governed by brittle connection failure. A timber member thickness distribution chosen to have the same stresses in the members lead to higher capacities as compared to a connection that is optimised for maximum plastic load-bearing capacity (Table 3: 311.15 kN > 243.65 kN and 345.28 kN > 253.43 kN).

Table 3: Summary of estimated ultimate loads on 95/90/95 and 60/160/60 multiple fastener connections considering the stiffness per shear plane given by Eurocode 5 and by a beam on elastic foundation model

	Optimisation for “plastic load-bearing capacity”, connection 95/90/95	Optimisation for “uniform stress distribution”, connection 60/160/60	Gain
Block shear failure and splitting in a sequential failure scenario: $F_{v,Rk}$ (K_{ser} EC5)	243.65 kN (Eq. (75))	311.15 kN (Eq. (102))	28%
Block shear failure and splitting in a sequential failure scenario: $F_{v,Rk}$ (K_{ser} beam on elastic foundation model)	253.43 kN (Eq. (116))	345.28 kN (Eq. (127))	36%

4.5 Beam on nonlinear foundation modelling: 95/90/95 and 60/160/60

The previous section confirmed that connection optimisation to obtain uniform stress distribution in multiple shear plane connections leads to higher load-bearing capacities of multiple fastener connections, but that the estimated connection stiffness influences the load-carrying capacity. It is therefore important to investigate this further by increasing the complexity of modelling of the connection. In the previous section, the foundation modulus of timber was considered to be linear-elastic. In this section, it is shown that it is possible to establish a non-linear model that takes into account the non-linear character of the foundation (i.e. embedment) as well as the non-linear behaviour of the steel. The same geometrical dimensions of the connection apply.

4.5.1 Characteristics of timber: embedment behaviour

In order to establish an embedment strength-displacement curve, the average embedment strength given by Eurocode 5 is calculated:

$$f_h = 0.082 \cdot (1 - 0.01 \cdot d) \cdot \rho_m = 0.082 \cdot (1 - 0.01 \cdot 16) \cdot 420 = 28.93\text{MPa} \tag{129}$$

Instead of a linear elastic foundation modulus, the following nonlinear function proposed by Sauvat [17] is applied:

$$m_{fh} = f_h \cdot \left(-ck \cdot \left(\arctan \left(\left((u \cdot fk) + dk \right)^{ek} + ak \right) + bk \right) \right) \tag{130}$$

Corresponding coefficients are determined from the mean response of a series of embedment tests established in a previous study [8]:

$$ak = 1.33,\ bk = -1.57,\ ck = 1.79,\ dk = -1.65,\ ek = 4.0,\ fk = 2.8 \tag{131}$$

By integrating Eq. (130) over the relative displacement, the shape of the evolution of the embedment strength with increasing displacements can be determined. Sauvat's function has the advantage of representing the stiffening at the beginning of the embedment due to the increase of the contact surface between the circular member and the timber (Fig. 31) [19].

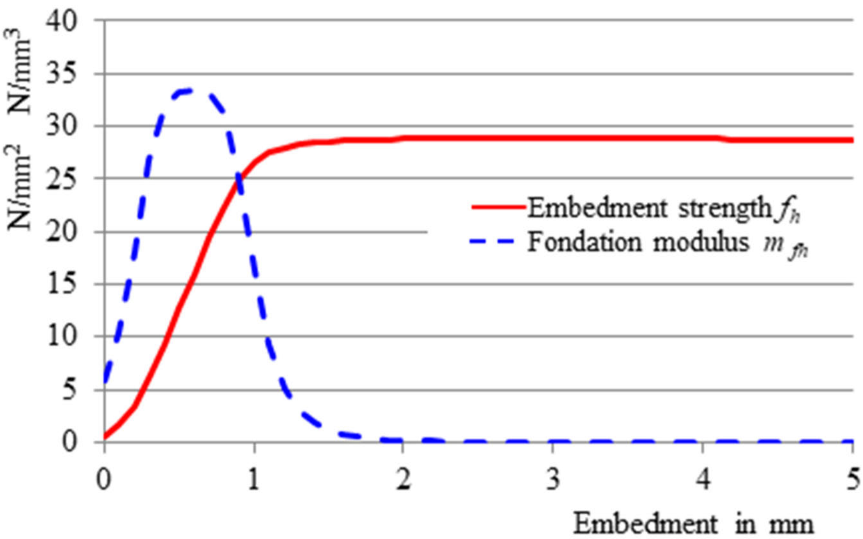

Fig. 31. Embedment strength and foundation modulus versus fastener displacement in the timber.

4.5.2 Characteristics of fasteners: bending moment

In order to take the nonlinear evolution of the bending moment of the fastener in the multiple shear plane connection into account, the following simplified model of plasticisation is applied. The steel is supposed to have an elastic-plastic behaviour. The parameters of the model are defined in Fig. 32 [8].

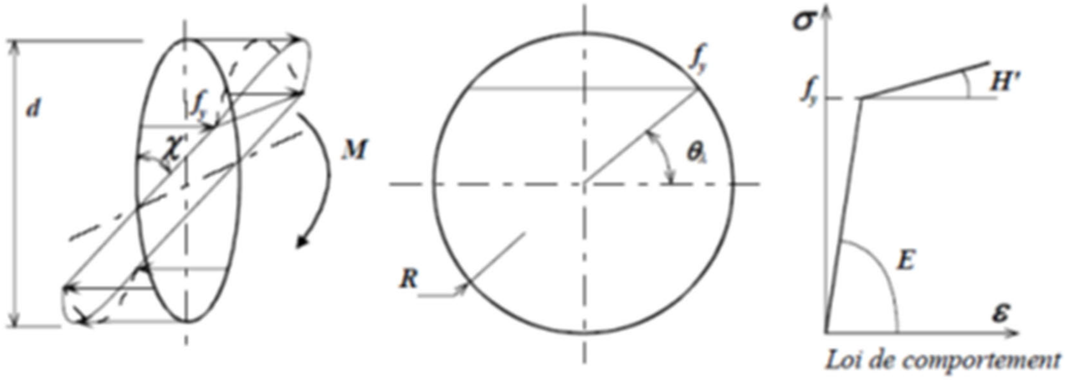

Fig. 32. Plasticisation model of the fastener's circular steel section and the model parameters: M the bending moment, R the radius, f_y the yield limit of the steel, E the modulus of elasticity of steel, H' the hardening modulus of the steel and finally χ the curvature of the section.

The nonlinear equations to calculate stress and plastic moment in the fastener section are given as:

$$M = R^3 \cdot f_y \left(\left(-\frac{5}{6} \cdot \cos\theta_\lambda + \frac{1}{3} \cdot \sin^2\theta_\lambda \cdot \cos\theta_\lambda + \frac{(\pi - 2 \cdot \theta_\lambda)}{4 \cdot \sin\theta_\lambda} \right) \frac{H'}{E} + \left(\frac{\theta_\lambda}{2} - \frac{1}{4} \cdot \sin 2\theta_\lambda + \cos\theta_\lambda \cdot \sin^3\theta_\lambda \right) \Big/ \sin\theta_\lambda + \left(\frac{4}{3} \cdot \cos\theta_\lambda \cdot \left(1 - \sin^2\theta_\lambda \right) \right) \right) \tag{132}$$

$$\chi = \frac{f_y}{E \cdot R \cdot \sin\theta_\lambda} \tag{133}$$

Steel of quality 4.6, i.e. with f_u = 400 MPa, and f_y = 240 MPa, is assumed in the calculation example. Furthermore, the modulus of elasticity and the hardening modulus are assumed to be equal to E = 210 000 MPa and H' = 1 800 MPa, respectively. Eqs. (132) and (133) yield the evolution of the moment as a function of the curvature as shown in Fig. 33.

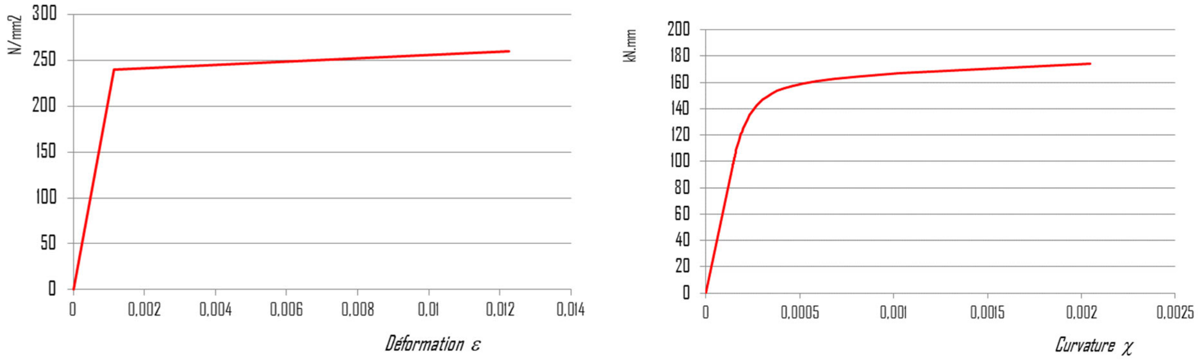

Fig. 33. The constitutive law (left) and the moment-curvature for a fastener diameter of 16 mm (right).

Since failure of the connection will occur before the plastic limit, it is not necessary to consider a rope effect in the investigated example. The fastener will not be subject to a tensile force, i.e. there will be no interaction between bending moment and normal force in the fastener. The presented plasticisation model will therefore be used for each of the sections of the modelled fasteners.

4.5.3 Modelling the multiple fastener connection with 8 bolts: 95/90/95

Fig. 34 illustrates that the model of the multiple fastener connection can be reduced to one quarter of the connection, when exploiting two symmetry planes. Each timber part is represented by a bar in the centre of the section, which is equal to the transverse dimensions of the timber without the drilling holes being taken into account (see vertical lines in Fig. 35). The bolts are represented by beams with nonlinear properties presented in the previous subsections (see horizontal lines in Fig. 35). Rotations and displacement at the end of the beams (fasteners) is constrained in order to account for the symmetry.

Beams that represent the bolts are connected to the beams representing the timber members by springs (see short dark vertical lines in Fig. 35). The stiffness of these springs that represent the embedment behaviour is determined as follows

$$K_{d\,OUT} = m_{fh} \cdot d \cdot \text{integer}\left(t_1 / (0.6 \cdot d)\right) \text{ (Outer part)} \tag{134}$$

$$K_{d\,IN} = m_{fh} \cdot d \cdot \text{integer}\left(\left(t_2 / 2\right) / (0.6 \cdot d)\right) \text{ (Inner part)} \tag{135}$$

A preliminary sensitivity study showed that this level of discretisation is sufficient for the model response to be insensitive to mesh size. The base of the springs is then connected to beam elements representing the timber members in between fasteners.

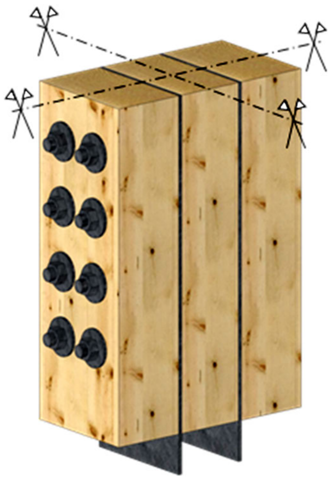

Fig. 34. Planes of symmetry of the multiple fastener connection used to reduce the model to ¼ of the structure.

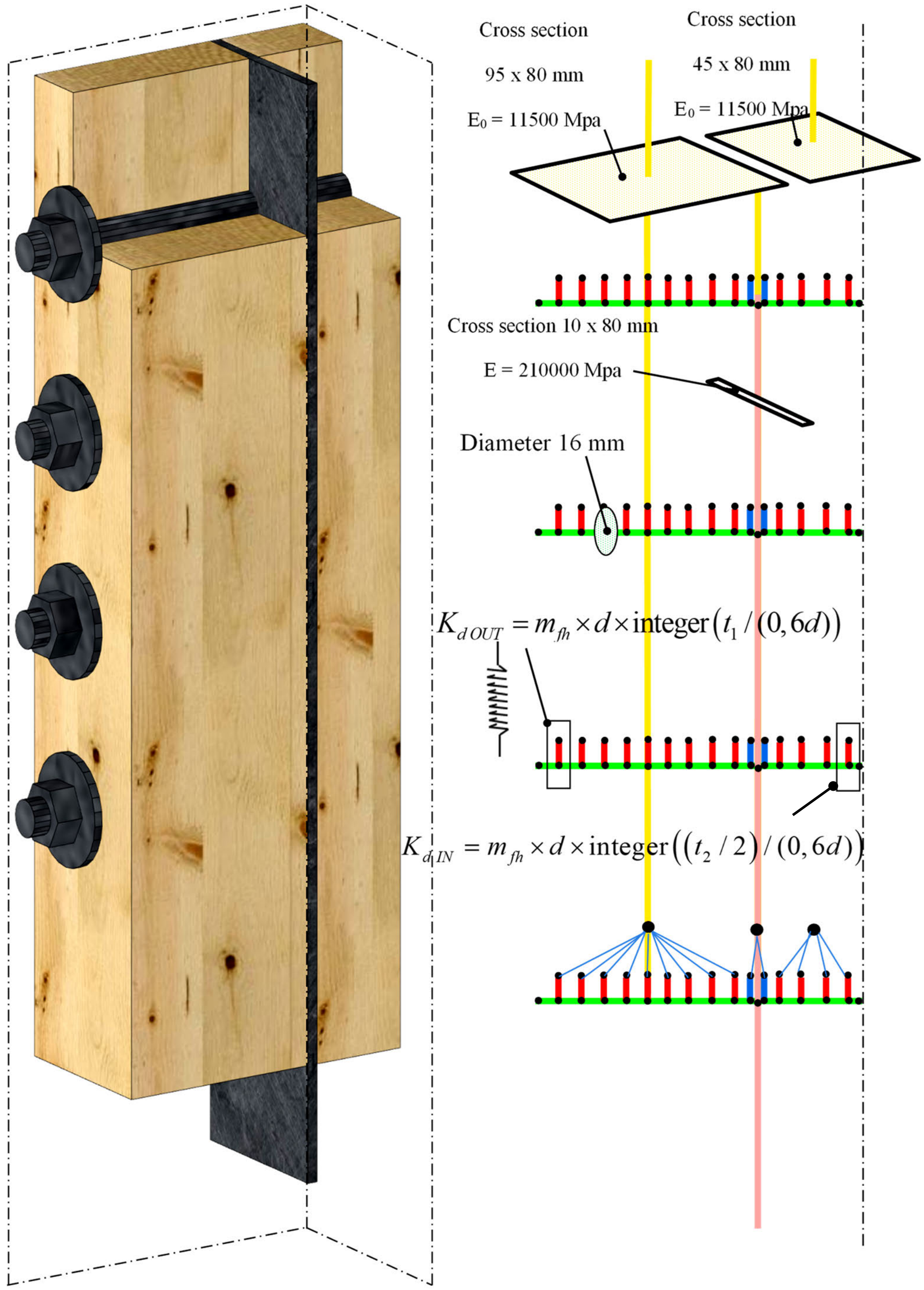

Fig. 35. 2D modelling of half of the multiple fastener connection 95/90/95 using beam elements and springs: presentation of dimensions and properties.

4.5.3.1 Analysis of connection failure: 95/90/95

Fig. 36 shows the nonlinear slip curve of the multiple fastener connection with forces per plane and displacement imposed on a steel plate. Fig. 36 also includes the linear elastic stiffness estimate using elastic beam on foundation modelling. The comparison shows the lower initial stiffness and the yield plateau of the nonlinear model compared to the linear elastic model.

It becomes obvious that failure occurs in a brittle way due to block shear failure in the inner part. For calculating the total capacity of the connection at failure, it is necessary to take into account the load in the outer part. Failure in one of the parts is considered to be the only possible scenario to prove in terms of design, it is unlikely to anticipate the evaluation of the strength of the connection after one of its parts is broken. To control load distribution, controlling the stiffness of the planes appears to be essential.

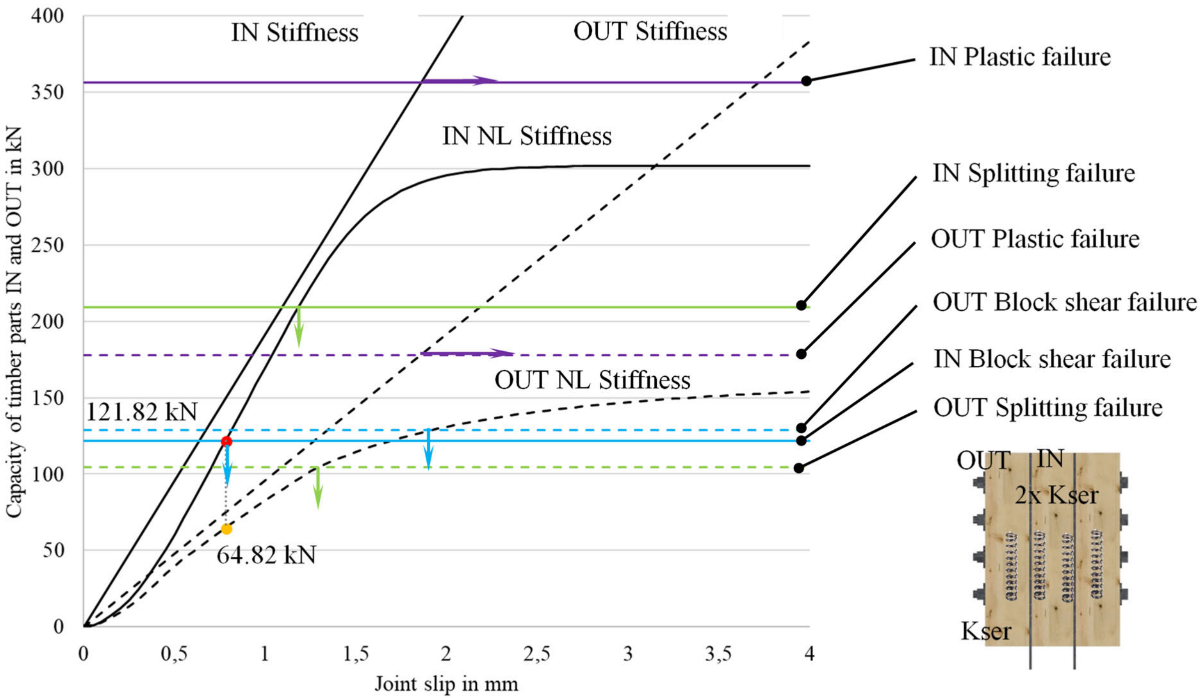

Fig. 36. Inner and outer stiffness of the joint 95/90/95 estimated with beam on nonlinear foundation model and capacity estimated with the Eurocode 5.

According to Fig. 36, failure occurs at a slip of 0.78 mm and the capacity of the multiple fastener connection is:

$$F_{v,Rk,\mathrm{model\_NL}} = F_{bs,Rk,IN} + 2 \cdot F_{v,OUT}\left(0.781\,mm\right) = 121.82 + 2 \cdot 64.82 = 251.48\,kN \quad (136)$$

4.5.4 Modelling the multiple fastener connection with 8 bolts: 60/160/60

The modelling of the 60/160/60 connection follows exactly the modelling of the 95/90/95 connection, only the different thicknesses are considered. Fig. 37 shows the model with parameters.

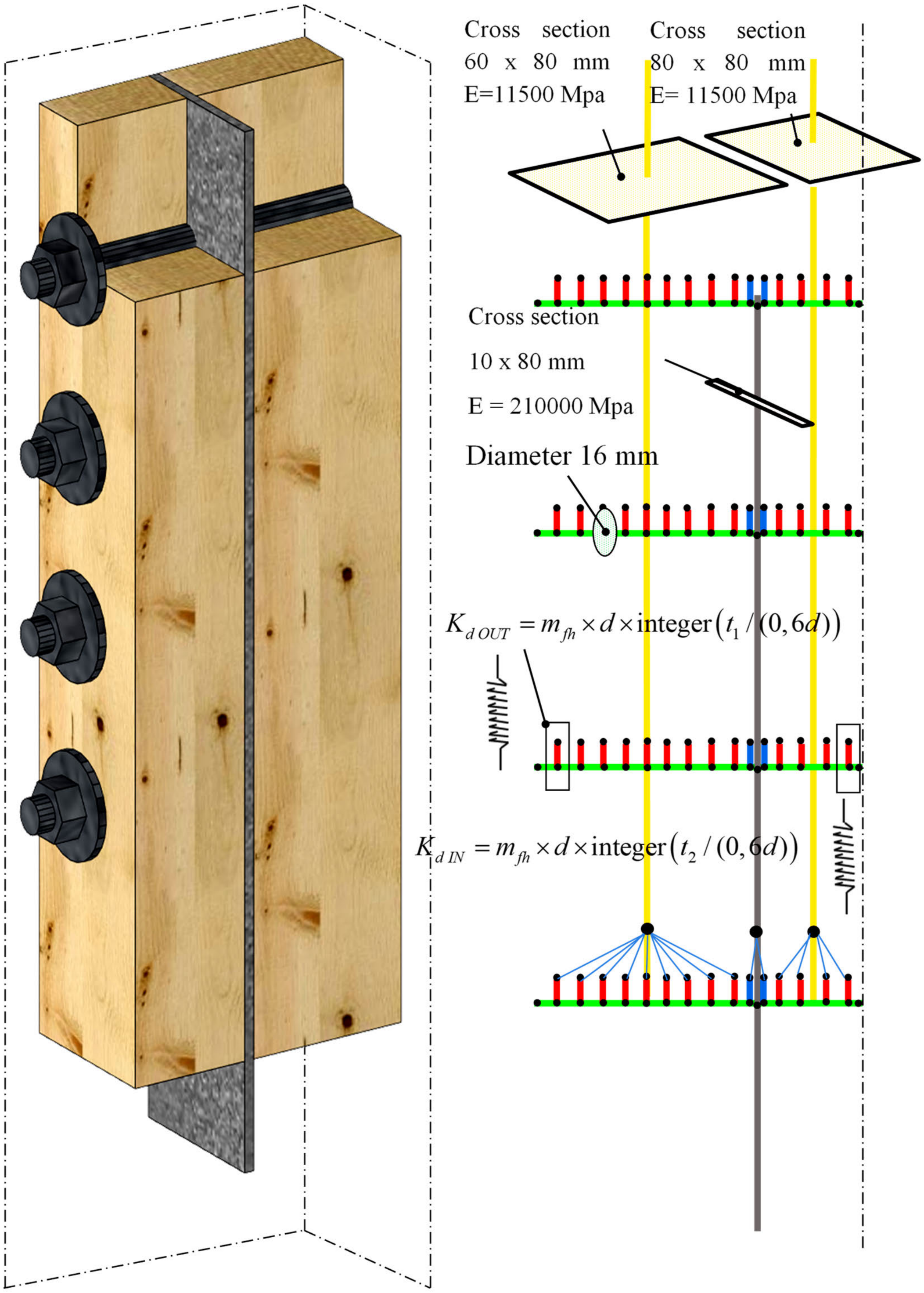

Fig 37. 2D modelling of half of the multiple fastener connection 60/160/60 using beam elements and springs: presentation of dimensions and properties.

4.5.4.1 Analysis of connection failure: 60/160/60

Fig. 36 shows the nonlinear slip curve of the multiple fastener connection with forces per plane and displacement imposed on a steel plate. Fig. 38 also includes the linear elastic stiffness estimate using elastic beam on foundation modelling. The comparison shows the lower initial stiffness and the yield plateau of the nonlinear model compared to the linear elastic model.

It becomes obvious that failure occurs in a brittle way due to block shear failure in the inner part. For calculating the total capacity of the connection at failure, it is necessary to take into account the load in the outer part. Failure in one of the parts is considered to be the only possible scenario to prove in terms of design, it is unlikely to anticipate the evaluation of the strength of the connection after one of its parts is broken. To control load distribution, controlling the stiffness of the planes appears to be essential.

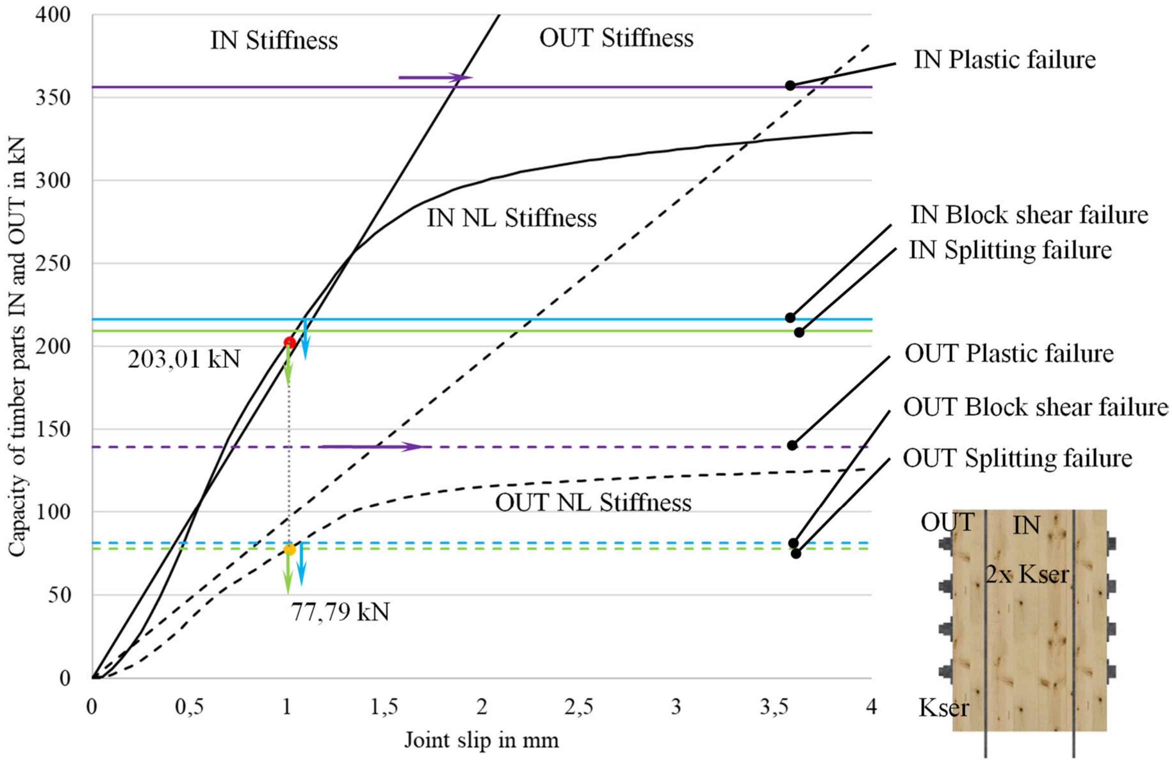

Fig 38. Inner and outer stiffness of the joint 60/160/60 estimated with beam on nonlinear foundation model and capacity estimated with the Eurocode 5.

According to Fig. 38, failure occurs at a slip of 1.10 mm and the capacity of the multiple fastener connection is:

$$F_{v,Rk,\text{model\_NL}} = F_{bs,Rk,IN} + 2 \cdot F_{v,OUT}\left(1.01\,mm\right) = 203.01 + 2 \cdot 77.79 = 358.59\ \text{kN} \quad (137)$$

4.5.5 Summary

Stiffness of the connection was calculated with a beam on nonlinear elastic foundation model (nonlinear BOF) and compared to values evaluated with a beam on elastic foundation model (elastic BOF) and those estimated based on Eurocode 5 equations. Higher stiffness was determined by the elastic and nonlinear BOF, which were able to take into account influences of fastener failure modes and timber member thickness. The nonlinear model can even consider lower initial stiffness. Results of a design example using all three approaches are given in Table 4. A dependence of capacities on the connection stiffness is obvious.

Conclusions drawn in sections 4.3.7 and 4.4.4 can be confirmed, i.e. the ultimate load-bearing capacity is governed by brittle connection failure. A timber member thickness distribution chosen to have the same stresses in the members lead to higher capacities as compared to a connection that is optimised for maximum plastic load-bearing capacity.

Analysis of the results in Table 4 (and all previous tables) shows that, whatever the way of modelling the multiple fastener connection, it will fail in a brittle manner. A timber member thickness distribution chosen to have a maximum plastic load-bearing capacity leads to lower capacities compared to a thickness distribution chosen to obtain a uniform stress distribution. The procedure to estimate connection stiffness per shear plane has a significant influence on the estimation of the capacity. It is therefore important that the designer has a reliable modelling tool when designing multiple shear plane connections. Without a reliable estimate of the stiffness, it is preferable to direct the designer to a solution where a uniform load distribution within the connection is guaranteed by cut fasteners (i.e. fasteners of half to total length inserted from both sides) as it was presented in section 4.2.1 (i.e. maximum of two shear planes per fastener); the connection capacity would be slightly lower. These conclusions are valid as long as the connection fails before reaching the ultimate plastic limit and as long as no reinforcement measures are applied.

It is interesting to note that nonlinear finite element modelling is a powerful tool for solving all types of multiple shear plane connections. It should also be noted that the estimation of the plastic load-carrying capacity of this type of connection still raises some questions when applying rules given in the current version of Eurocode 5.

Table 4. Summary of estimated ultimate load-carrying capacities of 95/90/95 and 60/160/60 joints BOF=beam on foundation model.

	Optimisation for “plastic load-bearing capacity”, connection 95/90/95	Optimisation for “uniform stress distribution”, connection 60/160/60	Gain
Sequential failure scenario: $F_{v,Rk}$ (K_{ser} EC5)	243.65 kN	311.15 kN	28%
Sequential failure scenario: $F_{v,Rk}$ (K_{ser} linear BOF)	253.43 kN	345.28 kN	36%
Sequential failure scenario: $F_{v,Rk}$ (K_{ser} nonlinear BOF)	251.48 kN	358.59 kN	42%

5 Discussion and Conclusions

The study presented in this document started from observations of the design process of some large timber structures that have been made thanks to the existence of Eurocode 5. This study has attempted to provide some initial answers to the questions and choice of solutions developed often in real time during the construction process. This study, which is based on experience with the design of timber structures and structural modelling of connections is summarised in the following. Three main recommendations that could be introduced in Eurocode 5 are proposed. Corresponding provision would help leading the designer in the dimensioning of multiple shear plane connections. These recommendations are expressed as follows:

- Lateral opening of connections due to fastener bending deformation and corresponding loads due to eccentricity in the load transfer in outer members have to be constrained until failure, in order to limit redistribution of loads between fasteners and shear planes.
- Structural measures have to be provided in order to avoid sequential failure of multiple fastener connections with multiple shear planes.
- Distribution of the load among the timber members in the connection has to be guaranteed until failure. Single- and double-shear dowel-type connections should be preferred instead of multiple shear plane connections. However, if the continuity of the dowel in a multiple shear plane connection is necessary, a uniform distribution of normal stresses between each timber part should be aimed at, unless the induced shear stresses are verified.

References

[1] Biger JP, Bocquet JF, Racher P (2000) *Testing and designing the joints for the pavilion of Utopia*. World Conference on Timber Engineering, Paper 4.3.3. Whistler, Canada.

[2] Perrin JP, Quost D, Bocquet JF, Racher P, Biger JP (1998) *The pavilion of Utopia*. World Conference on Timber Engineering, Vol. 2, pp. 80-87. Montreux, Switzerland.

[3] Racher P (2000) *Eléments mixtes dans les structures bois: Assemblages bois-métal et planchers bois-béton*. Forum Holzbau, http://www.forum-holzbau.com/pdf/p_racher_01.pdf.

[4] Cramer CO (1968) Load distribution in multiple-bolt tension joints. *Journal of the Structural Division* **94**(5):1101-1117.

[5] Lantos G (1969) Load distribution in a row of fasteners subjected to lateral load. *Wood Science* **1**(3):129-136.

[6] *STEP 1* (1995) Eurofortech, ISBN 90-5645-001-8.

[7] *STEP 1* (1995) Eurofortech, ISBN 90-5645-002-6.

[8] Bocquet JF (1997) *Modélisation des déformations locales du bois dans les assemblages brochés et boulonnés*. PhD thesis, Université Blaise Pascal, Clermont-Ferrand, France.

[9] Bocquet JF (2004) *Fiabilité et compétitivité des assemblages de structures en bois: Mécanismes de ruine associés aux assemblages à plans multiples de cisaillement: Détermination des paramètres du modèle de calcul des assemblages à plans multiples à plusieurs tiges sur les assemblages bois/bois du programme incendie*. Rapport d'études, 64 pages.

[10] Bocquet JF (2004) *Fiabilité et compétitivité des assemblages de structures en bois: Mécanismes de ruine associés aux assemblage à plans multiples de cisaillement: Détermination des dimensions optimales d'assemblages à quatre plans de cisaillement bois métal*. Rapport d'études, 39 pages.

[11] http://supermomo99.skyrock.com/3247855244-FONDATION-LOUIS-VUITTON-DETAIL-DES-SUPPORTS-DE-CHARPENTE-photo-SM99.html

[12] Bocquet JF, Barthram C, Pineur A (2012) *L-block failure of dowelled connections subject to bending reinforced with threated rods*. CIB-W18 Meeting 45, Paper 45-7-3. Växjö, Sweden.

[13] Bocquet JF (2012) *Solutions d'assemblages fréttés – Le projet Frank Gehry / Fondation Louis Vuitton*. 2ème Forum International Bois Construction Beaune.

[14] Deline E, Bocquet JF (2013) *La Fondation Louis Vuitton pour la Création: Une structure bois d'exception à Paris*. 3ème Forum International Bois Construction Beaune.

[15] Rossi S, Crocetti R, Honfi D, Frühwald Hansson E (2016) *Load-bearing capacity of ductile multiple shear steel-to-timber*. World Conference on Timber Engineering, Vienna, Austria.

[16] Sawata K, Kawamura H, Takanashi R, Ohashi Y, Sasaki Y (2016) *Effects of arrangement of steel plates on dowel type cross laminated timber joints with two slotted-in steel plates subjected to lateral force.* World Conference on Timber Engineering, Vienna, Austria.

[17] Sauvat N (2001) *Résistance d'assemblages de type tige en structure bois sous chargements cycliques complexes*. PhD thesis, LERMES/CUST, Université Blaise Pascal, Clermont-Ferrand, France.

[18] Bocquet JF, Sauvat N, Racher P (2004). *Fiabilité et compétitivité des assemblages de structures bois: Mécanismes de ruine associés aux assemblages à plans multiples*. Technical report, Centre Technique du Bois et de l'Ameublement, Paris.

[19] Schweigler M, Bader TK, Hochreiner G, Lemaître R (2018) Parameterization equations for the nonlinear connection slip applied to the anisotropic embedment behaviour of wood. *Composites Part B: Engineering* **142**:142-158.

[20] Hirai T (1983) Nonlinear load-slip relationship of bolted wood-joints with steel side members II. Application of the generalized theory of a beam on an elastic foundation. *Mokuzai Gakkaishi* **29**:839-844.

Design of three typologies of step joints – Review of European standardized approaches

Jorge M. Branco
University of Minho
Guimarães, Portugal

Maxime P. Verbist
University of Minho
Guimarães, Portugal

Thierry Descamps
University of Mons
Belgium

Summary

The present paper aims at investigating three different step joints which can often be encountered in existing timber trusses: single step joint, double step joint and single step joint with tenon-mortise. For each step joint, some design rules and geometrical recommendations have been gathered from different European standards and authors, since no design equation is conventionally defined. Therefore, design models have been determined for the three typologies of step joints according to their geometrical parameters and the emergence of two failure modes: shear cracking in the tie beam and crushing at the front-notch surface. In order to check the reliability of the design models, experiments on the single step joints have been performed by modifying the geometrical parameters.

1. Introduction

When assessing the roof of existing buildings, engineers have to deal with timber trusses made of badly preserved step joints (SJ) linking the rafter with the tie beam (Fig. 1). Since they are in contact with wet masonry walls, the SJ located at the foot of timber trusses between the rafter and the tie beam are continuously damaged over time. Therefore, the evaluation of these joints is a major issue for engineers involved in a restoration project. Before thinking about any intervention technique, engineers have to properly understand how the SJ fails, which parameters (geometry of the joint, mechanical properties of the wood) influence the failure modes and how the internal forces are distributed into the joint to finally figure out how to design the traditional carpentry joints. Hence, the present chapter aims at raising those questions by focusing on three SJ typologies: joints: single step joint (SSJ), double step joint (DSJ) and single step joint with tenon-mortise (SSJ-TM). Based on available geometrical recommendations from European Standards (e.g. Eurocode 5 [1], DIN 1052

[2], SIA 265 [3]) and authors (e.g. Siem and Jorissen [4], Bocquet [5]), design equations can be established for the three SJ typologies, in respect with both failure modes: shear cracking in the tie beam, and crushing at the front-notch surface. In order to check the reliability of the design equations and the emergence conditions of both failure modes, tests on several SSJ specimens from Verbist et al. [6] have been performed under monotonic compression tests in the rafter, by modifying the geometrical parameters. For the same purposes, DSJ and SSJ-TM specimens are going to be tested in the near future.

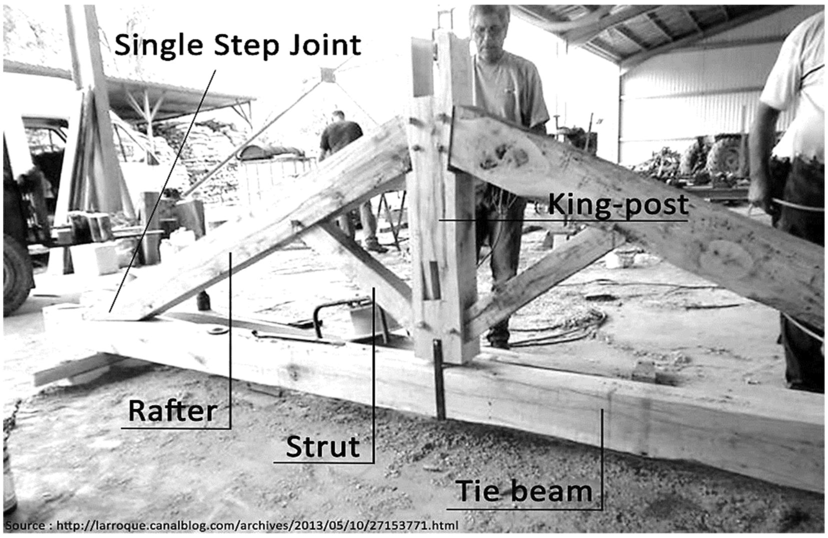

Fig. 1. Timber elements in traditional carpentry (king-post truss), from [6].

2. Single step joint without tenon-mortise

According to Yeomans [7], the single step joint (SSJ) is the most common step joint used to connect the rafter with the tie beam at the foot of timber trusses shown in Fig. 1. Even if the geometry of this joint (Fig. 2) is simple, one may pick up three SSJ families according to Oslet [8], from the past till today: the geometrical configuration *ideal design* (GCID), the geometrical configuration *perpendicular to the tie beam* (GCPTB) and the geometrical configuration *perpendicular to the rafter* (GCPR). Although it provides higher mechanical performances, the GCID is the most recent SSJ family since its geometry requires an accurate timber cutting, using new technologies (e.g. Computer Numerical Control (CNC)).

2.1 Geometrical parameters

As illustrated in Fig. 2, the single step joint (SSJ) is characterized by a single heel, including two contact surfaces, between the rafter and the tie beam. The first contact area called "front-notch surface'' is located in the front of the joint whereas the last one, called "bottom-notch surface", is situated at the bottom of the same joint. The front-notch (bottom-notch) surface is inclined under an angle α (γ) to the normal of the grain (parallel to the grain) in the tie beam. The SSJ is also characterized by the heel depth t_v, the shear length l_v, and the rafter skew angle β. From Siem and Jorissen [4], some recommendations about the geometrical SSJ parameters can be proposed from several European standards and National Annexes [2, 3, 9-16] as detailed in Table 1. If the prescriptions relative to the maximum heel depth t_v cannot be met, added design equations (not detailed in the present chapter) including the tensile strength parallel to the grain and the shear strength perpendicular to the grain should be checked when designing the cross-section of the tie beam (Allais et al. [17]).

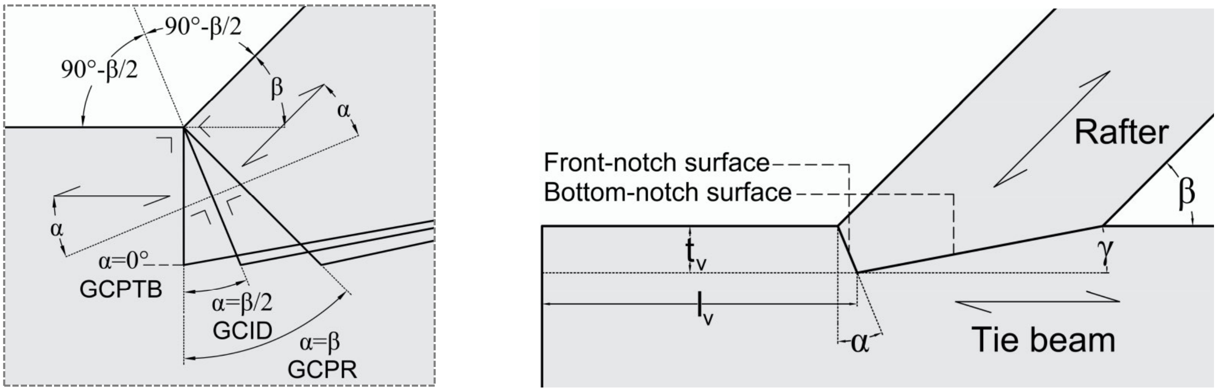

Fig. 2. General SSJ geometrical parameters, and inclination of the front-notch surface according to the three SSJ families from [6].

Table 1. Geometrical recommendations on SSJ parameters with respect to tie beam height h_{tb}, from different national standards according to Siem and Jorissen [4].

	Germany [2, 9-10], Italy [11], Switzerland [3]			Netherlands [12-15]		Norway [16]		
β	$\leq 50°$	$50° \leq \beta \leq 60°$	$\geq 60°$	$\leq 50°$	$\geq 60°$	$\leq 50°$	$50° \leq \beta \leq 60°$	$\geq 60°$
t_v	$\leq \frac{h_{tb}}{4}$	Linear interpolation	$\leq \frac{h_{tb}}{6}$	$\leq \frac{h_{tb}}{4}$	$\leq \frac{h_{tb}}{5}$	$\leq \frac{h_{tb}}{4}$	$\leq \frac{h_{tb}}{5}$	$\leq \frac{h_{tb}}{6}$
l_v	$\geq$ 150 mm [3]	$\leq 8 \cdot t_v$, $\geq$ 200 mm [2]		$\geq 6 \cdot t_v$		$\geq$ 150 mm		
α	$\beta/2$ [3]	$\gamma \leq \alpha \leq \beta$ [2]		$\beta/2 \leq \alpha \leq \beta$		$\beta/2$		

2.2 Review of design equations

2.2.1 Calculation of the characteristic compressive strength

According to Siem and Jorissen [4], Hankinson's and Norris's criteria can predict the characteristic compressive strength of the timber $f_{c,\alpha,k}$ under an angle α to the grain. Conform with Eurocode 5 [1], Hankinson's criterion (1) is based on the combination of the compressive strengths parallel $f_{c,0,k}$ and perpendicular $f_{c,90,k}$ to the grain. The factor $k_{c,90}$ depends on the loading geometrical configuration, involving the spreading of the compressive stress perpendicular to the grain. As the use conditions of this factor are not defined by Eurocode 5 [1] for traditional carpentry joints, Siem and Jorissen [4] suggest to not take it into account in the design equations of the joints ($k_{c,90} = 1$).

$$f_{c,\alpha,k} = \frac{f_{c,0,k}}{\frac{f_{c,0,k}}{k_{c,90} \cdot f_{c,90,k}} \cdot \sin^2\alpha + \cos^2\alpha} \quad (1)$$

Being very similar to Hankinson's criterion, Norris' criterion from DIN 1052 [2] includes the delamination of the timber grain due to the compressive stress $\sigma_{c,\alpha,k}$ on the surface inclined under an angle α to the grain, by introducing the characteristic shear strength $f_{v,k}$ parallel to the grain. The factor $k_{c,\alpha}$ (3) is related to the loading geometrical configuration, and to the spreading of the compressive stress under an angle α to the grain. Since this coefficient is not defined by the Standard DIN 1052 [2] when designing traditional carpentry joints, it can be given ($k_{c,\alpha} = 1$) as per Siem and Jorissen [4].

$$f_{c,\alpha,k} = \frac{f_{c,0,k} \cdot k_{c,\alpha}}{\sqrt{\left(\frac{f_{c,0,k}}{f_{c,90,k}} \cdot \sin^2 \alpha\right)^2 + \left(\frac{f_{c,0,k}}{1.5 \cdot f_{v,k}} \cdot \sin\alpha \cdot \cos\alpha\right)^2 + \cos^4 \alpha}} \tag{2}$$

$$k_{c,\alpha} = 1 + \sin\alpha \cdot \left(k_{c,90} - 1\right) \tag{3}$$

2.2.2 Design equation to account for shear cracking

As shown in Fig. 3, the design rafter load-bearing capacity, noted $N_{rafter,Rd}$, must be checked by the equations (4)-(5) below in order to avoid shear cracking in the tie beam for all SSJ geometrical configurations, according to Siem and Jorissen [4] and Bocquet [5]:

$$N_{rafter} \leq N_{rafter,Rd} = k_{v,red} \cdot \frac{k_{mod}}{\gamma_M} \cdot f_{v,k} \cdot \frac{b \cdot k_{cr} \cdot l_{v,eff}}{\cos\beta} \tag{4}$$

$$l_{v,eff} = \min\left(l_v \ , \ 8 \cdot t_v\right) \tag{5}$$

The reduction factor noted $k_{v,red}$ takes into account the non-uniform shear stress distribution along the grain in the tie beam which entails the decrease of the shear capacity in the single step joint. Conform with the Dutch National Annex from Eurocode 5 (Siem and Jorissen [4]), the reduction factor $k_{v,red} = 0.8$ can be applied to reduce the characteristic shear strength of timber parallel to the grain, noted $f_{v,k}$.

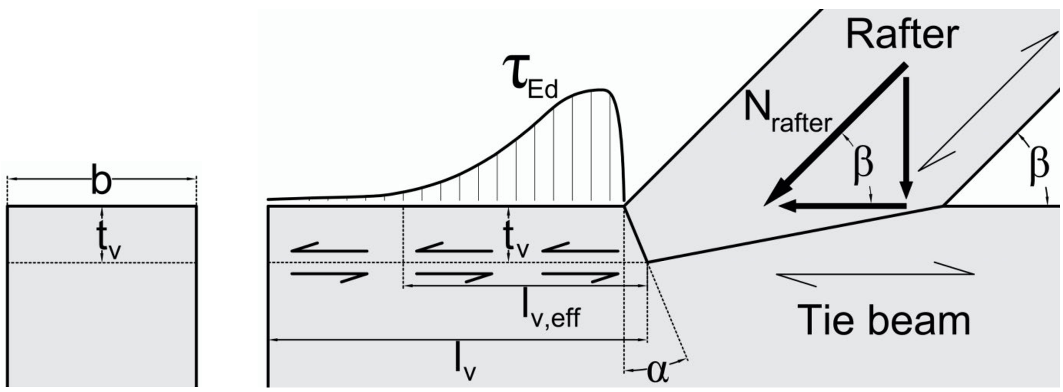

Fig. 3. Schema of the non-uniform shear stress distribution τ_{Ed} at the heel depth t_v, parallel to the grain in the tie beam, from [6].

Conform with Eurocode 5 [1], the parameters k_{mod} and γ_M are the modification factor and the partial coefficient of timber material, and k_{cr} is the reduction factor of the tie beam width b, which considers the influence of cracks on the shear strength along the grain for timber elements subject to bending. Based on Amendment 1 of Eurocode 5 [18], the reduction factor k_{cr} = 0.67 can be imposed for solid timber. When dealing with traditional timber carpentries, this reduction value can be given up if there is no significant eccentricity d_{supp} between the joint node and the support area. According to Allais et al. [17], the coefficient k_{cr} = 1 can be imposed if the condition $d_{supp} \leq h_{tb}$ is checked by considering the tie beam height h_{tb}. Based on the maximum limitation of the shear length ($l_{v,max} = 8 \cdot t_v$) imposed by DIN 1052 [2], the effective shear length $l_{v,eff}$ also takes into account the non-uniform shear stress distribution in the tie beam. From equation (5), the effective shear length then encompasses the shear stress distribution whose concentration peak is always located near the SSJ heel.

2.2.3 Design equation to account for crushing at the front-notch surface

As illustrated in Fig. 4, the design rafter load-bearing capacity, noted $N_{rafter,Rd}$, must be checked at the rafter and tie beam side respectively by equations (6)-(7) and (8)-(9) in order to avoid the crushing at the front-notch surface for the GCID ($\alpha = \beta/2$), according to Siem and Jorissen [4] and Bocquet [5]. Concerning the GCPTB characterized by an inclination angle of the front-notch surface $\alpha = 0°$, the crushing always occurs at the rafter side as the related compressive strength is lower than that at the tie beam side. Hence, the design rafter load-bearing capacity from the GCPTB, noted $N_{rafter,Rd}$, has to be checked only at the rafter side by equations (6)-(7). In contrast to the GCPTB, the crushing always appears at the tie beam side for the GCPR due to its inclination angle of the front-notch surface $\alpha = \beta$. Thereby, the design rafter load-bearing capacity from the GCPR, noted $N_{rafter,Rd}$, is required only at the tie beam side by equations (9)-(10) below.

$$N_{rafter} \leq N_{rafter,Rd} = \frac{k_{mod}}{\gamma_M} \cdot f_{c,\beta-\alpha,k} \cdot \frac{b \cdot t_{ef,1} \cdot \sin(90+\alpha-\gamma)}{\sin(90-\beta+\gamma)} \tag{6}$$

$$t_{ef,1} = \frac{t_v}{\cos\alpha} + 30 \cdot \sin(\beta-\alpha) + 30 \cdot \sin(\alpha-\gamma) \tag{7}$$

$$N_{rafter} \leq N_{rafter,Rd} = \frac{k_{mod}}{\gamma_M} \cdot f_{c,\alpha,k} \cdot \frac{b \cdot t_{ef,2} \cdot \sin(90+\alpha-\gamma)}{\sin(90-\beta+\gamma)} \tag{8}$$

$$t_{ef,2} = \frac{t_v}{\cos\alpha} + 30 \cdot \sin\alpha + 30 \tag{9}$$

$$N_{rafter} \leq N_{rafter,Rd} = f_{c,\alpha,k} \cdot \frac{k_{mod}}{\gamma_M} \cdot b \cdot t_{ef,2} \tag{10}$$

The mechanical property $f_{c,\alpha,k}$ ($f_{c,\beta-\alpha,k}$) stands for the characteristic compressive strength of timber at the front-notch surface under an angle α ($\beta - \alpha$) to the grain in the tie beam (rafter). The geometrical parameter $t_{ef,1}$ ($t_{ef,2}$) is the effective length of the front-notch surface, which considers the compressive stress spreading in the rafter (tie beam). Again, parameters k_{mod} and γ_M are respectively the modification factor and the partial safety coefficient.

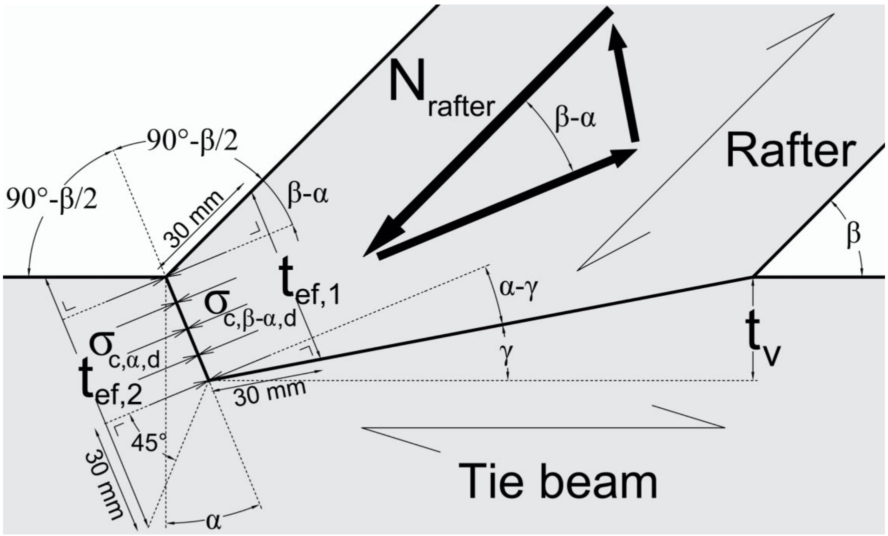

Fig. 4. Schema of the effective lengths $t_{ef,1}$ and $t_{ef,2}$, respectively in the rafter and tie beam for SSJ geometrical configurations, from [6].

2.3 Experimental Campaign

2.3.1 Experimental process and specimens

In Verbist et al. [6], several specimens of single step joints (SSJ) have been tested in the lab, under normal monotonic compression in the rafter, as shown in Fig. 5. In order to determine their mechanical behaviour (i.e. rafter load-bearing capacity, and the appearance conditions of both failure modes) and to check the reliability of design equations, the SSJ geometrical parameters have then been modified.

Because the GCPR and GCPTB are the most encountered SSJ in old traditional carpentries whereas the GCID is only present in new timber trusses, all three SSJ families have been tested by modifying the inclination angle α of the front-notch surface. Because the emergence of both failure modes is mainly conditioned by the rafter skew angle β in respect with design equations, two values have then been selected: $\beta = 30°$ for shear cracking in the tie beam, $\beta = 45°$ for crushing at the front-notch surface. Note that the following specimen labelling is used to describe each SSJ geometrical configuration: GCTB_30o_tv25_240SL. The first term deals with the three SSJ families (i.e. GCID, GCPR, and GCPTB). The second term is related to the rafter skew angle β [°]. The last two terms determine the size of the heel depth t_v [mm] and the shear length l_v [mm] respectively.

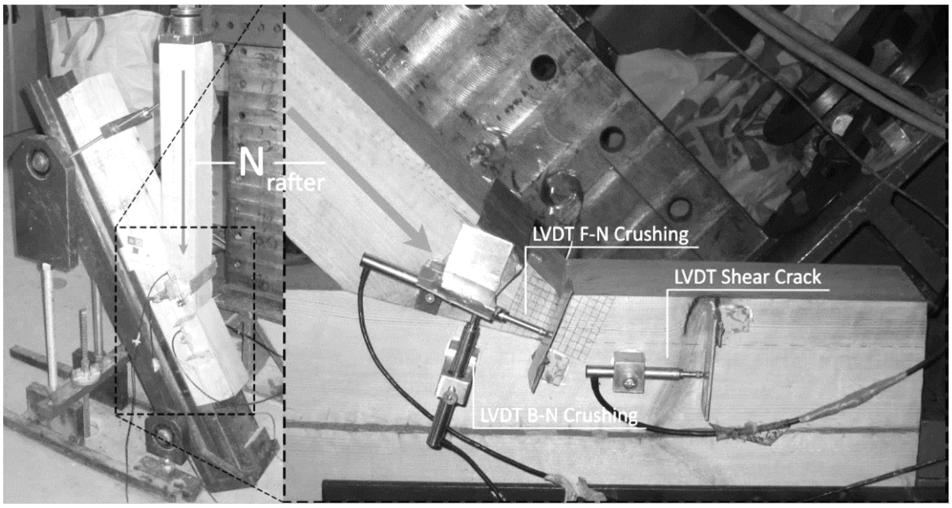

Fig. 5. Setup of SSJ specimens under normal monotonic compression tests [6].

Pinus sylvestris has been chosen as wood species for the experiments on SSJ specimens. From the mechanical characterization of small timber samples in compression (Verbist et al. [6]), *Pinus sylvestris* is featured by: the average compressive strengths $f_{c,0,m}$ = 29.4 MPa, $f_{c,15,m}$ = 20.7 MPa, $f_{c,30,m}$ = 12.9 MPa, $f_{c,90,m}$ = 3.7 MPa (parallel, inclined under 15° and 30° angles, and perpendicular to the grain respectively), and the average shear strength $f_{v,m}$ = 4 MPa parallel to the grain. Based on these wood mechanical properties, the theoretical rafter load-bearing capacities ($N_{rafter,theo}$) can then be calculated by the SSJ design equations previously defined for both failure modes, as detailed in Table 2.

2.3.2 Discussion about design equations

In order to check the reliability of SSJ design equations with respect to the failure modes, both maximum normal loads in the rafter $N_{rafter,exp}$ for each SSJ configuration tested can be compared with the theoretical rafter load-bearing capacity ($N_{rafter,theo}$) as detailed in Table 2. From the SSJ design equations, the following parameters have been chosen for all the SSJ geometrical configurations: k_{mod} = 0.9, γ_M = 1.3, $k_{c,\alpha}$ = 1 and $k_{v,red}$ = 0.8. Based on the general formulation COV = 100 · Deviation/Average, the coefficient of variation COV [%] is defined for the experimental results from a same SSJ geometrical configuration such as Deviation = $|N_{rafter,exp1} - N_{rafter,exp2}|$ and Average = $(N_{rafter,exp1} - N_{rafter,exp2})/2$. Besides, the relative variation $\Delta_{rel,rafter}$ [%] of maximum normal loads in the rafter between the smallest of both experimental results and the theoretical value is determined such as $\Delta_{rel,rafter} = 100 \cdot (N_{rafter,expmin} - N_{rafter,theo})/N_{rafter,theo}$ for each SSJ configuration, according to both failure modes.

As illustrated in Figs. 3 and 6, the shear crack emerges at the heel depth t_v in the tie beam and spreads along the shear length l_v to the tie beam end. From Verbist et al. [6], the shear crack may appear as the final failure mode after high crushing at the front-notch surface. In addition to the rafter skew angle β, the emergence of shear crack is conditioned by the inclination angle of the front-notch surface α (i.e. the three SSJ families) and by the geometrical proportion between the shear length and the heel depth l_v/t_v. The SSJ design equations against the shear crack can predict the maximum normal load in the rafter for the majority of $\beta = 30°$ specimens tested, apart from the tv30_160SL specimens and the GCPR for which they are too restrictive ($\Delta_{rel,rafter} \approx 50\%$). Moreover, the crushing at the front-notch sometimes emerges instead of the shear crack for the GCID and GCPR characterized by high geometrical proportions $l_v/t_v \geq 8$ while the shear crack is more likely to occur for the GCPTB. Hence, the reduction factor $k_{v,red}$ taking into account the non-uniform shear stress in the tie beam (Fig. 3) should vary according to the geometrical proportion l_v/t_v and to the inclination angle α of the front-notch surface. To simplify these correlations, the reduction factor $k_{v,red} = 0.8$ can be imposed in the design equations for all the SSJ geometrical configurations including $l_v/t_v \geq 6$ whereas it can be neglected for the other specimens ($k_{v,red} = 1$) checking $l_v/t_v < 6$. If further research aims at optimizing the SSJ design equation against shear cracking, the reduction factor $k_{v,red}$ should then be calculated by empirical equations such as $k_{v,red} = f(\alpha, l_v/t_v)$.

Fig. 6. Shear crack parallel to the grain at the heel depth in the tie beam [6]

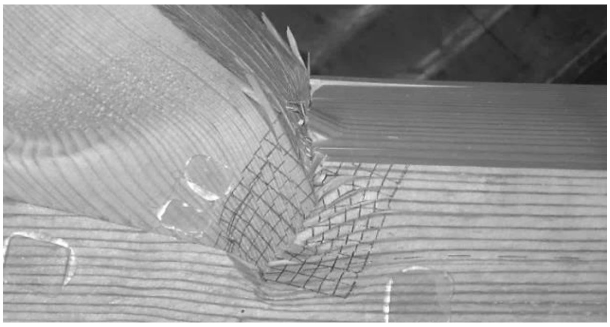

Fig. 7. Crushing at the front-notch surface in rafter and tie beam side [6]

As shown in Fig. 7, the compressive crushing occurs at the front-notch surface in the rafter and/or the tie beam. Regarding this failure mode, the relevance of design equations depends on the rafter skew angle β and the inclination angle α of the front-notch surface. Concerning the GCID, the design equations can predict the maximum normal load in the rafter although they are quite safe ($\Delta_{rel,rafter} \approx 35\%$) for the $\beta = 45°$ specimens. This safety may come from the assumption to neglect the friction forces at the contact surfaces of the SSJ in the design equations. Indeed, the higher the rafter skew angle β, the higher the friction forces and thus the rafter load-bearing capacity of the joint. Therefore, the friction forces should be taken into account to design the SSJ featuring high rafter skew angles $\beta \geq 30°$. However, the design equations cannot anticipate the experimental values $N_{rafter,exp}$ concerning the GCPR and the GCPTB because they are too restrictive ($\Delta_{rel,rafter} >> 50\%$) for the $\beta = 45°$ specimens. The underestimation of the rafter load-bearing capacity may come from the low reliability of the criteria from the state-of-the art of Siem and Jorissen [4] when calculating the characteristic compressive strength $f_{c,\alpha,k}$ under inclination angles $\alpha \geq 30°$ to the grain.

Because the loading factor $k_{c,\alpha}$ has been neglected ($k_{c,\alpha} = 1$) in the SSJ design equations, the theoretical approximations of the characteristic compressive strength $f_{c,\alpha,k}$ are too restrictive when the inclination angle α of the loading to the grain is superior to 30°. As the inclination angle α of the front-notch surface is equal to the rafter skew angle β for the GCPR at the tie beam side and for the GCPTB at the rafter side, the relative differences $\Delta_{rel,rafter}$ between $N_{rafter,exp}$ and $N_{rafter,theo}$ is higher than those for the GCID specimens featured by a lower inclination angle of compressive loading to the grain: $\alpha = \beta/2$. Hence, the factor $k_{c,\alpha}$ should be taken into account in the SSJ design equations ($k_{c,\alpha} > 1$) for the GCPTB and GCPR characterized by a moderate inclination angle of the front-notch surface ($\alpha \geq 30°$).

Table 2. Comparison between the experimental and theoretical results for the SSJ specimens tested, from [6].

Specimen labelling	$N_{rafter,exp}$ [kN]	COV [%]	$N_{rafter,theo}$ [kN]	$\Delta_{rel,rafter}$ [%]	Failure mode
GCID_30°_tv25_240SL	53 63	17	50 52	6 2	CFN SC
GCID_30°_tv30_160SL	65 75	14	42	55	SC
GCID_30°_tv30_240SL	52 67	25	55 62	5.5 8	CFN SC
GCID_30°_tv40_240SL	70 77	9.5	62	13	SC
GCID_45°_tv30_240SL	67 80	18	51	31	CFN
GCPR_30°_tv25_240SL	56 53	6	50	6	CFN
GCPR_30°_tv30_160SL	60 75	22	42	43	SC
GCPR_30°_tv30_240SL	85 90	6	54 62	57 37	CFN SC
GCPR_30°_tv40_240SL	78 90	14	62	26	CFN SC
GCPR_45°_tv30_240SL	80 95	17	41 76	95 5	CFN SC
GCPTB_30°_tv25_240SL	62 70	12	52	19	SC
GCPTB_30°_tv30_160SL	60 68	12.5	42	43	SC
GCPTB_30°_tv30_240SL	55 70	24	62	11	SC
GCPTB_30°_tv40_240SL	68 80	16	62	10	SC
GCPTB_45°_tv30_240SL	68 88	26	34	100	CFN

Legend: CFN = Crushing at the front-notch surface; SC = Shear crack.

3. Double step joint

Though the single step joint (SSJ) is the most common joint connecting the rafter and the tie beam, the double step joint (DSJ) is sometimes encountered within existing timber trusses, as illustrated in Fig. 8. When the limitation of the shear length l_v is too harsh (e.g. architectural geometrical restrictions), the DSJ is only used instead of the SSJ in order to prevent shear cracking by providing higher shear capacity to the step joint. Thanks to the wide joint including two heels between the rafter and the tie beam, the DSJ provides higher shear capacity than the SSJ does. Because the design requires accurate timber cutting using new technologies (e.g. CNC), the DSJ should be used only when necessary, for low rafter skew angle β according to Siem and Jorissen [4].

Fig. 8. Example of double step joint in-situ, from [19].

3.1 Geometrical parameters

As illustrated in Fig. 9, the "front heel" is located in the front whereas the last one called "rear heel" is situated in the rear of the DSJ. Similarly to the SSJ, each heel includes two contact surfaces between the rafter and the tie beam: the front-notch surface which is located in the front, and the bottom-notch surface which is situated in the bottom of each heel. Whereas the inclination angles of the front-notch and bottom-notch surfaces (i.e. α and γ) in the front heel are identical to the three SSJ families (Oslet [8]), those in the rear heel are related to the GCPR (i.e. $\alpha = \gamma = \beta$). Besides, the shear length at the front heel depth $t_{v,1}$, noted $l_{v,1}$, stands for the distance between the top of the front heel and the tie beam edge along the grain whereas the shear length at the rear heel depth $t_{v,2}$, noted $l_{v,2}$, is the distance between the top of both DSJ heels along the tie beam grain. From Siem and Jorissen [4], some recommendations about the geometrical DSJ parameters can be proposed from several European Standards [2, 3, 11, 12, 16] as detailed in Table 3.

Table 3. Recommendations on DSJ geometrical parameters, Siem and Jorissen [4].

	Netherlands [12]	DE [2], CH [3]	Italy [11]	Norway [16]
β	$\leq 50°$	–	–	$\leq 45°$
$t_{v,1}$	–	$\leq h_{tb}/6$	$\leq 0.8 \cdot t_{v,2}$	$\leq h_{tb}/4$
$t_{v,2}$	–	$\leq h_{tb}/4$	–	$\geq h_{tb}/4$
Δt_v	≥ 15 mm	≥ 10 mm	≥ 10 mm	15 mm $\leq \Delta t_v \leq$ 20 mm
$l_{v,1}$	$\geq 6 \cdot t_{v,1}$	$\leq 8 \cdot t_{v,1}$, ≥ 200 mm [2] ≥ 150 mm [3]	–	–
$l_{v,2}$	–	$\leq 8 \cdot t_{v,2}$ [2]	–	–

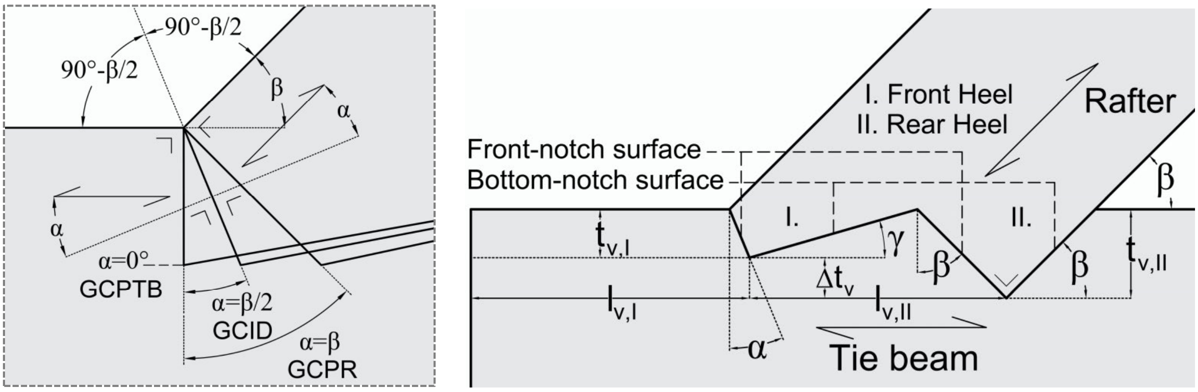

Fig. 9. General DSJ geometrical parameters and inclination of the front-notch surface in the front heel according to the three SSJ families, from [20].

3.2 Review of design equations

3.2.1 Design equation to account for shear cracking

As shown in Fig. 10, the design rafter load-bearing capacity, noted $N_{rafter,Rd,i}$, must be checked by the equations (11)-(12), similar to (4)-(5) from the SSJ design, in order to avoid shear cracking in the tie beam for each DSJ heel, according to Siem and Jorissen [4] and Bocquet [5]. The lowercase letter "i" from some geometrical parameters and coefficients stated in the equations (11)-(12) is related to the type of DSJ heel (i.e. i = I for the front heel; i = II for the rear heel).

$$N_{rafter,i} \leq N_{rafter,Rd,i} \cdot k_{v,red,i} \cdot f_{v,k} \cdot \frac{k_{mod}}{\gamma_M} \cdot \frac{b \cdot k_{cr} \cdot l_{v,eff,i}}{\cos\beta} \tag{11}$$

$$l_{v,eff,i} = \min\left(l_{v,i}\ ,\ 8 \cdot t_{v,i}\right) \tag{12}$$

Similar to the SSJ, the reduction factor $k_{v,red}$ takes into account the non-uniform shear stress distribution along the grain in the tie beam for each DSJ heel. The condition $k_{v,red} = 0.8$ should then be applied in the front and rear heels in order to reduce the characteristic shear strength $f_{v,k}$ of timber parallel to the grain in the tie beam. Based on the maximum limitation of the shear length ($l_{v,max,i} = 8 \cdot t_{v,i}$) imposed by DIN 1052 [2], the effective shear length $l_{v,eff,i}$ also takes into account the non-uniform shear stress distribution in the tie beam for each DSJ heel. With respect to the equation (12), the effective shear lengths $l_{v,eff,I}$ and $l_{v,eff,II}$ (equation (12)) encompass the non-uniform shear stress distribution whose concentration peaks are always located near the front and rear heels.

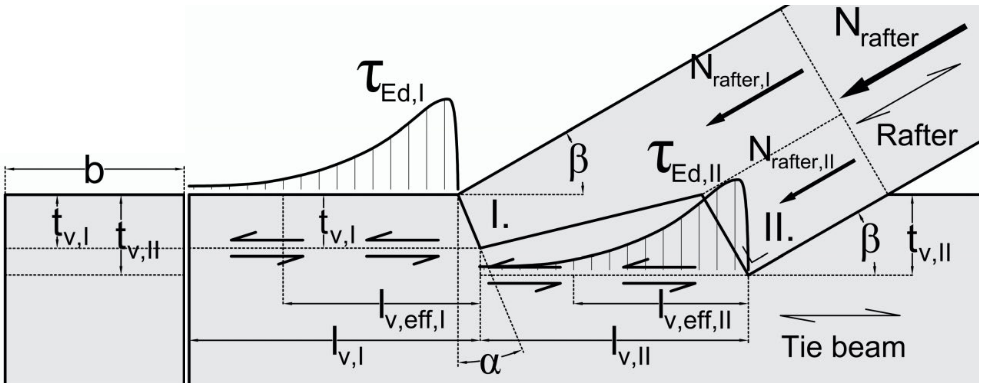

Fig. 10. Non-uniform shear stress distributions at both heels depths, from [20].

In Bocquet [5], a 2 mm gap is suggested at the front-notch surface in the front heel to optimize the rafter load-bearing capacity against shear cracking. If the geometrical recommendation is checked, the internal forces resolution in the DSJ becomes ideal and the rafter load-bearing capacities $N_{rafter,Rd,i}$ can reach their maximum values in both heels. Besides, shear cracking may emerge at the front and rear heel depths ($t_{v,\mathrm{I}}$ and $t_{v,\mathrm{II}}$) along their respective shear length ($l_{v,I}$ and $l_{v,II}$) as illustrated in Fig. 10. In order to prevent shear cracking in the tie beam at the front and rear heel depths, the maximum design rafter load-bearing capacity, noted $N_{rafter,max,Rd,max}$, must be checked by equation (13) such as a sum of design rafter load-bearing capacities related to both heels given by the equation (11).

$$N_{rafter,Rd,max} = N_{rafter,Rd,I} + N_{rafter,Rd,II} \tag{13}$$

If the recommendation from Bocquet [5] is not checked for the front-notch surface of the front heel, the internal forces resolution is not ideal. Thereby, the rafter load-bearing capacity from the rear heel doesn't reach its maximal value and the emergence of shear crack will only occur at the front heel depth $t_{v,1}$ in the tie beam. Hence, the total design rafter load-bearing capacity of double step joint (14), noted $N_{rafter,Rd,tot}$, is always between the design rafter load-bearing capacity the front heel ($N_{rafter,Rd,I}$) and the maximal design rafter load-bearing capacity ($N_{rafter,Rd,max}$) calculated by equations (11) and (13) respectively.

$$N_{rafter,Rd,I} \leq N_{rafter,Rd,tot} \leq N_{rafter,Rd,max} \tag{14}$$

3.2.2 Design equation to account for crushing at the front-notch surface

The design rafter load-bearing capacity against crushing at the front-notch surface in the front heel, noted $N_{rafter,Rd,I}$, must be checked by the equations (6) to (10) previously stated with respect to the three SSJ families. On the other hand, the design rafter load-bearing capacity against crushing at the front-notch surface in the rear heel, noted $N_{rafter,Rd,II}$, must be checked by the GCPR design equation (10), based on the effective length $t_{ef,II}$ (equation (15)) in the rear heel of DSJ as shown in Fig. 11.

$$t_{ef,II} = \frac{t_{v,II}}{\cos\beta} + 30 \cdot \sin(\beta - \gamma) + 30 \tag{15}$$

Similarly to the DSJ design model against the shear crack, both equations (13) and (14) must be satisfied in order to prevent crushing at the front-notch surfaces in the front and rear heels. When the internal force distribution is unbalanced between both DSJ heels, the rafter load-bearing capacity from the rear heel cannot reach its maximum value and the crushing will occur at the front-notch surface in the front heel. In the case of balanced internal forces, the value of the total design rafter load-bearing capacity of DSJ ($N_{rafter,Rd,tot}$) , should be taken as the value from the maximal design rafter load-bearing capacity ($N_{rafter,Rd,max}$), such as the sum of design rafter load-bearing capacities from the front and rear heels ($N_{rafter,Rd,I}$ and $N_{rafter,Rd,II}$ respectively).

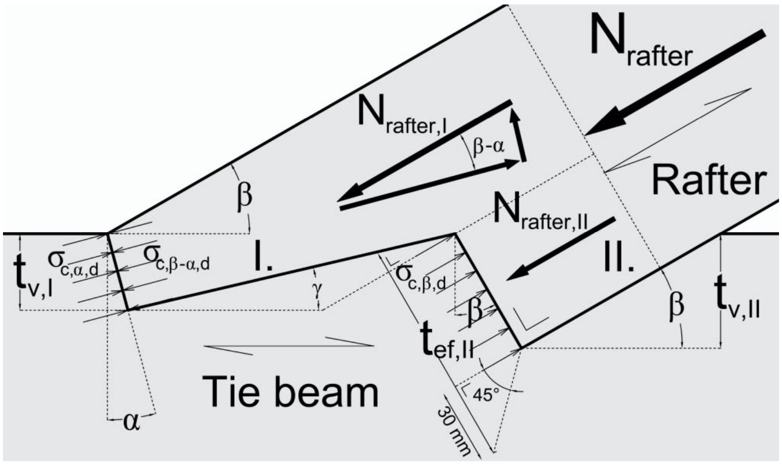

Fig. 11. Schema of the compressive stress spreading in both DSJ heels, and the effective length $t_{ef,II}$ in the rear heel at the tie beam side, from [20].

4. Single step joint with tenon-mortise

As the double step joint (DSJ), the single step joint with tenon-mortise (SSJ-TM) illustrated in Fig. 12 can be used instead of the single step joint (SSJ) to connect the tie beam with the rafter at the foot of timber trusses. The SSJ-TM can also provide compressive and/or shear capacities higher than those from the SSJ, by preventing better the emergence of failure modes, and thus guaranteeing the structural performances of timber carpentries. Because it is also featured by a complex geometry, the SSJ-TM has to be designed through accurate timber cutting ensured by experimented carpenters or new technologies use (e.g. CNC), and should then be promoted when necessary, alike the DSJ. Nevertheless, the SSJ-TM appears more often than the DSJ within existing timber trusses since the related knowledge and experience comes from the classical tenon-mortise connections which have commonly been used over time by the carpenters to link different elements in traditional timber structures (Grezel [21]).

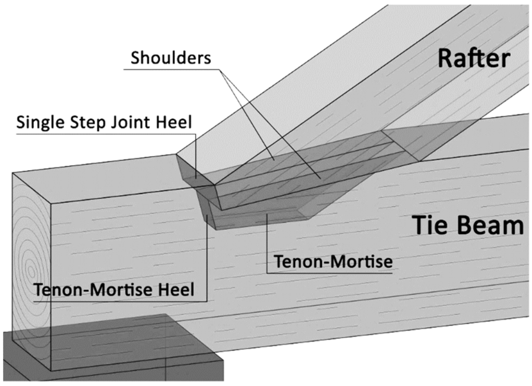

Fig. 12. Geometrical components of the SSJ-TM.

4.1 Geometrical parameters

As shown in Fig. 12, the single step joint with tenon-mortise (SSJ-TM) is featured by a tenon at the rafter side and by a mortise at the tie beam side. Among the three typologies of step joints, the SSJ-TM includes a higher amount of contact surfaces. From Figs. 12 and 13, it can be listed: (i) one front-notch surface and two bottom-notch surfaces called "shoulders" in the single step joint (SSJ) part; (ii) one front-notch surface, two bottom-notch surfaces and two lateral surfaces in the tenon-mortise (TM) part. Both lateral contact surfaces may bear off-plan loadings while the tenon-mortise provides significant bending moment capacity to the traditional joint. The inclination angle α of the front-notch surface and the inclination angle γ of the shoulders are identical to those related to the SSJ. Although several orientations of both bottom-notch surfaces in the TM part exist in the literature (Oslet [8], Grezel [21]), one of both bottom-notch surfaces (Fig. 13) is usually parallel to the grain in the tie beam whereas the other one is the extension from the rafter edge direction.

Two parts in the SSJ-TM heel should be distinguished: the SSJ heel, and the TM heel. The SSJ heel shown in Figs. 12 and 13 is characterised by the shoulder heel depth t_S (identical to the heel depth t_v from SSJ) whereas the TM heel is featured by the heel depth noted t_{TM}. According to Goss [22] and Descamps [23], the TM width b_{TM} illustrated in Fig. 13 cannot exceed one-third of the tie beam width b. Since the TM width b_{TM} is then inferior to the shoulder width b_S, the horizontal bottom-notch surface of the TM becomes the weakest part of the joint. To overcome this weakness, a 5 mm horizontal gap should be recommended at the bottom-notch surface between the tenon and the mortise in order to avoid any vertical loading transfer on that area (Descamps [23]). In that case, the internal forces of the joint can be distributed in the SSJ heel, namely at the front-notch surface and two bottom-notch surfaces (i.e. shoulders).

When the vertical component load rises in the shoulders with higher rafter skew angle ($\beta > 45°$), the mechanical behaviour of the single step joint with tenon-mortise is not optimal, by comparing it with the single or double step joints. For low rafter skew angle ($\beta \leq 45°$), it is better to increase the TM heel depth t_{TM} as much as possible, without exceeding the half-height of the tie beam h_{tb} in order to avoid entailing high tensile-shear stresses in the cross-section of the tie beam. Apart from these few recommendations, no conventional rule is defined for the other SSJ-TM geometrical parameters. However, the SSJ geometrical recommendations from the Table 1 can be used for the single step joint with tenon-mortise, by substituting the heel depth t_v by the shoulder heel depth t_S.

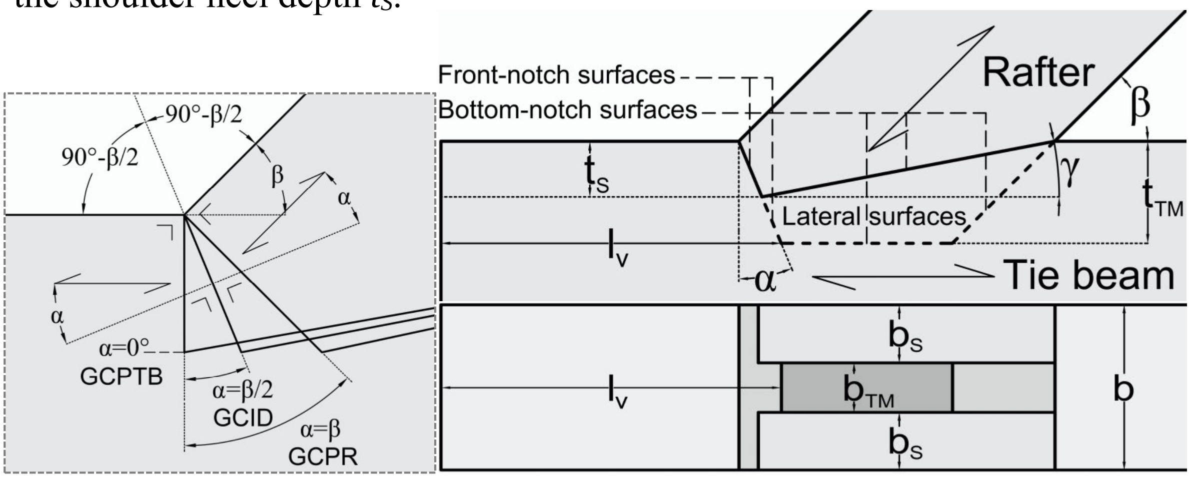

Fig. 13. General SSJ-TM geometrical parameters, and inclination of the front-notch surface according to the three SSJ families.

4.2 Review of design equations

4.2.1 Design equation to account for shear cracking

As shown in Fig. 14, shear cracking may occur at the TM heel depth t_{TM} along the grain in the tie beam. Similar to the other two step joints, the non-uniform shear stress distribution appears, by reducing the shear capacity of the joint. Therefore, the effective shear length $l_{v,eff}$ (equation (5)) and the reduction factor $k_{v,red}$ from the SSJ can be applied when designing the SSJ-TM.

The design rafter load-bearing capacity, $N_{rafter,Rd}$, must be checked by equation (16), in order to avoid shear cracking in the tie beam. Similar to the single step joint with double tenon-mortise (Bocquet [5]), two subcategories of failure modes related to shear cracking are taken into account in the SSJ-TM. As illustrated in Fig. 15, the overall shear crack at the TM heel depth in the tie beam can be induced either by the shear block along the path of both shoulders, or by the tensile crack in their cross-sections. Therefore, the overall shear crack, the shear block and the tensile crack have to be prevented by satisfying the equations (17), (18) and (19) respectively.

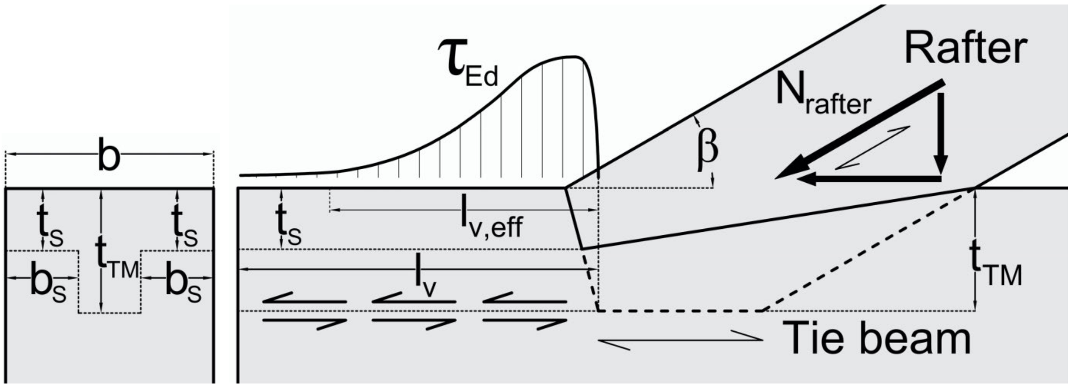

Fig. 14. Schema of the heterogeneous shear stress distribution at the tenon-mortise heel depth in the tie beam.

$$N_{rafter} \leq N_{rafter,Rd} = \max \begin{cases} F_{v,tb} \\ \min\left(F_{v,S}\ ,\ F_{t,S}\right) \end{cases} \tag{16}$$

$$F_{v,tb} = k_{v,red} \cdot \frac{k_{\text{mod}}}{\gamma_M} \cdot f_{v,k} \cdot \frac{b \cdot k_{cr} \cdot l_{v,eff}}{\cos\beta} \tag{17}$$

$$F_{v,S} = k_{v,red} \cdot \frac{k_{\text{mod}}}{\gamma_M} \cdot f_{v,k} \cdot \frac{2 \cdot \left(b_S + t_{TM} - t_S\right) \cdot k_{cr} \cdot l_{v,eff}}{\cos\beta} \tag{18}$$

$$F_{t,S} = \frac{k_{\text{mod}}}{\gamma_M} \cdot f_{t,0,k} \cdot \frac{2 \cdot b_S \cdot \left(t_{TM} - t_S\right)}{\cos\beta} \tag{19}$$

As for the other two typologies of step joints, the value $k_{v,red} = 0.8$ could be applied in order to reduce the characteristic shear strength $f_{v,k}$ of timber parallel to the grain in the tie beam at the TM heel depth. The mechanical property $f_{t,0,k}$ stands for the characteristic tensile strength of timber parallel to the grain in the tie beam.

The emergence of the T-shaped shear block and the tensile crack in the shoulders is conditioned by the difference between the TM and SSJ heel depths, noted Δt_v. The higher the geometrical parameter Δt_v, the higher the risk of the T-shaped shear block appearance. Besides, the load-bearing capacity of the joint against shear block along the shoulders, noted $F_{v,S}$, is higher (lower) than that against the overall shear crack in the tie beam noted $F_{v,tb}$ (the tensile crack in the shoulder cross-sections, noted $F_{t,S}$), when raising the difference of heel depths between the TM and the SSJ. Therefore, the T-shaped shear block in the tie beam should govern as the main subcategory of failure modes in order to optimize the SSJ-TM mechanical behaviour. To this end, ongoing research aims at determining the minimal value of Δt_v for which the shear capacity of the traditional joint is significantly higher than that from the SSJ.

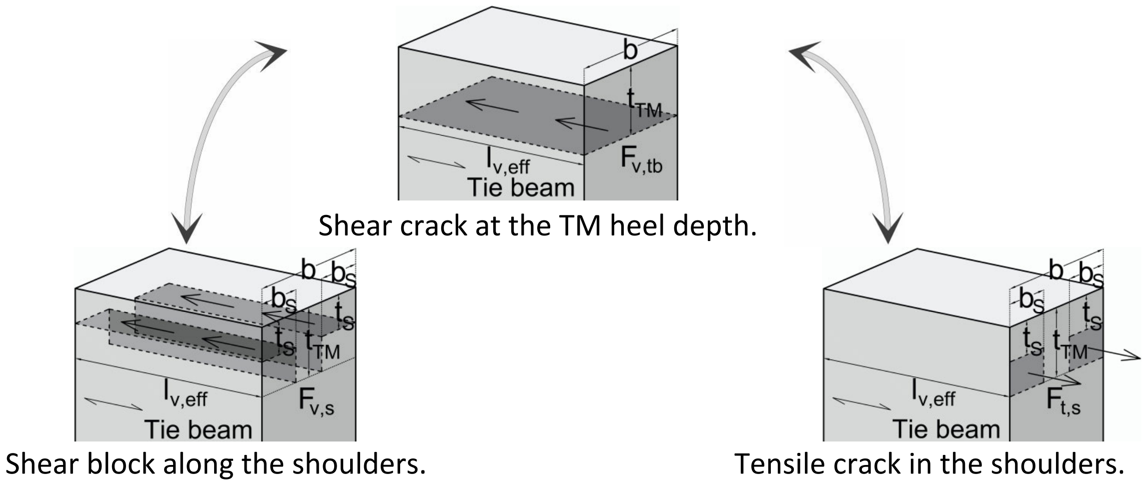

Fig. 15. Subcategories of failure modes related to the shear crack at the TM heel depth parallel to the grain of the tie beam.

4.2.2 Design equation to account for crushing at the front-notch surface

As illustrated in Fig. 16, the design rafter load-bearing capacity $N_{rafter,Rd}$ has to be checked at the rafter and tie beam side respectively by the equations (7), (20) to (22), (9) and (23) to (25) in order to avoid the crushing at the front-notch surface for the GCID ($\alpha = \beta / 2$). Concerning the GCPTB characterized by an inclination angle of the front-notch surface $\alpha = 0°$, the crushing always occurs at the rafter side as the related compressive strength is lower than that at the tie beam side. Hence, the checking of the design rafter load-bearing capacity from the GCPTB, $N_{rafter,Rd}$, is required only at the rafter side by the equations (7) and (20) to (22). In contrast to the GCPTB, the crushing always appears at the tie beam side for the GCPR as this SSJ configuration is featured by an inclination angle of the front-notch surface $\alpha = \beta$. Thereby, the design rafter load-bearing capacity from the GCPR, $N_{rafter,Rd}$, must be checked only at the tie beam side by the equations (9) and, (24) to (26) below.

$$N_{rafter} \le N_{rafter,Rd} = f_{c,\beta-\alpha,k} \cdot \frac{k_{mod}}{\gamma_M} \cdot \frac{A_{c,ef,1} \cdot \sin(90+\alpha-\gamma)}{\sin(90-\beta+\gamma)} \tag{20}$$

$$A_{c,ef,1} = b \cdot t_{S,ef,1} + (b - 2 \cdot b_S) \cdot t_{TM,ef,1} \tag{21}$$

$$t_{TM,ef,1} = \frac{t_{TM} - t_S}{\cos\alpha} + \frac{30 \cdot \sin\gamma}{\cos(\gamma-\alpha)} \tag{22}$$

$$N_{rafter} \le N_{rafter,Rd} = f_{c,\alpha,k} \cdot \frac{k_{mod}}{\gamma_M} \cdot \frac{A_{c,ef,2} \cdot \sin(90+\alpha-\gamma)}{\sin(90-\beta+\gamma)} \tag{23}$$

$$A_{c,ef,2} = b \cdot t_{S,ef,2} + (b - 2 \cdot b_S) \cdot t_{TM,ef,2} \tag{24}$$

$$t_{TM,ef,2} = \frac{t_{TM} - t_S}{\cos\alpha} \tag{25}$$

$$N_{rafter} \leq N_{rafter,Rd} = \frac{k_{mod}}{\gamma_M} \cdot f_{c,\alpha,k} \cdot A_{c,ef,2} \tag{26}$$

The mechanical property $f_{c,\alpha,k}$ ($f_{c,\beta-\alpha,k}$) stands for the characteristic compressive strength of timber at the front-notch surface under an angle α ($\beta - \alpha$) to the grain in the tie beam (rafter). The four geometrical parameters $t_{s,ef,1}$, $t_{TM,ef,1}$, $t_{S,ef,2}$, $t_{TM,ef,2}$ are the effective lengths of the front-notch surface related to the compressive stress spreading in the shoulders and tenon-mortise, at the rafter and tie beam sides respectively. Note that the effective lengths in the shoulders at the rafter and tie beam sides (respectively noted $t_{S,ef,1}$ and $t_{S,ef,2}$) are equivalent to the effective lengths in the rafter $t_{ef,1}$ (equation (9)) and in the tie beam $t_{ef,2}$ (equation (11)) calculated for the SSJ design to account the crushing at the front-notch surface.

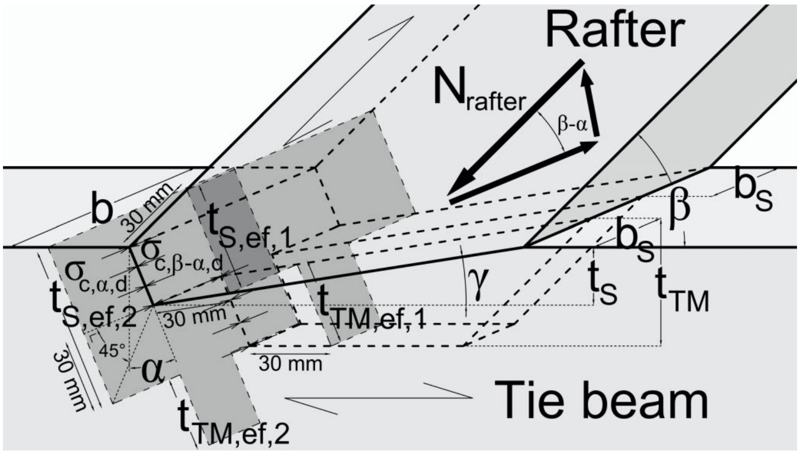

Fig. 16. Schema of the effective lengths $t_{s,ef,1}$, $t_{TM,ef,1}$, $t_{S,ef,2}$ and $t_{TM,ef,2}$, respectively in the shoulders and the tenon-mortise, at the rafter and tie beam sides.

4.2.3 Design equation to account for crushing at the bottom-notch surface

In contrast to the other two typologies of step joints, the crushing at the bottom-notch surface may occur as the third failure mode in the SSJ-TM. Because the bottom-notch surface is reduced to both shoulder areas as shown in Fig. 17, the rafter load-bearing capacity of the joint against the third failure mode is significantly lower than that from the SSJ and DSJ. Therefore, equations (27) and (28) must be satisfied in order to prevent the crushing at the bottom-notch surfaces in the shoulders:

$$N_{rafter} \leq N_{rafter,Rd} = \frac{k_{mod}}{\gamma_M} \cdot f_{c,90,k} \cdot \frac{2 \cdot b_s \cdot l_{c,eff}}{\sin \beta} \tag{27}$$

$$l_{c,eff} = \frac{t_S}{\tan \gamma} + 2.3 \tag{28}$$

The mechanical property $f_{c,90,k}$ stands for the characteristic compressive strength of timber at the bottom-notch surface perpendicular to the grain in the tie beam. The geometrical parameter $l_{c,eff}$ is the effective length of the bottom-notch surfaces, which considers the compressive stress spreading perpendicular to the grain in the shoulders at the tie beam side (Bocquet [5]).

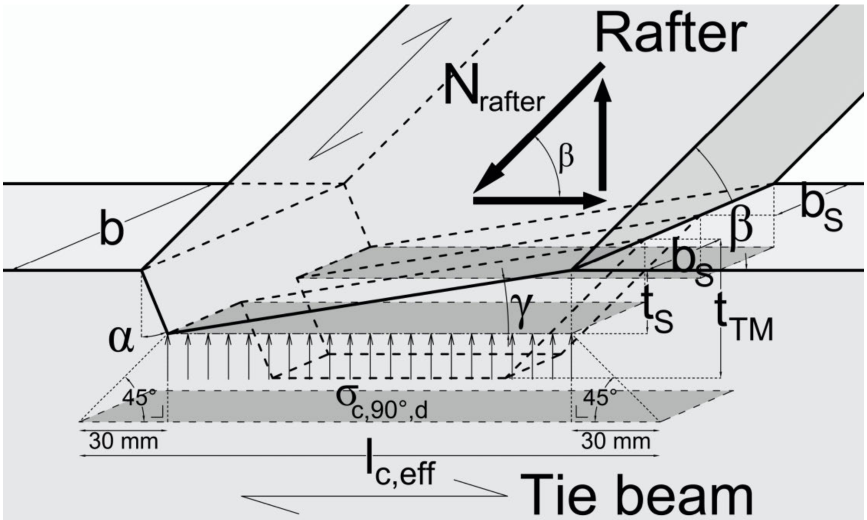

Fig. 17. Schema of the compressive stress spreading perpendicular to the grain and effective compressive length $l_{c,eff}$ in shoulders at the tie beam side.

5. Discussion

Based on geometrical and design recommendations from European standards and authors of works, design models of step joints (SJ) have been determined considering two failure modes: shear cracking in the tie beam, and crushing at the front-notch surface. Furthermore, three SJ typologies have been investigated: single step joint (SSJ), double step joint (DSJ) and single step joint with tenon-mortise (SSJ-TM). So far, several SSJ specimens have been tested under monotonic compression by modifying their geometrical parameters (Verbist et al [6]). Thereby, the reliability of SSJ design equations and the emergence conditions of both failure modes have been discussed and checked.

Relating to shear cracking, it has been shown that the reduction factor $k_{v,red} = 0.8$ with respect to the experimental results should be imposed for the SSJ geometrical configurations including the parameter $l_v / t_v \geq 6$ whereas it can be neglected for the other ones ($k_{v,red} = 1$). Following this recommendation, the design equations and the emergence of shear cracks can be checked as the final failure mode in the SSJ, independently of the rafter skew angle β. As further research on the non-uniform shear stress distribution in the tie beam, empirical equations giving $k_{v,red} = f\,(\alpha,\ l_v\ /\ t_v)$ should be established accurately in order to improve much more the reliability of the SSJ design model. Thereby, finite element modelling of the tested SSJ specimens should be developed in order to better predict shear cracking by determining the reduction factor $k_{v,red}$, as per the SSJ geometrical parameters and the experimental data.

The reliability of the SSJ design model against the crushing at the front-notch surface has been checked for all the GCID specimens. On the other hand, they show to be too restrictive for the GCPTB and GCPR with the rafter skew angle $\beta = 45°$, due to the poor theoretical approximation of the characteristic compressive strength $f_{c,\alpha,k}$. For moderate inclination angles of compressive loading to the grain ($\alpha \geq 30°$), the factor $k_{c,\alpha}$ should not be neglected ($k_{c,\alpha} > 1$) in the SSJ design equations when determining the characteristic compressive strength $f_{c,\alpha,k}$ of timber at the front-notch surface. Furthermore, the SSJ design equations are also restrictive because the friction at the contact surfaces of the joint has been disregarded as theoretical assumption. Hence, the friction forces at the front- and bottom-notch surfaces of the SSJ should be considered in the design equations for rafter skew angles $\beta \geq 30°$. In contrast to the SSJ-TM, the crushing at the bottom-notch surface is rarely a governing failure mode when designing the SJ for low rafter skew angles $\beta \leq 50°$ (Allais et al. [17]).

Based on the experimental and analytical results on the SSJ, similar design models have been proposed for the DSJ and SSJ-TM in respect with the shear crack in the tie beam and the crushing at the front-notch surface. Nevertheless, future experimental and numerical research on the other two SJ typologies are required to check the reliability of design models and the appearance conditions of both failure modes. Furthermore, the SJ design models have been established by considering several research assumptions. For instance, the SJ design models are relevant if the eccentricity of the joint node d_{supp} is inferior to the tie beam height h_{tb} (Allais et al. [17]). Otherwise, the eccentricity will entail additional shear, bending and tension stresses in the tie beam cross-section, which involves extra design models not detailed in the present work.

As a very last point, it should be mentioned that the SSJ specimens tested in laboratory come from young timber. Even if the wood mechanical properties can be approached with theoretical equations, it is not the case at all for timber trusses in existing buildings. In the field of built heritage restoration, the characterization of traditional timber elements and joints (e.g. strength, stiffness) can hardly happen without extracting some samples from the remaining structure. Moreover, the presence of damage inside timber elements and connections make harder the prediction of their mechanical behaviour, based only on the design models defined for sound SJ. In order to take into account the impact of damage on the SJ mechanical behaviour, some reduction values should then be introduced in the design models from the present research.

Acknowledgements

This work was financed by FEDER funds through the Competitively Factors Operational Programme – COMPETE and by national funds through FCT – Foundation for Science and Technology within the scope of the project PTDC/EPH-PAT/2401/2014. This work was partly financed in the framework of the Portuguese Public Procurement Code, LOTE 3ES2 – Escola Secundária de Loulé e Olhão. This work has been developed within the scope of the RILEM TC 245 RTE Reinforcement of Timber Elements in Existing Structures.

References

[1] *EN 1995-1-1:2004 (Eurocode 5)* Design of timber structures – Part 1.1: General – Common rules and rules for buildings. CEN Brussels.

[2] *DIN 1052:2004-08*. Design of timber structures – General rules and rules for buildings. DIN Berlin.

[3] *SIA 265:2012*. Bâtiment génie civil – Construction en bois. Swiss Standardisation Institute, Zurich.

[4] Siem J, Jorissen A (2015) *Can traditional carpentry joints be assessed and designed using modern standards?* 3rd International Conference on Structural Health Assessment of Timber Structures (SHATIS), Wroclaw, Poland.

[5] Bocquet JF (2015) *Les assemblages de charpentes traditionnelles dans le futur contexte réglementaire*. Formation ENSTIB. Université de Lorraine, France.

[6] Verbist MP, Branco JM, Poletti E, Descamps T, Lourenço PB (2017) Single step joint: Overview of European standardized approaches and experimentations. *Materials and Structures* **50**:161. DOI 10.1617/s11527-017-1028-4.

[7] Yeomans D (2003) *The repair of historic timber structures*. Thomas Telford Ltd, London.

[8] Oslet G (1890) *Traité de charpente en bois. Encyclopédie théorique & pratique des connaissances civiles et militaires*. Partie Civile, Cours de construction, Quatrième partie – Edited by Chairgrasse H. Fils, Paris, France. Digital reproduction. http://gallica.bnf.fr/ark:/12148/bpt6k872975z.r=Oslet,+Gustave.langF

[9] *DIN 1052:1988*. Mechanische Verbindungen, Teil 2. DIN Berlin.

[10] *DIN EN 1995-1-1/NA:2013*. National Annex. DIN Berlin.

[11] *CNR-DT 206* (2007) Istruzioni per la Progettazione, l'Esecuzione ed il Controllo delle Strutture di Legno, Italy.

[12] *NEN EN 1995-1-1/NA*. National Annex. NEN Delft.

[13] *NEN 3852:*1973. TGB 1972 – Houtconstructies. NEN Delft.

[14] *NEN 6760:*1991. TGB 1990 – Houtconstructies. NEN Delft.

[15] *NEN 6760:*2005. TGB 1990 – Houtconstructies. NEN Delft.

[16] *Norsk standard 446:*1957. Trekonstruksjoner. Standard Norge Oslo.

[17] Allais M, Kupferle F, Rossi F (2015) *Dimensionnement à froid des assemblages traditionnels bois conformément aux Eurocodes*. Guide Pratique. CODIFAB. Paris, France.

[18] *EN 1995-1-1/A1:2008*. Amendment 1 – Design of timber structures – Part 1.1: General – Common rules and rules for buildings. CEN, Brussels.

[19] Descamps T (2013) *Carpentry connections. Training school on assessment and reinforcement of timber elements*. COST FP1101, University of Mons, Belgium.

[20] Verbist MP, Branco JM, Poletti E, Descamps T, Lourenço PB (2017) *Single and double step joints design: Overview of European standard approaches compared to experimentation*. 3rd International Conference on Preservation, Maintenance and Rehabilitation of Historical Buildings and Structures (REHAB), pp. 1185-1194, Braga, Portugal.

[21] Grezel J (1950) *Les assemblages.* Annales de l'Institut Techniques du Bâtiment et des Travaux Publics, Manuel de la charpente en bois, n°9 – Institut Technique du Bâtiment et des Travaux Publics, Paris, France.

[22] Goss WFM (1890) *Bench work in wood. A course of study and practice designed for the use of schools and colleges*. Ginn & Company, Boston, USA. http://www.woodworkslibrary.com/repository/bench_work_in_wood.pdf.

[23] Descamps T (2015) *Dimensionnement et technologie des structures en bois. Introduction à l'Eurocode 5. Volume 1 – Matériau, vérification ELU et ELS et assemblages*. Université de Mons, Faculté Polytechnique.

Conclusions

Jørgen Munch-Andersen
Danish Timber Information
Copenhagen, Denmark

1. Results and deliverables

An important outcome of any COST Action is the exchange of knowledge between the participants during the meetings. In Working Group 3 *Connections* the exchange has been extensive, both between younger and more experienced people, between research and practice and between countries.

The deliverables to be handed over to the timber connection community consist of:

- This state-of-the-art report (STAR).
- 12 papers to appear in peer-reviewed journals, some in the special issue on COST FP 1402 of *Engineering Structures*.
- Proceedings of International Conference on Connections in Timber Engineering – From Research to Standards; held in Graz, Austria, in September 2017.
- 8 papers published in other conferences proceedings.
- 9 reports from Short Term Scientific Missions, where members from different countries have worked together on a subject.

This summary is mainly based on the papers in this STAR report (referred to by their title) and the proceedings of the conference held in Graz (referred to by their title and (Author, year)). It will focus on the contribution to the development of Eurocode 5 regarding connections.

2. Content and structure

The paper *Results from a questionnaire for practitioners about the connections chapter of the Eurocode 5* clearly demonstrates that the users find the present Chapter 8 both difficult to navigate in and insufficient for many practical problems. It is noticeable that the degree of satisfaction with the present content decreases with increased familiarities.

Insufficient rules were also pointed out by a practitioner at the Graz conference in the paper *The practical design of dowel-type connections in timber engineering structures according to EC5* (Brunauer, 2017).

The comments received from the National Standardization Bodies during the systematic review of Eurocode 5 also points out that many regularly used types of connections are not covered. It is not surprising that the present code is found insufficient as it mainly deals with softwood and glulam assembled with traditional types of fasteners. Rules for the nowadays very common self-tapping screws are incomplete and inconsistent and these screws are partly treated as nails, partly as lag screws. Furthermore, the treatment of engineered wood products is either incomplete or completely lacking.

The structure of the connection chapter is dealt with in *Proposal for a new structure of connections chapter*, where the focus in the proposed new structure is shifted from fastener type to application and design procedure. This is believed to enhance ease of use, as required in the Mandate and needed according to the questionnaire. The structure reflects the basic philosophy regarding design of connections with dowel-type fasteners firstly developed at a meeting of Working Group 3 in October 2015 and agreed in its present form by CEN TC 250/SC 5/WG 5 *Fasteners and connections* in 2016. The design process is divided into

a. Determine the load distribution among the fasteners

b. Check if the single fastener has sufficient load-carrying capacity

c. Check if the timber in the connection has sufficient load-carrying capacity

d. Adjust for group effects not comprised by *a*. and *c*.

e. Check that the fasteners can be installed without risk of splitting

3. Single fasteners

In the Action, the focus regarding single fasteners has been on determining the strength parameters needed to estimate the axial and lateral load-carrying capacities of a fastener (where the lateral capacity is determined by the European Yield Model, EYM). When Eurocode 5 was published this system was not in place but now the strength parameters should be taken from either a Declaration of Performance in accordance with a harmonized standard (in case: EN 14592) or from an ETA issued based on an EAD.

The different paths to obtain the parameters and their consequences are dealt with in *Technical specifications for fasteners*. For each strength parameter there might be several methods to determine it. *Test methods for determination of design parameters of fasteners* gives an overview which also include international alternatives to the European test methods.

The paper *Impact of standards and EADs on the determination of single fastener properties* (Munch-Andersen, 2017) from the Graz conference points out that a characteristic value based on tests with only 20 timber specimens is very uncertain, especially because the coefficient of variation (CoV) is very poorly determined. Further, it seems like most of the CoV of the strength parameter is related to other properties than the density of the timber used, so the influence of different brands of fasteners becomes negligible compared to that. This might imply that many strength parameters for normal fasteners could be determined without individual tests of each brand.

To that end databases are established with test results from many tests. The tests are primarily aimed at declaring strength parameters for specific products in the DoP and therefore not planned for research purposes. This means that not all properties are available that are relevant for generalization.

However, in *Nailed joints: Investigation on parameters for Johansen Model* it is made likely that the tension strength of nails can be used to determine the yield moment with high accuracy using a basic physical model. Using this relation will simplify the required testing. An attempt to determine general values for the withdrawal and head pull-through strengths for ring shank nails depending on the timber density were less successful, probably because of the great influence of timber properties other than the density. But the database should enable sound estimates of the mean values. The same will probably be possible using the information announced in *Database of screws* but the data remain to be studied.

Database of staples also includes edge distance and the results are discussed. Unfortunately, the number of tests available is small, so it is difficult to draw sound conclusions.

For CEN TC 250/SC 5/WG 5 there are two primary concerns regarding the strength parameters used in the equations for the load-carrying capacity of a single fastener. One is that outcome of the tests can be repeated by another testlab, another that the outcome ensures a correct estimation of the load-carrying capacity, i.e. that the test method is representative for the conditions in the connection. It is obvious that any alternative used for determining the same parameter might have a different outcome. In the Action it has not been possible to investigate which methods are most accurate, but more precise description of the test procedures is clearly desirable to increase repeatability.

Better estimates for stiffness of connections, known as the slip modulus, is highly needed, both for correct estimation of the load distribution in a connection and because this stiffness is crucial for members bracing slender timber structures.

Database and parameterization of embedment slip curves opens the discussion on how to express the slip in connections, which is most inadequately described in the present Eurocode 5. This subject is developed in *Beam-on-foundation modelling as an alternative design method for single fastener connections* with focus on numerical modelling of slip as basis for evaluation of load distribution in a connection. Embedment is also dealt with in *New criteria for the determination of the parallel-to-grain embedment strength of wood* (Yurrita and Cabrero, 2018).

4. Connection design

The key challenges in the proposed new structure of Eurocode 5 are items *a* (load distribution) and *c* (failure in timber) in the design process given above.

Valuable contributions to item *a* are *Stiffness and deformation of connections with dowel-type fasteners* as it also discusses load distribution and *Numerical modelling of the load distribution in multiple fastener connections* (Bader et al., 2017)

In *Design recommendations and example calculations for dowel-type connections with multiple shear planes* the importance of the load distribution is emphasized, including the optimal timber member thickness in multiple shear plane connections.

Failure in timber covered by item *c* will generally cause brittle failure modes. The international perspective on this is presented in the conference paper *Brittle failure of connections loaded parallel to grain* (Quenneville, 2017). This approach is developed towards a general European model based on the present Annex A in Eurocode 5, see *A review of the existing models for brittle failure in connections loaded parallel to the grain*. This is taken further in *Performance assessment of existing models to predict brittle failure modes of steel-to-timber connections loaded parallel-to-grain with dowel-type fasteners* (Yurrita and Cabrero, 2018).

A review of the existing models for brittle failure in connections loaded parallel to the grain summarizes existing models on this equally important topic. An improved approach is given in *Splitting of timber beams caused by perpendicular to grain forces of multiple connections* (Leijten, 2018).

CLT is a new material, so *Design approaches for dowel-type connections in CLT structures and their verification* fill in a major gap for using the possibilities of this material and contributes to include the special precautions for CLT in Eurocode 5.

Lastly, the paper *Design of three typologies of step joints – Review of European standardized approaches*, which also includes numerical studies, assists in fulfilling the strong desire from several countries to include modern carpentry joints in Eurocode 5.

5. Conclusions

The work of Working Group 3 *Connections* in COST Action FP1402 has already – and will in the years to come – contribute significantly to the development of the design basis for dowel-type connections in Eurocode 5. The Action has also established contact between individuals and research groups, which will contribute to the continued work to form a sound background for the revised Eurocode 5.

List of publications and STSM reports relevant to COST Action FP1402 Working Group 3

Peer-reviewed journal articles

Cabrero JM, Yurrita M (2018) Performance assessment of existing models to predict brittle failure modes of steel-to-timber connections loaded parallel-to-grain with dowel-type fasteners. *Engineering Structures*, in press. DOI: 10.1016/j.engstruct.2018.03.037.

Jockwer R, Dietsch P (2018) Review of design approaches and test results on brittle failure modes of connections loaded at an angle to the grain. *Engineering Structures* **171**:362-372.

Jockwer R, Fink G, Köhler J (2018) Assessment of the failure behaviour and reliability of timber connections with multiple dowel-type fasteners. *Engineering Structures* **172**:76-84.

Leijten AJM (2018a) A general bearing deformation model for timber: Compression perpendicular to grain. *Construction and Building Materials* **165**:707-716.

Leijten AJM (2018b) Splitting of timber beams caused by perpendicular to grain forces of multiple connections. *Engineering Structures* **171**:10-14.

Ringhofer A, Brandner R, Blass HJ (2018). Cross laminated timber (CLT): Design approaches for dowel-type fasteners and connections. *Engineering Structures*, in press. DOI: 10.1016/j.engstruct.2018.05.032.

Sandhaas C, Görlacher R (2018) Analysis of nail properties for joint design. *Engineering Structures* **173**:231-240.

Schweigler M, Bader TK, Vessby J, Eberhardsteiner J (2017) Constrained displacement boundary conditions in embedment testing of dowel-type fasteners in LVL. *Strain* **53**(6):e12238.

Schweigler M, Bader TK, Hochreiner G, Lemaître R (2018a) Parameterization equations for the nonlinear connection slip applied to the anisotropic embedment behavior of wood. *Composites Part B: Engineering* **142**:142–158.

Schweigler M, Bader TK, Hochreiner G (2018b) Engineering modeling of semi-rigid joints with dowel-type fasteners for nonlinear analysis of timber structures. *Engineering Structures* **171**:123-139.

Stepinac M, Cabrero JM, Ranasinghe K, Kleiber M (2018) Proposal for reorganization of the connections chapter of Eurocode 5. *Engineering Structures* **170**:135-145.

Yurrita M, Cabrero JM (2018) New criteria for the determination of the parallel-to-grain embedment strength of wood. *Construction and Building Materials* **173**:238-250.

Conference proceedings

Bader TK, Bocquet JF, Schweigler M, Lemaître R (2017) *Numerical modeling of the load distribution in multiple fastener joints*. Cost Action FP1402, International Conference on Connections in Timber Engineering – From Research to Standards. Graz University of Technology, Austria, pp. 136-152.

Brunauer A (2017) *The practical design of dowel-type connections in timber engineering structures according to EC5*. Cost Action FP1402, International Conference on Connections in Timber Engineering – From Research to Standards. Graz University of Technology, Austria, pp. 6-14.

Brühl F. Kuhlmann U (2017) *Consideration of connection ductility within the design of timber structures*. Cost Action FP1402, International Conference on Connections in Timber Engineering – From Research to Standards. Graz University of Technology, Austria, pp. 32-45.

Cabrero JM, Yurrita M (2018) *Performance of the different models for brittle failure in the parallel-to-grain direction for connections with dowel-type fasteners.* INTER Meeting 51, Paper 51-7-12, Tallinn, Estonia.

Cabrero JM, Rodriguez V (2017) *Avances de la Acción COST FP1402: de la investigación a la futura normativa*. Congreso sobre Construcción con Madera y otros Materiales Lignocelulósicos (LIGNOMAD 17), Barcelona, Spain.

Dias A (2017) *Performance of dowel-type fasteners for hybrid timber structures*. Cost Action FP1402, International Conference on Connections in Timber Engineering – From Research to Standards. Graz University of Technology, Austria, pp. 112-121.

Dietsch P, Brunauer A (2017) *Reinforcement of timber structures – a new section for EC5*. Cost Action FP1402, International Conference on Connections in Timber Engineering – From Research to Standards. Graz University of Technology, Austria, pp. 184-211.

Jockwer R, Dietsch P (2017) *Brittle failure of connections loaded perpendicular to grain*. Cost Action FP1402, International Conference on Connections in Timber Engineering – From Research to Standards. Graz University of Technology, Austria, pp. 166-182.

Jockwer R, Fink G, Köhler J (2017) *Assessment of existing safety formats for timber connections – How probabilistic approaches can influence connection design in timber engineering.* Cost Action FP1402, International Conference on Connections in Timber Engineering – From Research to Standards. Graz University of Technology, Austria, pp. 16-31.

Munch-Andersen J (2017) *Impact of standards and EADs on the determination of single fastener properties*. Cost Action FP1402, International Conference on Connections in Timber Engineering – From Research to Standards. Graz University of Technology, Austria, pp. 46-63.

Quenneville P (2017) *Brittle failure of connections loaded parallel to grain*. Cost Action FP1402, International Conference on Connections in Timber Engineering – From Research to Standards. Graz University of Technology, Austria, pp. 154-165.

Ranasinghe K, Cabrero JM, Stepinac M, Kleiber M (2018) *Practitioners' opinions about the EN 1995 – results from comprehensive online survey*. World Conference on Timber Engineering, Seoul, Korea.

Ringhofer A, Brandner R, Blass HJ (2017) *Design approaches for dowel-type connections in CLT structures and their verification*. Cost Action FP1402, International Conference on Connections in Timber Engineering – From Research to Standards. Graz University of Technology, Austria, pp. 80-111.

Sandhaas C, Görlacher R (2017) *Nailed joints: Investigation on parameters for Johansen model*. Proceedings INTER Meeting 49, Paper 50-7-3, Kyoto, Japan.

Schänzlin J, Mönch S (2017) *Push-out vs. beam: Can the results of experimental stiffness of TCC-connectors be transferred?* Cost Action FP1402, International Conference on Connections in Timber Engineering – From Research to Standards. Graz University of Technology, Austria, pp. 122-134.

Stepinac M, Rajčić V, Cabrero JM, Ranasinghe K, Kleiber M (2018) *Practitioners' opinions about the EN 1995 – German point of view in comparison with the rest of Europe*. Doktorandenkolloqium Holzbau Forschung + Praxis. Universität Stuttgart, Germany, pp. 185-190.

Tomasi R, Pasca D (2017) *Summary and recommendations regarding the seismic design of timber connections*. Cost Action FP1402, International Conference on Connections in Timber Engineering – From Research to Standards. Graz University of Technology, Austria, pp. 212-223.

Yurrita M, Cabrero JM, Quenneville P (2018) *Brittle failure mode in the parallel-to-grain direction on multiple shear dowelled timber connections with slotted-in steel plates*. INTER Meeting 51, Paper 51-7-10, Tallinn, Estonia.

Yurrita M, Cabrero JM (2017a) *The embedment strength as a system property*. INTER Meeting 50, Paper 50-7-2, pp. 83-93, Kyoto, Japan.

Yurrita M, Cabrero JM (2017b) *New concepts for the development of a formula for the embedment strength of timber*. Conference of Computational Methods in Wood Mechanics – from Material Properties to Timber Structures (CompWood 2017), Vienna, Austria.

STSM reports

Jockwer R (ETH Zurich, CH). *Review of design recommendations for connections loaded perpendicular to the grain*. STSM at Technical University Munich (DE), 08.02.-26.02.2016.

Jockwer R (ETH Zurich, CH). *Load-deformation behaviour and stiffness properties of lateral connections with multiple dowel-type fasteners*. STSM at TU Eindhoven (NL), 19.02.-02.03.2018.

Lemaître R (University of Lorraine, FR). *Works on different numerical modelling approaches to predict the load distribution in timber joints*. STSM at Linnaeus University (SE). 26.02.-23.03.2018.

Majano-Majano A (Technical University of Madrid, ES). *Splitting capacity of hardwood connections loaded at an angle to the grain*. STSM to University of Tras-os-Montes e Alto Douro (PT), 09.11.-16.12.2016.

Mergny E (Université Catholique de Louvain, BE). *Properties of single fasteners*. STSM at Karlsruhe Institute of Technology (DE), 16.11.-13.12.2015

de Proft K (Belgian Institute for Wood Technology, BE). *Properties of staples*. STSM at Karlsruhe Institute of Technology (DE), 20.06-30.06.2017.

Ringhofer A (Graz University of Technology, AT). *Stiffness properties of axially loaded self-tapping screws*. STSM at Karlsruhe Institute of Technology (DE), 11.01.-12.02.2016.

Rossi S (University of Trento, IT). *Load-bearing capacity of steel-to-timber dowelled joints with multiple slotted-in plates*. STSM to Lund University (SE). 01.04.-30.04.2016.

Schweigler M (Vienna University of Technology, AT). *Experimental characterisation and parameterisation of the load-to-grain angle dependent embedment behaviour of dowel-type fasteners in laminated veneer lumber (LVL).* STSM at Linnaeus University (SE). 09.05.-27.05.2016.